Mediators of Inflammation

Immunology and Infection by Protozoan Parasites

Guest Editors: Edecio Cunha-Neto, Christophe Chevillard, Mauricio M. Rodrigues, and Marcelo T. Bozza

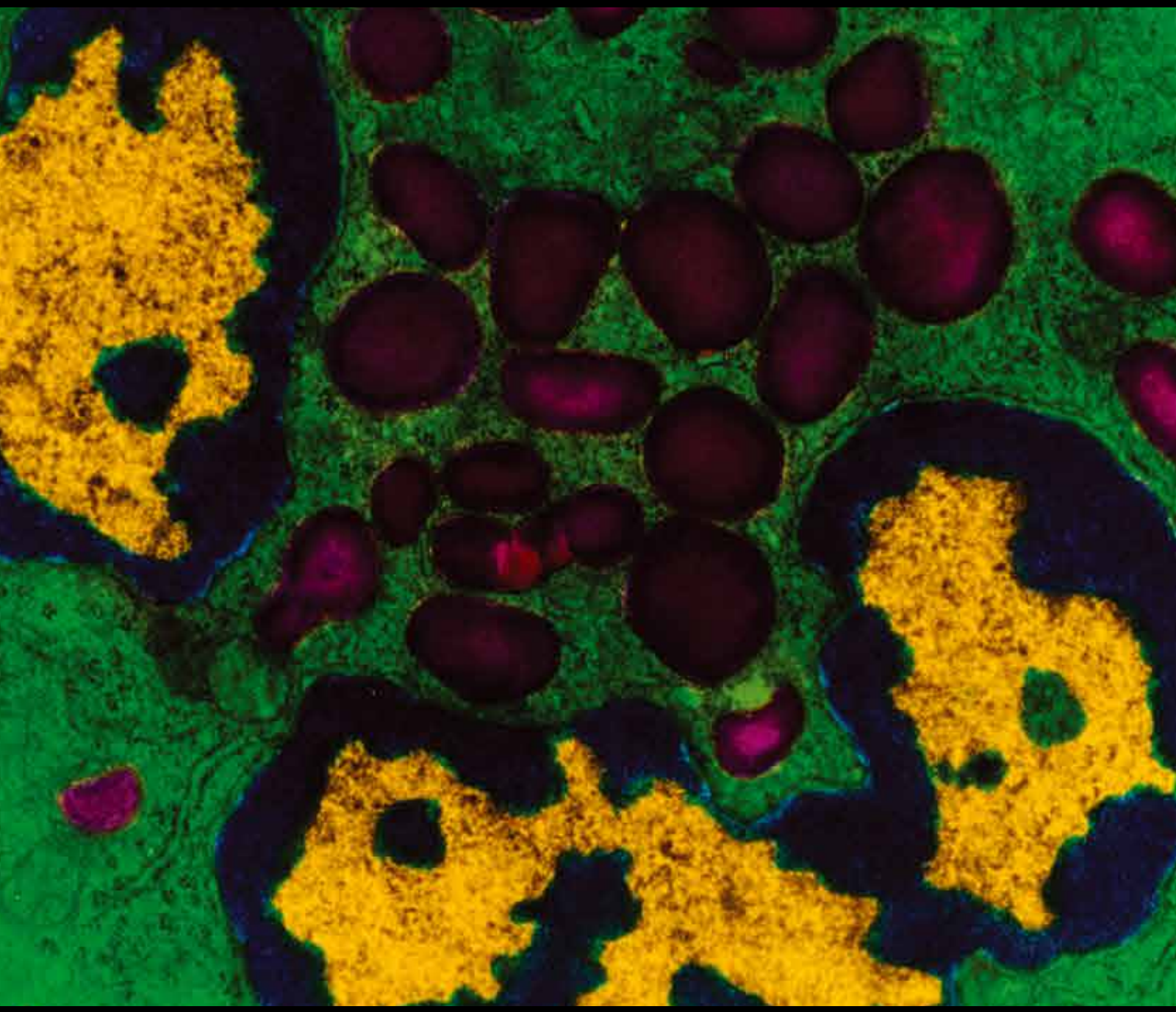

Immunology and Infection by Protozoan Parasites

Mediators of Inflammation

Immunology and Infection by Protozoan Parasites

Guest Editors: Edecio Cunha-Neto, Christophe Chevillard, Mauricio Martins Rodrigues, and Marcelo T. Bozza

Editorial Board

Contents

Hindawi Publishing Corporation
Mediators of Inflammation
Volume 2015, Article ID 504951, 2 pages
http://dx.doi.org/10.1155/2015/504951

Editorial

Immunology and Infection by Protozoan Parasites

Edecio Cunha-Neto,[1] Christophe Chevillard,[2] Mauricio Martins Rodrigues,[3] and Marcelo T. Bozza[4]

[1]*Heart Institute (Incor), University of São Paulo School of Medicine, 05403-000 São Paulo, SP, Brazil*
[2]*INSERM and Université Aix-Marseille, Marseille, France*
[3]*Escola Paulista de Medicina, Universidade Federal de São Paulo, 04044-010 São Paulo, SP, Brazil*
[4]*Departamento de Imunologia, Instituto de Microbiologia, Universidade Federal do Rio de Janeiro, 21941-902 Rio de Janeiro, RJ, Brazil*

Correspondence should be addressed to Edecio Cunha-Neto; edecunha@gmail.com

Received 1 December 2014; Accepted 1 December 2014

Protozoan infection is the cause of diseases of high morbidity and mortality. Most are non-self-limiting chronic infections and neglected diseases; emergent antimicrobial-resistant strains pose a substantial problem; for many of them treatment either is highly toxic or has limited effectiveness. Vaccine development is still a formidable task and there is no licensed vaccine for human protozoan infection. The key to the control of protozoan infection is the understanding of the host immune response to protozoan parasites, which will guide the development of effective vaccines and immunotherapeutic agents. In this special issue, there are important studies on the immunology of *T. cruzi* infection, tegumentary and visceral leishmaniasis, malaria, and toxoplasmosis, both in patients and in animal models, which promote the understanding of immunopathological/immunoprotective parameters in these diseases.

The reviews by J. M. Álvarez and colleagues and by E. Cunha-Neto and C. Chevillard cover fundamental findings, mechanisms, and questions concerning the immune response and pathology of mouse and human disease. In this line, L. G. Nogueira and colleagues characterize the myocardial expression of transcriptional factors involved in effector CD4+ T cell differentiation and the characteristic cytokines produced by the distinct lymphocyte subsets and demonstrate a profound predominance of local Th1 response. L. C. J. Abel and coworkers characterized the proinflammatory effects of glicophosphatidyl inositol-anchored *T. cruzi* mucin (GPI-mucins) on human immune cells. It was observed that IL-12 production by GPI-mucins was dependent on IFN-γ and CD40-CD40L interactions. F. C. Dias and colleagues investigated the HLA-G expression in tissues and HLA-G 147 3′ UTR polymorphic site typing in patients presenting Chagas disease and the role of the mouse functional homolog in *T. cruzi* infection. F. Vorraro and colleagues studied the susceptibility to *T. cruzi* of mouse strains previously selected based on inflammatory and antibody responses to complex antigens. Q. Miao and M. Ndao review the potential impact of *T. cruzi* infection on the status of host lipid metabolism. The role of lipid mediators in *T. cruzi* infection is explored in two research articles. A. M. C. Canavaci and colleagues revisit the pathological role of 5-lipoxygenase in the acute infection of mice and A. D. Malvezi and coworkers investigate the role of cyclooxygenase and lipoxins in macrophage invasion by *T. cruzi*. In mouse models of chronic myocardial disease by *T. cruzi*, I. R. Pereira and colleagues show that treatment with infliximab, an anti-human TNF monoclonal antibody, reduced the frequency of mice with arrhythmias and cardiac fibrosis, while M. B. de Cuba and coworkers show the beneficial effect of cholinergic stimulation in reducing inflammation and fibrosis in the heart. Importantly, A. F. Araújo and coworkers demonstrate the beneficial effects of prophylactic vaccination using *T. cruzi* genes against acute and chronic pathologies caused by myotropic strains of the parasite. W. H. K. Cabrera and colleagues have characterized mouse lines selected for maximal (AIRmax) or minimal (AIRmin) acute inflammatory reaction and for high (HIII)

or low (LIII) antibody (Ab) responses to complex antigens. Resistance to *T. cruzi* infection was found in female and in high responder lines AIRmax and HIII. It was correlated with enhanced production of IFN-γ and nitric oxide production by peritoneal and lymph node cells, in HIII males and females. Moreover, an Ab production QTL marker mapping to mouse chromosome 1 significantly cosegregated with survival after acute *T. cruzi* infection.

In the *Leishmania* field, M. F. Lopes and colleagues here review the interface between *Leishmania* and phagocytes, cells that are both targets and effector of the anti-*Leishmania* immune response. The study by E. Svensjö and colleagues suggests that a serine peptidase (ISP-2) from *L. major* regulates macrophage phagocytosis by inhibiting the pericellular release of proinflammatory kinins from surface bound kininogens. C. M. V. Vendrame and coworkers have shown that insulin-like growth factor- (IGF-) I decreased nitric oxide production but increased arginase expression and activity, which lead to increased *Leishmania* parasitism. However, IGF-I did not result in altered cytokine levels. Moreover, stimulation with IGF-I induced phosphatidylserine exposure on amastigotes led to increased arginase activity in macrophages, and this process was not blocked by anti-TGF-β antibodies. M. D. T. Carvalho and colleagues investigated risk markers of *L. infantum* visceral leishmaniasis and found that lipoprotein and triglyceride levels are risk factors for development of visceral leishmaniasis. They also found that genetic polymorphisms at the Lpl and Pparγ were associated with differential levels of lipoproteins and thus related to the disease outcome. I. Naouar and coworkers investigated granzyme-positive CD4+ T cells activated by *L. major* antigens, in *Leishmania*-healed subjects. They found that even CD4+CD25+CD127$^{\mathrm{dim/-}}$ Tregs expressed granzyme after exposure to *Leishmania* antigens.

A number of manuscripts published in this issue provide important new knowledge in the important field of malaria. A review from H. Zheng and colleagues highlighted important aspects of preerythrocytic stages biology and the immune evasion strategies of malaria parasites. The unraveling of these escape mechanisms may aid the development of a vaccine against malaria. In this same direction, the manuscript by the group of J. Huang and colleagues generated a new mouse model to study the immunity to these preerythrocytic stages. This new model employed transgenic MHC-I Kd mice. The results of their studies indicate that protective antimalaria immunity induced by radiation-attenuated sporozoites of *Plasmodium yoelii* in MHC-I-Kd-Tg mice is mediated by CS protein-specific, Kd-restricted CD8+ T cells. E. S. Fernandes and colleagues studied the effect of TRPV1 antagonism by capsazepine during mouse infection with *Plasmodium berghei* ANKA. Their result indicated that there was a modulation of the innate immune response in mice infected but it did not affect parasitemia. Two other studies dealt with malaria pathogenesis. L. S. Ortolan and coworkers described new predictive criteria to study the pathogenesis of malaria-2 associated ali/ards in mice. This method for accurately identifying mice suffering from ALI/ARDS before death will allow the use of this model to study the pathogenesis of this disease. Finally, J. C. Sánchez-Arcila and colleagues evaluated whether intestinal parasites coinfection would alter plasma cytokines profile elicited in acute malaria in subjects from endemic area of Brazil. They concluded that the infection with intestinal parasites (mainly protozoan) does not significantly modify the pattern of cytokine production in individuals infected with *P. falciparum* and *P. vivax*.

Finally, A. S. Machado and colleagues investigated the immunopathogenesis of toxoplasmosis in parturients and nonpregnant women. They measured the synthesis of Th1 and Th2 cytokines by mononuclear cells after culture with live *T. gondii* and identified Th17 (CD4+) and Tc17 (CD8+) cells in toxoplasma-seronegative and toxoplasma-seropositive parturient and nonpregnant women. They observed a lower level of IL-17-expressing CD4+ and CD8+ T lymphocytes in cultures of cells from seronegative and seropositive parturient and nonpregnant women that were stimulated with tachyzoites. It has been shown that the cytokine pattern and IL-17-expressing CD4+ and CD8+ T lymphocytes may have important roles in the inflammatory response to *T. gondii*, thus contributing to the maintenance of pregnancy and control of parasite invasion and replication. A. S. Machado and coworkers studied immunological and hematological biomarkers of ocular congenital toxoplasmosis in infants, finding differential immune parameter networks in each clinical group (active and cicatricial ocular toxoplasmosis).

Edecio Cunha-Neto
Christophe Chevillard
Mauricio Martins Rodrigues
Marcelo T. Bozza

Hindawi Publishing Corporation
Mediators of Inflammation
Volume 2015, Article ID 595829, 16 pages
http://dx.doi.org/10.1155/2015/595829

Research Article

Human Leucocyte Antigen-G (HLA-G) and Its Murine Functional Homolog Qa2 in the *Trypanosoma cruzi* Infection

Fabrício C. Dias,[1] Celso T. Mendes-Junior,[2] Maria C. Silva,[3] Fabrine S. M. Tristão,[4] Renata Dellalibera-Joviliano,[5] Philippe Moreau,[6] Edson G. Soares,[7] Jean G. Menezes,[7] André Schmidt,[1] Roberto O. Dantas,[1] José A. Marin-Neto,[1] João S. Silva,[3] and Eduardo A. Donadi[1,3]

[1] *Departamento de Clínica Médica, Faculdade de Medicina de Ribeirão Preto, Universidade de São Paulo, Avenida Bandeirantes 3900, 14049-900 Ribeirão Preto, SP, Brazil*
[2] *Departamento de Química, Faculdade de Filosofia, Ciências e Letras de Ribeirão Preto, Universidade de São Paulo, Avenida Bandeirantes 3900, 14049-900 Ribeirão Preto, SP, Brazil*
[3] *Departamento de Bioquímica e Imunologia, Faculdade de Medicina de Ribeirão Preto, Universidade de São Paulo, Avenida Bandeirantes 3900, 14049-900 Ribeirão Preto, SP, Brazil*
[4] *Departamento de Morfologia, Fisiologia e Patologia Básica, Faculdade de Odontologia de Ribeirão Preto, Universidade de São Paulo, Avenida Bandeirantes 3900, 14049-900 Ribeirão Preto, SP, Brazil*
[5] *Departamento de Cirurgia e Anatomia, Faculdade de Medicina de Ribeirão Preto, Universidade de São Paulo, Avenida Bandeirantes 3900, 14049-900 Ribeirão Preto, SP, Brazil*
[6] *CEA, Institute of Emerging Diseases and Innovative Therapies, Research Division in Hematology and Immunology, Saint-Louis Hospital, 1 Avenue Claude Vellefaux, 75475 Paris, France*
[7] *Departamento de Patologia e Medicina Legal, Faculdade de Medicina de Ribeirão Preto, Universidade de São Paulo, Avenida Bandeirantes 3900, 14049-900 Ribeirão Preto, SP, Brazil*

Correspondence should be addressed to Eduardo A. Donadi; eadonadi@fmrp.usp.br

Received 13 June 2014; Accepted 17 September 2014

Academic Editor: Marcelo T. Bozza

Genetic susceptibility factors, parasite strain, and an adequate modulation of the immune system seem to be crucial for disease progression after *Trypanosoma cruzi* infection. HLA-G and its murine functional homolog Qa2 have well-recognized immunomodulatory properties. We evaluated the *HLA-G* 3′ untranslated region (3′UTR) polymorphic sites (associated with mRNA stability and target for microRNA binding) and HLA-G tissue expression (heart, colon, and esophagus) in patients presenting Chagas disease, stratified according to the major clinical variants. Further, we investigated the transcriptional levels of Qa2 and other pro- and anti-inflammatory genes in affected mouse tissues during *T. cruzi* experimental acute and early chronic infection induced by the CL strain. Chagas disease patients exhibited differential *HLA-G* 3′UTR susceptibility allele/genotype/haplotype patterns, according to the major clinical variant (digestive/cardiac/mixed/indeterminate). HLA-G constitutive expression on cardiac muscle and colonic cells was decreased in Chagasic tissues; however, no difference was observed for Chagasic and non-Chagasic esophagus tissues. The transcriptional levels of *Qa2* and other anti and proinflammatory (*CTLA-4, PDCD1, IL-10, INF-γ*, and *NOS-2*) genes were induced only during the acute *T. cruzi* infection in BALB/c and C57BL/6 mice. We present several lines of evidence indicating the role of immunomodulatory genes and molecules in human and experimental *T. cruzi* infection.

1. Introduction

Chagas disease or American trypanosomiasis is caused by the parasite *Trypanosoma cruzi*, which may produce acute and chronic manifestations. During the acute phase, most cases are indeterminate, but some patients may develop severe myocarditis or meningoencephalitis, which can be lethal. The chronic phase exhibits four major clinical variants:

(i) the indeterminate form represents 50–70% of cases and develops without evident clinical and pathological signs [1]; (ii) the cardiac form encompasses 10–20% of cases and usually presents progressive congestive heart failure, various cardiac arrhythmias, thromboembolic events, and sudden death [1, 2]; (iii) the digestive form (8–10% of cases) is characterized by clinical signs of megaesophagus, megacolon, or both; (iv) the cardiodigestive or mixed form (8% of cases) comprises clinical and pathological signs of cardiac and digestive involvement. These clinical syndromes are considered to be a consequence of autonomic neuronal loss, microvascular derangements, and chronic organ inflammation directly dependent on parasite persistence or by immune system cells [3, 4].

In parallel with the chronic parasite infection, the immune response against parasite antigens is associated with the Chagas heart disease pathogenesis. Key features of the immunity in the Chagas disease include (i) predominance of partially activated T CD8 lymphocytes in cardiac inflammatory infiltrates [5], accompanied by high production of nitric oxide (NO), IL-12, monocyte chemoattractant protein-1 (MCP-1), and IFN-γ by infiltrating macrophages; (ii) preponderant IFN-γ production by cytolytic natural killer (NK) cells in the acute phase of the disease to control tissue and systemic parasite burden; and (iii) polyclonal B lymphocyte response [6–13].

Cytokine patterns in Chagas disease are characterized by T-helper (Th)1 polarization in the acute phase, with predominance of IFN-γ and TNF production. During the chronic phase, a coexistence of the Th1 (IL-12, IFN-γ, and TNF) and Th2 profiles (IL-4 and IL-10) may be observed, and the equilibrium between these profiles may be relevant to disease morbidity [3, 14, 15]; that is, a Th1 response aggravates and a Th2 response produces a better outcome in murine trypanosomiasis and human Chagas disease [16–20]. Besides cytokines, other immunomodulatory molecules such as PD-1 and CTLA-4 are also involved in acute and chronic trypanosomiasis [20–25]. In this context, immunomodulatory molecules may play an important role for disease evolution, controlling or exacerbating the immune response against *T. cruzi* itself or tissue modifications induced by parasites.

Among immunomodulatory molecules, the human leucocyte antigen- (HLA-) G is a nonclassical histocompatibility class Ib molecule, which has a well-recognized role in controlling several branches of the immune response, inhibiting T cell proliferation, NK, and cytotoxic T lymphocytes, inducing regulatory T cells and tolerizing dendritic cells [26]. These effects are primarily due to the preferential interaction of the HLA-G molecule with the Ig-like transcript (ILT)2, ILT4, and killer cell immunoglobulin-like (KIR2DL4) receptors, which induce inhibitory intracellular signals via tyrosine-based (ITIM) motifs [27].

HLA-G mRNA has restricted expression in nonpathological conditions, for organs such as the placenta, thymus, heart, intestines, brain, and skin [28], and the constitutive expression of the HLA-G molecule has been observed on placenta, thymus, cornea, pancreas, brain, erythroid cells, and blood cell surfaces [29–34]. On the other hand, HLA-G neoexpression has been observed in several situations, including tumors, viral infections, engrafted tissues, and autoimmune and inflammatory diseases. Depending on the underlying condition, the expression may be advantageous when the blockade of the immune response is desirable, such as in autoimmune disorders and in allografting, whereas HLA-G expression in tumors and chronic viral infections may be harmful [35, 36].

At the coding region, the *HLA-G* gene presents limited polymorphisms compared to classical HLA class I (*HLA-A/B/C*) genes, exhibiting only 50 alleles (The International Immunogenetics Database (IMGT), v3.16.0) and coding 16 different membrane-bound full length proteins. The regulatory regions also present several polymorphisms that coincide with or are close to binding sites for transcription factors (promoter region) or are targets for microRNA binding (3′ untranslated region (3′UTR)). At least 29 variation sites have been described at the promoter region [37] and 16 variants have been identified at the *HLA-G* 3′UTR [38]. Considering that the regulatory regions are involved on the magnitude of *HLA-G* gene expression, the study of these regions is relevant. In the healthy Brazilian population, at least eight *HLA-G* 3′UTR variation sites have been described [37, 39], and some of them have been associated with plasma soluble HLA-G (sHLA-G) levels [40].

The HLA-G murine functional homolog Qa2, encoded by *H2-Q7/Q9* gene, also presents restricted tissue expression, and Qa2 mRNA has been reported in thymus, liver, intestines, spleen, placenta, and brain. Qa2 also modulates the immune response by interacting with as yet unidentified NK cell receptors [41–45].

Little information is available regarding HLA-G and the Qa2 murine functional homolog in acute and chronic parasitic diseases. Considering that (i) no information is available regarding the role of these immunoregulatory molecules in *T. cruzi* infection; (ii) Chagas disease is a chronic disorder, in which several mechanisms of immunomodulation have been described in association with its pathogenesis; (iii) clinical variants of Chagas disease may depend on parasite and host genetic factors; (iv) experimental trypanosomiasis may help in the understanding of the human disease counterpart, we designed a study encompassing the HLA-G tissue expression and *HLA-G* 3′UTR polymorphic site typing in patients presenting Chagas disease, stratified according to major clinical variants. In addition, we evaluated the transcriptional level of the *H2-Q7/Q9* (Qa2), and other immunoregulatory *H2-T23* (Qa1), *CTLA-4,* and *PDCD1* (PD-1) genes in mouse (BALB/c and C57BL/6) affected tissues during experimental acute and early chronic infection caused by the CL strain of *T. cruzi* and correlated the expression of these genes with other mediators of inflammation, including *INF-γ*, inducible nitric oxide synthase (*NOS-2*), and *IL-10*.

2. Methods

2.1. Subjects. The protocol of the study was approved by the local Research Ethics Committee (Protocol number 11237/2009) and written informed consent was obtained from all participants. A total of 177 chronic Chagas disease patients exhibiting positive serology for *T. cruzi* antigens

followed at the Divisions of Cardiology and Gastroenterology of the Department of Medicine of the School of Medicine of Ribeirão Preto, University of São Paulo, Brazil, and 155 healthy individuals from the same region of patients, exhibiting negative serology for *T. cruzi* infection, were studied. The Chagas disease patients were submitted to clinical and laboratory examination. Electro- and echocardiography, esophagus and colon contrast X-ray examinations, and esophagus electromanometry were performed to classify patients into cardiac ($n = 52$, exhibiting or not heart failure), digestive ($n = 62$, exhibiting megaesophagus, megacolon, or both), cardiodigestive or mixed ($n = 24$, presenting any combination of cardiac and digestive forms), and indeterminate ($n = 39$) variants.

2.2. DNA Extraction and Genotyping. Genomic DNA was extracted from peripheral blood leucocytes using a standard salting-out procedure. Genotyping of the variation sites at *HLA-G* 3′UTR was performed by sequencing analyses as previously described [39].

2.3. Immunohistochemical Analysis of HLA-G. Fifty-four specimens of tissues obtained from Chagas disease deceased patients were analyzed, of which 30 were derived from heart, 13 from colon, and 11 from esophagus. In parallel, 20 tissue specimens (8 from heart, 6 from esophagus, and 6 from sigmoid colon) of deceased individuals without Chagas disease and exhibiting no histopathological tissue alteration were analyzed. Three specimens of trophoblast tissue (positive control for HLA-G expression) were also analyzed. The immunohistochemical analysis was performed using the primary antibody MEM/G9 (HLA-G1 and sHLA-G5 specific mouse IgG) (Exbio, Prague, Czech Republic), diluted 1 : 200, as previously described [46]. Briefly, after defining the range of brown color considered being positive, images were converted to 256 shades (8-bit) of gray. Then, the grayscale images were converted into a binary (black and white) variable to define the cutoff point. The threshold was adjusted, and the brown areas became black portions in the binary image [47]. Immunostained areas were evaluated using the ImageJ software (National Institutes of Health, Bethesda, MD).

2.4. Experimental Infections and Transcriptional Level Analysis. Male eight-week-old C57BL/6 and BALB/c mice were intraperitoneously (IP) injected with bloodstream CL strain forms of *T. cruzi*, using three infected and three noninfected animals in two independent experiments. The mice were cared for according to the institutional guidelines on ethics in animal experiments and all protocols were approved by the local Ethics Committee on Animal Care and Research (process number 172/2009).

For the acute infection, 10^3 bloodstream forms were IP injected. Mouse survival was verified daily for 30 days and the parasitemia was quantified microscopically by counting the parasites in 5 μL of citrated blood obtained from the tail lateral vein from day 7 until day 29 after infection. Parasite load was analyzed in the heart at day 24 after infection [48]. For the early chronic infection, 10^2 bloodstream forms of *T. cruzi* were IP injected and mouse survival was verified daily for 60 days. Parasite load was analyzed in the heart at day 60 after infection.

Gene expression was detected in the heart and esophagus at 24 and 60 days after infection (dpi), for acute and early chronic infections, respectively. Although Qa2, Qa1, and PD-1 are the encoded molecules of the *H2-Q7/Q9*, *H2-T23,* and *PDCD1* genes, respectively, to facilitate understanding we will refer in this text to *Qa2, Qa1,* and *PD-1* expression as synonyms of their respective gene expressions.

Total RNA was extracted from tissues using the TRIzol reagent (Invitrogen, Carlsbad, CA) and was reverse transcribed to obtain cDNA with the SuperScript III (Invitrogen) transcriptase reverse. SYBR Green Mix-based real-time quantitative PCR assays were performed using a StepOnePlus system (Applied Biosystems, Foster City, CA). Data were normalized according to the expression of the glyceraldehyde phosphate dehydrogenase (*GADPH*) housekeeping gene and relative expression of each mRNA was calculated with the $2^{-\triangle\triangle Ct}$ method [49]. Primer sequences included (i) *H2-Q7/Q9*-forward 5′-ATG GCG ACC ATT GCT GTT GT-3′, *H2-Q7/Q9*-reverse 5′-TCC AAT GAT GGC CAC AGC T-3′; (ii) *H2-T23*-fwd 5′-GCA CAA GTC AGA GGC AGT CG-3′, *H2-T23*-rev 5′-TGC AGG TAT GCC CTC TGT TG-3′; (iii) *CTLA-4*-fwd 5′-ACC TCT GCA AGG TGG AAC TCA-3′, *CTLA-4*-rev 5′-CCA TGC CCA CAA AGT ATG GC-3′; (iv) *PD-1*-fwd 5′-TTC AGG TTT ACC ACA AGC TGG-3′, *PD-1*-rev 5′-TGA CAA TAG GAA ACC GGG AA-3′; (v) *INF-γ*-fwd 5′-GCA TCT TGG CTT TGC AGC T-3′, *INF-γ*-rev 5′-CCT TTT TCG CCT TGC TGT TG-3′; (vi) *NOS-2*-fwd 5′-CGA AAC GCT TCA CTT CCA A-3′, *NOS-2*-rev 5′-TGA GCC TAT ATT GCT GTG GCT-3′; (vii) *IL-10*-fwd 5′-TGG ACA ACA TAC TGC TAA CC-3′, *IL-10*-rev 5′-GGA TCA TTT CCG ATA AGG CT-3′; (viii) *GAPDH*-fwd 5′-TGC AGT GGC AAA GTG GAG AT-3′, *GADPH*-rev 5′-CGT GAG TGG AGT CAT ACT GGA A-3′.

2.5. Statistical Analysis. Allele and genotype frequencies were estimated by direct counting, and adherences of phenotypical proportions to expectations under the Hardy-Weinberg equilibrium (HWE) were tested by the complete enumeration method using the GENEPOP 3.4 software [50]. Linkage disequilibrium (LD) between variation sites at *HLA-G* 3′UTR was evaluated by means of a likelihood ratio test of linkage disequilibrium implemented at the ARLEQUIN software [51]. *HLA-G* 3′UTR haplotypes of each individual were inferred for each group of patients (stratified according to the four clinical variants) and for the whole group of patients. Two distinct computational methods that do not take any prior information into account were used for this purpose: (1) the EM algorithm [52] implemented with the PL-EM software [53] and (2) a coalescence-based method implemented in the PHASE v2 software [54]. Therefore, the haplotype pair of each subject was independently inferred by four approaches; whenever these four approaches resulted in nonconsensual inference for a given subject, he was removed from all procedures that used haplotype data as input. The frequency

of each allele, genotype, or haplotype was compared between patients and controls by the two-sided Fisher exact test, with the aid of the GraphPad Instat 3.05 software, which was also used to estimate the Odds Ratio (OR) and its 95% Confidence Interval (CI).

For the HLA-G tissue expression, gene expression, and parasitism load, statistical analyses were performed using Student's t-test or Mann-Whitney tests and the relationship between immunomodulatory and mediators of inflammation genes was performed using the Spearman Correlation, both with the aid of the GraphPad Prism 5 v5.0b software. To facilitate data presentation, variables were expressed as mean ± SEM.

For all analyses, significance was defined at $P < 0.05$.

3. Results

3.1. Genotype and Allele Frequencies of Variation Sites at HLA-G 3′UTR. *HLA-G* 3′UTR variation sites were compared between (i) patients (considered as whole) with controls (healthy individuals); (ii) patients presenting clinically detectable disease (CDM) (cardiac (C) plus digestive (D) plus mixed (M) forms) with controls; (iii) patients presenting CDM with indeterminate patients (indeterminate form—I); and (iv) patients stratified according to the four clinical variants with each other and with controls. Association tests were performed for alleles and genotypes of each variation site.

The following *HLA-G* 3′UTR variation sites were observed in this study: 14-base pair insertion/deletion (I/D; rs66554220); +3001C/T (rs not available); +3003T/C (rs115689421); +3010C/G (rs116152775); +3027A/C (rs115810666); +3035C/T (rs115100128); +3142G/C (rs115928989); +3187A/G (rs114317070); and +3196C/G (rs115045214). Overall, these variation sites adhered to the Hardy-Weinberg Equilibrium, except +3010C/G in cardiac and whole group of patients and +3142G/C in digestive and whole group of patients. Table 1 shows the genotype and allele frequencies in patients with chronic Chagas disease and controls.

14-base pair I/D and +3001C/T: no significant differences were observed when the five types of comparisons were performed. The +3001T allele was observed in only one Chagas disease patient presenting exclusively the digestive form.

+3003T/C: the +3003CC genotype was not observed in Chagasic patients. Compared to controls, (i) the +3003TC genotype frequency was decreased in the whole group of patients ($P = 0.0131$) and in the digestive form ($P = 0.0462$); (ii) the frequency of the +3003C allele was decreased in the whole group of patients ($P = 0.0101$) and in patients exhibiting the digestive form ($P = 0.0448$); (iii) +3003TT genotype frequency was overrepresented in the whole group ($P = 0.0091$) and in digestive ($P = 0.0321$) patients; and (iv) +3003T allele frequency was increased in whole group ($P = 0.0101$) and in the digestive group ($P = 0.0448$) of patients.

+3010C/G: compared to controls, the +3010CG genotype was underrepresented in the whole group of patients ($P = 0.0322$) and in those presenting the cardiac variant ($P = 0.0098$).

+3027A/C: a decreased frequency of the +3027AC genotype was observed in the digestive form compared to control ($P = 0.0069$) and to patients with the indeterminate ($P = 0.0026$), cardiac ($P = 0.0076$), and mixed ($P = 0.0050$) forms. The frequency of the +3027CC genotype was increased in patients exhibiting the digestive form compared to indeterminate ($P = 0.0026$), cardiac ($P = 0.0076$), mixed ($P = 0.0050$), and control ($P = 0.0071$) groups. The +3027AA and +3027AC genotypes were not observed in patients with the digestive form. As consequence, the digestive group exhibited a decreased frequency of the +3027A allele compared to controls ($P = 0.0046$) and to patients with the indeterminate ($P = 0.0029$), cardiac ($P = 0.0083$), and mixed ($P = 0.0055$) forms. The +3027C allele presented the opposite association pattern.

+3035C/T: the +3035CC genotype was overrepresented in patients with the digestive form compared to control ($P = 0.0024$) and to patients with cardiac ($P = 0.0247$) and mixed ($P = 0.0404$) forms. A decreased frequency of the +3035CT genotype was observed in patients exhibiting the digestive form compared to mixed ($P = 0.0404$) and control ($P = 0.0095$) groups. The +3035C allele was overrepresented in the group of patients with the digestive form compared to control ($P = 0.0020$), indeterminate ($P = 0.0346$), cardiac ($P = 0.0118$), and mixed ($P = 0.0489$) groups. The +3035T allele presented the opposite association pattern.

+3142G/C: the +3142GG genotype frequency was significantly lower in digestive patients compared to indeterminate ($P = 0.0449$), cardiac ($P = 0.0363$), and mixed ($P = 0.0346$) forms. The +3142GC genotype frequency was lower in cardiac patients compared to digestive ($P = 0.0211$) and control ($P = 0.0061$) groups. In addition, +3142GC genotype frequency was decreased in the whole group of patients group compared to the control group ($P = 0.0459$).

+3187A/G: compared to controls, an increased frequency of the +3187GG genotype was observed in the whole group ($P = 0.0169$) and in the group of patients with the cardiac form ($P = 0.0459$).

+3196C/G: patients exhibiting the mixed form presented a decreased frequency of the +3196CC genotype ($P = 0.0499$) and an increased frequency of +3196GC genotype ($P = 0.0258$). In addition, +3196CG genotype was increased in the mixed group compared to the indeterminate variant ($P = 0.0188$).

When CDM patients (excluding the indeterminate group) were compared to controls, the following results were observed: (i) the +3003CT genotype frequency was decreased in patients ($P = 0.0128$); (ii) the frequency of the +3003TT genotype was increased in patients ($P = 0.0088$); (iii) +3003C allele frequency was decreased in patients ($P = 0.0097$) and +3003T allele presented the opposite association pattern ($P = 0.0097$); (iv) the +3187GG genotype frequency was overrepresented in patients ($P = 0.0282$); (v) +3196CC genotype frequency was decreased ($P = 0.0259$) and +3196GC genotype frequency was increased ($P = 0.0325$) in patients.

When CDM patients were compared to the indeterminate form, only the +3196GC genotype was increased in CDM patients ($P = 0.0440$). On the other hand, when indeterminate patients were compared to healthy controls, no significant results were observed.

Table 1: Genotype and allele frequencies of variation sites at *HLA-G* 3′ untranslated region (3′UTR) in patients with Chagas disease stratified according to clinical forms and healthy individuals.

3′UTR variation sites	Clinical forms													
	I		C		D		M		CDM		W		H	
	n	Freq.	*n*	Freq.	*n*	Freq.	*n*	Freq.	*n*	Freq.	*n*	Freq.	*n*	Freq.
14 bp I/D		(*n* = 39)		(*n* = 52)		(*n* = 62)		(*n* = 24)		(*n* = 138)		(*n* = 177)		(*n* = 155)
II	8	0.2051	14	0.2692	8	0.1290	5	0.2083	27	0.1957	35	0.1977	30	0.1935
DI	19	0.4872	20	0.3846	32	0.5161	12	0.5000	64	0.4638	83	0.4689	67	0.4323
DD	12	0.3077	18	0.3462	22	0.3548	7	0.2917	47	0.3406	59	0.3333	58	0.3742
I allele	35	0.4487	48	0.4615	48	0.3871	22	0.4583	118	0.4275	153	0.4322	127	0.4097
D allele	43	0.5513	56	0.5385	76	0.6129	26	0.5417	158	0.5725	201	0.5678	183	0.5903
+3001C/T		(*n* = 39)		(*n* = 52)		(*n* = 62)		(*n* = 24)		(*n* = 138)		(*n* = 177)		(*n* = 155)
CC	39	1.0000	52	1.0000	61	0.9839	24	1.0000	137	0.9928	176	0.9944	155	1.0000
CT	0	0.0000	0	0.0000	1	0.0161	0	0.0000	1	0.0072	1	0.0056	0	0.0000
TT	0	0.0000	0	0.0000	0	0.0000	0	0.0000	0	0.0000	0	0,0000	0	0.0000
C allele	78	1.0000	104	1.0000	123	0.9919	48	1.0000	275	0.9964	353	0.9972	310	1.0000
T allele	0	0.0000	0	0.0000	1	0.0081	0	0.0000	1	0.0036	1	0.0028	0	0.0000
+3003T/C		(*n* = 39)		(*n* = 52)		(*n* = 62)		(*n* = 24)		(*n* = 138)		(*n* = 177)		(*n* = 155)
TT	32	0.8205	45	0.8654	54	0.8710*	20	0.8333	119	0.8623*	151	0.8531*	114	0.7354*
CT	7	0.1795	7	0.1346	8	0.1290*	4	0.1667	19	0.1377*	26	0.1469*	40	0.2581*
CC	0	0.0000	0	0.0000	0	0.0000	0	0.0000	0	0.0000	0	0.0000	1	0.0065
T allele	71	0.9103	97	0.9327	116	0.9355*	44	0.9167	257	0.9312*	328	0.9266*	268	0.8645*
C allele	7	0.0897	7	0.0673	8	0.0645*	4	0.0833	19	0.0688*	26	0.0734*	42	0.1355*
+3010C/G		(*n* = 39)		(*n* = 52)		(*n* = 62)		(*n* = 24)		(*n* = 138)		(*n* = 177)		(*n* = 155)
CC	15	0.3846	21	0.4038	16	0.2581	10	0.4167	47	0.3406	62	0.3503	44	0.2839
GC	14	0.3590	16	0.3077*	31	0.5000	9	0.3750	56	0.4058	70	0.3955*	74	0.4774*
GG	10	0.2564	15	0.2885	15	0.2419	5	0.2083	35	0.2536	45	0.2542	37	0.2387
C allele	44	0.5641	58	0.5577	63	0.5081	29	0.6042	150	0.5435	194	0.5480	162	0.5226
G allele	34	0.4359	46	0.4423	61	0.4919	19	0.3958	126	0.4565	160	0.4520	148	0.4774
+3027A/C		(*n* = 39)		(*n* = 52)		(*n* = 62)		(*n* = 24)		(*n* = 138)		(*n* = 177)		(*n* = 155)
AA	0	0.0000	0	0.0000	0	0.0000	0	0.0000	0	0.0000	0	0.0000	1	0.0065
AC	6	0.1538*	6	0.1154*	0	0.0000*	4	0.1667*	10	0.0725	16	0.0904	15	0.0968*
CC	33	0.8462	46	0.8846	62	1.0000	20	0.8333	128	0.9275	161	0.9096	139	0.8967*
A allele	6	0.0769*	6	0.0577*	0	0.0000*	4	0.0833*	10	0.0362	16	0.0452	17	0.0548*
C allele	72	0.9231*	98	0.9423*	124	1.0000*	44	0.9167*	266	0.9638	338	0.9548	293	0.9452*
+3035C/T		(*n* = 39)		(*n* = 52)		(*n* = 62)		(*n* = 24)		(*n* = 138)		(*n* = 177)		(*n* = 155)
CC	30	0.7692	38	0.7308*	56	0.9032*	17	0.7083*	111	0.8043	141	0.7966	111	0.7161*
CT	7	0.1795	12	0.2308	6	0.0968*	7	0.2917*	25	0.1812	32	0.1808	40	0.2581*
TT	2	0.0513	2	0.0384	0	0.0000	0	0.0000	2	0.0145	4	0.0226	4	0.0258
C allele	67	0.8590*	88	0.8462*	118	0.9516*	41	0.8542*	247	0.8949	314	0.8870	262	0.8452*
T allele	11	0.1410*	16	0.1538*	6	0.0484*	7	0.1458*	29	0.1051	40	0.1130	48	0.1548*

Table 1: Continued.

3′ UTR variation sites	Clinical forms													
	I		C		D		M		CDM		W		H	
	n	Freq.	n	Freq.	n	Freq.	n	Freq.	n	Freq.	n	Freq.	n	Freq.
+3142G/C	($n = 39$)		($n = 51$)		($n = 60$)		($n = 24$)		($n = 135$)		($n = 174$)		($n = 155$)	
GG	16	0.4103*	21	0.4118*	13	0.2166*	11	0.4583*	45	0.3333	61	0.3505	44	0.2839
GC	15	0.3846	15	0.2941*	31	0.5167*	8	0.3333	54	0.4000	69	0.3966*	80	0.5161*
CC	8	0.2051	15	0.2941	16	0.2667	5	0.2084	36	0.2667	44	0.2529	31	0.2000
G allele	47	0.6026	57	0.5588	57	0.4750	30	0.6250	144	0.5333	191	0.5489	168	0.5419
C allele	31	0.3974	45	0.4412	63	0.5250	18	0.3750	126	0.4667	157	0.4511	142	0.4581
+3187A/G	($n = 39$)		($n = 50$)		($n = 61$)		($n = 24$)		($n = 135$)		($n = 174$)		($n = 155$)	
AA	22	0.5641	27	0.5400	26	0.4262	14	0.5833	67	0.4963	89	0.5115	82	0.5290
GA	12	0.3077	16	0.3200	29	0.4754	7	0.2917	52	0.3852	64	0.3678	66	0.4258
GG	5	0.1282	7	0.1400*	6	0.0984	3	0.1250	16	0.1185*	21	0.1207*	7	0.0452*
A allele	56	0.7179	70	0.7000	81	0.6639	35	0.7292	186	0.6889	242	0.6954	230	0.7419
G allele	22	0.2821	30	0.3000	41	0.3361	13	0.2708	84	0.3111	106	0.3046	80	0.2581
+3196C/G	($n = 39$)		($n = 50$)		($n = 61$)		($n = 24$)		($n = 135$)		($n = 174$)		($n = 155$)	
CC	22	0.5641	24	0.4800	25	0.4098	8	0.3333*	57	0.4222*	79	0.4540	86	0.5548*
GC	12	0.3077*	22	0.4400	31	0.5082	15	0.6250*	68	0.5037*	80	0.4598	58	0.3742*
GG	5	0.1282	4	0.0800	5	0.0820	1	0.0417	10	0.0741	15	0.0862	11	0.0710
C allele	56	0.7179	70	0.7000	81	0.6639	31	0.6458	182	0.6741	238	0.6839	230	0.7419
G allele	22	0.2821	30	0.3000	41	0.3361	17	0.3542	88	0.3259	110	0.3161	80	0.2581

I (indeterminate). C (cardiac). D (digestive). M (mixed). CDM (patients presenting clinically detected disease). W (whole group). H (healthy control). *frequencies that show statistical differences.

Table 2: Odds Ratio and 95% Confidence Interval values obtained from the comparisons of genotype and allele frequencies of variation sites at *HLA-G* 3′ untranslated region (3′UTR) between different presentation forms of Chagas disease and healthy controls.

Genotypes and alleles	Comparison	OR (95% CI)	Comparison	OR (95% CI)	Comparison	OR (95% CI)
+3003CT	W versus H	0.495 (0.29–0.86)	CDM versus H	0.459 (0.25–0.84)	D versus H	0.426 (0.19–0.97)
+3003TT	W versus H	2.089 (1.21–3.61)	CDM versus H	2.252 (1.23–4.11)	D versus H	2.428 (1.07–5.53)
+3003C	W versus H	0.506 (0.30–0.85)	CDM versus H	0.472 (0.27–0.83)	D versus H	0.440 (0.20–0.97)
+3003T	W versus H	1.977 (1.18–3.31)	CDM versus H	2.119 (1.20–3.74)	D versus H	2.272 (1.03–4.99)
+3010GC	W versus H	0.610 (0.39–0.95)	C versus H	0.414 (0.21–0.81)		
+3027AC	D versus I	0.041 (0.002–0.75)	D versus M	0.036 (0.002–0.71)	C versus D	17.473 (0.96–318.00)
	D versus H	0.073 (0.004–1.23)				
+3027CC	D versus I	24.254 (1.33–443.84)	D versus M	27.439 (1.42–531.65)	C versus D	0.057 (0.003–1.04)
	D versus H	14.785 (0.87–250.35)				
+3027A	D versus I	0.045 (0.002–0.81)	D versus M	0.040 (0.002–0.75)	C versus D	16.431 (0.91–295.23)
	D versus H	0.067 (0.004–1.13)				
+3027C	D versus I	22.324 (1.24–402.08)	D versus M	25.180 (1.33–477.12)	C versus D	0.061 (0.003–1.09)
	D versus H	14.847 (0.89–248.81)				
+3035CC	D versus M	3.843 (1.14–12.99)	C versus D	0.291 (0.10–0.82)	D versus H	3.700 (1.49–9.20)
+3035CT	D versus M	0.260 (0.08–0.88)	D versus H	0.308 (0.12–0.77)		
+3035C	D versus I	3.229 (1.14–9.13)	D versus M	3.358 (1.07–10.57)	C versus D	0.280 (0.11–0.74)
	D versus H	3.603 (1.50–8.65)				
+3035T	D versus I	0.310 (0.11–0.88)	D versus M	0.298 (0.09–0.94)	C versus D	3.576 (1.34–9.51)
	D versus H	0.278 (0.12–0.67)				
+3142GC	W versus H	0.616 (0.40–0.95)	C versus D	0.390 (0.18–0.86)	C versus H	0.391 (0.20–0.77)
+3142GG	D versus I	0.398 (0.16–0.96)	D versus M	0.327 (0.12–0.90)	C versus D	2.531 (1.10–5.80)
+3187GG	W versus H	2.902 (1.20–7.03)	CDM versus H	2.843 (1.13–7.14)	C versus H	3.442 (1.14–10.35)
+3196CC	CDM versus H	0.586 (0.37–0.93)	M versus H	0.401 (0.16–0.99)		
+3196GC	CDM versus H	1.697 (1.06–2.71)	CDM versus I	2.284 (1.07–4.88)	I versus M	0.267 (0.09–0.78)
	M versus H	2.787 (1.15–6.77)				

I (indeterminate). C (cardiac). D (digestive). M (mixed). CDM (patients presenting clinically detected disease). W (whole group). H (healthy control). OR, Odds Ratio. 95% CI, 95% Confidence Interval.

Table 2 shows the Odds Ratio and 95% Confidence Interval values obtained for all significant comparisons.

3.2. Haplotype Frequency of Variation Sites at HLA-G 3′UTR. To further understand how the ensemble of variation sites participate in Chagas disease susceptibility and considering that these variation sites were in linkage disequilibrium (results not shown), we analyzed the frequency of the *HLA-G* 3′UTR haplotypes observed for patients and controls, and the results of the statistical analyses are shown in Tables 3(a) and 3(b). Eleven out of 177 patients have been removed from all analyses that used haplotype data as input, since results for the four approaches of haplotype inference resulted in nonconsensual results. The names of the 3′UTR haplotypes (UTR-1, UTR-2, etc.) follow the nomenclature previously described by our group [39], which has been extensively used in the literature.

Compared to controls, (i) UTR-4 was underrepresented in the whole group of patients ($P = 0.0005$), CDM ($P = 0.0008$), digestive ($P = 0.0274$), and cardiac ($P = 0.0043$) forms; (ii) UTR-13 was overrepresented in the indeterminate group ($P = 0.0320$); (iii) UTR-14 was overrepresented in cardiac patients ($P = 0.0135$). A decreased frequency of the UTR-7 haplotype was observed in the digestive group compared to indeterminate ($P = 0.0056$), mixed ($P = 0.0053$), and control ($P = 0.0048$) groups. In addition, UTR-13 was also increased in patients presenting the indeterminate form when compared to CDM patients ($P = 0.0415$).

3.3. HLA-G Expression in Specimens Obtained from Chronic Chagas Disease Patients. HLA-G molecule expression was evaluated in the major organs affected by the disease, including heart, colon, and esophagus. Compared to non-Chagasic tissues, HLA-G expression was significantly decreased in Chagasic heart ($P = 0.0105$; Figures 1(a), 1(b), and 1(c)) and colon ($P = 0.0485$, Figures 1(d), 1(e), and 1(f)). HLA-G expression in individuals without Chagas disease was primarily observed on cardiac muscle cells and no cellular infiltration was observed (Figure 1(a)), whereas specimens from Chagas patients exhibiting cardiomegaly showed lesser HLA-G expression on cardiac muscle cells together with an infiltration of mononuclear cells (lymphocytes and plasma cells) exhibiting HLA-G expression (Figure 1(b)). The HLA-G immunolabeling in esophagus of Chagas patients with esophagomegaly was closely similar to that observed for individuals without Chagas disease (Figures 1(g), 1(h), and 1(i)).

Table 3: (a) Haplotype frequencies in patients with Chagas disease stratified according to clinical forms and healthy controls and (b) Odds Ratio and 95% Confidence Interval values obtained from the comparisons of haplotypes frequencies of variation sites at *HLA-G* 3′ untranslated region (3′UTR) between different presentation forms of Chagas disease and healthy controls.

(a)

Haplotype		Clinical forms													
		I		C		D		M		CDM		W		H	
		n	Freq.	*n*	Freq.	*n*	Freq.	*n*	Freq.	*n*	Freq.	*n*	Freq.	*n*	Freq.
UTR-1	DelCTGCCCGC	17	0.25	27	0.28	40	0.32	80	0.26	80	0.30	80	0.26	80	0.26
UTR-2	InsCTCCCGAG	20	0.29	28	0.29	37	0.31	75	0.24	80	0.30	75	0.24	75	0.24
UTR-3	DelCTCCCGAC	11	0.16	12	0.12	13	0.11	39	0.13	32	0.12	39	0.13	39	0.13
UTR-4	DelCCGCCCAC	4	0.06	3	0.03*	7	0.06*	41	0.13	13	0.05*	41	0.13*	41	0.13*
UTR-5	InsCTCCTGAC	3	0.04	11	0.11	5	0.04	29	0.09	18	0.07	29	0.09	29	0.09
UTR-6	DelCTGCCCAC	3	0.04	6	0.06	11	0.09	21	0.07	19	0.07	21	0.07	21	0.07
UTR-7	InsCTCATGAC	5	0.07*	3	0.03	0	0.00*	17	0.05*	7	0.03	17	0.05	17	0.05*
UTR-8	InsCTGCCGAG	1	0.02	0	0.00	0	0.00	4	0.01	0	0.00	4	0.01	4	0.01
UTR-10	DelCTCCCGAG	0	0.00	0	0.00	1	0.01	1	0.003	1	0.004	1	0.003	1	0.003
UTR-11	DelCCCCCGAC	0	0.00	0	0.00	0	0.00	1	0.003	0	0.00	1	0.003	1	0.003
UTR-13	DelCTCCTGAC	2	0.03*	0	0.00	0	0.00	0	0.00	0	0.00*	0	0.00	0	0.00*
UTR-14	DelCTGCCGGC	1	0.02	3	0.03*	0	0.00	0	0.00	3	0.01	0	0.00	0	0.00*
UTR-17	InsTTCCTGAC	0	0.00	0	0.00	1	0.01	0	0.00	1	0.004	0	0.00	0	0.00
Others[a]	DelCCGCCCGC	0	0.00	1	0.01	0	0.00	0	0.00	1	0.004	0	0.00	0	0.00
	DelCTCACCAC	0	0.00	1	0.01	0	0.00	0	0.00	1	0.004	0	0.00	0	0.00
	DelCTCCCCAC	0	0.00	0	0.00	1	0.01	0	0.00	1	0.004	0	0.00	0	0.00
	DelCTCCCCGC	0	0.00	0	0.00	1	0.01	0	0.00	1	0.004	0	0.00	0	0.00
	DelCCGACCGC	0	0.00	1	0.01	0	0.00	0	0.00	1	0.004	0	0.00	0	0.00
	InsCTCCCCAG	0	0.00	0	0.00	2	0.02	0	0.00	2	0.01	0	0.00	0	0.00
	InsCTGCCCAC	0	0.00	2	0.02	0	0.00	0	0.00	2	0.01	0	0.00	0	0.00
	InsCTGCCCGC	1	0.02	0	0.00	1	0.01	0	0.00	1	0.004	0	0.00	0	0.00

(b)

Haplotype	Comparison	OR (95% CI)	Comparison	OR (95% CI)	Comparison	OR (95% CI)
UTR-4	W versus H	0.354 (0.20–0.64)	CDM versus H	0.339 (0.18–0.65)	D versus H	0.406 (0.18–0.93)
	C versus H	0.207 (0.06–0.69)				
UTR-7	D versus I	0.048 (0.003–0.88)	D versus M	0.039 (0.002–0.74)	D versus H	0.070 (0.004–1.17)
UTR-13	CDM versus I	0.050 (0.002–1.06)	I versus H	23.346 (1.08–491.92)		
UTR-14	C versus H	22.759 (1.17–444.53)				

I (indeterminate). C (cardiac). D (digestive). M (mixed). CDM (patients presenting clinically detected disease). W (whole group). H (healthy control). Del (deletion), Ins (insertion), OR, Odds Ratio, 95% CI, 95% Confidence Interval. *frequencies that show statistical differences. [a]Group of haplotypes occurring at a frequency of ≤0.02.

3.4. Qa2 Expression during Experimental Acute and Early Chronic Infections. The transcriptional level of *Qa2* in acute and early chronic infections was studied in heart and esophagus specimens obtained from BALB/c and C57BL/6 infected mice, using the *T. cruzi* CL strain.

First, we characterized the acute and early chronic infections regarding the animal survival rate, tissue parasite load, and blood parasitism. Survival rates showed no significant differences for BALB/c and C57BL/6 mice for both acute (Figure 2(a)) and early chronic (Figure 2(b)) infections. During acute infection, the heart parasite load was 2-fold increased in C57BL/6 mice in relation to BALB/c group ($P < 0.05$; Figure 2(c)). No significant difference was observed between the two groups during the early chronic infection (Figure 2(d)). In addition, when we analyzed the bloodstream forms in the acute infection, BALB/c mice showed an increased parasitism level at days 21, 23, and 25 compared to C57BL/6 mice ($P < 0.05$; Figure 2(e)).

During acute infection, the heart and esophagus transcriptional levels of *Qa2* were significantly increased for both mouse strains, when compared to noninfected mice. Compared to the control group, the heart expression of *Qa2* in BALB/c and C57BL/6 was 28-fold and 25-fold increased, respectively ($P < 0.05$; Figure 3(a)), and the esophagus expression of *Qa2* was 17-fold and 16-fold increased in BALB/c and C57BL/6, respectively ($P < 0.05$; Figure 3(b)).

Acutely infected BALB/c mice showed increased transcriptional levels of *Qa2* in heart and esophagus, which

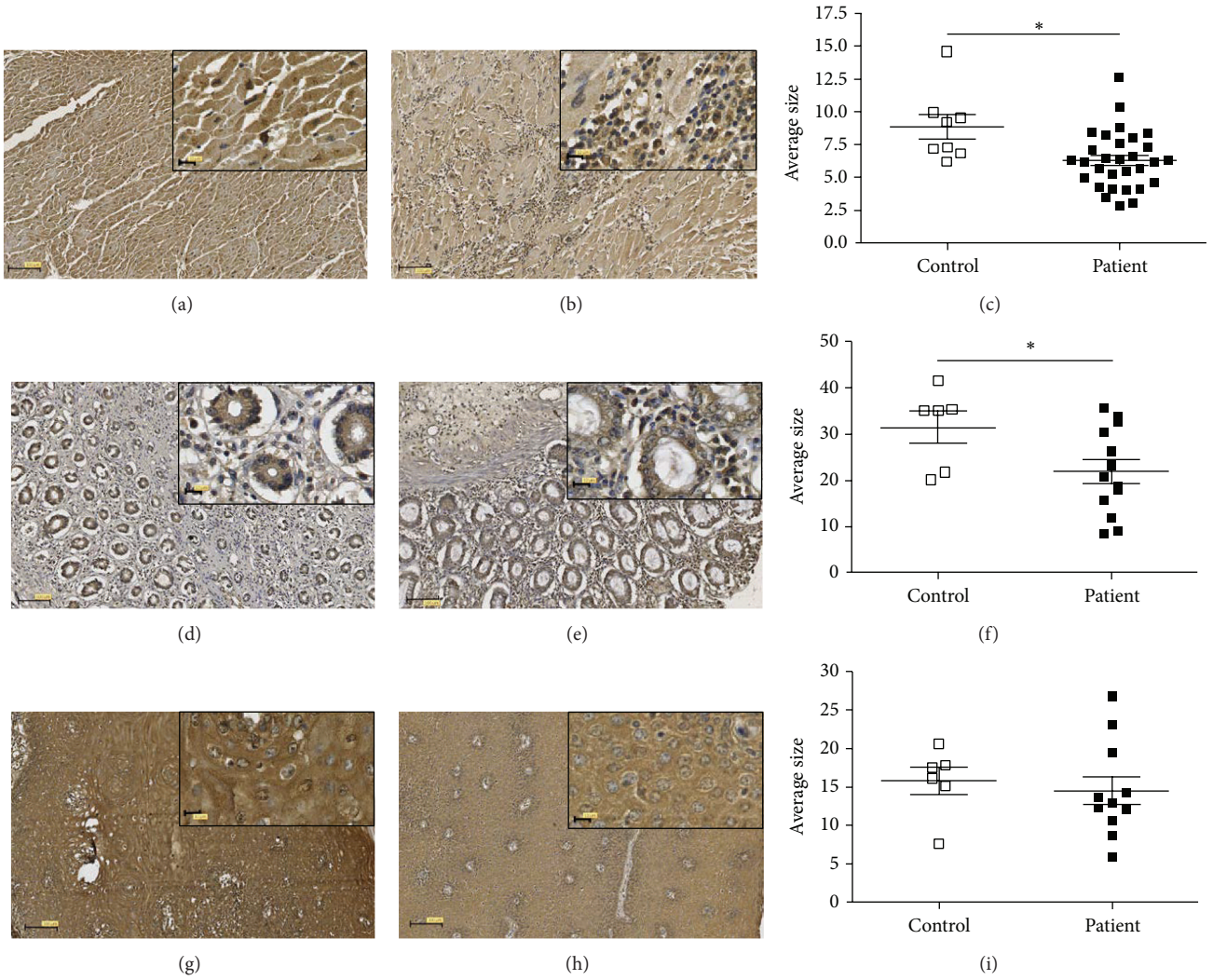

Figure 1: Immunohistochemical staining for HLA-G. Representative photomicrographs ((a), (b), (d), (e), (g), and (h)) and average size ((c), (f), and (i)) of HLA-G-stained cells in heart ((a)–(c)), colon ((d)–(f)), and esophagus ((g)–(i)) of controls ((a), (d), and (g)) and patients ((b), (e), and (h)). The insert boxes show a higher magnification of the HLA-G-stained cells in each tissue. Scale bar 100 μm, 12 μm (insert). ((c), (f), and (i)) Data are expressed as mean ± SEM. $^{*}P < 0.05$ indicating statistical significance compared with controls.

were 7-fold and 14-fold higher than early chronically infected mice, respectively ($P < 0.05$; Figures 3(a) and 3(b)). The transcriptional level of *Qa2* was 6-fold higher in heart of acutely infected C57BL/6 mice compared to early chronic infection ($P < 0.05$; Figure 3(a)). No significant difference in terms of *Qa2* expression was observed between noninfected and early chronically infected mice in heart and esophagus of BALB/c and C57BL/6 mice (Figures 3(a) and 3(b)).

To verify whether other known immunomodulatory genes were concomitantly modulated during the infection by CL strain of *T. cruzi*, we analyzed the transcriptional levels of *Qa1*, *CTLA-4* and *PD-1* genes. Our results showed that all of them were significantly augmented in heart and esophagus of BALB/c strain when compared to noninfected and early chronically infected mice ($P < 0.05$; Figures 3(a) and 3(b)). C57BL/6 mice showed an increased transcriptional level of *Qa1* in heart and increased levels of *CTLA-4* in esophagus and *PD-1* in both heart and esophagus, during the acute infection ($P < 0.05$), compared to controls and early chronically infected animals (Figures 3(a) and 3(b)). Moreover, during the acute infection, *Qa1* was 4-fold higher in esophagus of BALB/c strain compared to C57BL/6 animals, and *PD-1* expression was 2-fold higher in heart of C57BL/6 mice compared to BALB/c strain ($P < 0.05$; Figures 3(a) and 3(b)). No significant difference was observed between noninfected and early chronically infected mice in heart and esophagus specimens obtained from BALB/c and C57BL/6 mice (Figures 3(a) and 3(b)).

Considering that nonclassical histocompatibility genes may be influenced by the action of inflammatory mediators, we evaluated the transcriptional levels of *INF-γ*, *NOS-2,* and *IL-10* genes in the heart to observe the relationship between these genes and the nonclassical genes.

INF-γ, *NOS-2,* and *IL-10* expression was increased in both BALB/c and C57BL/6 strains during the acute infection compared to controls and early chronically infected animals

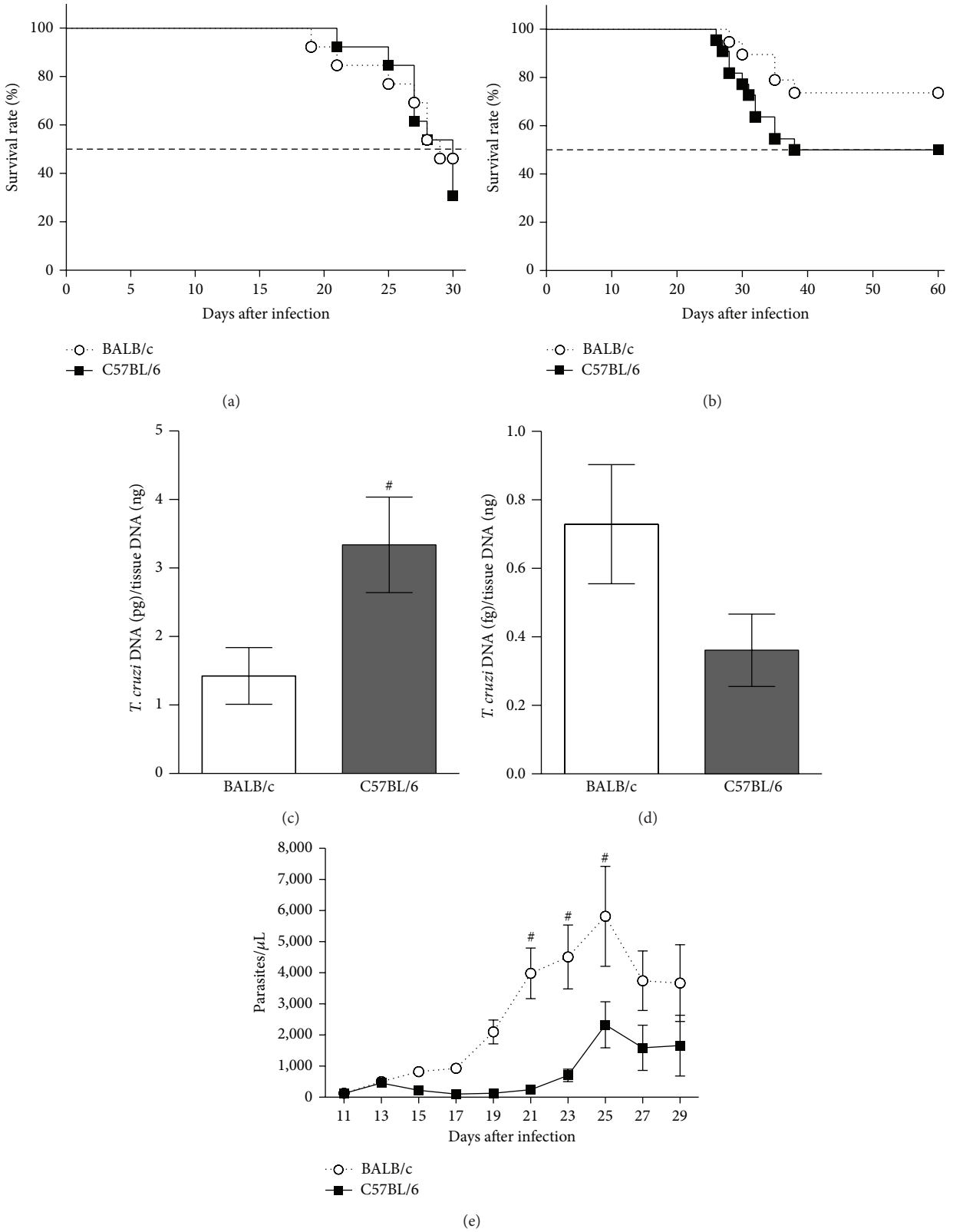

Figure 2: Survival, parasite load, and parasitism of *T. cruzi* infected mice. The male 8-week-old BALB/c and C57BL/6 mice were intraperitoneally infected with 10^3 or 10^2 bloodstream CL strain forms for acute and early chronic infections, respectively. For acute infection, the survival was observed daily during 35 days (a) and for early chronic infection the survival was observed daily during 60 days (b). The parasite load was determined in the heart at day 24 after infection for acute infection (c) and at day 60 after infection for early chronic infection (d). Parasitemia was quantified microscopically for 29 days (e). The data represent the mean ± SEM (n = 6 mice/group). $^{\#}P < 0.05$, comparison between BALB/c and C57BL/6 infected mice.

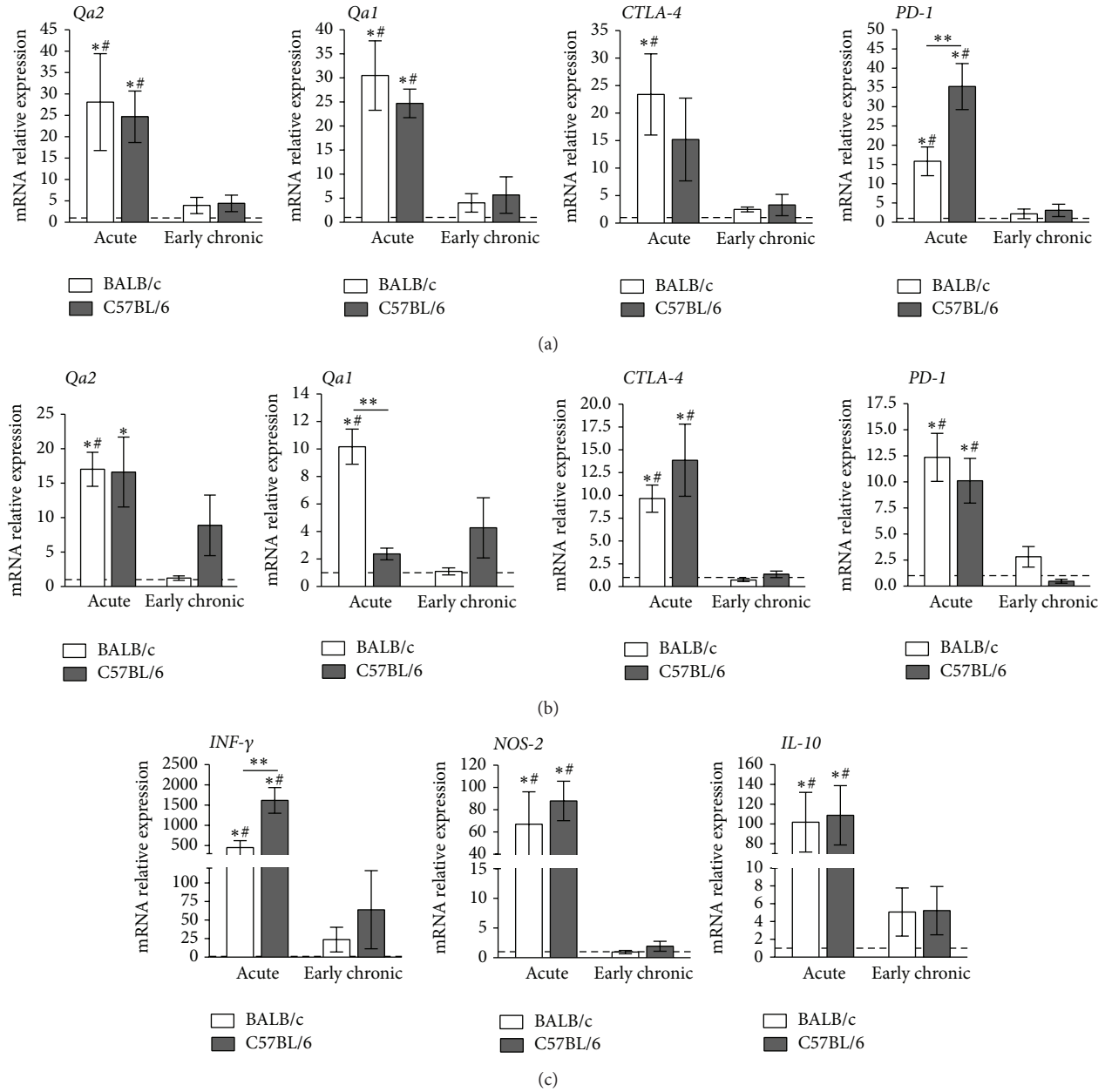

Figure 3: Transcriptional level in the heart and esophagus of *T. cruzi* infected mice. Transcript levels for immunomodulatory genes were measured by qRT-PCR in whole heart (a) and esophagus (b) homogenates obtained from infected mice at days 24 and 60 after infection for acute and early chronic infections, respectively. Transcriptional levels for INF-γ, NOS-2, and IL-10 were measured by qRT-PCR in whole heart homogenate (c). Uninfected mice are represented by dashed lines. The results are expressed as relative expression. The data represent the mean ± SEM (n = 6 mice/group). $^{*}P < 0.05$ indicating statistical significance compared with noninfected mice. $^{\#}P < 0.05$, comparison between acute and early chronic infections. $^{**}P < 0.05$, comparison between BALB/c and C57BL/6 infected mice.

($P < 0.05$; Figure 3(c)). The comparisons between strains showed that *INF-γ* expression was 4-fold higher in C57BL/6 than in BALB/c (Figure 3(c)). During the early chronic infection, the transcriptional levels of these genes were similar to noninfected mice for both BALB/c and C57BL/6 strains (Figure 3(c)). When we studied the relationship between these genes, we observed a positive correlation between *Qa2* and *INF-γ* ($P = 0.0417$; $r = 1.0000$) and *Qa2* and *NOS-2* ($P = 0.0417$; $r = 1.0000$) in heart specimens of both mouse strains during acute *T. cruzi* infection.

4. Discussion

The present study provides consistent data regarding the involvement of HLA-G and its Qa2 murine functional

homolog in the *T. cruzi* infection. *HLA-G* gene polymorphism and HLA-G tissue expression have been evaluated in several diseases; however, little is known about the role of these molecules in the human or experimental *T. cruzi* infections.

The association of genetic markers with infectious disease has posed intriguing questions regarding the comparisons of gene frequencies between individuals with the disease with healthy individuals who had never been exposed to the specific infectious agent. Due to the myriad of chronic clinical forms observed in Chagas disease, part of these concerns may be circumvented by the possibility of comparing patients presenting well recognized clinical variants with patients who were infected by *T. cruzi* and have not developed clinically detected forms (indeterminate). When patients as a whole were compared to healthy individuals, some *HLA-G* 3′UTR alleles/genotypes were overrepresented (+3003T allele and +3003TT and +3187GG genotypes), while others were underrepresented (+3003C allele, and +3003CT, +3010GC, +3042GC genotypes) in Chagas disease patients. When symptomatic patients (CDM) were compared to healthy controls, similar results were obtained, indicating that these polymorphic sites were indeed associated with the clinically detected Chagas disease. In contrast, when indeterminate patients were compared to controls, the frequency of the *HLA-G* 3′UTR alleles/genotypes was closely similar. This result corroborates the role of the aforementioned *HLA-G* 3′UTR alleles and genotypes in the clinically recognized Chagas variants.

The stratification of Chagas patients into clinical variants showed that the +3027CC and +3035CC genotypes and the +3027C and +3035C alleles were strongly associated with the digestive form of Chagas disease. In addition, the +3142GC genotype was associated with a decreased risk to cardiac form development, when compared to the digestive form. These results indicate that genetic susceptibility to digestive or cardiac forms may be distinct. Indeed, previous studies conducted by our group evaluating classical histocompatibility (HLA-A, -B, -DRB1 and DQB1) antigens/alleles [55] and other immunoregulatory genes, such as *CTLA-4* [25], also showed a differential pattern of susceptibility according to the Chagas clinical variant. No specific posttranscription regulation mechanism has been reported concerning the +3027A/C and +3035C/T polymorphic sites; however, in a previous *in silico* study, we reported several miRNAs that may target the +3027A/C and +3035C/T polymorphic sites [56].

When *HLA-G* 3′UTR polymorphic sites were considered as haplotypes, decreased UTR-4 and UTR-7 frequencies were associated with the clinically detectable Chagas disease and with the digestive form, respectively. On the other hand, UTR-14 was associated with the cardiac variant and UTR-13 with the indeterminate form. Noteworthy, particular posttranscription elements that are present in these UTRs also exhibited a similar differential behavior when their frequencies were individually evaluated, further corroborating the role of *HLA-G* 3′UTR sites in disease susceptibility. Our group demonstrated that specific *HLA-G* 3′UTR haplotypes are associated with differential soluble levels of HLA-G (sHLA-G), being UTR-1 associated with high sHLA-G and UTR-5 and UTR-7 with decreased sHLA-G levels [40]. However, there are no studies associating *HLA-G* 3′UTR haplotypes with tissue HLA-G expression.

Considering that cytokines, chemokine, and immunomodulatory molecules play an important role in the pathogenesis of many diseases, including Chagas disease, and gene polymorphisms may influence the expression of these molecules, different studies have reported the association between different clinical forms of Chagas disease and polymorphisms at *TNF* [57–61], *IL-1β* [62], *IL-10* [63], *IL-4* [64], *INF-γ* [65], *TGF-β1* [66], *IL-12B* [67], *CXCL9* [68], *CXCL10* [68], *CCR5* [68–70], *CCL2* [71], and *CTLA-4* [25] genes.

Regarding HLA-G expression on tissue cells, patients with the digestive form exhibited decreased expression in colon but not in esophagus specimens, contrasting with patients exhibiting the cardiac variant who presented a decreased expression on myocardium cells. Many segments of the digestive tract and normal myocardium fibers [28] may constitutively express HLA-G; however, the meaning of these findings has not been completely elucidated. The best characterized constitutive HLA-G expression is in the placenta, where it may provide protection to the fetus against the cytotoxic cell immune response against paternal antigens [72]. HLA-G constitutive expression in gut and heart may in fact present a similar protective effect. Indeed, increased plasma levels of sHLA-G and myocardium HLA-G expression have been associated with decreased cellular acute rejection and better graft survival in patients submitted to heart transplantation [73–75]. Then, the loss of HLA-G expression on myocardium cells may facilitate the action of infiltrating lymphomononuclear cells after tissue injury caused by *T. cruzi*. On the other hand, myocardium infiltrating lymphomononuclear cells also exhibited HLA-G expression, which could decrease their functional properties. Since myocardium damage has been primarily attributed to fiber losses due to the action of immune cytotoxic cells, one may consider that HLA-G lymphomononuclear cell expression may not be the only regulatory surface cell molecule. In addition, it is important to emphasize that all these findings were observed in heart specimens of deceased patients, and the temporal HLA-G expression during the chronic phase has not been evaluated as yet.

Overall, the outcome of the experimental *T. cruzi* infection may depend on several factors, including (i) the inoculated strain, (ii) the amount of parasites, and (iii) the genetic background of the animal. Several of these combinations have been used to induce acute or early chronic infection. BALB/c mouse has been considered to be susceptible to acute *T. cruzi* infection induced by the Y and Tulahuén strains, due to the predominance of a Th2 immune response, characterized by high production of IL-4 and IL-10 [3, 76]. On the other hand, C57BL/6 mouse is considered to be resistant to acute *T. cruzi* infection induced by Y and Tulahuén strains, since the mouse produces a Th1 immune response with the production of INF-γ, IL-12, TNF, and NO [3, 14, 15]. In the present study, we used the less virulent *T. cruzi* CL strain that depending on the dose may produce severe acute or lead to the development of early chronic infection. In BALB/c mice, the acute infection by CL strain induced higher heart parasitism and

parasitemia with increased production of proinflammatory mediators [77]. Since BALB/c is more susceptible to *T. cruzi* infection, chronic infection is difficult to be induced by more virulent strains. On the other hand, little is known about the acute and early chronic infection induced by CL strain in C57BL/6 mice. With the use of the CL strain we did not observe a differential susceptibility in BALB/c and C57BL/6 mice in terms of mouse survival; however, BALB/c showed higher parasitemia, whereas C57BL/6 presented higher heart parasitism. Therefore, the C57BL/6 controlled CL strain parasitemia but not heart tropism, and the inverse occurred with the BALB/c mouse.

Similarly to HLA-G, the Qa2 molecule may also control the immune response by inhibiting NK cells [45]. During acute *T. cruzi* infection, the transcriptional level of *Qa2* was increased in heart and esophagus in both BALB/c and C57BL/6 mouse strains, and the increased expression was not related to resistance or susceptibility to the acute infection. Although little attention has been devoted to the role of immunomodulatory nonclassical MHC molecules in experimental infection, *Qa2* expression may be induced to counterbalance the action of proinflammatory and other anti-inflammatory or immunomodulatory molecules. Indeed, the transcriptional levels of the *Qa1*, *CTLA-4*, *PDCD1*, *INF-γ*, *NOS-2,* and *IL-10* genes were also induced in the acute *T. cruzi* infection, as shown in this study. Additional literature findings corroborate this idea. Tissue damage observed in the affected tissues is due to the inflammatory process generated by an exacerbated immune response triggered against the parasite, and the high production of CTLA-4, PD-1, and IL-10 is related to control inflammatory process during *T. cruzi* infection [3, 14, 15, 23, 24, 78]. Our data suggest that the augmentation of immunomodulatory gene expression during the acute phase, including *Qa2* gene, may be associated with the control of tissue damage caused by inflammatory process, cytolysis, and fibrosis.

Regarding the early chronic infection, the expression of immunomodulatory, proinflammatory, and anti-inflammatory genes analyzed in this study was closely similar to noninfected mice in both BALB/c and C57BL/6 strains, and both animal groups were able to evolve into the early chronic infection, presenting only a little amount of *T. cruzi* in the heart. Considering that mice were exposed to decreased number of the less virulent CL strain, it is reasonable to conclude that both BALB/c and C57BL/6 mice had time and chance to mount an adequate immune response against the parasites.

5. Conclusion

We present several lines of evidence pointing to the participation of the immunomodulatory molecules HLA-G and its functional murine homolog Qa2 on human and experimental *T. cruzi* infection. In terms of Chagas disease susceptibility, *HLA-G* 3′UTR alleles/genotypes/haplotypes exhibited differential frequencies in infected/diseased patients when compared to only infected patients and healthy controls. The observation of a decreased HLA-G expression on cardiac muscle and colonic cells associated with the increased expression of HLA-G on myocardium infiltrating lymphomononuclear cells may reflect a lack of protection of these tissues that constitutively express HLA-G. In experimental infection, the mouse genetic background exerted only a mild influence on the overall response against the *T. cruzi* CL strain. The transcriptional levels of *Qa2*, *Qa1*, *CTLA-4*, *PDCD1*, *INF-γ*, *NOS-2,* and *IL-10* genes were induced only during the acute *T. cruzi* infection in BALB/c and C57BL/6 mice, indicating a fine balance between pro- and anti-inflammatory genes.

Conflict of Interests

The authors declare that there is no conflict of interests regarding the publication of this paper.

Acknowledgments

The authors thank Ana Maria da Rocha for technical assistance. This work was supported by Coordenação de Aperfeiçoamento de Pessoal de Nível Superior (Grant nos. CAPES/COFECUB 653/09, PRODOC 288/05-5, and PNPD 02883/09-0), Conselho Nacional de Desenvolvimento Científico e Tecnológico (CNPq Science Without Borders Program, Grant no. 236754/2012-2), and Núcleo de Apoio a Pesquisa em Doenças Inflamatórias (NAP-DIN). The funders had no role in study design, data collection and analysis, decision to publish, or preparation of the paper.

References

[1] J. A. Marin-Neto and A. Rassi Jr., "Update on chagas heart disease on the first centennial of its discovery," *Revista Española de Cardiología*, vol. 62, no. 11, pp. 1211–1216, 2009.

[2] S. B. Boscardin, A. C. T. Torrecilhas, R. Manarin et al., "Chagas' disease: an update on immune mechanisms and therapeutic strategies," *Journal of Cellular and Molecular Medicine*, vol. 14, no. 6, pp. 1373–1384, 2010.

[3] A. Rassi Jr., A. Rassi, and J. A. Marin-Neto, "Chagas disease," *The Lancet*, vol. 375, no. 9723, pp. 1388–1402, 2010.

[4] B. M. Ribeiro, E. Crema, and V. Rodrigues Jr., "Analysis of the cellular immune response in patients with the digestive and indeterminate forms of Chagas' disease," *Human Immunology*, vol. 69, no. 8, pp. 484–489, 2008.

[5] J. K. Leavey and R. L. Tarleton, "Cutting edge: Dysfunctional CD8+ T cells reside in nonlymphoid tissues during chronic *Trypanosoma cruzi* infection," *Journal of Immunology*, vol. 170, no. 5, pp. 2264–2268, 2003.

[6] J. Lannes-Vieira, "Trypanosoma cruzi-elicited $CD8^+$ T Cell-mediated Myocarditis: chemokine receptors and adhesion molecules as potential therapeutic targets to control chronic inflammation?" *Memorias do Instituto Oswaldo Cruz*, vol. 98, no. 3, pp. 299–304, 2003.

[7] M. A. Bryan, S. E. Guyach, and K. A. Norris, "Specific humoral immunity versus polyclonal B Cell activation in *Trypanosoma cruzi* infection of susceptible and resistant mice," *PLoS Neglected Tropical Diseases*, vol. 4, no. 7, article e733, 2010.

[8] I. Benítez-Hernández, E. Méndez-Enríquez, P. Ostoa et al., "Proteolytic cleavage of chemokines by *Trypanosoma cruzi's* cruzipain inhibits chemokine functions by promoting the

generation of antagonists," *Immunobiology*, vol. 215, no. 5, pp. 413–426, 2010.

[9] G. Gorelik, G. Cremashi, E. Borda, and L. Sterin-Borda, "Trypanosoma cruzi antigens down-regulate T lymphocyte proliferation by muscarinic cholinergic receptor-dependent release of PGE2," *Acta Physiologica Pharmacologica et Therapeutica Latinoamericana*, vol. 48, no. 3, pp. 115–123, 1998.

[10] M. Borges, A. C. Da Silva, D. Sereno, and A. Ouaissi, "Peptide-based analysis of the amino acid sequence important to the immunoregulatory function of *Trypanosoma cruzi* Tc52 virulence factor," *Immunology*, vol. 109, no. 1, pp. 147–155, 2003.

[11] E. Cunha-Neto, V. Coelho, L. Guilherme, A. Fiorelli, N. Stolf, and J. Kalil, "Autoimmunity in Chagas' disease: identification of cardiac myosin-B13 Trypanosoma cruzi protein crossreactive T cell clones in heart lesions of a chronic Chagas' cardiomyopathy patient," *Journal of Clinical Investigation*, vol. 98, no. 8, pp. 1709–1712, 1996.

[12] E. L. Khoury, V. Ritacco, P. M. Cossio et al., "Circulating antibodies to peripheral nerve in American trypanosomiasis (Chagas' disease)," *Clinical and Experimental Immunology*, vol. 36, no. 1, pp. 8–15, 1979.

[13] S. P. Kurup and R. L. Tarleton, "Perpetual expression of PAMPs necessary for optimal immune control and clearance of a persistent pathogen," *Nature Communications*, vol. 4, article 2616, 2013.

[14] Z. Brener and R. T. Gazzinelli, "Immunological control of *Trypanosoma cruzi* infection and pathogenesis of Chagas' disease," *International Archives of Allergy and Immunology*, vol. 114, no. 2, pp. 103–110, 1997.

[15] F. R. S. Gutierrez, T. W. P. Mineo, W. R. Pavanelli, P. M. M. Guedes, and J. S. Silva, "The effects of nitric oxide on the immune system during Trypanosoma cruzi infection," *Memorias do Instituto Oswaldo Cruz*, vol. 104, no. 1, pp. 236–245, 2009.

[16] L. C. J. Abel, L. V. Rizzo, B. Ianni et al., "Chronic Chagas' disease cardiomyopathy patients display an increased IFN-γ response to *Trypanosoma cruzi* infection," *Journal of Autoimmunity*, vol. 17, no. 1, pp. 99–107, 2001.

[17] J. A. S. Gomes, L. M. G. Bahia-Oliveira, M. O. C. Rocha, O. A. Martins-Filho, G. Gazzinelli, and R. Correa-Oliveira, "Evidence that development of severe cardiomyopathy in human Chagas' disease is due to a Th1-specific immune response," *Infection and Immunity*, vol. 71, no. 3, pp. 1185–1193, 2003.

[18] M. M. Teixeira, R. T. Gazzinelli, and J. S. Silva, "Chemokines, inflammation and *Trypanosoma cruzi* infection," *Trends in Parasitology*, vol. 18, no. 6, pp. 262–265, 2002.

[19] A. Talvani, M. O. C. Rocha, L. S. Barcelos, Y. M. Gomes, A. L. Ribeiro, and M. M. Teixeira, "Elevated concentrations of CCL2 and tumor necrosis factor-α in chagasic cardiomyopathy," *Clinical Infectious Diseases*, vol. 38, no. 7, pp. 943–950, 2004.

[20] W. O. Dutra, C. A. Menezes, L. M. Magalhaes, and K. J. Gollob, "Immunoregulatory networks in human Chagas disease," *Parasite Immunology*, vol. 36, no. 8, pp. 377–387, 2014.

[21] G. A. Martins, C. E. Tadokoro, R. B. Silva, J. S. Silva, and L. V. Rizzo, "CTLA-4 blockage increases resistance to infection with the intracellular protozoan *Trypanosoma cruzi*," *Journal of Immunology*, vol. 172, no. 8, pp. 4893–4901, 2004.

[22] S. E. B. Graefe, T. Jacobs, U. Wächter, B. M. Bröker, and B. Fleischer, "CTLA-4 regulates the murine immune response to Trypanosoma cruzi infection," *Parasite Immunology*, vol. 26, no. 1, pp. 19–28, 2004.

[23] P. E. A. Souza, M. O. C. Rocha, C. A. S. Menezes et al., "Trypanosoma cruzi infection induces differential modulation of costimulatory molecules and cytokines by monocytes and T cells from patients with indeterminate and cardiac Chagas' disease," *Infection and Immunity*, vol. 75, no. 4, pp. 1886–1894, 2007.

[24] F. R. Gutierrez, F. S. Mariano, C. J. F. Oliveira et al., "Regulation of *Trypanosoma cruzi*-induced myocarditis by programmed death cell receptor 1," *Infection and Immunity*, vol. 79, no. 5, pp. 1873–1881, 2011.

[25] F. C. Dias, T. D. S. Medina, C. T. Mendes-Junior et al., "Polymorphic sites at the immunoregulatory CTLA-4 gene are associated with chronic chagas disease and its clinical manifestations," *PLoS ONE*, vol. 8, no. 10, Article ID e78367, 2013.

[26] A. González, V. Rebmann, J. Lemaoult, P. A. Horn, E. D. Carosella, and E. Alegre, "The immunosuppressive molecule HLA-G and its clinical implications," *Critical Reviews in Clinical Laboratory Sciences*, vol. 49, no. 3, pp. 63–84, 2012.

[27] S. Rajagopalan, Y. T. Bryceson, S. P. Kuppusamy et al., "Activation of NK cells by an endocytosed receptor for soluble HLA-G," *PLoS Biology*, vol. 4, article e9, no. 1, 2006.

[28] M. Onno, T. Guillaudeux, L. Amiot et al., "The HLA-G gene is expressed at a low mRNA level in different human cells and tissues," *Human Immunology*, vol. 41, no. 1, pp. 79–86, 1994.

[29] M. T. McMaster, C. L. Librach, Y. Zhou et al., "Human placental HLA-G expression is restricted to differentiated cytotrophoblasts," *Journal of Immunology*, vol. 154, no. 8, pp. 3771–3778, 1995.

[30] V. Mallet, S. Fournel, C. Schmitt, A. Campan, F. Lenfant, and P. Le Bouteiller, "Primary cultured human thymic epithelial cells express both membrane-bound and soluble HLA-G translated products," *Journal of Reproductive Immunology*, vol. 43, no. 2, pp. 225–234, 1999.

[31] M. Le Discorde, P. Moreau, P. Sabatier, J.-M. Legeais, and E. D. Carosella, "Expression of HLA-G in human cornea, an immune-privileged tissue," *Human Immunology*, vol. 64, no. 11, pp. 1039–1044, 2003.

[32] V. Cirulli, J. Zalatan, M. McMaster et al., "The class I HLA repertoire of pancreatic islets comprises the nonclassical class Ib antigen HLA-G," *Diabetes*, vol. 55, no. 5, pp. 1214–1222, 2006.

[33] Y. H. Huang, L. Airas, N. Schwab, and H. Wiendl, "Janus head: the dual role of HLA-G in CNS immunity," *Cellular and Molecular Life Sciences*, vol. 68, no. 3, pp. 407–416, 2011.

[34] C. Menier, M. Rabreau, J.-C. Challier, M. Le Discorde, E. D. Carosella, and N. Rouas-Freiss, "Erythroblasts secrete the nonclassical HLA-G molecule from primitive to definitive hematopoiesis," *Blood*, vol. 104, no. 10, pp. 3153–3160, 2004.

[35] W.-H. Yan, "Human leukocyte antigen-G in cancer: are they clinically relevant?" *Cancer Letters*, vol. 311, no. 2, pp. 123–130, 2011.

[36] P. Tripathi and S. Agrawal, "The role of human leukocyte antigen E and G in HIV infection," *AIDS*, vol. 21, no. 11, pp. 1395–1404, 2007.

[37] E. C. Castelli, C. T. Mendes-Junior, L. C. Veiga-Castelli, M. Roger, P. Moreau, and E. A. Donadi, "A comprehensive study of polymorphic sites along the HLA-G gene: implication for gene regulation and evolution," *Molecular Biology and Evolution*, vol. 28, no. 11, pp. 3069–3086, 2011 (Italian).

[38] A. Sabbagh, P. Luisi, and E. C. Castelli, "Worldwide genetic variation at the 3′ untranslated region of the HLA-G gene: balancing selection influencing genetic diversity," *Genes and Immunity*, vol. 15, no. 2, pp. 95–106, 2014.

[39] E. C. Castelli, C. T. Mendes-Junior, N. H. S. Deghaide et al., "The genetic structure of 3′untranslated region of the HLA-G gene: polymorphisms and haplotypes," *Genes and Immunity*, vol. 11, no. 2, pp. 134–141, 2010.

[40] G. Martelli-Palomino, J. A. Pancotto, Y. C. Muniz et al., "Polymorphic sites at the 3′ untranslated region of the HLA-G gene are associated with differential hla -g soluble levels in the Brazilian and French population," *PLoS ONE*, vol. 8, no. 10, Article ID e71742, 2013.

[41] L. Flaherty, E. Elliott, J. A. Tine, A. C. Walsh, and J. B. Waters, "Immunogenetics of the Q and TL regions of the mouse," *Critical Reviews in Immunology*, vol. 10, no. 2, pp. 131–175, 1990.

[42] B. L. Melo-Lima, A. F. Evangelista, D. A. R. De Magalhães, G. A. Passos, P. Moreau, and E. A. Donadi, "Differential transcript profiles of MHC class Ib(Qa-1, Qa-2, and Qa-10) and aire genes during the ontogeny of thymus and other tissues," *Journal of Immunology Research*, vol. 2014, Article ID 159247, 12 pages, 2014.

[43] S. Joyce, P. Tabaczewski, R. H. Angeletti, S. G. Nathenson, and I. Stroynowski, "A nonpolymorphic major histocompatibility complex class Ib molecule binds a large array of diverse self-peptides," *Journal of Experimental Medicine*, vol. 179, no. 2, pp. 579–588, 1994.

[44] A. Kumánovics, A. Madan, S. Qin, L. Rowen, L. Hood, and K. F. Lindahl, "Quod erat faciendum: sequence analysis of the H2-D and H2-Q regions of 129/SvJ mice," *Immunogenetics*, vol. 54, no. 7, pp. 479–489, 2002.

[45] E. Y. Chiang, M. Henson, and I. Stroynowski, "The nonclassical major histocompatibility complex molecule Qa-2 protects tumor cells from NK cell- and lymphokine-activated killer cell-mediated cytolysis," *The Journal of Immunology*, vol. 168, no. 5, pp. 2200–2211, 2002.

[46] T. G. Silva, J. C. O. Crispim, F. A. Miranda et al., "Expression of the nonclassical HLA-G and HLA-E molecules in laryngeal lesions as biomarkers of tumor invasiveness," *Histology and Histopathology*, vol. 26, no. 12, pp. 1487–1497, 2011.

[47] F. S. M. Tristão, F. A. Rocha, A. P. Moreira, F. Q. Cunha, M. A. Rossi, and J. S. Silvaa, "5-Lipoxygenase activity increases susceptibility to experimental *Paracoccidioides brasiliensis* infection," *Infection and Immunity*, vol. 81, no. 4, pp. 1256–1266, 2013.

[48] K. L. Cummings and R. L. Tarleton, "Rapid quantitation of *Trypanosoma cruzi* in host tissue by real-time PCR," *Molecular and Biochemical Parasitology*, vol. 129, no. 1, pp. 53–59, 2003.

[49] S. A. Bustin, V. Benes, J. A. Garson et al., "The MIQE guidelines: minimum information for publication of quantitative real-time PCR experiments," *Clinical Chemistry*, vol. 55, no. 4, pp. 611–622, 2009.

[50] M. Raymond and F. Rousset, "Genepop (version 1.2): population-genetics software for exact tests and ecumenicism," *Journal of Heredity*, vol. 86, pp. 248–249, 1995.

[51] L. Excoffier and H. E. L. Lischer, "Arlequin suite ver 3.5: a new series of programs to perform population genetics analyses under Linux and Windows," *Molecular Ecology Resources*, vol. 10, no. 3, pp. 564–567, 2010.

[52] L. Excoffier and M. Slatkin, "Maximum-likelihood estimation of molecular haplotype frequencies in a diploid population," *Molecular Biology and Evolution*, vol. 12, no. 5, pp. 921–927, 1995.

[53] Z. S. Qin, T. Niu, and J. S. Liu, "Partition-ligation-expectation-maximization algorithm for haplotype inference with single-nucleotide polymorphisms," *The American Journal of Human Genetics*, vol. 71, no. 5, pp. 1242–1247, 2002.

[54] M. Stephens, N. J. Smith, and P. Donnelly, "A new statistical method for haplotype reconstruction from population data," *The American Journal of Human Genetics*, vol. 68, no. 4, pp. 978–989, 2001.

[55] N. H. S. Deghaide, R. O. Dantas, and E. A. Donadi, "HLA class I and II profiles of patients presenting with Chagas' disease," *Digestive Diseases and Sciences*, vol. 43, no. 2, pp. 246–252, 1998.

[56] E. C. Castelli, P. Moreau, A. O. E. Chiromatzo et al., "In silico analysis of microRNAS targeting the HLA-G 3′ untranslated region alleles and haplotypes," *Human Immunology*, vol. 70, no. 12, pp. 1020–1025, 2009.

[57] J. M. Rodríguez-Pérez, D. Cruz-Robles, G. Hernández-Pacheco et al., "Tumor necrosis factor-alpha promoter polymorphism in Mexican patients with Chagas' disease," *Immunology Letters*, vol. 98, no. 1, pp. 97–102, 2005.

[58] S. A. Drigo, E. Cunha-Neto, B. Ianni et al., "TNF gene polymorphisms are associated with reduced survival in severe Chagas' disease cardiomyopathy patients," *Microbes and Infection*, vol. 8, no. 3, pp. 598–603, 2006.

[59] V. Campelo, R. O. Dantas, R. T. Simões et al., "TNF microsatellite alleles in Brazilian chagasic patients," *Digestive Diseases and Sciences*, vol. 52, no. 12, pp. 3334–3339, 2007.

[60] C. W. Pissetti, D. Correia, R. F. de Oliveira et al., "Genetic and functional role of TNF-alpha in the development *Trypanosoma cruzi* infection," *PLoS Neglected Tropical Diseases*, vol. 5, no. 3, article e976, 2011.

[61] L. Criado, O. Flórez, J. Martín, and C. I. González, "Genetic polymorphisms in TNFA/TNFR2 genes and Chagas disease in a Colombian endemic population," *Cytokine*, vol. 57, no. 3, pp. 398–401, 2012.

[62] O. Flórez, G. Zafra, C. Morillo, J. Martín, and C. I. González, "Interleukin-1 gene cluster polymorphism in chagas disease in a Colombian case-control study," *Human Immunology*, vol. 67, no. 9, pp. 741–748, 2006.

[63] G. C. Costa, M. O. D. C. Rocha, P. R. Moreira et al., "Functional IL-10 gene polymorphism is associated with Chagas disease cardiomyopathy," *Journal of Infectious Diseases*, vol. 199, no. 3, pp. 451–454, 2009.

[64] L. E. Alvarado Arnez, E. N. Venegas, C. Ober, and E. E. Thompson, "Sequence variation in the IL_4 gene and resistance to *Trypanosoma cruzi* infection in Bolivians," *Journal of Allergy and Clinical Immunology*, vol. 127, no. 1, pp. 279.e3–282.e3, 2011.

[65] O. A. Torres, J. E. Calzada, Y. Beraún et al., "Role of the IFNG +874T/A polymorphism in Chagas disease in a Colombian population," *Infection, Genetics and Evolution*, vol. 10, no. 5, pp. 682–685, 2010.

[66] J. E. Calzada, Y. Beraún, C. I. González, and J. Martín, "Transforming growth factor beta 1 (TGFβ1) gene polymorphisms and Chagas disease susceptibility in Peruvian and Colombian patients," *Cytokine*, vol. 45, no. 3, pp. 149–153, 2009.

[67] G. Zafra, C. Morillo, J. Martín, A. González, and C. I. González, "Polymorphism in the 3′ UTR of the IL12B gene is associated with Chagas' disease cardiomyopathy," *Microbes and Infection*, vol. 9, no. 9, pp. 1049–1052, 2007.

[68] L. G. Nogueira, R. H. B. Santos, B. M. Ianni et al., "Myocardial chemokine expression and intensity of myocarditis in Chagas cardiomyopathy are controlled by polymorphisms in CXCL9 and CXCL10," *PLoS Neglected Tropical Diseases*, vol. 6, no. 10, Article ID e1867, 2012.

[69] J. E. Calzada, A. Nieto, Y. Beraún, and J. Martín, "Chemokine receptor CCR5 polymorphisms and Chagas' disease cardiomyopathy," *Tissue Antigens*, vol. 58, no. 3, pp. 154–158, 2001.

[70] O. Flórez, J. Martín, and C. I. González, "Genetic variants in the chemokines and chemokine receptors in Chagas disease," *Human Immunology*, vol. 73, no. 8, pp. 852–858, 2012.

[71] R. Ramasawmy, E. Cunha-Neto, K. C. Faé et al., "The monocyte chemoattractant protein-1 gene polymorphism is associated with cardiomyopathy in human Chagas disease," *Clinical Infectious Diseases*, vol. 43, no. 3, pp. 305–311, 2006.

[72] N. Rouas-Freiss, M. Kirszenbaum, J. Dausset, and E. D. Carosella, "Fetal-maternal tolerance: Role of HLA-G in protection of the fetus against maternal natural killer cell activity," *Comptes Rendus de l'Academie des Sciences III*, vol. 320, no. 5, pp. 385–392, 1997.

[73] R. Sheshgiri, N. Rouas-Freiss, V. Rao et al., "Myocardial HLA-G reliably indicates a low risk of acute cellular rejection in heart transplant recipients," *Journal of Heart and Lung Transplantation*, vol. 27, no. 5, pp. 522–527, 2008.

[74] N. Lila, A. Carpentier, C. Amrein, I. Khalil-Daher, J. Dausset, and E. D. Carosella, "Implication of HLA-G molecule in heart-graft acceptance," *The Lancet*, vol. 355, no. 9221, p. 2138, 2000.

[75] N. Lila, C. Amrein, R. Guillemain et al., "Human leukocyte antigen-G expression after heart transplantation is associated with a reduced incidence of rejection," *Circulation*, vol. 105, no. 16, pp. 1949–1954, 2002.

[76] D. F. Hoft, R. G. Lynch, and L. V. Kirchhoff, "Kinetic analysis of antigen-specific immune responses in resistant and susceptible mice during infection with *Trypanosoma cruzi*," *Journal of Immunology*, vol. 151, no. 12, pp. 7038–7047, 1993.

[77] C. M. Rodrigues, H. M. S. Valadares, A. F. Francisco et al., "Coinfection with different Trypanosoma cruzi strains interferes with the host immune response to infection," *PLoS Neglected Tropical Diseases*, vol. 4, no. 10, article e846, 2010.

[78] F. F. de Araújo, D. M. Vitelli-Avelar, A. Teixeira-Carvalho et al., "Regulatory T cells phenotype in different clinical forms of chagas' disease," *PLoS Neglected Tropical Diseases*, vol. 5, no. 5, article e992, 2011.

Hindawi Publishing Corporation
Mediators of Inflammation
Volume 2014, Article ID 910621, 13 pages
http://dx.doi.org/10.1155/2014/910621

Research Article

Biomarker Analysis Revealed Distinct Profiles of Innate and Adaptive Immunity in Infants with Ocular Lesions of Congenital Toxoplasmosis

Anderson Silva Machado,[1] Ana Carolina Aguiar Vasconcelos Carneiro,[1] Samantha Ribeiro Béla,[2] Gláucia Manzan Queiroz Andrade,[3] Daniel Vitor Vasconcelos-Santos,[4] José Nélio Januário,[5] Jordana G. Coelho-dos-Reis,[2] Eloisa Amália Vieira Ferro,[6] Andréa Teixeira-Carvalho,[2] Ricardo Wagner Almeida Vitor,[1] Olindo Assis Martins-Filho,[2] and UFMG Congenital Toxoplasmosis Brazilian Group —UFMG-CTBG[5]

[1] *Departamento de Parasitologia, Universidade Federal de Minas Gerais, Avenida Presidente Antônio Carlos, 6627, Pampulha, 31270-901 Belo Horizonte, MG, Brazil*
[2] *Laboratório de Biomarcadores de Diagnóstico e Monitoração, Centro de Pesquisas René Rachou, Fundação Oswaldo Cruz, Avenida Augusto de Lima, 1715 Barro Preto, 30190-002 Belo Horizonte, MG, Brazil*
[3] *Departamento de Pediatria, Universidade Federal de Minas Gerais, Avenida Professor Alfredo Balena 190, Santa Efigênia, 30130-100 Belo Horizonte, MG, Brazil*
[4] *Departamento de Oftalmologia e Otorrinolaringologia, Faculdade de Medicina da UFMG, Belo Horizonte, MG, Brazil*
[5] *Núcleo de Ações e Pesquisa em Apoio Diagnóstico (NUPAD), Universidade Federal de Minas Gerais, Avenida Professor Alfredo Balena 190, Santa Efigênia, 30130-100 Belo Horizonte, MG, Brazil*
[6] *Universidade Federal de Uberlândia, Avenida João Naves de Ávila 2121, Santa Mônica, 38408-100 Uberlândia, MG, Brazil*

Correspondence should be addressed to Olindo Assis Martins-Filho; oassismartins@gmail.com

Received 24 May 2014; Revised 14 July 2014; Accepted 18 July 2014; Published 18 September 2014

Academic Editor: Edecio Cunha-Neto

Toxoplasma gondii is the main infectious cause of human posterior retinochoroiditis, the most frequent clinical manifestation of congenital toxoplasmosis. This investigation was performed after neonatal screening to identify biomarkers of immunity associated with immunopathological features of the disease by flow cytometry. The study included infected infants without NRL and with retinochoroidal lesions (ARL, ACRL, and CRL) as well as noninfected individuals (NI). Our data demonstrated that leukocytosis, with increased monocytes and lymphocytes, was a relevant hematological biomarker of ARL. Immunophenotypic analysis also revealed expansion of $CD14^+CD16^+HLA\text{-}DR^{high}$ monocytes and $CD56^{dim}$ cytotoxic NK-cells in ARL. Moreover, augmented $TCR\gamma\delta^+$ and $CD8^+$ T-cell counts were apparently good biomarkers of morbidity. Biomarker network analysis revealed that complex and intricated networks underscored the negative correlation of monocytes with NK- and B-cells in NRL. The remarkable lack of connections involving B-cells and a relevant shift of NK-cell connections from B-cells toward T-cells observed in ARL were outstanding. A tightly connected biomarker network was observed in CRL, with relevant connections of NK- and $CD8^+$ T-cells with a broad range of cell subsets. Our findings add novel elements to the current knowledge on the innate and adaptive immune responses in congenital toxoplasmosis.

1. Introduction

Ocular toxoplasmosis is a common inflammatory eye disease and a major cause of posterior uveitis worldwide [1]. The importance of toxoplasmosis is even greater in Brazil, where the prevalence and severity of ocular disease are higher than those in the rest of the world [2]. A study conducted in Brazil showed that 90% of newborns with congenital

toxoplasmosis had clinical signs at birth. The main symptom observed was retinochoroiditis, present in 80% of newborns [3].

The success of infection caused by *T. gondii* is based on a delicate balance between the host immune response, which tries to clear the parasite, and the immune evasion strategies or immunomodulation elicited by the parasite, which enables the ultimate survival of both the parasite and the host [4]. A number of different host cells and compartments are involved in the immune response to *T. gondii,* and the interplay between these cells is crucial to resistance to the parasite [5–9].

Scarce immunological data on ocular disease in humans is available and these studies have mainly focused on the *T. gondii*-specific T-cell response *in vitro*. The analysis of systemic specific cellular response to *T. gondii* antigen in patients without and with active/cicatricial ocular lesions in acquired or congenital disease has described controversial data on the role of proinflammatory response in this scenario. Yamamoto and colleagues have characterized the immune response in adult patients with ocular disease due to congenital infection and have suggested that these patients may show tolerance toward the parasite by decreased proinflammatory response along with lower lymphoproliferative index [10]. In contrast, Fatoohi and colleagues show that systemic cellular response to *T. gondii* does not differ between adult patients without and with presumed congenital ocular toxoplasmosis in regard to T-cell activation and proinflammatory cytokine production [11]. Despite recent advances in toxoplasmosis immunology, relatively little attention has been focused on the immunological events related to the congenital toxoplasmic retinochoroiditis in infant patients. Considering these previous reports, this work aimed at characterizing the *ex vivo* systemic immunophenotypic profile of innate and adaptive cell subsets during the early phases of congenital toxoplasmosis and its association with the absence/presence of active/cicatricial retinochoroiditis in infants.

2. Methods

2.1. Study Population. The protocols conducted in this study were approved by the local Ethics Committee (Federal University of Minas Gerais, protocol 298/06) and written informed consent was obtained from all mothers of infants included in this study.

This study was part of a prospective investigation on neonatal screening for congenital toxoplasmosis conducted by a multidisciplinary research group (UFMG Congenital Toxoplasmosis Brazilian Group). From November 1, 2006, to May 31, 2007, a total of 146,307 children were tested for anti-*T. gondii* IgM antibodies in dried blood samples on filter paper using the Toxo IgM kit (Q-Preven, Symbiosis, Leme, Brazil). Confirmative plasma/serum tests were run in 220 infants and their mothers in cases with positive or underterminated screening results. The mothers and infants were tested for IgA (enzyme-linked immunosorbent assay) and IgG and IgM anti-*T. gondii* (enzyme-linked fluorometric assay, ELFA-VIDAS, BioMérieux SA, Lyon, France). Out of these 220 cases, 190 infants tested positive by confirmative exams and for the persistence of anti-*T. gondii* IgG antibodies in serum at the age of 12 months. All infants included in this study received medical care by a general clinical physician with experience with infectious diseases and the physical examination did not reveal any alteration. Ophthalmologic evaluation was performed by two retina/uveitis specialists assisted by a trained nursing professional according to a standardized protocol as reported elsewhere [3]. Infants also underwent a through pediatric examination, neuroimaging studies (cranial radiographs or transfontanel ultrasound; computer-assisted tomography in selected cases), hearing assessment, and ophthalmologic evaluation. Peripheral blood samples from 105 infants (45 ± 12 days of age; 53% male, 47% female) were collected to obtain leukocytes. These infants were classified into two groups: (i) group TOXO (infected infants), which comprised 83 infants diagnosed with congenital toxoplasmosis who had positive confirmative tests and persistent specific IgG antibodies, and (ii) group NI (control noninfected infants), which comprised 22 infants who tested negative by IgG anti-*T. gondii*. Among the 83 children from group TOXO, 15 infants presented active retinochoroidal lesions (ARL), 27 had simultaneous active and cicatricial retinochoroidal lesions (ACRL), 17 had cicatricial retinochoroidal lesions (CRL), and 24 had no retinochoroidal lesions (NRL). Infants from the NI group did not have any type of retinochoroidal lesions.

2.2. Flow Cytometric Acquisition and Analysis. Peripheral blood from infants with congenital toxoplasmosis (TOXO) and noninfected infants (NI) was processed, and leukocyteswere used for *ex vivo* protocols, as previously described [10]. Monoclonal antibodies (mAbs) were used for labeling cell surface molecules, for T and NKT lymphocytes (anti-CD3, anti-CD4, and anti-CD8), B lymphocytes (anti-CD5, anti-CD19, and anti-CD23), monocytes (anti-CD14, anti-CD16, anti-CD32, and anti-CD64), NK- and NKT-cells (anti-CD16, anti-CD56), anti-HLA-DR (activation), conventional T-cells (anti-TCR$\alpha\beta$), and gamma-delta T-cells (anti-TCR$\gamma\delta$), labeled with fluorescein isothiocyanate (FITC), phycoerythrin (PE), or TRI-COLOR (TC), which were purchased from Invitrogen Life Technologies (Carlsbad, CA, USA).

Cytofluorimetric data acquisition was performed with a Becton Dickinson FACSCalibur instrument. CELLQUEST software provided by the manufacturer was used for data analysis.

2.3. Data Analysis. This was a descriptive transversal study that applied three data analysis approaches for observational investigation of the immunological profile associated with distinct clinical manifestations of congenital toxoplasmosis, referred to as (1) conventional statistical analysis, (2) biomarker signature analysis, and (3) biomarkers network. The two later approaches have been shown as relevant to detect, with high sensitivity, putative minor changes in the immunological profiles that are not detectable by conventional statistical approaches.

2.3.1. Conventional Statistical Analysis. Statistical analyses were conducted using GraphPad Prism 5.0 software (GraphPad Software, San Diego, CA, USA). Differences between groups were first evaluated to test the normality. Considering the nonparametric nature of all data sets, statistical analyses between the TOXO and NI groups were performed by the Mann-Whitney test. Additional analyses among the TOXO subgroups were performed by the Kruskal-Wallis test, followed by Dunns' multiple comparison test. Data sets are presented as scatter distributions over median values (bars) for TOXO and NI groups. Data from the TOXO subgroups analysis were presented in box-plot format, highlighting the median together with the minimum and maximum values. In all cases, differences were considered significant at $P < 0.05$.

2.3.2. Biomarker Signature Analysis. The use of this approach was adapted from a pioneering study in order to identify relevant differences in the peripheral blood phenotypic signatures between the groups [11]. In this data analysis, initially, the whole universe of data of each cell subset was used to calculate the global median value used as the cut-off to classify infants as with "low" or "high" counts of a given biomarker. The following cut-offs were used to categorize each infant as presenting "low" or "high" levels of a given cell subset: MONCD16$^+$ = 125.0 cells/mm^3, MONCD16$^+$DR^{high} = 86.2 cells/mm^3, MONCD32$^+$ = 78.8 cells/mm^3, MONCD64$^+$ = 186.6 cells/mm^3, NK-cells = 1195.2 cells/mm^3, NKCD16$^+$CD56$^-$ = 441.2 cells/mm^3, NKCD16$^+$CD56$^+$ = 526.0 cells/mm^3, NKCD16$^-$CD56$^+$ = 85.4 cells/mm^3, CD3$^-$CD56^{dim} = 2.43%, CD3$^-$CD56^{bright} = 1.06%, CD3$^+$CD16$^+$ = 73.8 cells/mm^3, NKT-cells = 50.3 cells/mm^3, CD3$^+$ = 4590.5 cells/mm^3, TCR$\alpha\beta^+$ = 3991.6 cells/mm^3, TCR$\gamma\delta^+$ = 452.4 cells/mm^3, TCD4$^+$ = 2850.2 cells/mm^3, TCD8$^+$ = 1862.6 cells/mm^3, TCD4$^+$CD8$^+$ = 38.8 cells/mm^3, TCD4$^+$DR$^+$ = 466.5 cells/mm^3, TCD8$^+$DR$^+$ = 1471.6 cells/mm^3, BCD19$^+$ = 1523.0 cells/mm^3, BCD5$^+$ = 851.3 cells/mm^3, BCD5$^-$ = 576.7 cells/mm^3, and BCD23$^+$ = 959.0 cells/mm^3. Once the cut-offs for each biomarker were established, we selected infants with high biomarker counts and assembled the data using gray-scale diagrams to calculate the frequency of those for each clinical group. Relevant data (>50%) were then highlighted in bold/underline format. Radar charts were constructed to characterize the overall frequency of infants with high levels of a given innate or adaptive immune cell population. GraphPad Prism 5.00 software (San Diego, USA) was used for graphical arts.

2.3.3. Biomarker Network. Biomarker networks were assembled to assess the association between cell subpopulations (monocytes, NK-cells, NKT-cells, T-cells, and B-cells) and their subsets for each clinical group. The correlations were significant when Spearman's test resulted in a $P < 0.05$. Significant correlations representing the interaction between biomarkers tested were compiled using the open source software Cytoscape (version 2.8; http://www.cytoscape.org), as previously reported [12]. Biomarker networks were constructed using circle layouts with each biomarker being represented by a specific cartoon (monocytes; NK- and NKT-cells; T-cells and B-cells). Connecting edges display the underscore as negative, moderate, and strong, as proposed previously [13]. The correlation index (r) was used to categorize the correlation strength as negative ($r < 0$), moderate ($0.36 > r < 0.67$), or strong ($r > 0.68$). GraphPad Prism 5.00 software (San Diego, USA) was used for the data analysis.

3. Results

3.1. Leukocytosis with Increased Monocyte and Lymphocyte Counts is a Relevant Hematological Biomarker of Active Retinochoroidal Lesions in Congenital Toxoplasmosis. The analysis of hematological parameters demonstrated that TOXO is accompanied by relevant leukocytosis with increased monocyte and lymphocyte counts. Further categorization of infants, according to their ophthalmological records, showed that these changes were particularly observed in ARL patients. Relevant monocytosis was also observed in ACRL patients. No significant differences were observed in the NRL and CRL subgroups (Table 1).

3.2. Expansion of CD14$^+$CD16$^+$HLA-DR^{high} Proinflammatory Monocytes Is Present in Infants with Active Retinochoroidal Lesions in Congenital Toxoplasmosis. When evaluating monocyte subsets, our results demonstrated that infants in the TOXO group presented an increase of CD14$^+$CD16$^+$ macrophage-like and CD14$^+$CD16$^+$HLA-DR^{high} proinflammatory monocytes (Figure 1(a)). In fact, the increase in CD14$^+$CD16$^+$HLA-DR^{high} proinflammatory monocytes was particularly observed in the ARL subgroup when compared with NI controls (Figure 1(a)).

Furthermore, analysis of FCγ-R expression by monocytes (Figure 1(b)) showed that TOXO displayed relevant changes in CD32 and CD64 expression on the surface of these cells. Analysis of the TOXO subgroups demonstrated that the CRL infants, in particular, had decreased CD32 and increased CD64 expression when compared with NI control group (Figure 1(b)). Figure 1(c) shows representative flow cytometric histogram analyses of the CD32 and CD64 expression observed in the TOXO and NI groups.

3.3. NK- and NKT-Cell Subsets Are Expanded in the Peripheral Blood of Infants with Congenital Toxoplasmosis. Data regarding total CD3$^-$CD16$^{+/-}$CD56$^{+/-}$ NK-cells revealed an increased absolute count in peripheral blood samples from the TOXO group. Analysis of NK-cell subsets showed an increase in all NK-cell subsets in the TOXO group, including CD3$^-$CD16$^+$CD56$^-$, CD3$^-$CD16$^+$CD56$^+$, and CD3$^-$CD16$^-$CD56$^+$ cells (Figure 2(a)). Analysis of TOXO subgroups demonstrated that whereas total CD3$^-$CD16$^{+/-}$CD56$^{+/-}$ NK-cells were enhanced in the ARL subgroup, CD3$^-$CD16$^-$CD56$^+$ NK-cells were expanded in the ACRL and CRL subgroups compared with the NI and NRL patients, respectively (Figure 2(a)).

Analysis of NKT-cell subsets showed a significant increase in both the CD3$^+$CD16$^+$ and CD3$^+$CD56$^+$ cell subpopulations in the TOXO group compared with the NI

Table 1: Hematological records in infants with congenital toxoplasmosis*.

Parameters	NI ($n = 22$)	TOXO ($n = 76$)	TOXO subgroups			
			NRL ($n = 22$)	ARL ($n = 15$)	ACRL ($n = 24$)	CRL ($n = 15$)
WBC	9.3 (5.3–17.3) × 10^3	**11.6** (5.6–22.9) × 10^3	11.0 (6.2–17.3) × 10^3	**14.5** (7.6–23.0) × 10^3	11.8 (5.7–19.4) × 10^3	11.2 (5.7–18.2) × 10^3
Monocytes	0.8 (0.1–1.9) × 10^3	**1.2** (0.1–2.3) × 10^3	1.1 (0.2–2.1) × 10^3	**1.4** (0.5–1.7) × 10^3	**1.3** (0.2–2.3) × 10^3	1.0 (0.1–2.4) × 10^3
Neutrophils	1.8 (0.7–4.0) × 10^3	1.7 (0.5–5.7) × 10^3	1.8 (1.0–3.0) × 10^3	1.7 (0.8–3.6) × 10^3	1.6 (0.4–5.3) × 10^3	1.6 (0.9–5.7) × 10^3
Lymphocytes	6.2 (3.9–14.2) × 10^3	**7.5** (1.0–18.8) × 10^3	7.3 (4.3–14.2) × 10^3	**8.5** (5.4–18.1) × 10^3	7.5 (3.9–13.9) × 10^3	7.4 (1.0–13.9) × 10^3
Eosinophils	0.4 (0.1–0.8) × 10^3	0.4 (0.1–1.7) × 10^3	0.4 (0.08–0.8) × 10^3	0.5 (0.2–1.1) × 10^3	0.4 (0.003–1.7) × 10^3	0.3 (0.06–1.1) × 10^3
RBC	3.5 (2.8–4.5) × 10^6	3.6 (2.9–5.1) × 10^6	3.5 (2.5–4.4) × 10^6	3.68 (3.1–4.1) × 10^6	3.5 (2.4–4.5) × 10^6	3.71 (2.5–4.2) × 10^6
Hb (g/dL)	10.8 (8.5–13.1)	10.5 (8.1–13.9)	10.3 (7.8–13.0)	10.8 (8.3–12.2)	9.9 (7.7–12.9)	10.75 (7.2–12.9)
Hct (%)	31.0 (25.4–39.4)	31.9 (22.1–45.4)	30.6 (23.0–39.1)	32.8 (27.1–37.3)	29.4 (20.8–37.7)	31.8 (23.0–36.9)
PLT	4.8 (1.3–7.3) × 10^5	3.8 (1.1–7.9) × 10^5	4.31 (1.4–6.7) × 10^5	3.35 (1.4–6.3) × 10^5	3.61 (1.4–6.3) × 10^5	2.87 (1.7–4.9) × 10^5

*WBC = white blood cells; RBC = red blood cells; PLT = platelets. Results are expressed in cell counts/mm^3. Significant differences at $P < 0.05$ are highlighted by bold format.

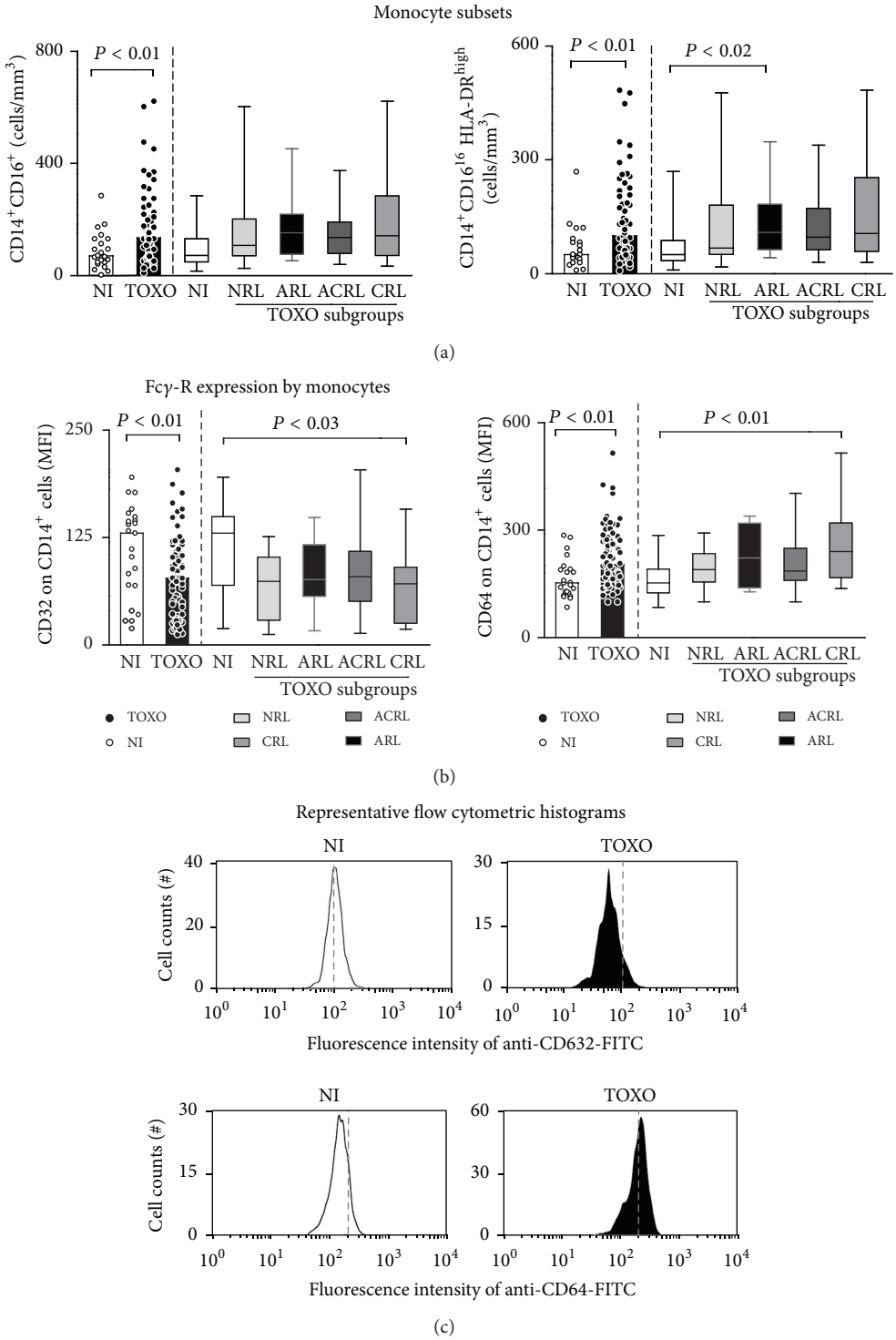

Figure 1: Monocyte subsets (a) and FCγ-R expression profile of monocytes (b) in the peripheral blood of congenital toxoplasmosis infants (TOXO) and noninfected controls (NI). Congenital toxoplasmosis was further categorized according to the clinical ocular status, referred to as no retinochoroidal lesions (NRL), active retinochoroidal lesions (ARL), active/cicatricial retinochoroidal lesions (ACRL), and cicatricial retinochoroidal lesions (CRL). The results are expressed as scatter plots of individual values and the medians of absolute cell counts/mm^3 (left side) or in box-plot format (right side), where the box stretches from the lower hinge (25th percentile) to the upper hinge (75th percentile), and the middle half represents the median of the distribution as a line across the box. Significant differences are highlighted by connecting lines, and P values are shown in the figure. (c) Representative histograms illustrating the downregulation of CD32 (top panels) and the upregulation of CD64 (bottom panels) on circulating monocytes from infants with congenital toxoplasmosis (black) compared to noninfected controls (white). The dashed lines were set to highlight the shift in the histogram distribution toward lower or higher FCγ-R expression by monocytes.

group. In fact, $CD3^+CD16^+$ cells were particularly expanded in the ARL and ACRL subgroups, whereas $CD3^+CD56^+$ cells were significantly increased in the ARL and CRL subgroups compared to NI controls (Figure 2(b)).

To characterize the major phenotypes related to the distinct functional features of NK-cells, we investigated the frequency of $CD56^{dim}$ cytotoxic and $CD56^{bright}$ immunoregulatory cell subsets. Our findings demonstrated a decreased percentage of $CD3^-CD16^+CD56^{bright}$ cells along with the expansion of $CD3^-CD16^+CD56^{dim}$ cells in the TOXO group compared to the NI group. Additional analysis revealed that $CD3^-CD16^+CD56^{bright}$ cells were reduced in all TOXO subgroups, while $CD3^-CD16^+CD56^{dim}$ cells were particularly expanded in the ARL subgroup compared to the NI group (Figure 2(a)).

3.4. Augmented Activation of $CD4^+$ T-Cells is Closely Related to the Presence of Active Retinochoroidal Lesions. Analysis of the adaptive immunity compartment is presented in Figure 3. Our data showed that TOXO patients presented increased counts of activated $CD4^+$HLA-DR^+ T-cells along with $CD4^+CD8^+$ T-cells, $CD19^+$ B-cells, and $CD19^+CD5^+$ B1-cells compared to NI patients (Figures 3(a) and 3(b)).

Additionally, our data demonstrated that $CD4^+$ T-cell counts were increased in the ARL subgroup compared to the CRL subgroup. Moreover, $CD4^+$HLA-DR^+ cells were particularly increased in the ARL and ACRL subgroups compared to the NI group (Figure 3(a)). No changes in B-cell subsets were observed among the TOXO subgroups (Figure 3(b)).

Our data demonstrated increased counts of TCR$\gamma\delta^+$ cells, $CD8^+$ T-cells, and particularly activated $CD8^+$HLA-DR^+ T-cells in the TOXO group. Analysis of TOXO subgroups demonstrated that TCR$\gamma\delta^+$ cells, $CD8^+$ T-cells, and activated $CD8^+$HLA-DR^+ T-cells, in particular, were increased in all groups with retinochoroidal lesions (ARL, ACRL, and CRL).

3.5. Expanded Frequency of Infants with High Levels of Innate and Adaptive Immune Cells Characterizes the Biomarker Signature Associated with the Presence of Active Retinochoroidal Lesions. To further characterize the immunological profile associated with distinct clinical manifestations of congenital toxoplasmosis, we assembled the overall phenotypic biomarker signature of peripheral blood innate/adaptive immune cells using the innovative/nonconventional data analysis approach referred to as the biomarker signature of innate and adaptive immunity compartments in the peripheral blood of infants with congenital toxoplasmosis (Figure 4).

Our data demonstrated that, in the NI group, most biomarkers were confined to frequencies below 50%, except $MONCD32^+$, CD3-$CD56^{bright}$, and $CD4^+$ T-cells. However, in all TOXO subgroups, most biomarkers were confined to frequencies above 50%. Specifically, the NRL subgroup predominantly showed enhancement of B-cell related biomarkers ($BCD19^+$, $BCD5^+$, $BCD5^-$, and $BCD23^+$) along with $TCD3^+$, TCR$\gamma\delta^+$, and NKT-cells in the innate immune compartment. By contrast, the CRL subgroups predominantly showed increases in the frequency of innate immunity biomarkers ($MONCD16^+$, $MONCD16^+DR^{high}$, $MONCD64^+$, NK-cells, $CD16^+CD56^-$, $CD16^+CD56^+$, $CD16^-CD56^+$, $CD3^-CD56^{dim}$, $CD3^+CD16^+$, and NKT-cells but not $MONCD32^+$ and $CD3^-CD56^{bright}$) along with T-cell related biomarkers (TCR$\gamma\delta^+$, $TCD4^+$, $TCD8^+$, $TCD4^+CD8^+$, and $TCD8^+DR^+$).

The profile of the ARL subgroup was of particular interest, with an enhanced frequency of biomarkers in both the innate and adaptive immune compartments. All biomarkers included in this investigation were found to be increased to above 50% in the ARL infants evaluated, except for $MONCD32^+$ and $CD3^-CD56^{bright}$. The ACRL subgroup showed an overall biomarker signature similar to that observed in the ARL subgroup, with minor changes mainly in the NK- and B-cell subsets.

3.6. Remarkable Lack of Connections Involving B-Cells Is Observed in Infants with Active Retinochoroidal Lesions. Exploratory analysis of biomarker networks demonstrated that although some axes intrinsic of innate and adaptive immunity were preserved in all clinical groups, some connections were lost in the TOXO subgroups (Figure 5).

In the NI group, NK- and B-cells clearly represent relevant foci of connections. A relevant shift of NK-cell connections toward T-cells was observed in the ARL subgroup along with a selective loss of connections with the B-cell compartment (Figure 5).

The ACRL subgroup clearly showed a transitional profile between the ARL and CRL subgroups with NK-cell connections focusing on T-cells and restoring the connections with B-cells (Figure 5).

3.7. Complex and Imbricated Biomarker Networks Underscore the Interaction of Monocytes with NK- and B-Cells in Protective Events, Whereas NK-Cells and $CD8^+$ T-Cells Appear Relevant to Mechanisms of Resolution. The fact that the NRL and CRL subgroups displayed a higher number of significant interactions and a more complex and imbricated biomarker network was outstanding. In fact, a rich number of connections were observed in these subgroups.

It was clear that the NRL subgroup showed relevant interaction between monocytes and other cell subsets (NKT-, NK-, and B-cells) mediated by negative correlations and a relevant role of NK-cell connections focusing on T- and B-cells (Figure 5).

In the CRL subgroup, a strong correlation axis could be identified, with the pivotal participation of several NK-cell subsets interacting with T- and B-cells along with strong connections of $CD8^+$ T-cells with a broad range of cell subsets (Figure 5).

4. Discussion

Retinochoroiditis in humans caused by *T. gondii* is the most frequent clinical manifestation of congenital and acquired parasite infection [14, 15]. The disease typically presents as a

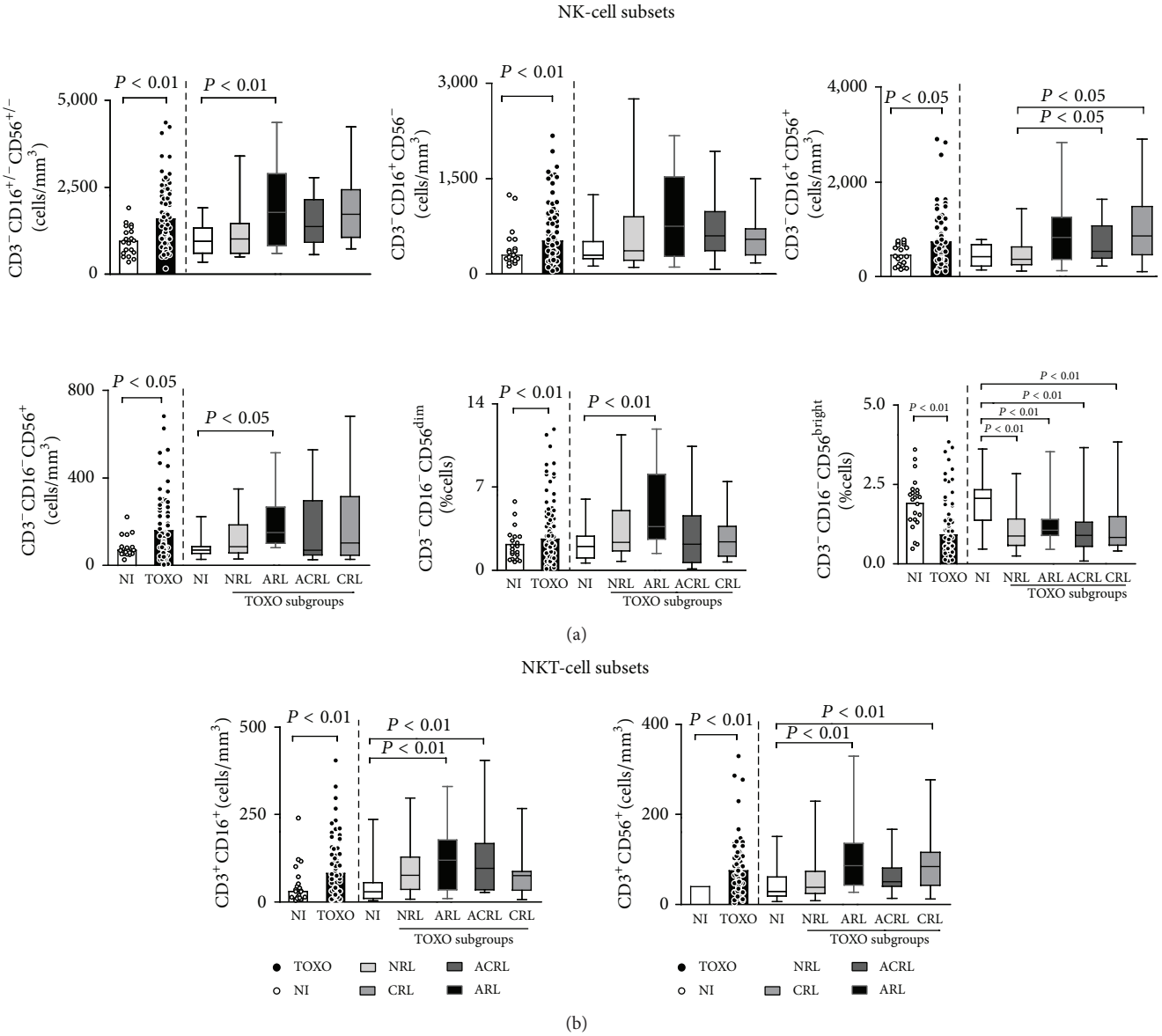

Figure 2: NK- (a) and NKT-cell subsets (b) in the peripheral blood of congenital toxoplasmosis infants (TOXO) and noninfected controls (NI). Congenital toxoplasmosis was further categorized according to the clinical ocular status, referred to as no retinochoroidal lesions (NRL), active retinochoroidal lesions (ARL), active/cicatricial retinochoroidal lesions (ACRL), and cicatricial retinochoroidal lesions (CRL). The results are expressed as scatter plots of individual values and the medians of absolute cell counts/mm^3 (left side) or in box-plot format (right side), where the box stretches from the lower hinge (25th percentile) to the upper hinge (75th percentile), and the middle half represents the median of the distribution as a line across the box. Significant differences are highlighted by connecting lines, and P values are shown in the figure.

unilateral focal necrotizing lesion in the presence of adjacent scars [1].

The common occurrence of toxoplasmic retinochoroiditis is believed to be under the influence of the status of the host immune response [16], the genotype of infective parasite strains [2], and the host genetic background [17, 18]; however, the participation of cellular components that lead to the establishment of this ocular manifestation has not been addressed well in humans.

The presence of active, active/cicatricial, or cicatricial lesions observed in the infants of our cohort is consequence of multiple factors, which may include parasite virulence and retinotropism of *T. gondii* in Brazil, individual susceptibility as well as the *T. gondii*-specific immune response in the infants of our cohort. Another possibility is that the time of infection during pregnancy may impact the outcome of distinct retinochoroidal lesions. The premise that putative infection by parasites with diverse virulence

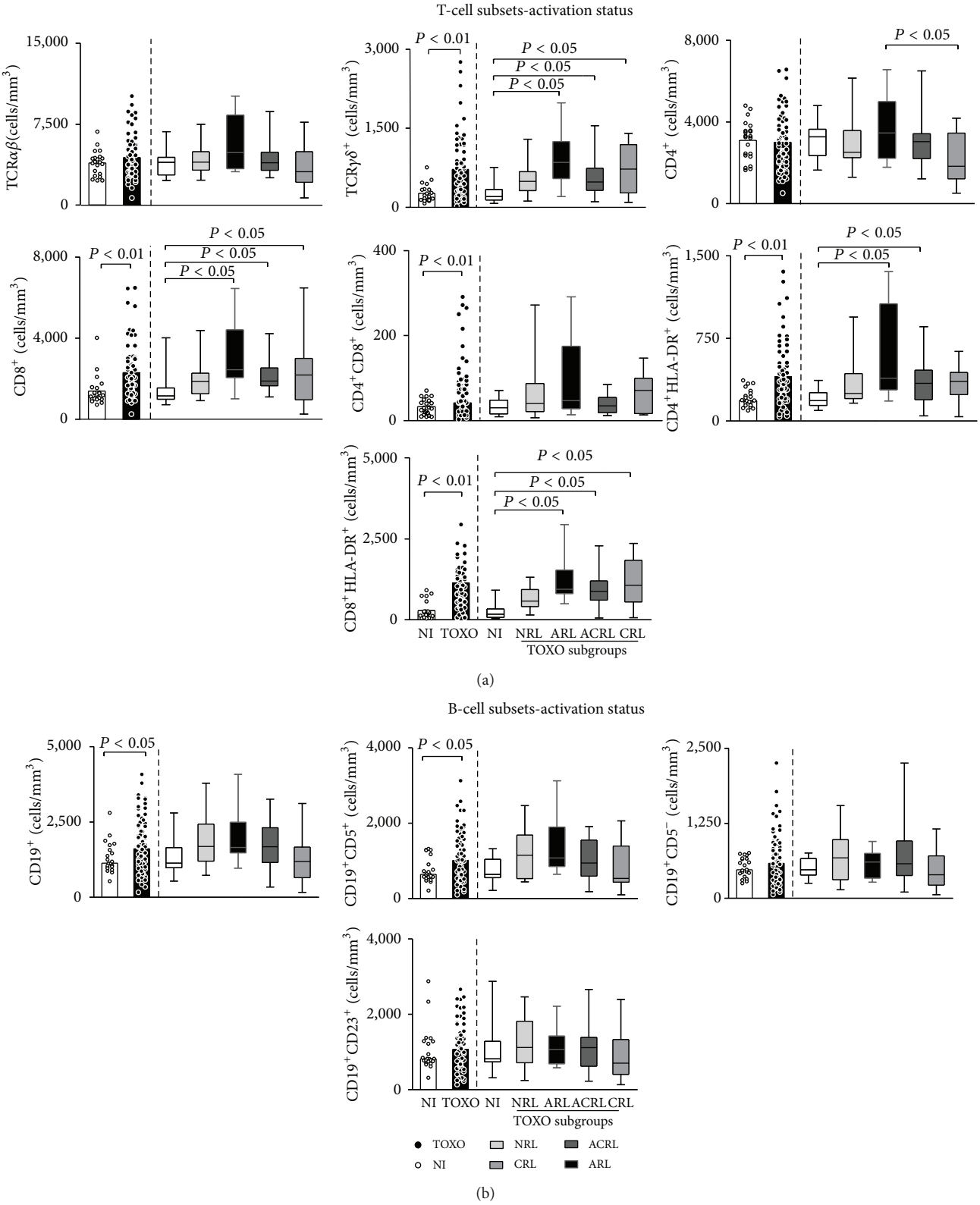

Figure 3: Major subsets and activation status of T- (a) and B-cells (b) in the peripheral blood of infants with congenital toxoplasmosis (TOXO) and noninfected controls (NI). Congenital toxoplasmosis was further categorized according to the clinical ocular status, referred to as no retinochoroidal lesions (NRL), active retinochoroidal lesions (ARL), active/cicatricial retinochoroidal lesions (ACRL), and cicatricial retinochoroidal lesions (CRL). The results are expressed as scatter plots of individual values and the medians of absolute cell counts/mm^3 (left side) or in box-plot format (right side), where the box stretches from the lower hinge (25th percentile) to the upper hinge (75th percentile), and the middle half represents the median of the distribution as a line across the box. Significant differences are highlighted by connecting lines, and P values are shown in the figure.

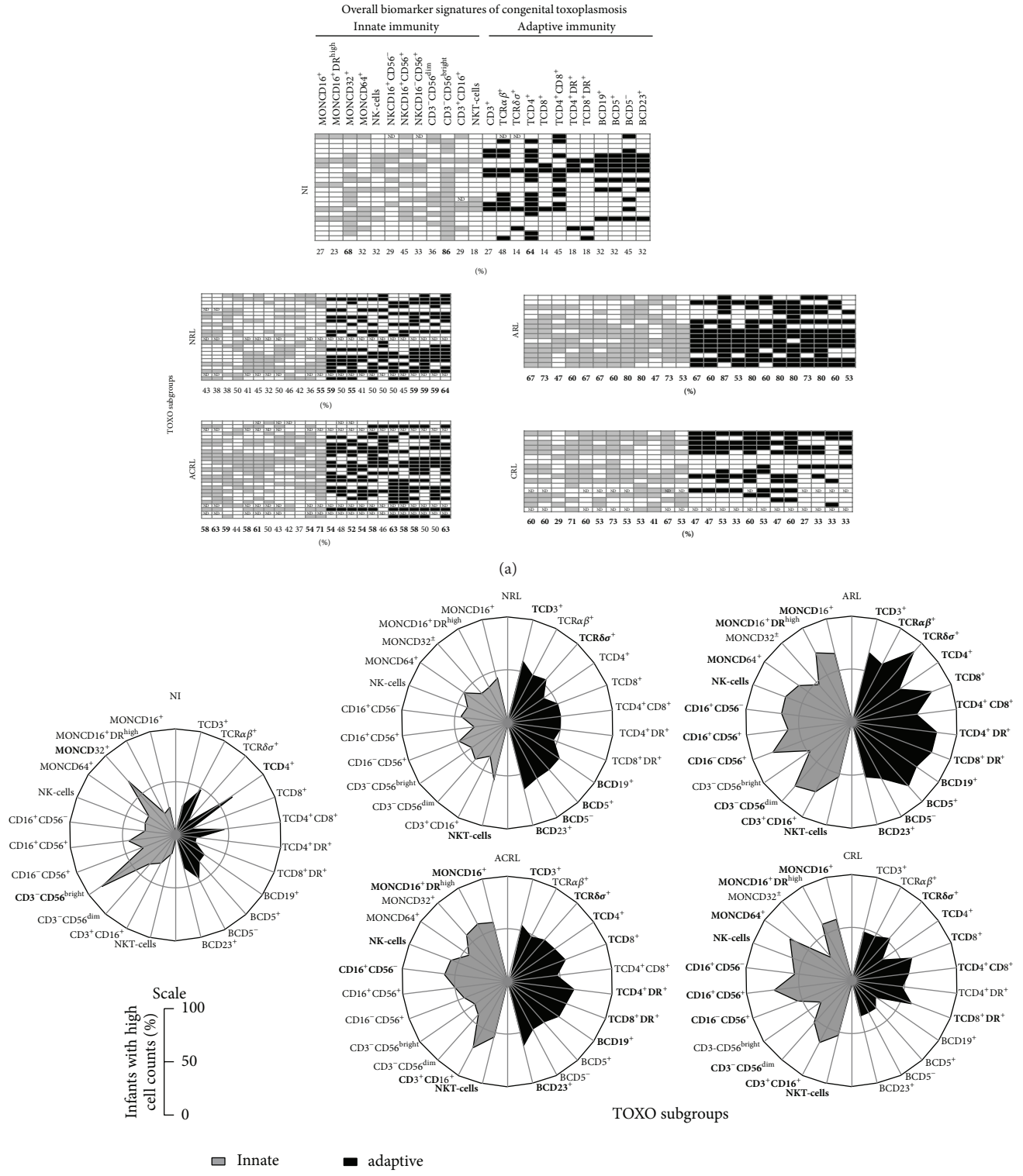

Figure 4: Biomarker signatures of innate and adaptive immunity in the peripheral blood of infants with congenital toxoplasmosis categorized as no retinochoroidal lesions (NRL), active retinochoroidal lesions (ARL), active/cicatricial retinochoroidal lesions (ACRL), and cicatricial retinochoroidal lesions (CRL) compared to noninfected controls (NI). (a) Gray-scale diagrams were assembled using the global median value of each cell subset as the cut-off mark to tag each infant as presenting "low" or "high" (innate; adaptive) levels of a given cell population. The frequency (%) of infants displaying high cell counts is provided, and the relevant data (>50%) are underscored in bold/underline format. (b) The radar charts summarize the biomarker signature of innate and adaptive immunity, where each axis displays the proportion of infants with high levels of a given cell population. The relevant data (>50%) are underscored in bold/underline format.

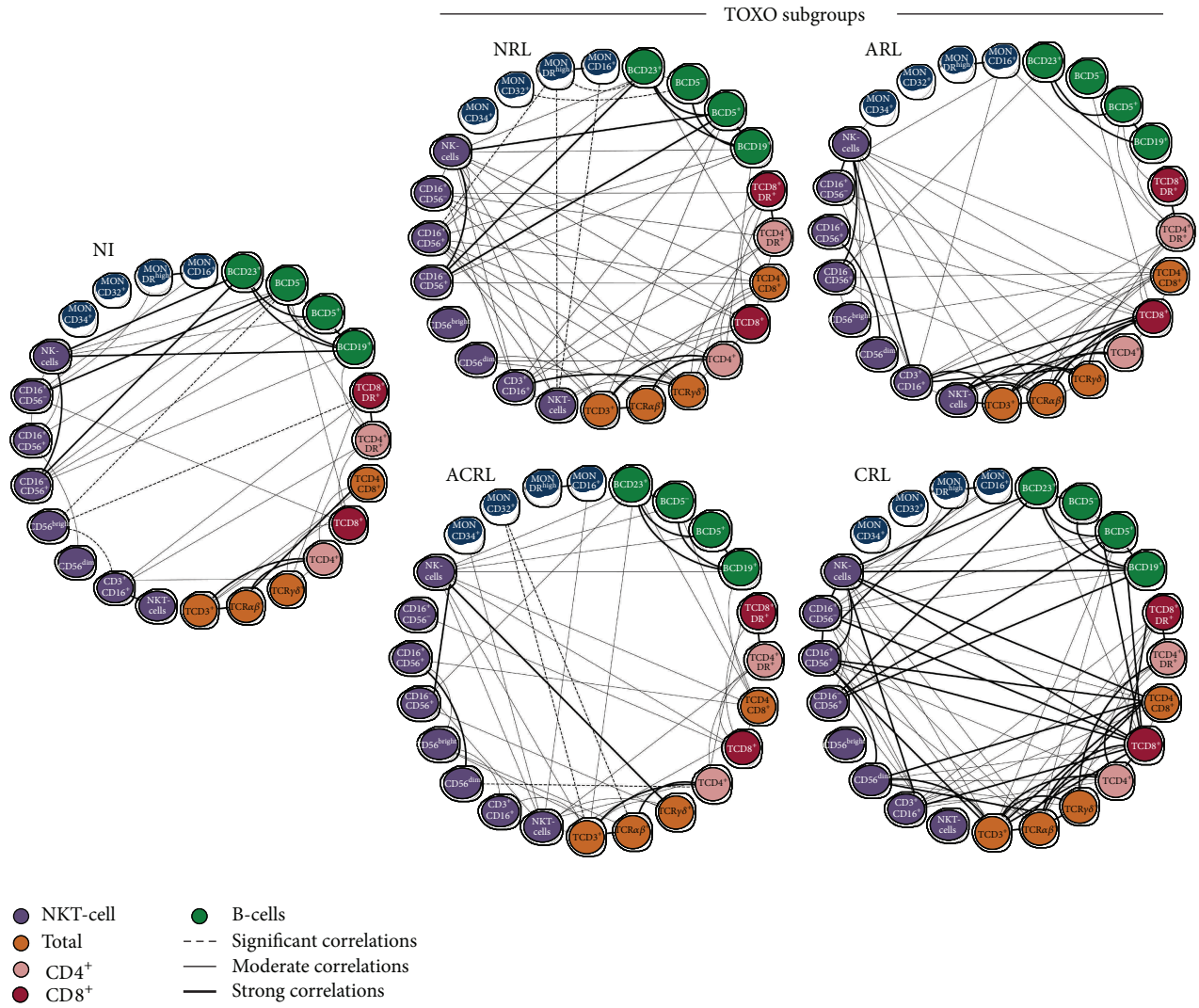

Figure 5: Biomarker networks of innate and adaptive immunity in the peripheral blood of infants with congenital toxoplasmosis categorized as no retinochoroidal lesions (NRL), active retinochoroidal lesions (ARL), active/cicatricial retinochoroidal lesions (ACRL), and cicatricial retinochoroidal lesions (CRL) compared to noninfected controls (NI). Networks were assembled to assess the association between leukocyte subpopulations, including monocytes, NK- and NKT-cells, T-cells (total, $CD4^+$, and $CD8^+$), and B-cells. Significant correlations at $P < 0.05$ are highlighted by connecting edges to underscore negative, moderate, and strong indexes.

and/or atypical/recombinant genotypes leads to different manifestation of ocular toxoplasmosis was not confirmed by our parasitology team, as shown by Carneiro et al., 2013 [19]. Moreover, preliminary results regarding IgM reactivity as well as IgG avidity do not support the hypothesis that time of infection during pregnancy may influence the occurrence of distinct patterns of retinochoroidal lesions (paper in preparation). The development of an adequate innate immune response is important for infection control and reduction of toxoplasmosis-associated injuries, primarily retinochoroiditis. However, the initial stages of congenital infection are unclear, and most studies mainly refer to work with experimental models [20–22]. The present study is a great opportunity to understand the major and minor changes in peripheral blood leukocyte subpopulations in infants with congenital toxoplasmosis. Although the analysis of *in vitro T. gondii*-specific immune response is highly relevant to understand the role of the parasite-derived antigens essential to elucidate the mechanism underlying the immunopathogenesis of ocular toxoplasmosis, we believe that the *ex vivo* analysis particularly in the absence of exogenous stimuli is highly relevant to map the events that take place *in vivo* and may point out putative biomarkers useful to comprehend the systemic network involved in the immunopathogenesis of ocular toxoplasmosis.

Infants were selected through a newborn screening program, and therefore, no information about gestational age when the congenital infection occurred was available. Our results showed an increase in the populations of monocytes and lymphocytes in infants with congenital toxoplasmosis. It is known that monocyte recruitment is essential in restricting the growth of *T. gondii* in murine models of

toxoplasmosis [6, 23]. However, other studies show that these cells as well as dendritic cells are strong candidates for the intracellular transport of *T. gondii* in the blood as a "Trojan Horse" [24]. Moreover, the activity of monocytes must be carefully controlled because excessive production of inflammatory cytokines and nitric oxide (NO) can result in severe immunopathology [25]. The increase in the population of monocytes was observed only in the active lesion groups, suggesting that the persistence of the immune response mediated by monocytes is directly related to the pathology observed in these infants.

After this previous analysis, we examined the changes in specific monocyte subsets. An increase in proinflammatory monocytes ($CD14^+CD16^+HLA\text{-}DR^{++}$) in infants with congenital toxoplasmosis was observed. Previous studies have shown that inflammatory monocytes produce IL-12 *in vitro* and *in vivo* when stimulated with *T. gondii* [6, 7], and it has also been proposed that these cells contribute to the direct control of *T. gondii* through the production of NO, which inhibits parasite replication [8]. Increased proinflammatory monocytes in infected infants, particularly in those with active retinochoroidal lesions, are indicative of a strong and persistent proinflammatory response.

NK-and NKT-cells are other innate populations involved in immunity against *T. gondii* that are increased in infants with congenital toxoplasmosis compared with noninfected children. Our results showed an increase in the population of $CD56^{dim}$ cells in infants with active lesions when compared with an important decrease in the immunoregulatory NK subset, expressing $CD56^{bright}$. The increase in this population and in subsets of NK- and NKT-cells is an important feature of the innate immune responses against the parasite [26].

Analysis of the adaptive immune response showed that $CD4^+$ T lymphocytes are apparently associated with the active lesion phenotype. Although several studies have demonstrated the importance of $CD4^+$ T-cells in infection control, the production of proinflammatory cytokines, mainly by $CD4^+$ T cells, is related to the morbidity of toxoplasmosis [27, 28]. Moreover, we observed that an increase in $CD8^+$ T-cells was associated with the presence of retinochoroiditis in infants. $CD8^+$ T-cells play a major role as effector lymphocytes against the parasite [29] and in killing infected macrophages and macrophages exposed to soluble parasite antigens [30]. Our results show that the increase in $CD8^+$ T-cells could also be an important biomarker of morbidity in infected infants.

The results observed in infected infants suggest maturation of the immune response against *T. gondii*. The increases in lymphocyte populations and in subpopulations of monocytes and NK-cells are important in controlling parasitemia. However, exacerbation of the proinflammatory response may also be damaging to infants and, therefore, a determining factor in the pathology observed. Only infants with active lesions showed increased leukocyte counts (specifically monocytes, NK-cells, and lymphocytes). Moreover, the same children also showed increased subpopulations of proinflammatory monocytes and active NK-cells. It is important to consider, however, that future studies with proper validation of the immunological subsets are still needed in order to support their predictive value and specificity as putative biomarkers of ocular involvement in congenital toxoplasmosis.

5. Conclusion

Studies on the immune response in human infections by *T. gondii*, particularly in newborns, are rare. This work provides important findings regarding the immune response to congenital toxoplasmosis, which indicated immunomodulation possibly associated with local control of retinochoroiditis. Future studies with proper validation of the immunological subsets are still needed in order to support their predictive value and specificity as putative biomarkers in the ocular congenital toxoplasmosis.

Conflict of Interests

The authors declare that there is no conflict of interests regarding the publication of this paper.

Authors' Contribution

Anderson Silva Machado and Ana Carolina Aguiar Vasconcelos Carneiro contributed equally to this work.

Acknowledgments

This work was supported by Fundação de Amparo à Pesquisa do Estado de Minas Gerais (FAPEMIG), Conselho Nacional de Desenvolvimento Científico e Tecnológico (CNPq), Secretaria de Saúde de Minas Gerais (SES-MG), and Núcleo de Ações e Pesquisa em Apoio Diagnóstico (NUPAD). CDRJG received fellowship from FAPEMIG-PMPD program. Ricardo Wagner Almeida Vitor, Andréa Teixeira-Carvalho, and Olindo Assis Martins-Filho are CNPq research fellows. The authors thank Rosalida Estevan Nazar Lopes for her technical assistance. The "UFMG Congenital Toxoplasmosis Brazilian Group" was responsible in their areas of expertise for the identification, treatment and follow-up of the children with congenital toxoplasmosis included in the study entitled "Newborn Screening for Congenital Toxoplasmosis in the State of Minas Gerais". The members of UFMG Congenital Toxoplasmosis Brazilian Group (UFMG CTBG) include Ana Carolina Aguiar Vasconcelos Carneiro, Ph.D., Department of Parasitology, Institute of Biological Sciences, UFMG; Daniel Vitor Vasconcelos-Santos, M.D. and Ph.D., Uveitis Unit, Hospital São Geraldo, Hospital das Clínicas, UFMG; Danuza O. Machado Azevedo, M.D. and Ph.D., Uveitis Unit, Hospital São Geraldo, Hospital das Clínicas, UFMG; Ericka V. Machado Carellos, M.D. and Ph.D., Department of Paediatrics, School of Medicine, UFMG; Fernando Orefice, M.D. and Ph.D., Uveitis Unit, Hospital São Geraldo, Hospital das Clínicas, UFMG; Gláucia Manzan Queriroz Andrade, M.D. and Ph.D., Department of Paediatrics, School of Medicine, UFMG; José Nélio Januário, M.D. and M.S., Department of Internal Medicine, School of Medicine, NUPAD, UFMG; Luciana Macedo Resende, Ph.D.,

Department of Phonoaudiology, School of Medicine, UFMG; Olindo Assis Martins-Filho, M.S. and Ph.D., Centro de Pesquisas René Rachou, FIOCRUZ, Belo Horizonte, Brazil; Ricardo Wagner Almeida Vitor, M.S. and Ph.D., Department of Parasitology, Institute of Biological Sciences, UFMG; Roberta M. Castro Romanelli, M.D. and Ph.D., Department of Paediatrics, School of Medicine, UFMG; Waleska Teixeira Caiaffa, M.D., M.P.H., and ScD, Department of Preventive, Medicine, School of Medicine, UFMG.

References

[1] G. N. Holland, "Ocular toxoplasmosis: a global reassessment: part II: disease manifestations and management," *The American Journal of Ophthalmology*, vol. 137, no. 1, pp. 1–17, 2004.

[2] R. E. Gilbert, K. Freeman, E. G. Lago et al., "Ocular sequelae of congenital toxoplasmosis in Brazil compared with Europe," *PLoS Neglected Tropical Diseases*, vol. 2, no. 8, article e277, 2008.

[3] D. V. Vasconcelos-Santos, D. O. Machado Azevedo, W. R. Campos et al., "Congenital toxoplasmosis in Southeastern Brazil: results of early ophthalmologic examination of a large cohort of neonates," *Ophthalmology*, vol. 116, no. 11, pp. 2199.e1–2205.e1, 2009.

[4] C. D. Dupont, D. A. Christian, and C. A. Hunter, "Immune response and immunopathology during toxoplasmosis," *Seminars in Immunopathology*, vol. 34, no. 6, pp. 793–813, 2012.

[5] S. K. Bliss, B. A. Butcher, and E. Y. Denkers, "Rapid recruitment of neutrophils containing prestored IL-12 during microbial infection," *The Journal of Immunology*, vol. 165, no. 8, pp. 4515–4521, 2000.

[6] D. G. Mordue and L. D. Sibley, "A novel population of Gr-1$^+$-activated macrophages induced during acute toxoplasmosis," *Journal of Leukocyte Biology*, vol. 74, no. 6, pp. 1015–1025, 2003.

[7] I. R. Dunay, A. Fuchs, and L. David Sibley, "Inflammatory monocytes but not neutrophils are necessary to control infection with Toxoplasma gondii in mice," *Infection and Immunity*, vol. 78, no. 4, pp. 1564–1570, 2010.

[8] I. R. Dunay and L. D. Sibley, "Monocytes mediate mucosal immunity to Toxoplasma gondii," *Current Opinion in Immunology*, vol. 22, no. 4, pp. 461–466, 2010.

[9] E. D. Tait, K. A. Jordan, C. D. Dupont et al., "Virulence of Toxoplasma gondii is associated with distinct dendritic cell responses and reduced numbers of activated CD8$^+$ T cells," *Journal of Immunology*, vol. 185, no. 3, pp. 1502–1512, 2010.

[10] J. H. Yamamoto, A. L. Vallochi, C. Silveira et al., "Discrimination between patients with acquired toxoplasmosis and congenital toxoplasmosis on the basis of the immune response to parasite antigens," *Journal of Infectious Diseases*, vol. 181, no. 6, pp. 2018–2022, 2000.

[11] F. Fatoohi, G. J. N. Cozon, M. Wallon, L. Kodjikian, and F. Peyron, "Systemic T cell response to *Toxoplasma gondii* antigen in patients with ocular toxoplasmosis," *Japanese Journal of Ophthalmology*, vol. 50, no. 2, pp. 103–110, 2006.

[12] P. Shannon, A. Markiel, O. Ozier et al., "Cytoscape: a software Environment for integrated models of biomolecular interaction networks," *Genome Research*, vol. 13, no. 11, pp. 2498–2504, 2003.

[13] R. Taylor, "Interpretation of the correlation coefficient: a basic review," *Journal of Diagnostic Medical Sonography*, vol. 6, no. 1, pp. 35–39, 1990.

[14] E. Delair, P. Latkany, A. G. Noble, P. Rabiah, R. McLeod, and A. Brézin, "Clinical manifestations of ocular toxoplasmosis," *Ocular Immunology and Inflammation*, vol. 19, no. 2, pp. 91–102, 2011.

[15] T. R. Olariu, J. S. Remington, R. McLeod, A. Alam, and J. G. Montoya, "Severe congenital toxoplasmosis in the United States: clinical and serologic findings in untreated infants," *Pediatric Infectious Disease Journal*, vol. 30, no. 12, pp. 1056–1061, 2011.

[16] L. M. Weiss and J. P. Dubey, "Toxoplasmosis: a history of clinical observations," *International Journal for Parasitology*, vol. 39, no. 8, pp. 895–901, 2009.

[17] D. G. MacK, J. J. Johnson, F. Roberts et al., "HLA-class II genes modify outcome of Toxoplasma gondii infection," *International Journal for Parasitology*, vol. 29, no. 9, pp. 1351–1358, 1999.

[18] M. S. Dutra, S. R. Béla, A. L. Peixoto-Rangel et al., "Association of a NOD2 gene polymorphism and T-helper 17 cells with presumed ocular toxoplasmosis," *Journal of Infectious Diseases*, vol. 207, no. 1, pp. 152–163, 2013.

[19] A. C. A. V. Carneiro, G. M. Andrade, J. G. L. Costa et al., "Genetic characterization of *Toxoplasma gondii* revealed highly diverse genotypes for isolates from newborns with congenital toxoplasmosis in Southeastern Brazil," *Journal of Clinical Microbiology*, vol. 51, no. 3, pp. 901–907, 2013.

[20] P. Escoffier, J. C. Jeanny, C. Marinach-Patrice et al., "Toxoplasma gondii: flat-mounting of retina as a new tool for the observation of ocular infection in mice," *Experimental Parasitology*, vol. 126, no. 2, pp. 259–262, 2010.

[21] A. Kikumura, T. Ishikawa, and K. Norose, "Kinetic analysis of cytokines, chemokines, chemokine receptors and adhesion molecules in murine ocular toxoplasmosis," *British Journal of Ophthalmology*, vol. 96, no. 9, pp. 1259–1267, 2012.

[22] A. Sauer, E. Rochet, I. Lahmar et al., "The local immune response to intraocular Toxoplasma re-challenge: less pathology and better parasite control through Treg/Th1/Th2 induction," *International Journal for Parasitology*, vol. 43, no. 9, pp. 721–728, 2013.

[23] P. M. Robben, M. LaRegina, W. A. Kuziel, and L. D. Sibley, "Recruitment of Gr-1+ monocytes is essential for control of acute toxoplasmosis," *Journal of Experimental Medicine*, vol. 201, no. 11, pp. 1761–1769, 2005.

[24] S. M. Lachenmaier, M. A. Deli, M. Meissner, and O. Liesenfeld, "Intracellular transport of Toxoplasma gondii through the blood-brain barrier," *Journal of Neuroimmunology*, vol. 232, no. 1-2, pp. 119–130, 2011.

[25] D. M. Mosser, "The many faces of macrophage activation," *Journal of Leukocyte Biology*, vol. 73, no. 2, pp. 209–212, 2003.

[26] A. R. French, E. B. Holroyd, L. Yang, S. Kim, and W. M. Yokoyama, "IL-18 acts synergistically with IL-15 in stimulating natural killer cell proliferation," *Cytokine*, vol. 35, no. 5-6, pp. 229–234, 2006.

[27] R. T. Gazzinelli, M. Wysocka, S. Hieny et al., "In the absence of endogenous IL-10, mice acutely infected with Toxoplasma gondii succumb to a lethal immune response dependent on CD4$^+$ T cells and accompanied by overproduction of IL-12, IFN-gamma and TNF-alpha," *The Journal of Immunology*, vol. 157, pp. 798–805, 1996.

[28] F. Lu, S. Huang, and L. H. Kasper, "$CD4^+$ T cells in the pathogenesis of murine ocular toxoplasmosis," *Infection and Immunity*, vol. 72, no. 9, pp. 4966–4972, 2004.

[29] Y. Suzuki, M. A. Orellana, R. D. Schreiber, and J. S. Remington, "Interferon-γ: the major mediator of resistance against Toxoplasma gondii," *Science*, vol. 240, no. 4851, pp. 516–518, 1988.

[30] F. T. Hakim, R. T. Gazzinelli, E. Denkers, S. Hieny, G. M. Shearer, and A. Sher, "$CD8^+$ T cells from mice vaccinated against Toxoplasma gondii are cytotoxic for parasite-infected or antigen-pulsed host cells," *Journal of Immunology*, vol. 147, no. 7, pp. 2310–2316, 1991.

Hindawi Publishing Corporation
Mediators of Inflammation
Volume 2014, Article ID 857245, 12 pages
http://dx.doi.org/10.1155/2014/857245

Research Article

Intestinal Parasites Coinfection Does Not Alter Plasma Cytokines Profile Elicited in Acute Malaria in Subjects from Endemic Area of Brazil

Juan Camilo Sánchez-Arcila,[1] Daiana de Souza Perce-da-Silva,[2] Mariana Pinheiro Alves Vasconcelos,[3] Rodrigo Nunes Rodrigues-da-Silva,[1] Virginia Araujo Pereira,[1] Cesarino Junior Lima Aprígio,[4] Cleoni Alves Mendes Lima,[5] Bruna de Paula Fonseca e Fonseca,[6] Dalma Maria Banic,[2] Josué da Costa Lima-Junior,[1] and Joseli Oliveira-Ferreira[1]

[1] *Laboratório de Imunoparasitologia, Instituto Oswaldo Cruz, Fundação Oswaldo Cruz, 21040-900 Rio de Janeiro, RJ, Brazil*
[2] *Laboratório de Simulídeos e Oncocercose, Instituto Oswaldo Cruz, Fundação Oswaldo Cruz, 21040-900 Rio de Janeiro, RJ, Brazil*
[3] *Instituto de Infectologia Emílio Ribas, 01246-900 São Paulo, SP, Brazil*
[4] *Agencia de Vigilância em Saúde da Secretaria de Estado da Saúde (AGEVISA), 78900-000 Porto Velho, RO, Brazil*
[5] *Centro Interdepartamental de Biologia Experimental e Biotecnologia, Universidade Federal de Rondonia, 78900-000 Porto Velho, RO, Brazil*
[6] *Laboratório de Tecnologia Diagnóstica, Bio-Manguinhos, Fundação Oswaldo Cruz, 21040-900 Rio de Janeiro, RJ, Brazil*

Correspondence should be addressed to Joseli Oliveira-Ferreira; lila@ioc.fiocruz.br

Received 13 June 2014; Accepted 1 September 2014; Published 16 September 2014

Academic Editor: Mauricio Martins Rodrigues

In Brazil, malaria is prevalent in the Amazon region and these regions coincide with high prevalence of intestinal parasites but few studies explore the interaction between malaria and other parasites. Therefore, the present study evaluates changes in cytokine, chemokine, C-reactive protein, and nitric oxide (NO) concentrations in 264 individuals, comparing plasma from infected individuals with concurrent malaria and intestinal parasites to individuals with either malaria infection alone and uninfected. In the studied population 24% of the individuals were infected with *Plasmodium* and 18% coinfected with intestinal parasites. Protozoan parasites comprised the bulk of the intestinal parasites infections and subjects infected with intestinal parasites were more likely to have malaria. The use of principal component analysis and cluster analysis associated increased levels of IL-6, TNF-α, IL-10, and CRP and low levels of IL-17A predominantly with individuals with malaria alone and coinfected individuals. In contrast, low levels of almost all inflammatory mediators were associated predominantly with individuals uninfected while increased levels of IL-17A were associated predominantly with individuals with intestinal parasites only. In conclusion, our data suggest that, in our population, the infection with intestinal parasites (mainly protozoan) does not modify the pattern of cytokine production in individuals infected with *P. falciparum* and *P. vivax*.

1. Introduction

The geographic distribution of *Plasmodium* and intestinal parasites are overlapped over the world; therefore malaria coinfection with intestinal parasites is common in tropical regions of the planet [1]. Although it is well known that polyparasitism is a common condition in human populations, its real impact on the immunopathology of other diseases, including malaria, has not been fully explored. In Brazil, malaria is endemic in the Amazon region and this

area coincides with high prevalence of other diseases. The prevalence of intestinal parasites has been largely reported in the Brazilian Amazon, mainly in studies involving indigenous populations or the impact of intestinal parasitism in nutritional status on Amazonian communities [2–9]. However, the interaction between malaria and other parasites has not been explored and to our knowledge only one work addressed malaria and helminthes coinfections in children infected with *P. vivax* in the Brazilian Amazon studying [10].

Studies from human populations conducted in Africa revealed that helminthic infection can have a negative effect on host response to malaria, including increased susceptibility to *Plasmodium* infection and increased severity of disease [11–14]. However, a protective effect, such as decreased risk of cerebral malaria and lower incidence of malaria, [15–17] and no effect in the susceptibility to malaria or in the pathologic effect of *Plasmodium* infections were also reported [18, 19]. The immunological interactions between helminthes and malarial parasites are unclear and there are little consensus on the effect of malaria and helminthes coinfection. During malaria infection, cytokines are reported to be important molecular markers of cell-mediated immune response and known to be critical players in the regulation of diseases. A T helper 1 (Th1) response predominantly characterizes human malaria infection and the production of proinflammatory cytokines such as interferon gamma (IFN-γ), IL-6, tumor necrosis factor (TNF-α), and other inflammatory cytokines [20, 21]. These inflammatory cytokines are considered critical for the resolution of parasitemia and control of malaria infection, especially during the early stages of *P. falciparum* infection [22, 23]. Conversely, if these robust inflammatory responses are not regulated during chronic malaria infection, they can lead to immunopathology and severe forms of the disease response [24–26]. Regulatory cytokines, including interleukin (IL)-10 and transforming growth factor beta (TGF-β), were shown to have an important role as an immunoregulator of the infection caused by *P. falciparum* in neutralizing the effects of Th1 inflammatory responses associated with immune pathology and the more severe forms of *P. falciparum* infection [24]. There also a range of other mediators, such as IL-4 and nitric oxide, that have been linked to disease severity in malaria-infected individuals [27, 28].

On the other hand, helminths infections have a profound effect on the immune system, resulting in a strong immunoregulatory and Th2 response that can inhibit the ability of the host to mount a Th1 type immune response. Indeed, *Ascaris* sp. infection induces anti-inflammatory Th2 responses [29–31] and is also associated with an immunoregulatory immune response, defined by elevated levels of interleukin (IL)-10 and transforming growth factor-β (TGF-β) [32, 33]. Therefore, it is expected that the influence of helminthic infection on the immune system could extend to the immune response against malaria due to the anti-inflammatory effect of cytokines induced by helminthes and thereby possibly affect the course of malaria infection [12, 34, 35].

Due to the recognized ability of some helminths to elicit anti-inflammatory cytokines and that many parasites manipulate host cytokine pathways for their own benefit [36], we hypothesized that there may be a counterbalance between proinflammatory cytokines, associated to malaria, and anti-inflammatory cytokines, associated to helminths or protozoa intestinal parasites. Although cytokine responses have been extensively described in *P. falciparum* infection, few studies have looked at systemic cytokine concentration in coinfection of intestinal parasites and malaria. We believe that comprehensive profiling of serum levels of multiple inflammatory markers such as cytokines, chemokine, C-reactive protein, and nitric oxide (NO) would provide greater insight into their utility to differentiate infected individuals with concurrent malaria and intestinal parasites to individuals with either infection alone. In this regard, the ability to measure numerous molecules in a single sample and to visualize changes in inflammatory markers, including cytokine networks in single and malaria and intestinal parasites coinfected individuals is critical to advance our understanding of the immune response to pathogens. Therefore, we applied both traditional univariate and multivariate analysis to the data in order to identify the type of response that develops during coinfection and which inflammatory markers are important.

2. Material and Methods

2.1. Study Area and Study Design. We conducted a cross-sectional survey in a rural settlement community of Porto Velho, municipality of Rondonia State, Brazilian Amazon. The settlement called Joana D'Arc is located 120 km of Porto Velho and the Brazilian Government in 2001 created it in order to give land to people. Joana D'Arc settlers were mostly rain forest native migrants, some with previous agricultural experience, but most with no knowledge of agricultural potential or techniques necessary for farming in a tropical rain forest area. They were low-income people attracted by free land and promised government support. Despite being a place where people lived for over 10 years, there is no health infrastructure in the area and the source of income of residents is from agriculture and small livestock to manufacture cheese. Samples and survey data were collected in 2010 and 2011, during the dry months of June-August, coinciding with the period of increased malaria transmission in Rondonia State. In order to be included in the study, participants had to meet the following criteria: (1) have been resident in the study area; (2) provided a stool samples; and (3) have given a blood sample for the collection of plasma and malaria diagnosis. A total of 264 participants met these criteria and formed our study population.

2.2. Sample Size. The sample size was estimated to determine prevalence of malaria using the formula for estimating single proportion at 95% confidence interval. The prevalence of coinfection is unknown in the area, so we used 0.50, to maximize sample size. Based on these entities and expected margin of error to be 0.1, 264 subjects were included in our study. All epidemiological, hematological, and cytokine quantification results were stored in Epi-Info version 3.2. Prior to analysis, the data were centered and standardized

to ensure equal contribution of each parameter and to avoid differences due to scale.

2.3. Collection and Examination of Blood. The study team visited houses selected randomly to invite participation. After written informed consent and an epidemiological survey from all adult donors or from parents of donors in the case of minors, blood was drawn by venipuncture. At the time of blood sampling, thick and thin blood smears were performed and stained with 10% Giemsa to examine for the presence of malaria parasites. Parasitological evaluation was done by examination of 200 fields at 1000x magnification under oil-immersion. The parasitemia was expressed as the number of parasites/μL of blood in the thick blood smear. Using the oil immersion objective, 500 leucocytes were counted at the same time as the number of parasites. Then, the number of parasites/μL of blood was calculated by multiplying the number of parasites counted against 500 leucocytes and the number of leukocytes of the subject and dividing the product by 500. A researcher expert in malaria diagnosis examined all slides. To confirm the parasitological diagnosis, we performed molecular analyses of all samples using primers specific for genus (*Plasmodium* sp.) and species (*P. falciparum* and *P. vivax*). The amplification protocols were described previously by Snounou et al. [37]. Subjects were considered to have malaria if they were positive in the thick blood smear and/or PCR. Blood counts, including hematologic indices, were done using an automatic hematology analyzer (Pentra, Horiba Medical, Montpellier, France) and peripheral smears of blood samples were made for routine differential blood cellular quantification. A manual differential white blood cells count was also performed to distinguish the immature neutrophils.

2.4. Collection and Examination of Stool Samples. All individuals were requested to provide a morning fecal sample and a labeled screw-capped plastic container was provided. A single stool sample was collected from each subject on the following day and examined by a direct unstained wet smear in normal saline and Lugol's iodine solution at 100x and 400x by a technician with expertise in intestinal parasites identification. The physicians in our team provided medication after assessing the exams results of the participants and examining them. All participants found suffering from intestinal parasites infections were given complete treatment.

2.5. ELISA Specific for Protein C-Reactive. The CRP levels were determined in all plasma samples using an in-house ELISA. Microtiter plates (Nunc/MaxiSorp, Rochester, NY, USA) were coated with a goat anti-human-CRP antibody (Sigma, USA; catalogue C8284) in carbonate-bicarbonate buffer (TCO_4) overnight at 4°C. The plates were then washed three times with phosphate-buffered saline-0.05% Tween 20 (PBST) and plasma samples diluted 1 : 500 in PBST were incubated with the plates for 1 h at 37°C. The plates were then washed three times and incubated with rabbit anti-human-CRP antibody (Sigma, USA; catalogue C3527) in PBST for 1 h at 37°C. The plates were washed three times and peroxidase-conjugated goat anti-rabbit-IgG antibodies (Sigma, USA; A0545) were added. The wells were thoroughly washed to remove all unbound horseradish peroxidase (HRP)-conjugated antibodies and an o-phenylendyamine substrate solution was added to each well. The enzyme (HRP) and substrate were allowed to react for a short incubation period. The enzyme-substrate reaction was terminated by the addition of 2 N $H_2SO_4$and the degree of color change was measured at 492 nm ± 2 nm in a spectrophotometer (SpectraMax 250; Molecular Devices, Sunnyvale, CA). The plasma concentration of CRP was determined by comparison to standard concentrations of purified human CRP (Sigma, St. Louis, USA). The range of detection of CRP was 0.01–320 μg/mL. Sera from noninfected individuals were used on every plate as negative controls. Specific CRP optical density values were converted to concentration values (μg/mL) using sigmoidal curve-fit equations derived from CRP standard curves.

2.6. Griess Microassay Detection of Nitrite and Nitrate. A modified Griess reaction was used to detect nitrite and nitrate ([38], modified by [39]). The NO levels in samples were indirectly measured after first converting nitrates to nitrites with a nitrate reductase treatment (*Aspergillus* species NAD [P] H, Sigma, UK) and NADPH β-nicotinamide adenine dinucleotide phosphate (Sigma Diagnostics, St. Louis, USA). Griess reagent [5% phosphoric acid, 1% sulphanilic acid, and 0.1% N-(1-naphthyl-1)-ethylendiamine dihydrochloride, all from Sigma, UK, dissolved in 100 mL deionized water] was added and proteins were subsequently precipitated by trichloroacetic acid (BDH, England). The tube contents were mixed and centrifuged (Eppendorf centrifuge 5415 C, Germany); two samples of each supernatant were transferred to a flat-bottomed microplate and their absorbencies were read at 520 nm using a microplate reader (SpectraMax, Molecular Devices Inc). NO values were calculated from standard calibration plots [39].

2.7. Multiplex Microsphere Cytokine Immunoassay. Cytokine concentrations in plasma samples were determined using high throughput magnetic bead-based BioPlex assay. Thirteen cytokines IL-1β, IL-2, IL-4, IL-5, IL-6, IL-7, IL-10, IL-12 p70, IL-17A, IFN-γ, TNF-α, G-CSF, and granulocyte-macrophage colony-stimulating factor (GM-CSF)] and three chemokines (IL-8, MCP-1, and MIP-1β) were analyzed using a BioPlex Kit assay (Bio-Rad Laboratories, Hercules, CA, USA) following the manufacturer instructions as described in [40]. Briefly, 50 μL of standard or test sample along with 50 μL of mixed beads was added into the wells of a prewetted 96-well microtiter plate. After 1 h of incubation and washing, 25 μL of detection antibody mixture was added and the samples were incubated for 30°C min and then washed. Finally, 50 μL of streptavidin-PE was added and, after 10°C min of incubation and washing, the beads were ressuspended in 125 μL assay buffer and analyzed using a BioPlex suspension array system (Bio-Rad Laboratories) and the BioPlex manager software (v.3.0). A minimum of 100 beads per region were analyzed. A curve fit was applied

to each standard curve according to the manufacturer's manual and sample concentrations were interpolated from the standard curves. The lower limits of cytokines detection using this method were MIP-1β, 1.69 pg/mL; IL-6 1.25 pg/mL; IFN-γ, 0.88 pg/mL; IL-5, 0.84 pg/mL; GM-CSF, 0.47 pg/mL; TNF-α, 0.82 pg/mL; IL-2, 0.29 pg/mL; IL-1β, 0.73 pg/mL; IL-13, 1.1 pg/mL; IL-4, 0.78 pg/mL; MCP-1, 1.64 pg/mL; IL-8, 1.01 pg/mL; IL-10, 0.4 pg/mL; G-CSF, 1.89 pg/mL; IL-7, 1.1 pg/mL; IL-12p70, 0.57 pg/mL; and IL-17A, 0.38 pg/mL TNF-α, 0.10 pg/mL. For all samples, the quantification of the analytes was done in a single day to avoid freeze-thaw cycles.

2.8. Statistical Analysis. We compared epidemiological and hematological parameters and cytokine production between groups, using a permutation-based ANOVA (999 permutations) followed by a post hoc test (Tukey HSD), to test for pairwise differences. Permutation-based ANOVA generates the null distributions from the data, avoiding the problems related to the violation of normality and homogeneity [41]. We also used Chi-squared test to determine the significant differences between proportions in binary variables (sex). A principal component analysis (PCA) was applied to the dataset containing cytokines, chemokines, and inflammation markers, to detect the variation patterns related to the studied groups and to identify variables accounting for the majority of the variation within the dataset. PCA is a widely used ordination methodology that reduces dimensionality of multivariate data and detects variables that are more important to explain the variance structure of the data, generating orthogonal (independent) axes using linear combinations of the original variables. PCA can be interpreted numerically: each axis (principal component, PC) is described by an eigenvalue related to the amount of variation that it explains, so that the first PC will always explain more variation than the second, and so on. In addition, variables and units have coordinates ("loadings") along these PCs, which indicate their contribution to each PC. PCA can be also interpreted visually, from the origin of the graph: variables cytokines, chemokines, CRP, and NO (inflammatory mediators) and experimental units (patients) will be located according to their correlations, and distance from the origin means higher contributions to the overall variation (higher absolute loadings). Angles from the origin are roughly proportional to correlation: collinear vectors (approaching 0° or 180°) can be interpreted as positively or negatively correlated and right angles indicate independence (orthogonality).

To further investigate the relationship between infection groups and cytokine profile, we elaborated a heatmap that relates two hierarchical cluster analyses in a bidimensional plot. *Z*-scores were calculated from transformed values of cytokine levels and represent standard deviations from the population mean: *Z*-score = [(individual cytokine values − population cytokine mean value)/population cytokine standard deviation]. Cluster analyses were performed from *Z*-scores using Euclidean distance metrics and Ward as the linkage algorithm. All analyses were performed using *R* statistical environment [42]. Permutation ANOVA was performed with *lmPerm* package [43] and PCA analysis with *vegan* [44] and *gplots* package [45] was used to build the heatmaps.

2.9. Ethical Consideration. The study was conducted after obtaining ethical clearance from Fundação Oswaldo Cruz Ethical Committee (CEP/FIOCRUZ, 492/08). Individual oral and written consents were obtained from all participants. Donors positive for *P. vivax* and/or *P. falciparum* at the time of blood collection were subsequently treated using the chemotherapeutic regimen recommended by the Brazilian Ministry of Health.

3. Results

3.1. Malaria and Intestinal Parasites Infections. Of the 353 individuals analyzed at baseline, 264 subjects were included in our study, 16 (6.1%) were infected with malaria only, 48 (18.2%) were coinfected with malaria and intestinal parasites, 98 (37%) were infected with intestinal parasites only, and 102 (38.7%) were uninfected with either malaria or intestinal parasites. *P. vivax* was more prevalent in both malaria infected only (81.2%) and coinfected with intestinal parasites (75%). Protozoan parasites comprised the bulk of the infections in subjects infected with intestinal parasites only (70.4%) or coinfected with malaria and intestinal parasites (81.2%). The prevalence of intestinal parasites was significantly higher in individuals infected with malaria than with those who were not infected (adjusted OR = 3.1, 95% CI = 1.66–5.86 $P = 0.0003$). The most prevalent protozoan was *Giardia intestinalis* and helminths were *Ancylostoma duodenale* and *Strongyloides stercoralis*. Multiple protozoa species were common in both intestinal parasites only (14.5%) and coinfected with malaria (33.3%) while only one subject presented multiple helminthes species infection. Dual, triple, and quadruple protozoan and helminthes infections were observed. Data in Table 1 summarizes the prevalence of single and multiple parasites species infections. In coinfected subjects, the prevalence of *P. vivax* malaria was 75% (36) and *P. falciparum* was 23% (11) whereas 2% (1) had mixed species infection. *G. intestinalis* was the most prevalent intestinal parasite in both *P. falcilparum* and *P. vivax* coinfections. However, in *P. vivax* coinfected subjects the species of protozoans and helminthes were more diverse (Figure 1).

3.2. Infection Groups, Epidemiological, and Hematological Data. As shown in Table 2, the infection groups were defined by the presence or absence of malaria infection and/or intestinal parasites infection, resulting in the following groups: malaria (M), coinfected (CI), intestinal parasites (IP), and uninfected (UN). The majority of the subjects infected with malaria was male and presented general clinical malaria symptoms such as history of fever and headache. We did not observe differences in parasitemia between Malaria and coinfected groups. There were no differences in age, years of residence in endemic area (TR), years of residence in Rondonia (TRO), and months since last malaria episode (LME). However the number of past malaria episodes (PME)

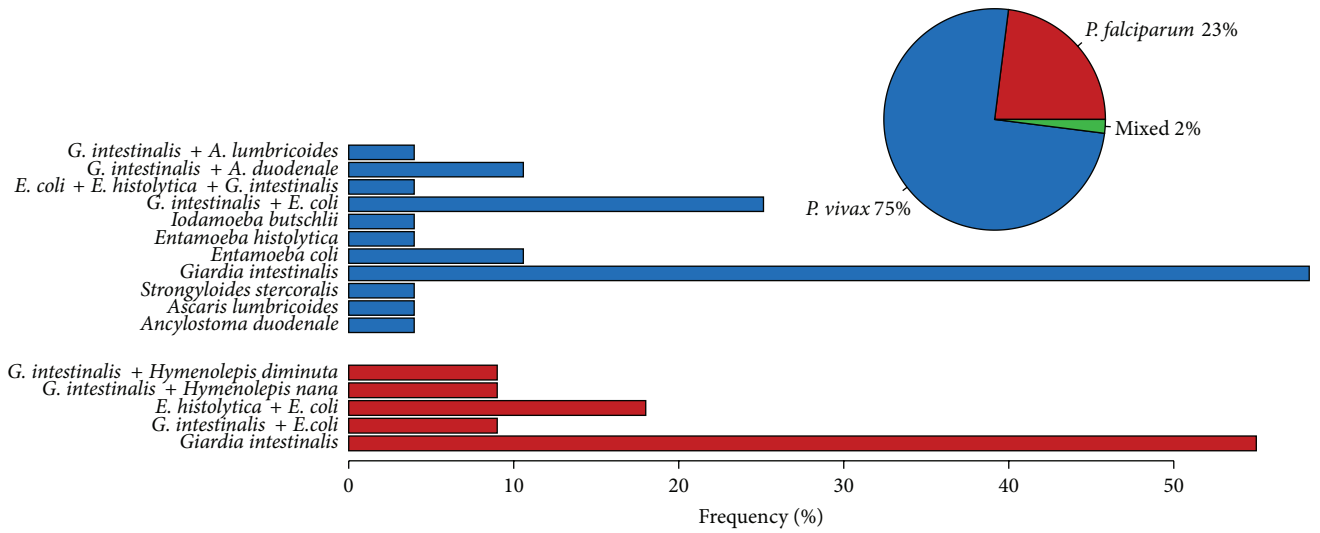

Figure 1: Frequency of individuals infected with *P. vivax* (blue) and *P. falciparum* (red) in the population of study. In the barplot the specific frequency of each species of intestinal parasites discriminated by *P. vivax* and *P. falciparum* is represented.

was higher in the groups negative for malaria when compared with malaria group (intestinal parasite $P < 0.0001$ and uninfected $P < 0.05$). The analysis of some hematological parameters revealed that malaria and coinfected groups were similar and no differences were observed in the median hemoglobin, platelets, lymphocytes, band cells values, and *Plasmodium* parasites counts. However, they differ from intestinal parasites and uninfected groups presenting lower mean lymphocytes and platelets counts while band cells counts were higher. Hemoglobin levels in malaria and coinfected groups were slightly higher when compared with the uninfected group.

3.3. Levels of Inflammatory Mediators. Firstly, we analyzed the median plasma levels of individual cytokines, chemokines, NO, and CRP comparing the concentration between groups (Figure 2). Cytokines levels varied widely among the cytokines ranging from 0.3 pg to 6952 pg. The cytokines IL-5, IL-7, and GM-CSF were low in most plasma samples (data not shown). Most remarkably, Malaria group presented the highest levels of CRP and intestinal parasites the highest level of IL-12p70, IL-17A, and NO. In both malaria and coinfected groups the median levels of TNF-α, IL-2, IL-10, IL1-β, MCP-1, and IL-6 were observed to be mostly significantly increased compared with those intestinal parasites and uninfected groups ($P < 0.001$ for all comparisons). The median levels of IFN-γ and IL-8 were increased in all groups compared to uninfected group. Changes in cytokine and chemokine levels were very similar in malaria and coinfected groups and with this analysis we could not associate changes in cytokine profile that could be due to coinfection.

3.4. Principal Component Analysis (PCA) and Cluster Analysis of Inflammatory Mediators. In order to assess differences in the whole multivariate set of cytokines, chemokines, NO, and CRP data in individuals between the groups, we performed an exploratory principal component analysis (PCA), a multivariate technique to identify whether inflammatory mediators could indicate coinfection. Figure 3(a) displays a PCA of inflammatory mediator for the groups M, CI, IP, and UN. The dotted line connects each individual to the centroid of its group and the position of the centroids indicates that there was an overall difference in the mediators between two groups: M and CI and IP and UN groups. In these two groups, the individuals were gathered by their similar inflammatory mediator's profiles. The differences in the inflammatory mediators between M and CI groups from IP and UN groups were higher levels of IL-1β, IL-6, TNF-α IL-10, and CRP and decreased levels of IL-17A and NO while IP and UN presented higher levels of IL-17A and NO and decreased levels of IL-10 and CRP (Figure 3(b)). In order to characterize cytokine inflammatory mediators in each studied individual, we applied a two-dimensional clustering analysis (Figure 4) using the cytokines that presented the largest loading values in the PCA analysis (IL-6, IL-1β, TNF-α, MCP1, IFN-γ, IL-17A, CRP, and IL-10). This method allows coupled clustering of both the subject and the measured parameters without taking in account the groups. Interestingly, the clustering algorithm could discriminate two major clusters: one cluster included increased levels of IL-6, TNF-α, IL-10, and CRP and low levels of IL-17A predominantly in individuals from M and CI groups and the second cluster included low levels of almost all inflammatory mediators predominantly in individuals from UN group and increased levels of IL-17A predominantly in individuals from IP group.

4. Discussion

Overlapping distribution of intestinal parasites and malaria might result in high rate of coinfection. In the studied

Table 1: Prevalence of malaria and intestinal parasites in the studied population.

	Number of cases	Prevalence (%)
Infected with malaria only		
P. vivax	**13**	**81.2**
P. falciparum	**3**	**18.8**
Total	**16**	**6.1**
Infected with intestinal parasites only		
Protozoa	**69**	**70.4**
Giardia intestinalis	48	69.6
Entamoeba coli	7	10.1
Entamoeba histolytica	3	4.3
Iodamoeba butschlii	1	1.5
G. intestinalis + (*I. butschlii* or *E. histolytica* or *E. coli*)	3	4.3
E. histolytica + (*I. butschlii* or *E. coli*)	2	2.9
E. coli + *E. histolytica* + *G. intestinalis*	3	4.3
E. coli + *E. histolytica* + *I. butschlii*	1	1.5
E. coli + *E. histolytica* + *G. intestinalis* + *I. butschlii*	*1*	1.5
Helminths	**17**	**17.4**
Ancylostoma duodenale	6	35.3
Strongyloides stercoralis	5	29.4
Ascaris lumbricoides	3	17.6
Trichuris trichiura	2	11.8
S. stercoralis + *T. trichiura*	1	5.9
Protozoa + Helminthes	**12**	**12.2**
E. coli + *A. lumbricoides*	2	16.7
G. intestinalis + (*A. duodenale* or *T. trichiura* or *S. stercoralis*)	7	58.4
G. intestinalis + *I. butschlii* + *A. lumbricoides*	1	8.3
E. coli + *E. histolytica* + *A. duodenale*	1	8.3
E. coli + *E. histolytica* + *I. butschlii* + *S. stercoralis*	1	8.3
Total	**98**	**37.1**
Coinfected with malaria + intestinal parasites		
Malaria + Protozoa	**39**	**81.2**
G. intestinalis	23	59.0
E. coli	3	7.7
E. histolytica or *I. butschlii*	2	5.2
E. coli + (*G. intestinalis* or *E. histolytica*)	10	25.6
E. coli + *E. histolytica* + *G. intestinalis*	1	2.6
Malaria + Helminths	***3***	***6.3***
A. duodenale or *A. lumbricóides* or *S. stercoralis*	3	100
Malaria + Protozoa + helminthes	*6*	*12.5*
G. intestinalis + (*A. duodenale* or *A. lumbricoides*)	4	66.7
G. intestinalis + (*Hymenolepis nana* or *Hymenolepis diminuta*)	2	33.3
Total	**48**	**18.2**
Uninfected	**102**	**38.6**

population 24% of the individuals were infected with *Plasmodium*, 55% with intestinal parasites, and 18% with malaria and intestinal parasites. In the studied area, the likelihood of being infected with malaria was significantly higher in individuals infected with intestinal parasites. Several studies from human populations conducted in Africa reveal that helminthic infection can have a negative effect on host response to malaria, including increased susceptibility to *Plasmodium* infection and increased severity of disease [11–14]. In our study, although malaria was more frequent in

Table 2: Epidemiological and hematological data in the studied groups.

	Infection groups			
	Malaria	Coinfected	Intestinal parasites[a]	Uninfected[b]
	$N = 16$	$N = 48$	$N = 98$	$N = 102$
	n (%)	n (%)	n (%)	n (%)
Gender n (%)				
M	11 (69)	34 (71)	49 (50)	48 (47)
F	5 (31)	14 (29)	49 (50)	54 (53)
Age	24 (21–33)	31 (22–41)	30 (14–43)	29 (14–38)
TR	22 (16–27)	23 (18–32)	23 (14–34)	24 (13–31)
TRO	21 (10–24)	22 (15–27)	18 (11–30)	24 (13–30)
LME	6 (0–66)	3 (0–16)	24 (6–60)	10 (1–36)
PME	5 (2–8)^{a***b*}	4 (1–10)^{a*}	4 (2–60)^{b*}	5 (2–14)
Hematological				
Lymphocytes (mm^3)	1316 (863–1982)^{b***}	1170 (789–1826)^{a***b***}	2178 (1813–2725)	2068 (1697–2467)
Platelets (mm^3)	166 (148–204)^{a*b***}	152 (106–197)^{a***b***}	214 (173–245)^{b*}	233 (193–286)
Band cells (mm^3)	34 (0–141)^{a***b***}	26 (0–143)^{a***b***}	0 (0-0)	0 (0-0)
Eosinophils (mm^3)	73 (36.75–138.75)^{a*}	104 (42.5–328.5)^{a*}	328 (185–720)^{b*}	245 (146.75–484.00)
Hemoglobin (g/dL)	12.7 (12–14)^{b*}	13.2 (12.2–14)^{b*}	13.8 (12.8–15)	13.8 (13–14.7)
Parasitemia (parasites/μL)	2740 (738–5591)	1816 (641–5700)	—	—

n (%): number of samples (percentage); TR: Years of residence in endemic area; TRO: Years of residence in Rondonia; LME: Months since last malaria episode and PME: number of past malaria episodes. The variables Age, TR, TRO, LME and PME, values are expressed as Median (25%–75%). Differences were calculated using a TukeyHSD from a permutation based ANOVA. Differences of parasitemia between Coinfected and Malaria group were calculated using a permutation t test. [a]differences between indicated group and Intestinal parasites; [b]differences between indicated group and Uninfected. Statistical differences of epidemiological parameters were expressed as $^{***}P < 0.0001$, $^{**}P < 0.001$, $^{*}P < 0.05$.

individuals infected with intestinal parasites, hematological parameters and parasitemia did not differ between coinfected and malaria single infected individuals. In both groups anemia was not frequent and changes in lymphocytes, and platelets and band cells seem to be due to acute malaria infections while eosinophil levels were high only in intestinal parasites group. Although anemia and thrombocytopenia are the most prominent alterations in acute malaria infection and in coinfections with helminths, hematological changes in these infections are a wide and contradictory event [40, 46–50].

Differences in results obtained in different studies might depend on the species of the intestinal parasites and the age of studied population. While most of the coinfection studies are with helminthes and in children [1, 10], in our study the most prevalent intestinal parasites in the population were protozoans and the participants were adults. In addition, our sample size may be small and could not allow the stratification of the intestinal infections by helminthes and protozoans, a factor which may account for these differences.

The influence of intestinal parasites (mainly helminthes) in *Plasmodium* coinfection has gained interest because it has been hypothesized that Th2 polarized immune response elicited by helminthes could alter the natural immune response of the host to *Plasmodium* parasites [12, 34, 36]. Most of the studies associate cytokine profile mainly with the immunopathology of severe/complicated malaria [24, 51]. Few studies looked at systemic cytokines concentration in coinfection comparing plasma of infected individuals with concurrent malaria and intestinal parasites with either infection alone [52–55]. To our knowledge, this is the first study that evaluates 16 cytokines, CRP, and NO in malaria coinfection with intestinal parasites. In our study, the analysis of individual cytokines, chemokines, CRP, and NO could not detect changes associated to coinfection. However, the use of principal component analysis and cluster analysis provided evidence that groups of individuals with malaria (M and CI) could be discriminated from the groups of individuals negative for malaria (IP and UN) based on inflammatory mediators profile. They formed two separate groups based on the levels of cytokines, CRP, and NO. For malaria infected individuals (M and CI) the profile was high levels of IL-1β, IL-6, TNF-α IL-10, and CRP and decreased levels of IL-17A while for malaria negative individuals (IP and UN) the profile was high levels of IL-17A, NO and decreased levels of IL-10 and CRP.

The high production of CRP, IL-10, TNF-α, and IL-6 observed in our analysis in M and CI groups is reported in several studies in acute malaria infections [50, 56, 57]. In Brazilian populations, IL-10 and CRP are an important marker of acute malaria caused by *P. vivax* [40, 50, 56].

The role of cytokines production in acute malaria is far from being understood and little is known about their effect in coinfection with other parasites. In our study, the levels of inflammatory mediators in individuals with acute malaria did not differ from individuals coinfected with intestinal parasites when compared with individuals single infected with malaria. However, few reports demonstrated altered cytokines levels

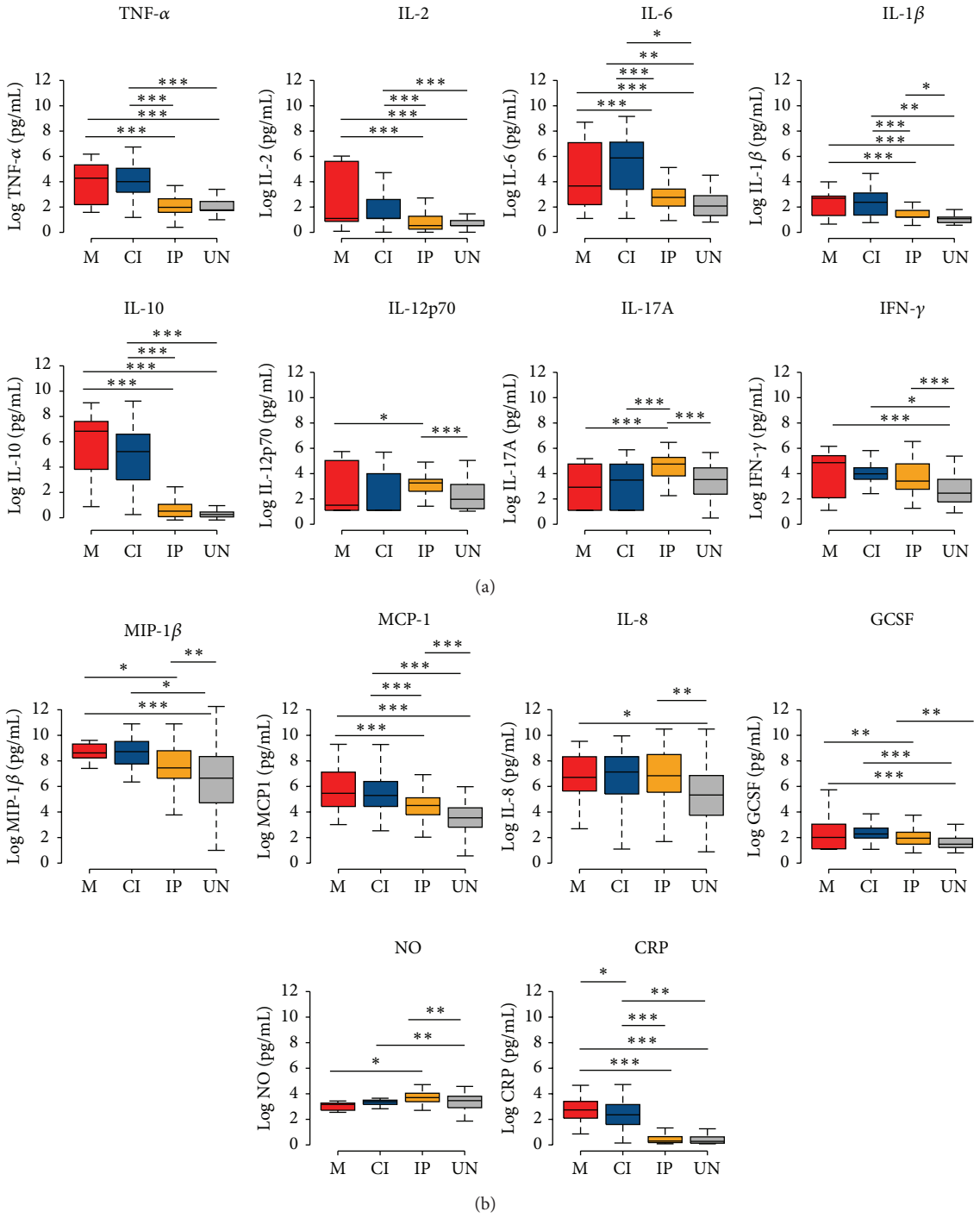

Figure 2: Boxplots of the levels of (a) cytokines, (b) chemokines, and inflammation markers in the groups (M = red, CI = blue, IP = orange, and UN = gray). Differences were calculated using a TukeyHSD from a permutation ANOVA over cytokine values transformed with Log. Significant statistical differences are represented in the bars and the level of significance expressed as $^{***}P < 0.0001$, $^{**}P < 0.001$, and $^{*}P < 0.05$.

in children and adults coinfected with *P. falciparum* and *Schistosoma haematobium*. Higher IFN-γ and similar TNF-α, TGF-β, and IL-10 levels were found when comparing coinfected and single *P. falciparum* infected children [52] while, in adults, higher IFN-γ, TNF-α, and TGF-β levels were detected [53]. Elevated IL-6 and IL-10 were also associated with acute malaria in children but the levels were lower in children coinfected with *S. haematobium* when compared to children infected with *S. haematobium* alone [54]. In these studies the question of whether the high concentration of

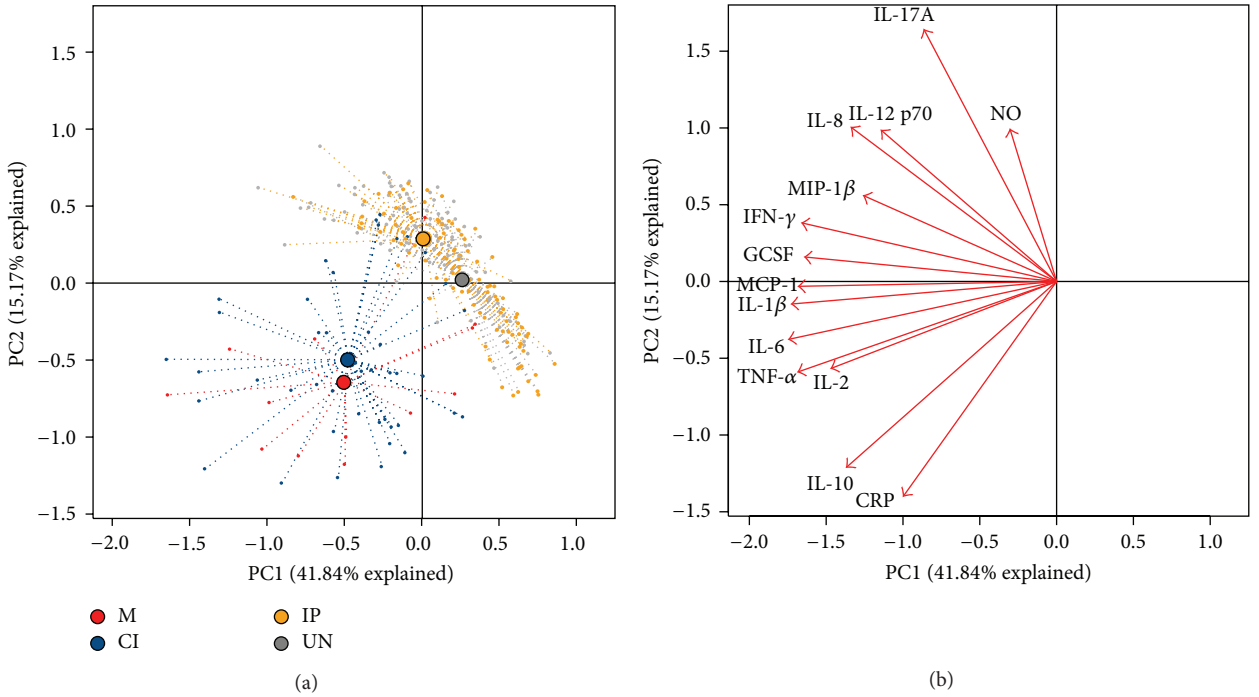

Figure 3: Principal component analysis (PCA) of inflammatory mediators (cytokine, chemokines, CRP, and NO). (a) Results are shown for M, CI, IP, and UN groups. Each point represents an individual from a group and each group has a color code: M = red, CI = orange, IP = blue, and UN = gray. (b) Arrows indicating the direction of maximum change while the length of arrows represents the magnitude of the change. The explanation of the first principal component (PC1) explained 41.84% of the variation of the data and the second principal component (PC2) explained 15.17%. The separation of CI and M individuals from IP and EXP and the association of some cytokines with the different groups can be observed.

cytokines in coinfected individuals had a negative or positive effect on malaria was not addressed.

It is worth it to highlight that, specifically using PCA analysis, we observed the importance of the contribution of IL-17A to separate the M and CI from IP and UN, although IL-17A seems to be higher in IP individuals. It has been observed that IL-17 is an important marker of intestinal inflammation contributing to enhance innate barrier defenses at mucosal surfaces [58, 59]. Interestingly in the groups CI and M we also detected decreased levels of NO. This inflammatory marker has been described to be protective against *P. falciparum in vitro*, and low levels of this marker have been associated with suppression of NO synthesis depending of the gravity in malaria [27]. The contribution of intestinal parasites coinfection in the pathogenesis of malaria is still controversial, and its role is probably specific depending on the type of parasite involved in the coinfection. In our study in spite of the great amount of inflammatory markers evaluated, the use of multivariate analysis techniques proved to be an excellent tool to find hidden patterns in complex data systems including cytokine studies [57, 60–62]. Indeed, using cluster analysis, Prakash et al. [61] detected differences of plasmatic cytokines between individuals with mild, severe noncerebral, and cerebral malaria. In our study, this analysis was able to detect differences between individuals with malaria versus without malaria but was not able to detect differences between malaria versus intestinal parasites coinfected individuals. Therefore, it seems that intestinal parasites coinfection (mainly protozoan) does influence in the plasmatic cytokine levels of individuals with acute malaria and the real influence of these infections could be perceived in regions highly endemic for specific parasites such as *Ascaris lumbricoides* and *Schistosoma mansoni*.

5. Conclusion

In conclusion, our data suggest that, in our population, the infection with intestinal parasites (mainly protozoan) does not modify the pattern of cytokine production in individuals infected with *Plasmodium*.

Conflict of Interests

The authors declare that there is no conflict of interest regarding the publication of this paper.

Acknowledgments

The authors are in debt to the individuals who participated in this study and Andrea Sánchez Tapia for revising the paper. This work was supported by Fundação de Amparo à Pesquisa do Estado do Rio de Janeiro (FAPERJ, Brazil), Pronex Malaria, Conselho Nacional de Desenvolvimento Científico e Tecnológico (CNPq, Brazil), Instituto Oswaldo Cruz (FIOCRUZ, Brazil), Pronex Malaria/CNPq/DECIT/MS. JOF

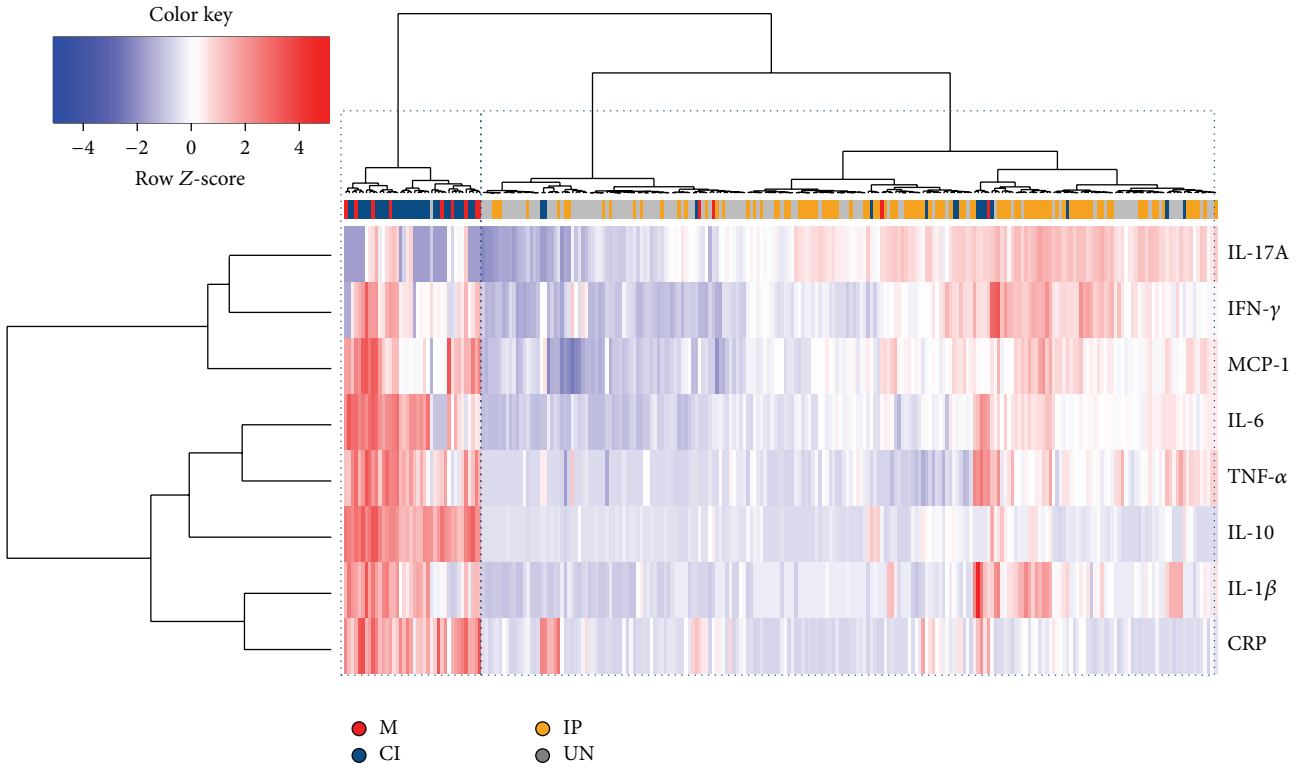

Figure 4: Two-way coupled cluster analysis (heatmap). Each cell indicates the value of a single mediator of inflammation among the studied individuals. The horizontal cluster illustrates the grouping of individuals considering seventeen cytokines, C-reactive protein, and nitric oxide. The vertical cluster shows the grouping of mediator of inflammation such as cytokines meaning that cytokines that presented more similar responses are closer in the clusters. The red color in the cells indicates high values and the blue color indicates low values in the production of cytokines and inflammatory proteins. The white color indicates no changes in the cytokine levels. The colors under the horizontal cluster represent the groups (M = red, CI = orange, IP = blue, and UN = gray) of each individual. Sample clustering resulting from the algorithm applied is shown at the top of the graph as a horizontal dendrogram, with an indication of the group to which each individual sample belongs. The horizontal-dotted boxes show the clusters of individuals obtained. The first vertical box with dotted lines represents the group of individuals with malaria only (M) and malaria-intestinal parasites coinfected (CI). The second box shows the uninfected (UN) and IP individuals.

is recipient of a Research Productivity Fellowship from CNPq, and JCSA is recipient of a fellowship from Instituto Oswaldo Cruz and VAR from CNPq.

References

[1] R. Pullan and S. Brooker, "The health impact of polyparasitism in humans: are we under-estimating the burden of parasitic diseases?" *Parasitology*, vol. 135, no. 7, pp. 783–794, 2008.

[2] C. Fernández Araujo and C. Leite Fernández, "Prevalence of intestinal parasitosis in the city of Eirunepé, Amazon," *Revista da Sociedade Brasileira de Medicina Tropical*, vol. 38, no. 1, p. 69, 2005.

[3] F. M. Fleming, S. Brooker, S. M. Geiger et al., "Synergistic associations between hookworm and other helminth species in a rural community in Brazil," *Tropical Medicine and International Health*, vol. 11, no. 1, pp. 56–64, 2006.

[4] E. A. De Souza, M. Da Silva-Nunes, R. Dos Santos Malafronte, P. T. Muniz, M. A. Cardoso, and M. U. Ferreira, "Prevalence and spatial distribution of intestinal parasitic infections in a rural Amazonian settlement, Acre State, Brazil," *Cadernos de Saúde Pública*, vol. 23, no. 2, pp. 427–434, 2007.

[5] J. G. Valverde, A. Gomes-Silva, C. J. M. de Carvalho et al., "Prevalence and epidemiology of intestinal parasitism, as revealed by three distinct techniques in an endemic area in the Brazilian Amazon," *Annals of Tropical Medicine and Parasitology*, vol. 105, no. 6, pp. 413–424, 2011.

[6] J. O. Ferrari, M. U. Ferreira, L. M. Camargo, and C. S. Ferreira, "Intestinal parasites among Karitiana Indians from Rondônia State, Brazil.," *Revista do Instituto de Medicina Tropical de Sao Paulo*, vol. 34, no. 3, pp. 223–225, 1992.

[7] M. A. Cardoso, M. U. Ferreira, L. M. A. Camargo, and S. C. Szarfarc, "Anaemia, iron deficiency and malaria in a rural community in Brazilian Amazon," *European Journal of Clinical Nutrition*, vol. 48, no. 5, pp. 326–332, 1994.

[8] E. Eve, E. Ferraz, and V. E. Thatcher, "Parasitic infections in villagers from three districts of the Brazilian Amazon," *Annals of Tropical Medicine and Parasitology*, vol. 92, no. 1, pp. 79–87, 1998.

[9] M. A. Cardoso, M. U. Ferreira, L. M. Camargo, and S. C. Szarfarc, "Anemia in a population from an endemic area of malaria, Rondônia (Brazil)," *Revista de Saude Publica*, vol. 26, no. 3, pp. 161–166, 1992.

[10] G. C. Melo, R. C. Reyes-Lecca, S. Vitor-Silva et al., "Concurrent helminthic infection protects schoolchildren with *Plasmodium*

vivax from anemia," *PLoS ONE*, vol. 5, no. 6, Article ID e11206, 2010.

[11] J.-G. Tshikuka, M. E. Scott, K. Gray-Donald, and O.-N. Kalumba, "Multiple infection with *Plasmodium* and helminths in communities of low and relatively high socio-economic status," *Annals of Tropical Medicine and Parasitology*, vol. 90, no. 3, pp. 277–293, 1996.

[12] M. Nacher, P. Singhasivanon, S. Yimsamran et al., "Intestinal helminth infections are associated with increased incidence of *Plasmodium vivax* malaria in Thailand," *Journal of Parasitology*, vol. 88, no. 1, pp. 55–58, 2002.

[13] A. Spiegel, A. Tall, G. Raphenon, J.-F. Trape, and P. Druilhe, "Increased frequency of malaria attacks in subjects co-infected by intestinal worms and *Plasmodium falciparum* malaria," *Transactions of the Royal Society of Tropical Medicine and Hygiene*, vol. 97, no. 2, pp. 198–199, 2003.

[14] C. Sokhna, J.-Y. Le Hesran, P. A. Mbaye et al., "Increase of malaria attacks among children presenting concomitant infection by *Schistosoma mansoni* in Senegal," *Malaria Journal*, vol. 3, article 43, 2004.

[15] M. J. Murray, A. B. Murray, M. B. Murray, and C. J. Murray, "Parotid enlargement, forehead edema, and suppression of malaria as nutritional consequences of ascariasis," *The American Journal of Clinical Nutrition*, vol. 30, no. 12, pp. 2117–2121, 1977.

[16] V. Briand, L. Watier, J. Y. Le Hesran, A. Garcia, and M. Cot, "Coinfection with Plasmodium falciparum and Schistosoma haematobium: protective effect of schistosomiasis on malaria in Senegalese children?" *The American Journal of Tropical Medicine and Hygiene*, vol. 72, no. 6, pp. 702–707, 2005.

[17] K. E. Lyke, A. Dicko, A. Dabo et al., "Association of *Schistosoma haematobium* infection with protection against acute *Plasmodium vivax* malaria in Malian children," *The American Journal of Tropical Medicine and Hygiene*, vol. 73, no. 6, pp. 1124–1130, 2005.

[18] A. E. Shapiro, E. M. Tukahebwa, J. Kasten et al., "Epidemiology of helminth infections and their relationship to clinical malaria in southwest Uganda," *Transactions of the Royal Society of Tropical Medicine and Hygiene*, vol. 99, no. 1, pp. 18–24, 2005.

[19] P. Bejon, T. W. Mwangi, B. Lowe, N. Peshu, A. V. S. Hill, and K. Marsh, "Helminth infection and eosinophilia and the risk of *Plasmodium vivax* malaria in 1- to 6-year-old children in a malaria endemic area," *PLoS Neglected Tropical Diseases*, vol. 2, no. 1, p. e164, 2008.

[20] K. Artavanis-Tsakonas, J. E. Tongren, and E. M. Riley, "The war between the malaria parasite and the immune system: Immunity, immunoregulation and immunopathology," *Clinical and Experimental Immunology*, vol. 133, no. 2, pp. 145–152, 2003.

[21] E. M. Riley, S. Wahl, D. J. Perkins, and L. Schofield, "Regulating immunity to malaria," *Parasite Immunology*, vol. 28, no. 1-2, pp. 35–49, 2006.

[22] Z. Su, M. Segura, K. Morgan, J. C. Loredo-Osti, and M. M. Stevenson, "Impairment of protective immunity to blood-stage malaria by concurrent nematode infection," *Infection and Immunity*, vol. 73, no. 6, pp. 3531–3539, 2005.

[23] D. L. Doolan, C. Dobaño, and J. K. Baird, "Acquired immunity to malaria," *Clinical Microbiology Reviews*, vol. 22, no. 1, pp. 13–36, 2009.

[24] N. P. J. Day, T. T. Hien, T. Schollaardt et al., "The prognostic and pathophysiologic role of pro- and antiinflammatory cytokines in severe malaria," *Journal of Infectious Diseases*, vol. 180, no. 4, pp. 1288–1297, 1999.

[25] D. Dodoo, F. M. Omer, J. Todd, B. D. Akanmori, K. A. Koram, and E. M. Riley, "Absolute levels and ratios of proinflammatory and anti-inflammatory cytokine production in vitro predict clinical immunity to *Plasmodium falciparum* malaria," *Journal of Infectious Diseases*, vol. 185, no. 7, pp. 971–979, 2002.

[26] C. Noone, M. Parkinson, D. J. Dowling et al., "Plasma cytokines, chemokines and cellular immune responses in pre-school Nigerian children infected with *Plasmodium falciparum*," *Malaria Journal*, vol. 12, no. 1, article 5, 2013.

[27] N. M. Anstey, J. B. Weinberg, M. Y. Hassanali et al., "Nitric oxide in Tanzanian children with malaria: inverse relationship between malaria severity and nitric oxide production/nitric oxide synthase type 2 expression," *The Journal of Experimental Medicine*, vol. 184, no. 2, pp. 557–567, 1996.

[28] S. Cabantous, B. Poudiougou, A. A. Oumar et al., "Genetic evidence for the aggravation of *Plasmodium vivax* malaria by interleukin 4," *Journal of Infectious Diseases*, vol. 200, no. 10, pp. 1530–1539, 2009.

[29] S. M. Geiger, C. L. Massara, J. Bethony, P. T. Soboslay, O. S. Carvalho, and R. Corrêa-Oliveira, "Cellular responses and cytokine profiles in *Ascaris lumbricoides* and *Trichuris trichiura* infected patients," *Parasite Immunology*, vol. 24, no. 11-12, pp. 499–509, 2002.

[30] J. D. Turner, H. Faulkner, J. Kamgno et al., "Th2 cytokines are associated with reduced worm burdens in a human intestinal helminth infection," *Journal of Infectious Diseases*, vol. 188, no. 11, pp. 1768–1775, 2003.

[31] C. A. Figueiredo, M. L. Barreto, L. C. Rodrigues et al., "Chronic intestinal helminth infections are associated with immune hyporesponsiveness and induction of a regulatory network," *Infection and Immunity*, vol. 78, no. 7, pp. 3160–3167, 2010.

[32] J. D. Turner, J. A. Jackson, H. Faulkner et al., "Intensity of intestinal infection with multiple worm species is related to regulatory cytokine output and immune hyporesponsiveness," *The Journal of Infectious Diseases*, vol. 197, no. 8, pp. 1204–1212, 2008.

[33] T. Supali, J. J. Verweij, A. E. Wiria et al., "Polyparasitism and its impact on the immune system," *International Journal for Parasitology*, vol. 40, no. 10, pp. 1171–1176, 2010.

[34] M. Nacher, F. Gay, P. Singhasivanon et al., "*Ascaris lumbricoides* infection is associated with protection from cerebral malaria," *Parasite Immunology*, vol. 22, no. 3, pp. 107–113, 2000.

[35] M. Nacher, P. Singhasivanon, U. Silachamroon et al., "Helminth infections are associated with protection from malaria-related acute renal failure and jaundice in Thailand," *American Journal of Tropical Medicine and Hygiene*, vol. 65, no. 6, pp. 834–836, 2001.

[36] R. M. Maizels, A. Balic, N. Gomez-Escobar, M. Nair, M. D. Taylor, and J. E. Allen, "Helminth parasites—masters of regulation," *Immunological Reviews*, vol. 201, no. 1, pp. 89–116, 2004.

[37] G. Snounou, S. Viriyakosol, W. Jarra et al., "High sensitivity of detection of human malaria parasites by the use of nested polymerase chain reaction," *Molecular and Biochemical Parasitology*, vol. 61, no. 2, pp. 315–320, 1993.

[38] K. A. Rockett, M. M. Awburn, E. J. Rockett, and I. A. Clark, "Tumor necrosis factor and interleukin-1 synergy in the context of malaria pathology," *The American Journal of Tropical Medicine and Hygiene*, vol. 50, no. 6, pp. 112–118, 1994.

[39] H. Nahrevanian and M. J. Dascombe, "Nitric oxide and reactive nitrogen intermediates during lethal and nonlethal strains of

murine malaria," *Parasite Immunology*, vol. 23, no. 9, pp. 491–501, 2001.

[40] R. N. Rodrigues-da-Silva, J. D. C. Lima-Junior, B. D. P. Fonseca e Fonseca et al., "Alterations in cytokines and haematological parameters during the acute and convalescent phases of *Plasmodium vivax* and *Plasmodium vivax* infections," *Memorias do Instituto Oswaldo Cruz*, vol. 109, no. 2, pp. 154–162, 2014.

[41] J. Ludbrook and H. Dudley, "Why permutation tests are superior to t and f tests in biomedical research," *American Statistician*, vol. 52, no. 2, pp. 127–132, 1998.

[42] R Core Team, *A Language and Environment for Statistical Computing*, R Foundation for Statistical Computing, Vienna, Austria, 2013, http://www.R-project.org/.

[43] "Wheeler B. lmPerm: permutation tests for linear models," 2010, http://cran.r-project.org/web/packages/lmPerm/index.html.

[44] J. Oksanen, F. G. Blanchet, R. Kindt et al., vegan: Community Ecology Package, 2010, http://CRAN.R-project.org/package=vegan.

[45] G. R. Warnes, B. Bolker, L. Bonebakker et al., "Various R programming tools for plotting data," 2014, http://CRAN.R-project.org/package=gplots.

[46] E. N. T. Meeusen and A. Balic, "Do eosinophils have a role in the killing of helminth parasites?" *Parasitology Today*, vol. 16, no. 3, pp. 95–101, 2000.

[47] A. D. Klion and T. B. Nutman, "The role of eosinophils in host defense against helminth parasites," *The Journal of Allergy and Clinical Immunology*, vol. 113, no. 1, pp. 30–37, 2004.

[48] N. Tangpukdee, H.-S. Yew, S. Krudsood et al., "Dynamic changes in white blood cell counts in uncomplicated *Plasmodium falciparum* and *P. vivax* malaria," *Parasitology International*, vol. 57, no. 4, pp. 490–494, 2008.

[49] W. R. J. Taylor, H. Widjaja, H. Basri et al., "Changes in the total leukocyte and platelet counts in Papuan and non Papuan adults from northeast Papua infected with acute *Plasmodium vivax* or uncomplicated *Plasmodium falciparum* malaria," *Malaria Journal*, vol. 7, article 259, 2008.

[50] J. D. C. Lima-Junior, R. N. Rodrigues-da-Silva, V. A. Pereira et al., "Cells and mediators of inflammation (C-reactive protein, nitric oxide, platelets and neutrophils) in the acute and convalescent phases of uncomplicated *Plasmodium vivax* and *Plasmodium falciparum* infection," *Memórias do Instituto Oswaldo Cruz*, vol. 107, no. 8, pp. 1035–1041, 2012.

[51] P. Kern, C. J. Hemmer, J. van Damme, H.-J. Gruss, and M. Dietrich, "Elevated tumor necrosis factor alpha and interleukin-6 serum levels as markers for complicated *Plasmodium vivax* malaria," *The American Journal of Medicine*, vol. 87, no. 2, pp. 139–143, 1989.

[52] F. Remoue, T. O. Diallo, V. Angeli et al., "Malaria co-infection in children influences antibody response to schistosome antigens and inflammatory markers associated with morbidity," *Transactions of the Royal Society of Tropical Medicine and Hygiene*, vol. 97, no. 3, pp. 361–364, 2003.

[53] T. O. Diallo, F. Remoue, A. M. Schacht et al., "Schistosomiasis co-infection in humans influences inflammatory markers in uncomplicated *Plasmodium falciparum* malaria," *Parasite Immunology*, vol. 26, no. 8-9, pp. 365–369, 2004.

[54] K. E. Lyke, A. Dabo, L. Sangare et al., "Effects of concomitant *Schistosoma haematobium* infection on the serum cytokine levels elicited by acute *Plasmodium vivax* malaria infection in Malian children," *Infection and Immunity*, vol. 74, no. 10, pp. 5718–5724, 2006.

[55] N. Imai, N. Rujeni, N. Nausch et al., "Exposure, infection, systemic cytokine levels and antibody responses in young children concurrently exposed to schistosomiasis and malaria," *Parasitology*, vol. 138, no. 12, pp. 1519–1533, 2011.

[56] R. M. Gonçalves, K. C. Salmazi, B. A. N. Santos et al., "$CD4^+$ $CD25^+$ $Foxp3^+$ regulatory T cells, dendritic cells, and circulating cytokines in uncomplicated malaria: do different parasite species elicit similar host responses?" *Infection and Immunity*, vol. 78, no. 11, pp. 4763–4772, 2010.

[57] R. M. Gonçalves, K. K. G. Scopel, M. S. Bastos, and M. U. Ferreira, "Cytokine balance in human Malaria: does *Plasmodium vivax* elicit more inflammatory responses than *Plasmodium vivax*?" *PLoS ONE*, vol. 7, no. 9, Article ID e44394, 2012.

[58] D. J. Cua and C. M. Tato, "Innate IL-17-producing cells: the sentinels of the immune system," *Nature Reviews Immunology*, vol. 10, no. 7, pp. 479–489, 2010.

[59] S. J. Rubino, K. Geddes, and S. E. Girardin, "Innate IL-17 and IL-22 responses to enteric bacterial pathogens," *Trends in Immunology*, vol. 33, no. 3, pp. 112–118, 2012.

[60] H. Helmby, M. Kullberg, and M. Troye-Blomberg, "Altered immune responses in mice with concomitant *Schistosoma mansoni* and *Plasmodium chabaudi* infections," *Infection and Immunity*, vol. 66, no. 11, pp. 5167–5174, 1998.

[61] D. Prakash, C. Fesel, R. Jain, P.-A. Cazenave, G. C. Mishra, and S. Pied, "Clusters of cytokines determine malaria severity in *Plasmodium falciparum*-infected patients from endemic areas of central India," *Journal of Infectious Diseases*, vol. 194, no. 2, pp. 198–207, 2006.

[62] S. Roy, J. Lavine, F. Chiaromonte et al., "Multivariate statistical analyses demonstrate unique host immune responses to single and dual lentiviral infection," *PLoS ONE*, vol. 4, no. 10, Article ID e7359, 2009.

Hindawi Publishing Corporation
Mediators of Inflammation
Volume 2014, Article ID 143450, 12 pages
http://dx.doi.org/10.1155/2014/143450

Research Article

Ecotin-Like ISP of *L. major* Promastigotes Fine-Tunes Macrophage Phagocytosis by Limiting the Pericellular Release of Bradykinin from Surface-Bound Kininogens: A Survival Strategy Based on the Silencing of Proinflammatory G-Protein Coupled Kinin B_2 and B_1 Receptors

Erik Svensjö,[1] Larissa Nogueira de Almeida,[1] Lucas Vellasco,[1] Luiz Juliano,[2] and Julio Scharfstein[1]

[1] *Instituto de Biofísica Carlos Chagas Filho, Universidade Federal do Rio de Janeiro, 21990-400 Rio de Janeiro, RJ, Brazil*
[2] *Escola Paulista de Medicina, Universidade Federal de São Paulo, 04044-020 São Paulo, SP, Brazil*

Correspondence should be addressed to Julio Scharfstein; jscharf2@gmail.com

Received 13 June 2014; Accepted 17 August 2014; Published 10 September 2014

Academic Editor: Marcelo T. Bozza

Inhibitors of serine peptidases (ISPs) expressed by *Leishmania major* enhance intracellular parasitism in macrophages by targeting neutrophil elastase (NE), a serine protease that couples phagocytosis to the prooxidative TLR_4/PKR pathway. Here we investigated the functional interplay between ISP-expressing *L. major* and the kallikrein-kinin system (KKS). Enzymatic assays showed that NE inhibitor or recombinant ISP-2 inhibited KKS activation in human plasma activated by dextran sulfate. Intravital microscopy in the hamster cheek pouch showed that topically applied *L. major* promastigotes (WT and Δ*isp*2/3 mutants) potently induced plasma leakage through the activation of bradykinin B_2 receptors (B_2R). Next, using mAbs against kininogen domains, we showed that these BK-precursor proteins are sequestered by *L. major* promastigotes, being expressed at higher % in the Δ*isp*2/3 mutant population. Strikingly, analysis of the role of kinin pathway in the phagocytic uptake of *L. major* revealed that antagonists of B_2R or B_1R reversed the upregulated uptake of Δ*isp*2/3 mutants without inhibiting macrophage internalization of WT *L. major*. Collectively, our results suggest that *L. major* ISP-2 fine-tunes macrophage phagocytosis by inhibiting the pericellular release of proinflammatory kinins from surface bound kininogens. Ongoing studies should clarify whether *L. major* ISP-2 subverts TLR_4/PKR-dependent prooxidative responses of macrophages by preventing activation of G-protein coupled B_2R/B_1R.

1. Introduction

Integrated by 3 serine proteases, factor XII (FXII), factor XI (FXI), and plasma prekallikrein (PK) and by one nonenzymatic cofactor, high molecular weight kininogen (HK), the kallikrein-kinin system (KKS), also referred to as the plasma contact pathway of coagulation, is assembled and activated when the blood comes in contact with negatively charged polymers of endogenous origin or microbial surfaces [1, 2]. Upon binding to these negatively charged structures, the zymogen FXII undergoes a conformational change that endows the unstable proenzyme with limited enzymatic activity. Activated FXII (FXIIa) then cleaves prekallikrein (complexed to the cofactor HK), generating PKa. Reciprocal cleavage reactions between FXIIa and PKa amplify the proteolytic cascade, leading to downstream (i) generation of fibrin via the FXIIa/FXIa-dependent procoagulative pathway, (ii) release of the internal bradykinin (BK) moiety of HK by PKa. Once liberated, the short-lived BK induces vasodilation and increases microvascular permeability through the activation of bradykinin B_2 receptors (B_2R) expressed in the endothelium lining [1]. In addition, the multifunctional PKa generates

plasmin, an effector of fibrinolysis, and cleaves native C3 of the complement system C3 [3, 4].

Although HK is classically regarded as the parental precursor of proinflammatory kinins, the cleaved form of HK (HKa), a disulfide linked two-chain structure, has additional biological functions. For example, it has been reported that HKa reduces neutrophil adhesive functions upon binding to β2-integrin Mac-1 (CR3, CD11b/CD18, $\alpha M\beta 2$) [1, 5]. More recently, Yang et al. [6] appointed HK/HKa as the plasma-borne opsonins that drive efferocytosis of apoptotic cells via plasminogen activator receptor (uPAR)/RAC1-pathway. After binding to phosphatidyl serine (PS) exposed by apoptotic neutrophils, the surface-bound HK binds to uPAR before switching off proinflammatory responses of macrophages [6]. In contrast to this novel immunoregulatory function, HK (and low molecular weight kininogen, LK) are traditionally viewed as precursors of proinflammatory kinins. Once leaked into extravascular tissues, the plasma-borne HK/LK undergo proteolytic cleavage by tissue kallikrein, releasing the B_2R agonist lysyl-BK (LBK) in inflammatory exudates [1]. It is noteworthy that oxidized forms of kininogens may release bioactive kinins as result of cooperation between neutrophil elastase (NE) and mast cell tryptase [7, 8]. Acting as paracrine hormones, the short-lived kinins (BK or LBK) swiftly activate G-protein coupled bradykinin B_2 receptors (B_2R), a subtype of receptor constitutively expressed by endothelial cells, nociceptive neurons, macrophages, and DCs [1, 9–11]. The long-range signaling activity of intact kinins is controlled by kinin-degrading metallopeptidases, such as the angiotensin converting enzyme (ACE/kininase II) [1]. In addition, the liberated kinin peptides are metabolized by kininase I (carboxypeptidase N or M); removal of the C-terminal Arg residue generates des-Arg-kinins, the high-affinity ligands of B_1R, a GPCR subtype whose expression is strongly upregulated in injured/inflamed tissues [12].

During the last decade, research conducted in our laboratory showed that kinins proteolytically released in peripheral sites of *T. cruzi* or *Leishmania chagasi* infection reversibly couple inflammation to antiparasite immunity [13–17]. Another interesting twist came from studies showing that activation of the contact system/KKS promotes bacterial entrapment within fibrin meshes, thus providing a physical barrier against the systemic spread of microbial pathogens [18]. To this date, however, it is unclear whether the contact pathway modulates immunity at early stages of cutaneous leishmaniasis. Intravital microscopy studies conducted in the mouse ear model of *L. major* infection [19–21] have shown that infiltrating neutrophils engulf the promastigotes before expressing the apoptotic markers required for efferocytosis by dermal DCs. After internalizing the parasitized/apoptotic neutrophils, the dermal DCs are no longer capable of steering protective TH1-responses in the draining lymph node [19–21]. Although efferocytosis has strong impact on DC function and TH development in *L. major* infection, independent studies showed that macrophage clearance of apoptotic neutrophils may either induce pro- or anti-inflammatory responses in NE-dependent manner, the intracellular fate of the parasite being influenced by the host genetic background [22, 23].

In natural infection by blood-feeding arthropods, insect proboscis inevitably causes bleeding, which then causes the mixing of plasma and sandfly saliva substances with parasites deposited in the injured dermis [24]. Interestingly, *Phlebotomy duboscq*, a vector of *Leishmania* species, contains high levels of a salivary protein (PdSP15) that inhibits the contact pathway [25] by binding to negatively charged polymers of endogenous origin—such as platelet-derived polyphosphates [2, 18, 26]. Considering that activation of the procoagulative contact system induces microvascular leakage through PKa-mediated release of BK, it is conceivable that sandfly-transmitted *Leishmania* promastigotes have evolved the means to subvert the innate effector function of the kinin pathway at early stages of infection.

The current study was motivated by the recent discovery that *Leishmania* has three genes encoding ecotin-like inhibitors of serine peptidases (ISPs) [27]. Previous studies with the archetype of the family *Escherichia coli* ecotin [28] showed that this inhibitor targets neutrophil elastase (NE) [29]—a member of the trypsin-fold serine peptidases of clan PA/family S_{1A}. After noting that the *Leishmania* genome [30] lacks these endogenous serine peptidase targets, Eschenlauer et al. [27] predicted that *L. major* ISPs might target S_{1A}-family serine peptidases expressed by cells of the innate immune system, such as NE, tryptase, and cathepsin G [30]. In a series of elegant studies, Eschenlauer et al. [27] and Faria et al. [31, 32] addressed this issue using *L. major* lines lacking ISP2 and ISP3 ($\Delta isp2/3$). After studying the outcome of interactions between *L. major* promastigotes and elicited macrophages, these authors found that these phagocytes internalized the $\Delta isp2/3$ promastigotes far more efficiently than ISP-expressing wild-type (WT) parasites [27, 31] and linked the upregulated CR3-dependent phagocytosis of the $\Delta isp2/3$ *L. major* mutants to NE-dependent activation of innate immunity via the TLR_4/PKR/TNF-α/IFN-β, a prooxidative pathway that limits intracellular parasite survival [31, 32]. Notably, the phenotype of $\Delta isp2/3$ promastigotes was reversed by supplementing the macrophage cultures with purified (recombinant) ISP-2 or with the synthetic NE inhibitor (MeOSuc-AAPV-CMK), at the onset of infection [31]. Based on these collective findings, these authors suggested that ISP-2 expressing *L. major* promastigotes might downmodulate phagocytosis and limit microbicidal responses of macrophages by preventing NE-dependent activation of TLR_4 [31, 32]. More recently, we have documented that macrophages internalize and limit intracellular *T. cruzi* growth in resident macrophages through activation pathways forged by the cross-talk between bradykinin B_2 receptors and C5a receptors [33]. Intrigued by the similarities that exist between the phenotype of the *L. major* $\Delta isp2/3$ mutant and *L. chagasi* promastigotes [15] and *T. cruzi* trypomastigotes (Dm28 strain) [33, 34], in the current work we interrogated whether ISP-expressing *L. major* and the ISP-2 $\Delta isp2/3$ mutants differ in their ability to activate the KKS *in vivo* and *in vitro*. Using intravital microscopy, we first showed that *L. major* promastigotes topically applied to the hamster cheek pouch potently activate the KKS extravascularly, irrespective of presence/absence of ISP. In the second part of this study, we present evidence indicating that ISP-expressing *L. major*

may subvert innate immunity by targeting kinin-releasing serine proteases (S_{1A} family) exposed at the cell-surface of macrophages.

2. Materials and Methods

2.1. Parasites. *L. major* Promastigotes of Friedlin (MHOM/JL/80/Friedlin) were grown in modified Eagle's medium (HOMEM, Sigma) supplemented with 10% heat-inactivated fetal bovine serum (FBS, Gibco) at 25°C, as previously described [31, 32]. Suspensions of promastigotes were washed twice with PBS before being used either *in vitro* or *in vivo*. *Leishmania major* deficient in ISP2 and ISP3 (Δ*isp*2/3) were generated as previously described by Eschenlauer et al. [27]. The following antibiotics were used at the indicated concentration for the selection of transfectants: 50 mg/mL hygromycin B (Roche), 25 mg/mL G418 (Invitrogen), 10 mg/mL phleomycin (InvivoGen), and 50 mg/mL puromycin dihydrochloride (Calbiochem).

2.2. Intravital Digital Microscopy. Syrian hamsters, 3-month-old males, were maintained and anesthetized according to regulations given by the local ethical committee (IBCCF, protocol-014, 23/02/2008). Altogether 65 hamsters (114 ± 18 g) (Anilab, São Paulo, Brazil) were used. Anesthesia was induced by intraperitoneal injection of sodium pentobarbital 3% that was supplemented with i.v. α-chloralose (2.5% W/V, solution in saline) through a femoral vein catheter. A tracheal cannula (PE 190) was inserted to facilitate spontaneous breathing and the body temperature was maintained at 37°C by a heating pad monitored with a rectal thermistor. The hamster cheek pouch (HCP) was prepared and used for intravital microscopy as previously reported [34, 35]. The microcirculation of the HCP was observed using an Axioskop 40 microscope, objective 4x, and oculars 10x equipped with a LED light source Colibri (Carl Zeiss, Germany) and appropriate filters (490/520 nm and 540/580 nm, rhodamine) for observations of fluorescence in epiluminescence. A digital camera, AxioCam HRc, and a computer with the AxioVision 4.4 software program (Carl Zeiss, Germany) were used for image analysis of arteriolar diameter and total fluorescence in a representative rectangular area (5 mm^2) of the prepared HCP. Fluorescence was recorded for 30 min prior to experimental interventions to secure normal blood flow and unaltered vascular permeability and the fluorescence measured at 30 min after FITC-dextran (FITC-dextran 150 kDa, 100 mg/kg bodyweight, TdB Consultancy, Uppsala, Sweden) injection was adjusted to 2000 fluorescent units (RFU = Relative Fluorescent Units) for statistical reasons. Leukocytes were labeled *in vivo* by injecting rhodamine 100 μg/kg b.w i.v. (10 min prior to experimental interventions), reinforced by injection of the same tracer at 10 μg/kg b.w. every 10 min until 60 min. The recorded fluorescence at 10 min after rhodamine injection in each experiment was adjusted to 3000 fluorescent units (RFU) for statistical reasons. Two images of exactly the same area were recorded at every 5 min interval during the entire experiment. One was used to measure plasma leakage and arteriolar diameter (490/520 nm) and the other to measure total fluorescence of rhodamine-labeled leukocytes in circulation, rolling, adherence, and migration (540/580 nm) in the observed area (5 mm^2) here defined as leukocyte accumulation. Exposure time was limited to 15 s for each captured image in order to avoid phototoxicity. Following 30 min control period after FITC-dextran injection HCPs were topically exposed to WT *L. major* promastigotes or Δ*isp*2/3 (7.5×10^6/500 μL) during interruption of the superfusion for 10 min. Cromoglycate was injected i.p. (40 mg/kg b.w.) at time of pentobarbital anesthesia and dextran sulfate 500 kDa (TdB Consultancy, Uppsala, Sweden) was injected i.v. (2 mg/kg) prior to parasite application. HOE-140 tested at 0.5 μM and the histamine receptor H1 mepyramine (10 μM) were applied locally via a syringe pump into the superfusion during 10 min prior to application of promastigotes.

2.3. Isolation of Peritoneal Macrophages and Invasion Assays. C57BL/6 mice received an intraperitoneal injection of 2 mL of 3% thioglycolate and macrophages were harvested from peritoneal lavage 3 days later. Macrophages were plated on 13 mm coverslips in 24-well plate and after 20 h of incubation at 37°C in complete medium (RPMI + 10% FBS, 100 U/mL penicillin, and 100 μg/mL streptomycin) the nonadherent cells were removed by washing the monolayer of cells with PBS. Invasion assays were performed by adding stationary phase promastigotes to the monolayers at a ratio of 5 : 1 (parasite/macrophage) in medium containing 1 mg/mL albumin from bovine serum (BSA, Sigma). The interaction was performed during 3 h in a humidified chamber containing 5% CO_2 at 37°C. When indicated, the culture medium was supplemented with 100 nM of B_2R antagonist (HOE-140, Sigma) or 1 μM of B_1R antagonist des-Arg^9-[Leu^8]-BK (DAL^8-BK; Sigma), 5 minutes before addition of parasites. After interaction, extracellular promastigotes were removed by washing the monolayers twice with PBS, which were then fixed with Bouin overnight and stained with Giemsa (Merck). The number of intracellular amastigotes was determined by counting at least 100 cells per replicate under the light microscope. All assays were done in triplicates and results were expressed as mean values ± SD.

2.4. Parasite Surface Staining. Promastigotes were preincubated with PBS-1% BSA for 1 hour to avoid unspecific binding and then incubated for 1 h with monoclonal antibody MBK_3 (IgG1—1 : 50) or HKH4 (IgG_{2a}—1 : 50), kindly provided by Dr. W. Müller-Esterl from Frankfurt University. MBK_3 recognizes the BK epitope in domain D4 of human and bovine H-/L-kininogens whereas HKH_4 binds to the D1 domain [36]. Isotype-matched monoclonal antibodies were used as negative controls. Parasites were washed three times with PBS-1% BSA and incubated with secondary fluorescent antibody (FITC—1 : 50) for 30 min at 4°C, protected from light. After washing, the samples were acquired by flow cytometry (FACSCan; BD Biosciences), and data analyses were done with Summit software (Dako Colorado, Inc). Assays were done in duplicates and results are representative of two independent experiments.

2.5. Contact Phase Activation of Human Plasma. The activation of FXII/PK in human citrated (platelet free) plasma treated (or not) with dextran sulfate (DXS; 500 kDa, TdB Consultancy) was monitored by spectrofluorimetry as previously described [37], using internally quenched fluorescent substrates whose sequences correspond to the C-terminal (Abz-GFSPFRSVTVQ-EDDnp) or N-terminal flanking region (Abz-MTEMARRPQ-EDDnp m) of BK of mouse kininogen. The hydrolysis of the cleaved substrate Abz-peptidyl-EDDnp (Abz = o-aminobenzoyl and EDDnp = ethylenediamine 2,4-dinitrophenyl) was monitored by measuring the fluorescence at $\lambda_{ex.} = 320$ nm and $\lambda_{em.} = 420$ nm in a Spectramax M5 fluorescence spectrophotometer. The reaction was carried out in PBS, pH 7.4, using citrated human plasma 1 : 20, 4 μM of the Abz-peptidyl-EDDnp substrate and 20 nM of the contact system activator DXS (500 kDa). As internal controls, the plasma was pretreated with the synthetic PKa inhibitor (PKSI-527—5 μM) [38]. Assays with recombinant ISP-2 (kindly supplied by A. P. C. A. Lima) were performed at final concentrations of 142, 177, 240, and 355 nM; the neutrophil elastase (NE) inhibitor MeOSuc-AAPV-CMK (Calbiochem) was tested at 10, 20, and 30 μM. PKSI or recombinant ISP2 and MeOSuc-AAPV-CMK were preincubated with human plasma for 15 min, at 37°C, prior to the addition of DXS and the substrate. Plasma was prepared by centrifugation of blood samples at 2500 g for 20 min at 4°C. After centrifugation, plasma samples were filtered using a 0.2 μm membrane.

2.6. Statistical Analyses. Statistical analyses were done using PRISM 5.0 (GraphPad Software). Comparisons of the means of the different groups were done by one-way analysis of variance (ANOVA). When the mean values of the groups showed a significant difference, pairwise comparison was performed with the Tukey test. A P value of 0.05 or less was considered to indicate a statistically significant difference. For intravital experiments, we used ANOVA or pairwise t-test, when appropriate.

3. Results

3.1. Analysis of the Dynamics of Inflammation in HCP Topically Sensitized with L. major Promastigotes. Intravital microscopy in HCP has provided a wealth of information about the interplay between the KKS and the topically applied pathogens because this method dispenses the use of needles, thus ruling out the influence of bleeding and collateral activation of the contact system in the analysis of microcirculatory parameters. As a starting point in this work, we asked whether the proinflammatory responses evoked by ISP-expressing *L. major* promastigotes or ISP-deficient parasites were comparable. Our results (Figures 1–3) revealed that *L. major* (WT) promastigotes induced a very robust and reversible microvascular leakage that was detectable at 20 min and reached its maximal value 45 min after pathogen application (Figures 1(a)–1(c)). In 4 out of 15 experiments we measured leukocyte accumulation in and around postcapillary venules and noted that these circulating cells were promptly mobilized locally, the response being detectable up to 90 min after pathogen application (Figure 1(b)). The temporal course and dynamics of the plasma leakage response evoked by WT promastigotes were quite different from the classical responses elicited by BK, histamine, or leukotrienes, all of which cause a maximal increase within 10 min and reversed to steady-state conditions within 30 min [39, 40]. Intriguingly, we found that the leakage responses evoked by *L. major* (WT) promastigotes were generally more robust than those induced by the same inoculum of *L. donovani* promastigotes (Figure 1(c)) [16] or *T. cruzi* (tissue culture trypomastigotes, Dm28c strain) [35]. Akin to the findings made in the above-mentioned studies, we found that topically applied HOE-140 (B_2R antagonist) markedly reduced *L. major* (WT-) induced plasma leakage (Figure 1(a)).

Considering that mast cells are innate sentinel cells strategically localized in the perivascular tissues, we next interrogated whether *L. major* promastigotes might evoke plasma leakage in mast cell-dependent manner. As shown in Figure 1(a), the topical addition of mepyramine (histamine-1-receptor blocker) markedly inhibited the macromolecular leakage induced by *L. major* promastigotes. In a limited series of studies, we found that cromoglycate, a well-known mast cell stabilizer, abolished the *L. major*-induced leakage of plasma (Figure 1(b), lower panel). Of further interest, cromoglycate prevented leukocyte accumulation in the parasite-laden microvascular beds, reducing this parameter to levels below controls (Figure 1(b), top panel). It is noteworthy that the doses of mepyramine and HOE-140 that were topically added to the HCP at the onset of infection were sufficient to block the leakage induced by standard solutions of histamine (4 μM) and BK (0.5 μM) [35]. Further expanding this investigation, we next explored the possibility that the microvascular leakage elicited by *L. major* promastigotes requires the participation of circulating neutrophils. To this end, we injected separate group of hamsters intravenously with DXS, a negatively charged polymer (500 kDa) and found that it profoundly inhibited plasma leakage induced by *L. major* promastigotes. Although DXS was initially thought to inhibit neutrophil-dependent microvascular permeability by blocking endothelial interaction with neutrophil-derived cationic proteins [41–44], there is now awareness that these effects might result from DXS-mediated activation of the KKS, a systemic reaction that leads to hypotension as result of excessive BK formation [45].

Finally, we sought to compare the microvascular responses elicited by WT *L. major* with their counterparts genetically deficient in ISP-2/ISP-3. As shown in Figure 1(d), the dynamics of plasma leakage induced by topically applied Δ*isp*2/3 mutants was similar to that evoked by WT parasites, the peak response being observed at 45–50 min after pathogen application. However, somewhat surprisingly, the Δ*isp*2/3 mutants were 20% less effective in eliciting transendothelial leakage of plasma as compared to WT promastigotes (Figure 1(d)); the difference in their proinflammatory phenotypes ($P < 0.05$) was already noticeable at 25 min after parasite application.

3.2. Bradykinin Receptors Selectively Fuel Macrophage Internalization of ISP-Deficient L. major. Studies in mice models

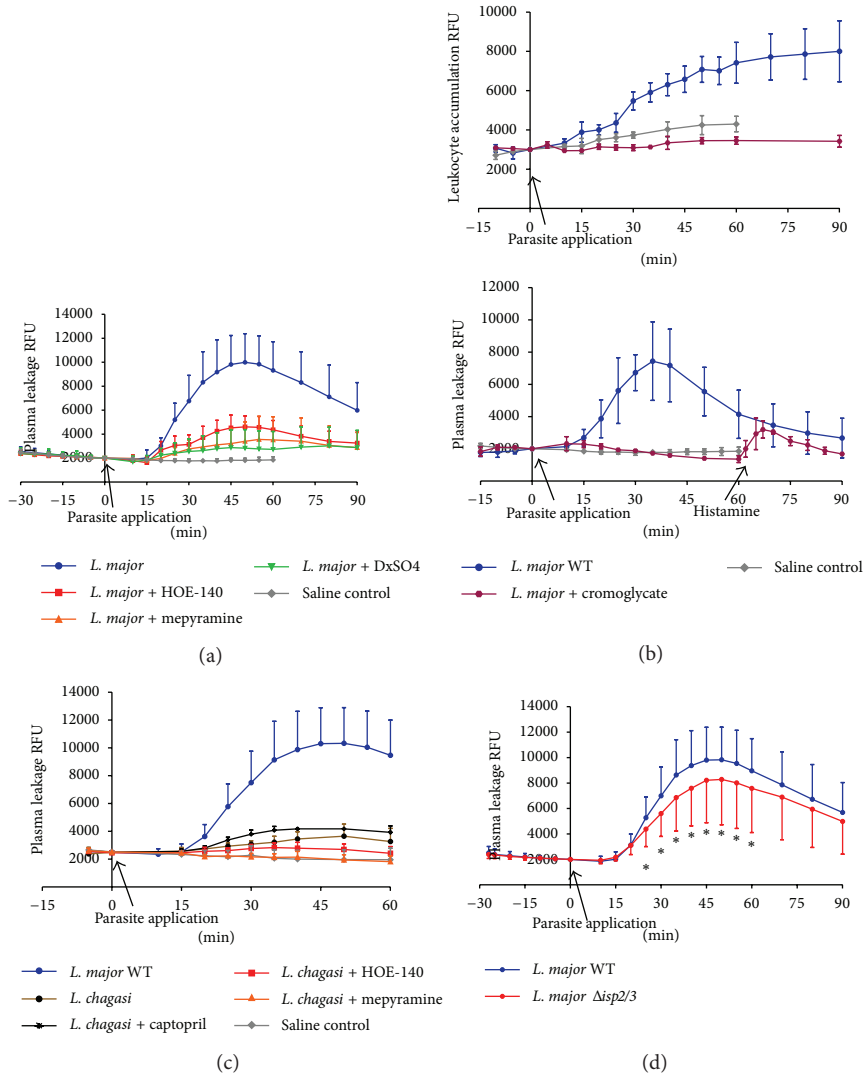

Figure 1: Microvascular plasma leakage and leukocyte accumulation in the HCP sensitized with *Leishmania*. The data represent relative fluorescence units (RFU: mean ± SD) induced by the topical application of *L. major* promastigotes (MHOM/JL/80/Friedlin, 500 μL of 1,5 × 10^7/mL) on hamster cheek pouch preparations (HCPs) after 30 min of stabilization period without significant increase in RFU. Applications of promastigotes were made during 10 min of interrupted superfusion of the HCPs. (a) Pharmacological interventions. Four groups of HCP were sensitized with *L. major* WT promastigotes, whereas one group (saline control; $n = 6$) served as untreated control. The first group ($n = 15$) corresponds to the positive controls, that is, profile of HCP exposed to *L. major* alone; the second group ($n = 5$) received HOE-140 (0.5 μM) 5 min prior to promastigote application; the third group ($n = 4$) received the antagonist of histamine receptor (H1R) mepyramine (10 μM) 5 min prior to challenge with promastigotes; and the fourth group ($n = 7$) was pretreated (i.v.) with dextran sulfate 500 (DXS-500; 2 mg/kg) at time of FITC-dextran injection. Plasma leakage was significantly reduced ($P < 0.05$) in all experimental groups subjected to pharmacological interventions. (b) Effect of the mast cell stabilizer cromoglycate. Data represent mean values ± SD obtained in HCP sensitized by *L. major* WT ($n = 4$) and a saline control group ($n = 6$). Two hamsters were given cromoglycate 40 mg/kg i.p. at time of anesthesia induction, and this treatment resulted in a complete inhibition of plasma leakage and leukocyte accumulation elicited by *L. major* despite the fact that the HCPs responded to histamine stimuli (4 μM) at the end of the experiment, that is, 60 min after topical application of *L. major* promastigotes. As an internal control, one hamster from the DXS-treated group ($n = 7$, Figure 1(a)) received rhodamine i.v. prior to parasite challenge. Measurements of leukocyte accumulation showed that DXS-500 reduced the *Leishmania* response to levels below the saline control group while plasma leakage decreased to the level of controls depicted in Figure 1(a) (data not shown). (c) Comparative analysis of kinin/B_2R-driven microvascular plasma leakage induced by different *Leishmania* species. The graph depicts responses evoked by *L. major* WT and *L. chagasi* promastigotes (500 μL de 1,5 × 10^7/mL). *L. major* WT (blue filled circles, $n = 19$); *L. chagasi* (brown filled circles, $n = 6$); *L. chagasi* + captopril 1 μM (black crosses, $n = 4$); *L. chagasi* + 0.5 μM HOE-140 (red squares, $n = 4$); *L. chagasi* + 10 μM mepyramine (orange triangles, $n = 4$); and saline control (grey diamonds, $n = 3$). The maximal microvascular response to *L. major* was 5-fold higher than *L. chagasi* at 50 min after parasite application. The tests involving pharmacological interventions in HCP sensitized with *L. chagasi* groups were different ($P < 0.05$) from the *L. chagasi* control at 40 min. (d) Microvascular plasma leakage elicited by *L. major* Δ*isp*2/3. The data represent mean values ± SD. One group represents the microvascular responses evoked by WT *L. major* (MHOM/JL/80/Friedlin, $n = 19$) whereas the second group represents responses induced by *L. major* Δ*isp*2/3 ($n = 16$). The plasma leakage induced by WT versus Δ*isp*2/3 promastigotes was significantly different ($^*P < 0.05$) between 25 and 60 min after topical application of the pathogens.

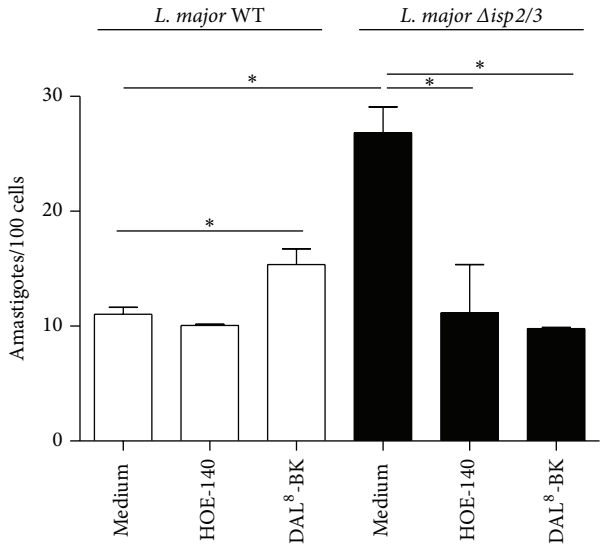

Figure 2: Differential role for bradykinin receptors in the phagocytic response of macrophages infected by WT *L. major* promastigotes and Δ*isp*2/3 mutants. Thioglycolate elicited (peritoneal) macrophages were incubated in medium containing 1 mg/mL BSA in the presence or absence of 100 nM of HOE-140 or 1 μm of des-Arg^9-[Leu^8]-BK (DAL^8-BK). Promastigotes were added (parasite/cell ratio 5 : 1) and incubated for 3 h at 37°C. White bars represent *L. major* WT and black bars represent Δ*isp*2/3. Data represent numbers of intracellular amastigotes per 100 macrophages (means ± SD) for triplicates and represent two different experiments ($^*P < 0.05$).

of acute Chagas disease [14] and visceral leishmaniasis [16] have recently showed that B_2R-deficient mice exhibited impaired development of type-1 effector T cells, the immune dysfunction of the transgenic strain being ascribed to primary deficiency in the maturation of $B_2R^{-/-}$ DCs in chagasic mice [14]. In a third study, we examined the role of the kinin pathway in the *in vitro* outcome of macrophage interactions with *L. chagasi* promastigotes [15]. Interestingly, these studies revealed that activation of the kinin/B_2R pathway may either fuel intracellular parasite outgrowth in splenic macrophages from hamsters, a species that is susceptible to visceral leishmaniasis, or limit parasite survival in thioglycolate-elicited mouse peritoneal macrophages [16]. Motivated by this groundwork, in the next series of experiments we examined the outcome of macrophage interaction (3 h in the absence of serum) with *L. major* promastigotes or Δ*isp*2/3 mutants. Consistent with the phenotypic properties of Δ*isp*2/3 promastigotes originally described by Eschenlauer et al. [27], we found that the phagocytic uptake of these mutants was strongly upregulated as compared to WT promastigotes (Figure 2). Next, we asked whether B_2R (constitutively expressed) or B_1R (NFκ-B inducible; [35]) contributed to the phagocytic uptake of *L. major*. Infection assays performed in the presence of HOE-140 or DAL^8-BK (B_1R antagonist) revealed that none of these GPCR antagonists inhibited macrophage uptake of ISP-expressing (WT) *L. major*. In striking contrast, however, both GPCR antagonists efficiently reduced the phagocytic uptake of Δ*isp*2/3 promastigotes by the phagocytes (resp., to 58% and 63%; Figure 2). For reasons that are not clear, the B_1R antagonist had a mild but significant stimulatory effect (39% increase compared with medium) on the uptake of WT *L. major*.

3.3. Surface Exposure of the BK Epitope Differs in WT and Δisp2/3 Promastigotes. Since the studies of macrophage infection by *L. major* promastigotes were routinely performed in the absence of serum, we reasoned that the kinin agonists should either originate from kininogens molecules bound to the surface of macrophages [46] or alternatively from kininogen molecules eventually sequestered from serum by promastigotes. To test the latter possibility, we washed stationary phase *L. major* promastigotes extensively as described for infection assays and then stained the parasites with two different domain-specific mAbs: (i) MBK_3, a monoclonal antibody that recognizes the BK epitope (domain D_4) of kininogens (HK/LK), and (ii) HKH_4, a mAb that recognizes domain D_1 of HK/LK [36]. FACS analysis showed that almost 70% of Δ*isp*2/3 promastigotes are positive stained for HKH4, compared to less than 50% of the WT parasites (Figure 3(a)). Along similar lines, MBK_3 antibody showed that the BK epitope of kininogens was present in a higher proportion of Δ*isp*2/3 promastigotes as compared to WT promastigotes (Figure 3(b), 82,4%) as compared to WT parasites (Figure 3(b), 73.1%). These results suggest that both ISP-expressing *L. major* promastigotes and Δ*isp*2/3 mutants are able to sequester kininogens (retaining the intact BK molecule) from FCS. According to our working hypothesis (Figure 5), the kininogen opsonins tethered on ISP-deficient parasites may be cleaved by pericellular serine proteases (S_{1a} family) of macrophages, whereas the surface-bound kininogens associated to ISP-expressing (WT) *L. major* should be protected from proteolytic cleavage.

3.4. Targeting Activation of the Contact Phase/KKS in Human Plasma with Recombinant ISP-2 or Synthetic Inhibitor of Neutrophil Elastase. Considering that ISP-2 is hardly detected in the supernatants of *L. major* promastigotes (A. P. C. A. Lima, personal communication), we reasoned that we reasoned that this ecotin-like inhibitor may target S_{1A} serine proteases within the secluded spaces formed by the juxtaposition of host cell/parasite plasma membranes. Given the technical obstacles to monitor KKS activation and kinin release in this intercellular compartment, we first asked whether soluble (recombinant) ISP-2 or MeOSuc-AAPV-CMK (NE inhibitor) could inhibit the activation of the human contact system by DXS. This was addressed using a novel enzymatic assay that we recently used to detect the *P. duboscq* sandfly protein inhibitor of the contact system [25]. Briefly, the addition of DXS (500 kDa) to human plasma induces the reciprocal activation of FXII/PK, leading to the accumulation of PKa, the major kinin-releasing (S_{1A} family) in the plasma. Using as-read-outs synthetic substrates spanning the N-terminal or C-terminal flanking sequences of BK in the kininogen molecule, the kinetic measurements shown in our positive controls (Figure 4) reflect DXS-induced hydrolysis of

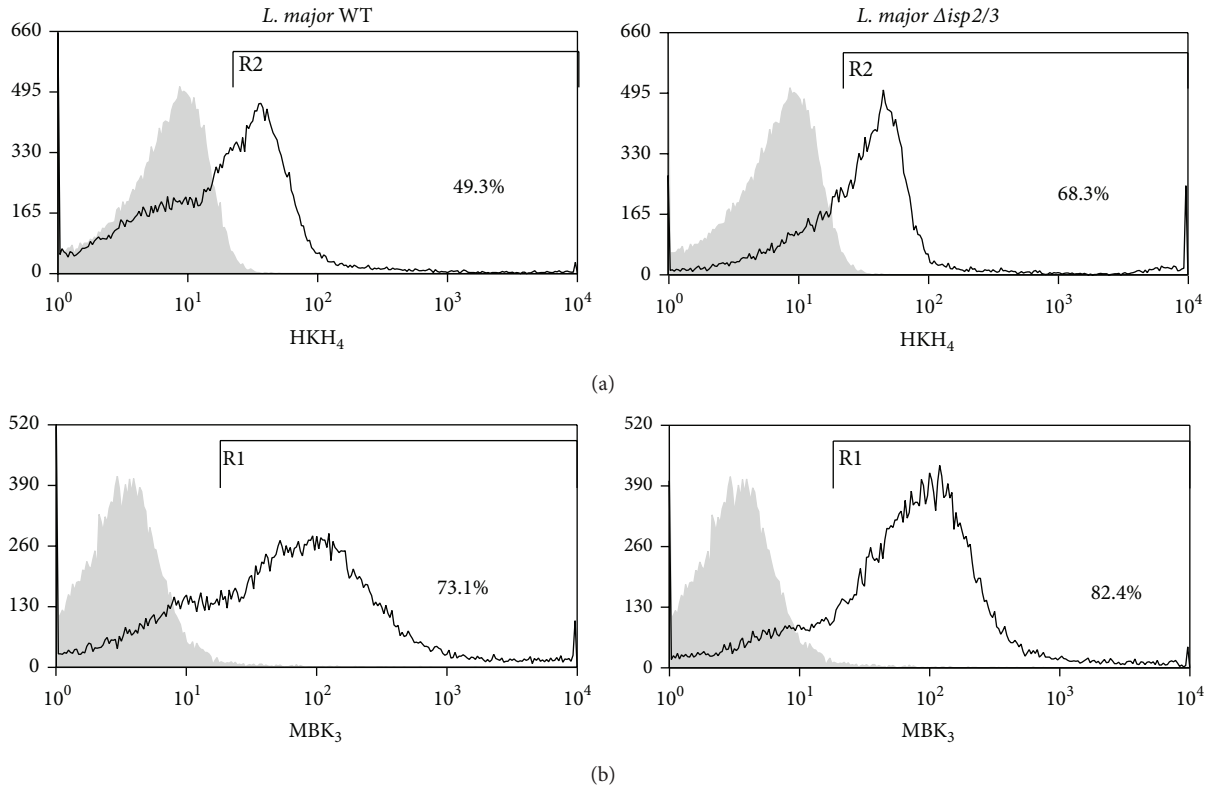

Figure 3: Evidence of differential display of kininogens and BK epitopes on surface of WT *L. major* versus Δ*isp*2/3 promastigotes. WT and Δ*isp*2/3 promastigotes were washed 3x before incubation with mAbs against D1 or D4 (BK epitope) of kininogens, HK/LK (HKH_4 (a) or MBK_3 (b), resp.) for 1 h. Unrelated Ab (IgG_{2a} for HKH_4 or IgG1 for MBK_3 staining) were used as specificity controls. Binding of primary IgG was assessed by incubating the cells with a secondary FITC-labeled anti-mouse IgG antibody for 1 h. The graphs represent the percentage of HK/LK adsorption and are representative of two independent experiments performed in duplicates.

the kininogen-like substrate by PKa [25]. Internal controls run in the presence of the synthetic PKa inhibitor (PKSI-257) show, as expected, pronounced inhibition of the contact phase enzyme by DXS. Assays performed with soluble ISP-2 revealed that the onset of hydrolysis was consistently delayed, in dose-dependent manner (range 142–355 nM; Figures 4(a) and 4(b)). A similar trend was observed when we added MeOSuc-AAPV-CMK (NE inhibitor) to the citrated plasma (range 10–30 μM; Figures 4(c) and 4(d)). Collectively, these findings are consistent with the proposition that the activity of the contact phase enzyme complex (FXIIa/PKa) is at least partially inhibited by ISP-2 (soluble) or by the synthetic NE inhibitor.

4. Discussion

In the current study, we used genetically modified Δ*isp*2/3 mutants of *L. major* to determine whether these ecotin-like inhibitors regulate the proinflammatory activity of the kinin/B_2R pathway *in vivo* and *in vitro*. In the first group of studies, we demonstrated that *L. major* promastigotes potently evoke plasma leakage and induce leukocyte accumulation in microvascular beds through mast cell-dependent activation of the kinin/B_2R pathway, irrespective of the presence or absence of ISP-2. Extending this analysis to *in vitro* infection models, we showed that antagonists of B_2R (HOE-140) or B_1R (DAL^8-BK) efficiently reversed the upregulated phagocytic uptake of *L. major* Δ*isp*2/3 by TG-macrophages without interfering with the internalization of ISP-expressing (WT) promastigotes. As discussed further below, these findings suggested that, upon attachment to the macrophage surface, ISP-expressing promastigotes might suppress the activation of B_2R/B_1R-dependent proinflammatory responses by inhibiting the kinin-releasing activity of serine proteases (S_{1A} family).

While studying the functional interplay between NE and ISP-2 during macrophage infection by *Leishmania*, Faria et al. [31, 32] demonstrated that two prominent phenotypes of Δ*isp*2/3 mutants (upregulated phagocytosis and induction of ROS via the elastase/TLR_4/PKR pathway) were completely reversed in cultures supplemented with three different inhibitors of serine peptidases: aprotinin [27], a non-specific inhibitor of Arg-hydrolyzers, MeOSuc-AAPV-CMK (NE inhibitor), and the *L. major* ISP-2 (soluble/recombinant). Given the precedent that NE and mast cell tryptase (acting cooperatively) liberate bioactive kinin from oxidized kininogens [7], our findings that HOE-140 and DAL^8-BK also reversed the phenotype of Δ*isp*2/3 mutants suggest that ISP-expressing *L. major* might inhibit the pericellular processing of surface-bound HK through the targeting of

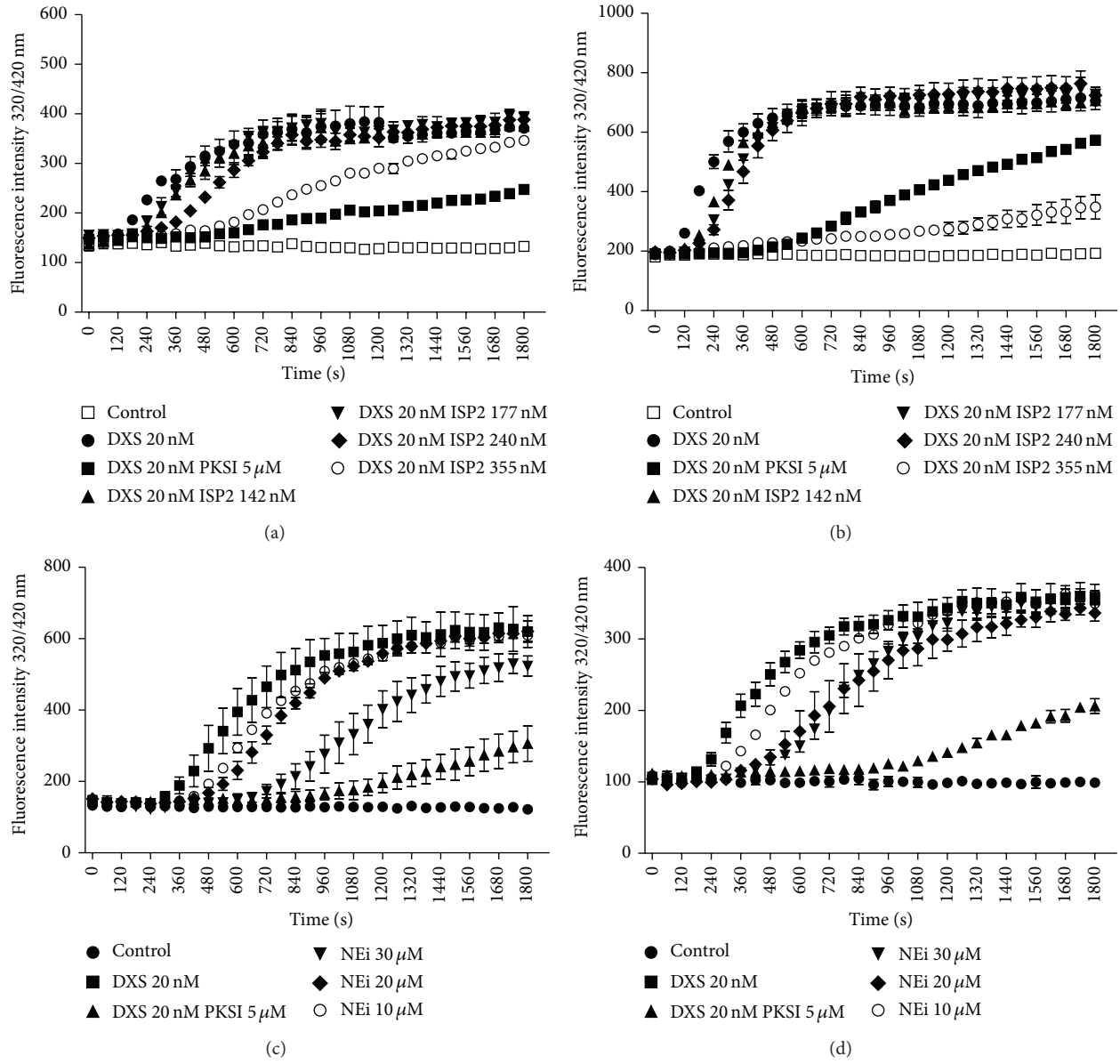

Figure 4: Effect of ISP2 on DXS-induced contact phase activation of human plasma. Citrated human platelet free plasma diluted 1 : 20 in buffer (described in methods) was supplemented with (i) 4 μM Abz-MTEMARRPQ-EDDnp (a, c) or 4 μM Abz-GFSPFRSVTVQ-EDDnp (b, d), intramolecular quenched fluorescent substrates whose sequences span the N-terminal or the C-terminal flanking sites (resp.) of BK in mHK (ii) dextran sulfate 500 kDa (DXS; 20 nM). The substrate was also tested in the absence of DXS (Control). Assays with the elastase inhibitor (NEi—MeOSuc-AAPV-CMK-10, 20, and 30 μM), the synthetic PKa inhibitor (PKSI-527—5 μM), and the inhibitor of serine peptidase 2 (ISP2—142, 177, 240, and 355 nM) were performed using two different schemes. (a, b) PKSI or the elastase inhibitor was added to the plasma together with DXS and the substrate. (c, d) PKSI or ISP2 was preincubated with plasma for 15 min, at 37°C, prior to the addition of DXS and the substrate. Hydrolysis was followed by measuring the fluorescence at $\lambda_{ex.}$ = 320 nm and $\lambda_{em.}$ = 420 nm (up to 1800 seconds). The plot shows the increase of fluorescence with time, reflecting substrate hydrolysis. The values in the figures represent the mean ± SE of duplicate determinations performed within 1 representative experiment of 2.

NE. Alternatively, our finding that soluble ISP-2 (or the NE inhibitor MeOSuc-AAPV-CMK) partially inhibit DXS-induced activation of the contact system in human citrated plasma (i.e., PKa-mediated hydrolysis of the flanking sites of BK in kininogen-like substrates) suggests that ISP-expressing promastigotes might rely on their surface-associated ISP-2 to target the contact phase enzymatic complex (FXIIa/PKa/HK) assembled on macrophage surfaces [46]. Admittedly, genetic studies will be required to dissect whether ISP-2 subverts innate immunity by protecting surface kininogens from the kinin-releasing activity of NE and/or by targeting surface assembled contact phase peptidases (FXII/PK). Although we have not systematically analyzed the impact of pharmacological blockade of B_2R/B_1R on the intracellular parasitism

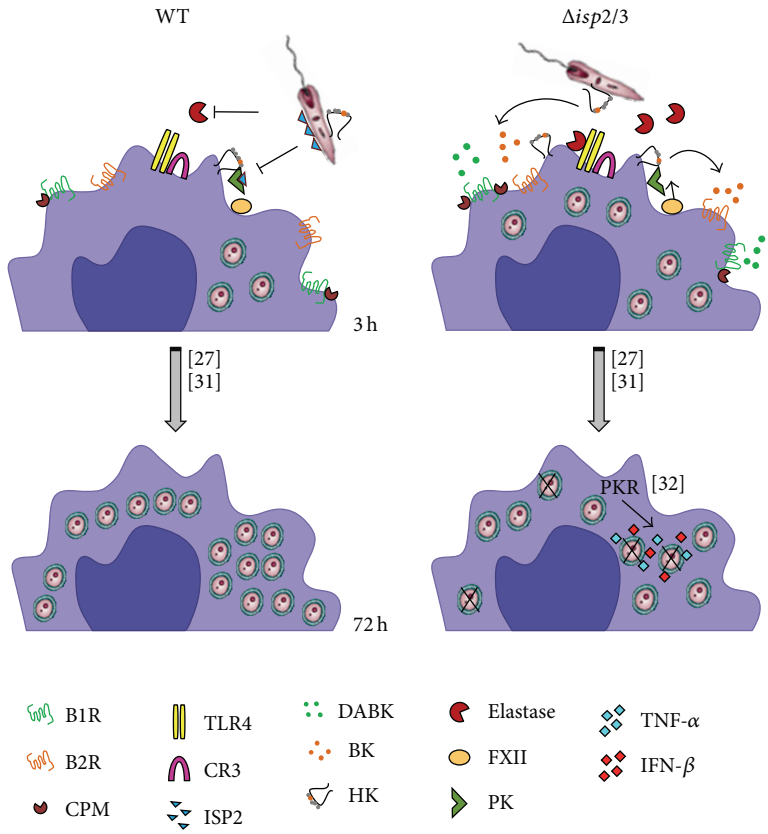

FIGURE 5: Scheme shows how ISP-2 limits the kinin-releasing activity of surface S_1A-proteases of macrophages. As an extension of recently published studies [27, 31, 32], here we propose that the proinflammatory phenotype of the Δ*isp*2/3 mutant (right side of scheme) is due to increased pericellular release of kinins mediated by NE and/or contact phase serine proteases (FXIIa/PKa). In the absence of ISP-2, the "eat me signal" of kininogen tethered on *L. major* mutants might be inactivated by S_1A-family proteases. In addition, the released kinin peptides fuel phagocytosis and microbicidal function of macrophages via activation of B_2R and B_1R, a subtype of GPCR upregulated in inflamed tissues.

of TG-macrophages, preliminary results suggest that HOE-140 (tested at 100 nM) upregulates the outgrowth/survival of Δ*isp*2/3 mutants in TG-macrophages. If confirmed by genetic studies, our results may imply that *L. major* promastigotes might limit ROS formation via the NE/TLR_4/PKR/TNF-α/IFN-β pathway originally described by Faria et al. [32] through ISP-2-dependent targeting of kinin-releasing peptidases assembled at the surface of macrophages.

A key event in many inflammatory processes is the adhesive interaction of circulating neutrophils and activated endothelial cells in postcapillary venules, a process that is often coupled to increased microvascular permeability, which in turn leads to the progressive accumulation of protein-rich edema fluid in interstitial tissues. Although conceding that the dynamics of the inflammatory responses that sand-fly-transmitted *Leishmania* induces in the injured dermis is far more complex than what is described in our intravital microscopy studies, the analysis of microvascular leakage and leukocyte accumulation in HCP topically sensitized with *L. major* promastigotes (WT or ISP2/3-deficient parasites) revealed that these parasites are far more potent inducers of plasma leakage and leukocyte accumulation than *L. donovani* [15], *L. chagasi* promastigotes (Figure 1(c)), or *T. cruzi* trypomastigotes [35]. Although the mechanisms underlying the discrepant phenotypes of *L. major* and *L. chagasi* or *T. cruzi* remain unknown, we were intrigued to find out that a 3X-fold higher dose of *L. chagasi* promastigotes did not evoke such a strong microvascular response, not even after treating the HCP with captopril, an inhibitor of kinin degradation by angiotensin-converting enzyme (Figure 1(c), black curve). In contrast, *T. cruzi* and *L. chagasi* are potentially lethal pathogens that disseminate systemically and preferentially target tissue in organs irrigated by fenestrated capillaries. Under these circumstances, plasma-borne substrates, such as kininogens, diffuse freely into the visceral tissues invaded by these visceralizing species of pathogenic trypanosomatids, both of which were empowered with kinin-releasing cysteine proteases [15, 47–49]. It is noteworthy that B_2R-deficient mice acutely infected by *T. cruzi* [14] or *L. chagasi* [16] display heightened disease susceptibility, implying that the activation of the kinin/B_2R pathway may preferentially shift the host/parasite balance towards protective immunity, at least during the acute phase.

Since proboscis inevitably provokes some extent of bleeding, we may predict plasma proteins and anti-inflammatory substances derived from the insect saliva are rapidly mixed

with metacyclic parasites. Our studies in HCP topically sensitized with *L. major* promastigotes (which prevents bleeding and KKS activation due to pathogen inoculation through needles) suggest that these parasites potently evoke plasma leakage and leukocyte accumulation in microvascular beds via the kinin/B_2R pathway. For reasons that are unclear, we found that Δ*isp*2/3 promastigotes evoked a somewhat milder inflammatory response (20%). Incidentally, Eschenlauer et al. [27] have reported that mice subcutaneously infected with *L. major* promastigotes transiently displayed higher tissue burden of ISP2/ISP-3-deficient parasites as compared to WT parasites. Lasting 3 days, the parasite burden subsequently equalized, implying that the selective advantage conferred to ISP-deficient promastigotes has waned as the infection progressed.

Based on pharmacological approaches, we showed evidences that *L. major* activates the KKS via mechanisms that involve transcellular cross-talk between neutrophils (intravascularly) and mast cells, a subset of innate sentinel cells that are mostly localized in perivascular tissues. Beyond the vasoactive role of histamine, a potent inducer of vascular permeability, mast cells also release heparin and polyphosphates, both of which were recently characterized as endogenous activators of the contact system [50, 51]. Given the interdependent nature of inflammatory circuits, it is likely that mast cells and the KKS/complement cascades are reciprocally activated and fueled in the HCP sensitized with *L. major* promastigotes. Although we have not studied the impact of the influx of complement into peripheral sites of *L. major* infection, it is well-documented that *Leishmania* lipophosphoglycan is opsonized by C3bi [52]. In the absence of other potent inflammatory cues, the engagement of macrophage CR3 by ISP-expressing *L. major* (WT) promastigotes may drive phagocytosis without necessarily stimulating the production of reactive oxygen intermediates, thereby creating a hospitable environment for the intracellular growth of *L. major* [31, 32]. Although studies in CD11b-deficient BALB/c mice have recently confirmed that activation of the C3bi/CR3 pathway increases host susceptibility to *L. major* infection [53], it will be interesting to know whether CR3-dependent suppression of IL-12 responses might depend on parasite-evoked extravasation of complement components to the extravascular compartment, as proposed here for plasma-borne kininogens.

Studies in the mouse ear model of sandfly-transmitted infection showed that *L. major* metacyclic promastigotes deposited in the dermis are engulfed by the infiltrating neutrophils within approximately 3 h [19–21]. Based on the results described in HCP topically sensitized with *L. major* promastigotes, it is conceivable that the proteolytic release of vasoactive kinins may further stimulate the transendothelial migration of neutrophils at very early stages of the infection. Furthermore, given evidence that parasitized neutrophils expose the apoptotic markers required for efferocytosis, it will be interesting to know whether plasma leakage may contribute to DC efferocytosis and to the ensuing suppression of Th1-inductive functions of DCs in the draining lymph nodes [19–21]. Beyond the impact on adaptive immunity, it is well established that efferocytosis of apoptotic neutrophils has profound effect on parasite survival in infected macrophages [22]. In this context, our finding that kininogen epitopes (N-terminal D1 and internal/BK/D4 domain) are tethered at the surface of *Leishmania* promastigotes is an intriguing finding because it raises the possibility that ISP-expressing promastigotes might "protect" the integrity of surface bound kinin precursors from premature proteolytic degradation by host proteolytic enzymes. This hypothesis is worth exploring in light of recent studies showing that HK (an abundant protein in the bloodstream; 660 nM) binds to PS exposed on apoptotic neutrophils before stimulating uPAR-dependent efferocytosis by macrophages via the p130Cas-CrkII-Dock-180-Rac1 pathway [6]. In other words, ISPs may protect the integrity of HK opsonins "eat me signals" while at the same time preventing the liberation of proinflammatory kinins (see scheme, Figure 5) within sites of parasite attachment to phagocytes. Although we have not explored the potential significance of *L. major* opsonization by kininogens, it will be interesting to know whetherparasite subsets bearing the uPAR ligand HK/HKa "eat me signal" might render macrophage permissive to intracellular survival, perhaps reminiscent of the apoptotic mimicry paradigm originally described by Barcinski and coworkers [54].

5. Conclusions

Extending the breadth of our previous investigations about the role of the kallikrein-kinin system in the immunopathogenesis of experimental Chagas disease and visceral leishmaniasis, the studies reported in this paper suggest that ecotin-like inhibitors expressed by *L. major* promastigotes fine-tune phagocytosis and may limit amastigote survival by inhibiting the pericellular activity of kinin-releasing serine proteases (S_{1a} family) of macrophages.

Conflict of Interests

The authors declare that there is no conflict of interests regarding the publication of this paper.

Acknowledgments

This study was supported by grants from CNPq/INBEB, Faperj, and PRONEX. The authors thank Professor Ana Paula Cabral de Araujo Lima (Instituto de Biofísica Carlos Chagas Filho, Universidade Federal do Rio de Janeiro) for kindly providing WT and Δ*isp*2/3 *L. major* and inhibitor of serine peptidase 2 (ISP2) and Professor Werner Müller-Esterl (University of Frankfurt) for donation of anti-kininogen antibodies. They also wish to thank Dr. Marilia Faria (Instituto de Biofísica Carlos Chagas Filho, Universidade Federal do Rio de Janeiro) for independently testing the B_2R and B_1R antagonists in infection assays with macrophages (unpublished data).

References

[1] A. P. Kaplan and K. Joseph, "Pathogenic mechanisms of bradykinin mediated diseases: dysregulation of an innate

inflammatory pathway," *Advances in Immunology*, vol. 121, pp. 41–89, 2014.

[2] C. Maas and T. Renné, "Regulatory mechanisms of the plasma contact system," *Thrombosis Research*, vol. 129, no. 2, pp. S73–S76, 2012.

[3] U. Amara, M. A. Flierl, D. Rittirsch et al., "Molecular intercommunication between the complement and coagulation systems," *Journal of Immunology*, vol. 185, no. 9, pp. 5628–5636, 2010.

[4] D. Ricklin, G. Hajishengallis, K. Yang, and J. D. Lambris, "Complement: a key system for immune surveillance and homeostasis," *Nature Immunology*, vol. 11, no. 9, pp. 785–797, 2010.

[5] Y. T. Wachtfogel, R. A. deLa Cadena, S. P. Kunapuli et al., "High molecular weight kininogen binds to Mac-1 on neutrophils by its heavy chain (domain 3) and its light chain (domain 5)," *Journal of Biological Chemistry*, vol. 269, no. 30, pp. 19307–19312, 1994.

[6] A. Yang, J. Dai, Z. Xie et al., "High molecular weight kininogen binds phosphatidylserine and opsonizes urokinase plasminogen activator receptor-mediated efferocytosis," *The Journal of Immunology*, vol. 192, no. 9, pp. 4398–4408, 2014.

[7] A. Kozik, R. B. Moore, J. Potempa, T. Imamura, M. Rapala-Kozik, and J. Travis, "A novel mechanism for bradykinin production at inflammatory sites: Diverse effects of a mixture of neutrophil elastase and mast cell tryptase versus tissue and plasma kallikreins on native and oxidized kininogens," *Journal of Biological Chemistry*, vol. 273, no. 50, pp. 33224–33229, 1998.

[8] K. M. Heutinck, I. J. M. ten Berge, C. E. Hack, J. Hamann, and A. T. Rowshani, "Serine proteases of the human immune system in health and disease," *Molecular Immunology*, vol. 47, no. 11-12, pp. 1943–1955, 2010.

[9] J. Aliberti, J. P. B. Viola, A. Vieira-de-Abreu, P. T. Bozza, A. Sher, and J. Scharfstein, "Cutting edge: bradykinin induces IL-12 production by dendritic cells: a danger signal that drives Th1 polarization," *Journal of Immunology*, vol. 170, no. 11, pp. 5349–5353, 2003.

[10] C. M. Bertram, S. Baltic, N. L. Misso et al., "Expression of kinin B1 and B2 receptors in immature, monocyte-derived dendritic cells and bradykinin-mediated increase in intracellular Ca^{2+} and cell migration," *Journal of Leukocyte Biology*, vol. 81, no. 6, pp. 1445–1454, 2007.

[11] R. Gulliver, S. Baltic, N. L. Misso, C. M. Bertram, P. J. Thompson, and M. Fogel-Petrovic, "Lys-des[Arg9]-bradykinin alters migration and production of interleukin-12 in monocyte-derived dendritic cells," *American Journal of Respiratory Cell and Molecular Biology*, vol. 45, no. 3, pp. 542–549, 2011.

[12] F. Marceau and D. R. Bachvarov, "Kinin receptors," *Clinical Reviews in Allergy and Immunology*, vol. 16, no. 4, pp. 385–401, 1998.

[13] A. C. Monteiro, V. Schmitz, E. Svensjö et al., "Cooperative activation of TLR2 and bradykinin B2 receptor is required for induction of type 1 immunity in a mouse model of subcutaneous infection by *Trypanosoma cruzi*," *Journal of Immunology*, vol. 177, no. 9, pp. 6325–6335, 2006.

[14] A. C. Monteiro, V. Schmitz, A. Morrot et al., "Bradykinin B2 Receptors of dendritic cells, acting as sensors of kinins proteolytically released by *Trypanosoma cruzi*, are critical for the development of protective type-1 responses," *PLoS Pathogens*, vol. 3, no. 11, pp. 1730–1744, 2007.

[15] E. Svensjö, P. R. Batista, C. I. Brodskyn et al., "Interplay between parasite cysteine proteases and the host kinin system modulates microvascular leakage and macrophage infection by promastigotes of the *Leishmania donovani* complex," *Microbes and Infection*, vol. 8, no. 1, pp. 206–220, 2006.

[16] D. Nico, D. F. Feijó, and N. Maran, "Resistance to visceral leishmaniasis is severely compromised in mice deficient of bradykinin B2-receptors," *Parasites and Vectors*, vol. 5, no. 1, article 261, 2012.

[17] J. Scharfstein, D. Andrade, E. Svensjö, A. C. Oliveira, and C. R. Nascimento, "The kallikrein-kinin system in experimental Chagas disease: a paradigm to investigate the impact of inflammatory edema on GPCR-mediated pathways of host cell invasion by *Trypanosoma cruzi*," *Frontiers in Immunology*, vol. 3, no. 396, pp. 1–20, 2007.

[18] B. Engelmann and S. Massberg, "Thrombosis as an intravascular effector of innate immunity," *Nature Reviews Immunology*, vol. 13, no. 1, pp. 34–45, 2013.

[19] N. C. Peters, J. G. Egen, N. Secundino et al., "In vivo imaging reveals an essential role for neutrophils in leishmaniasis transmitted by sand flies," *Science*, vol. 321, no. 5891, pp. 970–974, 2008.

[20] N. C. Peters, "In vivo imaging reveals an essential role for neutrophils in Leishmaniasis transmitted by sand flies," *Science*, vol. 322, no. 5908, p. 1634, 2008.

[21] F. L. Ribeiro-Gomes, N. C. Peters, A. Debrabant, and D. L. Sacks, "Efficient capture of infected neutrophils by dendritic cells in the skin inhibits the early anti-leishmania response," *PLoS Pathogens*, vol. 8, no. 2, Article ID e1002536, 2012.

[22] F. L. Ribeiro-Gomes, M. C. A. Moniz-de-Souza, M. S. Alexandre-Moreira et al., "Neutrophils activate macrophages for intracellular killing of *Leishmania major* through recruitment of TLR4 by neutrophil elastase," *The Journal of Immunology*, vol. 179, no. 6, pp. 3988–3994, 2007.

[23] A. A. Filardy, D. R. Pires, and G. A. Dosreis, "Macrophages and neutrophils cooperate in immune responses to Leishmania infection," *Cellular and Molecular Life Sciences*, vol. 68, no. 11, pp. 1863–1870, 2011.

[24] R. G. Titus and J. M. C. Ribeiro, "The role of vector saliva in transmission of arthropod-borne disease," *Parasitology Today*, vol. 6, no. 5, pp. 157–160, 1990.

[25] P. H. Alvarenga, X. Xu, F. Oliveira et al., "Novel family of insect salivary inhibitors blocks contact pathway activation by binding to polyphosphate, heparin, and dextran sulfate," *Arteriosclerosis, Thrombosis, and Vascular Biology*, vol. 33, no. 12, pp. 2759–2770, 2013.

[26] F. Müller, N. J. Mutch, W. A. Schenk et al., "Platelet polyphosphates are proinflammatory and procoagulant mediators in vivo," *Cell*, vol. 139, no. 6, pp. 1143–1156, 2009.

[27] S. C. P. Eschenlauer, M. S. Faria, L. S. Morrison et al., "Influence of parasite encoded inhibitors of serine peptidases in early infection of macrophages with *Leishmania major*," *Cellular Microbiology*, vol. 11, no. 1, pp. 106–120, 2009.

[28] C. H. Chung, H. E. Ives, S. Almeda, and A. L. Goldberg, "Purification from *Escherichia coli* of a periplasmic protein that is a potent inhibitor of pancreatic proteases," *The Journal of Biological Chemistry*, vol. 258, no. 18, pp. 11032–11038, 1983.

[29] C. T. Eggers, I. A. Murray, V. A. Delmar, A. G. Day, and C. S. Craik, "The periplasmic serine protease inhibitor ecotin protects bacteria against neutrophil elastase," *The Biochemical Journal*, vol. 379, no. 1, pp. 107–118, 2004.

[30] A. C. Ivens, C. S. Peacock, and E. A. Worthey, "The genome of the kinetoplastid parasite, *Leishmania major*," *Science*, vol. 309, no. 5733, pp. 436–442, 2005.

[31] M. S. Faria, F. C. G. Reis, R. L. Azevedo-Pereira, L. S. Morrison, J. C. Mottram, and A. P. C. A. Lima, "Leishmania inhibitor of serine peptidase 2 prevents TLR4 activation by neutrophil elastase promoting parasite survival in murine macrophages," *The Journal of Immunology*, vol. 186, no. 1, pp. 411–422, 2011.

[32] M. S. Faria, T. C. Calegari-Silva, A. de Carvalho, J. C. Vivarini, U. G. Lopes, and A. P. Lima, "Role of protein kinase R in the killing of Leishmania major by macrophages in response to neutrophil elastase and TLR4 via TNFα and IFNβ," *The FASEB Journal*, vol. 28, no. 7, pp. 3050–3063, 2014.

[33] V. Schmitz, L. N. Almeida, E. Svensjö, A. C. Monteiro, J. Köhl, and J. Scharfstein, "C5a and bradykinin receptor cross-talk regulates innate and adaptive immunity in *Trypanosoma cruzi* infection," *The Journal of Immunology*. In press.

[34] V. Schmitz, E. Svensjö, R. R. Serra, M. M. Teixeira, and J. Scharfstein, "Proteolytic generation of kinins in tissues infected by *Trypanosoma cruzi* depends on CXC chemokine secretion by macrophages activated via Toll-like 2 receptors," *Journal of Leukocyte Biology*, vol. 85, no. 6, pp. 1005–1014, 2009.

[35] D. Andrade, R. Serra, E. Svensjö et al., "*Trypanosoma cruzi* invades host cells through the activation of endothelin and bradykinin receptors: a converging pathway leading to chagasic vasculopathy," *British Journal of Pharmacology*, vol. 165, no. 5, pp. 1333–1347, 2012.

[36] J. Kaufmann, M. Haasemann, S. Modrow, and W. Müller-Esterl, "Structural dissection of the multidomain kininogens. Fine mapping of the target epitopes of antibodies interfering with their functional properties," *The Journal of Biological Chemistry*, vol. 268, no. 12, pp. 9079–9091, 1993.

[37] B. Korkmaz, S. Attucci, M. A. Juliano et al., "Measuring elastase, proteinase 3 and cathepsin G activities at the surface of human neutrophils with fluorescence resonance energy transfer substrates," *Nature Protocols*, vol. 3, no. 6, pp. 991–1000, 2008.

[38] A. Fukumizu and Y. Tsuda, "Amino acids and peptides. LIII. Synthesis and biological activities of some pseudo-peptide analogs of PKSI-527, a plasma kallikrein selective inhibitor: the importance of the peptide backbone," *Chemical and Pharmaceutical Bulletin*, vol. 47, no. 8, pp. 1141–1144, 1999.

[39] E. Svensjö, "Bradykinin and prostaglandin E1, E2 and F2α-induced macromolecular leakage in the hamster cheek pouch," *Prostaglandines and Medicine*, vol. 1, no. 5, pp. 397–410, 1978.

[40] E. Svensjö, K. E. Andersson, E. Bouskela, F. Z. G. A. Cyrino, and S. Lindgren, "Effects of two vasodilatory phosphodiesterase inhibitors on bradykinin-induced permeability increase in the hamster cheek pouch," *Agents and Actions*, vol. 39, no. 1-2, pp. 35–41, 1993.

[41] S. Rosengren, K. Ley, and K.-E. Arfors, "Dextran sulfate prevents LTB4-induced permeability increase, but not neutrophil emigration, in the hamster cheek pouch," *Microvascular Research*, vol. 38, no. 3, pp. 243–254, 1989.

[42] D. C. Höcking, T. J. Ferro, and A. Johnson, "Dextran sulfate inhibits PMN-dependent hydrostatic pulmonary edema induced by tumor necrosis factor," *Journal of Applied Physiology*, vol. 70, no. 3, pp. 1121–1128, 1991.

[43] R. A. Brown, R. Lever, N. A. Jones, and C. P. Page, "Effects of heparin and related molecules upon neutrophil aggregation and elastase release in vitro," *British Journal of Pharmacology*, vol. 139, no. 4, pp. 845–853, 2003.

[44] K. Ley, M. Cerrito, and K.-E. Arfors, "Sulfated polysaccharides inhibit leukocyte rolling in rabbit mesentery venules," *American Journal of Physiology. Heart and Circulatory Physiology*, vol. 260, no. 5, pp. H1667–H1673, 1991.

[45] M. Siebeck, J. C. Cheronis, E. Fink et al., "Dextran sulfate activates contact system and mediates arterial hypotension via B2 kinin receptors," *Journal of Applied Physiology*, vol. 77, no. 6, pp. 2675–2680, 1994.

[46] A. Barbasz and A. Kozik, "The assembly and activation of kinin-forming systems on the surface of human U-937 macrophage-like cells," *Biological Chemistry*, vol. 390, no. 3, pp. 269–275, 2009.

[47] E. del Nery, M. A. Juliano, A. P. C. A. Lima, J. Scharfstein, and L. Juliano, " Kininogenase activity by the major cysteinyl proteinase (cruzipain) from *Trypanosoma cruzi*," *Journal of Biological Chemistry*, vol. 272, no. 41, pp. 25713–25718, 1997.

[48] A. P. C. A. Lima, P. C. Almeida, I. L. S. Tersariol et al., "Heparan sulfate modulates kinin release by *Trypanosoma cruzi* through the activity of cruzipain," *The Journal of Biological Chemistry*, vol. 277, no. 8, pp. 5875–5881, 2002.

[49] J. Scharfstein, V. Schmitz, V. Morandi et al., "Host cell invasion by *Trypanosoma cruzi* is potentiated by activation of bradykinin B2 receptors," *The Journal of Experimental Medicine*, vol. 192, no. 9, pp. 1289–1299, 2000.

[50] C. Oschatz, C. Maas, B. Lecher et al., "Mast cells increase vascular permeability by heparin-initiated bradykinin formation *in vivo*," *Immunity*, vol. 34, no. 2, pp. 258–268, 2011.

[51] D. Moreno-Sanchez, L. Hernandez-Ruiz, F. A. Ruiz, and R. Docampo, "Polyphosphate is a novel pro-inflammatory regulator of mast cells and is located in acidocalcisomes," *Journal of Biological Chemistry*, vol. 287, no. 34, pp. 28435–28444, 2012.

[52] G. F. Späth, L. A. Garraway, S. J. Turco, and S. M. Beverley, "The role(s) of lipophosphoglycan (LPG) in the establishment of *Leishmania major* infections in mammalian hosts," *Proceedings of the National Academy of Sciences of the United States of America*, vol. 100, no. 16, pp. 9536–9541, 2003.

[53] C. R. Carter, J. P. Whitcomb, J. A. Campbell, R. M. Mukbel, and M. A. McDowell, "Complement receptor 3 deficiency influences lesion progression during *Leishmania major* infection in BALB/c Mice," *Infection and Immunity*, vol. 77, no. 12, pp. 5668–5675, 2009.

[54] J. L. M. Wanderley and M. A. Barcinski, "Apoptosis and apoptotic mimicry: the *Leishmania* connection," *Cellular and Molecular Life Sciences*, vol. 67, no. 10, pp. 1653–1659, 2010.

Hindawi Publishing Corporation
Mediators of Inflammation
Volume 2014, Article ID 475919, 13 pages
http://dx.doi.org/10.1155/2014/475919

Research Article

Insulin-Like Growth Factor-I Induces Arginase Activity in *Leishmania amazonensis* Amastigote-Infected Macrophages through a Cytokine-Independent Mechanism

Celia Maria Vieira Vendrame,[1] Marcia Dias Teixeira Carvalho,[1,2] Andre Gustavo Tempone,[3] and Hiro Goto[1,4]

[1] *Laboratório de Soroepidemiologia e Imunobiologia, Instituto de Medicina Tropical de São Paulo, Universidade de São Paulo, Avenida Dr. Enéas de Carvalho Aguiar 470, Predio II, 4° Andar, 05403-000 São Paulo, SP, Brazil*
[2] *Laboratório de Imunofisiopatologia, Instituto de Ciências Biomédicas IV, Universidade de São Paulo, 05508-900 São Paulo, SP, Brazil*
[3] *Departamento de Parasitologia, Instituto Adolfo Lutz, 01246-903 São Paulo, SP, Brazil*
[4] *Departamento de Medicina Preventiva, Faculdade de Medicina, Universidade de São Paulo, 01246-903 São Paulo, SP, Brazil*

Correspondence should be addressed to Hiro Goto; hgoto@usp.br

Received 25 April 2014; Revised 18 July 2014; Accepted 1 August 2014; Published 9 September 2014

Academic Editor: Christophe Chevillard

Leishmania (Leishmania) amazonensis exhibits peculiarities in its interactions with hosts. Because amastigotes are the primary form associated with the progression of infection, we studied the effect of insulin-like growth factor (IGF)-I on interactions between *L. (L.) amazonensis* amastigotes and macrophages. Upon stimulation of infected macrophages with IGF-I, we observed decreased nitric oxide production but increased arginase expression and activity, which lead to increased parasitism. However, stimulation of amastigote-infected macrophages with IGF-I did not result in altered cytokine levels compared to unstimulated controls. Because IGF-I is present in tissue fluids and also within macrophages, we examined the possible effect of this factor on phosphatidylserine (PS) exposure on amastigotes, seen previously in tissue-derived amastigotes leading to increased parasitism. Stimulation with IGF-I induced PS exposure on amastigotes but not on promastigotes. Using a PS-liposome instead of amastigotes, we observed that the PS-liposome but not the control phosphatidylcholine-liposome led to increased arginase activity in macrophages, and this process was not blocked by anti-TGF-β antibodies. Our results suggest that in *L. (L.) amazonensis* amastigote-infected macrophages, IGF-I induces arginase activity directly in amastigotes and in macrophages through the induction of PS exposure on amastigotes in the latter, which could lead to the alternative activation of macrophages through cytokine-independent mechanisms.

1. Introduction

Leishmaniases are diseases with tegumentary or visceral forms that are caused by protozoans of the genus *Leishmania* and are transmitted via insect vectors and affect more than 12 million people in tropical and subtropical areas of the world [1]. *Leishmania (Leishmania) amazonensis* is one of the most prevalent species that causes tegumentary leishmaniasis in the New World causing localized cutaneous, mucosal, or diffuse cutaneous leishmaniases [2]. The control or progression of leishmaniasis in the vertebrate host depends on nonspecific and specific factors of the immune response as well as the ability of the parasite to evade the host response [3]. However, the various disease manifestations and outcomes may result from diverse *Leishmania* species-related immune and immunopathogenic responses and *L. (L.) amazonensis* exhibits peculiarities that distinguish it from other species.

The differences in the immunopathogenic mechanisms of patients infected with either *L. (Viannia) braziliensis* or *L. (L.) amazonensis*, the species that are prevalent in Brazil, are evident. While the response to *L. (V.) braziliensis* infection is related to the exacerbation of the Th1-type response [4–6] or to defects in the modulation of IFN-γ production or decreased IL-10 receptor expression in severe mucosal cases

[6, 7], *L. (L.) amazonensis* infection tends to elicit a less effective or limited T cell-response against the parasite [5, 8], which could explain the development of diffuse cutaneous leishmaniasis in certain cases. These differences are also noticeable in cutaneous leishmaniasis in mice. Compared to *L. major* infection, to which the BALB/c mouse strain is susceptible and the C57BL/6 strain is resistant [9], both mouse strains are resistant to *L. (V.) braziliensis* [10] and both are susceptible to *L. (L.) amazonensis* [11]. The development of lesions in *L. (L.) amazonensis*-infected mice is not only dependent on the Th2 immune response [12] but rather on the presence of Th1 $CD4^+$ T cells [13] and IFN-γ, which promotes parasite growth in amastigote-infected macrophages in vitro [14]. The diverse outcomes and development of specific immune responses during *L. (L.) amazonensis* infection could be attributed to alterations observed during early innate *Leishmania*-host interactions involving inflammatory cytokines, chemokines, Toll-like receptors, dendritic cell activation, and so forth [15]. Thus in the present study, we focused on the effect of a growth factor in the nonspecific interaction between *L. (L.) amazonensis* and macrophages.

Among nonspecific elements, we have been studying the effect of insulin-like growth factor (IGF)-I on *Leishmania* and in leishmaniases. IGFs are polypeptides with a molecular mass of approximately 7.5 kDa, that exist in two major forms, IGF-I and IGF-II, which share 60% similarity and are found in circulation associated with IGF binding proteins and in tissues. IGFs affect cell metabolism and are important endocrine growth and differentiation factors [16]. Based on these characteristics, we previously studied the effect of IGFs on leishmaniasis during their initial interactions as nonspecific factors, though the Th1 cytokine IFN-γ is known to inhibit IGF-I [17], and the Th2 cytokines IL-4 and IL-13 to increase IGF-I expression [18].

We have previously shown that adding physiological concentrations of extrinsic IGF-I into cultures induces proliferation of different species of *Leishmania* promastigotes and axenic amastigotes, which is an effect that is not observed with IGF-II despite its high similarity to IGF-I [19, 20]. In experimental models, extrinsic IGF-I significantly increases lesion sizes and the number of viable parasites [21].

During infection however, the interaction between amastigotes and host cells is critical for the progression of infection and the establishment of disease, which is different to promastigotes. This fact was elegantly proven recently using axenic *Leishmania major* amastigotes [22]. Specifically, comparing *Leishmania (L.) amazonensis* promastigotes and amastigotes showed differences in dendritic cell activation [22], parasitism after IFN-γ stimulation [14], susceptibility to histone proteins [23], and intracellular signaling after IGF-I stimulation [24]. Therefore, in the present study, we analyzed the effects of IGF-I on the interaction between *Leishmania (L.) amazonensis* amastigotes and macrophages.

Because our previous data show that IGF-I favors parasite growth and arginase activation using *Leishmania (L.) amazonensis* promastigotes [25], we initially evaluated parasitism and arginase activity on amastigote-infected macrophages and on cell-free-amastigotes upon IGF-I stimulation. Then, we analyzed inflammatory and Th1 and Th2 cytokine production in infected macrophages upon IGF-I stimulation because of their potential role in macrophage activation [26]. Another phenomenon related to the progression of *L. (L.) amazonensis* infection is the phosphatidylserine (PS) exposure that was observed only on tissue-derived amastigotes [27–29]. Because no induction factor was identified before and IGF-I is present in tissue fluids, we evaluated PS exposure upon IGF-I stimulation and the possible role of the PS molecule on macrophage activation.

In the present study, we thus show that IGF-I induces arginase activity directly in *Leishmania (L.) amazonensis* amastigotes and in amastigote-infected macrophages, the latter through the induction of PS exposure on amastigotes that could lead to the alternative activation of macrophages through cytokine-independent mechanisms.

2. Material and Methods

2.1. Parasites. *Leishmania (Leishmania) amazonensis* (MHOM/BR/73/M2269) was kindly provided by Professor Clara Lucia Barbieri from Universidade Federal de São Paulo and was maintained through regular passage inBALB/c mice. Amastigotes were obtained from footpad lesions of BALB/c mice infected one month earlier. The lesions were aseptically dissected and washed in 0.01 M phosphate-buffered saline pH 7.4 (PBS) and cut and ground in a Petri dish containing PBS. Then, the suspension was disrupted by four passages through 22-gauge needles and centrifuged 3 times at 250 ×g for 10 min; the resulting supernatant was centrifuged at 1,400 ×g for 30 minutes and the parasites were suspended in RPMI 1640 medium (Gibco, Carlsbad, CA, USA). The purified amastigotes were used immediately in the experiments or were expanded to promastigotes and maintained in 199 medium (Gibco) supplemented with 10% heat-inactivated fetal calf serum (Cultilab, Campinas, SP, Brazil) at 26°C. The promastigotes used in these experiments were in the stationary-phase of growth and had undergone no more than four passages in culture.

2.2. Mice. BALB/c mice of both sexes, aged 6–8 weeks, were obtained from the Animal Facility of the Faculdade de Medicina da Universidade de São Paulo and used as a source of peritoneal macrophages or for the in vivo maintenance of *L. (L.) amazonensis.* This study was approved by the Ethical Committee for Animal Research (CEEA), at Biomedical Sciences Institute/Universidade de Sao Paulo, protocol number 041/03, adhering to the Ethical Principles in Animal Research adopted by Brazilian College of Animal Experimentation (COBEA).

2.3. Macrophage Culture, Infection and Stimulation. Resident peritoneal cells were obtained from the peritoneal cavities of BALB/c mice and suspended in RPMI 1640 medium supplemented with 100 UI/mL penicillin, 100 μg/mL streptomycin, and 2% heat-inactivated BALB/c mouse serum (complete medium). The concentration was adjusted to 4-5 × 10^6 cells/mL and the cells were plated in different amounts either on round 13 mm^2glass cover slips placed in the wells

of 24-well plates (Corning Life sciences Tewksbury, MA, USA) or directly into the wells and incubated for 2 h to adhere on the plate at 37°C in a humidified atmosphere containing 5% CO_2. Thereafter, the wells were washed twice with RPMI 1640 medium to remove any nonadherent cells. Then, either adherent cells (macrophages) or *Leishmania* amastigotes or promastigotes were preincubated for 5 minutes with 50 ng/mL recombinant human IGF-I or IGF-II (R & D Systems, Minneapolis, MN, USA) and then washed out. The parasite suspension (2 parasites/1 cell ratio) was dispensed into the wells and allowed to infect for 2 h at 33°C in a humidified atmosphere containing 5% CO_2 and then the noninternalized parasites were washed out and the culture was maintained at 33°C in a humidified atmosphere containing 5% CO_2. In some cases, the IGF-I and IGF-II were maintained throughout the experimental period. Controls were maintained without IGF-I. In some experiments, 100 μM N^G-hydroxy-L-arginine acetate salt (NOHA) (Sigma-Aldrich Co., St. Louis, MO, USA) was added to the culture or used to preincubate the amastigotes for 5 minutes and was washed out [30]. Tests were run in sextuplicate and incubated for 2, 24, 48, or 72 h. The coverslips, supernatants, or cell lysates were recovered for different evaluations. In the experiments for the evaluation of H_2O_2 production, phenol red free medium was used.

2.4. Parasite Burden in Macrophages. The cover slips were removed from the plates, mounted and stained with Giemsa dye and processed for the evaluation of parasitism under a light microscope (Carl Zeiss, Göttingen, Germany). Six hundred cells were counted for each treatment condition. The data are presented as the number of parasites in 100 cells from the formula [(number of parasites: number of infected cells) × (number of infected cells/total number of cells) × 100]. This analysis was performed by two independent observers who were blinded to the experimental conditions.

2.5. Cell and Parasite Lysates: Sample Preparations. Four million cells in 500 μL were plated in 24-well culture plates and infected and stimulated with IGF-I as described previously. Some sets were stimulated with IFN-γ (10 ng/mL) or lipopolysaccharide (LPS) from *Escherichia coli* (Sigma Co., Ltd. (St Louis, MO, USA)) (1 μg/mL) or NOHA (100 μM). After 24 h of incubation, the cells were washed twice with ice-cold PBS and then lysed for 10 minutes with ice-cold lysis buffer (10 mM Tris-HCl pH 7.6, 150 mM NaCl, 2% NP-40 substitute (octylphenoxypolyethoxyethanol), 1 mM 4-(2-aminoethyl)-benzenesulfonyl fluoride and 5 μM leupeptin). The lysed cell preparation was centrifuged at 10,000 ×g for 5 minutes at 4°C and the protein concentration in the supernatant was determined using a Lowry protein assay [31] to adjust the concentrations before analysis. These lysates were used in western blot analyses and arginase expression and activity assays. For the analysis of *Leishmania* amastigote arginase activity, the same lysate preparation protocol was used.

2.6. SDS-PAGE and Western Blot Analysis. Cell lysates (20 μg protein in 20 μL) were run on sodium dodecyl sulphate-10% polyacrylamide gels. The separated proteins were electrotransferred onto 0.2 mm pore size nitrocellulose membranes using transblot SD-semidry transfer cells (Bio Rad, CA, USA; 30 minutes at 15 mV). The membranes were blocked with 150 mM NaCl, 20 mM Tris, 0.01% Tween 20, pH 7.4 buffer (TBS-T buffer) containing 5% fat-free milk for one hour. The membranes were reacted with a monoclonal anti-arginase-I antibody (1 : 1000 in PBS) (BD Biosciences Pharmigen, San Diego, CA, USA) for 2 h at room temperature, washed three times with TBS-T and incubated with a peroxidase-conjugated polyclonal anti-mouse IgG (1 : 1000) (Sigma-Aldrich, Saint Louis, MO, USA) for one hour at room temperature. Rainbow protein molecular weight markers (Bio-Rad Laboratories, Hercules, CA, USA) were used. Bound antibodies were detected by an ECL chemiluminescence kit (Amersham Biosciences, Piscataway, NJ, USA) following the manufacturer's instruction.

2.7. Arginase Activity. Cells and amastigotes were taken from the culture and the obtained lysates were assayed for arginase activity as described previously [32]. Briefly, to activate the arginase, 50 μL of the lysates were treated with the same volume of 5 mM $MnCl_2$, 25 mM Tris-HCl pH 7.4 at 56°C for 10 min. Then, to 25 μL of the activated lysate, 25 μL of 0.5 M L-arginine pH 9.7 were added and incubated at 37°C for 60 min. The reaction was stopped with 400 μL of $H_2SO_4/H_3PO_4/H_2O$ (1/3/7, v/v/v). The urea concentration was measured at 540 nm in a Multiskan MCC/340 P version 2.20 plate reader spectrophotometer (Labsystems, Vantaa, Finland) after the addition of 25 μL of 9% α-isonitrosopropiophenone in 100% methanol and incubation at 100°C for 45 min. One unit of enzyme activity is defined as the amount of enzyme that catalyzes the formation of 1 μmol of urea per minute.

2.8. Detection of Nitrite. Nitrite (NO_2^-) accumulation in the cell culture supernatants was used as an indicator of nitric oxide production and it was determined by the Griess reaction [33]. The absorbance of the reaction product at 570 nm was measured using an ELISA reader. The nitrite concentration was determined using sodium nitrite as a standard.

2.9. Detection of H_2O_2. The assay is based on the horseradish peroxidase (HRPO)-mediated oxidation of phenol red by H_2O_2as described by Pick and Keisari [34]. A standard curve was established using a H_2O_2 solution of known concentration. Phorbol myristate acetate (PMA) 2 mM (Sigma Co., Ltd., St Louis, MO, USA) was used as positive control. Tests were run in sextuplicate.

2.10. Measurement of Cytokines. The cell culture supernatants were harvested after 24 h for the analysis of IL-1β, 48 h for IL-6 and TNF and 72 h for TGF-β and IFN-γ by ELISA according to the manufacturer's instructions using BD OptEIA kits (BD Biosciences, USA) in 96-well tissue culture plates (Corning Costar Co., USA) and read at 450 nm in a Multiskan MCC/340 P version 2.20 spectrophotometer (Labsystems, Vantaa, Finland). The sensitivity of the cytokine

assays was as follows: IFN-γ, 8 pg/mL; IL1-β, 8 pg/mL; IL-6, 16 pg/mL; TGF-β, 20 pg/mL; and TNF, 8 pg/mL. The concentrations were determined by comparison with a curve generated from each cytokine standard. All of the cytokine measurements were performed in triplicate and at the same time to avoid intertest variations.

2.11. Measurement of Prostaglandin E_2 (PGE_2). The assay is based on the competitive binding technique in which the PGE_2 present in the supernatant competes with a fixed amount of alkaline phosphatase-labeled PGE_2 for sites on mouse monoclonal anti-PGE_2 antibodies. The analysis was performed according to the manufacturer's instructions using a Prostaglandin E_2 immunoassay (R&D System, Inc. Minneapolis, MN, USA). The sensitivity of the PGE_2 assay was 15.9 pg/mL. The concentrations were determined by comparison with a standard curve.

2.12. Effect of IGF-I on Phosphatidylserine-Exposure. Annexin V binds to negatively charged phospholipid surfaces with a higher specificity for PS. The detection of annexin V was made by flow cytometry after staining with fluorescein isothiocyanate-conjugated annexin V and propidium iodide (PI) using a commercially available kit (Annexin V FITC Apoptosis Detection KIT II-BD Biosciences). Amastigotes (10^6 parasite/mL) were treated in the same way as described above with 50 or 100 ng/mL IGF-I or with H_2O_2 (4 or 8 mM) [35] as a positive control for 24 h. Then, the cells were washed twice with cold PBS and 100 μL of the solution (10^5cells) was resuspended in annexin V binding buffer (10 mM HEPES, 140 mM NaCl, 2.5 mM $CaCl_2$, pH 7.4) and incubated with 5 μL of annexin V FITC and 5 μL of PI at 4°C for 15 minutes in the dark. After this period, 400 μL of binding buffer was added to each tube and the cells were collected in a BD FACSCalibur (Becton Dickinson, Franklin, NJ, USA) and analyzed by Cell Quest. A total of 10,000 events were harvested from each sample. We evaluated annexin V positive and PI negative populations.

2.13. Effect of the Negatively Charged Lipid PS-Liposome on Arginase Activity of BALB/c Macrophages

2.13.1. Liposome Preparation. Liposomes were prepared by the film-hydration method, using hydrogenated phospholipids (LIPOID Gmbh, Germany) [36]. For the preparation of the negatively charged liposomes (PS-liposomes), saturated egg phosphatidylcholine, saturated egg phosphatidylserine, and cholesterol (Sigma-Aldrich) (7 : 2 : 1 molar ratio) or neutral liposomes (PC-liposomes-control group), phosphatidylcholine, and cholesterol (9 : 1) were dissolved in chloroform : methanol (1 : 1 ratio). The solution was further sonicated for 10 minutes. The mixture was evaporated in a rotary evaporator at 55°C at 60 rpm for 40 minutes in a vacuum and protected from light. A preheated (55°C) solution of 2.25% glycerol (9 mL) was added to the lipid film using glass beads. The swelling process of the preformed liposomes was performed in a rotary evaporator at 55°C at 80 rpm for 60 minutes without a vacuum. The surface charge of neutral and negatively charged liposomes was previously confirmed using the zeta potential analysis, in a Zeta Plus Analyzer (BrookHaven Instr. Corp.). The samples were diluted in 1 mL of 3 mM KCl as recommended by the manufacturer. The diluted samples were then analyzed for ten cycles with a voltage of 4 mV. The phospholipid content of the liposomal formulations was determined by the Stewart assay [37].

2.13.2. Arginase Activity with Liposome. Macrophages (2×10^6/500 μL RPMI 1640 medium) were plated in a 24-well plate and incubated for 2 h to allow adherence at 37°C in a humidified atmosphere containing 5% CO_2. Thereafter, the wells were washed twice with RPMI 1640 to remove any non-adherent cells. Then, we infected some wells with amastigotes (2 parasites/1 cell ratio) or used 30 μL of phosphatidylcholine-(PC-) liposome 30%, 30 μL of PS-liposome 30%, or 30 μL of 2.25% glycerol as stimuli. Unstimulated macrophages were used as a control. We performed the same experiment in parallel using 3 μL of an anti-TGF-β antibody (15 μg/mL) in each well (R&D Systems, Inc., USA). After 24 h, the cells were treated to obtain the lysates and the arginase activity reaction was performed as described above.

2.14. Statistical Analysis. The statistical analyses were performed using GraphPad Prism 5 (GraphPad Software, Inc., San Diego, CA, USA). The data were analyzed by ANOVA with the Student Newman-Keuls contrast post-test and were considered significant when $P < 0.05$. The cytokine absorbances were analyzed after transformation and linear regression. The results are expressed as medians and percentiles (25–75). The Kruskal-Wallis test with the Student Newman-Keuls contrast post-test was used for statistical comparisons among groups using SigmaStat for Windows Version 3.10 (Systal Software, Inc., San Jose, CA, USA). A 0.05 confidence level was considered significant.

3. Results

Using tissue-derived *Leishmania (L.) amazonensis* amastigotes, we initially analyzed the parasitism and arginase activity in infected macrophages and extracellular amastigotes. The effects of IGF-I were assayed in the following three different ways: preincubation of amastigotes or macrophages for 5 minutes with IGF-I that was washed out or with the factor maintained in the culture medium throughout the experimental period. We observed an increase in the number of parasites within macrophages after 48 h of amastigote infection in all IGF-I stimulation conditions tested (Figure 1(a)), as observed previously with promastigotes [25]. We did not observe any effect when IGF-II was used with *L. (L) amazonensis* amastigotes (data not shown).

We observed increased arginase expression after IGF-I stimulation in infected macrophages (Figure 1(b)). To demonstrate that the enzyme activity was present after IGF-I stimulation, we measured the arginase activity by urea determination, and the activity increased after IGF-I treatment (Figure 1(c)). To confirm that the urea was derived from

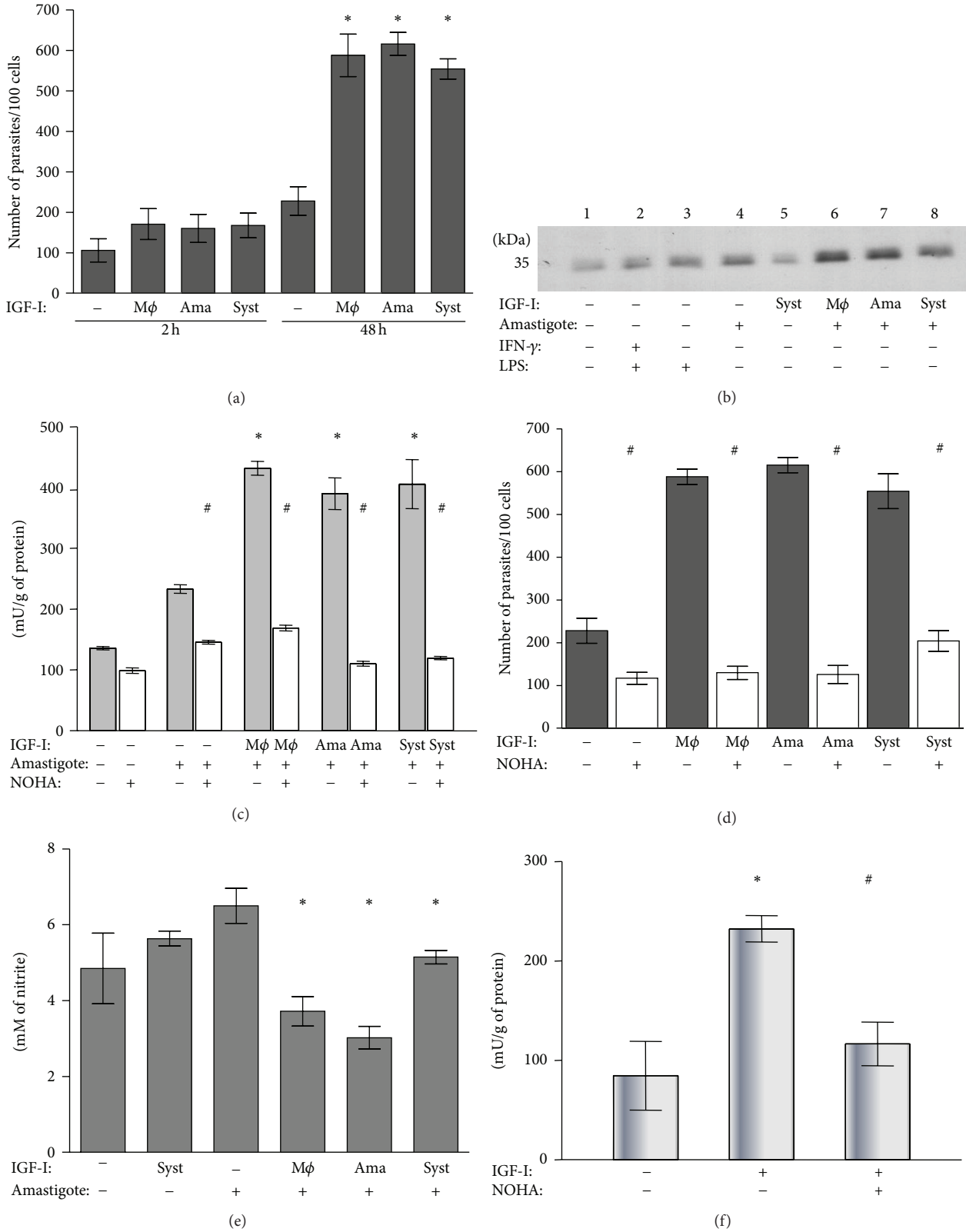

Figure 1: Effect of IGF-I on the *Leishmania* amastigote-macrophage interaction. (a) Parasite burden evaluated after 2 and 48 h of culture. (b) Arginase expression analyzed in infected macrophages at 24 h with western blotting using an anti-arginase-I antibody. (c) Arginase activity evaluated in the interaction measuring urea production with and without the arginase inhibitor NOHA. (d) Effect of inhibition by NOHA on the parasite burden in *Leishmania* amastigote-infected macrophages. (e) Measurement of nitrite production in the culture supernatant by the Griess method. (f) Effect of IGF-I on the arginase activity of *Leishmania* amastigotes. BALB/c peritoneal macrophages were infected with amastigotes of *Leishmania (L.) amazonensis.* Amastigotes (ama) or macrophages (mϕ) were prestimulated for 5 min with IGF-I (50 ng/mL) before interaction or the factors were maintained in the culture system (syst) throughout the experiment period. For further details see Material and Methods Section. $^{*}P < 0.05$ compared with amastigote-infected macrophage without IGF-I stimulation (ANOVA and Student Newman-Keuls tests). $^{\#}P < 0.05$ compared with culture without NOHA (ANOVA and Student Newman-Keuls tests).

arginase activity, a specific arginase inhibitor (NOHA) was used to inhibit urea formation (Figure 1(c)). Urea formation increased relative to unstimulated parasites and was inhibited by NOHA. Parasitism increased with arginase activity and was inhibited by NOHA (Figure 1(d)). However, nitric oxide production decreased significantly compared to that of controls that lack IGF-I (Figure 1(e)). Neither IGF-I nor IGF-II altered the production of hydrogen peroxide in *L. (L.) amazonensis*-infected macrophages (data not shown). Furthermore, arginase activity in IGF-I-stimulated cell-free-amastigotes was also evaluated and arginase activity increased in these conditions (Figure 1(f)).

The balance between Th1 and Th2 cytokines is known to be an important determinant in the activation of the L-arginine metabolic pathways that leads to the production of nitric oxide or polyamines [26] and macrophage stimulation with IL-4, IL-10, and TGF-β induces arginase-I activation and leads to the increased growth of amastigotes within macrophages [30, 38]. In addition to those cytokines, the production of other inflammatory cytokines (IFN-γ, IL-1β, IL-6, IL-10, IL-l2, TGF-β, TNF, and PGE_2) was analyzed in the *Leishmania amazonensis* amastigote-infected macrophages after IGF-I stimulation. IGF-I did not alter cytokine production by amastigote-infected macrophages compared to the controls without IGF-I (Figures 2(a), 2(c), 2(e), 2(g), and 2(i)). Then, as a comparison, we extended the study to analyze cytokine production by *Leishmania* promastigote-infected macrophages upon IGF-I stimulation. No alteration in IL-10, IL-12, and PGE_2 was observed in either *Leishmania* form (data not shown); however, we observed decreased IFN-γ (Figure 2(b)) but increased TGF-β (Figure 2(h)) and TNF (Figure 2(j)) levels compared with those of the nonstimulated promastigote infected-macrophage controls. IGF-I increased production of IL-6 in uninfected macrophages, but while amastigote infection (Figure 2(e)) led to its decrease in IGF-I-stimulated cells, promastigote infection did not promote IL-6 decrease in IGF-I-stimulated cells (Figure 2(f)). IL-1β levels remained low in the amastigote-infected cells (Figure 2(a)) compared with the high levels in the promastigote-infected cells with or without IGF-I stimulation (Figure 2(b)).

Because we did not observe effects due to IGF-I on cytokine production in the amastigote-infected macrophages, we looked for an alternative mechanism that could explain the alternative macrophages activation, focusing on PS exposure on amastigotes described before [27]. We investigated the possible effect of IGF-I on PS exposure on *L. (L.) amazonensis* after IGF-I stimulation. We used hydrogen peroxide stimulation as a positive control [35] that induced PS exposure on control promastigotes but not on control amastigotes. However IGF-I clearly increased PS exposure on amastigotes (Figure 3) but not on promastigotes (data not shown).

We then determined whether PS is involved in inducing arginase activity in macrophages. To restrict the analysis to the effect of this molecule, we used a negatively charged PS-liposome instead of amastigotes. As controls, we used the neutral lipids phosphatidylcholine- (PC-) liposome and glycerol. PS-liposomes have been previously characterized and have exhibited a zeta potential of −88 mV (±20), which is a considerable negative charge when compared to PC-liposomes, which demonstrated a zeta potential of +1.25 mV (±0.2). Exposure to the PS-liposome led to an increase in macrophage arginase activity. Neither the PC-liposome nor glycerol induced arginase activity in macrophages (Figure 4). Additionally, we observed no change in the arginase activity induced by the PS-liposomes in the macrophages using an anti-TGF-β antibody (Figure 4).

4. Discussion

In the present study, we used tissue-derived amastigotes to simulate conditions similar to those in infected tissues in vivo. Initially, we observed the alternative activation of macrophages with increased arginase expression and activity and decreased nitric oxide production in *L. (L.) amazonensis* amastigote-infected macrophages, which lead to increased parasitism after IGF-I stimulation. These findings were similar to previous observations of promastigote-infected macrophages [25]. Reactive oxygen and reactive nitrogen intermediates are important nonspecific parasiticidal elements [39] and both superoxide and nitric oxide have been previously shown to be necessary for *L. (L.) amazonensis* amastigote killing within macrophages [40]. In our experiments, we evaluated hydrogen peroxide production and found that it was not increased during amastigote or promastigote infection and was not altered upon IGF-I stimulation (data not shown). However, in the present study, only the decrease in NO production upon IGF-I exposure was sufficient to increase parasitism in the macrophage. Regarding this result, we should consider the additional effect of IGF-I on activation of *Leishmania* arginase in our system. The parasite arginase is vital for its growth and arginase gene deletion has been shown to impair the progression of infection in vitro and in vivo [41, 42]. Factors that activate *Leishmania* arginase were unknown, but in our previous study with promastigotes [25] as well as in our present study with amastigotes, we show that a host IGF-I does activate parasite arginase.

Because the observed alternative macrophage activation could have been due to the modulation of cytokine production [26], we analyzed cytokine production after IGF-I stimulus [25]. In *L. (L.) amazonensis* amastigote-infected macrophages, we observed no alteration of cytokines production after IGF-I stimulation compared to unstimulated infected controls, suggesting that macrophage arginase activation due to amastigote infection does not involve the modulation of cytokine production. Interestingly, in a parallel analysis, the production of the same cytokines in *L. (L.) amazonensis* promastigote-infected macrophages showed alterations upon IGF-I stimulus. We observed decreased IFN-γ but increased TGF-β and TNF levels compared with those in unstimulated promastigote-infected macrophages, which suggest that increased TGF-β and decreased IFN-γ lead to the alternative activation of macrophages upon IGF-I stimulus in *L. (L.) amazonensis* promastigote-infected macrophages. TGF-β production was already increased during infection with *L. (L.) amazonensis* promastigotes as previously observed [43] and was further increased by IGF-I

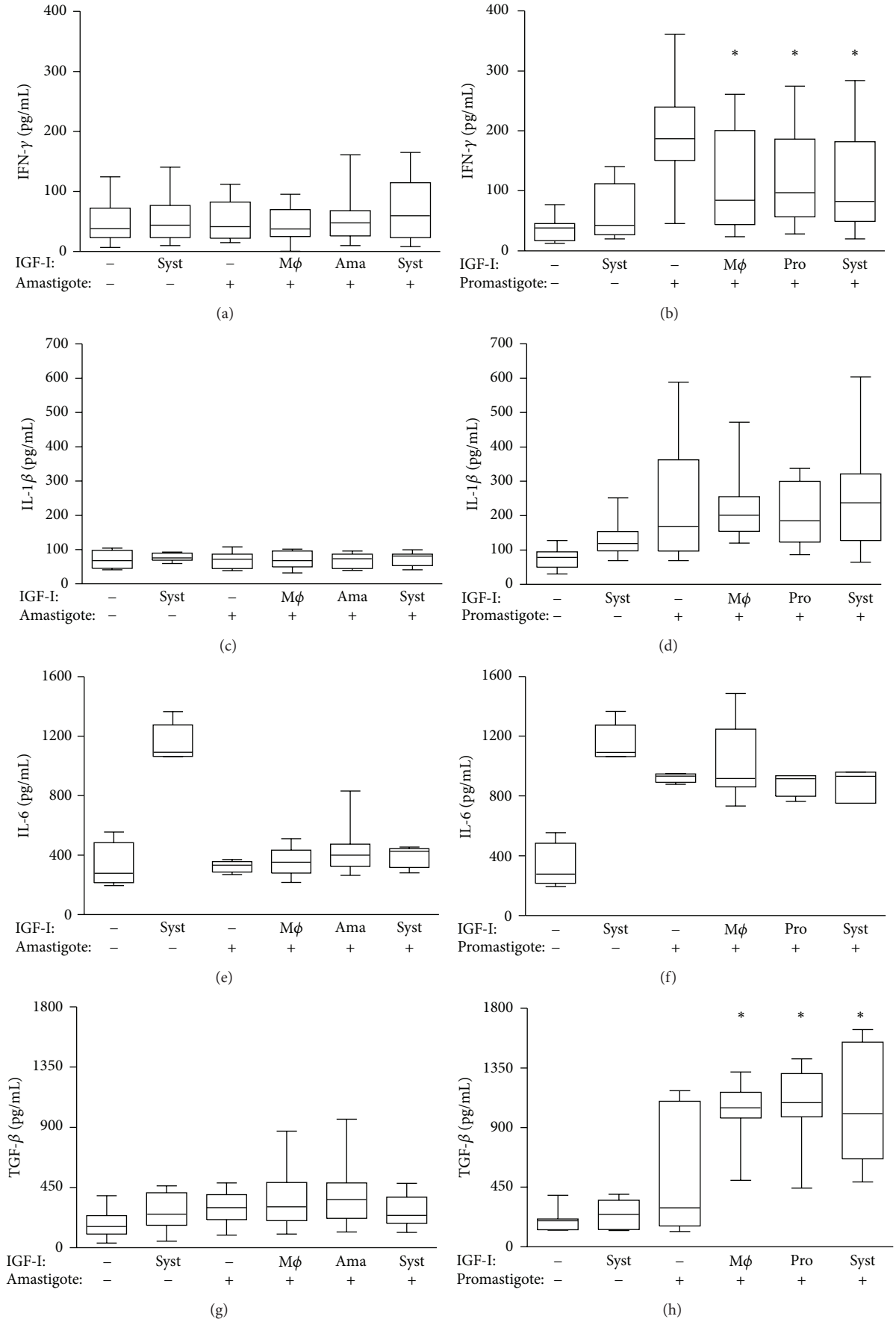

Figure 2: Continued.

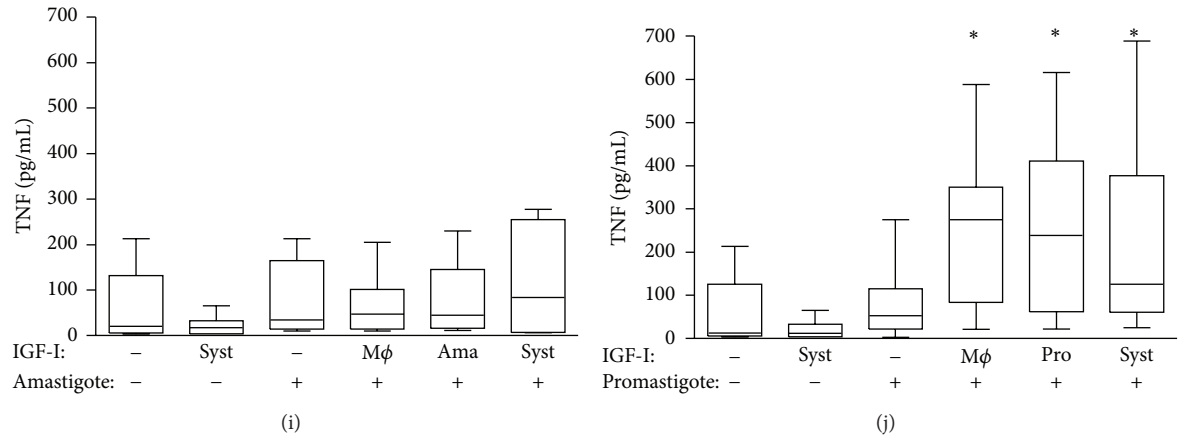

Figure 2: Effect of IGF-I on cytokine production by BALB/c peritoneal macrophages infected with amastigotes or promastigotes of *L. (L.) amazonensis*. Cytokine levels were determined in the culture supernatant by ELISA: IFN-γ: (a) and (b); IL1-β: (c) and (d); IL-6: (e) and (f); TGF-β: (g) and (h); TNF: (i) and (j). Boxes represent the median values and the 25th and 75th percentiles (3 experiments, $n = 6$). Mϕ = macrophage, ama = amastigote, pro = promastigote and Syst = System. $^{*}P < 0.05$ compared with promastigote-infected macrophage without IGF-I stimulation. (Kruskal-Wallis test with the Student Newman-Keuls contrast post-test).

exposure in the present study. The presence of IFN-γ in the culture supernatant could have originated from contaminant lymphocytes because peritoneal macrophages were used; however, such lymphocyte contamination, if any, would be very low and the production of IFN-γ by macrophages has been shown previously [44]; therefore, we believe that the IFN-γ originated from macrophages and that its production decreased after IGF-I stimulation.

Although cytokine production was not altered by IGF-I stimulation in amastigote-infected macrophages, when compared with the promastigote-infected macrophages, we observed differences in the production of IL-1β and IL-6. IL-1β production was not altered in amastigote-infected macrophages but increased in promastigote-infected macrophages, and no changes were observed after IGF-I stimulation. We also observed increased IL-6 upon IGF-I stimulus in uninfected macrophages that remained increased at the same level in promastigote-infected cells but decreased in amastigote-infected cells to the level of the uninfected, unstimulated cells. These data suggest that amastigotes suppress cytokine production in general. In line with our results, IL-1β production was previously shown to be suppressed in *Leishmania donovani* amastigote-infected human monocytes [45]. Moreover, *L. major* amastigotes did not induce the production of the proinflammatory cytokine TNF and the chemokines CCL3 and CCL4, which is in contrast to the higher production during promastigote infection [22]. Similarly, with *Leishmania donovani* amastigotes, a significant proportion of genes were shown to be suppressed in host cells [46].

No alteration in cytokine production that we observed in the amastigote-infected macrophages was also observed in a study with *Leishmania major* where parasite arginase was further shown to affect host cell arginase activation [42]. This finding would be interesting to confirm with *L. (L.) amazonensis* but here we investigated PS exposure on tissue-derived *L (L.) amazonensis* amastigotes as it relates to the progression of the infection and is called apoptotic mimicry [27]. The induction factor was previously unknown, and because IGF-I is present in tissue fluids [47] and within macrophages [48] which is the amastigotes niche, we considered the possible effect of this factor on PS exposure in amastigotes. In fact, IGF-I stimulation induced PS exposure on *L. amazonensis* amastigotes but, interestingly, not on promastigotes. A recent publication regarding *Leishmania* promastigotes shows the absence of PS in this form of the parasite [49] although in our experiment with promastigotes the hydrogen peroxide induced exposure of PS or some similar molecule that has bound to anexin V (data not shown). However, we should emphasize that apoptotic mimicry [27] and the present results refer to PS exposure on amastigotes, and the presence of PS is considered to be likely in other growth phases by the same authors [49].

In the study on apoptotic mimicry, increased parasite growth was attributed to TGB-β production [27]; however, in the present study, we explored the effect of PS exposure on arginase activity in macrophages. Using PS-liposomes to restrict the analysis to this particular molecule, we were able to show that in fact PS-liposomes but not the control PC-liposomes led to increased arginase activity in the macrophages. Furthermore, neutralization of TGF-β using an anti-TGF-β antibody had no effect on arginase activity. Of note, PS-liposomes were previously shown to have an effect on L-arginine metabolism, leading to a decrease in NO production by lipopolysaccharide-stimulated macrophages [50]. In the present study, we also observed decreased nitric oxide production but increased arginase activity after IGF-I stimulation in amastigote-infected cells, suggesting the preferential activation of the alternative macrophage pathway, possibly due to PS exposure on amastigotes after stimulation. Further studies must be performed to clarify how PS-liposomes activate macrophage arginase, but because

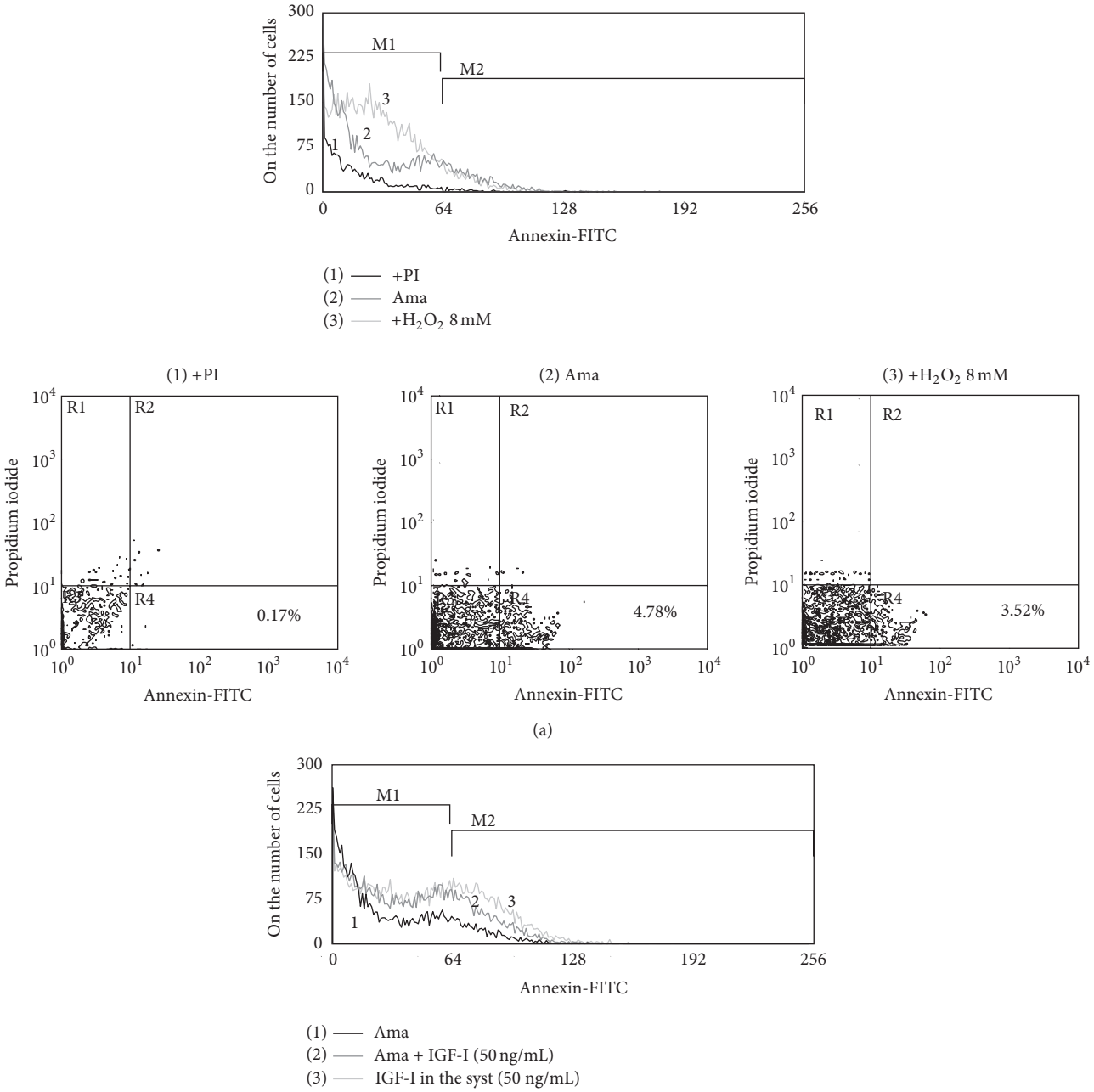

Figure 3: Continued.

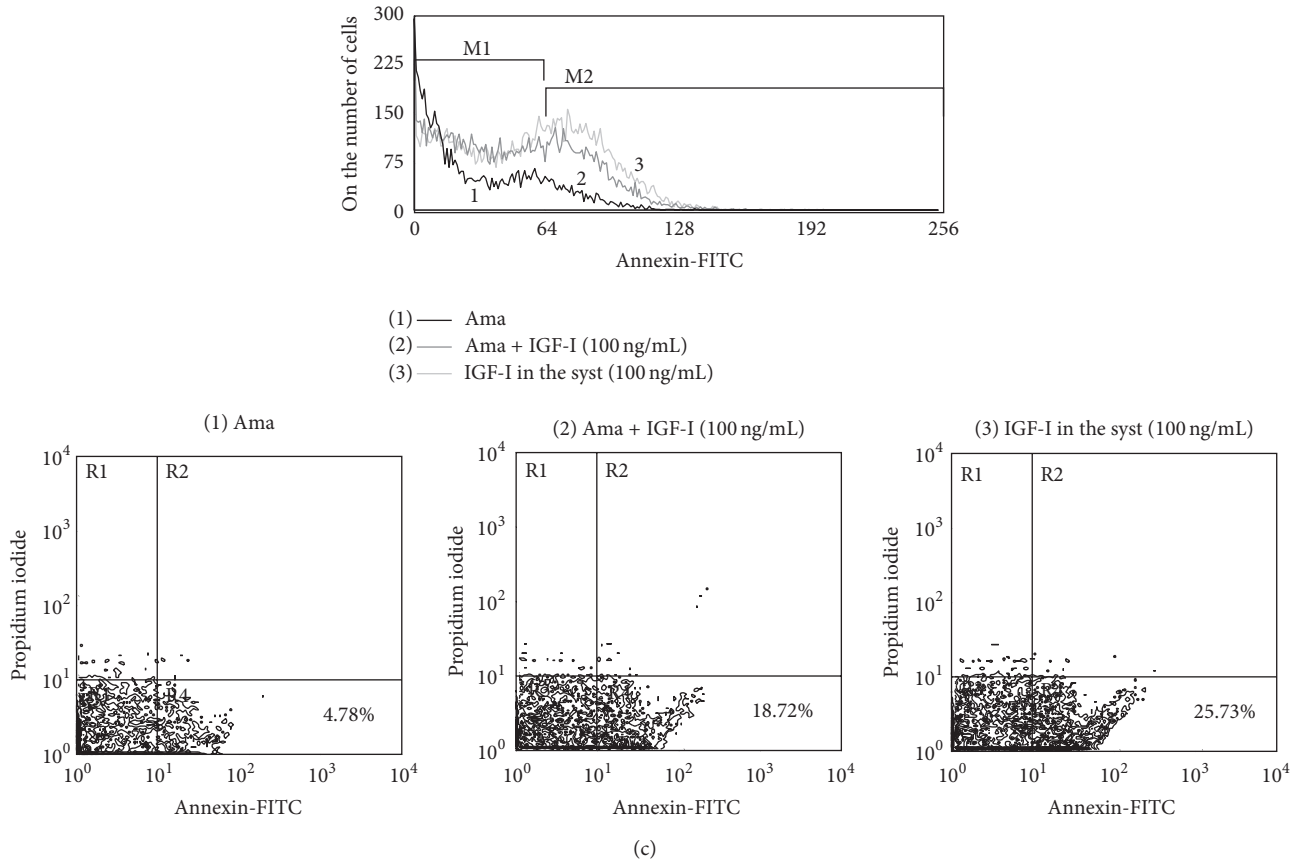

Figure 3: Effect of IGF-I on Annexin V binding to *L. (L.) amazonensis* after IGF-I stimulation. Annexin V-FITC binding to parasites by flow cytometry. (a) Controls. (1) Negative control-amastigotes without Annexin V-FITC label; only with propidium iodide (PI) stain; (2) Unstimulated amastigotes. (3) Positive control-amastigotes after 8 mM H_2O_2 stimulation. (b) IGF-I (50 ng/mL) stimulation and (c) IGF-I (100 ng/mL) stimulation. (1) Unstimulated amastigotes. (2) Amastigotes prestimulated for 5 min and maintained in culture without IGF-I for 24 h. (3) Amastigotes maintained in culture (syst) with IGF-I for 24 h. The results are representative of 3 independent experiments. Data were collected in a BD FACScalibur and analyzed by CellQuest Pro (BD Biosciences). A total of 10,000 events were harvested from each sample.

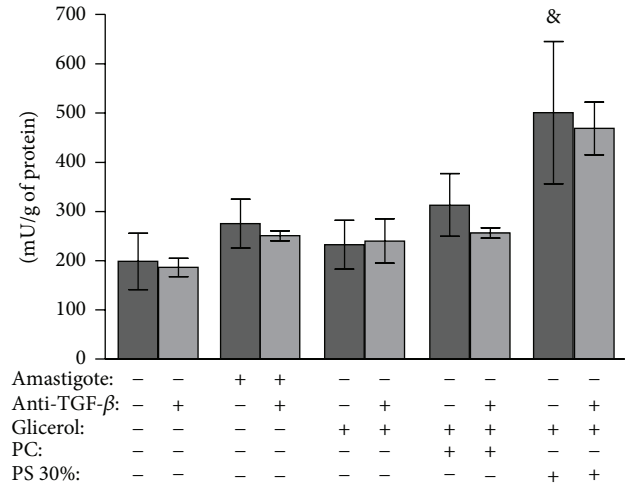

Figure 4: Effect of negatively charged lipid phosphatidylserine (PS)-liposomes on arginase activity of BALB/c macrophages. Peritoneal macrophages were infected with phosphatidylserine- (PS-) liposomes, phosphatidylcholine- (PC-) liposome or glycerol. Amastigotes of *Leishmania (L.) amazonensis* were used as controls. In parallel, an anti-TGF-β antibody was used in all interaction conditions. Macrophages were lysed and the arginase activity was determined by measuring the urea level. Assays were run in triplicate. The data are presented as the mean ± standard deviation of enzyme activity units (amount of enzyme that catalyzes the formation of 1 μmol urea/min). The results are representative of two similar experiments. $^{\&}P < 0.05$ compared with control without liposome (ANOVA and Student Newman-Keuls tests).

arginase is a trimeric metalloenzyme that contains a binuclear manganese cluster in the active site [51], we can speculate that the negative charge of the PS-liposome could carry manganese through cell membrane when PS-liposomes are internalized by macrophages [37], providing manganese to the enzyme and activating it.

Studies using mouse [52] and human cells [53] show an increased *Leishmania* parasite burden when apoptotic neutrophils are ingested by macrophages. This increased burden occurs when using neutrophils derived from the *Leishmania major*-susceptible BALB/c mouse strain. Considering the data from the present study, we can speculate that this phenomenon may be related to the arginase activation induced by PS exposure on apoptotic cells. In the above-mentioned studies, the effect was related to the induction of PGE_2 and TGF-β production [52, 53]; however, our data contradict this observation as a possible mechanism in the present experiments.

The present data suggest that in *L. (L.) amazonensis* amastigote-infected macrophages, IGF-I induces arginase activity directly on amastigotes and also in macrophages. The cytokine production data suggest that amastigote infection leads to the suppression of cytokine production with no contribution to macrophage activation upon IGF-I stimulation. A phenomenon that is seemingly peculiar to *L. (L.) amazonensis* is the induction of PS exposure on amastigotes, which was previously observed on tissue-derived amastigotes and was induced by IGF-I and contributes to the progression of the infection in the present study. Finally, we should emphasize that the activation of macrophage arginase by PS-liposomes leads to the alternative activation of macrophages through cytokine-independent mechanisms.

Conflict of Interests

The authors declare that there is no conflict of interests regarding the publication of this paper.

Acknowledgments

This study was supported by Fundação de Amparo à Pesquisa do Estado de São Paulo (Grant no. 01/13009-9 and fellowship 01/08799-0 to CMVV), Conselho Nacional de Pesquisa (research fellowship 304064/2005-0 to HG and Grant no. 484499/2006-8), and the Seropidemiology and Immunobiology Laboratory LIM/38 (HC-FMUSP). The authors thank Fabrício Pettito-Assis for help with liposome experiments.

References

[1] P. Desjeux, "Leishmaniasis: current situation and new perspectives," *Comparative Immunology, Microbiology and Infectious Diseases*, vol. 27, no. 5, pp. 305–318, 2004.

[2] H. Goto and J. A. Lauletta Lindoso, "Cutaneous and mucocutaneous leishmaniasis," *Infectious Disease Clinics of North America*, vol. 26, no. 2, pp. 293–307, 2012.

[3] A. C. Cunningham, "Parasitic adaptive mechanisms in infection by Leishmania," *Experimental and Molecular Pathology*, vol. 72, no. 2, pp. 132–141, 2002.

[4] A. M. Da-Cruz, R. Bittar, M. Mattos et al., "T-cell-mediated immune responses in patients with cutaneous or mucosal leishmaniasis: long-term evaluation after therapy," *Clinical and Diagnostic Laboratory Immunology*, vol. 9, no. 2, pp. 251–256, 2002.

[5] F. T. Silveira, R. Lainson, C. M. de Castro Gomes, M. D. Laurenti, and C. E. P. Corbett, "Immunopathogenic competences of Leishmania (V.) braziliensis and L. (L.) amazonensis in American cutaneous leishmaniasis," *Parasite Immunology*, vol. 31, no. 8, pp. 423–431, 2009.

[6] L. P. Carvalho, S. Passos, O. Bacellar et al., "Differential immune regulation of activated T cells between cutaneous and mucosal leishmaniasis as a model for pathogenesis," *Parasite Immunology*, vol. 29, no. 5, pp. 251–258, 2007.

[7] D. R. Faria, K. J. Gollob, J. Barbosa Jr. et al., "Decreased in situ expression of interleukin-10 receptor is correlated with the exacerbated inflammatory and cytotoxic responses observed in mucosal leishmaniasis," *Infection and Immunity*, vol. 73, no. 12, pp. 7853–7859, 2005.

[8] A. B. B. Macedo, J. C. Sánchez-Arcila, A. O. Schubach et al., "Multifunctional CD4+T cells in patients with American cutaneous leishmaniasis," *Clinical and Experimental Immunology*, vol. 167, no. 3, pp. 505–513, 2012.

[9] W. J. Beil, G. Meinardus-Hager, D.-C. Neugebauer, and C. Sorg, "Differences in the onset of the inflammatory response to cutaneous leishmaniasis in resistant and susceptible mice," *Journal of Leukocyte Biology*, vol. 52, no. 2, pp. 135–142, 1992.

[10] F. J. S. Rocha, U. Schleicher, J. Mattner, G. Alber, and C. Bogdan, "Cytokines, signaling pathways, and effector molecules required for the control of Leishmania (Viannia) braziliensis in mice," *Infection and Immunity*, vol. 75, no. 8, pp. 3823–3832, 2007.

[11] B. A. S. Pereira and C. R. Alves, "Immunological characteristics of experimental murine infection with Leishmania (Leishmania) amazonensis," *Veterinary Parasitology*, vol. 158, no. 4, pp. 239–255, 2008.

[12] L. C. C. Afonso and P. Scott, "Immune responses associated with susceptibility of C57BL/10 mice to Leishmania amazonensis," *Infection and Immunity*, vol. 61, no. 7, pp. 2952–2959, 1993.

[13] L. Soong, C.-H. Chang, J. Sun et al., "Role of CD4+ T cells in pathogenesis associated with Leishmania amazonensis infection," *Journal of Immunology*, vol. 158, no. 11, pp. 5374–5383, 1997.

[14] H. Qi, J. Ji, N. Wanasen, and L. Soong, "Enhanced replication of Leishmania amazonensis amastigotes in gamma interferon-stimulated murine macrophages: implications for the pathogenesis of cutaneous leishmaniasis," *Infection and Immunity*, vol. 72, no. 2, pp. 988–995, 2004.

[15] L. Soong, "Subversion and utilization of host innate defense by Leishmania amazonensis," *Frontiers in Immunology*, vol. 3, article 58, 2012.

[16] J. I. Jones and D. R. Clemmons, "Insulin-like growth factors and their binding proteins: biological actions," *Endocrine Reviews*, vol. 16, no. 1, pp. 3–34, 1995.

[17] S. Arkins, N. Rebeiz, D. L. Brunke-Reese, A. Biragyn, and K. W. Kelley, "Interferon-gamma inhibits macrophage insulin-like growth factor-I synthesis at the transcriptional level," *Molecular Endocrinology*, vol. 9, no. 3, pp. 350–360, 1995.

[18] M. W. Wynes and D. W. H. Riches, "Induction of macrophage insulin-like growth factor-I expression by the Th2 cytokines IL-4 and IL-13," *Journal of Immunology*, vol. 171, no. 7, pp. 3550–3559, 2003.

[19] H. Goto, C. M. C. Gomes, C. E. P. Corbett, H. P. Monteiro, and M. Gidlund, "Insulin-like growth factor I is a growth-promoting factor for Leishmania promastigotes and amastigotes," *Proceedings of the National Academy of Sciences of the United States of America*, vol. 95, no. 22, pp. 13211–13216, 1998.

[20] C. M. C. Gomes, H. Goto, C. E. P. Corbett, and M. Gidlund, "Insulin-like growth factor-1 is a growth promoting factor for Leishmania promastigotes," *Acta Tropica*, vol. 64, no. 3-4, pp. 225–228, 1997.

[21] C. M. D. C. Gomes, H. Goto, V. L. Ribeiro Da Matta, M. D. Laurenti, M. Gidlund, and C. E. P. Corbett, "Insulin-like growth factor (IGF)-I affects parasite growth and host cell migration in experimental cutaneous leishmaniasis," *International Journal of Experimental Pathology*, vol. 81, no. 4, pp. 249–255, 2000.

[22] U. A. Wenzel, E. Bank, C. Florian et al., "Leishmania major parasite stage-dependent host cell invasion and immune evasion," *The FASEB Journal*, vol. 26, no. 1, pp. 29–39, 2012.

[23] Y. Wang, Y. Chen, L. Xin et al., "Differential microbicidal effects of human histone proteins H2A and H2B on Leishmania promastigotes and amastigotes," *Infection and Immunity*, vol. 79, no. 3, pp. 1124–1133, 2011.

[24] C. M. C. Gomes, H. P. Monteiro, M. Gidlund, C. E. P. Corbett, and H. Goto, "Insulin-like growth factor-I induces phosphorylation in Leishmania (Leishmania) mexicana promastigotes and amastigotes," *Journal of Eukaryotic Microbiology*, vol. 45, no. 3, pp. 352–355, 1998.

[25] C. M. V. Vendrame, M. D. T. Carvalho, F. J. O. Rios, E. R. Manuli, F. Petitto-Assis, and H. Goto, "Effect of insulin-like growth factor-I on Leishmania amazonensis promastigote arginase activation and reciprocal inhibition of NOS2 pathway in macrophage in vitro," *Scandinavian Journal of Immunology*, vol. 66, no. 2-3, pp. 287–296, 2007.

[26] F. O. Martinez and S. Gordon, "The M1 and M2 paradigm of macrophage activation: time for reassessment," F1000Prime Rep, 2014.

[27] J. M. De Freitas Balanco, M. E. Costa Moreira, A. Bonomo et al., "Apoptotic mimicry by an obligate intracellular parasite downregulates macrophage microbicidal activity," *Current Biology*, vol. 11, no. 23, pp. 1870–1873, 2001.

[28] A. Tripathi and C. M. Gupta, "Transbilayer translocation of membrane phosphatidylserine and its role in macrophage invasion in Leishmania promastigotes," *Molecular and Biochemical Parasitology*, vol. 128, no. 1, pp. 1–9, 2003.

[29] J. França-Costa, J. L. M. Wanderley, P. Deolindo et al., "Exposure of phosphatidylserine on Leishmania amazonensis isolates is associated with diffuse cutaneous leishmaniasis and parasite infectivity," *PloS one*, vol. 7, no. 5, Article ID e36595, 2012.

[30] V. Iniesta, L. C. Gómez-Nieto, and I. Corraliza, "The inhibition of arginase by N(omega)-hydroxy-l-arginine controls the growth of Leishmania inside macrophages," *Journal of Experimental Medicine*, vol. 193, no. 6, pp. 777–784, 2001.

[31] O. H. Lowry, N. J. Rosebrough, A. L. Farr, and R. J. Randall, "Protein measurement with the folin phenol reagent," *The Journal of Biological Chemistry*, vol. 193, no. 1, pp. 265–275, 1951.

[32] I. M. Corraliza, M. L. Campo, G. Soler, and M. Modolell, "Determination of arginase activity in macrophages: a micromethod," *Journal of Immunological Methods*, vol. 174, no. 1-2, pp. 231–235, 1994.

[33] L. C. Green, D. A. Wagner, J. Glogowski, P. L. Skipper, J. S. Wishnok, and S. R. Tannenbaum, "Analysis of nitrate, nitrite, and [15N]nitrate in biological fluids," *Analytical Biochemistry*, vol. 126, no. 1, pp. 131–138, 1982.

[34] E. Pick and Y. Keisari, "A simple colorimetric method for the measurement of hydrogen peroxide produced by cells in culture," *Journal of Immunological Methods*, vol. 38, no. 1-2, pp. 161–170, 1980.

[35] M. Das, S. B. Mukherjee, and C. Shaha, "Hydrogen peroxide induces apoptosis-like death in Leishmania donovani promastigotes," *Journal of Cell Science*, vol. 114, no. 13, pp. 2461–2469, 2001.

[36] A. G. Tempone, R. A. Mortara, H. F. de Andrade, and J. Q. Reimão, "Therapeutic evaluation of free and liposome-loaded furazolidone in experimental visceral leishmaniasis," *International Journal of Antimicrobial Agents*, vol. 36, no. 2, pp. 159–163, 2010.

[37] A. G. Tempone, D. Perez, S. Rath, A. L. Vilarinho, R. A. Mortara, and H. F. de Andrade Jr., "*Targeting Leishmania* (L.) chagasi amastigotes through macrophage scavenger receptors: the use of drugs entrapped in liposomes containing phosphatidylserine," *Journal of Antimicrobial Chemotherapy*, vol. 54, no. 1, pp. 60–68, 2004.

[38] V. Iniesta, L. C. Gómez-Nieto, I. Molano et al., "Arginase I induction in macrophages, triggered by Th2-type cytokines, supports the growth of intracellular Leishmania parasites," *Parasite Immunology*, vol. 24, no. 3, pp. 113–118, 2002.

[39] C. Bogdan, M. Rollinghoff, and A. Diefenbach, "Reactive oxygen and reactive nitrogen intermediates in innate and specific immunity," *Current Opinion in Immunology*, vol. 12, no. 1, pp. 64–76, 2000.

[40] R. M. Mukbel, C. Patten Jr., K. Gibson, M. Ghosh, C. Petersen, and D. E. Jones, "Macrophage killing of Leishmania amazonensis amastigotes requires both nitric oxide and superoxide," *The American Journal of Tropical Medicine and Hygiene*, vol. 76, no. 4, pp. 669–675, 2007.

[41] S. C. Roberts, M. J. Tancer, M. R. Polinsky, K. Michael Gibson, O. Heby, and B. Ullman, "Arginase plays a pivotal role in polyamine precursor metabolism in Leishmania: characterization of gene deletion mutants," *The Journal of Biological Chemistry*, vol. 279, no. 22, pp. 23668–23678, 2004.

[42] H. M. Muleme, R. M. Reguera, A. Berard et al., "Infection with arginase-deficient Leishmania major reveals a parasite number-dependent and cytokine-independent regulation of host cellular arginase activity and disease pathogenesis," *Journal of Immunology*, vol. 183, no. 12, pp. 8068–8076, 2009.

[43] P. K. Ramos, V. Brito Mde, F. T. Silveira et al., "In vitro cytokines profile and ultrastructural changes of microglia and macrophages following interaction with Leishmania," *Parasitology*, vol. 141, no. 8, pp. 1052–1063, 2014.

[44] M. Munder, M. Mallo, K. Eichmann, and M. Modolell, "Murine macrophages secrete interferon γ upon combined stimulation with interleukin (IL)-12 and IL-18: a novel pathway of autocrine macrophage activation," *Journal of Experimental Medicine*, vol. 187, no. 12, pp. 2103–2108, 1998.

[45] N. E. Reiner, W. Ng, C. B. Wilson, W. R. McMaster, and S. K. Burchett, "Modulation of in vitro monocyte cytokine responses to Leishmania donovani: interferon-γ prevents parasite-induced inhibition of interleukin 1 production and primes monocytes to respond to Leishmania by producing both tumor necrosis factor-α and interleukin 1," *Journal of Clinical Investigation*, vol. 85, no. 6, pp. 1914–1924, 1990.

[46] S. Buates and G. Matlashewski, "General suppression of macrophage gene expression during Leishmania donovani infection," *Journal of Immunology*, vol. 166, no. 5, pp. 3416–3422, 2001.

[47] D. A. Rappolee, D. Mark, M. J. Banda, and Z. Werb, "Wound macrophages express TGF-α and other growth factors in vivo: analysis by mRNA phenotyping," *Science*, vol. 241, no. 4866, pp. 708–712, 1988.

[48] L. C. Reis, E. M. Ramos-Sanchez, and H. Goto, "The interactions and essential effects of intrinsic insulin-like growth factor-I on Leishmania (Leishmania) major growth within macrophages," *Parasite Immunology*, vol. 35, no. 7-8, pp. 239–244, 2013.

[49] A. Weingärtner, G. Kemmer, F. D. Müller et al., "Leishmania promastigotes lack phosphatidylserine but bind annexin V upon permeabilization or miltefosine treatment," *PLoS ONE*, vol. 7, no. 8, Article ID e42070, 2012.

[50] Y. Aramaki, R. Matsuno, and S. Tsuchiya, "Involvement of p38 MAP kinase in the inhibitory effects of phosphatidylserine liposomes on nitric oxide production from macrophages stimulated with LPS," *Biochemical and Biophysical Research Communications*, vol. 280, no. 4, pp. 982–987, 2001.

[51] E. Cama, F. A. Emig, D. E. Ash, and D. W. Christianson, "Structural and functional importance of first-shell metal ligands in the binuclear manganese cluster of arginase I," *Biochemistry*, vol. 42, no. 25, pp. 7748–7758, 2003.

[52] F. L. Ribeiro-Gomes, A. C. Otero, N. A. Gomes et al., "Macrophage interactions with neutrophils regulate Leishmania major infection," *Journal of Immunology*, vol. 172, no. 7, pp. 4454–4462, 2004.

[53] L. Afonso, V. M. Borges, H. Cruz et al., "Interactions with apoptotic but not with necrotic neutrophils increase parasite burden in human macrophages infected with Leishmania amazonensis," *Journal of Leukocyte Biology*, vol. 84, no. 2, pp. 389–396, 2008.

Hindawi Publishing Corporation
Mediators of Inflammation
Volume 2014, Article ID 902038, 10 pages
http://dx.doi.org/10.1155/2014/902038

Review Article

Trypanosoma cruzi Infection and Host Lipid Metabolism

Qianqian Miao[1,2] and Momar Ndao[1,2]

[1] *National Reference Centre for Parasitology, Research Institute of McGill University Health Centre, Montreal General Hospital, Montreal, QC, Canada H3G 1A4*
[2] *Department of Microbiology and Immunology, McGill University, Montreal, QC, Canada H3A 2B4*

Correspondence should be addressed to Momar Ndao; momar.ndao@mcgill.ca

Received 26 April 2014; Accepted 5 August 2014; Published 3 September 2014

Academic Editor: Marcelo T. Bozza

Trypanosoma cruzi is the causative agent of Chagas disease. Approximately 8 million people are thought to be affected worldwide. Several players in host lipid metabolism have been implicated in *T. cruzi*-host interactions in recent research, including macrophages, adipocytes, low density lipoprotein (LDL), low density lipoprotein receptor (LDLR), and high density lipoprotein (HDL). All of these factors are required to maintain host lipid homeostasis and are intricately connected via several metabolic pathways. We reviewed the interaction of *T. cruzi* with each of the relevant host components, in order to further understand the roles of host lipid metabolism in *T. cruzi* infection. This review sheds light on the potential impact of *T. cruzi* infection on the status of host lipid homeostasis.

1. Introduction

Trypanosoma cruzi (*T. cruzi*) is the etiological agent of Chagas disease (CD). It is estimated that 8 million people are infected worldwide [1]. In the endemic area of South and Central America, CD is transmitted through contact with the feces of the triatomine bug (the kissing bug). When taking a blood meal from a human, the bug defecates on the skin where *T. cruzi* can enter the wound or the mucosal membrane by scratching. Effective vector-control programs have greatly decreased disease transmission in these areas [2, 3]. However, CD was brought to North America, Europe, and Asia by infected individuals, through migration in recent years. In nonendemic area, CD is transmitted through blood transfusion, organ transplantation, and congenital transmission [4].

During the *T. cruzi* infection process, the parasite interacts with a wide range of host immunological and metabolic factors. In the past decade, special attention was given to the close relationship between *T. cruzi* infection and host lipid metabolism. Several research groups have uncovered the interaction between *T. cruzi* and players in the host cholesterol transport and storage system such as macrophage [5–7], adipocytes [8], low density lipoprotein (LDL), and high density lipoprotein (HDL) [9–11]. The molecular landscape and impact of these relationships in *T. cruzi* infection and pathogenesis, as well as host immunological responses and inflammatory reactions, will be reviewed in this paper.

There are three stages in CD progression: acute, indeterminate, and chronic. Although the majority of infected individuals are asymptomatic while carrying the life-long infection, some develop severe symptoms upon infection. During the acute stage, infected individuals may develop unspecific symptoms such as fever, nausea, diarrhea, and rash, as well as severe symptoms such as a raised inflammatory lesion at the site of parasite entry (chagoma), unilateral periorbital edema (Romana's sign), lymphadenopathy, and hepatosplenomegaly [12]. The majority of patients survive the acute stage and enter the prolonged indeterminate stage without overt symptoms of disease, which lasts for life. However, thirty percent of patients develop chronic CD, which includes grave symptoms such as megaesophagus, megacolon, and chronic heart disease [13].

T. cruzi has a complex life cycle and undergoes several transformations during the infection process. The parasite exists mainly in its epimastigote form in the triatomine vector. It transforms into metacyclic trypomastigote in the hind

gut of the vector which is then defecated to infect human host. Once in the host, the metacyclic form infects a wide range of phagocytic (i.e., monocytes, neutrophils, mast cells, and macrophages) and nonphagocytic cells (i.e., epithelial cells, endothelial cells, fibroblasts, and mesenchymal cells). Upon infection, trypomastigotes transform into intracellular amastigotes and divide by binary fission. Once the division process is complete, amastigotes transform back into blood trypomastigotes which escape the cell to infect neighbouring cells or enter the blood circulation [14].

2. *T. cruzi* Infection and Macrophage Lipid Bodies

Lipid bodies (LB), also named lipid droplets or adiposomes, are lipid-rich organelles existing in almost all organisms. Unlike other organelles, lipid bodies are uniquely surrounded by a monolayer of phospholipids [15]. The core of the lipid body is rich in neutral lipids, mainly triacylglycerol and sterol esters, as well as other putative membranous structures [15]. Historically, lipid bodies were thought to function in neutral lipid storage and transport; however, recent research has uncovered their importance in regulation of host immune responses. Lipid bodies are involved in the formation of paracrine mediator eicosanoids in cells involved in inflammatory processes [16, 17]. The number of lipid bodies in leukocytes increases in response to a variety of inflammatory conditions, such as atherosclerosis and mycobacterial infections [18, 19].

During acute *T. cruzi* infection, host macrophages are strongly activated and will inhibit parasite replication [20]. It has been demonstrated that activated murine macrophages are capable of killing the parasites *in vitro* [5–7]. The macrophage inhibition of parasite replication also correlated positively with increases in the oxidative burst activity [21], tumor necrosis factor-alpha production (TNF-α) [7], and nitric oxide secretion [22]. Macrophages from more resistant C57/BL6 mice strain also secreted higher TNF-α in the *in vivo* experiments compared to macrophages from the susceptible strains, such as C3H and BALB [23]. In macrophage-depleted *T. cruzi* infected rats, myocardial parasite load as well as blood parasitemia was significantly increased compared to control [24]. When irradiate rats, which have very low numbers of T and B lymphocytes, were treated with recombinant Interferon-γ (IFN-γ), which classically activates host macrophages, *T. cruzi* parasite load was significantly reduced [25]. These findings demonstrated the importance of macrophage in the clearance of parasites. However, the roles of macrophage in *T. cruzi* infection may not be as simple as previously thought. Certain features of macrophage activation may aid in parasite survival in the host. Melo showed that, during acute *T. cruzi* infection, there is a prominent increase in the number of lipid bodies in macrophages [26]. This increase in lipid body formation correlated with increased parasite load *in vivo* [27]. It was further demonstrated that the induction of lipid body formation during *T. cruzi* infection was Toll-like receptor (TLR-2) dependent and was enhanced by the uptake of apoptotic cells, which causes macrophage to interact with $\alpha_v\beta 3$ integrin and activates TGF-β-dependent lipid body formation [27, 28]. Increased levels of TGF-β are known to cause phagocytic cells to become permissive to *T. cruzi* infection [29, 30] (Figure 1(a)).

Increased lipid body formation also led to increased eicosanoid prostaglandin E_2 (PGE_2) production in inflammatory macrophages. Prostaglandins are known to inhibit TNF-α and IFN-γ production, while enhancing TGF-β secretion [31–33]. Release of prostaglandins reduces macrophage trypanocidal function [31, 34]. Although the impact of PGE_2 release in *T. cruzi* infection is contradictory, the release of PGE_2 was correlated in resistance against certain strains of *T. cruzi* infection [35]. In addition, treatment with nonsteroidal anti-inflammatory drugs (NSAIDs) or cyclooxygenase (COX) inhibitors was able to modulate lipid body formation and decrease PGE_2 production, which led to decreased parasite growth in macrophages [27, 36].

Furthermore, these newly formed lipid bodies also varied significantly in size and light density, which indicated the structural participation of these organelles in immune responses to *T. cruzi* infection. The structural alterations of LB in macrophages may be related to the different lipid compositions in the organelle, stage of new LB formation, or fluctuation of the arachidonate production and concentration [37]. Ultrastructural investigation revealed that the newly formed lipid bodies are localized in close proximity to macrophage phagolysosomes or even within these structures. This suggests that lipid bodies may interact with the phagolysosomes during acute *T. cruzi* infection [38]. Lipid bodies are known to provide nutrients to intracellular parasites such as *Leishmania chagasi,* which are located in the phagolysosome [39]. The relationship between lipid body and phagolysosome can also be beneficial to the host. As reviewed by Melo et al., lipids recruited during lipid body formation, such as arachidonic acid (AA), are able to activate actin assembly, phagosome-lysosome fusion, and phagosome maturation [40, 41]. In addition, these lipids can activate phagosomal nicotinamide adenine dinucleotide phosphate-(NADPH-) oxidase, which leads to pathogen elimination [42]. The implication of the close localization of lipid bodies and phagolysosome in *T. cruzi* infected macrophages needs to be further investigated.

3. *T. cruzi* Infection and Host Adipose Tissue

Adipose tissue is one of the largest organs in the host. It is comprised of a wide range of cell types including adipocytes, pericytes, monocytes, macrophages, and endothelial cells [43]. The function of adipose tissue has long been considered to be energy storage. More than 95% of adipocyte cell mass is lipid droplets where triglycerides and cholesterol esters are stored [44]; however, it was recently uncovered that the functions of adipose tissue include not only energy storage, but also metabolic regulation, neuroendocrine, and immune regulations [45]. Adipose tissue is home to a variety of adipokines, such as adiponectin [46], leptin [47], and resistin

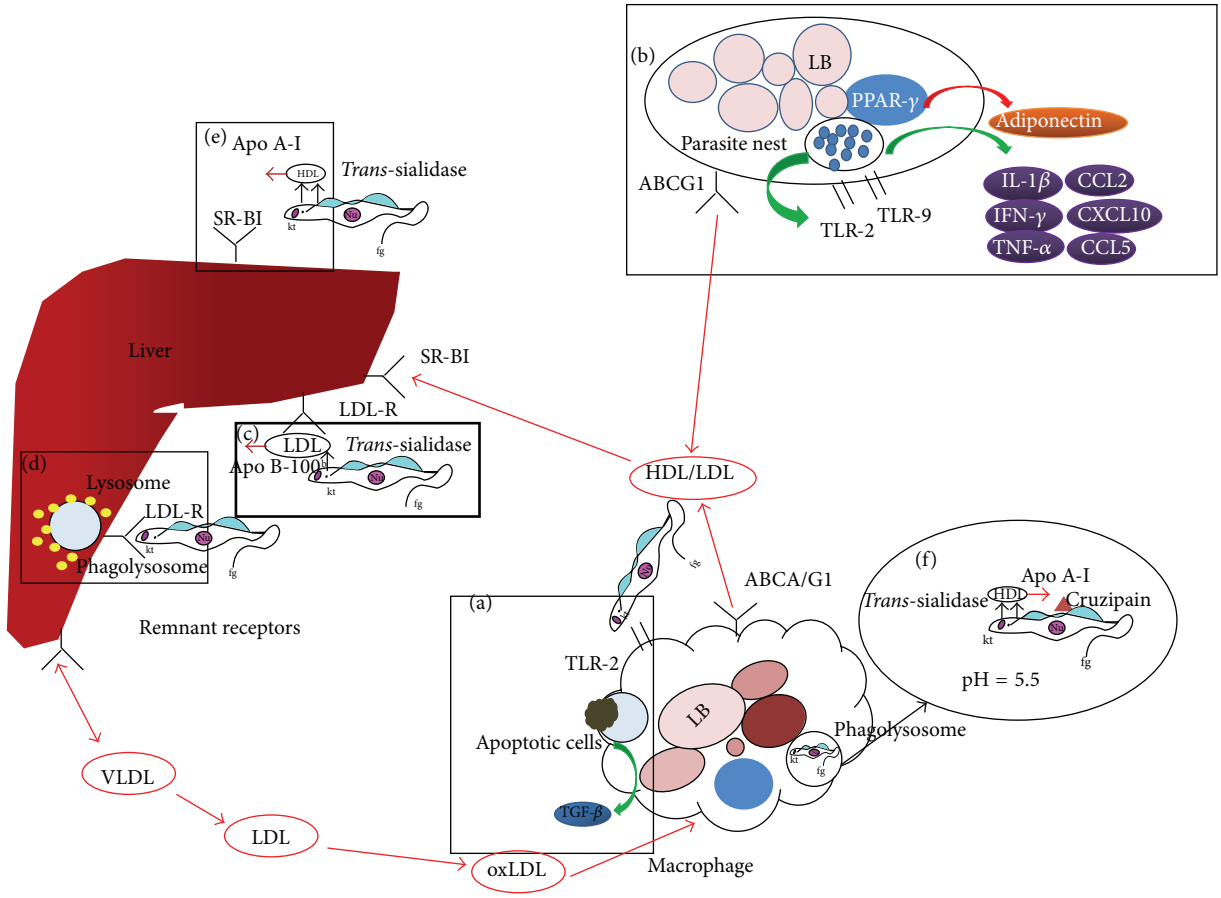

FIGURE 1: *Trypanosoma cruzi* interacting with various components of host lipid metabolism. (a) *T. cruzi* infects macrophage and activates TLR-2 signaling which causes the increased lipid bodies (LB) number and altered LB morphology. This effect is further enhanced by macrophage uptake of apoptotic cells. Increased LB number causes increased eicosanoid production, which leads to upregulation of TGF-β and increased cell susceptibility to *T. cruzi* infection. (b) *T. cruzi* uses adipocytes as a reservoir for chronic infection. *T. cruzi* infection causes adipocytes to display an inflammatory phenotype, upregulating cytokines such as IL-1β, IFN-γ, TNF-α, CCL2, CXCL10, and CCL5. TLR-2 and 9, which are essential to *T. cruzi* infection, are also upregulated. The infection also causes downregulation of adiponectin secretion via PPAR-γ expression. (c) Host LDL inhibits *T. cruzi trans*-sialidase and increases *T. cruzi* infection *in vitro*. LDL can be taken up by the liver and extrahepatic cells by LDLR. It is unknown whether LDL-LDLR interaction plays a role in *T. cruzi* infection. (d) *T. cruzi* enters host cell via LDLR. LDL-R activation leads to lysosomal recruitment to parasitophorous vacuole and parasite internalization. (e) HDL inhibits *T. cruzi trans*-sialidase activity and increases *T. cruzi* infection *in vitro*. HDL is uptaken by host cells via receptor mediated interaction with SR-BI. Whether this interaction can be utilized by *T. cruzi* cell entry process is not known. (f) Apo A-I in the HDL complex is cleaved by the major cysteine protease of *T. cruzi*, cruzipain. Cruzipain and *trans*-sialidase are similarly expressed and located during different life stages of *T. cruzi*. It is possible that HDL is bound to the surface of *T. cruzi* trypomastigotes by *trans*-sialidase and is cleaved by cruzipain in the acidic environment in the parasitophorous vacuole. Host cholesterol transport by VLDL, LDL, and HDL is indicated in red arrows. Host VLDL and lipid-poor nascent HDL particles are produced in the liver. By effluxing cholesterol, host VLDL transforms to become LDL and nascent HDL becomes mature HDL. LDL particles can be oxidized and uptaken by macrophage. Lipid-laden macrophages are termed foam cells and are major contributors in host atherosclerosis development. HDL effluxes cholesterol from peripheral tissue via the action of ABCA1 or ABCG1 and returns cholesterol to hepatic tissues for storage or excretion.

[48], which are prominent regulators of lipid homeostasis and immunological functions.

Recently, metabolic dysfunction was linked to CD pathogenesis by the observation that there are greater incidences of diabetes in *T. cruzi* infected individuals [49]. Later research showed decreased insulin level and dysregulated glucose responses among CD patients [50, 51], which further demonstrated the dysregulation of energy metabolism in these patients. It was also shown that chemically induced diabetic mice as well as genetically predisposed *db*/*db* diabetic mice with defective leptin receptors had higher parasitemia and mortality after *T. cruzi* infection, which suggests that the dysregulation of host metabolism may be beneficial to parasitic survival in the host [52].

Adipocytes are the key cell type in metabolic dysregulations such as diabetes [53]. The role of adipocytes in CD pathogenesis was therefore investigated. Mice infected with *T. cruzi* showed symptoms of hypoglycemia during the acute

stage of infection; however, insulin sensitivity was unaltered [54]. Levels of adiponectin and leptin were significantly reduced in *T. cruzi* infected mice, which further suggest the altered state of glucose regulation and possible adipocyte involvement in disease progression [54]. Adiponectin is the only adipokine secreted exclusively by adipocytes and is strongly associated with insulin resistance and hyperglycemia. High parasite load was detected in the adipose tissue at the chronic stage, 300 days postinfection, as measured by quantitative polymerase chain reaction (qPCR). Decreased levels of adiponectin in the plasma and adipose tissue of infected mice were also observed during the chronic stage. Microscopic investigation revealed the preferred localization of *T. cruzi* in the brown fat of adipose tissue, where lipid bodies are higher in number and smaller in size compared to white adipocytes. These findings suggest that adipose tissues may serve as the parasitic reservoir during chronic infection and adipokine synthesis was disrupted possibly due to the infection [54]. Observations that *T. cruzi* parasite is present in the adipose tissue biopsy of chronically infected human patients have further confirmed the finding that adipose tissue is the reservoir of chronic *T. cruzi* infection [55]. Several follow-up studies have also shown the susceptible nature of adipocytes to *T. cruzi* infection [8, 56].

In vitro infection of cultured adipocytes with *T. cruzi* revealed that a panel of proinflammatory cytokines was upregulated; these include IL-1β, IFN-γ, TNF-α, chemokine ligand (CCL2), CCL5, and C-X-C motif chemokine 10 (CXCL10) The expressions of TLR-2 and 9 are also upregulated [8]. Other pathways, such as notch, extracellular signaling-regulated kinases (ERK), and phosphoinositide-3-kinases (PI3K), were also activated. It was shown that both ERK and PI3K pathways were activated upon *T. cruzi* infection [57, 58]. Furthermore, PPAR-γ is highly expressed in adipose tissue and, along with adiponectin, exerts anti-inflammatory effect [59]. Levels of peroxisome proliferator-activated receptor (PPAR-γ) were decreased in the infected cells, which may have led to the decreased secretion of adiponectin and increased inflammatory reactions. These findings suggest that infection of adipocytes with *T. cruzi* may contribute to the systemic proinflammatory immune responses as well as metabolic dysregulation [8] (Figure 1(b)).

In summary, recent research has revealed that adipose tissue may be the most important reservoir for *T. cruzi* chronic infection and these infected adipocytes display a proinflammatory phenotype. Altered activation profile of several kinase pathways in adipose tissues may also contribute to host metabolic dysregulation. However, questions remain unanswered. It is clear that chronic *T. cruzi* infection displays tissue tropism; however the evolutionary benefits of *T. cruzi* residing in adipocytes are unknown. *T. cruzi* may utilize the lipid stores within the adipocytes for its multiplication and survival. It is also possible that *T. cruzi* chooses adipocytes for its prolonged life-span. In addition, the specific mechanism of *T. cruzi*-adipocyte interaction is unknown. Further research is needed to unravel the biological processes behind the relationship between *T. cruzi* and adipocytes.

4. *T. cruzi* Infection and Host Cholesterol Transport Pathways

T. cruzi glycoprotein 85 (gp85)/*trans*-sialidase is similar to that of viral and bacterial neuraminidases. However, unlike other neuraminidases, upon hydrolysis of α-linked sialic acid from glycoconjugates on cell surfaces, *T. cruzi trans*-sialidase transfers the sialic acid onto parasitic receptors [60]. The expression and activity of *trans*-sialidase are developmentally regulated and are present at about the same extent in epimastigotes and trypomastigotes. Minimal *trans*-sialidase activity was detected in amastigotes [61]. *Trans*-Sialidase is known to be involved in trypomastigote cell adhesion and invasion process by interacting with a wide range of ligands, such as laminin, fibronectin, and collagen [62–65]. Inhibition of *T. cruzi trans*-sialidase by specific antibodies led to the increased rate of infection [66].

Cholesterol transport chains are the major components of maintaining host lipid homeostasis and lipoproteins are essential players in these pathways. Lipoproteins are categorized based on their density and protein content into high density lipoproteins (HDL, density 1.603–1.210), low density lipoproteins (LDL, density 1.019–1.603), intermediate density lipoproteins (IDL, density 1.006–1.019), very low density lipoproteins (VLDL, density 0.95–1.006), and chylomicrons (density < 0.95). All lipoproteins allow the transport of hydrophobic lipid contents, such as cholesterol, triglycerides, and phospholipids, within the hydrophilic blood circulation system.

LDL is characterized by the presence of a single copy of apolipoprotein B-100 (Apo B-100) molecule on its surface. It is generated from liver-derived VLDL by a process mediated by lipoprotein lipase and hepatic lipase as well as lipid exchange proteins [67, 68]. LDL has been shown to be a potent inhibitor of *T. cruzi trans*-sialidase and enhances the infection of human fibroblasts *in vitro* in a dose-dependent manner [10]. The enhanced infection rate seen upon the addition of LDL *in vitro* is comparable to that of the enhancement caused by *trans*-sialidase inhibition [10]. LDL particles were seen covering the parasite cellular surface of *T. cruzi* trypomastigotes, but not amastigotes [69]. The localization of LDL particles correlates with *trans*-sialidase localization on the parasite surface and suggests that LDL may directly inhibit *T. cruzi* surface *trans*-sialidase to enhance rate of infection (Figure 1(c)). However, the exact molecular mechanism of this interaction has yet been demonstrated.

Previous reports have also shown that LDL can be endocytosed by *T. cruzi* epimastigotes [69]. Gold-labelled LDL particles were found within flagellar pockets. Immunoelectron microscopy showed that *trans*-sialidase expression is most concentrated in the flagellar pocket region, which suggested that despite LDL inhibition of *T. cruzi trans*-sialidase, *trans*-sialidase may also facilitate LDL endocytosis by the parasite [70]. Reservosomes are the site of accumulated endocytosed proteins and lipids in *T. cruzi*. This organelle in the parasite provides support for metacyclogenesis from epimastigotes to trypomastigotes [71, 72]. LDL particles were also found in the *T. cruzi* membrane enclosed vesicles and reservosome within the parasite. LDL may be stored and

processed in the reservosome for usage during this transformation and infection process [73]. Similar process of LDL uptake was also demonstrated in *Leishmania amazonensis*, a parasite closely related to *T. cruzi* in the Trypanosomatidae family [74].

Another important molecule in the LDL metabolic cycle is the LDL receptor (LDLR). LDLR plays an essential role in the internalization of circulating LDL in the host liver and peripheral cells. A significant amount of cholesterol is delivered to these organs via the interaction of LDL-LDLR [75]. Approximately 50% of LDL is removed at the liver [76]. LDLR also facilitates the endocytosis of a variety of other ligands, such as proteinases and proteinase-inhibitor complexes, as well as interacting with cytoplasmic adaptor proteins which have signaling transduction functions [77]. The expression of LDLR by the host cell is regulated by a wide range of lipid metabolic and immune regulatory stimuli, such as intracellular cholesterol level, oxysterols, various growth factors, and cytokines [78, 79]. Ruan et al. demonstrated that, in human mesangial cells, increased levels of TNF-α, TGF-β, and IL1-β caused increased transcription of LDLR [80]. LDLR was previously shown to be a potential host receptor for Hepatitis C virus (HCV) and other flaviviridae viruses [81, 82]. However, this direct interaction was not documented in parasitic infections until recently.

The *T. cruzi* parasite specifically binds to LDLR during the infection process [83]. Activation of LDLR facilitates the recruitment of lysosomes to the parasitophorous vacuole, which leads to the internalization of *T. cruzi* into the cytoplasm. Disruption of LDLR by genetic knockout resulted in 62% reduction in *T. cruzi* infection, which suggests LDLR is essential for *T. cruzi* cell invasion process (Figure 1(c)). Furthermore, upregulation of LDLR expression was also seen in the heart of *T. cruzi* infected CD1 mice [83]. Moreover, in *Toxoplasma gondii* infection, LDLR functions to uptake LDL particles and support intracellular parasite growth [84]. It is recently demonstrated that *T. cruzi* interaction with LDL receptor leads to the increased accumulation of LDL-cholesterol in host tissue in both acute and chronic CD [85].

Alterations in the micro- and macrovascular circulations and atherosclerosis-like symptoms are commonly seen in cardiomyopathic patients [86, 87]. Bestetti et al. reported that *T. cruzi* infection in combination with a high cholesterol diet can induce early symptoms of atherosclerosis in mice [88, 89]. LDL and LDLR were implicated extensively in atherosclerosis pathology and progression. It is known that LDL particles are transported across the endothelium and become trapped in the matrix of arterial wall cells, which leads to the production of highly cytotoxic oxidized LDL and subsequently activates inflammatory pathways, such as NFκB [90]. The interaction of *T. cruzi* with LDLR may increase host susceptibility to atherosclerosis and arterial pathology.

In addition to the parasite interaction with LDL and LDLR, *T. cruzi* also interacts with HDL (originally named cruzin in *T. cruzi* research [91]), the major component of the reverse cholesterol transport pathway. HDL is a complex, multistructured particle consisting of two layers of phospholipids that are held together by two molecules of apolipoprotein A-I (Apo A-I). The main function of HDL is to remove excess cholesterol from peripheral tissues and return it to the liver for storage and excretion [92]. Other functions of HDL also include inhibiting LDL oxidation, platelet aggregation and coagulations, and endothelial inflammation, as well as promoting endothelial nitric oxide production and prostacyclin bioavailability [93, 94].

Similar to LDL-*T. cruzi* interaction, HDL was shown to bind to and inhibit *T. cruzi* trypomastigotes *trans*-sialidase activity [11, 95]. Interestingly, this interaction is specific for *T. cruzi* and was not found in *Trypanosoma rangeli,* an infectious agent nonpathogenic to human hosts. *T. cruzi* and *T. rangeli* overlap geographically, share antigenic protein, and are able to infect the same triatominae vector and vertebrate hosts. HDL inhibition of *T. cruzi trans*-sialidase functions in a dose-dependent manner through a reversible noncompetitive mechanism [95]. Maximum association between HDL and *T. cruzi trans*-sialidase occurs in less than 5 min and lasts more than 120 min [11]. More importantly, HDL inhibition of *T. cruzi trans*-sialidase enhances parasite infection *in vitro* [10]. Recently, Weizong et al. have discovered similar interaction between Apo A-I and Dengue virus. The research group showed that Apo A-I is associated with the virus particles and preincubation of dengue virus with HDL enhances viral infection through a scavenger receptor-BI- (SR-BI-) mediated mechanism [96]. These findings may also provide a possible mechanism for the enhancement of *T. cruzi* infection by HDL (Figure 1(e)). Furthermore, our research has shown that, during the intracellular amastigote stage of infection, groups infected in the presence of HDL had lower number of intracellular parasites than groups without HDL (Q. Miao & M. Ndao, personal communication). It is possible that HDL inhibition of *T. cruzi trans*-sialidase led to the decreased rate of trypomastigotes escaping from the parasitophorous vacuole and delaying the process of trypomastigote transformation [97].

In the *T. cruzi* epimastigote form, HDL may also be endocytosed and function as nutritional supply [10]. HDL endocytosis was first observed in *Trypanosoma brucei brucei* (*T. b. brucei*). *T. brucei* (African trypanosome) is closely related to *T. cruzi* (American trypanosome) in evolutionary lineage and shares a high level of biological resemblance. In the interaction of HDL with *T. brucei*, HDL is named trypanolytic factor (TLF), because endocytosis of certain HDL subspecies, which contain haptoglobin-related protein (Hpr, TLF-1 [98]) and apolipoprotein L-I (Apo L-I, TLF-2 [99]), causes lysis of *T. b. brucei* and protects mammalian hosts from infection [100]. However, *T. cruzi* has developed resistance to TLFs. The exact mechanism of this resistance is currently unknown.

The interaction between HDL and *T. cruzi* was recently reinforced by the discovery that the major structural component of HDL, apolipoprotein A-I (Apo A-I, full-length 28.1 kDa), is truncated into fragments (24.7, 13.6, 10.3, and 9.3 kDa) in sera of *T. cruzi* infected patients [101]. Apo A-I (243 amino acids) accounts for ~75% of HDL protein content [102]. Both the N- and the C-termini of Apo A-I are involved in lipid binding functions [103–105]. The central domain of the Apo A-I protein is involved in the activation of lecithin-cholesterol acyltransferase (LCAT), which is responsible for

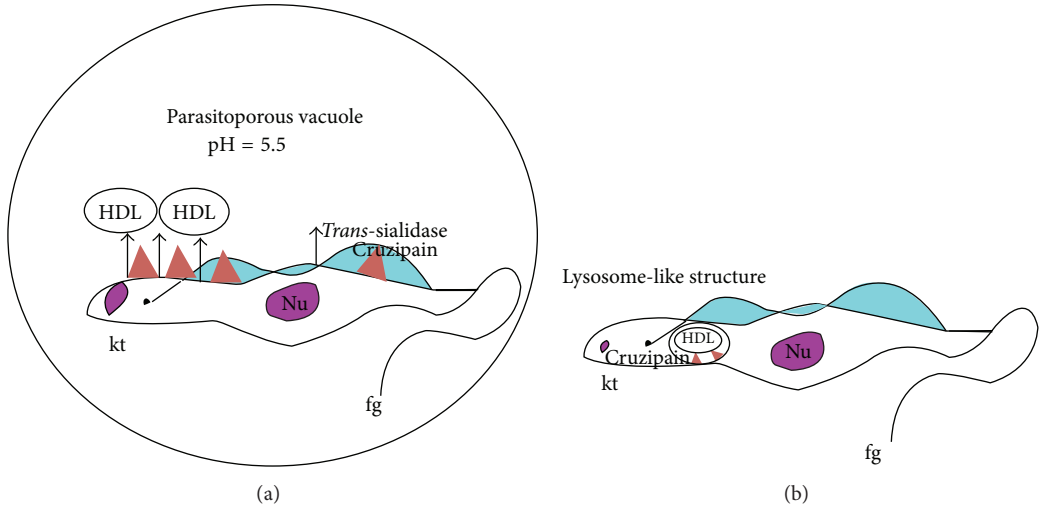

Figure 2: Possible mechanisms of *T. cruzi* cruzipain cleaving Apo A-I in HDL. *T. cruzi* cruzipain is expressed in the parasitic surface as well as in the lysosomal-like structure/reservosome. Both cruzipain fractions are required to produce the full Apo A-I truncation profile seen in *T. cruzi* infected human patients. This implies that Apo A-I within the HDL complex may be (a) truncated during the infection process on the parasitic surface and also (b) endocytosed by *T. cruzi* and processed in the reservosome for possible lipid utilization.

the esterification and storage of cholesterol within HDL particles [106]. Minor changes in the Apo A-I amino acid sequence or structure could seriously affect HDL function [107]. Therefore, Apo A-I truncation seen in *T. cruzi* infection may contribute to the dysregulation of host lipid metabolism. The effect of this dysregulation needs to be further investigated. However, the unique truncation pattern seen in these patients has high discriminatory power between infected and uninfected patients and can be used as *T. cruzi* diagnostic biomarkers [101, 108, 109].

Our research has revealed that the series of Apo A-I truncations was facilitated by the major cysteine protease of *T. cruzi*, cruzipain [56], which is also known as GP 57/51 or cruzain. This protease which belongs to the mammalian papain superfamily is known to cleave immunoglobulin class G proteins [110, 111]. Cruzipain has an essential function in the invasion and survival processes of *T. cruzi* and is expressed in all developmental stages of the parasite life cycle [110]. At each stage, cruzipain is differentially located within the parasite to carry out stage specific functions [112, 113]. In the *T. cruzi* trypomastigote form, cruzipain is located on the parasite surface, flagellar pocket, and lysosome-like structure [114, 115].

It was also shown that cruzipain was only able to cleave Apo A-I at an acidic pH, which suggests that the cleavage may take place within acidic environments. Furthermore, cruzipain from parasite surface (Figure 2(a)) and cruzipain within the lysosome-like structure (Figure 2(b)) are both required in order to produce the truncation pattern [56]. It is interesting to note that the localization of cruzipain highly resembles that of *trans*-sialidase. Therefore, it is possible that HDL is both endocytosed by trypomastigotes and bound to the surface of the parasite via *trans*-sialidase. During the infection process, the parasite bound HDL is cleaved by cruzipain in the acidic parasitophorous vacuole.

With the emerging evidence, it is becoming obvious that *T. cruzi* exploits the complex cholesterol transport system via a variety of molecules such as LDL, LDL-R, and HDL. The results of these interactions seem to all lead to the establishment of *T. cruzi* infection and Chagas disease chronicity. The impact of these relationships on host lipid metabolism is yet to be investigated.

5. Conclusion

Host lipid metabolism is a intricate system involving a wide range of factors. It interacts with other energy metabolic systems as well as the immune system. The role of host lipid metabolism in response to infectious agents is drawing increasing attention. This review may aid in deeper understanding of *T. cruzi* interacting with host lipid metabolism with a more systematic approach, as well as the role of lipids in *T. cruzi* pathogenesis. We have clearly illustrated that *T. cruzi* interacts with several specific factors in host lipid metabolism. Further research in these interactions and the role of lipids in *T. cruzi* pathogenesis will be highly useful in the future.

Conflict of Interests

The authors declare that there is no conflict of interests regarding the publication of this paper.

Acknowledgments

The National Reference Centre for Parasitology is supported by Public Health Agency of Canada/National Microbiology Laboratory Grant HT070-010033 and by the Research Institute of McGill University Health Centre.

References

[1] L. V. Kirchhoff, "Epidemiology of American Trypanosomiasis (Chagas Disease)," *Advances in Parasitology*, vol. 75, pp. 1–18, 2011.

[2] J. C. P. Dias, A. C. Silveira, and C. J. Schofield, "The impact of Chagas disease control in Latin America: a review," *Memorias do Instituto Oswaldo Cruz*, vol. 97, no. 5, pp. 603–612, 2002.

[3] G. A. Schmunis and J. R. Cruz, "Safety of the blood supply in Latin America," *Clinical Microbiology Reviews*, vol. 18, no. 1, pp. 12–29, 2005.

[4] J. A. Perez-Molina, F. Norman, and R. Lopez-Velez, "Chagas disease in non-endemic countries: epidemiology, clinical presentation and treatment," *Current Infectious Disease Reports*, vol. 14, no. 3, pp. 263–274, 2012.

[5] N. Nogueira and Z. A. Cohn, "Trypanosoma cruzi: in vitro induction of macrophage microbicidal activity," *Journal of Experimental Medicine*, vol. 148, no. 1, pp. 288–300, 1978.

[6] S. G. Reed, "In vivo administration of recombinant IFN-γ induces macrophage activation, and prevents acute disease, immune suppression, and death in experimental Trypanosoma cruzi infections," *Journal of Immunology*, vol. 140, no. 12, pp. 4342–4347, 1988.

[7] J. S. Silva, G. N. R. Vespa, M. A. G. Cardoso, J. C. S. Aliberti, and F. Q. Cunha, "Tumor necrosis factor alpha mediates resistance to Trypanosoma cruzi infection in mice by inducing nitric oxide production in infected gamma interferon-activated macrophages," *Infection and Immunity*, vol. 63, no. 12, pp. 4862–4867, 1995.

[8] F. Nagajyothi, M. S. Desruisseaux, N. Thiruvur et al., "Trypanosoma cruzi Infection of cultured adipocytes results in an inflammatory phenotype," *Obesity*, vol. 16, no. 9, pp. 1992–1997, 2008.

[9] Q. Miao, C. Santamaria, D. Bailey et al., "Apolipoprotein A-I truncations in Chagas disease are caused by cruzipain, the major cysteine protease of Trypanosoma cruzi," *American Journal of Pathology*, vol. 184, no. 4, pp. 976–984, 2014.

[10] R. P. Prioli, I. Rosenberg, and M. E. A. Pereira, "High- and low-density lipoproteins enhance infection of *Trypanosoma cruzi* in vitro," *Molecular and Biochemical Parasitology*, vol. 38, no. 2, pp. 191–198, 1990.

[11] R. P. Prioli, I. Rosenberg, S. Shivakumar, and M. E. A. Pereira, "Specific binding of human plasma high density lipoprotein (cruzin) to Trypanosoma cruzi," *Molecular and Biochemical Parasitology*, vol. 28, no. 3, pp. 257–263, 1988.

[12] R. Hoff, R. S. Teixeira, J. S. Carvalho, and K. E. Mott, "Trypanosoma cruzi in the cerebrospinal fluid during the acute stage of Chagas' disease," *The New England Journal of Medicine*, vol. 298, no. 11, pp. 604–606, 1978.

[13] M. A. Miles, "New world trypanosomiasis," in *Topley and Wilson's Microbiology and Microbial Infections*, K. J. P. Cox and D. Wakelin, Eds., pp. 283–302, Arnold, London, UK, 1998.

[14] K. M. Tyler, C. L. Olson, and D. M. Engman, "The life cycle of *Trypanosoma cruzi*," in *American Trypanomiasis*, vol. 7, pp. 1–11, Kluwer Academic Publishers, 2003.

[15] K. Tauchi-Sato, S. Ozeki, T. Houjou, R. Taguchi, and T. Fujimoto, "The surface of lipid droplets is a phospholipid monolayer with a unique fatty acid composition," *The Journal of Biological Chemistry*, vol. 277, no. 46, pp. 44507–44512, 2002.

[16] P. F. Weller, P. T. Bozza, W. Yu, and A. M. Dvorak, "Cytoplasmic lipid bodies in eosinophils: central roles in eicosanoid generation," *International Archives of Allergy and Immunology*, vol. 118, no. 2–4, pp. 450–452, 1999.

[17] C. Bandeira-Melo, P. T. Bozza, and P. F. Weller, "The cellular biology of eosinophil eicosanoid formation and function," *Journal of Allergy and Clinical Immunology*, vol. 109, no. 3, pp. 393–400, 2002.

[18] D. J. McGookey and R. G. W. Anderson, "Morphological characterization of the cholesteryl ester cycle in cultured mouse macrophage foam cells," *Journal of Cell Biology*, vol. 97, no. 4, pp. 1156–1168, 1983.

[19] H. D'Avila, R. C. N. Melo, G. G. Parreira, E. Werneck-Barroso, H. C. Castro-Faria-Neto, and P. T. Bozza, "Mycobacterium bovis bacillus Calmette-Guérin induces TLR2-mediated formation of lipid bodies: Intracellular domains for eicosanoid synthesis in vivo," *Journal of Immunology*, vol. 176, no. 5, pp. 3087–3097, 2006.

[20] Z. Brener and R. T. Gazzinelli, "Immunological control of *Trypanosoma cruzi* infection and pathogenesis of Chagas' disease," *International Archives of Allergy and Immunology*, vol. 114, no. 2, pp. 103–110, 1997.

[21] C. F. Nathan, "Secretion of oxygen intermediates: role in effector functions of activated macrophages," *Federation Proceedings*, vol. 41, no. 6, pp. 2206–2211, 1982.

[22] G. N. R. Vespa, F. Q. Cunha, and J. S. Silva, "Nitric oxide is involved in control of Trypanosoma cruzi-induced parasitemia and directly kills the parasite in vitro," *Infection and Immunity*, vol. 62, no. 11, pp. 5177–5182, 1994.

[23] M. Russo, N. Starobinas, R. Ribeiro-Dos-Santos, P. H. Minoprio Eisen, and M. Hontebeyrie-Joskowicz, "Susceptible mice present higher macrophage activation than resistant mice during infections with myotropic strains of Trypanosoma cruzi," *Parasite Immunology*, vol. 11, no. 4, pp. 385–395, 1989.

[24] R. C. N. Melo and C. R. S. Machado, "*Trypanosoma cruzi*: peripheral blood monocytes and heart macrophages in the resistance to acute experimental infection in rats," *Experimental Parasitology*, vol. 97, no. 1, pp. 15–23, 2001.

[25] S. Revelli, G. Didoli, E. Roggero et al., "Macrophage activity, IL-6 levels, antibody response and heart histology in rats undergoing an attenuated Trypanosoma cruzi acute infection upon treatment with recombinant interferon γ," *Cytokines, Cellular and Molecular Therapy*, vol. 4, no. 3, pp. 153–159, 1998.

[26] R. C. N. Melo, "Depletion of immune effector cells induces myocardial damage in the acute experimental Trypanosoma cruzi infection: ultrastructural study in rats," *Tissue and Cell*, vol. 31, no. 3, pp. 281–290, 1999.

[27] H. D'Avila, C. G. Freire-de-Lima, N. R. Roque et al., "Host cell lipid bodies triggered by Trypanosoma cruzi infection and enhanced by the uptake of apoptotic cells are associated with prostaglandin E2 generation and increased parasite growth," *Journal of Infectious Diseases*, vol. 204, no. 6, pp. 951–961, 2011.

[28] C. G. Freire-de-Lima, Q. X. Yi, S. J. Gardai, D. L. Bratton, W. P. Schiemann, and P. M. Henson, "Apoptotic cells, through transforming growth factor-β, coordinately induce anti-inflammatory and suppress pro-inflammatory eicosanoid and NO synthesis in murine macrophages," *The Journal of Biological Chemistry*, vol. 281, no. 50, pp. 38376–38384, 2006.

[29] J. S. Silva, D. R. Twardzik, and S. G. Reed, "Regulation of *Trypanosoma cruzi* infections in vitro and in vivo by transforming growth factor β (TGF-β)," *Journal of Experimental Medicine*, vol. 174, no. 3, pp. 539–545, 1991.

[30] M. Ming, M. E. Ewen, and M. E. A. Pereira, "Trypanosome invasion of mammalian cells requires activation of the TGFβ signaling pathway," *Cell*, vol. 82, no. 2, pp. 287–296, 1995.

[31] M. M. Borges, J. K. Kloetzel, H. F. Andrade Jr., C. E. Tadokoro, P. Pinge-Filho, and I. Abrahamsohn, "Prostaglandin and nitric oxide regulate TNF-α production during Trypanosoma cruzi infection," *Immunology Letters*, vol. 63, no. 1, pp. 1–8, 1998.

[32] G. O. Ramirez-Yañez, S. Hamlet, A. Jonarta, G. J. Seymour, and A. L. Symons, "Prostaglandin E2 enhances transforming growth factor-beta 1 and TGF-beta receptors synthesis: an in vivo and in vitro study," *Prostaglandins Leukotrienes and Essential Fatty Acids*, vol. 74, no. 3, pp. 183–192, 2006.

[33] S. G. Harris, J. Padilla, L. Koumas, D. Ray, and R. P. Phipps, "Prostaglandins as modulators of immunity," *Trends in Immunology*, vol. 23, no. 3, pp. 144–150, 2002.

[34] H. D'Avila, D. A. M. Toledo, and R. C. N. Melo, "Lipid bodies: inflammatory organelles implicated in host-trypanosoma cruzi interplay during innate immune responses," *Mediators of Inflammation*, vol. 2012, Article ID 478601, 11 pages, 2012.

[35] A. M. Celentano, G. Gorelik, M. E. Solana, L. Sterin-Borda, E. Borda, and S. M. González Cappa, "PGE2 involvement in experimental infection with Trypanosoma cruzi subpopulations," *Prostaglandins*, vol. 49, no. 3, pp. 141–153, 1995.

[36] C. G. Freire-de-Lima, C. G. Freire-de-Lima et al., "Uptake of apoptotic cells drives the growth of a pathogenic trypanosome in macrophages," *Nature*, vol. 403, no. 6766, pp. 199–203, 2000.

[37] R. C. N. Melo, D. L. Fabrino, F. F. Dias, and G. G. Parreira, "Lipid bodies: structural markers of inflammatory macrophages in innate immunity," *Inflammation Research*, vol. 55, no. 8, pp. 342–348, 2006.

[38] R. C. N. Melo, H. D. Ávila, D. L. Fabrino, P. E. Almeida, and P. T. Bozza, "Macrophage lipid body induction by Chagas disease in vivo: putative intracellular domains for eicosanoid formation during infection," *Tissue and Cell*, vol. 35, no. 1, pp. 59–67, 2003.

[39] N. E. Rodríguez, U. Gaur, and M. E. Wilson, "Role of caveolae in Leishmania chagasi phagocytosis and intracellular survival in macrophages," *Cellular Microbiology*, vol. 8, no. 7, pp. 1106–1120, 2006.

[40] R. C. N. Melo and A. M. Dvorak, "Lipid body-phagosome interaction in macrophages during infectious diseases: host defense or pathogen survival strategy?" *PLoS Pathogens*, vol. 8, no. 7, Article ID e1002729, 2012.

[41] E. Anes, M. P. Kühnel, E. Bos, J. Moniz-Pereira, A. Habermann, and G. Griffiths, "Selected lipids activate phagosome actin assembly and maturation resulting in killing of pathogenic mycobacteria," *Nature Cell Biology*, vol. 5, no. 9, pp. 793–802, 2003.

[42] C.-I. Suh, N. D. Stull, J. L. Xing et al., "The phosphoinositide-binding protein p40 phox activates the NADPH oxidase during FcγIIA receptor-induced phagocytosis," *Journal of Experimental Medicine*, vol. 203, no. 8, pp. 1915–1925, 2006.

[43] M. S. Desruisseaux, M. E. Trujillo, H. B. Tanowitz, and P. E. Scherer, "Adipocyte, adipose tissue, and infectious disease," *Infection and Immunity*, vol. 75, no. 3, pp. 1066–1078, 2007.

[44] S. W. Cushman, "Structure-function relationships in the adipose cell. I. Ultrastructure of the isolated adipose cell.," *Journal of Cell Biology*, vol. 46, no. 2, pp. 326–341, 1970.

[45] J. R. Koethe, T. Hulgan, and K. Niswender, "Adipose tissue and immune function: a review of evidence relevant to HIV infection," *Journal of Infectious Diseases*, vol. 208, no. 8, pp. 1194–1201, 2013.

[46] P. E. Scherer, S. Williams, M. Fogliano, G. Baldini, and H. F. Lodish, "A novel serum protein similar to C1q, produced exclusively in adipocytes," *The Journal of Biological Chemistry*, vol. 270, no. 45, pp. 26746–26749, 1995.

[47] Y. Zhang, R. Proenca, M. Maffei, M. Barone, L. Leopold, and J. M. Friedman, "Positional cloning of the mouse obese gene and its human homologue," *Nature*, vol. 372, no. 6505, pp. 425–432, 1994.

[48] C. M. Steppan, S. T. Bailey, S. Bhat et al., "The hormone resistin links obesity to diabetes," *Nature*, vol. 409, no. 6818, pp. 307–312, 2001.

[49] V. M. dos Santos, S. F. da Cunha, V. P. Teixeira et al., "Frequency of diabetes mellitus and hyperglycemia in chagasic and non-chagasic women," *Revista da Sociedade Brasileira de Medicina Tropical*, vol. 32, no. 5, pp. 489–496, 1999.

[50] M. E. Guariento, M. J. A. Saad, E. O. A. Muscelli, and J. A. R. Gontijo, "Heterogenous insulin response to an oral glucose load by patients with the indeterminate clinical form of Chagas' disease," *Brazilian Journal of Medical and Biological Research*, vol. 26, no. 5, pp. 491–495, 1993.

[51] L. C. Oliveira, Y. Juliano, N. F. Novo, and M. M. Neves, "Blood glucose and insulin response to intravenous glucose by patients with chronic Chagas' disease and alcoholism.," *Brazilian Journal of Medical and Biological Research*, vol. 26, no. 11, pp. 1187–1190, 1993.

[52] H. B. Tanowitz, B. Amole, D. Hewlett, and M. Wittner, "Trypanosoma cruzi infection in diabetic mice," *Transactions of the Royal Society of Tropical Medicine and Hygiene*, vol. 82, no. 1, pp. 90–93, 1988.

[53] A. Guilherme, J. V. Virbasius, V. Puri, and M. P. Czech, "Adipocyte dysfunctions linking obesity to insulin resistance and type 2 diabetes," *Nature Reviews Molecular Cell Biology*, vol. 9, no. 5, pp. 367–377, 2008.

[54] T. P. Combs, S. Mukherjee, C. J. G. de Almeida et al., "The adipocyte as an important target cell for *Trypanosoma cruzi* infection," *Journal of Biological Chemistry*, vol. 280, no. 25, pp. 24085–24094, 2005.

[55] A. V. Matos Ferreira, M. Segatto, Z. Menezes et al., "Evidence for Trypanosoma cruzi in adipose tissue in human chronic Chagas disease," *Microbes and Infection*, vol. 13, no. 12-13, pp. 1002–1005, 2011.

[56] Q. Miao, C. Santamaria, D. Bailey et al., "Apolipoprotein A-I truncations in chagas disease are caused by cruzipain, the major cysteine protease of trypanosoma cruzi," *American Journal of Pathology*, vol. 184, no. 4, pp. 976–984, 2014.

[57] S. Mukherjee, H. Huang, S. B. Petkova et al., "Trypanosoma cruizi infection activates extracellular signal-regulated kinase in cultured endothelial and smooth muscle cells," *Infection and Immunity*, vol. 72, no. 9, pp. 5274–5282, 2004.

[58] S. E. Wilkowsky, M. A. Barbieri, P. Stahl, and E. L. D. Isola, "Trypanosoma cruzi: Phosphatidylinositol 3-kinase and protein kinase B activation is associated with parasite invasion," *Experimental Cell Research*, vol. 264, no. 2, pp. 211–218, 2001.

[59] E. Hovsepian, F. Penas, G. A. Mirkin, and N. B. Goren, "Role of PPARs in trypanosoma cruzi infection: implications for chagas disease therapy," *PPAR Research*, vol. 2012, Article ID 528435, 8 pages, 2012.

[60] M. J. M. Alves and W. Colli, "Role of the gp85/*trans*-sialidase superfamily of glycoproteins in the interaction of *Trypanosoma cruzi* with host structures," *Sub-cellular biochemistry*, vol. 47, pp. 58–69, 2008.

[61] M. E. A. Pereira, "A developmentally regulated neuraminidase activity in Trypanosoma cruzi," *Science*, vol. 219, no. 4591, pp. 1444–1446, 1983.

[62] A. Ouaissi, J. Cornette, A. Taibi, P. Velge, and A. Capron, "Major surface immunogens of *Trypanosoma cruzi* trypomastigotes," *Memorias do Instituto Oswaldo Cruz*, vol. 83, supplement 1, p. 502, 1988.

[63] R. R. Tonelli, R. J. Giordano, E. M. Barbu et al., "Role of the gp85/*trans*-sialidases in *Trypanosoma cruzi* tissue tropism: preferential binding of a conserved peptide motif to the vasculature in vivo," *PLoS Neglected Tropical Diseases*, vol. 4, no. 11, article e864, 2010.

[64] R. Giordano, R. Chammas, S. S. Veiga, W. Colli, and M. J. M. Alves, "An acidic component of the heterogeneous Tc-85 protein family from the surface of Trypanosoma cruzi is a laminin binding glycoprotein," *Molecular and Biochemical Parasitology*, vol. 65, no. 1, pp. 85–94, 1994.

[65] P. Velge, M. A. Ouaissi, J. Cornette, D. Afchain, and A. Capron, "Identification and isolation of Trypanosoma cruzi trypomastigote collagen-binding proteins: possible role in cell-parasite interaction," *Parasitology*, vol. 97, no. 2, pp. 255–268, 1988.

[66] R. Cavallesco and M. E. A. Pereira, "Antibody to Trypanosoma cruzi neuraminidase enhances infection in vitro and identifies a subpopulation of trypomastigotes," *Journal of Immunology*, vol. 140, no. 2, pp. 617–625, 1988.

[67] G. J. de Grooth, A. H. E. M. Klerkx, E. S. G. Stroes, A. F. H. Stalenhoef, J. J. P. Kastelein, and J. A. Kuivenhoven, "A review of CETP and its relation to atherosclerosis," *Journal of Lipid Research*, vol. 45, no. 11, pp. 1967–1974, 2004.

[68] J. Huuskonen, V. M. Olkkonen, M. Jauhiainen, and C. Ehnholm, "The impact of phospholipid transfer protein (PLTP) on HDL metabolism," *Atherosclerosis*, vol. 155, no. 2, pp. 269–281, 2001.

[69] M. J. Soares and W. de Souza, "Endocytosis of gold-labeled proteins and LDL by Trypanosoma cruzi," *Parasitology Research*, vol. 77, no. 6, pp. 461–468, 1991.

[70] R. P. Prioli, J. S. Mejia, T. Aji, M. Aikawa, and M. E. A. Pereira, "Trypanosoma cruzi: localization of neuraminidase on the surface of trypomastigotes," *Tropical Medicine and Parasitology*, vol. 42, no. 2, pp. 146–150, 1991.

[71] M. J. Soares, T. Souto-Padron, M. C. Bonaldo, S. Goldenberg, and W. de Souza, "A stereological study of the differentiation process in Trypanosoma cruzi," *Parasitology Research*, vol. 75, no. 7, pp. 522–527, 1989.

[72] M. J. Soares and W. De Souza, "Cytoplasmic organelles of trypanosomatids: a cytochemical and stereological study," *Journal of Submicroscopic Cytology and Pathology*, vol. 20, no. 2, pp. 349–361, 1988.

[73] M. G. Pereira, E. S. Nakayasu, C. Sant'Anna et al., "Trypanosoma cruzi epimastigotes are able to store and mobilize high amounts of cholesterol in reservosome lipid inclusions," *PLoS ONE*, vol. 6, no. 7, Article ID e22359, 2011.

[74] N. N. de Cicco, M. G. Pereira, J. R. Corrêa et al., "LDL uptake by Leishmania amazonensis: involvement of membrane lipid microdomains," *Experimental Parasitology*, vol. 130, no. 4, pp. 330–340, 2012.

[75] B. R. Carr and E. R. Simpson, "Lipoprotein utilization and cholesterol synthesis by the human fetal adrenal gland.," *Endocrine Reviews*, vol. 2, no. 3, pp. 306–326, 1981.

[76] J. E. Vance, "Assembly and secretion of lipoproteins," in *Biochemistry of Lipids, Lipoproteins and Membrane*, J. E. Vance and D. Vance, Eds., pp. 505–526, Elsevier, Amsterdam, The Netherlands, 2002.

[77] D. K. Strickland, S. L. Gonias, and W. S. Argraves, "Diverse roles for the LDL receptor family," *Trends in Endocrinology and Metabolism*, vol. 13, no. 2, pp. 66–74, 2002.

[78] A. Kumar, A. Middleton, T. C. Chambers, and K. D. Mehta, "Differential roles of extracellular signal-regulated kinase-1/4 and p38(MAPK) in interleukin-1β- and tumor necrosis factor-α-induced low density lipoprotein receptor expression in HepG2 cells," *The Journal of Biological Chemistry*, vol. 273, no. 25, pp. 15742–15748, 1998.

[79] A. C. Nicholson and D. P. Hajjar, "Transforming growth factor-β up-regulates low density lipoprotein receptor-mediated cholesterol metabolism in vascular smooth muscle cells," *Journal of Biological Chemistry*, vol. 267, no. 36, pp. 25982–25987, 1992.

[80] X. Z. Ruan, Z. Varghese, R. Fernando, and J. F. Moorhead, "Cytokine regulation of low-density lipoprotein receptor gene transcription in human mesangial cells," *Nephrology Dialysis Transplantation*, vol. 13, no. 6, pp. 1391–1397, 1998.

[81] P. André, F. Komurian-Pradel, S. Deforges et al., "Characterization of low- and very-low-density hepatitis C virus RNA-containing particles," *Journal of Virology*, vol. 76, no. 14, pp. 6919–6928, 2002.

[82] V. Agnello, G. Ábel, M. Elfahal, G. B. Knight, and Q.-X. Zhang, "Hepatitis C virus and other flaviviridae viruses enter cells via low density lipoprotein receptor," *Proceedings of the National Academy of Sciences of the United States of America*, vol. 96, no. 22, pp. 12766–12771, 1999.

[83] F. Nagajyothi, L. M. Weiss, D. L. Silver et al., "*Trypanosoma cruzi* utilizes the host low density lipoprotein receptor in invasion," *PLoS Neglected Tropical Diseases*, vol. 5, no. 2, article e953, 2011.

[84] L. R. Portugal, L. R. Fernandes, V. S. Pietra Pedroso, H. C. Santiago, R. T. Gazzinelli, and J. I. Alvarez-Leite, "Influence of low-density lipoprotein (LDL) receptor on lipid composition, inflammation and parasitism during *Toxoplasma gondii* infection," *Microbes and Infection*, vol. 10, no. 3, pp. 276–284, 2008.

[85] C. Johndrow, R. Nelson, H. Tanowitz et al., "*Trypanosoma cruzi* infection results in an increase in intracellular cholesterol," *Microbes and Infection*, vol. 16, no. 4, pp. 337–344, 2014.

[86] E. Cunha-Neto, M. Duranti, A. Gruber et al., "Autoimmunity in Chagas disease cardiopathy: biological relevance of a cardiac myosin-specific epitope crossreactive to an immunodominant Trypanosoma cruzi antigen," *Proceedings of the National Academy of Sciences of the United States of America*, vol. 92, no. 8, pp. 3541–3545, 1995.

[87] M. A. Rossi, "Aortic endothelial cell changes in the acute septicemic phase of experimental Trypanosoma cruzi infection in rats: Scanning and transmission electron microscopic study," *The American Journal of Tropical Medicine and Hygiene*, vol. 57, no. 3, pp. 321–327, 1997.

[88] R. B. Bestetti, M. T. Ariolli, J. L. do Carmo et al., "Clinical characteristics of acute myocardial infarction in patients with Chagas'disease," *International Journal of Cardiology*, vol. 35, no. 3, pp. 371–376, 1992.

[89] D. Sunnemark, R. A. Harris, J. Frostegård, and A. Örn, "Induction of early atherosclerosis in CBA/J mice by combination of Trypanosoma cruzi infection and a high cholesterol diet," *Atherosclerosis*, vol. 153, no. 2, pp. 273–282, 2000.

[90] P. Nievelstein-Post, G. Mottino, A. Fogelman, and J. Frank, "An ultrastructural study of lipoprotein accumulation in cardiac

valves of the rabbit," *Arteriosclerosis and Thrombosis*, vol. 14, no. 7, pp. 1151–1161, 1994.

[91] R. P. Prioli, J. M. Ordovas, I. Rosenberg, E. J. Schaefer, and M. E. A. Pereira, "Similarity of cruzin, an inhibitor of *Trypanosoma cruzi* neuraminidase, to high-density lipoprotein," *Science*, vol. 238, no. 4832, pp. 1417–1419, 1987.

[92] A. R. Tall, "An overview of reverse cholesterol transport," *European Heart Journal*, vol. 19, pp. A31–A35, 1998.

[93] P. J. Barter, S. Nicholls, K.-A. Rye, G. M. Anantharamaiah, M. Navab, and A. M. Fogelman, "Antiinflammatory properties of HDL," *Circulation Research*, vol. 95, no. 8, pp. 764–772, 2004.

[94] C. Mineo, H. Deguchi, J. H. Griffin, and P. W. Shaul, "Endothelial and antithrombotic actions of HDL," *Circulation Research*, vol. 98, no. 11, pp. 1352–1364, 2006.

[95] R. P. Prioli, I. Rosenberg, and M. E. A. Pereira, "Specific inhibition of *Trypanosoma cruzi* neuraminidase by the human plasma glycoprotein "cruzin"," *Proceedings of the National Academy of Sciences of the United States of America*, vol. 84, no. 10, pp. 3097–3101, 1987.

[96] W. Weizong, W. Zhongsu, Z. Yujiao et al., "Effects of right ventricular nonapical pacing on cardiac function: a meta-analysis of randomized controlled trials," *Pacing and Clinical Electrophysiology*, vol. 36, no. 8, pp. 1032–1051, 2013.

[97] S. S. C. Rubin-de-Celis, H. Uemura, N. Yoshida, and S. Schenkman, "Expression of trypomastigote *trans*-sialidase in metacyclic forms of Trypanosoma cruzi increases parasite escape from its parasitophorous vacuole," *Cellular Microbiology*, vol. 8, no. 12, pp. 1888–1898, 2006.

[98] A. B. Smith, J. D. Esko, and S. L. Hajduk, "Killing of trypanosomes by the human haptoglobin-related protein," *Science*, vol. 268, no. 5208, pp. 284–286, 1995.

[99] L. Vanhamme, F. Paturiaux-Hanocq, P. Poelvoorde et al., "Apolipoprotein L-I is the trypanosome lytic factor of human serum," *Nature*, vol. 422, no. 6927, pp. 83–87, 2003.

[100] S. L. Hajduk, D. R. Moore, J. Vasudevacharya et al., "Lysis of Trypanosoma brucei by a toxic subspecies of human high density lipoprotein," *The Journal of Biological Chemistry*, vol. 264, no. 9, pp. 5210–5217, 1989.

[101] M. Ndao, T. W. Spithill, R. Caffrey et al., "Identification of novel diagnostic serum biomarkers for chagas' disease in asymptomatic subjects by mass spectrometric profiling," *Journal of Clinical Microbiology*, vol. 48, no. 4, pp. 1139–1149, 2010.

[102] A. R. Tall and J. L. Breslow, *Plasma High Density Lipoproteins and Atherogenesis*, Lipincott Raven, Philadelphia, Pa, USA, 1996.

[103] M. N. Palgunachari, V. K. Mishra, S. Lund-Katz et al., "Only the two end helixes of eight tandem amphipathic helical domains of human Apo A-I have significant lipid affinity: implications for HDL assembly," *Arteriosclerosis, Thrombosis, and Vascular Biology*, vol. 16, no. 2, pp. 328–338, 1996.

[104] V. K. Mishra, M. N. Palgunachari, G. Datta et al., "Studies of synthetic peptides of human apolipoprotein A-I containing tandem amphipathic α-helixes," *Biochemistry*, vol. 37, no. 28, pp. 10313–10324, 1998.

[105] K. L. Gillotte, M. Zaiou, S. Lund-Katz et al., "Apolipoprotein-mediated plasma membrane microsolubilization: role of lipid affinity and membrane penetration in the efflux of cellular cholesterol and phospholipid," *Journal of Biological Chemistry*, vol. 274, no. 4, pp. 2021–2028, 1999.

[106] H. J. Pownall, Q. Pao, and J. B. Massey, "Isolation and specificity of rat lecithin:cholesterol acyltransferase: comparison with the human enzyme using reassembled high-density lipoproteins containing ether analogs of phosphatidylcholine," *Biochimica et Biophysica Acta*, vol. 833, no. 3, pp. 456–462, 1985.

[107] P. G. Frank and Y. L. Marcel, "Apolipoprotein A-I: structure-function relationships," *Journal of Lipid Research*, vol. 41, no. 6, pp. 853–872, 2000.

[108] Y. Jackson, E. Chatelain, A. Mauris et al., "Serological and parasitological response in chronic Chagas patients 3 years after nifurtimox treatment," *BMC Infectious Diseases*, vol. 13, no. 1, article 85, 2013.

[109] C. Santamaria, C. E. Jackson, Q. Miao et al., "Serum biomarkers predictive of cure in Chagas disease patients after nifurtimox treatment," *BMC Infectious Diseases*, vol. 14, article 302, 2014.

[110] A. C. M. Murta, P. M. Persechini, T. De Souto Padron, W. De Souza, J. A. Guimaraes, and J. Scharfstein, "Structural and functional identification of GP57/51 antigen of Trypanosoma cruzi as a cysteine proteinase," *Molecular and Biochemical Parasitology*, vol. 43, no. 1, pp. 27–38, 1990.

[111] P. Berasain, C. Carmona, B. Frangione, J. J. Cazzulo, and F. Goñi, "Specific cleavage sites on human IgG subclasses by cruzipain, the major cysteine proteinase from Trypanosoma cruzi," *Molecular and Biochemical Parasitology*, vol. 130, no. 1, pp. 23–29, 2003.

[112] J. Vernal, J. Muoz-Jordán, M. Müller, J. José Cazzulo, and C. Nowicki, "Sequencing and heterologous expression of a cytosolic-type malate dehydrogenase of *Trypanosoma brucei*," *Molecular and Biochemical Parasitology*, vol. 117, no. 2, pp. 217–221, 2001.

[113] F. Parussini, V. G. Duschak, and J. J. Cazzulo, "Membrane-bound cysteine proteinase isoforms in different developmental stages of Trypanosoma cruzi," *Cellular and Molecular Biology*, vol. 44, no. 3, pp. 513–519, 1998.

[114] J. Scharfstein, M. Schechter, M. Senna, J. M. Peralta, L. Mendonça-Previato, and M. A. Miles, "Trypanosoma cruzi: characterization and isolation of A 57/51,000 m.w. surface glycoprotein (GP57/51) expressed by epimastigotes and blood-stream trypomastigotes," *Journal of Immunology*, vol. 137, no. 4, pp. 1336–1341, 1986.

[115] J. J. Cazzulo, "Proteinases of Trypanosoma cruzi: patential targets for the chemotherapy of Changas desease," *Current Topics in Medicinal Chemistry*, vol. 2, no. 11, pp. 1261–1271, 2002.

Hindawi Publishing Corporation
Mediators of Inflammation
Volume 2014, Article ID 872464, 12 pages
http://dx.doi.org/10.1155/2014/872464

Research Article

Predictive Criteria to Study the Pathogenesis of Malaria-Associated ALI/ARDS in Mice

Luana S. Ortolan,[1,2] Michelle K. Sercundes,[3] Renato Barboza,[4] Daniela Debone,[3] Oscar Murillo,[5] Stefano C. F. Hagen,[6] Momtchilo Russo,[1] Maria Regina D' Império Lima,[1] José M. Alvarez,[1] Marcos Amaku,[7] Claudio R. F. Marinho,[5] and Sabrina Epiphanio[1,8]

[1] *Departamento de Imunologia, Instituto de Ciências Biomédicas, Universidade de São Paulo, Edifício Biomédicas IV, Avenida Professor Lineu Prestes, No. 1730, 05508-900 São Paulo, SP, Brazil*
[2] *Departamento de Ciências Biológicas, Universidade Federal de São Paulo, Rua Professor Artur Riedel, No. 275, Jardim Eldorado, 09972-270 Diadema, SP, Brazil*
[3] *Instituto de Medicina Tropical de São Paulo, Universidade de São Paulo, Avenida Dr. Enéas Carvalho de Aguiar, No. 470, 05403-000 São Paulo, SP, Brazil*
[4] *Departamento de Ciências Exatas e da Terra, Universidade Federal de São Paulo, Rua Professor Artur Riedel, No. 275, Jardim Eldorado, 09972-270 Diadema, SP, Brazil*
[5] *Departamento de Parasitologia, Instituto de Ciências Biomédicas, Universidade de São Paulo, Avenida Professor Lineu Prestes, No. 1374, Edifício Biomédicas II Cidade Universitária "Armando Salles Oliveira", 05508-000 São Paulo, SP, Brazil*
[6] *Departamento de Cirurgia, Faculdade de Medicina Veterinária e Zootecnia da Universidade de São Paulo, Avenida Professor Dr. Orlando Marques de Paiva, No. 87, Cidade Universitária, 05508 270 São Paulo, SP, Brazil*
[7] *Departamento de Medicina Veterinária Preventiva e Saúde Animal, Faculdade de Medicina Veterinária e Zootecnia da Universidade de São Paulo, Avenida Professor Dr. Orlando Marques de Paiva, No. 87, Cidade Universitária, 05508 270 São Paulo, SP, Brazil*
[8] *Departamento de Análises Clínicas e Toxicológicas, Faculdade de Ciências Farmacêuticas, Universidade de São Paulo, Avenida Professor Lineu Prestes, No. 580, Bloco 17, Cidade Universitária "Armando Salles Oliveira", 05508-000 São Paulo, SP, Brazil*

Correspondence should be addressed to Sabrina Epiphanio; sabrinae@usp.br

Received 5 June 2014; Accepted 16 July 2014; Published 2 September 2014

Academic Editor: Mauricio Martins Rodrigues

Malaria-associated acute lung injury/acute respiratory distress syndrome (ALI/ARDS) often results in morbidity and mortality. Murine models to study malaria-associated ALI/ARDS have been described; we still lack a method of distinguishing which mice will develop ALI/ARDS before death. This work aimed to characterize malaria-associated ALI/ARDS in a murine model and to demonstrate the first method to predict whether mice are suffering from ALI/ARDS before death. DBA/2 mice infected with *Plasmodium berghei* ANKA developing ALI/ARDS or hyperparasitemia (HP) were compared using histopathology, PaO_2 measurement, pulmonary X-ray, breathing capacity, lung permeability, and serum vascular endothelial growth factor (VEGF) levels according to either the day of death or the suggested predictive criteria. We proposed a model to predict malaria-associated ALI/ARDS using breathing patterns (enhanced pause and frequency respiration) and parasitemia as predictive criteria from mice whose cause of death was known to retrospectively diagnose the sacrificed mice as likely to die of ALI/ARDS as early as 7 days after infection. Using this method, we showed increased VEGF levels and increased lung permeability in mice predicted to die of ALI/ARDS. This proposed method for accurately identifying mice suffering from ALI/ARDS before death will enable the use of this model to study the pathogenesis of this disease.

1. Introduction

Malaria is an infectious disease with a huge impact on public health and a high mortality rate. According to the World Health Organization, approximately 3.3 billion people were at risk of contracting malaria in 2011 [1–3]. In some individuals, *Plasmodium* infection may result in severe malaria that can lead to ALI/ARDS [4, 5]. Patients infected with

P. falciparum, *P. vivax*, and *P. knowlesi* can develop ALI or ARDS with mortality rates of approximately 80% [6, 7]. Malaria-associated ALI/ARDS is thought to be due, in part, to increased alveolar permeability, parasite sequestration, and host immune response; however, the mechanisms behind it are largely unknown [4].

ALI/ARDS can occur at any time during an infection, even after treatment with antimalarial drugs when parasitemia has been reduced (reviewed in [4]). The development of ALI/ARDS, along with its negative outcomes, makes the prospective identification and effective treatment of those who develop this syndrome very important. Though, there is little information on malaria-associated ALI/ARDS progression, resulting in a lack of knowledge of the mechanisms of pathogenesis; therefore, the understanding of mouse models is essential.

Several reports have observed lung injury in mice infected with *P. berghei* (*Pb*) strains [8–19]. The observations have highlighted possible roles for many factors, including platelet-activating factor receptor [8], urokinase receptor [9], ICAM-1 [10, 11], CD40 [12], neutrophils [13], vascular endothelial growth factor (VEGF) [14], epithelium sodium channel activity [15], CD36-dependent parasite sequestration [16], hemozoin deposition [17], and CD8+ T lymphocytes [18], in malaria-associated lung injury.

Recently, there have been many models described that focus on the pulmonary pathology associated with malaria, including the classical C57BL/6 susceptible mouse model of cerebral malaria infection with *Pb*ANKA [16, 19]. Other models have used different parasite/mouse combinations that result in the mice surviving for longer periods of time (without signs of cerebral malaria), theoretically allowing the investigation of disease progression over time [14, 15, 18]. However, none of them were able to identify ALI/ARDS before death. Here, we have characterized a murine model of malaria-associated ALI/ARDS that shows similarities between humans and murine ALI/ARDS. Moreover, we proposed a method for classifying mice suffering from ALI/ARDS before the time of death as a predictive model for malaria-associated ALI/ARDS.

2. Materials and Methods

2.1. Mice and Parasites. DBA/2 male mice 6–10 weeks old (purchased from the Department of Parasitology, University of São Paulo, Brazil) were infected with 1×10^6 *P. berghei* ANKA (clone 1.49 L) infected red blood cells (iRBCs), as previously described [14]. Parasitemia and mortality were monitored daily. Parasitemia levels were analyzed using Giemsa-stained peripheral blood smears.

2.2. Anesthesia and Euthanasia. All efforts were made to prevent undue stress or pain to the mice. Mice with signs of imminent death were euthanized to avoid suffering. Before restraint for X-rays, the mice were given ketamine (100 mg/kg) and xylazine (5 mg/kg). The mice were euthanized with ketamine (300 mg/kg) (Vetbrands, Brazil) and xylazine (22.5 mg/kg) (Syntec, Brazil), and consciousness was checked by testing the pedal reflex, heartbeats and breathing movements.

2.3. Histological Evaluations. Necropsy was performed in mice dying naturally from the malaria or mice sacrificed on the 20th days after infection (DAI) to complete the experiment and to avoid animal suffering. The lungs were collected, fixed in buffered 10% formalin and then embedded in paraffin, sectioned at 5 μm onto slides and stained with hematoxylin-eosin (HE) and phosphotungstic acid hematoxylin (PTAH), to emphasize fibrin, as previously described [20].

2.4. Arterial Blood Analyses and Measurements of Body Temperature. Mice were placed near a heat lamp for three minutes to increase peripheral blood flow. The mice were then restrained by hand, the ventral artery of the tail was nicked with a small scalpel blade, and capillary tubes containing lithium-heparin (50 IU/mL) were placed underneath the cut to collect approximately 100 μL of blood. The blood was immediately placed in an i-STAT EG 8+ cartridge and analyzed using the *iSTAT* System Analyzer (Abbott group). The PaO_2/FiO_2 was calculated assuming that the fraction of inspired O_2 (FiO_2) was 0.21. In a subset of mice, the inguinal temperatures were assessed on day 0 and on the 5th, 7th and 9th DAI using a DT-203/60SEC digital thermometer (Becton Dickinson, Franklin Lakes, New Jersey, EUA).

2.5. X-Ray. Mice received light anesthesia on the 7th DAI and were X-rayed for 0.066 seconds in a mA100 fine focus Bucky V mAs 6.6 (RAYtech machine KV37, USA). A trained technician blinded to the infection status of the mice examined the X-rays, which were scored for signs of lung injury: 0, no change; 1, discrete and/or light opacification; and 2, diffuse opacification. The mice were later classified as suffering from ALI/ARDS or HP at death by the presence or absence of pleural effusion, respectively.

2.6. Determination of Respiratory Pattern. Respiratory patterns (respiratory frequency (RF) and enhanced pause (Penh)) were monitored on the 5th, 7th, 9th, 15th, and 20th DAI by placing the mice in an unrestrained whole-body plethysmography chamber (WBP, Buxco Electronics, Wilmington, North Carolina, USA) for 10 minutes (basal level). The data were collected using Biosystems XA software and included the RF (breaths/minute) and variables to calculate the Penh, a theoretical variable that correlates with both pulmonary resistance and intrapleural pressure [21]. The Penh is calculated by [22]

$$\text{Penh} = \frac{\text{peak expiration speed}}{\text{peak inspiration speed}} \times \left(\frac{\text{expiratory time}}{\text{relaxation time}} - 1 \right). \quad (1)$$

2.7. Identifying ALI/ARDS in Mice before Death. To identify ALI/ARDS in mice before death, we used two groups of infected mice: the survival group (infected control) and the sacrificed group in which the mice were sacrificed on the

7th DAI (10–12 mice per group). In the survival group, any mouse showing pleural effusion or red and congested lungs at necropsy, the cause of death was attributed to ALI/ARDS. In contrast, at necropsy, in mice without pleural effusion that died after 13th DAI with pale lungs and high levels of parasitemia, the cause of death was attributed to HP and consequently anemia.

Individual mice sacrificed on the 7th DAI were classified as having been likely to die of ALI/ARDS or HP, by comparing their respiratory patterns and parasitemia levels with the survival group, in which the *causa mortis* was known (Supplementary Figure S1 in Supplementary Material available online at http://dx.doi.org/10.1155/2014/872464).

In each individual experiment, using the survival group, we established three cut-offs using receiver operating characteristic (ROC) curves for the Penh, RF, and parasitemia measured on the 7th DAI, which were used as predictive criteria. The cut-offs from this group were chosen based on the maximum sensitivity and specificity for each parameter. The mice sacrificed on day 7 were also screened for the same parameters before sacrifice, and they were grouped based on the cut-offs from the ROC curves generated using data from the survival group. The same cut-offs were used to retrospectively classify the sacrificed group as suffering from ALI/ARDS or HP. The mice were said to have suffered from ALI/ARDS if they were above the cut-off for at least two of the three variables. For this method to work, it was necessary that three or more animals died by ALI/ARDS in the survival group/per experiment. In all of the experiments, we calculated the sensitivity and specificity from the survival group.

2.8. Confirming the Accuracy of the Groupings. To confirm if and when the mice could be grouped using the respiratory pattern cut-offs and parasitemia, confirmation experiments were performed. Two survival groups were assessed for pleural effusion and reddish lungs, which were used as the gold standards for mice dying of lung injury. These criteria constitute a practical phenotype for assessing ALI/ARDS because they are not arbitrary and can be assessed immediately during the necropsy; furthermore, previous results have shown that 100% of the mice that die between 7–12 DAI with clear signs of ALI, including the presence of pulmonary edema, hemorrhages, and hypoxemia [14]. The survivors were monitored until the 20th DAI, and the cause of death was determined. At the end of the experiment, the data from one group were used to generate the ROC curves that were then used to classify the mice in the second group on the 7th DAI; these results were then compared with observations of the pathology from necropsy of the second group (Supplementary Figure S2). Confirmation that the second mouse groupings were likely to be correct was performed in experiments in which the sensitivity and specificity of the groupings using the ROC curves were calculated.

2.9. Lung Permeability and Edema. To investigate lung permeability, on the 7th DAI, mice were injected intravenously with 0.2 mL of 1% Evans Blue (Sigma). The mice were sacrificed 45 minutes later, and the lungs were weighed and placed in 2 mL of formamide (Merck) for 48 hours at 37°C. The absorbance of the formamide was then measured at λ620 nm. The amount of Evans Blue staining per gram of lung tissue was calculated from a standard curve. The sacrificed mice were classified as suffering from ALI/ARDS by the ROC curves generated from a survival group as described above. The lung permeability of the ALI/ARDS and HP mice was expressed as fold increase in relation to that of the NI mice. To further investigate the presence of edema, in a group of survival mice, the lungs were weighed immediately after natural death, and the wet weights were recorded and compared between ALI/ARDS and HP mice of the same age. The mice were confirmed as suffering from ALI/ARDS or HP at death by the presence or absence of pleural effusion, respectively.

2.10. VEGF in Serum. On the 7th DAI, mice were anesthetized, and their serum was collected by cardiac puncture. An ELISA kit (R&D Systems) was used to quantify VEGF levels in the serum according to the manufacturer's instructions. The VEGF level of the ALI/ARDS and HP mice was expressed as fold increase in relation to that of the NI mice. The mice were classified as suffering from ALI/ARDS or HP by comparing the predictive criteria and VEGF levels.

2.11. Hematological Parameters Determination. Blood samples were collected in tubes containing sodium citrate as anticoagulant. Total number of red blood cells, hemoglobin, and hematocrit were measured using V-53 reagent kit (Mindray, P.R. China) and Auto Hematology Analyzer BC-5300Vet (Mindray, Nanshan, Shenzhen, P.R. China).

2.12. Statistical Analysis. The data were analyzed by D'Agostino-Pearson normality test. Nonparametric variables were compared using Mann-Whitney test. The simultaneous effects of two factors were analyzed by two-way ANOVA following Bonferroni post-hoc test. The differences between the groups were considered significant when $P \leq 0.05$. Statistical analyses were performed in GraphPad Prism version 5.0, including assessments of sensitivity and specificity. To establish cut off from data, ROC curves were generated using the results of the control group in MedCalc version 8.2.1.0. The Penh, RF and, EP data were analyzed using SPSS for Microsoft version 19.0 through a Pearson correlation (Penh versus RF: −0.827, P: 0.001; Penh versus EP: −0.152, P: 0.001; RF versus EP: 0.200, P: 0.05) for further grouping. The cluster analysis was developed by case grouping using Ward's method with a Euclidean distance analysis, which generated a dendrogram grouping each of the subjects studied and their physiologic characteristics analyzed into a particular cluster.

3. Results

3.1. Overview of Pathology at Death in PbANKA-Induced ALI/ARDS. To characterize and discriminate the pathology associated with ALI/ARDS or HP, DBA/2 mice were infected with *P. berghei* ANKA-infected red blood cells (iRBCs) and

followed until their deaths. Subsequently, the animals were necropsied and the *causa mortis* determined. Survival analysis revealed an average of 49.2% (25–75%) of the mice had died of ALI/ARDS between the 7th and 12th DAI, whereas the HP mice died between the 13th and 21st DAI (Figure 1(a)). Although parasitemias were increased in both groups, the HP group had higher levels of parasitemia, at approximately 40–50% on the day of death (Figure 1(b)). Comparing the lung weights, we observed that the mice that died with ALI/ARDS had heavier lungs (averaging 40% more mass) than the mice that died with HP, suggesting edema (Figure 1(c)).

At necropsy, noninfected (NI) mice had light pink lungs, and no liquid inside of the thoracic cavity was observed (Figure 1(d)). However, mice that died with ALI/ARDS had reddish lungs and pleural effusion (Figure 1(e)). In these mice, the histological changes where characterized by marked alveolar edema and hemorrhage, along with neutrophil-dominant inflammatory cellular infiltration, foamy macrophages in the alveolar and interstitial sites, and destruction of the alveolar septa (Figure 1(h)), as previously described [14]. In contrast to the ALI/ARDS mice, the animals that died with HP after the 13th DAI had grayish lungs and a darkened spleen and liver but no pleural effusion (Figure 1(f)) and severe anemia, with decreases in the number of erythrocytes, hemoglobin level, and hematocrit percentage (Supplementary Figure S3). These HP mice had interstitial pneumonia with mononuclear inflammatory cells but at a later time in the infection, diagnosed on the day of death (Figure 1(i)). Interestingly, in the lungs of ALI/ARDS mice we observed the presence of acellular eosinophilic membranes that adhered to the alveolar ducts and walls and hyaline membranes, a hallmark of ALI/ARDS in humans (Figures 1(j) and 1(k)).

3.2. Chest Radiography Shows Lung Opacity in PbANKA-Induced ALI/ARDS. Bilateral infiltrates observed on frontal chest radiographs are recognized as a criterion for the diagnosis of ALI and ARDS [23]. In our work, X-ray analysis on the 7th DAI revealed lung opacification, which was more prominent in the ALI/ARDS group than in the HP group (Figures 2(a) and 2(b)). NI mice had no changes in the lungs.

3.3. PbANKA-Induced ALI/ARDS Is Associated with Hypoxemia and Decreased Body Temperature. Hypoxemia is not a direct assessment of damage *per se* but is often a manifestation of injury [24]. In humans, the hypoxemia was defined by The American-European Consensus Conference as $PaO_2/FiO_2 \leq 300$ mmHg (for ALI) or ≤200 mmHg (for ARDS) [25]. In agreement with previous results [14], we show that the majority of the DBA/2 mice infected with *Pb*ANKA who died of ALI/ARDS had PaO_2/FiO_2 values between 200 and 300 mmHg, and we further demonstrate that mice that developed the more severe form of ARDS, presented PaO_2/FiO_2 values of ≤200 mmHg. On the 7th DAI, the PaO_2/FiO_2 in the ALI/ARDS group (234.3 ± 21.38) was significantly lower than the level in the HP group (303±17.26; $P = 0.029$) (Figure 2(c)). NI mice showed PaO_2/FiO_2 values above 300 mmHg with average 371.42 (SD ± 24.27). There are no agreed-upon validated PaO_2/FiO_2 data in animal models of lung injury [26]; thus, we categorized all of the animals in the group with lung injury as ALI/ARDS.

The infected mice had slightly increased body temperatures between day 0 and the 5th DAI; however, between the 7th and 9th DAI, their temperatures dropped and the mice became hypothermic (Figure 2(d)). Mice that would start to develop ALI/ARDS and die had the lowest temperatures on the 7th DAI compared with the HP mice. We hypothesized that the reduction in body temperature could be related to decreased survival of the animals, especially those that developed ALI/ARDS.

3.4. Respiratory Patterns and Parasitemia Are Correlated in PbANKA-Induced ALI/ARDS. To characterize the lung physiopathology during infection, we analyzed the enhanced pause (Penh), respiratory frequency (RF), and parasitemia (EP) levels at five different time points. On the 5th DAI the ALI/ARDS group had breathing patterns and parasitemia similar to the HP group and NI mice. However, by the 7th DAI, the ALI/ARDS group had increased Penh, decreased RF, and a tendency to increase the parasitemia even if not significantly, compared with the HP mice (Figures 3(a)–3(c)). After the 9th DAI, the statistical comparison between the ALI/ARDS and HP mice could not be performed in the individual experiments due to the minimal numbers of surviving ALI/ARDS mice. Interestingly, animals that survived for longer periods, that is, animals that did not develop ALI/ARDS and subsequently died by HP, breathing patterns returned nearly to baseline levels. NI mice had no changes in breathing patterns over time.

Parasitemia increased over the course of infection (Figure 3(c)). On the day of death, parasitemia in the ALI/ARDS group was 20.8% (SD ± 4.6), while parasitemia in mice that died of HP was 40.9% (SD ± 9.21; $P \leq 0.0001$). However, on the 7th DAI, the mice that went on to die of ALI/ARDS had 17.0% (SD ± 5.0) iRBCs, while the mice that would go on to die with HP were 12.2% (SD ± 4.5) parasitemic (Supplementary Figure S4a).

Aiming to perform a correlation study examining the respiratory parameters (Supplementary Figure S4b and S4c) and EP (Supplementary Figure S4a), we conducted experiments on the 7th DAI, when the onset of important pulmonary pathology occurred, rather than using the 5th DAI when we did not observe consistent differences in respiratory patterns between the study groups.

The high correlation between Penh, RF, and EP and the development of ALI/ARDS or HP (Pearson correlation Penh *versus* RF: −0.827, $P = 0.001$; Penh *versus* EP: −0.152, $P = 0.001$; RF *versus* EP: 0.200, P: 0.05) led us to identify four groups based on the cluster analysis (group 1 consisted of 88.46% of individuals with ALI/ARDS and 11.53% with HP; group 2 included 57.77% of individuals with ALI/ARDS and 42.22% with HP; group 3 consisted of 19.35% individuals with ALI/ARDS and 80.64% with HP; group 4 included 21.42% of individuals with ALI/ARDS and 78.57% with HP) (Figure 4). Such clustering highlights that the physiological conditions evaluated in groups 1 and 2 were dominated by ALI/ARDS,

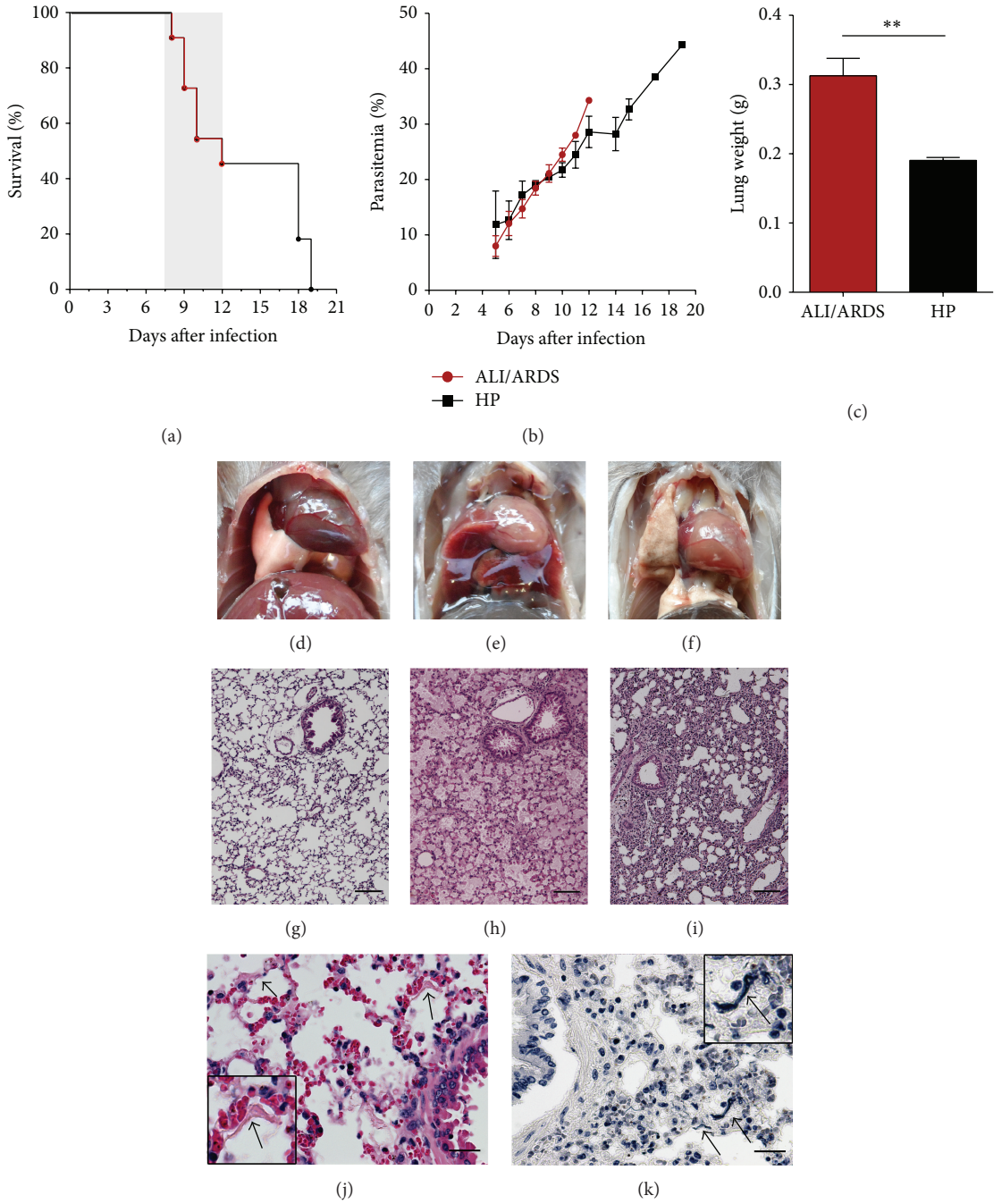

Figure 1: Infection of DBA/2 mice with *P. berghei* ANKA constitutes a rodent model for malaria-associated ALI/ARDS. (a) Survival and (b) parasitemia curves from the ALI/ARDS and HP mice over time. The red line was the mice that died with ALI/ARDS. The gray area represents the period when the mice die of ALI/ARDS. The data presented are representative of 13 independent experiments; $n = 10–12$ mice/experiment. (c) The lungs of mice that died with ALI/ARDS weighed 40% more than the lungs of mice that died with HP ($^{**}P \leq 0.005$; Mann-Whitney test of lung weights are representative of four separate experiments). Data ((b) and (c)) represent means and SEM; $n = 10–12$ mice/experiment. (d) Representative pictures of a NI mouse, (e) an infected mouse that died with ALI/ARDS showing hemorrhagic lungs and a large amount of pleural effusion, and (f) a mouse that died with HP showing pale and grayish lungs and no pleural effusion. Representative histopathological images of lungs from (g) NI mice and infected DBA/2 mice that died with (h) ALI/ARDS and (i) HP on the 10th and 21st days after infection, respectively. The arrow points to the hyaline membranes in the lungs of the DBA/2 mice that died with (j) ALI/ARDS stained with hematoxylin-eosin and (k) stained with phosphotungstic acid hematoxylin. The bar corresponds to 100 μm. HP: hyperparasitemia; ALI/ARDS: acute lung injury/acute respiratory distress syndrome.

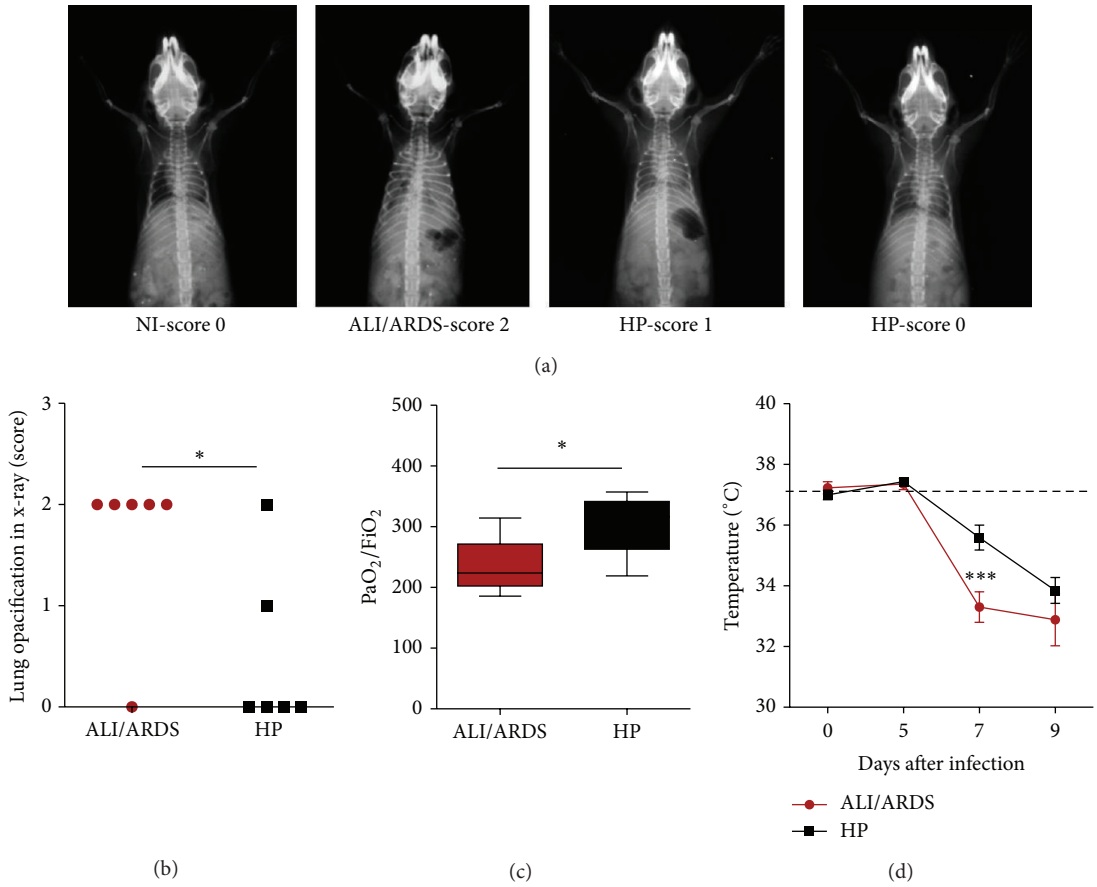

Figure 2: Radiography of the lungs, hypoxemia, and body temperature over time. (a) From left to right, X-rays from NI and infected DBA/2 mice that died with ALI/ARDS and HP showing different lung opacification scores on the 7th DAI. (b) Lung opacification scores on the 7th DAI. Mice that will later die with ALI/ARDS have a higher lung opacification score compared with mice that will die with HP ($n = 12$; $^{*}P \leq 0.05$, Mann-Whitney test of scores taken from two separate experiments). NI mice do not have any lung opacification and are assigned score zero. (c) PaO_2/FiO_2 values in *P. berghei* ANKA-infected mice on the 7th DAI. Results from three grouped experiments ($n = 13$ mice, $^{*}P \leq 0.05$; Mann-Whitney test). (d) Body temperatures in DBA/2 mice infected with *P. berghei* ANKA slightly increased on the 5th DAI from 37.1°C in the NI mice to 37.3 in the ALI/ARDS mice and 37.4°C in the HP mice). However, the temperatures dropped and the mice became hypothermic (especially the ALI/ARDS mice), with mean temperatures of 33.0°C on the 7th DAI and 32.8°C on the 9th DAI. Results are from three grouped experiments ($n = 31$ mice; $^{***}P \leq 0.001$, two-way ANOVA with Bonferroni post test). Data (d) represents means and SEM. The dashed line represents the mean value of NI mice. NI: noninfected mice; ALI/ARDS: acute lung injury/acute respiratory distress syndrome; HP: hyperparasitemia.

while groups 3 and 4 were dominated by HP, with a difference of 25%. Additionally between the groups with major higher frequencies of one of the two pathologies (groups 1 and 2 or groups 3 and 4), the difference between the analyzed characteristics was 10%.

3.5. A Murine Model to Predict Malaria-Associated ALI/ARDS at an Early Time Point. Mice that die from ALI/ARDS present altered Penh, RF, and EP values from the mice that die from HP; thus, we hypothesized that those parameters could be used as predictive criteria for the *causa mortis*. As described in the materials and methods, for each individual experiment, we used an infected control group (survival group) and established cut-offs using ROC curves for Penh, RF, and EP (Supplementary Table S1) measured on the 7th DAI and applied these cut-offs to classify the sacrifice group (Supplementary Figure S1). Following this procedure, the mice sacrificed on the 7th DAI could be classified as likely to die with ALI/ARDS or HP. We compared their respiratory patterns and parasitemia with a survival group that was not sacrificed and for which the cause of death was known. The sensitivity (≤100% and ≥67%; average 88.31%; SD ± 11.95) and specificity (100% ≤ and ≥71%; average 90.85%; SD ± 10.81) were calculated from the survival group for each individual experiment. In addition, we observed that the respiratory patterns and parasitemia were similar between the survival group and the sacrificed group (Figures 5(a)–5(c)).

To confirm the accuracy of the grouping, the cut-offs from the ROC curves of the respiratory patterns and parasitemia were performed using the two infected control groups (survival groups) on the 7th DAI. The groups were monitored until the 20th DAI, and the cause of death was determined

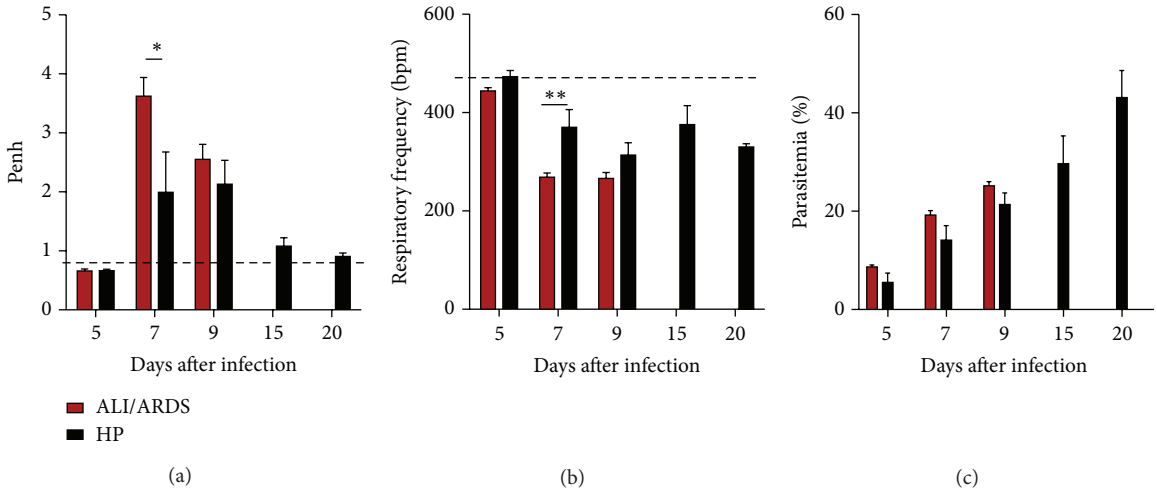

Figure 3: Breathing patterns and parasitemia from ALI/ARDS and HP mice over time. (a) and (b) Breathing patterns and (c) parasitemia from DBA/2 mice infected with *P. berghei* ANKA that developed ALI/ARDS and HP over time. (a) There was no evidence on the 5th and 9th DAI that the ALI/ARDS and HP mice had different breathing patterns. However, on the 7th DAI, there was evidence that the ALI/ARDS mice had a higher enhanced pause (Penh) (a) and a lower respiratory frequency (b) than the HP mice. Parasitemia increased over time in both groups (c). Results are representative from three independent experiments ($n = 11$ mice/experiment; $^{*}P \leq 0.05$, two way ANOVA with Bonferroni post test). The dashed line represents the mean value of NI mice; NI: noninfected mice; ALI/ARDS: acute lung injury/acute respiratory distress syndrome; HP: hyperparasitemia.

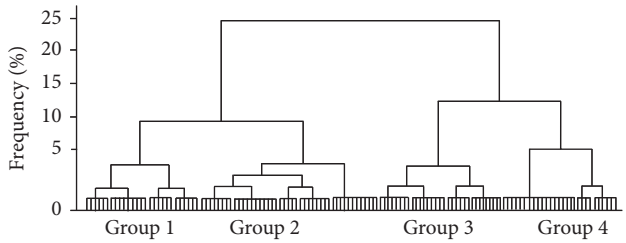

Figure 4: Breathing patterns and parasitemia could be used to group mice into two main clusters. Ward's linkage cluster analysis illustrates the distance between the physiological cluster patterns in DBA/2 mice infected with *P. berghei* ANKA that developed ALI/ARDS and HP. Values were measured on the 7th DAI. The data are from 13 independent experiments; $n = 142$ mice. Group 1 = 88.46% of individuals with ALI/ARDS and 11.53% with HP; group 2 = 57.77% of individuals with ALI/ARDS and 42.22% with HP; group 3 = 19.35% individuals with ALI/ARDS and 80.64% with HP; group 4 = 21.42% of individuals with ALI/ARDS and 78.57% with HP. ALI/ARDS: acute lung injury/acute respiratory distress syndrome; HP: hyperparasitemia.

(Supplementary Figure S2). On the 7th DAI, we were able to group the mice in the ALI/ARDS or HP groups with 91% sensitivity and 76% specificity in the three grouped experiments (Table 1). Among the experiments, the best result was 100% sensitivity and 100% specificity, and the worst result was 66.6% sensitivity and 60% specificity. On the 9th DAI, we were not able to group the mice, as no ALI/ARDS mice from the survival group were alive.

3.6. PbANKA-Induced ALI/ARDS Causes Breakdown of the Alveolar-Capillary Barrier. In a previous study, we demonstrated that VEGF promotes malaria-associated ALI in mice and that expression of this growth factor is increased in mice that died of ALI [14]. Here, using blood samples from mice sacrificed on the 7th DAI, we confirmed that mice classified as likely to die with ALI/ARDS and HP had VEGF serum levels 3.3-fold and 1.7-fold higher than those in the NI group, respectively (Figure 6(a)). Furthermore, the pulmonary vascular permeability measured by Evans blue uptake in the lungs on the 7th DAI was higher in mice predicted to die of ALI/ARDS (10.6-fold higher than NI mice) than in those classified as suffering from HP (5.5-fold higher than NI mice) (Figures 6(b)–6(e)).

Table 1: Confirming the accuracy of the groupings. True and false pathologies checked by the ROC curves from the predictive criteria* on the 7th DAI and the *causa mortis*.

	Pathology		
Test	ALI/ARDS	HP	Total
Hits	11	13	24
Errors	1	4	5
Total	12	17	29

*Penh, respiratory frequency, and parasitemia.

4. Discussion

According to The American-European Consensus Conference, the recommended criteria to define both ALI and ARDS are acute onset, hypoxemia levels of $PaO_2/FiO_2 \leq 300$ mmHg (for ALI) or ≤200 mmHg (for ARDS), bilateral infiltrates seen on a frontal chest radiograph, and pulmonary artery wedge pressure (≤18 mmHg when measured or no clinical evidence of left atrial hypertension) (revised by Thompson and Moss,

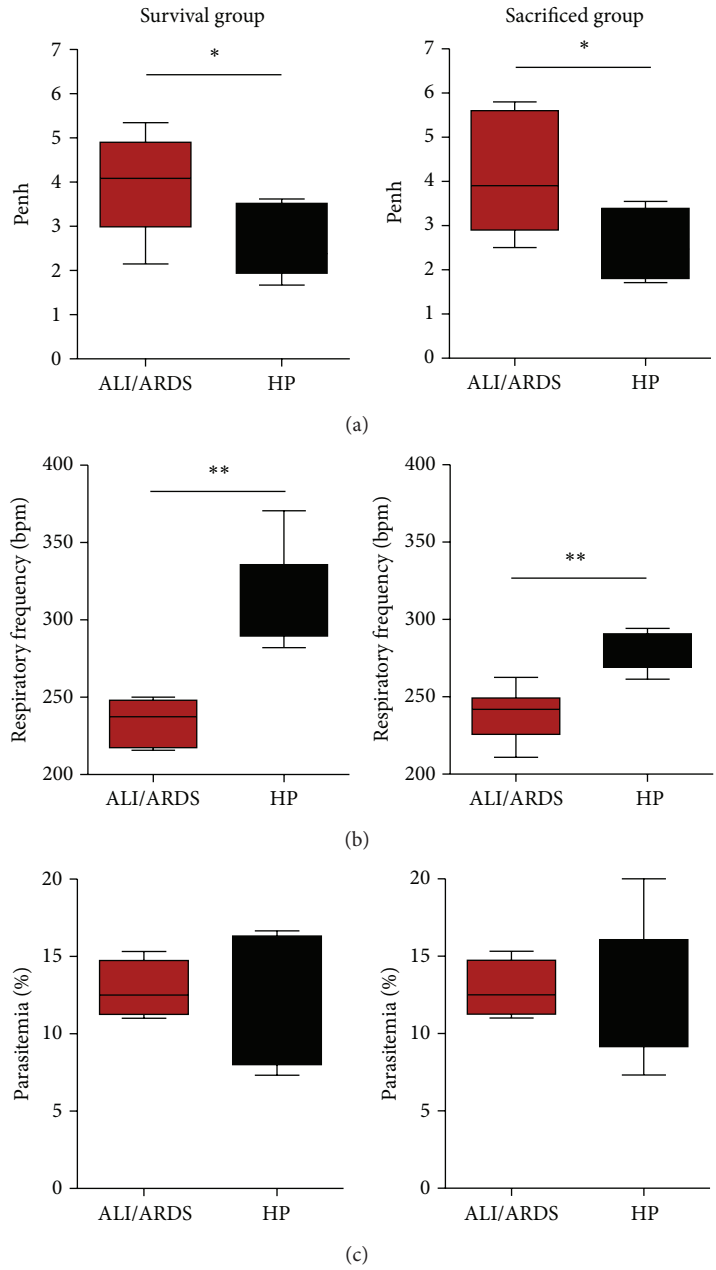

FIGURE 5: A murine model to predict malaria-associated ALI/ARDS. (a) Penh (enhanced pause), (b) respiratory frequency, and (c) parasitemia measured on the 7th DAI. The sacrificed mice were classified according predictive model, using the parameter cut-offs measured from the survival mice and applied to the sacrificed mice. DBA/2 mice infected with *P. berghei* ANKA and their breathing parameters were measured in plethysmograph chambers (BUXCO Electronics, USA). Note that these three parameters are similar between the survival group and sacrificed group; (n = 11 mice/group; $^{*}P < 0.05$, $^{**}P < 0.005$, Mann-Whitney test). ALI/ARDS: acute lung injury/acute respiratory distress syndrome; HP: hyperparasitemia; bpm: beats per minute. Results are representative of more than 5 independent experiments.

2010). Recently, in accord with The Berlin Definition, the ALI term was abolished and the ARDS was defined based on oxygenation: mild ARDS (200 mmHg $PaO_2/FiO_2 \leq 300$ mmHg), moderate ARDS (100 mmHg $PaO_2/FiO_2 \leq 200$ mmHg), and severe ARDS (bellow 100 mmHg PaO_2/FiO_2, among other criteria [27]. However, The Berlin Definition was not validated by a later study [28] and ALI is still used for lung injury in mice. Despite the discussion in the field, some consensual parameters are used to study ALI in mice such as kinetics of injury, radiographic evaluation, physiological assessment, histological evidence of lung injury, and assessment of increased permeability of the alveolar-capillary membrane [26].

Malaria-associated ALI/ARDS is progressively more frequently reported, is often fatal and is still not fully understood [29], thus an animal model would be essential to address

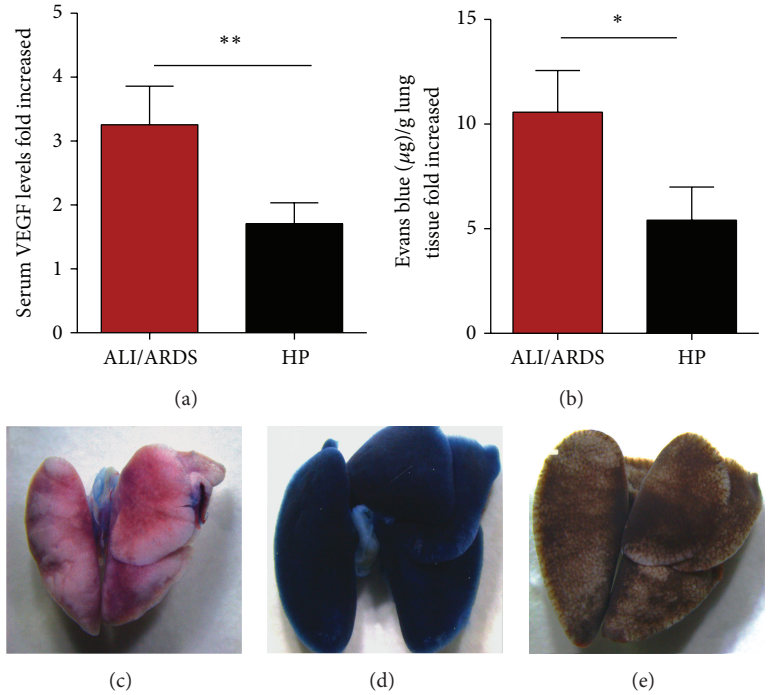

Figure 6: Increased vascular permeability and serum VEGF protein confirmed the predictive criteria for malaria-associated ALI/ARDS. (a) Serum VEGF protein in DBA/2 mice infected with *P. berghei* ANKA on the 7th DAI was measured by ELISA. The VEGF levels are higher in the mice classified as likely to die with ALI/ARDS compared with HP mice (according to the proposed predictive criteria). The data represent fold increases in relation to NI mice taken from three experiments; ($n = 28$ mice; $^{**}P < 0.005$, Mann-Whitney test). (b) Lung vascular permeability in DBA/2 mice infected with *P. berghei* ANKA 7th DAI, assessed using Evans Blue. The vascular permeability is higher in the mice classified as likely to die with ALI/ARDS compared with the HP mice (according to the proposed predictive criteria). The data represent fold increased in relation to NI mice taken from three experiments; ($n = 51$ mice; $^{*}P < 0.05$, Mann-Whitney test). Bars represent means and SEM. The images represent (c) NI: noninfected mice, (d) ALI/ARDS: acute lung injury acute respiratory distress syndrome, and (e) HP: hyperparasitemia.

such a complex disease [30]. We showed that DBA/2 mice infected with *Pb*ANKA constitute a rodent model of malaria-associated ALI/ARDS [14], and here, we approach respiratory and parasitological parameters to devise a mathematical model able to predict development of ALI/ARDS during *Pb*ANKA infection.

This murine model clearly showed edema in ALI/ARDS mice, indicating that these animals had more severe disease and that they were dying during the exudative phase of ALI/ARDS. In addition, we observed local destruction of the alveolar epithelium, with denuded areas covered by fibrin-containing hyaline membranes, a hallmark of ALI/ARDS in humans [23], along with neutrophils, alveolar macrophages, mononuclear cells, and iRBC. The presence of edema observed in the ALI/ARDS mice is also reflected by the increased wet weight of the lungs [31], although the increased weight of the lungs could be partially due to cellular accumulation [18]. The opaque appearance of the lungs in X-rays and the opaque pulmonary alveolar pattern were sometimes bilateral and other times unilateral. However, we did not observe type II cell hyperplasia in the ALI/ARDS mice or the interstitial fibrosis characteristic of the proliferative phase of ARDS, denoting the early stage of the acute syndrome.

Pleural effusion was used as a gold standard for mice dying of lung injury, as it is a practical nonarbitrary phenotype to assess. Even though this finding is infrequent in human malaria, pleural effusion has been observed in malaria-associated ARDS in humans and in a nonmalarial setting and has previously been correlated with reduced gas exchange in the lungs [32–34].

Here, we showed that respiratory patterns and parasitemia differ between the mice that would go on to die with ALI/ARDS or HP in a model of malaria-associated lung injury. We further show that we could use these differences to accurately group the mice as likely to die with ALI/ARDS as early as the 7th DAI but not on the 5th DAI. On the 7th DAI, there were significant differences in these parameters between the two groups, and the use of a cut-off from the ROC curves enabled us to identify the mice that would die with ALI/ARDS, with 88.5% (SD ± 11.52) sensitivity and 90.7% (SD ± 11.45) specificity at this point using the cut-off for Penh, RF, and EP from the survival group as a template for the sacrificed group.

The ability to identify mice as being likely to die of ALI/ARDS accurately based on respiratory patterns and parasitemia opens up the possibility of studying this disease without concerns for confounding data generated from mice that would never go on to develop the disease or having to wait until death is imminent. Altered respiratory patterns are associated with lung injury and have been observed in

a number of respiratory models, including Penh data that have been used in different murine models [35–37]. The high parasitemia that is associated with adverse outcomes has been shown in a number of murine malaria models [38, 39], further supporting our choice to use these parameters to distinguish mice suffering from ALI/ARDS. Despite some controversy regarding the use of Penh [20], our results clearly show that this parameter varies between mice that will or will not die of ALI/ARDS.

ARDS in humans causes tachypnea [23]. Nevertheless, the current data showed the ALI/ARDS mice had a lower RF than the HP mice. In addition, our results showed that animals with ALI/ARDS experienced a sharp decline in body temperature, especially on the 7th DAI. Despite malaria being traditionally known as a febrile illness [40, 41], murine malaria, including ARDS, can lead to hypothermia [18, 42, 43]. This symptom may be an interesting effort to reduce inflammation-mediated damage to the endothelium, as it has been shown that increased temperatures result in increased sensitivity of endothelial cells to proinflammatory factors such as tumor necrosis factor [44]. We suggest that decreased RF may be a side effect of hypothermia; it may also be associated with the increased effort required by the mice to breathe due to the lung damage, edema and/or hypothermia that may have contributed to the development of ALI/ARDS and the death of these animals.

Even though the parasitemia average was higher in the ALI/ARDS group on the 7th DAI in the 13 experiments observed (Supplementary Figure S4a), it was the most variable analyzed parameter. In our predictive model, even small differences often helped to define whether an animal would be classified with ALI/ARDS or HP because the proposed method combines two or three parameters at the same time. The high correlation identified between the Penh, RF, and EP and the development of ALI/ARDS or HP exhibited in the development of these pathologies by cluster analysis (Figure 4) with any differentiation factors studied under 5% could allow a positive identification of ALI/ARDS with an accuracy varying from 57.77% to 88.46% or of HP with an accuracy varying from 78.57% to 80.64%. Furthermore, these experiments revealed a large difference in these variables between the groups ranging from 25% to 10% in terms of physiological conditions studied, enabling us to establish parameters to predict the presence or absence of ALI/ARDS or HP with greater accuracy in our study model either with a refinement of the data or with the inclusion of one or more variables.

Previously, it was shown that lung vessel permeability and VEGF levels were significantly higher in infected DBA/2 mice exhibiting ALI symptoms when death is imminent [14]. Here, we confirmed similar these results using this new predictive criteria to classify these mice.

How *Plasmodium* infection causes ALI/ARDS remains largely unknown. Animal models have the potential to elucidate the mechanisms of disease and identify prognostic markers and therapeutic targets. The results presented in this paper describe a murine model of ALI/ARDS and, most importantly, describe how it is possible to accurately identify mice with lung injury before death. The study of mechanisms involved in the genesis of ALI/ARDS on earlier time points is essential for the elucidation of the pathogenic events underlying the development of this severe disease.

Ethical Approval

All experiments were performed in accordance with the ethical guidelines for experiments with mice, and the protocols were approved by the Animal Health Committee of the Biomedical Sciences Institute of the University of São Paulo (CEUA no. 003 page 98 book2) and of the Federal University of São Paulo (CEP 1712/09). The guidelines for animal use and care were based on the standards established by the The Brazilian College of Animal Experimentation (COBEA).

Conflict of Interests

The authors declare no commercial or other associations that might pose conflict of interests.

Authors' Contribution

Luana S. Ortolan, Michelle K. Sercundes, Renato Barboza, Oscar Murillo, Daniela Debone, and Stefano C. F. Hagen designed and performed the experiments, discussed the results, and analyzed the data. José M. Alvarez, Marcos Amaku, Claudio R. F. Marinho, and Sabrina Epiphanio conceived and designed the study, discussed the results, and wrote the paper. Maria Regina D' Império Lima and Momtchilo Russo reviewed the paper. Claudio R. F. Marinho and Sabrina Epiphanio funded this work.

Acknowledgments

The authors thank Maria M. Mota and Silvia Portugal for critically reviewing the paper and Bernardo Paulo Albe and Erika Paula Machado Peixoto for their technical support. Financial support was provided by Grants 2009/53256-7 (Sabrina Epiphanio) and 2009/53889-0 (Claudio R. F. Marinho) from the São Paulo Research Foundation (FAPESP) and the Conselho Nacional de Desenvolvimento Científico e Tecnológico (CNPq) 306668/2012-2 and 470590/2009-2 (Sabrina Epiphanio).

References

[1] World Health Organization, *World Malaria Report*, 2012.

[2] S. Antinori, L. Galimberti, L. Milazzo, and M. Corbellino, "Biology of human malaria plasmodia including *Plasmodium knowlesi*," *Mediterranean Journal of Hematology and Infectious Diseases*, vol. 4, no. 1, 2012.

[3] N. J. White, "Plasmodium knowlesi: the fifth human malaria parasite," *Clinical Infectious Diseases*, vol. 46, no. 2, pp. 172–173, 2008.

[4] A. Mohan, S. K. Sharma, and S. Bollineni, "Acute lung injury and acute respiratory distress syndrome in malaria," *Journal of Vector Borne Diseases*, vol. 45, no. 3, pp. 179–193, 2008.

[5] L. H. Miller, D. I. Baruch, K. Marsh, and O. K. Doumbo, "The pathogenic basis of malaria," *Nature*, vol. 415, no. 6872, pp. 673–679, 2002.

[6] W. R. J. Taylor, J. Hanson, G. D. H. Turner, N. J. White, and A. M. Dondorp, "Respiratory manifestations of malaria," *Chest*, vol. 142, no. 2, pp. 492–505, 2012.

[7] N. J. White, S. Pukrittayakamee, T. T. Hien et al., "Malaria," *The Lancet*, vol. 383, no. 9918, pp. 723–735, 2013.

[8] N. Lacerda-Queiroz, M. A. Rachid, M. M. Teixeira, and A. L. Teixeira, "The role of platelet-activating factor receptor (PAFR) in lung pathology during experimental malaria," *International Journal for Parasitology*, vol. 43, no. 1, pp. 11–15, 2013.

[9] P. F. Piguet, C. Da Laperrousaz, C. Vesin, F. Tacchini-Cottier, G. Senaldi, and G. E. Grau, "Delayed mortality and attenuated thrombocytopenia associated with severe malaria in urokinase- and urokinase receptor-deficient mice," *Infection and Immunity*, vol. 68, no. 7, pp. 3822–3829, 2000.

[10] J. Li, W. Chang, G. Sun et al., "Intercellular adhesion molecule 1 is important for the development of severe experimental malaria but is not required for leukocyte adhesion in the brain," *Journal of Investigative Medicine*, vol. 51, no. 3, pp. 128–140, 2003.

[11] N. Favre, C. Da Laperousaz, B. Ryffel et al., "Role of ICAM-1 (CD54) in the development of murine cerebral malaria," *Microbes and Infection*, vol. 1, no. 12, pp. 961–968, 1999.

[12] P. F. Piguet, C. D. Kan, C. Vesin, A. Rochat, Y. Donati, and C. Barazzone, "Role of CD40-CD40L in mouse severe malaria," *The American Journal of Pathology*, vol. 159, no. 2, pp. 733–742, 2001.

[13] G. Senaldi, C. Vesin, R. Chang, G. E. Grau, and P. F. Piguet, "Role of polymorphonuclear neutrophil leukocytes and their integrin CD11a (LFA-1) in the pathogenesis of severe murine malaria," *Infection and Immunity*, vol. 62, no. 4, pp. 1144–1149, 1994.

[14] S. Epiphanio, M. G. Campos, A. Pamplona et al., "VEGF promotes malaria-associated acute lung injury in mice," *PLoS Pathogens*, vol. 6, no. 5, Article ID e1000916, 2010.

[15] L. Hee, A. Dinudom, A. J. Mitchell et al., "Reduced activity of the epithelial sodium channel in malaria-induced pulmonary oedema in mice," *International Journal for Parasitology*, vol. 41, no. 1, pp. 81–88, 2011.

[16] F. E. Lovegrove, S. A. Gharib, L. Peña-Castillo et al., "Parasite burden and CD36-mediated sequestration are determinants of acute lung injury in an experimental malaria model," *PLoS Pathogens*, vol. 4, no. 5, Article ID e1000068, 2008.

[17] K. Deroost, A. Tyberghein, N. Lays et al., "Hemozoin induces lung inflammation and correlates with malaria-associated acute respiratory distress syndrome," *The American Journal of Respiratory Cell and Molecular Biology*, vol. 48, no. 5, pp. 589–600, 2013.

[18] P. E. van den Steen, N. Geurts, K. Deroost et al., "Immunopathology and dexamethasone therapy in a new model for malaria-associated acute respiratory distress syndrome," *American Journal of Respiratory and Critical Care Medicine*, vol. 181, no. 9, pp. 957–968, 2010.

[19] M. C. Souza, J. D. Silva, T. A. Pádua, V. L. Capelozzi, P. R. M. Rocco, and M. D. G. Henriques, "Early and late acute lung injury and their association with distal organ damage in murine malaria," *Respiratory Physiology and Neurobiology*, vol. 186, no. 1, pp. 65–72, 2013.

[20] M. Cotovio, L. Monreal, L. Armengou, J. Prada, J. M. Almeida, and D. Segura, "Fibrin deposits and organ failure in newborn foals with severe septicemia," *Journal of Veterinary Internal Medicine*, vol. 22, no. 6, pp. 1403–1410, 2008.

[21] E. Hamelmann, J. Schwarze, K. Takeda et al., "Noninvasive measurement of airway responsiveness in allergic mice using barometric plethysmography," *The American Journal of Respiratory and Critical Care Medicine*, vol. 156, no. 3 I, pp. 766–775, 1997.

[22] M. Lomask, "Further exploration of the Penh parameter," *Experimental and Toxicologic Pathology*, vol. 57, supplement 2, pp. 13–20, 2006.

[23] B. T. Thompson and M. Moss, *Acute Respiratory Distress Syndrome*, Informa Healh Care, New York, NY, USA, 2nd edition, 2010.

[24] G. Matute-Bello, C. W. Frevert, and T. R. Martin, "Animal models of acute lung injury," *The American Journal of Physiology—Lung Cellular and Molecular Physiology*, vol. 295, no. 3, pp. L379–L399, 2008.

[25] G. R. Bernard, A. Artigas, K. L. Brigham et al., "The American-European Consensus Conference on ARDS: definitions, mechanisms, relevant outcomes, and clinical trial coordination," *The American Journal of Respiratory and Critical Care Medicine*, vol. 149, part 1, no. 3, pp. 818–824, 1994.

[26] G. Matute-Bello, G. Downey, B. B. Moore et al., "An official american thoracic society workshop report: features and measurements of experimental acute lung injury in animals," *The American Journal of Respiratory Cell and Molecular Biology*, vol. 44, no. 5, pp. 725–738, 2011.

[27] V. M. Ranieri, G. D. Rubenfeld, B. T. Thompson et al., "Acute respiratory distress syndrome: the Berlin definition," *The Journal of the American Medical Association*, vol. 307, no. 23, pp. 2526–2533, 2012.

[28] R. Hernu, F. Wallet, F. Thiollière et al., "An attempt to validate the modification of the American-European consensus definition of acute lung injury/acute respiratory distress syndrome by the Berlin definition in a university hospital," *Intensive Care Medicine*, vol. 39, no. 12, pp. 2161–2170, 2013.

[29] P. E. van den Steen, K. Deroost, J. Deckers, E. van Herck, S. Struyf, and G. Opdenakker, "Pathogenesis of malaria-associated acute respiratory distress syndrome," *Trends in Parasitology*, vol. 29, no. 7, pp. 346–358, 2013.

[30] J. A. Bastarache and T. S. Blackwell, "Development of animal models for the acute respiratory distress syndrome," *Disease Models and Mechanisms*, vol. 2, no. 5-6, pp. 218–223, 2009.

[31] J. C. Parker and M. I. Townsley, "Evaluation of lung injury in rats and mice," *The American Journal of Physiology—Lung Cellular and Molecular Physiology*, vol. 286, no. 2, pp. L231–L246, 2004.

[32] M. S. Al-Ibrahim and R. S. Holzman, "Bilateral pleural effusion with *Plasmodium falciparum* infection," *The American Journal of Tropical Medicine and Hygiene*, vol. 24, no. 6, part 1, pp. 910–912, 1975.

[33] C. Sirivichayakul, P. Chanthavanich, W. Chokejindachai, K. Pengsaa, K. Kabkaew, and R. Saelim, "Pleural effusion in childhood falciparum malaria," *Southeast Asian Journal of Tropical Medicine and Public Health*, vol. 31, no. 1, pp. 187–189, 2000.

[34] S. Luh and C. Chiang, "Acute lung injury/acute respiratory distress syndrome (ALI/ARDS): the mechanism, present strategies and future perspectives of therapies," *Journal of Zhejiang University Science B*, vol. 8, no. 1, pp. 60–69, 2007.

[35] A. M. Sciuto, R. B. Lee, J. S. Forster, M. B. Cascio, D. L. Clapp, and T. S. Moran, "Temporal changes in respiratory dynamics in mice exposed to phosgene," *Inhalation Toxicology*, vol. 14, no. 5, pp. 487–501, 2002.

[36] X. Ci, X. Chu, X. Xu, H. Li, and X. Deng, "Short-term roxithromycin treatment attenuates airway inflammation via MAPK/NF-κB activation in a mouse model of allergic asthma," *Inflammation Research*, vol. 61, no. 7, pp. 749–758, 2012.

[37] J. M. Stark, A. M. Khan, C. L. Chiappetta, H. Xue, J. L. Alcorn, and G. N. Colasurdo, "Immune and functional role of nitric oxide in a mouse model of respiratory syncytial virus infection," *Journal of Infectious Diseases*, vol. 191, no. 3, pp. 387–395, 2005.

[38] J. V. Harris, T. M. Bohr, C. Stracener et al., "Sequential Plasmodium chabaudi and Plasmodium berghei infections provide a novel model of severe malarial anemia," *Infection and Immunity*, vol. 80, no. 9, pp. 2997–3007, 2012.

[39] K. E. Schmidt, B. Schumak, S. Specht, B. Dubben, A. Limmer, and A. Hoerauf, "Induction of pro-inflammatory mediators in Plasmodium berghei infected BALB/c mice breaks blood-brain-barrier and leads to cerebral malaria in an IL-12 dependent manner," *Microbes and Infection*, vol. 13, no. 10, pp. 828–836, 2011.

[40] I. A. Clark, A. C. Budd, L. M. Alleva, and W. B. Cowden, "Human malarial disease: a consequence of inflammatory cytokine release," *Malaria Journal*, vol. 5, article no. 85, 2006.

[41] C. L. MacKintosh, J. G. Beeson, and K. Marsh, "Clinical features and pathogenesis of severe malaria," *Trends in Parasitology*, vol. 20, no. 12, pp. 597–603, 2004.

[42] M. Hernandez-Valladares, J. Naessens, S. Nagda et al., "Comparison of pathology in susceptible A/J and resistant C57BL/6J mice after infection with different sub-strains of *Plasmodium chabaudi*," *Experimental Parasitology*, vol. 108, no. 3-4, pp. 134–141, 2004.

[43] C. E. Cross and J. Langhorne, "Plasmodium chabaudi chabaudi (AS): inflammatory cytokines and pathology in an erythrocytic-stage infection in mice," *Experimental Parasitology*, vol. 90, no. 3, pp. 220–229, 1998.

[44] J. D. Hasday, D. Bannerman, S. Sakarya et al., "Exposure to febrile temperature modifies endothelial cell response to tumor necrosis factor-α," *Journal of Applied Physiology*, vol. 90, no. 1, pp. 90–98, 2001.

Hindawi Publishing Corporation
Mediators of Inflammation
Volume 2014, Article ID 230129, 10 pages
http://dx.doi.org/10.1155/2014/230129

Research Article

Lipoprotein Lipase and PPAR Alpha Gene Polymorphisms, Increased Very-Low-Density Lipoprotein Levels, and Decreased High-Density Lipoprotein Levels as Risk Markers for the Development of Visceral Leishmaniasis by *Leishmania infantum*

Márcia Dias Teixeira Carvalho,[1] Diego Peres Alonso,[2] Célia Maria Vieira Vendrame,[1] Dorcas Lamounier Costa,[3] Carlos Henrique Nery Costa,[3] Guilherme Loureiro Werneck,[4,5] Paulo Eduardo Martins Ribolla,[2] and Hiro Goto[1,6]

[1] *Laboratório de Soroepidemiologia e Imunobiologia, Instituto de Medicina Tropical de São Paulo, Universidade de São Paulo, Avenida Dr. Enéas de Carvalho Aguiar 470, Prédio II, 4° Andar, 05403-000 São Paulo, SP, Brazil*
[2] *Departamento de Parasitologia, Instituto de Biociências, Universidade Estadual Paulista, 18618-970 Botucatu, SP, Brazil*
[3] *Instituto de Doenças Tropicais Natan Portella, Universidade Federal do Piauí, 64001-450 Teresina, PI, Brazil*
[4] *Departamento de Epidemiologia, Instituto de Medicina Social, Universidade do Estado do Rio de Janeiro, 20550-900 Rio de Janeiro, RJ, Brazil*
[5] *Instituto de Estudos em Saúde Coletiva, Universidade Federal do Rio de Janeiro, 21941-598 Rio de Janeiro, RJ, Brazil*
[6] *Departamento de Medicina Preventiva, Faculdade de Medicina, Universidade de São Paulo, 01246-903 São Paulo, SP, Brazil*

Correspondence should be addressed to Hiro Goto; hgoto@usp.br

Received 22 May 2014; Accepted 2 August 2014; Published 27 August 2014

Academic Editor: Christophe Chevillard

In visceral leishmaniasis (VL) endemic areas, a minority of infected individuals progress to disease since most of them develop protective immunity. Therefore, we investigated the risk markers of VL within nonimmune sector. Analyzing infected symptomatic and, asymptomatic, and noninfected individuals, VL patients presented with reduced high-density lipoprotein cholesterol (HDL-C), elevated triacylglycerol (TAG), and elevated very-low-density lipoprotein cholesterol (VLDL-C) levels. A polymorphism analysis of the lipoprotein lipase (LPL) gene using HindIII restriction digestion ($N = 156$ samples) (H+ = the presence and H− = the absence of mutation) revealed an increased adjusted odds ratio (OR) of VL versus noninfected individuals when the H+/H+ was compared with the H−/H− genotype (OR = 21.3; 95% CI = 2.32–3335.3; $P = 0.003$). The H+/H+ genotype and the H+ allele were associated with elevated VLDL-C and TAG levels ($P < 0.05$) and reduced HDL-C levels ($P < 0.05$). An analysis of the L162V polymorphism in the peroxisome proliferator-activated receptor alpha (PPARα) gene ($n = 248$) revealed an increased adjusted OR when the Leu/Val was compared with the Leu/Leu genotype (OR = 8.77; 95% CI = 1.41–78.70; $P = 0.014$). High TAG ($P = 0.021$) and VLDL-C ($P = 0.023$) levels were associated with susceptibility to VL, whereas low HDL ($P = 0.006$) levels with resistance to infection. The mutated LPL and the PPARα Leu/Val genotypes may be considered risk markers for the development of VL.

1. Introduction

Visceral leishmaniasis (VL) is a systemic disease that is prevalent in tropical and subtropical regions. VL is caused by various species of protozoa within the genus *Leishmania* and of the *Leishmania donovani* complex, including *Leishmania infantum* (previously referred to as *L. chagasi*), in the new world [1]. In a VL-endemic area, the most infected individuals remain asymptomatic. Individuals with infection may present

with mild symptoms and a minority of infected individuals, approximately 10–20%, progress to active severe disease that is characterized by fever, hepatosplenomegaly, pancytopenia, hypergammaglobulinemia, and severe weight loss [2, 3]. However, the factors that are associated with susceptibility to infection progression are not well known.

The immune system has been the natural focus of previous studies that assessed the risk markers for VL development. Most studies have focused on genes that are related to the immune system. In studies with approaches that were based mainly on family groups with VL infection, the SLC11A1 (formerly called as the natural resistance-associated macrophage protein-1, NRamp-1) gene on chromosome 2q35 [4, 5], interleukin-4/interleukin-9 [6], the TNF locus [7], a locus on chromosome 22q12 [8, 9], IL-18 [10], and IL-1beta [11] polymorphisms have been associated with VL infection. However, in their 2009 review [12], Blackwell et al. suggested that most of these polymorphisms had marginal effects on infection progression. Recently, the IL-10 819 C/T genotype was associated with susceptibility to VL development in Iran [13]. In well-powered population-based studies, the CXCR2 gene [14] and DLL1, which encode delta-like 1, the ligand for Notch 3 [15], were associated with susceptibility to VL development but not SLC11A1 in India [16]. More recently, another well-powered population-based study revealed a consistent contribution of the HLA-DRB1-HLA-DQA1 HLA class II region to VL susceptibility in the Indian subcontinent and Brazil [17]. However, the role of these genetic determinants in the pathogenesis of VL was not addressed in these studies.

In *L. infantum* infection, protective immunity develops in the majority of individuals who reside in VL-endemic areas [2]. During active disease, immune derangement occurs; however, the immune system remains highly activated [3]. Therefore, nonspecific factors may play important roles in infections by parasites that can efficiently evade effective immune responses. Furthermore, a study has indicated that factors not related to acquired cell-mediated immunity may explain the progression of VL [18]. Therefore, in this study, we focused on nonimmune sector, that is, lipid metabolism.

Several studies have reported on lipid alterations in human VL cases [19–22]. In this study, we initially analyzed serum-lipid profiles in a large number of patients with clinical manifestations of VL. We found high triacylglycerol (TAG) levels, high very-low-density lipoprotein cholesterol (VLDL-C) levels, and low high-density lipoprotein cholesterol (HDL-C) levels in infected symptomatic individuals. These alterations may have resulted from the inflammatory infectious process; however, we investigated the possible role of these lipoprotein fractions in susceptibility to *L. infantum* infection because previous results have suggested that amastigotes are largely dependent on protein and lipids as an energy source within host cells [23]. In addition to the analysis of lipoprotein fraction alterations, we extended the study to analyze the factors that modulate TAG and HDL levels. These additional factors included lipoprotein lipase (LPL), which hydrolyzes TAG from TAG-rich lipoprotein particles in plasma [24] and reduces the uptake of a TAG-rich artificial emulsion [25], apolipoprotein E (apoE), which mediates the binding of lipoprotein particles to receptors in the liver that mediate their clearance [26], and peroxisome proliferator-activated receptor alpha (PPARα), which is involved in lipid metabolism, including roles in oxidation pathways, the uptake and transport of fatty acids, and lipoprotein synthesis routes [27]. Therefore, we focused on LPL, apoE, and PPARα gene polymorphisms as candidates for genetic risk markers for disease development in *L. infantum* infection. LPL gene polymorphisms were searched using HindIII and PVuII restriction enzymes known to reveal mutated genes that correlate with TAG level alteration and the former also with HDL level alteration [28, 29]. We found that the H+/H+ genotype and the H+ allele, which were identified using HindIII restriction in the LPL gene, were more frequent in infected symptomatic individuals and were notably associated with high levels of VLDL-C, TAG, and HDL-C. The apoE gene is presented in three main isoforms (apoE2, apoE3, and apoE4) that are coded by three common alleles (E2, E3, and E4) [26]. We found that the E3/E3 genotype and the E3 allele were more frequent in infected symptomatic individuals than in infected asymptomatic or noninfected individuals, and these factors were associated with high levels of VLDL cholesterol and TAG. We found that the Leu/Val genotype and the Val allele of the L162V polymorphism in the PPARα gene were more frequent in infected symptomatic individuals than in infected asymptomatic or noninfected individuals but with no apparent association with alterations in lipoprotein levels.

We hypothesized that certain lipid fractions may play a role in the development of *L. infantum* infection. In this study, we found that high levels of triglycerides and VLDL and low levels of HDL favor the development of active disease. Therefore, we suggest that related lipoprotein lipase and apolipoprotein E genotypes that lead to alterations in these lipoprotein levels as well as the presence of the PPARα L162V allele may be susceptibility factors and markers of VL development.

2. Materials and Methods

2.1. Study Design and Subjects. The individuals who were included in this study were from Teresina, Piaui State, Northeastern Brazil. The inclusion criteria were as follows: unrelated individuals who presented with active VL (referred to as infected symptomatic), healthy individuals who had been infected with *L. infantum* as determined by a positive anti-*Leishmania* (Montenegro) delayed-type hypersensitivity skin test and/or the presence of anti-*Leishmania* antibodies (referred to as infected asymptomatic), and healthy individuals who had no evidence of present or past infection with *L. infantum* as determined by both a negative Montenegro skin test and the absence of specific antibodies. The subjects and materials in this study were similar to those in the previous study by Alonso et al. [30] in which possible ethnic and environmental biases were analyzed and deemed not to be confounding factors.

2.2. Ethics Statement. This study was approved by the ethics committees of the participating institutions (Comissão de Ética em Pesquisa da Universidade Federal do Piauí and Comissão de Ética para Análise de Projetos de Pesquisa da

Diretoria Clínica do Hospital das Clínicas e da Faculdade de Medicina da Universidade de São Paulo). Written informed consent was obtained from all of the participants or their parents or guardians. Additionally, the samples and data were treated anonymously.

2.3. Analysis of Biochemical Parameters. After 12 hours of fasting, venous blood samples were drawn from 81 individuals to measure lipid parameters. The total cholesterol (TC), low-density lipoprotein cholesterol (LDL-C), HDL-C, and TAG concentrations were measured using automated methods (Roche Diagnostics Co., Indianapolis, IN, USA), and the VLDL-C concentrations were calculated (TAG concentration/5) using the Friedewald equation.

2.4. Genetic Analysis of the LPL Polymorphism. DNA was extracted from peripheral blood white cells using the GFX Genomic Blood DNA Purification Kit (GE Healthcare, Piscataway, NJ, USA) and subjected to amplification by polymerase chain reaction (PCR) using a Bio-Rad Laboratories DNA Thermal Cycler (Hercules, CA, USA).

The variations were confirmed using a restriction fragment length polymorphism (RFLP) assay in which the PCR-amplified products were digested by HindIII for 156 individuals or by PvuII for 130 individuals. Due to the availability, not all samples were analyzed using both enzymes. One primer set was used to amplify the sequence around a HindIII restriction site in intron 8 (the forward primer was 5′-TTTAGGCCTGAAGTTTCCAC-3′, and the reverse primer was 5′-CTCCCTAGAACAGAAGATC-3′) [31]. The amplified fragment was 1.3 kb in size. The other primer set was obtained from the DNA sequences that flanked a PvuII restriction site in intron 6 (the forward primer was 5′-TAGAGGTTGAGGCACCTGTGC-3′, and the reverse primer was 5′-GTGGGTGAATCACCTGAGGTC-3′) [32]. The amplified fragment was 858 bp long. The amplification of the region that flanked the HindIII site was performed over 33 cycles at 95°C for 1 min, 60°C for 2 min, and 72°C for 2 min. The amplification of the sequence that surrounded the PvuII site was performed over 32 cycles at 95°C for 1 min, 68°C for 2 min, and 72°C for 2 min. The PCR-amplified products were digested with HindIII or PvuII. HindIII yielded fragments that were 600 bp and 700 bp long, and PvuII yielded fragments that were 266 bp and 592 bp long [28].

2.5. Genetic Analysis of the apoE Polymorphism. Using extracted DNA, the variations were confirmed by a single-nucleotide polymorphism (SNP) assay in which the PCR-amplified products were analyzed using the SNaPshot Multiplex Kit (Applied Biosystems, Foster City, CA, USA) for 115 individuals. We used one set of primers that were derived from exon 4 in the apoE gene, and PCR was used to amplify a 244 bp region that spanned the E2, E3, and E4 allelic sites (the forward primer was 5′-TAAGCTTGGCACGGCTGTCCAAGGA-3′, and the reverse primer was 5′-ACAGAATTCGCCCCGGCCTGGTACAC-3′) [26]. The amplification of the apoE site was performed with an initial denaturation at 95°C for 2 min, which was followed by 35 cycles at 95°C for 1 min, 60°C for 1 min, and 72°C for 30 s. The SNaPshot Multiplex Kit was used to investigate the presence of the E2, E3, and E4 alleles in the amplified products. Two specific primers for apoE SNPs were utilized (the forward primer was 5′-GCGCGGACATGGAGGACGTG-3′, and the reverse primer was 5′-CCCCCGGCCTGGTACACTGCCAGGC-3′). The SNaPshot Multiplex Kit reactions were performed in the ABI 377 Automatic Sequencer (Applied Biosystems) following the manufacturer's recommendations.

2.6. Genotyping of the PPARα L162V Polymorphism. Using extracted DNA, the PPARα gene L162V polymorphism was genotyped by allelic discrimination using TaqMan probes on a custom assay-on-demand basis by Applied Biosystems. A pair of oligos was custom-designed to amplify a fragment that contained the L162V SNP together with different allele-specific fluorescent probes using PCR. Genotyping was performed using a real-time PCR reaction (StepOnePlus Applied Biosystems) according to the following protocol: in a 10 μL reaction, 5 μL of Maxima Probe/ROX qPCR Master Mix (2X) (Fermentas) was mixed with 0.5 μL of TaqMan reagents (a 20X master mix that contained the probes and the pair of oligos) and 4.5 μL of autoclaved Milli-Q water. The reaction was performed following the cycling protocol, initial denaturation for 10 min at 95°C, followed by 40 cycles of denaturation at 95°C for 15 s, and annealing and extension for 60 s at 60°C. After cycling, a graph of allelic discrimination was generated.

2.7. Statistical Analysis. The data were expressed as means and standard deviations and compared using ANOVA tests. The Student Newman-Keuls posttest was used for post hoc statistical comparisons among the groups, and the t-test was used for statistical comparisons between the groups. The frequencies and comparison distributions of the genotypes and alleles for each polymorphic site were estimated by gene counting. Consistency with the Hardy-Weinberg proportions was tested by the log-likelihood ratio. We used the Pearson χ^2 test for trends to analyze differences in the frequency of the LPL genotypes and alleles between the outcome groups (infected symptomatic, infected asymptomatic, and noninfected). Associations between levels of lipids and different genotypes and the patient outcomes were expressed as odds ratios (OR) and their respective 95% confidence intervals (95% CI), adjusted for age and gender, estimated by means of exact logistic regression models. Models compared the infected (both symptomatic and asymptomatic) individuals to the noninfected individuals. The levels of lipids were analyzed both as continuous and dichotomous variables. For the dichotomous analyses, the cut-off points used for TC, LDL-C, HDL-C, TAG, and VLDL-C were established by selecting the point of the ROC curve that maximized the sensitivity and specificity for separating noninfected and infected symptomatic individuals. Data were analyzed using Stata statistical software (Stata for Windows 13.0, StataCorp, College Station, TX), Systat version 10 (Point Richmond, Richmond, CA), and GraphPad Prism 3.0 (GraphPad Software Inc., San Diego, CA, USA). A P value <0.05 was considered to be significant.

Table 1: Levels of serum lipids in individuals exposed to *Leishmania infantum* from endemic area.

Lipids	Infected symptomatic individuals		Infected asymptomatic individuals		Noninfected individuals		P value
	n	mg/dL	n	mg/dL	n	mg/dL	
TC	17	121.2 ± 34.6	28	143.0 ± 42.1	36	139.9 ± 36.1	0.152
LDL-C	17	59.5 ± 30.8	28	85.5 ± 42.2	36	77.1 ± 36.0	0.083
HDL-C	17	38.3 ± 4.3*	28	39.0 ± 5.8*	36	43.0 ± 7.2	**0.012**
TAG	17	219.4 ± 84.9*,†	28	169.1 ± 62.7	36	157.9 ± 67.6	**0.013**
VLDL-C	17	43.8 ± 16.9*,†	28	33.9 ± 12.4	36	31.6 ± 13.5	**0.013**

TC = total cholesterol; LDL-C = low-density lipoprotein cholesterol; HDL-C = density lipoprotein cholesterol; TAG = triacylglycerol; VLDL = very-low-density lipoprotein cholesterol. Lipid values expressed as the mean ± SD. P value analyzed by ANOVA test with the Student Newman-Keuls posttest. $^{*}P < 0.05$ versus noninfected individuals; $^{\dagger}P < 0.05$ versus infected asymptomatic individuals. P values in bold indicate statistically significant differences.

3. Results

In this study, using a candidate gene approach to reveal the genetic traits and the resulting phenotypic expressions, that is, lipoprotein levels, we aimed to identify the risk markers for the development of *L. infantum* infection.

The assessment of the lipid fraction levels revealed elevated triacylglycerol (TAG) levels and elevated very-low-density lipoprotein cholesterol (VLDL-C) levels in all of the infected symptomatic individuals compared with the infected asymptomatic and noninfected individuals ($P < 0.05$) (Table 1) (according to the III Brazilian Guidelines on Dyslipidemia [33], the optimal TAG level is <130 mg/dL for individuals up to 20 years of age and <150 mg/dL in individuals who are older than 20 years of age). Because the ideal age-matched endemic controls for this approach could not be obtained due to technical and ethical reasons, the average age (mean ± standard deviation) of the infected symptomatic individuals ($n = 17$; 6.2 ± 7.6 years of age) was significantly lower than the average ages of the infected asymptomatic ($n = 28$; 30.2 ± 12.4 years of age) and noninfected individuals ($n = 36$; 27.9 ± 19.2 years of age). To circumvent bias, we separately examined the individuals who were younger than 20 years of age when the differences between the groups were still maintained (data not shown). Additionally, we observed reduced high-density lipoprotein cholesterol (HDL-C) levels in both the infected symptomatic and asymptomatic individuals compared with the noninfected individuals ($P < 0.05$) (Table 1).

We analyzed the polymorphisms of the LPL, apoE, and PPARα genes. The genotype distributions for all of the polymorphisms were in Hardy-Weinberg equilibrium for all of the groups (Table 2). Significant differences were observed in the frequencies of the polymorphic HindIII-restricted genotypes (H+/H+ versus H+/H−, $P < 0.05$; H+/H+ versus H−/H−, $P < 0.01$) and the HindIII-restricted alleles (H+ versus H−, $P < 0.01$) (Table 1). However, no differences were detected between the groups according to the frequencies of either the genes or the alleles of the PvuII restriction products (Table 2). In the apoE gene, the analysis of the three common apoE alleles (E2, E3, and E4) that code the three main apoE isoforms (apoE2, apoE3, and apoE4) indicated that the E3/E3 genotype was the most frequent, followed by the E3/E4, E2/E3, E2/E4, and E4/E4 genotypes. The E2/E2 genotype was not detected in any of the individuals. In the analysis of the apoE alleles, the E3 allele was the most frequent, followed by the E4 and E2 alleles. Significant differences were observed between the frequency of the E4 allele and that of the E3 allele ($P < 0.05$) (Table 2). We found that the E3/E3 genotype and the E3 allele were more frequent in infected symptomatic individuals than in infected asymptomatic or noninfected individuals (Table 2). In the PPARα gene L162V polymorphism, we found significant differences in the frequencies of the Leu/Leu and Leu/Val ($P < 0.05$) genotypes and the Leu and Val alleles ($P < 0.01$) between the groups (Table 2).

In the analysis of the association between the genotypes and the lipoprotein levels in all of the individuals regardless of the outcome, the TAG and VLDL-C levels were significantly higher in the H+/H+ individuals ($P < 0.01$) (Table 3). The individuals with the H+/H+ genotype had significantly lower HDL-C levels than the individuals with the H+/H− genotype ($P < 0.05$). The serum-lipid levels were measured in only two H−/H− individuals, which was insufficient for the statistical analysis (the means are presented in the legend of Table 3). In the individuals with the P1/P1 genotype, no significant differences in the lipid profiles were observed between the P1/P2 and P2/P2 individuals (Table 3). In the analysis of the apoE genotypes and alleles, we found that the TAG and VLDL-C levels in the individuals with the E2/E3 genotype were significantly higher than those in the E3/E3 and E3/E4 ($P < 0.05$) individuals (Table 3). The serum-lipid data were available in only one E4/E4 individual (all of the variables are shown in the legend of Table 3). The serum-lipid levels were not evaluated in the E2/E4 and E2/E2 individuals. Furthermore, the TAG and VLDL-C levels were significantly higher in the E2 individuals than in the E3 and E4 individuals ($P < 0.05$), but the TC levels were higher in the E3 individuals than in the E2 and E4 individuals ($P < 0.05$) (Table 3). The E3 allele was associated with higher TC levels than with the E2 and E4 alleles; however, the levels were still optimal [33]. The lipid profiles were not associated with either the genotypes or the alleles of the L162V polymorphism in the PPARα gene (Table 3).

To analyze the association between the genotypic and phenotypic expressions and the outcomes, we performed a multivariate analysis to calculate the adjusted odds ratio (OR) because of the significant differences in the ages and gender distribution among the studied groups. The results of this

Table 2: Frequency of genotypes and alleles of LPL, apoE, and PPARα genes in individuals exposed to *Leishmania infantum*.

	Polymorphisms[§§]	Infected symptomatic individuals		Infected asymptomatic individuals		Noninfected individuals		P value
		n	% of total	n	% of total	n	% of total	
HindIII	H+/H+[(a)]	24	46.2	17	35.4	13	23.2	**0.040**[(a vs. b)]
	H+/H−[(b)]	26	50.0	27	56.3	34	60.7	0.103[(b vs. c)]
	H−/H−[(c)]	2	3.8	4	8.3	9	16.1	**0.006**[(a vs. c)]
		HWE[†]	*0.116*		*0.138*		*0.099*	
	H+[(d)]	74	71.5	61	63.5	60	53.6	
	H−[(e)]	30	28.8	35	36.5	52	46.4	**0.008**[(d vs. e)]
PvuII	P1/P1[(f)]	12	28.6	13	29.5	16	37.2	0.429[(f vs. g)]
	P1/P2[(g)]	25	59.5	27	61.4	23	53.5	0.835[(g vs. h)]
	P2/P2[(h)]	5	11.9	4	9.1	4	9.3	0.507[(f vs. h)]
		HWE[†]	*0.146*		*0.062*		*0.294*	
	P1[(i)]	49	58.3	53	60.2	55	64.0	
	P2[(j)]	35	41.7	35	39.8	31	36.0	0.452[(i vs. j)]
ApoE	E2/E3[(k)]	3	8.1	4	10.5	2	5.0	0.833[(k vs. l)]
	E3/E3[(l)]	30	81.1	24	63.2	26	65.0	0.116[(l vs. m)]
	E3/E4[(m)]	4	10.8	10	26.3	10	25.0	0.214[(k vs. m)]
	E2/E4	0	0.0	0	0.0	1	2.5	
	E4/E4	0	0.0	0	0.0	1	2.5	
	E2[(n)]	3	4.1	4	5.3	3	3.7	0.953[(n vs. o)]
	E3[(o)]	67	90.5	62	81.6	64	80.0	**0.038**[(o vs. p)]
	E4[(p)]	4	5.4	10	13.1	13	16.3	0.230[(n vs. p)]
PPPARα	Leu/Leu[(q)]	48	80.0	61	87.1	92	93.9	**0.022**[(q vs. r)]
	Leu/Val[(r)]	11	18.3	8	11.4	6	6.1	
	Val/Val	1	1.7	1	1.4	0	0.0	
		HWE[†]	*0.693*		*0.247*		*0.745*	
	Leu[(s)]	107	89.2	130	92.9	190	96.9	
	Val[(t)]	13	10.8	10	7.1	6	3.1	**0.008**[(s vs. t)]

[§§] P value analyzed by χ^2 test for trend; [†] P value in Hardy-Weinberg equilibrium (HWE).
Note: H+ indicates presence and H− indicates absence of the HindIII restriction site. P1 indicates absence and P2 indicates presence of the PvuII restriction site. Apo E polymorphism results in six genotypes (E2/E2, E2/E3, E2/E4, E3/E3, E3/E4, and E4/E4). E2/E4 and E4/E4 did not have sufficient number to be analyzed. E2/E2 was not detected. PPARα L162V polymorphism results in three genotypes (Leu/Leu, Leu/Val, and Val/Val). Bold text indicates statistically significant differences.

analysis suggested that the presence of the lipoprotein lipase H+/H+ genotype (adjusted OR = 21.3; 95% CI = 2.32–335.3; $P = 0.003$), the PPARα Leu/Val genotype (adjusted OR = 8.77; 95% CI = 1.41–78.7; $P = 0.014$), and elevated levels of VLDL-C (adjusted OR = 1.08; 95% CI = 1.01–1.17; $P = 0.023$) and TAG (adjusted OR = 1.02; 95% CI = 1.00–1.03; $P = 0.021$) were associated with symptomatic *L. infantum* infection. In contrast, the HDL levels were inversely associated with symptomatic (adjusted OR = 0.84; 95% CI = 0.71–0.96; $P = 0.006$) and asymptomatic (adjusted OR = 0.92; 95% CI = 0.84–0.99; $P = 0.027$) *L. infantum* infection (Table 4). When the lipoprotein levels were analyzed using the cut-off value established by selecting the point on the ROC curve that maximized the sensitivity and specificity for separating noninfected and infected symptomatic individuals, the association with symptomatic infection became more evident for elevated levels of VLDL-C (cut-off value = 33 mg/dL; adjusted OR = 18.8; 95% CI = 1.71–1014.4; $P = 0.009$) and TAG (cut-off value = 168 mg/dL; adjusted OR = 18.8; 95% CI = 1.71–1014.4; $P = 0.009$).

4. Discussion

Discovering reliable markers for the assessment of individual and population risks of disease development is a major challenge for the scientific community. In this study, we evaluated potential markers of VL development. In areas that are endemic for VL, most infected individuals develop a protective immune response. Therefore, we focused on the nonimmune lipid elements as potential susceptibility factors based on the hypothesis that these alterations in VL patients may favor parasite growth and disease development. We further analyzed the polymorphisms of certain genes that may lead to such alterations in lipoprotein levels.

In a significant number of patients with clinical manifestations of VL, we found high TAG levels, high VLDL-C levels, and low HDL-C levels in infected symptomatic individuals

Table 3: Levels of lipids (mg/dL) according to genotypes and alleles of LPL and of apoE in individuals exposed to *Leishmania infantum*.

		Polymorphisms	Age	Lipids (mg/dL)				
				TC[a]	LDL-C[a]	HDL-C[a]	TAG[a]	VLDL-C[a]
HindIII	Genotypes	H+/H+ (n = 19)	22.6 ± 15.4	150.8 ± 42.2	91.0 ± 44.0	38.1 ± 5.6	207.6 ± 82.7	41.5 ± 16.5
		H+/H− (n = 33)	22.1 ± 18.2	138.8 ± 34.8	77.4 ± 35.6	41.9 ± 6.4	157.9 ± 52.8	31.6 ± 10.5
		P value[#]	0.914	0.274	0.228	**0.037**	**0.011**	**0.010**
	Alleles	H+ (n = 71)	22.4 ± 16.6	145.3 ± 38.8	84.7 ± 40.3	39.9 ± 6.2	184.5 ± 73.6	36.9 ± 14.6
		H− (n = 37)	22.7 ± 17.5	135.2 ± 34.7	74.4 ± 34.7	42.5 ± 6.3	154.5 ± 50.8	30.9 ± 10.1
		P value[#]	0.919	0.187	0.191	**0.040**	**0.029**	**0.029**
PvuII	Genotypes	P1/P1 (n = 15)	22.4 ± 14.0	24.6 ± 16.7	81.7 ± 37.1	40.0 ± 4.7	159.4 ± 50.9	31.9 ± 10.1
		P1/P2 (n = 27)	24.6 ± 16.7	141.8 ± 38.7	84.3 ± 39.7	39.9 ± 6.3	173.0 ± 77.7	34.6 ± 15.5
		P2/P2 (n = 4)	16.5 ± 17.8	132.8 ± 40.3	71.7 ± 28.8	41.5 ± 5.7	230.5 ± 89.0	46.0 ± 17.6
		P value[§]	0.622	0.878	0.828	0.878	0.217	0.220
	Alleles	P1 (n = 57)	23.5 ± 15.1	142.8 ± 36.5	82.9 ± 37.7	40.0 ± 5.4	165.8 ± 64.4	165.8 ± 64.4
		P2 (n = 35)	22.8 ± 16.7	139.7 ± 38.1	81.4 ± 37.1	40.3 ± 6.1	186.1 ± 81.4	37.2 ± 16.2
		P value[#]	0.840	0.706	0.853	0.793	0.188	0.191
apoE	Genotypes	E2/E3 (n = 4)	23.7 ± 14.3	120.0 ± 36.2	65.7 ± 30.4	41.7 ± 7.8	275.3 ± 113.5[*,†]	54.7 ± 22.7[*,†]
		E3/E3 (n = 29)	19.1 ± 14.8	152.1 ± 40.1	91.5 ± 41.6	39.2 ± 5.8	166.9 ± 58.5	33.4 ± 11.6
		E3/E4 (n = 6)	35.5 ± 18.1	119.0 ± 11.9	65.7 ± 23.9	39.0 ± 3.0	177.3 ± 100.4	35.5 ± 19.9
		P value[§]	0.068	0.069	0.205	0.692	**0.026**	**0.028**
	Alleles	E2 (n = 4)	23.7 ± 14.3	120.0 ± 36.2	65.7 ± 30.4	41.7 ± 7.8	275.3 ± 113.5[*,†]	54.7 ± 22.7[*,†]
		E3 (n = 68)	20.8 ± 15.5	147.3 ± 39.4[†,‡]	87.7 ± 40.2	39.2 ± 5.7	174.2 ± 69.6	34.8 ± 13.8
		E4 (n = 8)	32.1 ± 16.5	113.0 ± 15.0	59.5 ± 23.2	38.7 ± 2.6	165.5 ± 87.7	33.1 ± 17.4
		P value[§]	0.152	**0.029**	0.099	0.661	**0.029**	**0.031**
PPARα	Genotypes	Leu/Leu (n = 54)	26.7 ± 17.6	137.9 ± 39.7	78.2 ± 38.8	40.9 ± 6.5	173.2 ± 81.2	34.6 ± 16.2
		Leu/Val (n = 8)	23.1 ± 18.3	146.9 ± 32.6	83.3 ± 31.1	40.3 ± 5.7	166.1 ± 35.7	33.4 ± 6.9
		P value[#]	0.589	0.545	0.728	0.794	0.809	0.830
	Alleles	Leu (n = 116)	26.5 ± 17.5	138.5 ± 39.0	78.6 ± 38.1	40.8 ± 6.4	172.7 ± 78.5	34.5 ± 15.6
		Val (n = 8)	23.1 ± 18.3	146.9 ± 32.6	83.3 ± 31.1	40.3 ± 5.7	166.1 ± 35.7	33.4 ± 6.9
		P value[#]	0.599	0.555	0.735	0.798	0.814	0.834

All values are expressed as the mean ± SD in individuals exposed to *Leishmania chagasi*.

[a]values in mg/dL. [#]P value analyzed by Student t-test; [§]P value analyzed by ANOVA test with the Student Newman-Keuls posttest. In relation to genotypes: [*]$P < 0.05$ versus E3/E3; [†]$P < 0.05$ versus E3/E4. In relation to alleles: [*]$P < 0.05$ versus E3; [†]$P < 0.05$ versus E4; [‡]$P < 0.05$ versus E2. H−/H− did not have sufficient number to be analyzed (n = 2). Age = 28.0 ± 12.7; TC = 105.0 ± 14.1; LDL-C = 50.0 ± 7.1; HDL-C = 47.5 ± 2.1; TAG = 126.5 ± 9.2; VLDL-C = 25.5 ± 2.1. E4/E4 did not have sufficient number to be analyzed (n = 1). Age = 22.0; TC = 95.0; LDL-C = 41.0; HDL-C = 38.0; TAG = 130.0; VLDL = 26.0. H+ indicates presence and H− indicates absence of the HindIII restriction site. P1 indicates absence and P2 indicates presence of the PvuII restriction site.

Note: Apo E polymorphism results in six genotypes ranking (E2/E2, E2/E3, E2/E4, E3/E3, E3/E4, and E4/E4) and three alleles (E2, E3, and E4). Bold text indicates statistically significant differences.

Table 4: Adjusted odds ratios (OR) and respective 95% confidence intervals for the association between levels of lipids (mg/dL) and genotypes of LPL, apoE, and PPARα and infected symptomatic and asymptomatic *L. infantum* infection.

Variable	Infected symptomatic infection			Infected asymptomatic infection		
	OR*	95% CI*	*P* value	OR*	95% CI*	*P* value
HindIII						
H−/H−	1.00			1.00		
H+/H−	6.37	0.84–83.4	0.083	2.04	0.49–10.4	0.435
H+/H+	21.3	2.32–335.3	**0.003**	3.48	0.72–20.4	0.143
PvuII						
P1/P1	1.00			1.00		
P1/P2	1.86	0.55–6.68	0.395	1.42	0.52–3.98	0.593
P2/P2	0.71	0.10–5.28	1.000	1.20	0.18–7.81	1.000
ApoE						
E3/E4	1.00			1.00		
E3/E3	2.66	0.52–16.1	0.312	0.91	0.28–2.93	1.000
E2/E3	4.31	0.23–113.7	0.515	1.90	0.22 –25.3	0.825
PPARα						
Leu/Leu	1.00			1.00		
Leu/Val	8.77	1.41–78.7	**0.014**	2.76	0.56–17.9	0.272
TC	0.99	0.97–1.01	0.301	1.00	0.99–1.01	0.787
LDL-C	0.99	0.97–1.01	0.353	1.01	0.99–1.02	0.414
HDL-C	0.84	0.71–0.96	**0.006**	0.92	0.84–0.99	**0.027**
TAG	1.02	1.00–1.03	**0.021**	1.00	0.99–1.01	0.597
VLDL-C	1.08	1.01–1.17	**0.023**	1.01	0.97–1.05	0.580

* Adjusted for age (≤ or >20 years) and gender.
P values in bold indicate statistically significant differences.

as previously reported in the literature [19–22]. LPL, apoE, and PPARα are known as important components of lipid metabolism with roles in the homeostasis of different lipoprotein fractions and their transport, and the polymorphisms of these genes have been associated with cardiovascular diseases [28, 29, 34–36]. Therefore, these gene polymorphisms were analyzed in this study. We targeted LPL, apoE, and PPARα genes with polymorphisms and alleles that were analyzed in relation to symptomatic *L. infantum* infection. Importantly, an association between these polymorphisms and the expected phenotypes was observed, excluding the L162V polymorphism in the PPARα gene. This finding is in contrast to most studies on gene polymorphisms in which the resulting phenotypes were unidentified. In the studied population, the H+/H+ genotype and the H+ allele were associated with elevated VLDL-C and TAG levels ($P < 0.05$) and reduced HDL-C levels ($P < 0.05$). For the apoE genes and alleles, the genotype and expected phenotype association was unclear because the TAG and VLDL-C levels were significantly higher in individuals with the E2 allele than in individuals with the E3 and E4 alleles but not in individuals with the E3 allele. This finding may be due to the restricted number of samples and to the different roles of the six apoE allotypes. However, the association between the E2 allele and the alterations in lipoprotein levels may not have been uncovered because apoE2 carries significantly less VLDL cholesterol than apoE4 [35], and apoE2 impairs the lipolytic conversion of VLDL to LDL through inhibiting LPL activity [34].

The association between the H+/H+ genotype and the H+ allele with higher TAG and lower HDL-C levels was stronger in the infected symptomatic group than in the infected asymptomatic group. PvuII has been associated with variations in serum lipids in other diseases [29, 36]; however, we did not detect any significant associations between the PvuII-restricted LPL genotypes and the presence of active VL or lipid fraction levels. This finding reinforces our suggestion that the HindIII-restricted LPL genotypes that were identified in this study are risk markers for the development of symptomatic *L. infantum* infection.

In the literature, high TAG and low HDL-C levels have been suggested as parameters for the diagnosis and follow-up of patients with VL [37]. However, in addition to a single study that suggested a role for LDL in the development of VL through tumor necrosis factor-α (TNF-α) production [22], our study is the first to clearly find that the LPL genotype that leads to a phenotype of high VLDL-C levels, high TAG levels, and low HDL-C levels is a risk factor for active visceral leishmaniasis. Interestingly, we observed reduced high-density lipoprotein cholesterol (HDL-C) levels in both the infected symptomatic and asymptomatic individuals compared with the noninfected individuals, which may suggest that decreased HDL levels initially favor infection. When TG and VLDL levels increase, progression to symptomatic infection may occur.

The biological roles of VLDL and HDL in *Leishmania* infection need to be further analyzed; however, as an initial approach, we assessed the role of lipoprotein fractions in the mechanism of cell infection in vitro by examining the phagocytosis of promastigotes by macrophages. We observed 29% more parasites within the macrophages that were incubated for six hours with VLDL ($P < 0.05$) than in culture without the addition of lipoprotein. The coaddition of HDL significantly reduced (37%) the parasite burden compared with VLDL ($P < 0.05$).

The PPARα L162V polymorphism has been demonstrated to be a risk marker for symptomatic infection; however, the mutated gene was not associated with altered lipoprotein levels. In a functional study of the Val-mutated PPARα allele, this mutation in the DNA binding domain for PPARα impacted the function of this transcription factor by preventing its proper binding to the region of DNA that is under its transcriptional control [38]. The frequency of this mutated allele was significantly higher in individuals who presented with symptomatic infection; therefore, the inefficient activation of lipid metabolism genes may lead to higher serum levels of lipid fractions. However, the results of this study did not indicate a relationship between the polymorphisms and the lipid profiles. A possible explanation for this finding is the low number of individuals who presented with the Val allele. This variant allele is relatively rare (an observed frequency of 10.8%), and the lipid profiles of only 8 individuals who were carrying this allele were measured. Therefore, any statistical evidence for a relationship between this mutation and the lipid profiles would be unlikely. Besides the PPARα gene can modulate lipid pathways, which may not be reflected in serum-lipid levels, and indirectly affect the outcome of *Leishmania infantum* infection. In addition, PPARα is known for its major role in the upregulation of cholesterol trafficking and efflux in macrophages [39]. Interestingly, in transcriptomic studies with *Leishmania*-infected mouse macrophages, cholesterol accumulation was clearly observed within host cells, which was achieved by the upregulation of genes that are implicated in the uptake of LDL (CD36 and the LDL receptor) and by the downregulation of genes that mediate cholesterol efflux (ABCA1 and CYP27) [40, 41]. In this scenario, a PPARα variant allele may contribute to the modulation of infection by enhancing the accumulation of cholesterol in infected cells and by shuttling cholesterol to *Leishmania* parasites. We cannot rule out either the modulation of infection by PPARα functions in inflammatory processes [39].

The results of this study and those from two previous studies [30, 42] support the presupposition that the genotypes for molecules that are not related to the adaptive immune system, that is, LPL, PPARα, and mannan-binding lectin (MBL) genotypes, have a significant correlation with *L. infantum* infection or disease. Notably, in addition to the roles of MBL in the complement system [43] and the autoimmune process [44], MBL levels are affected by the activation of PPARα [45], which induces LPL expression [46].

These genetic markers and the more easily accessible lipid levels may be used to evaluate the risk of *L. infantum* infection and disease in endemic areas and may be used to follow up patients who present with active-phase infection. Furthermore, our results suggest that we should consider studying lipid-lowering drugs as a complementary treatment for VL patients.

Conflict of Interests

The authors declare that there is no conflict of interests regarding the publication of this paper.

Authors' Contribution

Márcia Dias Teixeira Carvalho and Diego Peres Alonso and the senior authors Paulo Eduardo Martins Ribolla and Hiro Goto had, respective equal participation in this study.

Acknowledgments

The authors would like to acknowledge the Conselho Nacional de Desenvolvimento Científico e Tecnológico (Grant 154581/2006-2, research fellowship to H. Goto), the Fundação de Amparo à Pesquisa do Estado de São Paulo (Fellowship 06/60006-9 to M, Dias Teixeira Carvalho), and the Laboratório de Investigação Médica (LIM/38 HC-FMUSP). They also would like to thank Valéria Sutti Nunes, Maria das Graças Prianti, Letícia Amaral Nogueira Alonso, and Débora Colombi for providing laboratory assistance and all of the study participants for agreeing to contribute to this research. In addition, they would like to thank Isac Castro for the excellent statistical assistance and are grateful to the Laboratório de Lípides (LIM/10 HC-FMUSP) for its assistance.

References

[1] I. L. Mauricio, M. W. Gaunt, J. R. Stothard, and M. A. Miles, "Genetic typing and phylogeny of the Leishmania donovani complex by restriction analysis of PCR amplified gp63 intergenic regions," *Parasitology*, vol. 122, no. 4, pp. 393–403, 2001.

[2] R. Badaro, T. C. Jones, R. Lorenco et al., "A prospective study of visceral leishmaniasis in an endemic area of Brazil," *Journal of Infectious Diseases*, vol. 154, no. 4, pp. 639–649, 1986.

[3] H. Goto and M. D. G. Prianti, "Immunoactivation and immunopathogeny during active visceral leishmaniasis," *Revista do Instituto de Medicina Tropical de Sao Paulo*, vol. 51, no. 5, pp. 241–246, 2009.

[4] B. Bucheton, L. Abel, M. M. Kheir et al., "Genetic control of visceral leishmaniasis in a Sudanese population: candidate gene testing indicates a linkage to the NRAMP1 region," *Genes & Immunity*, vol. 4, no. 2, pp. 104–109, 2003.

[5] H. S. Mohamed, M. E. Ibrahim, E. N. Miller et al., "*SLC11A1* (formerly *NRAMP1*) and susceptibility to visceral leishmaniasis in the Sudan," *European Journal of Human Genetics*, vol. 12, no. 1, pp. 66–74, 2004.

[6] H. S. Mohamed, M. E. Ibrahim, E. N. Miller et al., "Genetic susceptibility to visceral leishmaniasis in The Sudan: linkage and association with IL4 and IFNGR1," *Genes and Immunity*, vol. 4, no. 5, pp. 351–355, 2003.

[7] T. M. Karplus, S. M. B. Jeronimo, H. Chang et al., "Association between the tumor necrosis factor locus and the clinical outcome of Leishmania chagasi infection," *Infection and Immunity*, vol. 70, no. 12, pp. 6919–6925, 2002.

[8] B. Bucheton, L. Abel, S. El-Safi et al., "A major susceptibility locus on chromosome 22q12 plays a critical role in the control of kala-azar," *American Journal of Human Genetics*, vol. 73, no. 5, pp. 1052–1060, 2003.

[9] B. Bucheton, L. Argiro, C. Chevillard et al., "Identification of a novel G245R polymorphism in the IL-2 receptor β membrane proximal domain associated with human visceral leishmaniasis," *Genes and Immunity*, vol. 8, no. 1, pp. 79–83, 2007.

[10] A. Moravej, M. Rasouli, S. Asaei, M. Kalani, and Y. Mansoori, "Association of interleukin-18 gene variants with susceptibility to visceral leishmaniasis in Iranian population," *Molecular Biology Reports*, vol. 40, no. 6, pp. 4009–4014, 2013.

[11] A. Moravej, M. Rasouli, M. Kalani et al., "IL-1β (-511T/C) gene polymorphism not IL-1β (+3953T/C) and LT-α (+252A/G) gene variants confers susceptibility to visceral leishmaniasis," *Molecular Biology Reports*, vol. 39, no. 6, pp. 6907–6914, 2012.

[12] J. M. Blackwell, M. Fakiola, M. E. Ibrahim et al., "Genetics and visceral leishmaniasis: Of mice and man," *Parasite Immunology*, vol. 31, no. 5, pp. 254–266, 2009.

[13] M. Hajilooi, K. Sardarian, M. Dadmanesh et al., "Is the IL-10 -819 polymorphism associated with visceral leishmaniasis?" *Inflammation*, pp. 1–6, 2013.

[14] S. Mehrotra, M. Fakiola, J. Oommen et al., "Genetic and functional evaluation of the role of CXCR1 and CXCR2 in susceptibility to visceral leishmaniasis in North-East India," *BMC Medical Genetics*, vol. 12, article 162, 2011.

[15] S. Mehrotra, M. Fakiola, A. Mishra et al., "Genetic and functional evaluation of the role of DLL1 in susceptibility to visceral leishmaniasis in India," *Infection, Genetics and Evolution*, vol. 12, no. 6, pp. 1195–1201, 2012.

[16] S. Mehrotra, J. Oommen, A. Mishra et al., "No evidence for association between SLC11A1 and visceral leishmaniasis in India," *BMC Medical Genetics*, vol. 12, article 71, 2011.

[17] M. Fakiola, A. Strange, H. J. Cordell et al., "Common variants in the HLA-DRB1-HLA-DQA1 HLA class II region are associated with susceptibility to visceral leishmaniasis," *Nature Genetics*, vol. 45, no. 2, pp. 208–213, 2013.

[18] C. R. Davies and A. S. M. Gavgani, "Age, acquired immunity and the risk of visceral leishmaniasis: a prospective study in Iran," *Parasitology*, vol. 119, no. 3, pp. 247–257, 1999.

[19] E. D. Bekaert, E. Dole, D. Y. Dubois et al., "Alterations in lipoprotein density classes in infantile visceral Leishmaniasis: presence of apolipoprotein SAA," *European Journal of Clinical Investigation*, vol. 22, no. 3, pp. 190–199, 1992.

[20] E. D. Bekaert, R. Kallel, M.-. Bouma et al., "Plasma lipoproteins in infantile visceral Leishmaniasis: deficiency of apolipoproteins A-I and A-II," *Clinica Chimica Acta*, vol. 184, no. 2, pp. 181–191, 1989.

[21] C. S. Lal, A. Kumar, S. Kumar et al., "Hypocholesterolemia and increased triglyceride in pediatric visceral leishmaniasis," *Clinica Chimica Acta*, vol. 382, no. 1-2, pp. 151–153, 2007.

[22] N. M. Soares, T. F. Leal, M. C. Fiúza et al., "Plasma lipoproteins in visceral leishmaniasis and their effect on Leishmania-infected macrophages," *Parasite Immunology*, vol. 32, no. 4, pp. 259–266, 2010.

[23] D. Rosenzweig, D. Smith, F. Opperdoes, S. Stern, R. W. Olafson, and D. Zilberstein, "Retooling Leishmania metabolism: From sand fly gut to human macrophage," *The FASEB Journal*, vol. 22, no. 2, pp. 590–602, 2008.

[24] H. Jansen, B. Breedveld, and K. Schoonderwoerd, "Role of lipoprotein lipases in postprandial lipid metabolism," *Atherosclerosis*, vol. 141, no. 1, pp. S31–S34, 1998.

[25] M. D. T. Carvalho, L. M. Harada, M. Gidlund, D. F. J. Ketelhuth, P. Boschcov, and E. C. R. Quintão, "Macrophages take up triacylglycerol-rich emulsions at a faster rate upon co-incubation with native and modified LDL: an investigation on the role of natural chylomicrons in atherosclerosis," *Journal of Cellular Biochemistry*, vol. 84, no. 2, pp. 309–323, 2001.

[26] M. Emi, L. L. Wu, M. A. Robertson et al., "Genotyping and sequence analysis of apolipoprotein E isoforms," *Genomics*, vol. 3, no. 4, pp. 373–379, 1988.

[27] C. Duval, M. Muller, and S. Kersten, "PPARalpha and dyslipidemia," *Biochimica et Biophysica Acta*, vol. 1771, no. 8, pp. 961–971, 2007.

[28] Y. I. Ahn, M. I. Kamboh, R. F. Hamman, S. A. Cole, and R. E. Ferrell, "Two DNA polymorphisms in the lipoprotein lipase gene and their associations with factors related to cardiovascular disease," *Journal of Lipid Research*, vol. 34, no. 3, pp. 421–428, 1993.

[29] E. Socquard, A. Durlach, C. Clavel, P. Nazeyrollas, and V. Durlach, "Association of HindIII and PvuII genetic polymorphisms of lipoprotein lipase with lipid metabolism and macrovascular events in type 2 diabetic patients," *Diabetes & Metabolism*, vol. 32, no. 3, pp. 262–269, 2006.

[30] D. P. Alonso, A. F. B. Ferreira, P. E. M. Ribolla et al., "Genotypes of the mannan-binding lectin gene and susceptibility to visceral leishmaniasis and clinical complications," *Journal of Infectious Diseases*, vol. 195, no. 8, pp. 1212–1217, 2007.

[31] T. G. Kirchgessner, J.-. Chuat, C. Heinzmann et al., "Organization of the human lipoprotein lipase gene and evolution of the lipase gene family," *Proceedings of the National Academy of Sciences of the United States of America*, vol. 86, no. 24, pp. 9647–9651, 1989.

[32] K. Oka, G. T. Tkalcevic, J. Stocks, D. J. Galton, and W. V. Brown, "Nucleotide sequence of PvuII polymorphic site at the human lipoprotein lipase gene locus," *Nucleic Acids Research*, vol. 17, no. 16, p. 6752, 1989.

[33] R. D. Santos, "III Brazilian Guidelines on Dyslipidemias and Guideline of Atherosclerosis Prevention from Atherosclerosis Department of Sociedade Brasileira de Cardiologia," *Arquivos Brasileiros de Cardiologia*, vol. 77, supplement 3, pp. 1–48, 2001.

[34] Y. Huang, X. Q. Liu, S. C. Rail Jr., and R. W. Mahley, "Apolipoprotein E2 reduces the low density lipoprotein level in transgenic mice by impairing lipoprotein lipase-mediated lipolysis of triglyceride-rich lipoproteins," *The Journal of Biological Chemistry*, vol. 273, no. 28, pp. 17483–17490, 1998.

[35] L. Dong and K. H. Weisgraber, "Human apolipoprotein E4 domain interaction. Arginine 61 and glutamic acid 255 interact to direct the preference for very low density lipoproteins," *Journal of Biological Chemistry*, vol. 271, no. 32, pp. 19053–19057, 1996.

[36] J. L. Anderson, G. J. King, T. L. Bair et al., "Association of lipoprotein lipase gene polymorphisms with coronary artery disease," *Journal of the American College of Cardiology*, vol. 33, no. 4, pp. 1013–1020, 1999.

[37] G. Seçmeer, A. B. Cengiz, A. Gürgey et al., "Hypertriglyceridemia and decreased high-density lipoprotein could be a clue for visceral leishmaniasis," *Infectious Diseases in Clinical Practice*, vol. 14, no. 6, pp. 401–402, 2006.

[38] A. Sapone, J. M. Peters, S. Sakai et al., "The human peroxisome proliferator-activated receptor α gene: Identification and functional characterization of two natural allelic variants," *Pharmacogenetics*, vol. 10, no. 4, pp. 321–333, 2000.

[39] E. Rigamonti, G. Chinetti-Gbaguidi, and B. Staels, "Regulation of macrophage functions by PPAR- α, PPAR- γ, and LXRs in mice and men," *Arteriosclerosis, Thrombosis, and Vascular Biology*, vol. 28, no. 6, pp. 1050–1059, 2008.

[40] J. Osorio y Fortéa, E. de La Llave, B. Regnault et al., "Transcriptional signatures of BALB/c mouse macrophages housing multiplying *Leishmania amazonensis* amastigotes," *BMC Genomics*, vol. 10, article 119, 2009.

[41] I. Rabhi, S. Rabhi, R. Ben-Othman et al., "Transcriptomic signature of Leishmania infected mice macrophages: a metabolic point of view," *PLoS Neglected Tropical Diseases*, vol. 6, no. 8, Article ID e1763, 2012.

[42] S. Hamdi, R. Ejghal, M. Idrissi et al., "A variant in the promoter of MBL2 is associated with protection against visceral leishmaniasis in Morocco," *Infection, Genetics and Evolution*, vol. 13, no. 1, pp. 162–167, 2013.

[43] W. K. Eddie Ip, K. Takahashi, R. Alan Ezekowitz, and L. M. Stuart, "Mannose-binding lectin and innate immunity," *Immunological Reviews*, vol. 230, no. 1, pp. 9–21, 2009.

[44] S. Saevarsdottir, T. Vikingsdottir, and H. Valdimarsson, "The potential role of mannan-binding lectin in the clearance of self-components including immune complexes," *Scandinavian Journal of Immunology*, vol. 60, no. 1-2, pp. 23–29, 2004.

[45] M. Rakhshandehroo, R. Stienstra, N. J. de Wit et al., "Plasma mannose-binding lectin is stimulated by PPARα in humans," *The American Journal of Physiology—Endocrinology and Metabolism*, vol. 302, no. 5, pp. E595–E602, 2012.

[46] M. Panadero, C. Bocos, and E. Herrera, "Relationship between lipoprotein lipase and peroxisome proliferator-activated receptor-α expression in rat liver during development," *Journal of Physiology and Biochemistry*, vol. 62, no. 3, pp. 189–198, 2006.

Hindawi Publishing Corporation
Mediators of Inflammation
Volume 2014, Article ID 506450, 12 pages
http://dx.doi.org/10.1155/2014/506450

Research Article

TRPV1 Antagonism by Capsazepine Modulates Innate Immune Response in Mice Infected with *Plasmodium berghei* ANKA

Elizabeth S. Fernandes,[1,2] Carolina X. L. Brito,[1] Simone A. Teixeira,[3] Renato Barboza,[4] Aramys S. dos Reis,[3] Ana Paula S. Azevedo-Santos,[5] Marcelo Muscará,[3] Soraia K. P. Costa,[3] Claudio R. F. Marinho,[3] Susan D. Brain,[2] and Marcos A. G. Grisotto[1,6]

[1] *Universidade CEUMA, 65075-120 São Luís, MA, Brazil*
[2] *Cardiovascular Division, King's College London, London, UK*
[3] *Universidade de São Paulo, São Paulo, Brazil*
[4] *Universidade Federal de São Paulo, Diadema, Brazil*
[5] *Universidade Federal do Maranhão, São Luís, Brazil*
[6] *Instituto Florence de Ensino Superior, São Luís, Brazil*

Correspondence should be addressed to Elizabeth S. Fernandes; elizabeth.soares@ceuma.br

Received 3 June 2014; Accepted 8 July 2014; Published 24 August 2014

Academic Editor: Mauricio Martins Rodrigues

Thousands of people suffer from severe malaria every year. The innate immune response plays a determinant role in host's defence to malaria. Transient receptor potential vanilloid 1 (TRPV1) modulates macrophage-mediated responses in sepsis, but its role in other pathogenic diseases has never been addressed. We investigated the effects of capsazepine, a TRPV1 antagonist, in malaria. C57BL/6 mice received 10^5 red blood cells infected with *Plasmodium berghei* ANKA intraperitoneally. Noninfected mice were used as controls. Capsazepine or vehicle was given intraperitoneally for 6 days. Mice were culled on day 7 after infection and blood and spleen cell phenotype and activation were evaluated. Capsazepine decreased circulating but not spleen $F4/80^+Ly6G^+$ cell numbers as well as activation of both $F4/80^+$and $F4/80^+Ly6G^+$ cells in infected animals. In addition, capsazepine increased circulating but not spleen $GR1^+$ and natural killer (NK) population, without interfering with natural killer T (NKT) cell numbers and blood NK and NKT activation. However, capsazepine diminished CD69 expression in spleen NKT but not NK cells. Infection increased lipid peroxidation and the release of TNFα and IFNγ, although capsazepine-treated group exhibited lower levels of lipid peroxidation and TNFα. Capsazepine treatment did not affect parasitaemia. Overall, TRPV1 antagonism modulates the innate immune response to malaria.

1. Introduction

Malaria is an infectious disease caused by intracellular protozoans of the genus *Plasmodium* and transmitted from person to person through bites of infected mosquitoes. It affects millions of people annually and is a leading cause of child mortality in underdevelopment countries [1]. Severe malaria such as cerebral malaria is frequently fatal and outcome of infection depends on host's immune response, with innate immunity playing a determinant role in it [2, 3]. Available antimalarial therapy targets the *Plasmodium*. However, elimination of the parasite does not halt the clinical consequences of disease as surviving patients from severe malaria can develop a range of neurological deficits [4, 5]. In this context, an effective immune response is essential for patient's recovery. Innate response is the major immunity component of patients who have been infected with *Plasmodium* for the first time, being essential to the development of an effective acquired immune response [6].

Recently, a protective role for transient receptor vanilloid 1 (TRPV1), a nonselective cation channel found on both neuronal and nonneuronal cells, was suggested in bacteria-induced sepsis [7–10]. Indeed, in the absence of TRPV1 activation, macrophage functions such as their ability to

phagocytose and to release inflammatory mediators (nitric oxide (NO), reactive oxygen species (ROS), and cytokines) are impaired [9]. Also, TRPV1 has been linked to macrophage survival [9]. Evidence suggests a feedback between TRPV1 activation and ROS production may exist; in addition to modulating oxidative stress by downregulating ROS generation, this receptor can be directly activated by hydrogen peroxide (H_2O_2) [11] and regulated by superoxide anion (O_2^-) release [12–14]. Oxidative stress generation has a direct impact on macrophage-erythrocyte-endothelium interactions and imbalances of this pathway may trigger excessive damage and impaired host's immune response to malaria [15, 16].

Herein, the role of TRPV1 in malaria was investigated for the first time. We used the TRPV1 antagonist, capsazepine, to assess whether TRPV1 is able to modulate the innate immune response to malaria in animals infected with *Plasmodium berghei* ANKA.

2. Materials and Methods

2.1. Animals. Inbred male C57BL/6 mice (8 weeks old) were used. Mice were obtained from the animal's facility of the Department of Parasitology, Institute of Biomedical Sciences, University of São Paulo. Mice were kept in a climatically controlled environment and given food and water *ad libitum*. All procedures were approved by the Ethics Committee of the University of São Paulo and carried out in accordance with the Brazilian society for animal welfare (SBCAL).

2.2. Malaria Induction. Malaria was induced by a single intraperitoneal (i.p.) injection of 10^5 red blood cells (RBCs) infected with *Plasmodium berghei* ANKA (clone 1.49L) as described by Elias et al. [17]. Parasitaemia was assessed daily in a blood smear stained by Giemsa, by microscopy, from day 5 to day 7 following infection and was expressed as % of infected RBCs. Mice were terminally anaesthetised with a mixture of ketamine (75 mg/kg; Dopalen, Ceva, Brazil) and xylazine (1 mg/kg; i.p.; Sigma-Aldrich, Brazil), and exsanguinated by cardiac puncture on day 7 after infection (premortality end point; [18, 19]). Their blood and spleen were collected for further analysis. The plasma was separated and stored at −70°C for further quantitation of plasma aldehydes and cytokines. Cell population phenotype and activation were evaluated by flow cytometry. Noninfected mice were used as controls.

2.3. Pharmacological Treatment. In order to assess the role of TRPV1 in malaria, animals received the TRPV1 antagonist, capsazepine (Sigma-Aldrich, Brazil; $n = 5$, uninfected (control) group and $n = 8$, infected group), intraperitoneally from 24 h following infection, for 6 days (2x day, 50 μg/animal; [9]). Vehicle (10% DMSO in saline, 120 μL/animal; $n = 5$, uninfected (control) group and $n = 8$, infected group) was used as controls.

2.4. Flow Cytometry Analysis. Blood and spleen samples from infected and uninfected mice and single-cell suspensions were prepared. Peripheral blood cells were isolated by Percoll gradient (Sigma-Aldrich, Brazil). Spleens were homogenized and passed through a nylon mesh of 70 μm to create a single-cell suspension. Cells were stained with Trypan blue (Sigma-Aldrich, Brazil) and assessed for viability in a haemocytometer. Cells (10^6) were washed, resuspended in flow cytometry buffer (2% foetal calf serum (Invitrogen, Brazil) in phosphate buffered saline-PBS (Sigma-Aldrich, Brazil)), and stained with directly conjugated monoclonal antibodies (BD Biosciences or eBiosciences, Brazil): anti-F4/80 FITC, anti-IAb PE, anti-Ly6G PerCP, anti-GR1 Pe-Cy7, anti-CD3 PE and APC, anti-NK1.1 FITC, and anti-CD69 PECy5. Events were acquired on a BD FACSCanto (BD Biosciences-Immunocytometry Systems) and analyzed using FlowJo software (Tree Star Inc.). In order to analyze monocyte/macrophage and neutrophil populations, cells expressing $CD3^+$, $CD4^+$, $CD8^+$, and $CD19^+$ were gated out and the phenotypic F4/80, GR1, and Ly6G lineage markers were evaluated. Results are expressed as representative two-colour dot-plots as well as number of cells ($\times 10^6$), except for IAb, expressed as mean fluorescence.

2.5. Plasma Cytokine Levels. The plasma levels of TNFα, IFNγ, IL-4, IL-6, IL-2, IL-10, and IL-17 were evaluated by using a cytometric bead array (CBA) mouse Th1/Th2/Th17 cytokine kit (BD Biosciences, Brazil) according to manufacturer's instructions. Analysis was performed on a Facscalibur cytometer flow cytometer (BD Biosciences-Immunocytometry Systems). Results were calculated in CBA FCAP Array software (BD Biosciences, Brazil) as pg/mL and are expressed as fold-increase relative to uninfected controls.

2.6. Plasma Aldehydes. Total plasma aldehyde (mainly malondialdehyde) concentrations were quantified as an index of lipid peroxidation and oxidative stress, as previously described [20, 21]. Briefly, 100 μL of sample were incubated with 100 μL of PBS and 400 μL of thiobarbituric acid (0.67%; Sigma-Aldrich, Brazil), at 90°C for 45 min. Samples were then centrifuged at 1,000 xg for 10 min. Three hundred μL of the supernatant was incubated with 300 μL of butanol (Sigma-Aldrich, Brazil) and 30 μL of a saturated solution of sodium chloride (Sigma-Aldrich, Brazil). Samples were mixed in a vortex, centrifuged at 1,000 xg for 2 min and then added to a 96-well plate (200 μL/well). Absorbance was read at 535 and 572 nm and the difference between the absorbance was used to calculate the aldehyde concentrations, using the molar extinction coefficient of the chromophore ($1.56 \times 10^5\ M^{-1}/cm^{-1}$). Results are expressed as fold-increase relative to uninfected controls.

2.7. Data Analysis. The results are presented as the mean ± standard deviation (SD). The percentages of inhibition are reported as mean ± SD of inhibitions obtained in each individual experiment compared with control samples. Statistical comparisons of the data were performed by ANOVA followed

by Bonferroni and unpaired t-test when appropriate. The P values < 0.05 were considered significant.

3. Results

3.1. Capsazepine Does Not Affect Parasitaemia. Figure 1 shows parasitaemia levels up to day 7 after infection, in mice treated with either vehicle or capsazepine. Parasitaemia progressively increased in both groups. Repeated treatment with capsazepine had no effect on parasitaemia. Experiments were performed with a premortality end-point. Thus, no signs of cerebral malaria such as reduced responsiveness to stimulation, ataxia, respiratory distress or prostration, paralysis, and convulsions were observed in either capsazepine- or vehicle-infected mice. However, both groups of animals displayed piloerection and/or abnormal posture, as a result of infection.

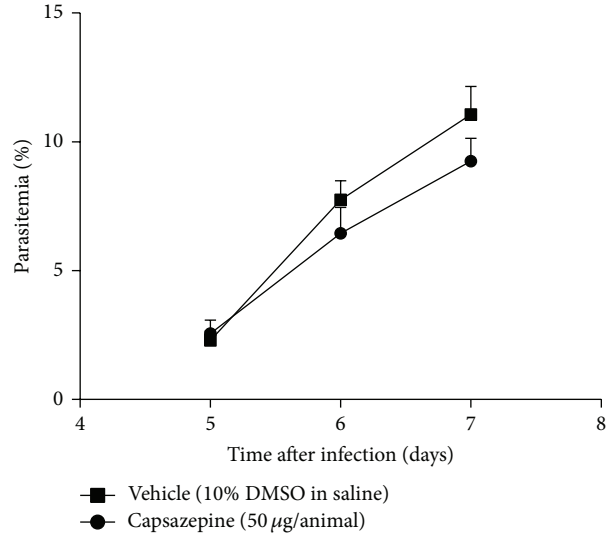

Figure 1: Effect of capsazepine on parasitaemia levels. Parasitaemia was measured daily, from day 5 to day 7 after infection in blood smear samples obtained from C57BL/6 mice infected with *Plasmodium berghei* ANKA (10^5 infected RBCs/animal; i.p.) treated with either capsazepine (50 μg/animal, 2x day, for 6 days) or vehicle (10% DMSO in saline) from 24 h after infection (n = 8 per group).

3.2. Capsazepine Alters Circulating Monocyte but Not Spleen Macrophage Population Number and Activation. As represented in Figures 2(a)–2(e), three distinct populations of peripheral blood leukocytes were detected in all groups of uninfected and infected animals: F4/80$^+$, F4/80$^+$Ly6G$^+$ and Ly6G$^+$ cells. Malaria induction had no effect on Ly6G$^+$ cell population as no statistical significance was found between any of the evaluated groups. Mean ± SD values for Ly6G$^+$ populations are as follows: vehicle-uninfected group 2.0 ± 0.6, capsazepine uninfected group 1.3 ± 0.4, vehicle-infected group 0.9 ± 1.1, and capsazepine infected group 1.3 ± 0.8. On the other hand, *P. berghei* ANKA infection increased F4/80$^+$Ly6G$^+$ cell numbers in both vehicle- (3.9-fold increase) and capsazepine- (1.9-fold increase) treated groups when compared to uninfected controls, whilst no effects were observed on F4/80$^+$ cell population (Figures 2(b) and 2(c)). In addition, malaria caused increased activation of both F4/80$^+$ (5.1-fold increase) and F4/80$^+$Ly6G$^+$ (6.6-fold increase) circulating cells when compared to uninfected animals, as denoted by expression of IAb on these cells (Figures 2(d) and 2(e)). Repeated administration of capsazepine in infected animals caused reduction of F4/80$^+$Ly6G$^+$ population expansion by 25.0 ± 5.2% but did not affect F4/80$^+$ cell numbers (Figures 2(b) and 2(c)). In addition, *P. berghei* ANKA-induced activation of F4/80$^+$ and F4/80$^+$Ly6G$^+$ cells was halted by capsazepine. As depicted in Figures 2(d) and 2(e), capsazepine treatment reduced by 75 ± 22.7% and 90.3 ± 7.1%, the expression of IAb on F4/80$^+$ and F4/80$^+$Ly6G$^+$ cells, respectively, when compared to vehicle-treated infected controls. As infection raised the number of circulating F4/80$^+$Ly6G$^+$ cells, a decline was noticed in the GR1$^+$ cell population (34.1 ± 15.1%). However, infected mice treated with capsazepine exhibited a higher number of these cells when compared with both their uninfected- (1.8-fold increase) and infected- (2.4-fold increase) control animals. Mean ± SD values for GR1$^+$ populations are as follows: vehicle-uninfected group 2.9 ± 0.6, capsazepine uninfected group 2.5 ± 0.4, vehicle-infected group 1.9 ± 0.4, and capsazepine infected group 4.6 ± 0.5 ($P < 0.05$). Capsazepine treatment in uninfected animals had no effects in regard to expansion or activation of both F4/80$^+$ and F4/80$^+$Ly6G$^+$ cells (Figures 2(a)–2(e)) and neither on GR1$^+$ cells.

Similarly, F4/80$^+$, F4/80$^+$Ly6G$^+$ and Ly6G$^+$ cells were detected in spleen samples obtained from both infected and uninfected mice whether or not they were treated with capsazepine (Figures 3(a)–3(e)). As observed for circulating Ly6G$^+$ cells, malaria induction had no effects on spleen Ly6G$^+$ cells. Mean ± SD values for spleen Ly6G$^+$ populations are as follows: vehicle-uninfected group 0.7 ± 0.2, capsazepine uninfected group 1.1 ± 0.4, vehicle-infected group 1.0 ± 0.6, and capsazepine infected group 0.9 ± 0.3. However, *P. berghei* ANKA injection raised the numbers of F4/80$^+$ and F4/80$^+$Ly6G$^+$ cells in both vehicle- (2.0- and 5.8-fold increase, resp.) and capsazepine- (1.5- and 4.9-fold increase, resp.) treated groups when compared to their respective uninfected controls (Figures 3(b) and 3(c)). Also, *P. berghei* ANKA infection augmented F4/80$^+$ and F4/80$^+$Ly6G$^+$ cells in both vehicle- (5.5- and 2.0-fold increase, resp.) and capsazepine- (2.3- and 1.8-fold increase, resp.) treated groups when compared to their respective uninfected controls (Figures 3(d) and 3(e)). Capsazepine had no effects on the number or activation of spleen F4/80$^+$ and F4/80$^+$Ly6G$^+$ cells (Figures 3(a)–3(e)). Spleen GR1$^+$ cell population remained unaltered irrespective of treatments and mean ± SD values are as follows: vehicle-uninfected group 0.9 ± 0.2, capsazepine uninfected group 1.3 ± 0.6, vehicle-infected group 0.8 ± 0.3, and capsazepine infected group 1.3 ± 0.4. Moreover, capsazepine had no effects on F4/80$^+$ and F4/80$^+$Ly6G$^+$ cells (Figures 3(a)–3(e)) when administered to uninfected mice.

3.3. Capsazepine Modulates Blood and Spleen NK and NKT Population Number and Activation. We also evaluated

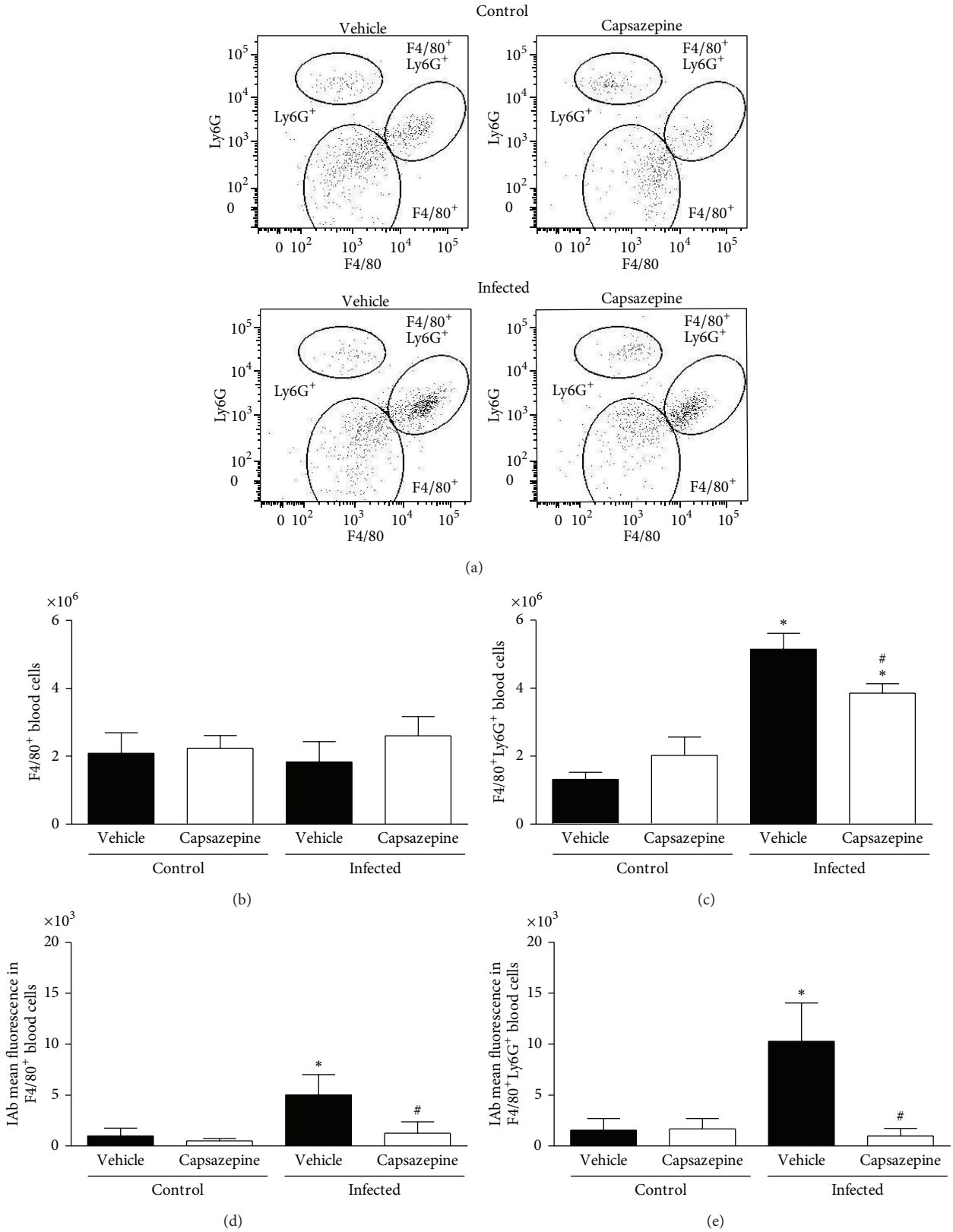

FIGURE 2: Effect of capsazepine on peripheral blood F4/80$^+$, F4/80$^+$Ly6G$^+$, and Ly6G$^+$ cells. (a) Representative two-colour dot-plots for peripheral blood F4/80$^+$, F4/80$^+$Ly6G$^+$, and Ly6G$^+$ cell populations from uninfected and *Plasmodium berghei* ANKA-infected mice (10^5 infected RBCs/animal; i.p.). Circulating (b) F4/80$^+$ and (c) F4/80$^+$Ly6G$^+$ cell numbers in uninfected and *Plasmodium berghei* ANKA-infected mice (10^5 infected RBCs/animal; i.p.). Expression of IAb (mean fluorescence) on circulating (d) F4/80$^+$ and (e) F4/80$^+$Ly6G$^+$ cell populations. Capsazepine (50 μg/animal, 2x day, for 6 days) was administered from 24 h infection. Vehicle- (10% DMSO in saline) treated animals were used as controls. Data are expressed as mean ± SD, $n = 5$ per group. $^*P < 0.05$ compared with respective uninfected (control) groups; $^\#P < 0.05$ compared with vehicle-treated infected group.

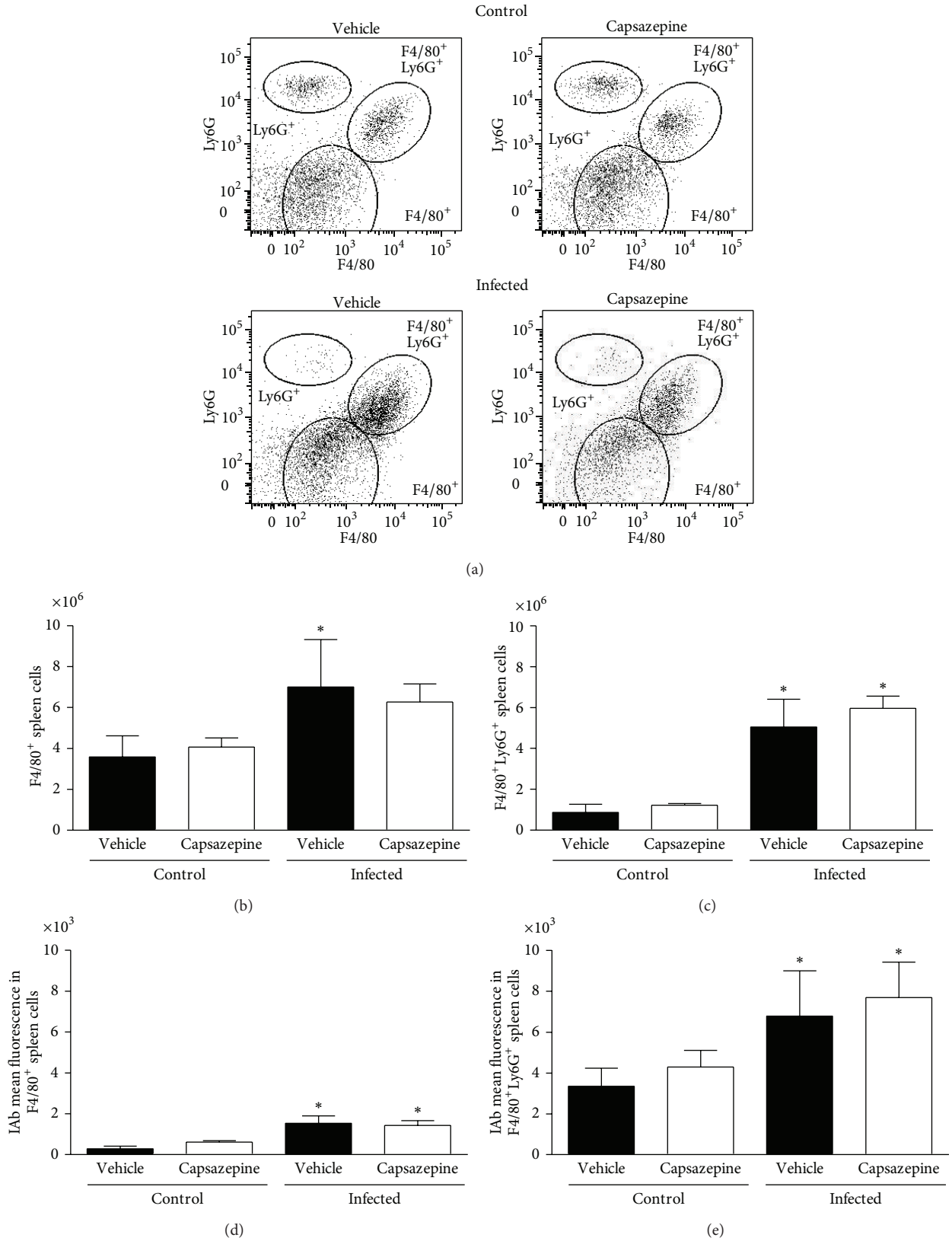

FIGURE 3: Effect of capsazepine on spleen F4/80$^+$, F4/80$^+$Ly6G$^+$, and Ly6G$^+$ cells. (a) Representative two-colour dot-plots for spleen F4/80$^+$, F4/80$^+$Ly6G$^+$, and Ly6G$^+$ cell populations from uninfected and *Plasmodium berghei* ANKA-infected mice (10^5 infected RBCs/animal; i.p.). Spleen (b) F4/80$^+$ and (c) F4/80$^+$Ly6G$^+$ cell numbers in uninfected and *Plasmodium berghei* ANKA-infected mice (10^5 infected RBCs/animal; i.p.). Expression of IAb (mean fluorescence) on spleen (d) F4/80$^+$ and (e) F4/80$^+$Ly6G$^+$ cell populations. Capsazepine (50 μg/animal, 2x day, for 6 days) was administered from 24 h after infection. Vehicle- (10% DMSO in saline) treated animals were used as controls. Data are expressed as mean ± SD, $n = 5$ per group. $^*P < 0.05$ compared with respective uninfected (control) groups.

the effects of capsazepine on circulating and spleen NK ($CD3^{-}NK1.1^{+}$) and NKT ($CD3^{+}NK1.1^{+}$) cells. Peripheral blood NK and NKT cells were detected in all groups of uninfected and infected animals (Figures 4(a)–4(e)). Malaria induction had no effects on either NK or NKT cell numbers when compared to uninfected control mice (Figures 4(b) and 4(d)). On the other hand, NK, but not NKT activation via CD69 expression, was increased in both vehicle- (11.1-fold increase) and capsazepine- (11.5-fold increase) treated groups when compared to their respective uninfected controls (Figure 4(c)). However, capsazepine treatment significantly increased NK cell population (Figure 4(b)) when compared to either its uninfected control group (1.8-fold increase) or vehicle-treated infected animals (1.5-fold increase). Also, capsazepine was able to enhance activation of NKT-infected cells (2.7-fold increase; Figure 4(e)). Importantly, NK cells account for the majority of circulating and activated $NK1.1^{+}$ cells in infected animals (Figure 4).

Similarly, spleen NK and NKT cells were detected in all groups of uninfected and infected animals (Figures 5(a)–5(e)). Malaria induction caused spleen NKT but not NK cell population expansion when compared to uninfected control mice (Figures 5(b) and 5(d)). This was observed for both vehicle- (5.6-fold increase) and capsazepine- (4.1-fold increase) treated mice (Figure 5(d)). Figures 5(c) and 5(e) demonstrate that CD69 expression was augmented on both spleen NK and NKT cells obtained from infected mice treated with either vehicle (5.3- and 6.9-fold increase, resp.) or capsazepine (5.6- and 3.1-fold increase, resp.). However, NKT activation was 45.7±17.5% lower in capsazepine-treated mice when compared to vehicle-infected controls (Figure 5(e)). Capsazepine treatment in infected mice had no effects on spleen NK and NKT cell numbers or NK activation (Figure 5). Similarly, capsazepine did not alter spleen NK and NKT profile (cell number and activation) in samples obtained from uninfected mice (Figure 5).

3.4. Capsazepine Reduces Lipid Peroxidation and Plasma TNFα Levels in P. berghei ANKA-Infected Mice. *P. berghei* ANKA infection increased lipid peroxidation in both vehicle- and capsazepine-treated mice, as demonstrated by the levels of plasma aldehydes (Figure 6(a)). However, this increase was less pronounced in the capsazepine-treated group (20.5±6.4% reduction). Malaria also triggered the release of TNFα and IFNγ in both infected groups (Figures 6(b) and 6(c)). TNFα production was markedly reduced by capsazepine treatment (70.8 ± 14.5%; Figure 6(b)). On the other hand, capsazepine treatment did not affect IFNγ release triggered by malaria (Figure 6(c)). Vehicle- and capsazepine-treated uninfected mice exhibited similar levels of plasma aldehydes, TNFα, and IFNγ (data not shown). Production of IL-4, IL-6, IL-2, IL-10, and IL-17 was not detected in any of the evaluated groups.

4. Discussion

Since its discovery, evidence has accumulated that TRPV1 has the potential to play a key role in a variety of pathologies, especially those associated with imbalances of the immune and inflammatory response, such as asthma [22–24] and rheumatoid arthritis [25–27]. Recent reports demonstrated that TRPV1 is expressed on immune cells such as macrophages and peripheral-blood mononuclear cells in inflammatory conditions [9, 28–30]. More recently, TRPV1 was suggested to modulate a range of macrophage-mediated responses to bacterial infection [9]. Indeed, TRPV1 deletion or antagonism has been associated with poorer outcome of experimental sepsis as TRPV1 blockade increases pathogen load and also facilitates the transition from a local to a systemic inflammatory response to bacteria [7, 9, 10, 31–34]. In addition, TRPV1 knockout (TRPV1 KO) mice challenged with intestinal bacteria or LPS present with a dysregulated production of inflammatory mediators, including NO, ROS, and cytokines such as TNFα, IL-10, and IL-6 [7–9]. So far, there are no reports of TRPV1 playing any roles in the immune response to other pathogens.

Here, we show for the first time that TRPV1 antagonism by capsazepine, a nonselective antagonist, modulates the innate immune response to malaria. Reports have shown that capsazepine presents species- and modality-specific activity on TRPV1 and also inhibits acetylcholine receptors, voltage-gated calcium channels, and hyperpolarization-activated cyclic nucleotide-gated channels, in addition to TRPV1 [35–38]. However, it is important to highlight that capsazepine was administered in this study, as described by Fernandes and collaborators [9] who showed that repeated treatment with this drug *in vivo* produces a similar profile to that of TRPV1 KO mice in response to bacterial infection [9]. Herein, we induced malaria by injecting *P. berghei* ANKA in a susceptible strain of mice known to develop cerebral malaria-like symptoms and to present with 60–100% mortality within the second week following injection (for review see [19]). Our studies were carried out at a premortality end-point, that is, 7 days following infection. At this time point, parasitaemia had reached 11%, in agreement with previous studies [17, 22].

Evidence suggests that the innate immune response plays an important role during the early phase of infection, with activated monocytes and neutrophils releasing nonspecific inflammatory mediators such as ROS and cytokines [2, 39] and exerting their roles as phagocytes and antigen-presenting cells when in contact with circulating infected RBCs [40]. Indeed, phagocytosis of infected RBCs by peripheral blood and tissue phagocytes is suggested to be the major mechanism of *Plasmodium* removal [41]. As a result of this interaction, phagocytes may damage the endothelium, thus contributing to the collapse of the circulation and in the case of cerebral malaria, damaging the brain microvasculature [4, 42]. During infection, monocytes differentiate into macrophages in the spleen and also in the brain, becoming available in the brain microvasculature [4]. Activated macrophages contribute to pathogen clearance and activation of lymphocytes, in an attempt to stimulate the generation of an acquired immune response capable of improving parasite removal and fighting a secondary infection [2, 43].

As previously mentioned, TRPV1 can be found on immune cells. It is then expected that antagonism of TRPV1 channels expressed on these cells would affect their phenotypes. Our results show that at 7 days after infection, there

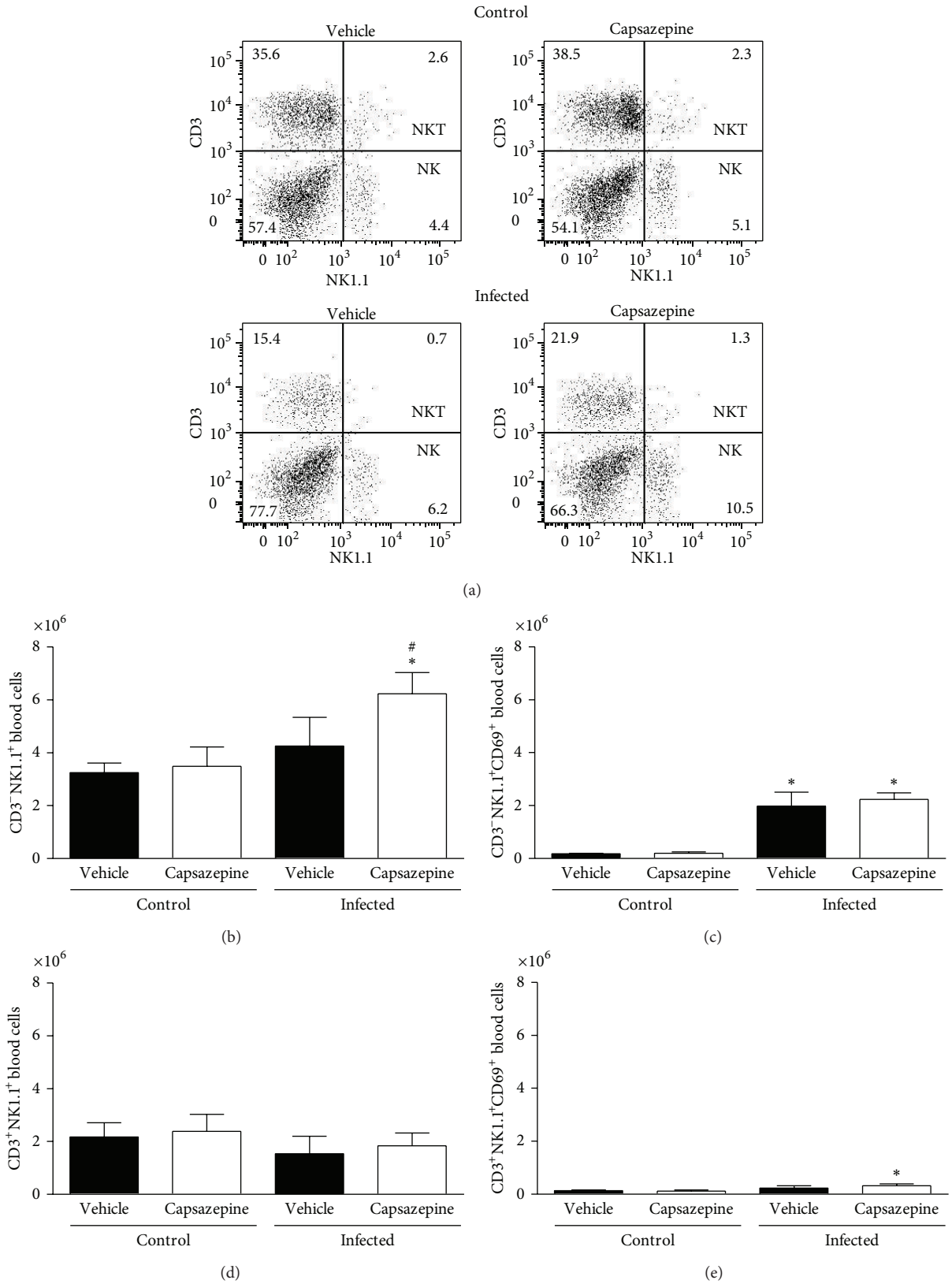

Figure 4: Effect of capsazepine on peripheral blood $CD3^{-}NK1.1^{+}$ and $CD3^{+}NK1.1^{+}$ cells. (a) Representative two-colour dot-plots for peripheral blood $CD3^{-}NK1.1^{+}$ (NK) and $CD3^{+}NK1.1^{+}$ (NKT) cell populations from uninfected and *Plasmodium berghei* ANKA-infected mice (10^5 infected RBCs/animal; i.p.). Circulating (b) $CD3^{-}NK1.1^{+}$ and (c) $CD3^{-}NK1.1^{+}$ cell numbers in uninfected and *Plasmodium berghei* ANKA-infected mice (10^5 infected RBCs/animal; i.p.). Expression of CD69 on circulating (d) $CD3^{-}NK1.1^{+}$ and (e) $CD3^{-}NK1.1^{+}$ cells. Capsazepine (50 μg/animal, 2x day, for 6 days) was administered from 24 h after infection. Vehicle- (10% DMSO in saline) treated animals were used as controls. Data are expressed as mean ± SD, $n = 5$ per group. $^{*}P < 0.05$ compared with respective uninfected (control) groups.

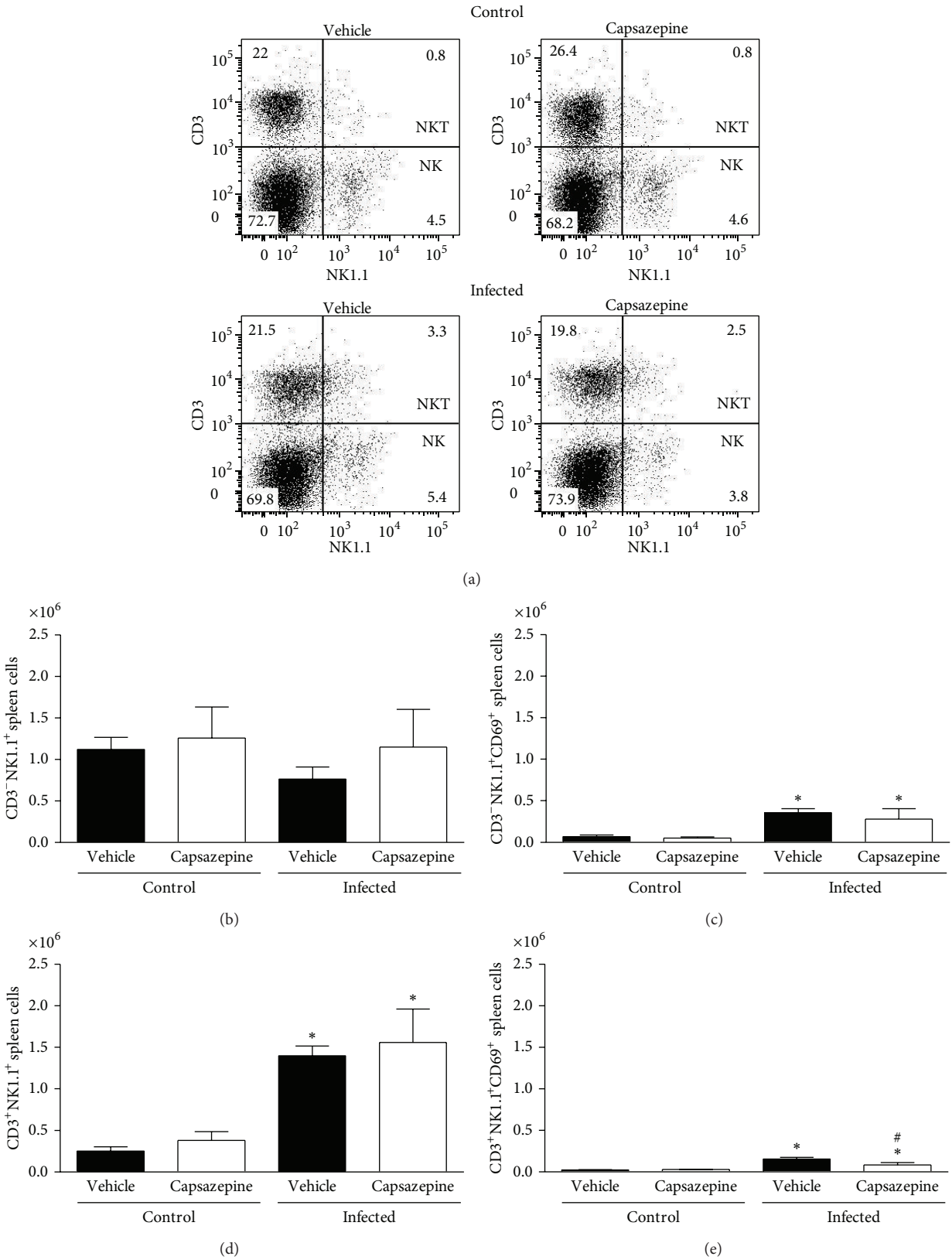

FIGURE 5: Effect of capsazepine on spleen $CD3^-NK1.1^+$ and $CD3^+NK1.1^+$ cells. (a) Representative two-colour dot-plots for spleen $CD3^-NK1.1^+$ (NK) and $CD3^+NK1.1^+$ (NKT) cell populations from uninfected and *Plasmodium berghei* ANKA-infected mice (10^5 infected RBCs/animal; i.p.). Spleen (b) $CD3^-NK1.1^+$ and (c) $CD3^-NK1.1^+$ cell numbers in uninfected and *Plasmodium berghei* ANKA-infected mice (10^5 infected RBCs/animal; i.p.). Expression of CD69 on circulating (d) $CD3^-NK1.1^+$ and (e) $CD3^-NK1.1^+$ cells. Capsazepine (50 μg/animal, 2x day, for 6 days) was administered from 24 h after infection. Vehicle- (10% DMSO in saline) treated animals were used as controls. Data are expressed as mean ± SD, $n = 5$ per group. $^*P < 0.05$ compared with respective uninfected (control) groups.

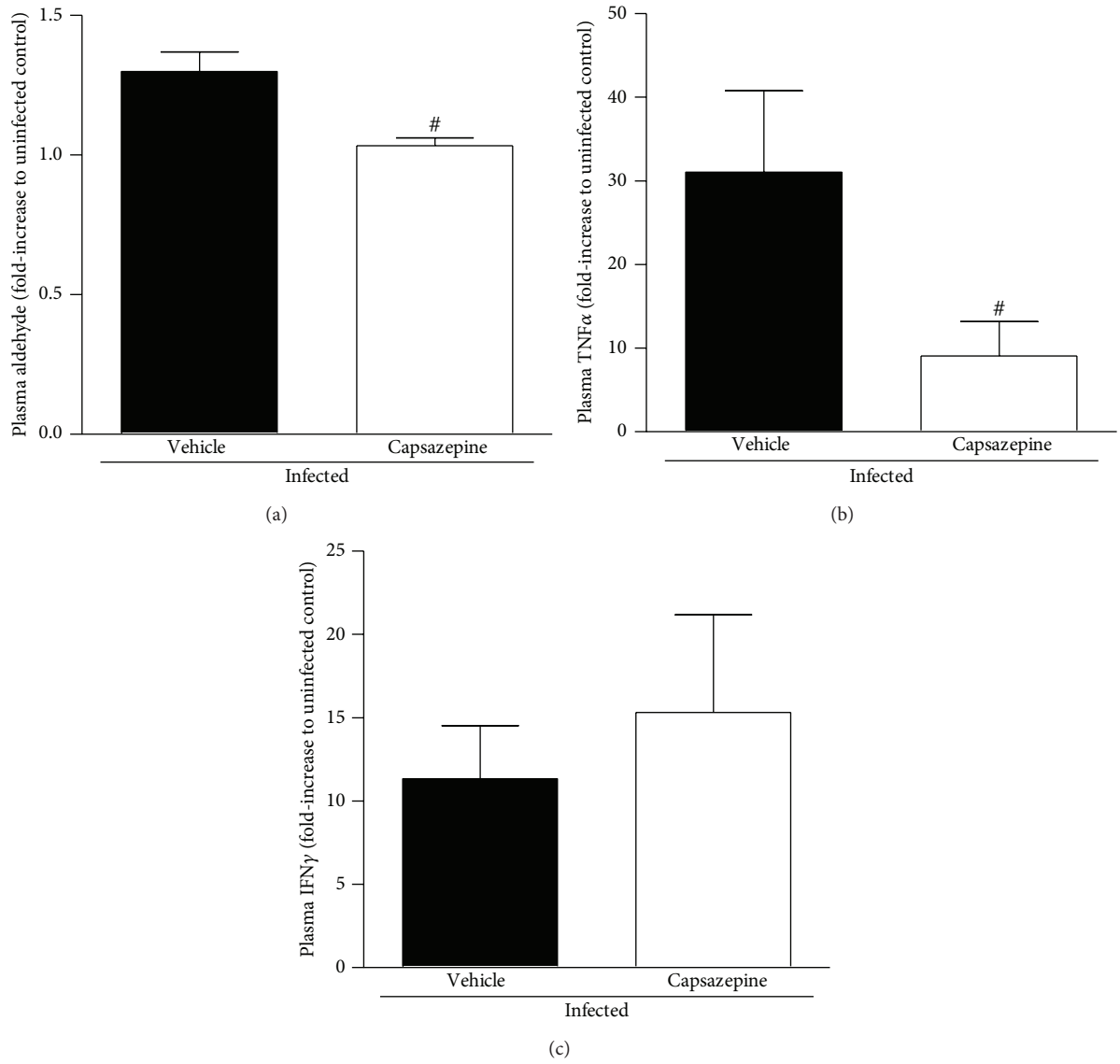

Figure 6: Effect of capsazepine on systemic lipid peroxidation and cytokine release. (a) Aldehyde; (b) TNFα and (c) IFNγ levels in plasma samples obtained from uninfected and *Plasmodium berghei* ANKA-infected mice (10^5 infected RBCs/animal; i.p.). Capsazepine (50 μg/animal, 2x day, for 6 days) was administered from 24 h after infection. Vehicle- (10% DMSO in saline) treated animals were used as controls. Data are expressed as mean ± SD, $n = 5$–8 per group. $^{\#}P < 0.05$ compared with vehicle-treated infected group.

is activation of both monocytes and spleen macrophages ($F4/80^+$). Interestingly, we detected a group of circulating $F4/80^+Ly6G^+$ cells which became markedly expanded and activated (as denoted by IAb expression) following infection. This is the first report to our knowledge of their contribution to malaria. However, it was recently suggested in a model of infection caused by vaccinia virus inoculation in C57BL/6 mice that $F4/80^+Ly6G^+$ cells are indeed monocytes with a great capacity of producing ROS and IFNγ whilst $Ly6G^-$ monocytes produce NO and TNFα [44]. In addition, the same study suggested that $F4/80^+Ly6G^+$ cells replace $Ly6G^-$ monocytes as infection progresses. Herein, we show the existence of $F4/80^+Ly6G^+$ cells also in the spleen and that they exhibit a similar profile (in terms of number and activation pattern) to that of $Ly6G^-$ cells in this tissue. As the population of $F4/80^+Ly6G^+$ cells rises, $GR1^+$ cells (myeloid-derived suppressor cells) decline with infection. This is expected as an increase of mature monocytes and neutrophils normally occurs as a result of infection [45, 46]. However, at 7 days after infection, these changes in the balance and/or activation of $F4/80^+$, $F4/80^+Ly6G^+$, and $GR1^+$ cells could not be noticed at spleen level. However, it is possible that these alterations may occur in this organ at a different time point not addressed by this study.

Repeated treatment with capsazepine caused inhibition of activation of both $F4/80^+$ and $F4/80^+Ly6G^+$ cells as well as reduction of the number of circulating $F4/80^+Ly6G^+$ cells in infected mice. Interestingly, $GR1^+$ cell number is

markedly increased in the same group of animals, suggesting that, as capsazepine shuts down F4/80$^+$- and F4/80$^+$Ly6G$^+$-mediated responses, either by deactivating them or decreasing their availability in the circulation, these cells are progressively replaced by GR1$^+$ cells in order to restore the immune responses that may be dependent on F4/80$^+$- and F4/80$^+$Ly6G$^+$ monocytes. Indeed, GR1$^+$ cells are suggested to be recruited in order to compensate "the loss" of monocytes that undergo polarization following *Plasmodium* or bacterial infection [47, 48]. These cells are also called regulatory monocytes/macrophages and have a potent ability to suppress T cell proliferation and Th1 responses [49]. On the other hand, the definite role of these cells in critical illness is still of debate (for review see [47]).

To evaluate the impact this shift on monocyte profile had on inflammatory mediator release, we measured the levels of plasma aldehydes (index of lipid peroxidation secondary to oxidative stress) and cytokines such as TNFα and IFNγ. Indeed, high systemic levels of inflammatory mediators such as TNFα, IFNγ, and aldehydes are correlated with severe malaria in humans [50]. In fact, lipid peroxidation is produced during malaria as a result of the interactions between monocytes/macrophages and infected erythrocytes, and also the endothelium [51, 52]. In addition, cytokines are also released in response to malaria, triggering suppression of erythropoiesis and activation of a variety of circulating and spleen cells [2, 53, 54]. We found that whilst diminished levels of lipid peroxidation-derived aldehydes and TNFα were detected in animals with malaria that had been treated with capsazepine, IFNγ production remained similar to that observed for samples obtained from vehicle-infected mice. A reduction of oxidative stress was expected as capsazepine was previously suggested to inhibit oxidative stress in cultured RAW264 monocytes/macrophages in a TRPV1 independent manner, although this data was obtained from cells that had not been challenged with any pathogen product [55]. Later, TRPV1 deletion was shown to decrease ROS production by macrophages in sepsis [9] and to modulate the release of these mediators in other inflammatory conditions [14, 56]. However, loss of TRPV1 function has been associated with increased production of TNFα upon bacterial infection [7, 9, 32]. It is possible that TRPV1 differently modulates monocytes and macrophages with respect to their ability to produce TNFα. Also, TRPV1 effects on TNFα production may vary at different stages of malaria.

NK and NKT cells are important effectors of the innate immune response to malaria, directly recognizing *Plasmodium*-infected RBCs and malarial antigens, in addition to producing IFNγ in order to contain parasitaemia [2, 18, 40]. Indeed, these cells rise early during malaria and have been suggested to mediate the differentiation of Th1/Th2 responses and to be essential for the trafficking of leukocytes to the brain in cerebral malaria (for review see [2]). In addition, similarly to macrophages, they can accumulate into the brain during cerebral malaria, contributing to a worse outcome [18]. NK cells have also been linked to dendritic cell maturation and T cell activation in the spleen by releasing of cytokines [53, 57]. Also, evidence has shown that during malaria, NK cells may undergo an intense turnover or even migrate out of the spleen [18]. This was investigated at a similar time-point to that used in our study (1 week following infection). Here, we assessed the dynamics between circulating and spleen NK and NKT cells. We found that *P. berghei* ANKA-induced infection caused expansion of spleen NKT but not NK cell population. This was not accompanied by any change on circulating NK and NKT cell numbers. It is possible that at this time-point, NK and NKT cells have already migrated to the brain. Indeed, Hansen and collaborators showed that NK cells accumulate into the brain of C57BL/6 mice as early as 4 days following infection with *P. berghei* ANKA, triggering the migration of T cells to the brain microvasculature [18]. On the other hand, we show that both NK and NKT cells became activated in response to infection, with NK cells representing the majority of activated cells. Disappointingly, expansion of spleen NKT cells did not translate in their activation as only few of these cells expressed CD69. Capsazepine treatment in infected mice led to a further expansion of the circulating NK population, but its activation was similar to that of vehicle-infected group. In addition, capsazepine treatment reduced by half the activation of spleen NKT cells when compared to its infected-control. We would expect that the reduction of activation of spleen NKT cells and F4/80$^+$Ly6G$^+$ monocytes by capsazepine would impair IFNγ release. However, we show capsazepine inhibitory effects on these populations do not affect IFNγ production in malaria, indicating that either TRPV1 may not play a role on IFNγ production or NK cells become the sole source of IFNγ once TRPV1 is blocked. In addition, the lack of effect of capsazepine on parasitaemia may be related to the similar levels of IFNγ detected in both groups of animals.

Our study provides the first evidence that TRPV1 modulates malaria by mediating innate immune response, specifically by interfering with the expansion and activation of effector cells, especially monocytes. We also show that TRPV1 regulates the immunological balance between different monocyte populations in addition to modulating mediator release by them. It is possible that blocking TRPV1 may be either beneficial, as a reduction of oxidative stress may reflect on reduced vascular dysfunction, or deleterious, as impairment of innate response may lead to an inefficient removal of the parasite in addition to an inefficient acquired immune response to malaria. However, the impact TRPV1 antagonism may have on severe malaria outcome is of importance and remains to be investigated.

Conflict of Interests

The authors declare no conflict of interests.

Acknowledgments

This work was supported by the Conselho Nacional de Desenvolvimento Científico e Tecnológico (CNPq; Brazil), Coordenação de Aperfeiçoamento de Pessoal de Nivel Superior (CAPES; Brazil), Fundação de Amparo à Pesquisa e Desenvolvimento Científico do Maranhão (FAPEMA;

Brazil), and Fundação de Amparo à Pesquisa do Estado de São Paulo (FAPESP; Brazil).

References

[1] World Health Organization, *World Malaria Report: 2013*, 2013.

[2] L. Schofield, "Intravascular infiltrates and organ-specific inflammation in malaria pathogenesis," *Immunology and Cell Biology*, vol. 85, no. 2, pp. 130–137, 2007.

[3] V. Pradhan and K. Ghosh, "Immunological disturbances associated with malarial infection," *Journal of Parasitic Diseases*, vol. 37, no. 1, pp. 11–15, 2013.

[4] H. J. Shikani, B. D. Freeman, M. P. Lisanti, L. M. Weiss, H. B. Tanowitz, and M. S. Desruisseaux, "Cerebral malaria: we have come a long way," *The American Journal of Pathology*, vol. 181, no. 5, pp. 1484–1492, 2012.

[5] A. Moulick, S. Maitra, B. S. Sarkar, A. Jana, and S. Sarkar, "Vivax malaria presenting with myelitis: a rare complication," *Journal of Clinical and Diagnostic Research*, vol. 7, no. 5, pp. 914–916, 2013.

[6] M. M. Stevenson and E. M. Riley, "Innate immunity to malaria," *Nature Reviews Immunology*, vol. 4, no. 3, pp. 169–180, 2004.

[7] I. A. Clark, "How TNF was recognized as a key mechanism of disease," *Cytokine and Growth Factor Reviews*, vol. 18, no. 3-4, pp. 335–343, 2007.

[8] E. S. Fernandes, M. A. Fernandes, and J. E. Keeble, "The functions of TRPA1 and TRPV1: moving away from sensory nerves," *British Journal of Pharmacology*, vol. 166, no. 2, pp. 510–521, 2012.

[9] E. S. Fernandes, L. Liang, S. Smillie et al., "TRPV1 deletion enhances local inflammation and accelerates the onset of systemic inflammatory response syndrome," *Journal of Immunology*, vol. 188, no. 11, pp. 5741–5751, 2012.

[10] V. Guptill, X. Cui, A. Khaibullina et al., "Disruption of the transient receptor potential vanilloid 1 can affect survival, bacterial clearance, and cytokine gene expression during murine sepsis," *Anesthesiology*, vol. 114, no. 5, pp. 1190–1199, 2011.

[11] K. Susankova, K. Tousova, L. Vyklicky, J. Teisinger, and V. Vlachova, "Reducing and oxidizing agents sensitize heat-activated vanilloid receptor (TRPV1) current," *Molecular Pharmacology*, vol. 70, no. 1, pp. 383–394, 2006.

[12] E. S. Fernandes, C. T. Vong, S. Quek et al., "Superoxide generation and leukocyte accumulation: key elements in the mediation of leukotriene B4-induced itch by transient receptor potential ankyrin 1 and transient receptor potential vanilloid 1," *The FASEB Journal*, vol. 27, no. 4, pp. 1664–1673, 2013.

[13] P. Puntambekar, D. Mukherjea, S. Jajoo, and V. Ramkumar, "Essential role of Rac1/NADPH oxidase in nerve growth factor induction of TRPV1 expression," *Journal of Neurochemistry*, vol. 95, no. 6, pp. 1689–1703, 2005.

[14] A. Starr, R. Graepel, J. Keeble et al., "A reactive oxygen species-mediated component in neurogenic vasodilatation," *Cardiovascular Research*, vol. 78, no. 1, pp. 139–147, 2008.

[15] C. K. B. Ferrari, P. C. S. Souto, E. L. França, and A. C. Honorio-França, "Oxidative and nitrosative stress on phagocytes' function: from effective defense to immunity evasion mechanisms," *Archivum Immunologiae et Therapiae Experimentalis*, vol. 59, no. 6, pp. 441–448, 2011.

[16] S. Percário, D. R. Moreira, B. A. Q. Gomes et al., "Oxidative stress in Malaria," *International Journal of Molecular Sciences*, vol. 13, no. 12, pp. 16346–16372, 2012.

[17] R. M. Elias, M. Correa-Costa, C. R. Barreto et al., "Oxidative stress and modification of renal vascular permeability are associated with acute kidney injury during P. berghei ANKA infection," *PLoS ONE*, vol. 7, no. 8, Article ID e44004, 2012.

[18] D. S. Hansen, N. J. Bernard, C. Q. Nie, and L. Scholeld, "NK cells stimulate recruitment of CXCR3$^+$ T cells to the brain during *Plasmodium berghei*-mediated cerebral malaria," *Journal of Immunology*, vol. 178, no. 9, pp. 5779–5788, 2007.

[19] L. Rénia, S. W. Howland, C. Claser et al., "Cerebral malaria Mysteries at the blood-brain barrier," *Virulence*, vol. 3, no. 2, pp. 193–201, 2012.

[20] R. P. Bird and H. H. Draper, "Comparative studies on different methods of malonaldehyde determination," *Methods in Enzymology*, vol. 105, pp. 299–305, 1984.

[21] L. Sharma, J. Kaur, and G. Shukla, "Role of oxidative stress and apoptosis in the placental pathology of plasmodium berghei infected mice," *PLoS ONE*, vol. 7, no. 3, Article ID e32694, 2012.

[22] R. Nassini, P. Pedretti, N. Moretto et al., "Transient receptor potential ankyrin 1 channel localized to non-neuronal airway cells promotes non-neurogenic inflammation," *PLoS ONE*, vol. 7, no. 8, Article ID e42454, 2012.

[23] F. Tsuji and H. Aono, "Role of transient receptor potential vanilloid 1 in inflammation and autoimmune diseases," *Pharmaceuticals*, vol. 5, no. 8, pp. 837–852, 2012.

[24] J. Yang, H. M. Yu, X. D. Zhou, V. P. Kolosov, and J. M. Perelman, "Study on TRPV1-mediated mechanism for the hypersecretion of mucus in respiratory inflammation," *Molecular Immunology*, vol. 53, no. 1-2, pp. 161–171, 2013.

[25] E. S. Fernandes, F. A. Russell, D. Spina et al., "A distinct role for transient receptor potential ankyrin 1, in addition to transient receptor potential vanilloid 1, in tumor necrosis factor α-induced inflammatory hyperalgesia and Freund's complete adjuvant-induced monarthritis," *Arthritis and Rheumatism*, vol. 63, no. 3, pp. 819–829, 2011.

[26] J. Keeble, F. Russell, B. Curtis, A. Starr, E. Pinter, and S. D. Brain, "Involvement of transient receptor potential vanilloid 1 in the vascular and hyperalgesic components of joint inflammation," *Arthritis and Rheumatism*, vol. 52, no. 10, pp. 3248–3256, 2005.

[27] F. A. Russell, E. S. Fernandes, J. Courade, J. E. Keeble, and S. D. Brain, "Tumour necrosis factor α mediates transient receptor potential vanilloid 1-dependent bilateral thermal hyperalgesia with distinct peripheral roles of interleukin-1β, protein kinase C and cyclooxygenase-2 signalling," *Pain*, vol. 142, no. 3, pp. 264–274, 2009.

[28] T. K. Finney-Hayward, M. O. Popa, P. Bahra et al., "Expression of transient receptor potential C6 channels in human lung macrophages," *The American Journal of Respiratory Cell and Molecular Biology*, vol. 43, no. 3, pp. 296–304, 2010.

[29] C. I. Saunders, R. G. Fassett, and D. P. Geraghty, "Up-regulation of TRPV1 in mononuclear cells of end-stage kidney disease patients increases susceptibility to *N*-arachidonoyl-dopamine (NADA)-induced cell death," *Biochimica et Biophysica Acta: Molecular Basis of Disease*, vol. 1792, no. 10, pp. 1019–1026, 2009.

[30] J. Zhao, L. Ching, Y. R. Kou et al., "Activation of TRPV1 prevents OxLDL-induced lipid accumulation and TNF-α-Induced inflammation in macrophages: role of liver X receptor α," *Mediators of Inflammation*, vol. 2013, Article ID 925171, 14 pages, 2013.

[31] P. Bryant, M. Shumate, G. Yumet, C. H. Lang, T. C. Vary, and R. N. Cooney, "Capsaicin-sensitive nerves regulate the metabolic response to abdominal sepsis," *The Journal of Surgical Research*, vol. 112, no. 2, pp. 152–161, 2003.

[32] N. Clark, J. Keeble, E. S. Fernandes et al., "The transient receptor potential vanilloid 1 (TRPV1) receptor protects against the onset of sepsis after endotoxin," *The FASEB Journal*, vol. 21, no. 13, pp. 3747–3755, 2007.

[33] T. Iida, I. Shimizu, M. L. Nealen, A. Campbell, and M. Caterina, "Attenuated fever response in mice lacking TRPV1," *Neuroscience Letters*, vol. 378, no. 1, pp. 28–33, 2005.

[34] Y. Wang, M. Novotný, V. Quaiserová-Mocko, G. M. Swain, and D. H. Wang, "TRPV1-mediated protection against endotoxin-induced hypotension and mortality in rats," *American Journal of Physiology: Regulatory Integrative and Comparative Physiology*, vol. 294, no. 5, pp. R1517–R1523, 2008.

[35] R. J. Docherty, J. C. Yeats, and A. S. Piper, "Capsazepine block of voltage-activated calcium channels in adult rat dorsal root ganglion neurones in culture," *British Journal of Pharmacology*, vol. 121, no. 7, pp. 1461–1467, 1997.

[36] L. Liu and S. A. Simon, "Capsazepine, a vanilloid receptor antagonist, inhibits nicotinic acetylcholine receptors in rat trigeminal ganglia," *Neuroscience Letters*, vol. 228, no. 1, pp. 29–32, 1997.

[37] C. H. Gill, P. J. Strijbos, S. A. Bates, W. Cairns, D. Owen, and C. H. Davies, "Capsazepine inhibits a recombinant human HCN1-mediated current," *British Journal of Pharmacology*, vol. 135, no. 5, p. 251, 2001.

[38] P. McIntyre, L. M. McLatchie, A. Chambers et al., "Pharmacological differences between the human and rat vanilloid receptor 1 (VR1)," *British Journal of Pharmacology*, vol. 132, no. 5, pp. 1084–1094, 2001.

[39] U. Frevert and A. Nacer, "Immunobiology of Plasmodium in liver and brain," *Parasite Immunology*, vol. 35, no. 9-10, pp. 267–282, 2013.

[40] C. Coban, K. J. Ishii, T. Horii, and S. Akira, "Manipulation of host innate immune responses by the malaria parasite," *Trends in Microbiology*, vol. 15, no. 6, pp. 271–278, 2007.

[41] V. Gallo, O. A. Skorokhod, E. Schwarzer, and P. Arese, "Simultaneous determination of phagocytosis of *Plasmodium falciparum*-parasitized and non-parasitized red blood cells by flow cytometry," *Malaria Journal*, vol. 11, article 428, 2012.

[42] F. M. S. de Leoratti, S. C. Trevelin, F. Q. Cunha et al., "Neutrophil paralysis in *Plasmodium vivax* malaria," *PLoS Neglected Tropical Diseases*, vol. 6, no. 6, Article ID e1710, p. e1710, 2012.

[43] C. L. L. Chua, G. Brown, J. A. Hamilton, S. Rogerson, and P. Boeuf, "Monocytes and macrophages in malaria: protection or pathology?" *Trends in Parasitology*, vol. 29, no. 1, pp. 26–34, 2013.

[44] M. A. Fischer, M. L. Davies, I. E. Reider et al., "CD11b+, Ly6G+ cells produce type I interferon and exhibit tissue protective properties following peripheral virus infection," *PLoS Pathogens*, vol. 7, no. 11, Article ID e1002374, 2011.

[45] J. A. Villadangos, "Hold On, the Monocytes Are Coming!," *Immunity*, vol. 26, no. 4, pp. 390–392, 2007.

[46] Q. Yang, P. Ghose, and N. Ismaila, "Neutrophils mediate immunopathology and negatively regulate protective immune responses during fatal bacterial infection-induced Toxic Shock," *Infection and Immunity*, vol. 81, no. 5, pp. 1751–1763, 2013.

[47] J. N. Fullerton, A. J. O'Brien, and D. W. Gilroy, "Pathways mediating resolution of inflammation: when enough is too much," *The Journal of Pathology*, vol. 231, no. 1, pp. 8–20, 2013.

[48] J. A. van Ginderachter, A. Beschin, P. D. Baetselier, and G. Raes, "Myeloid-derived suppressor cells in parasitic infections," *European Journal of Immunology*, vol. 40, no. 11, pp. 2976–2985, 2010.

[49] D. I. Gabrilovich and S. Nagaraj, "Myeloid-derived suppressor cells as regulators of the immune system," *Nature Reviews Immunology*, vol. 9, no. 3, pp. 162–174, 2009.

[50] K. E. Lyke, R. Burges, Y. Cissoko et al., "Serum levels of the proinflammatory cytokines interleukin-1 beta (IL-1β), IL-6, IL-8, IL-10, tumor necrosis factor alpha, and IL-12(p70) in Malian children with severe *Plasmodium falciparum* malaria and matched uncomplicated malaria or healthy controls," *Infection and Immunity*, vol. 72, no. 10, pp. 5630–5637, 2004.

[51] S. L. Hazen, "Oxidized phospholipids as endogenous pattern recognition ligands in innate immunity," *Journal of Biological Chemistry*, vol. 283, no. 23, pp. 15527–15531, 2008.

[52] E. Schwarzer, H. Kühn, E. Valente, and P. Arese, "Malaria-parasitized erythrocytes and hemozoin nonenzymatically generate large amounts of hydroxy fatty acids that inhibit monocyte functions," *Blood*, vol. 101, no. 2, pp. 722–728, 2003.

[53] M. Vitale, M. Della Chiesa, S. Carlomagno et al., "NK-dependent DC maturation is mediated by TNFα and IFNγ released upon engagement of the NKp30 triggering receptor," *Blood*, vol. 106, no. 2, pp. 566–571, 2005.

[54] F. Gimenez, S. B. De Lagerie, C. Fernandez, P. Pino, and D. Mazier, "Tumor necrosis factor α in the pathogenesis of cerebral malaria," *Cellular and Molecular Life Sciences*, vol. 60, no. 8, pp. 1623–1635, 2003.

[55] M. J. Garle, A. Knight, A. T. Downing, K. L. Jassi, R. H. Clothier, and J. R. Fry, "Stimulation of dichlorofluorescin oxidation by capsaicin and analogues in RAW 264 monocyte/macrophages: lack of involvement of the vanilloid receptor," *Biochemical Pharmacology*, vol. 59, no. 5, pp. 563–572, 2000.

[56] T. Schilling and C. Eder, "Importance of the non-selective cation channel TRPV1 for microglial reactive oxygen species generation," *Journal of Neuroimmunology*, vol. 216, no. 1-2, pp. 118–121, 2009.

[57] F. Gerosa, B. Baldani-Guerra, C. Nisii, V. Marchesini, G. Carra, and G. Trinchieri, "Reciprocal activating interaction between natural killer cells and dendritic cells," *The Journal of Experimental Medicine*, vol. 195, no. 3, pp. 327–333, 2002.

Hindawi Publishing Corporation
Mediators of Inflammation
Volume 2014, Article ID 475946, 13 pages
http://dx.doi.org/10.1155/2014/475946

Research Article

Effects of Cholinergic Stimulation with Pyridostigmine Bromide on Chronic Chagasic Cardiomyopathic Mice

Marília Beatriz de Cuba,[1] Marcus Paulo Ribeiro Machado,[1] Thais Soares Farnesi,[1] Angelica Cristina Alves,[1] Livia Alves Martins,[1] Lucas Felipe de Oliveira,[1] Caroline Santos Capitelli,[1] Camila Ferreira Leite,[1] Marcos Vinícius Silva,[1] Juliana Reis Machado,[1] Henrique Borges Kappel,[1] Helioswilton Sales de Campos,[1] Luciano Paiva,[1] Natália Lins da Silva Gomes,[2] Ana Carolina Guimarães Faleiros,[1] Constança Felicia de Paoli de Carvalho Britto,[2] Wilson Savino,[2] Otacílio Cruz Moreira,[2] Virmondes Rodrigues Jr.,[1] Nicola Montano,[3] Eliane Lages-Silva,[1] Luis Eduardo Ramirez,[1] and Valdo Jose Dias da Silva[1]

[1] *Natural and Biological Sciences Institute, Triangulo Mineiro Federal University, Praca Manoel Terra 330, Centro, 38025-015 Uberaba, MG, Brazil*
[2] *Oswaldo Cruz Institute, 21040-900 Rio de Janeiro, RJ, Brazil*
[3] *Department of Clinical Sciences, Internal Medicine II, L. Sacco Hospital, University of Milan, 20157 Milan, Italy*

Correspondence should be addressed to Valdo Jose Dias da Silva; valdo@mednet.com.br

Received 25 April 2014; Revised 16 July 2014; Accepted 20 July 2014; Published 24 August 2014

Academic Editor: Marcelo T. Bozza

The aim of the present study was to assess the effects of an anticholinesterase agent, pyridostigmine bromide (Pyrido), on experimental chronic Chagas heart disease in mice. To this end, male C57BL/6J mice noninfected (control:Con) or chronically infected (5 months) with *Trypanosoma cruzi* (chagasic:Chg) were treated or not (NT) with Pyrido for one month. At the end of this period, electrocardiogram (ECG); cardiac autonomic function; heart histopathology; serum cytokines; and the presence of blood and tissue parasites by means of immunohistochemistry and PCR were assessed. In NT-Chg mice, significant changes in the electrocardiographic, autonomic, and cardiac histopathological profiles were observed confirming a chronic inflammatory response. Treatment with Pyrido in Chagasic mice caused a significant reduction of myocardial inflammatory infiltration, fibrosis, and hypertrophy, which was accompanied by a decrease in serum levels of IFNγ with no change in IL-10 levels, suggesting a shift of immune response toward an anti-inflammatory profile. Lower nondifferent numbers of parasite DNA copies were observed in both treated and nontreated chagasic mice. In conclusion, our findings confirm the marked neuroimmunomodulatory role played by the parasympathetic autonomic nervous system in the evolution of the inflammatory-immune response to *T. cruzi* during experimental chronic Chagas heart disease in mice.

1. Introduction

Chagas disease, also known as American Trypanosomiasis, an endemic parasitic disease caused by a flagellate protozoan (*Trypanosoma cruzi*), is highly prevalent throughout Latin America. Its major clinical manifestation is the chronic chagasic cardiomyopathy (CCC), which affects 1/3 of the chronically infected patients and may present severe symptoms and signs, such as congestive heart failure, thromboembolic phenomena, cardiac arrhythmias, and sudden death [1–4]. Pathological processes in the heart include mononuclear inflammatory infiltration, focal myocarditis, epicarditis, and neuroganglionitis, associated with variable focal fibrosis and a paucity of parasites, which is poorly correlated with myocardial inflammatory infiltration [2, 4].

The pathogenesis of CCC includes the balance between parasite invasiveness and the host immune response, particularly the Th1/Th2 balance, which affects the resistance/susceptibility to *T. cruzi* infection [5–7]. Even though

an imbalanced, excessive production of Th1 proinflammatory cytokines is critical to control of the parasite levels in blood and tissue [8], this type of response can also be capable of destroying functional cardiomyocytes [8] and intracardiac autonomic neurons [2, 4, 9]. This autonomic denervation, involving mainly parasympathetic postganglionic neurons causes a marked cardiac autonomic dysfunction [2, 4, 9–11], which may be involved in initiating life-threatening cardiac arrhythmias and sudden death [2, 4]. Curiously, this vagal parasympathetic autonomic dysfunction is strongly associated with inflammatory infiltration and immune activation not only in Chagas heart disease but also in other types of cardiopathy [12–15].

Although these data support a direct role of the immune system in mediating both cardiac and autonomic nervous disturbances, recent data indicate that changes in the autonomic nervous system also affect the pattern of immune response and inflammation in several cardiac and noncardiac disease states [15–17], including Chagas disease [18]. Both the sympathetic and parasympathetic branches of the autonomic nervous system can exert substantial modulatory effects on the immune response, mainly by inhibiting the Th1 response profile [17, 19–21]. This new evidence also indicates that cardiac sympathetic and particularly parasympathetic autonomic denervation/dysfunction may also contribute to an increased inflammatory response and possibly to enhanced parasite elimination [22]. Data from our laboratory collected in the context of acute Chagas disease in mice has recently confirmed that cardiac autonomic denervation/dysfunction might contribute to increased inflammation [18].

Taking into account the concepts described above, new therapies based on manipulations of vagal neuroimmunomodulation of the heart may be beneficial for treating heart diseases in general and chronic chagasic cardiomyopathy in particular [17, 23]. For example, therapeutic approaches for increasing cardiac vagal function, thereby potentiating or stimulating the vagal anti-inflammatory reflex, might have a positive impact on chronic chagasic cardiomyopathy. In fact, for other cardiopathies, these strategies, in both an experimental and clinical context, including chronic electric vagal stimulation [24] or pharmacological potentiation [25], have successfully improved cardiac outcomes.

Pyridostigmine bromide, an anticholinesterasic agent that has been used for many years to treat *myasthenia gravis*, exhibits protective cardiovascular effects during short-term administration that lead to a reduction of cardiovascular risk markers and an improvement of autonomic dysfunction [26, 26, 27, 27–29]. By potentiating vagal parasympathetic function, this compound is thought to provoke sinus bradycardia, to reduce AV nodal conduction and the refractory period of action potentials and to increase the cardiac excitation threshold, among other direct cardiac effects. It is also believed that pyridostigmine bromide, via potentiation of the cholinergic anti-inflammatory pathway, causes a reduction in myocardial inflammation and fibrosis associated with an improvement in cardiac hypertrophy and remodeling. However, there have been no reports regarding the effects of pyridostigmine bromide on the chronic phase of Chagas heart disease.

Therefore, the main aim of the present study was to evaluate the effects of cholinergic potentiation with the anticholinesterase agent pyridostigmine bromide on electrocardiographical, cardiac autonomic, histological (inflammatory infiltration and fibrosis), immunological, and parasitological parameters in C57BL/6j mice infected with the Romildo strain of *Trypanosoma cruzi* during the chronic phase of Chagas heart disease.

2. Methods

All experiments were performed on wild-type C57BL/6j mice obtained from the animal facility of the Department of Physiology of Triangulo Mineiro Federal University, Uberaba, MG. All animals were males, weighed 20–30 g, and were maintained in the animal facility of the Department of Physiology at the Triangulo Mineiro Federal University on a rodent diet (Nuvilab CR1, Nuvital Nutrientes Ltda, Curitiba, PR, Brazil) and were given water *ad libitum* until the beginning of the experimental protocols. All the experiments were carried out according to the "Principles of Laboratory Animal Care" formulated by the National Society for Medical Research, England, and "The Guide for the Care and Use of Laboratory Animals" published by the US National Institutes of Health (NIH publication number 85-23, revised in 1996). All procedures were also submitted to and approved by the Commission for Ethics in the Use of Animals in Research of the Triangulo Mineiro Federal University.

2.1. Parasite Inoculation. To induce experimental Chagas disease, mice were intraperitoneally inoculated with 15,000 trypomastigote forms of the Romildo strain of *T. cruzi*. An additional set of animals matched for gender and weight received intraperitoneal injections of the vehicle, and these were designated as the control noninfected group. After inoculation, all of the animals were observed at least twice daily to monitor their general state and to assess mortality during the acute phase. On the 12th day after inoculation, levels of parasitemia were measured by the microhematocrit method for the peripheral tail blood of all inoculated animals, according to Brenner's technique [30], to confirm infection. All subsequent surgical procedures and experimental protocols were performed at the 5th and 6th months of infection, during the chronic phase of infection, which is characterized by light tissue invasion and low mortality.

2.2. Experimental Groups. The experimental groups were divided according to the presence of Chagas disease and the administration of pyridostigmine bromide during the month from the 5th to the 6th month of observation (chronic phase), as described below. The numbers of animals used in each group are indicated in the Results section. The following groups were investigated:

Group I—Con-NT: wild-type C57BL/6j mice were injected with vehicle as a control (Con), not treated (NT) with pyridostigmine bromide and evaluated after six months at the end of the observation period;

Group II—Con-Pyrido: wild-type C57BL/6j were injected with vehicle as a control (Con) and treated with 30 mg/kg pyridostigmine bromide (Pyrido), an anticholinesterase agent, dissolved in tap water, for 30 days from the 5th to the 6th month of observation;

Group III—Chg-NT: wild-type C57BL/6j mice were inoculated with 15,000 trypomastigote forms of the Romildo strain of *T. cruzi* (Chg), not treated (NT) with pyridostigmine bromide and evaluated after six months at the end of the observation period;

Group IV—Chg-Pyrido: wild-type C57BL/6j mice were inoculated with 15,000 trypomastigote forms of the Romildo strain of *T. cruzi* (Chg) and treated with 30 mg/kg pyridostigmine bromide (Pyrido), an anticholinesterase agent, dissolved in tap water, for 30 days from the 5th to the 6th month of observation.

The solution drinking volume was monitored daily, and the pyridostigmine bromide concentration (approximately 0.084 mg/mL) was adjusted daily according to the drinking volume to maintain a daily mean ingested dose of 30 mg/kg.

2.3. Conventional Electrocardiographic (ECG) Monitoring in Anesthetized Mice. Immediately prior to inoculation (ECG1), at the 5th (ECG2, immediately prior to the pyridostigmine bromide treatment) and at the 6th months of observation (ECG3, at the end of the experimental protocol, prior to the surgical procedures), all of the animals were submitted to a conventional ECG study under tribromoethanol (250 mg/kg, i.p.) anesthesia. Needle electrodes were placed under the skin to record the conventional bipolar limb leads (I, II, and III), the unipolar limb leads (aVR, aVL, and aVF), and the unipolar precordial (chest) leads (VA: the needle was placed immediately to the right of the sternum in the 4th intercostal space; VB: the needle was placed just to the left of the sternum in the 4th intercostal space; and VC; the needle was positioned in the 5th intercostal space at the midaxillary line). To avoid errors in the positioning of the leads, the same individual consistently placed the electrodes on the animals. The ECG was recorded using an ECG amplifier (model 8811A, Hewlett-Packard Med. Inst., Waltham, MA, USA) coupled to a 12-bit analogue-to-digital interface (DI-720-USB, Dataq Instruments, Inc., Akron, OH, USA) at the sampling rate of 3 KHz on an IBM personal computer with the analysis performed by Windaq-Pro+ software (Dataq Instruments, Inc., Akron, OH, USA). The ECG was recorded for 2 minutes. The intervals and wavelengths (ms) were calculated automatically using customized software following wave identification and cursor placement. The ECG tracings were consistently analyzed by the same individual, who was blinded to the study protocol. The following ECG parameters were examined: (1) RR interval (RRi), (2) P wave duration (Pd), (3) PR interval (PR), (4) QRS duration (QRSd), (5) QT interval (QT), and (6) corrected QT interval (cQT, defined as the QT interval corrected for heart rate using Bazett's equation, where the corrected QTc was equal to QT (in s)/RR (in s)$^{1/2}$). In contrast to humans, the T wave in small rodents is not well characterized and appears as a shoulder of the QRS complex. Accordingly, to measure the QT interval, we used the apex of the T wave, which can be determined with high accuracy. The ECG parameters were determined from each lead and were averaged. Additionally, the presence of cardiac arrhythmias and atrioventricular or intraventricular blockades, among other alterations, was analyzed by visual inspection of ECG tracings by a blinded ECG specialist.

2.4. Long-Term Electrocardiographic Recordings in Freely Moving Mice. After the third ECG recording, at the 6th month of observation, the animals were reanesthetized with tribromoethanol (250 mg/kg, i.p.), and a pair of stainless steel electrodes were implanted inside the subcutaneous tissue to collect chronic recordings of conventional bipolar limb ECG lead II. The animals were also cannulated with polyethylene tubing placed in the jugular vein for drug administration. After the surgical procedures, the animals were left to recover in individual cages for at least 48–72 h.

After 48–72 h of surgical recovery and in the absence of anesthesia, the electrodes were connected to an ECG amplifier (model 8811A, Hewlett Packard, Waltham, MA, USA), and the baseline ECG was sampled continuously (3 KHz) for a period of 30 minutes with a personal computer (IBM/PC) equipped with a 12-bit analogue-to-digital interface (DI-720-USB, Dataq Instruments, Inc., Akron, OH, USA). All animals were always recorded between 8:00 AM and 5:00 PM in a quiet condition and in a freely moving state. The time series of RR intervals derived from these chronic ECG recordings were used to study the cardiac autonomic modulation in heart rate variability.

2.5. Heart Rate Variability Analysis. From the baseline chronic ECG recordings (30 minutes), the RR interval time series were derived automatically by the detection of the R wave peaks using customized linear analysis software, which was kindly provided by Dr. Alberto Porta (University of Milan, Italy). The time series of the RR intervals were divided into contiguous segments of 300 beats overlapping by half (Welch protocol). After calculating the mean and variance for each segment, a model-based autoregressive spectral analysis was performed, as described elsewhere [31, 32]. Briefly, a model of the oscillatory components present in the stationary segments of the beat-to-beat time series of the RR intervals was calculated based on the Levinson-Durbin recursion, and the order for the model was chosen according to Akaike's criterion [32]. This procedure allows for the automatic quantification of the center frequency and power of each relevant oscillatory component in the time series. The oscillatory components were labeled as very low frequency (VLF), low frequency (LF), or high frequency (HF) when the central frequencies were within the bands of 0.01–0.10 Hz, 0.10–1.00 Hz, or 1.00–5.00 Hz, respectively [18]. The power of the LF and HF components of the heart rate variability was also expressed in normalized units, which were obtained by calculating the percentage of the LF and HF variability with respect to the total power after subtracting the power of the VLF component (frequencies $<$ 0.10 Hz). The normalization procedure tends to minimize the effect of changes in the total power on the absolute values of the LF and HF variabilities [31, 32].

2.6. Pharmacological Autonomic Blockade. After 30 minutes of baseline chronic ECG recording, half of the animals were given an intravenous injection of atropine sulfate (1 mg/kg, i.v.) followed by an injection of propranolol (1 mg/kg, i.v.) 15 minutes later, whereas the other half received injections in the reverse sequence (propranolol followed by atropine sulfate). This procedure allowed for the quantification of the cardiac parasympathetic and sympathetic autonomic effects, in the former and latter group, respectively, measured as the differences between heart rate (HR) after atropine and baseline HR (parasympathetic effect) or as the differences between HR after propranolol and baseline HR (sympathetic effect), as well as the measurement of intrinsic pacemaker heart rate (IHR), quantified as the heart rate after the double blockade with atropine sulfate followed by propranolol or propranolol followed by atropine sulfate.

2.7. Histopathological Examination. At the end of the experimental protocol, all animals were euthanized with an excess dose of sodium thiopental (100 mg/kg, resp., i.p.), and the chest cavity was then opened to remove the heart for histopathological analysis. To evaluate the extent of inflammatory infiltration, tissue damage, fibrosis, and parasite nests, excised hearts from all animals were cleaned in 0.9% saline solution and fixed in phosphate-buffered 10% formalin solution for 48 h.

After embedding the samples in paraffin, five 5–7 μm thick longitudinal (four-chamber) sections of the hearts were stained with hematoxylin-eosin and analyzed using an upright light microscope (Axiolab, Carl Zeiss Inc., Germany). All regions of the hearts were examined by two blinded observers. The inflammatory infiltration and parasite nests were characterized using a semiquantitative approach and the scoring system described by Chapadeiro et al. [33]. A global myocardial inflammation score was defined for each animal as the sum of the scores from different regions of the heart.

To quantify the fibrotic area in the myocardium, contiguous longitudinal sections of the hearts were stained with Picrosirius Red, which binds the collagen present in the tissue matrix, and the slides were analyzed with polarized light microscopy using KS300 software (Karl Zeiss, Inc., Germany).

To enhance the visualization of parasite nests or antigens in cardiac tissue, an immunohistochemistry technique based on the detection of the diaminobenzidine (DAB-) derived chromogen was performed. The chromogen was generated by a secondary antibody labeled with peroxidase, which binds to a primary antibody against *T. cruzi* antigens. After antibody labeling, peroxidase reaction, and costaining with hematoxylin, slides were analyzed with an upright light microscope (Axiolab, Carl Zeiss Inc., Germany).

2.8. Quantification of Serum Levels of Cytokines. At the end of the experimental protocol, serum samples for each animal were collected by means of cardiac puncture to perform cytokine profiling (IFN-γ, TNF-α, IL-2, IL-4, IL-5, and IL-10) via ELISA or the cytometric bead array (CBA) technique.

Enzyme-Linked Immune Assay (ELISA). Serum concentrations of IFN-γ and IL-10 were measured by ELISA using pairs of monoclonal antibodies in accordance with the manufacturer's specifications (BD Pharmingen). Briefly, high-affinity 96-well plates (Nunc, Roskilde, Denmark) were sensitized with cytokine-specific monoclonal antibodies followed by blocking with PBS containing 2% BSA (Sigma). The sera and recombinant cytokines were then added, and the plates were incubated for 4 h at room temperature. The plates were washed and incubated with 1 μg/mL biotinylated anticytokine monoclonal antibody at 37°C for 2 h followed by washing and incubation with alkaline phosphatase-conjugated streptavidin at 37°C for 2 h. The reaction was developed using disodium-p-nitrophenyl phosphate (Sigma) in diethanolamine buffer. Absorbance was measured at 405 nm in a microplate reader (Bio-Rad, 2550 Reader EIA, CA, USA). The cytokine concentration was calculated using a linear regression analysis of the absorbance values obtained for the recombinant cytokines, and it was expressed as pg/mL. The sensitivity of the tests ranged from 2 to 20 pg/mL.

2.8.1. Flow Cytometry Using a Cytometric Bead Array (CBA). Measurement of the cytokines TNF-α and IL-2 (Th1 cytokines) and IL-4 and IL-5 (Th2 cytokines) in serum samples was performed using the cytometric bead array (CBA) kit (BD Biosciences, USA) according to the manufacturer's instructions. Briefly, 50 μL of bead populations with discrete fluorescence intensities and coated with cytokine-specific capture antibodies was added to 50 μL of mice sera and 50 μL of phycoerythrin-conjugated anti-mouse Th1/Th2 cytokine antibodies. Simultaneously, standards for each cytokine (0–5000 pg/mL) were mixed with cytokine capture beads and the phycoerythrin-conjugated reagent. The vortexed mixtures were incubated for 3 h. Beads were washed and analyzed using flow cytometry (FACSCalibur, BD Biosciences, USA). The quantity (pg/mL) of each cytokine was calculated using CellQuest software (BD Biosciences, USA). Standard curves were derived from the cytokine standards supplied with the kit. The lower limit of detection ranged from 1 to 2.1 pg/mL for different cytokines.

2.9. Parasite DNA Detection in the Blood and in the Heart with Conventional PCR. For parasite DNA isolation from the blood, total blood samples of mice were collected in tubes containing 6 M guanidine HCl with 0.2 M EDTA (pH 8) (V/V). DNA was extracted using the phenol-chloroform-isoamyl alcohol method according to Macedo et al. [34].

For parasite DNA isolation from the heart, half of the hearts excised at the end of the experimental protocol were homogenized, and DNA was extracted by the alkaline lysis method.

PCR specific for *T. cruzi* was performed according to Wincker et al. [35] using the following primers to amplify a fragment of 330 bp: 121 (5′-AAA TAA TGT ACG GG(G/T) GAG ATG CAT GA-3′) and 122 (5′-GGT TCG ATT GGG GTT GGT GTA ATA TA-3′) from a nonvariant region of the kinetoplast DNA minicircles of *T. cruzi*. The cycling conditions were as follows: 95°C for 5 minutes followed by 35

Table 1: Electrocardiogram before treatment with pyridostigmine bromide. Electrocardiographical parameters (expressed as mean ± S.E.M.) collected after five months follow-up in noninoculated control (Con) or *T. cruzi*-inoculated (Chg) anesthetized C57BL/6j mice before treatment with pyridostigmine bromide (Pyrido) or vehicle (NT: nontreated animals).

	Con-NT ($n = 10$)	Con-Pyrido ($n = 12$)	Chg-NT ($n = 13$)	Chg-Pyrido ($n = 17$)
RR (ms)	139.73 ± 5.22	150.83 ± 6.02	139.04 ± 5.62	133.35 ± 4.04
Pd (ms)	13.87 ± 1.50	13.8 ± 1.37	18.56 ± 0.51$^{*\#}$	18.84 ± 0.72$^{*\#}$
PR (ms)	38.83 ± 2.61	38.72 ± 2.28	40.64 ± 0.98	40.17 ± 1.29
QRSd (ms)	14.6 ± 1.86	13.61 ± 1.43	17.53 ± 1.08$^{*\#}$	17.06 ± 1.00$^{*\#}$
QT (ms)	20.74 ± 2.26	17.14 ± 1.60	22.28 ± 0.96$^{*\#}$	21.2 ± 1.01$^{\#}$
cQT ($ms^{1/2}$)	1.74 ± 0.51	1.42 ± 0.50	1.9 ± 0.08$^{*\#}$	1.84 ± 0.09$^{\#}$

RR: RR interval; Pd: P wave duration; PR: PR interval; QRSd: QRS complex duration; QT: QT interval; cQT: corrected QT interval; ms: milliseconds; $^{*}P < 0.05$ versus Con-NT; and $^{\#}P < 0.05$ versus Con-Pyrido.

Table 2: Electrocardiogram after treatment with pyridostigmine bromide. Electrocardiographical parameters (expressed as mean ± S.E.M.) collected at the 6th month of observation and after one month of treatment (from the 5th to 6th month of infection) in noninoculated control (Con) or *T. cruzi*-inoculated (Chg) anesthetized C57BL/6j mice treated with pyridostigmine bromide (Pyrido) or vehicle (NT: nontreated animals).

	Con-NT ($n = 10$)	Con-Pyrido ($n = 12$)	Chg-NT ($n = 10$)	Chg-Pyrido ($n = 17$)
RR (ms)	137.56 ± 3.37	141.05 ± 5.38	152.54 ± 5.01*	152.98 ± 12.93
Pd (ms)	14.01 ± 1.53	13.38 ± 1.51	18.68 ± 0.52$^{*\&\#}$	14.63 ± 0.53
PR (ms)	37.93 ± 1.96	44.38 ± 2.51*	45.45 ± 2.22*	43.2 ± 0.99
QRSd (ms)	14.45 ± 1.39	13.47 ± 1.37	15.04 ± 0.53	14.5 ± 0.41
QT (ms)	17.77 ± 1.87	17.35 ± 1.38	22.47 ± 1.04$^{*\#}$	18.21 ± 0.59
cQT ($ms^{1/2}$)	1.51 ± 0.51	1.49 ± 0.47	1.83 ± 0.09$^{*\&\#}$	1.51 ± 0.06

RR: RR interval; Pd: P wave duration; PR: PR interval; QRSd: QRS complex duration; QT: QT interval; cQT: corrected QT interval; $^{*}P < 0.05$ versus Con-NT; ms: milliseconds; $^{\&}P < 0.05$ versus Chg-Pyrido; and $^{\#}P < 0.05$ versus Con-Pyrido.

cycles at 95°C for 1 minute and 65°C for 1 minute. The products of the reaction were revealed by electrophoresis in a 6.0% polyacrylamide gel and stained with silver nitrate, which was photographed with a digital camera.

2.10. Statistical Analysis. All numerical data are expressed as the means (±S.E.M.), whereas the semiquantitative data from the histological examinations are expressed as the medians and the 25th and 75th percentiles. According to the normality and variance homogeneity of the distribution, a parametric statistic, such as two-way ANOVA followed by Tukey's multiple comparison test, or a nonparametric test, such as the Mann-Whitney test, was performed. Categorical variables were analyzed using the Fisher exact test. All statistical calculations were performed using SigmaStat 2.0.3 software (SPSS Inc., Chicago, IL, USA). The differences were considered significant when $P < 0.05$.

3. Results

Parasite detection in peripheral tail blood samples by the microhematocrit technique performed on the 12th day after infection was positive for all *T. cruzi*-inoculated animals and negative for all control noninfected mice.

Electrocardiographical parameters measured in the first ECG recording (ECG1) at the beginning of the experimental protocol before *T. cruzi* inoculation and treatment did not show any significant difference among all experimental groups, as expected. However, after five months of infection and before the pyridostigmine bromide treatment, chagasic animals (from Chg-NT and Chg-Pyrido groups) presented significant elongations of Pd, QRSd, QT, and cQT (Table 1), indicating a global functional disturbance of heart.

Interestingly, as shown in Table 2, after one month of the pyridostigmine bromide treatment and six months of infection, Chg-Pyrido mice presented a significant reduction in Pd (an atrial parameter) and cQT (a ventricular parameter), suggesting an improvement in the electrical function of the heart. In contrast, in Chg-NT mice, most of the ECG parameters were significantly different compared to Con-NT mice. It is worth noting that, in the Con-Pyrido group, a significant increase in PR was observed, as expected, because pyridostigmine bromide might be increasing vagal neural transmission in the atrioventricular node, with a consequent reduction in the conduction velocity of the action potential. These results suggest that pyridostigmine bromide treatment can be effective in improving electrical disorders induced by chronic chagasic cardiomyopathy.

The results of heart rate variability analysis in time- (variance) and frequency-domain (spectral) parameters are shown in Table 3. A significant reduction in the absolute values of total variability (variance) and the spectral components VLF, LF, and HF was observed in Chg-NT mice compared to Con-NT and Con-Pyrido mice. The LF and HF com-

Table 3: Heart rate variability after treatment with pyridostigmine bromide. Heart rate variability parameters (expressed as mean ± S.E.M.) collected at the 6th month of observation and after one month of treatment (from the 5th to 6th month of infection) in noninoculated control (Con) or *T. cruzi*-inoculated (Chg) freely moving C57BL/6j mice treated with pyridostigmine bromide (Pyrido) or vehicle (NT: nontreated animals).

	Con-NT ($n = 9$)	Con-Pyrido ($n = 9$)	Chg-NT ($n = 9$)	Chg-Pyrido ($n = 12$)
RR (ms)	117.97 ± 3.97	112.67 ± 4.14	104.27 ± 4.32	113.74 ± 4.33
HR (bpm)	516.81 ± 8.35	543.57 ± 9.06	590.61 ± 9.82	539.07 ± 8.76
Variance (ms^2)	218.61 ± 12.35	148.96 ± 9.91	32.13 ± 5.12$^{*\&}$	63.57 ± 6.11
VLF (ms^2)	106.06 ± 8.93	69.37 ± 7.23	11.76 ± 2.84$^{*\&}$	22.60 ± 3.90
LF (ms^2)	57.84 ± 6.28	52.31 ± 6.23	11.10 ± 3.77*	21.99 ± 5.09
LF (nu)	51.83 ± 4.13	56.24 ± 4.09	47.80 ± 4.57	39.25 ± 4.91
HF (ms^2)	54.71 ± 6.86	27.19 ± 4.44	9.01 ± 3.19$^{*\&}$	18.78 ± 3.53
HF (nu)	47.54 ± 4.11	41.80 ± 3.97	48.05 ± 4.49	58.70 ± 4.86
LF/HF	2.31 ± 1.53	4.04 ± 1.48	2.60 ± 1.54	2.92 ± 2.01

RR: RR interval; HR: heart rate; VLF: very low frequency spectral component; LF: low frequency spectral component; HF: high frequency spectral component; ms: milliseconds; bpm: beats per minute; nu: normalized units; $^{*}P < 0.05$ versus Con-NT; and $^{\&}P < 0.05$ versus Chg-Pyrido.

ponents expressed in normalized units and the LF/HF ratio were not different from Con-NT mice. In contrast, chagasic mice treated with pyridostigmine bromide (the Chg-Pyrido group) presented values of variance and VLF and HF spectral components that were significantly higher compared to Chg-NT mice, suggesting an improvement of some autonomic parameters that changed during chronic chagasic cardiomyopathy (Table 3).

The autonomic dysfunction observed in the heart rate variability analysis of Chg-NT mice and its improvement in Chg-Pyrido mice was confirmed by pharmacological autonomic blockade with atropine sulfate or propranolol. The use of these autonomic blockers showed that vagal parasympathetic effects significantly decreased without a change in sympathetic effects in Chg-NT mice compared with Con-NT mice (Figure 1). Chagasic mice treated with pyridostigmine bromide showed values of vagal parasympathetic effects that were significantly higher compared to Chg-NT mice and similar to those found in Con-NT mice (Figure 1). Additionally, noninfected control mice treated with pyridostigmine bromide showed vagal parasympathetic effects that markedly increased without any changes in sympathetic effects compared with Con-NT mice (Figure 1). No changes in the intrinsic pacemaker heart rate (IHR) were found in any of the experimental groups after the six-month observation period.

The relative cardiac weight of Chg-NT mice was significantly higher than that observed in the other groups (Figure 2), indicating that cardiac hypertrophy was induced by Chagas disease in mice and that pyridostigmine bromide treatment was able to reverse or impair the development of cardiac hypertrophy in chagasic mice.

A semiquantitative examination of cardiac inflammatory infiltration indicated discrete to mild diffuse myocarditis (average inflammatory score was equal to 0.5, $P25\% = 0.5$, and $P75\% = 0.5$, $P < 0.0001$ versus Con-NT), which was observed in the atria (Figures 3(g) and 3(h)), the ventricles (Figures 3(e) and 3(f)), and the neural ganglia (Figure 3(g)) in the CHG-NT mice in comparison to normal CON-NT mice (Figures 3(a), 3(b), 3(c), and 3(d)), which presented no inflammatory infiltration (average inflammatory score was equal to 0.0, $P25\% = 0.0$ and $P75\% = 0.0$). In Chg-Pyrido mice, reduced inflammatory infiltration, which was categorized as very discrete to discrete (average inflammatory score was equal to 0.125, $P25\% = 0.0$, and $P75\% = 0.25$, $P < 0.001$ versus Chg-NT), was observed in the atria, the ventricles (Figures 3(i), 3(j), 3(k), and 3(l)), and the neural ganglia. As expected in this mouse model of chronic Chagas disease, no amastigote nests in the myocardium were found in either Chg-NT or Chg-Pyrido mice.

In different sections of the heart stained by Picrosirius Red, the morphometry of fibrosis revealed a marked and diffuse increase in the fibrotic area in both absolute (μm^2) and relative (%) values in the Chg-NT group compared to Chg-NT mice (Figure 4). Interestingly, Chg-Pyrido mice presented significantly reduced fibrotic areas in all cardiac chambers (Figure 4) compared to Chg-NT mice. Despite these reduced values, the fibrotic areas were still larger than those found in Con-NT mice (Figure 4).

The serum levels of the cytokines IL-2, IL-4, IL-5, and TNF-α, measured with the CBA technique, did not reveal any change in any of the experimental groups. In fact, the serum levels of IL-2 and IL-4 were undetectable, with values near 0 pg/mL. However, using the ELISA technique, serum levels of IFN-γ were significantly higher in Chg-NT mice compared to Chg-Pyrido mice ($P < 0.05$). No IFN-γ was detected in Con-NT mice. Serum levels of IL-10, measured with ELISA technique, were significantly higher in both Chg-NT and Chg-Pyrido mice compared to Con-NT mice ($P < 0.05$). No differences were found in the serum IL-10 levels between Chg-NT and Chg-Pyrido mice (Figure 5).

The immunohistochemical technique using peroxidase to label *T. cruzi* parasite nests or antigens revealed a complete absence of parasites in control noninfected mice, whereas *T. cruzi* labeling was positive for 62.50% of Chg-NT and 81.81% of Chg-Pyrido mice ($P = 0.603$, not significant using the Fisher exact test). The parasite antigens were diffusely distributed throughout the heart tissue (Figure 6).

Using a conventional PCR method to detect parasite DNA in blood and heart during the chronic phase of Chagas disease

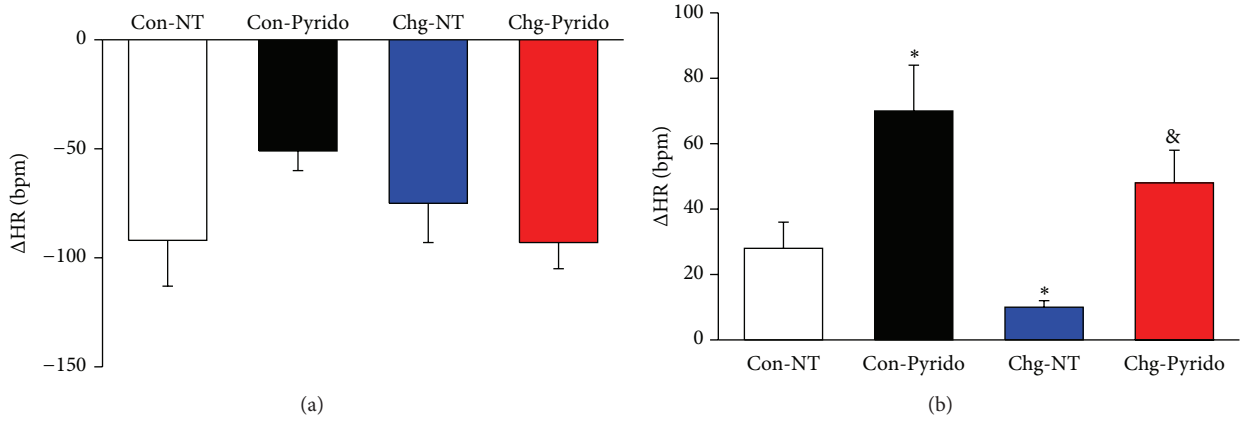

Figure 1: Heart rate responses to pharmacological autonomic blockade. Heart rate responses (ΔHR) to propranolol (sympathetic effect) (Panel (a)) or to atropine sulfate (vagal parasympathetic effect) (Panel (b)) expressed as mean ± S.E.M. and measured at the 6th month of observation and after one month of treatment (from the 5th to 6th month of infection) in noninoculated control (Con) or in *T. cruzi*-inoculated (Chg) freely moving C57BL/6j mice treated with pyridostigmine bromide (Pyrido) or vehicle (NT: nontreated animals). ($^{*}P < 0.05$ versus Con-NT; $^{\&}P < 0.05$ versus Chg-NT).

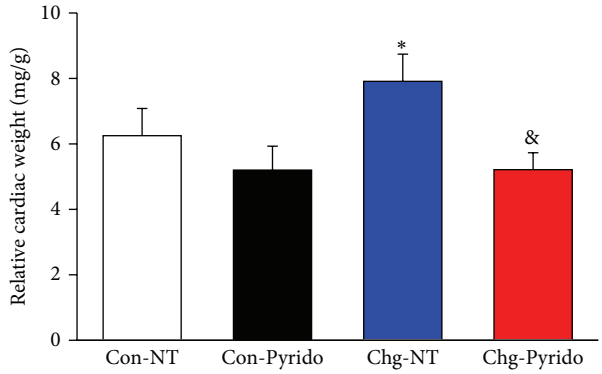

Figure 2: Relative cardiac weights after treatment with pyridostigmine bromide. Relative cardiac weights (in mg/g) expressed as mean ± S.E.M. calculated at the 6th month of observation and after one month of treatment (from the 5th to 6th month of infection) in noninoculated control (Con) or in *T. cruzi*-inoculated (Chg) C57BL/6j mice treated with pyridostigmine bromide (Pyrido) or vehicle (NT: non treated animals). ($^{*}P < 0.05$ versus Con-NT and $^{\&}P < 0.05$ versus Chg-NT).

in mice, a complete absence of parasite DNA in noninfected control mice was observed, whereas *T. cruzi* DNA was found in 16.67% and 42.9% ($P = 0.559$) in the blood of Chg-NT and Chg-Pyrido mice, respectively, and in 72.73% and 86.67% ($P = 0.614$) of heart samples from Chg-NT and Chg-Pyrido mice, respectively.

4. Discussion

To our knowledge, the present study is the first to analyze the effects of the deliberate potentiation of cholinergic signaling using pyridostigmine bromide, an anticholinesterase agent, during the chronic phase of experimental Chagas disease in mice. Furthermore, this study evaluated the effects of pyridostigmine bromide treatment on electrocardiographic, autonomic, histopathological, immunoinflammatory, and parasitological parameters of Chagas disease.

The present study is, to our knowledge, the first to demonstrate autonomic dysfunction induced by chronic Chagas disease in an experimental mouse model. This dysfunction was characterized by a marked reduction in heart rate variability, with reduced variance (time-domain parameter) and the VLF, LF, and HF components (frequency-domain parameters) of heart rate variability, as well as a concurrent reduction in the cardiac vagal effect, without an apparent change in sympathetic effects, as measured by pharmacological blockade in chronic control chagasic animals. Only morphological reports describing the ganglia and nerve lesions in chagasic mice have been published in the literature [36]. This finding follows our previous report of a similar autonomic dysfunction in mice with acute Chagas disease [18]. This autonomic dysfunction was accompanied by electrocardiographic changes associated with mild diffuse inflammatory infiltration of mononuclear cells as well as fibrosis and hypertrophy in the atrial and ventricular myocardium and the elevation of IFN-γ and IL-10 in the blood serum of wild-type and untreated chagasic C57BL/6j mice, which confirms the presence of chronic myocarditis six months following infection with *T. cruzi*. This increase in serum levels of IFN-γ and IL-10 in chronic chagasic mice matches similar previous reports in human beings [37–39]. Additionally, parasite antigens and DNA were detected by immunohistochemical labeling in the heart and by PCR in blood and heart, respectively, reinforcing the role played by parasites in inducing and/or maintaining chronic infection. Because our findings are consistent with previous observations in hamsters, rabbits, dogs, and humans during the chronic phase of Chagas disease [10, 40], the mouse model used here appears to represent a suitable tool for future experimental studies in Chagas heart disease.

During the chronic phase of Chagas heart disease, this report revealed a significant increase in cardiac vagal parasympathetic autonomic modulation associated with a significant reduction of inflammatory infiltration in the myocardium of infected mice treated with pyridostigmine bromide during the last month of a six-month observation period.

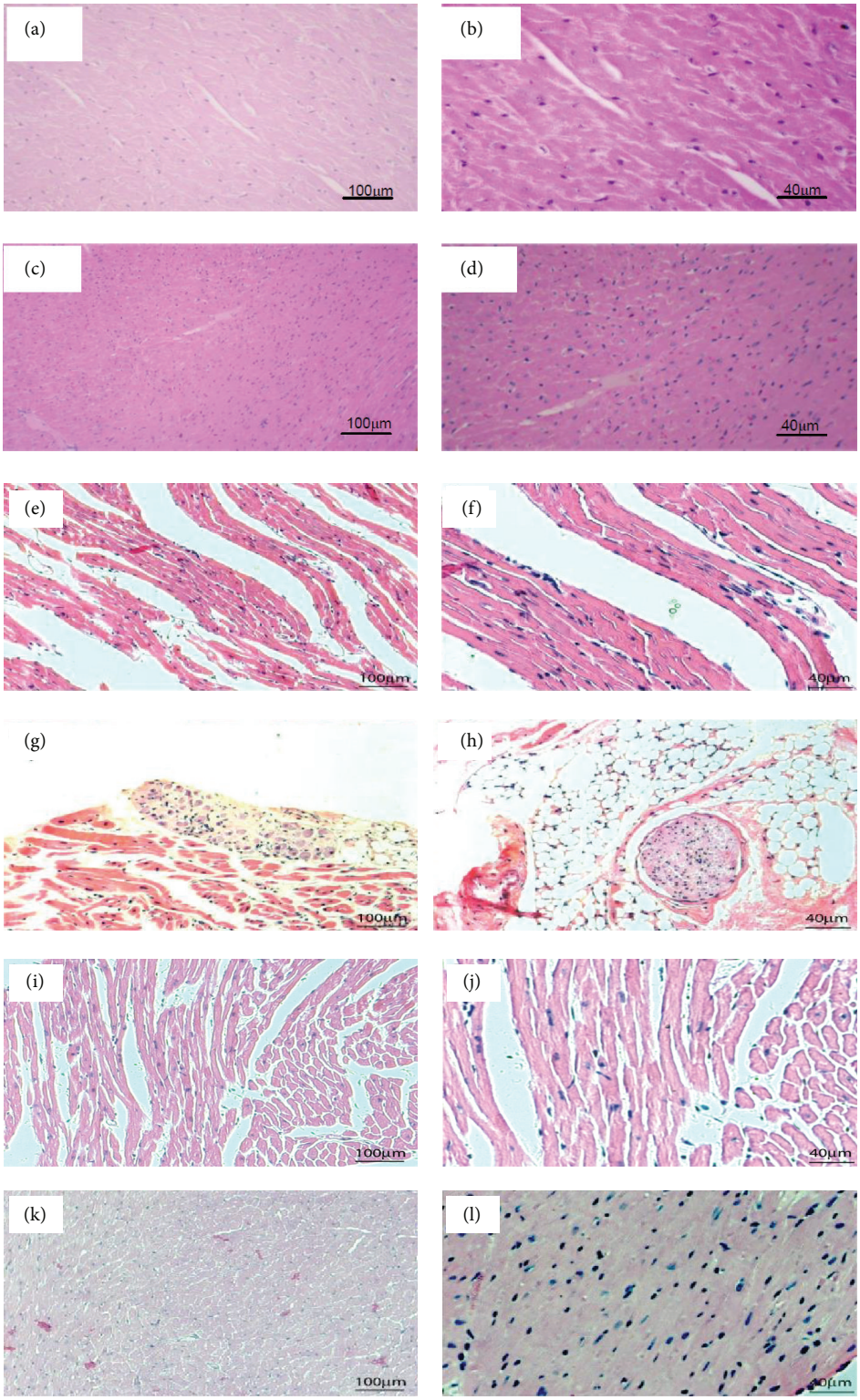

Figure 3: Cardiac histopathology after treatment with pyridostigmine bromide. Photomicrographs of cardiac sections stained with H-E. Panels (a) and (b): ventricular sections from a control nontreated mouse. Panels (c) and (d): ventricular sections from a pyridostigmine bromide-treated control mouse. Panels (e) and (f): ventricular sections from a chagasic nontreated mouse. Panels (g) and (h): atrial sections from a nontreated chagasic mouse showing, respectively, a ganglionitis and neuritis focus. Panels (i), (j), (k), and (l): different ventricular sections from a chagasic mouse treated with pyridostigmine bromide. Note the lower inflammatory infiltration into heart tissues from a chagasic mouse treated with pyridostigmine bromide. (Left panels: magnification = 100x; right panels: magnification = 200x.)

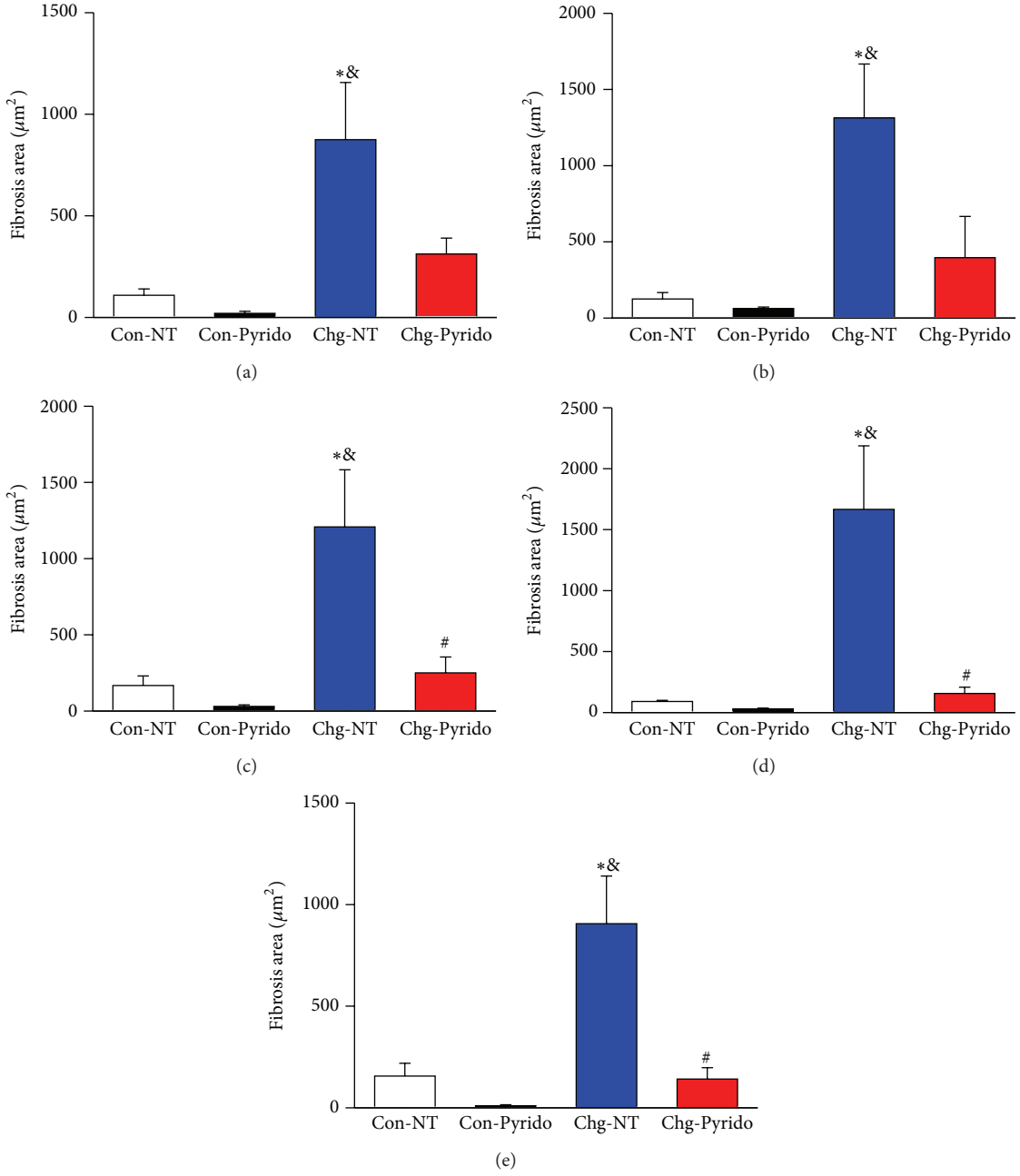

Figure 4: Cardiac fibrosis after treatment with pyridostigmine bromide. Fibrotic areas (in μm^2) expressed as mean ± S.E.M. for the right (Panel (a)) and left (Panel (b)) atria, the right (Panel (c)) and left (Panel (d)) ventricles, and the atrioventricular septum (Panel (e)), measured after Picrosirius Red staining at the 6th month of observation and after one month of treatment (from the 5th to 6th month of infection) in noninoculated control (Con) or in *T. cruzi*-inoculated (Chg) C57BL/6j mice treated with pyridostigmine bromide (Pyrido) or vehicle (NT: nontreated animals). ($^*P < 0.05$ versus Con-NT; $^\&P < 0.05$ versus Chg-Pyrido; and $^\#P < 0.05$ versus Con-Pyrido).

Because pyridostigmine bromide is an anticholinesterasic agent, which increases the bioavailability of acetylcholine in the synaptic varicosities, the increase in cardiac vagal parasympathetic autonomic function, demonstrated by the higher heart rate variability and cardiac vagal effect, was expected and was verified after treatment. This vagal stimulation effect of pyridostigmine bromide confirms previous reports in other experimental contexts [41].

The anti-inflammatory effect of pyridostigmine bromide was associated with a marked reduction of myocardial fibrosis and hypertrophy. Serum levels of IFN-γ also decreased, whereas TNA-α trended to decrease, both of which are Th1 proinflammatory cytokines, without any change in the augmented serum levels of IL-10.

The combined analysis of these results suggests that pyridostigmine bromide may act on the heart, at least partially

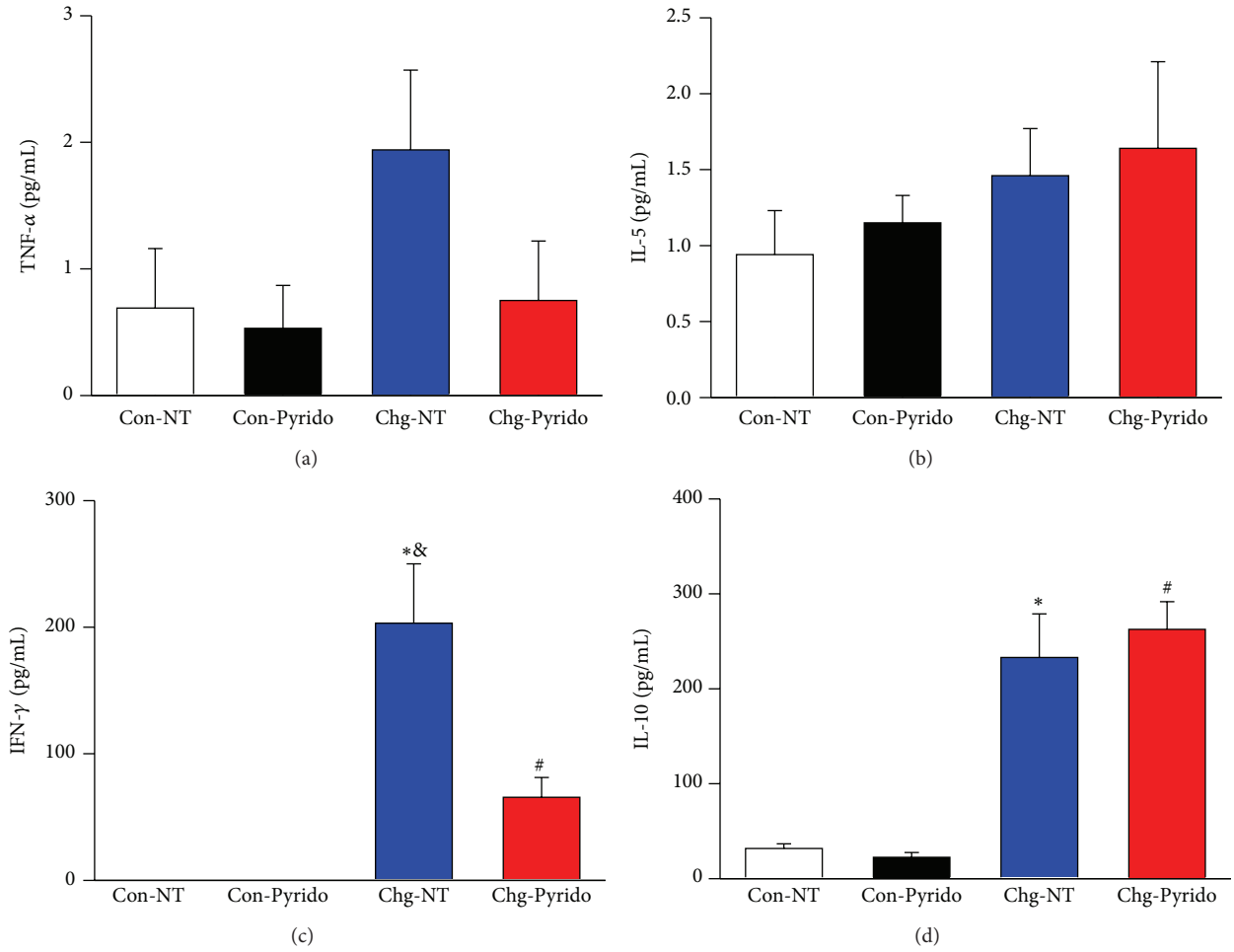

Figure 5: Serum cytokines after treatment with pyridostigmine bromide. Serum levels (in pg/mL) expressed as mean ± S.E.M. of tumor necrosis factor-α (TNF-α: Panel (a)), interleukin-5 (IL-5: Panel (b)) measured by the cytometric bead array technique, interferon-γ (IFN-γ: Panel (c)), and interleukin-10 (IL-10: Panel (d)) measured by ELISA at the 6th month of observation and after one month of treatment (from the 5th to 6th month of infection) in noninoculated control (Con) or *T. cruzi*-inoculated (Chg) C57BL/6j mice treated or not (NT) with pyridostigmine bromide (Pyrido). ($^{*}P < 0.05$ versus Con-NT; $^{\&}P < 0.05$ versus Chg-Pyrido; and $^{\#}P < 0.05$ versus Con-Pyrido).

increasing the vagal parasympathetic activity, via the accumulation of acetylcholine in the myocardium. This accumulation was confirmed by improvements in heart rate variability and vagal parasympathetic effect, which, acting on immune cells, may exert immunomodulatory effects, thereby shifting the immune response toward the predominance of an anti-inflammatory response.

These new findings in the chronic Chagas disease context reinforce the idea of an intimate interplay between the immune and autonomic nervous systems and the potential use of parasympathetic stimulation to treat chagasic myocarditis [18, 23]. Additionally, the improvement of cardiac inflammation, fibrosis, and hypertrophy in pyridostigmine bromide-treated chronic chagasic animals suggests that the decrease of vagal autonomic function due to ganglionic neuronal lesions and denervation, which occur precociously during the acute phase, may play an important immunomodulatory role in the increased Th1 immune response and inflammatory infiltration, as verified during the chronic phase of the disease.

Even though our results support the immunomodulatory role played by the cholinergic vagal parasympathetic nervous system in the heart, we cannot rule out a possible role of pyridostigmine bromide in increasing local acetylcholine levels via its release from nonneural local structures, such as endothelial cells, cholinergic lymphocytes, and cardiomyocytes [42]. In fact, these nonneural sources of acetylcholine, potentiated by pyridostigmine bromide treatment, may explain the substantial improvement in ECG abnormalities, inflammation, fibrosis, and hypertrophy observed in both ventricles of the heart, which are poorly innervated by vagal parasympathetic fibers.

Data from the immunohistochemical labeling of *T. cruzi* antigens and *T. cruzi* DNA detection by PCR showed that parasites are present in the heart tissue and blood of the chagasic mice six months after infection, confirming previous reports [38, 43]. The number of animals positive for parasite antigens or DNA did not differ between pyridostigmine bromide-treated and nontreated chagasic animals. The persistence of the parasite in the chronic phase, even at a very

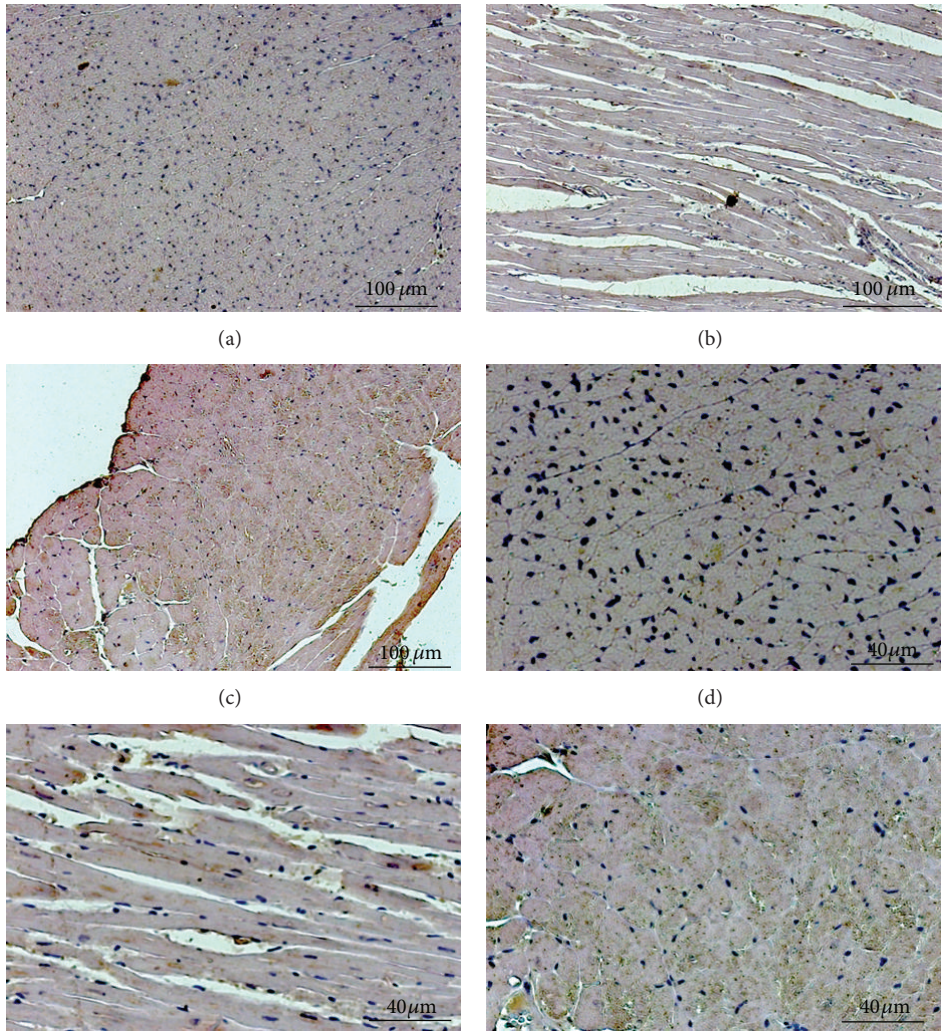

Figure 6: Immunohistochemistry for parasite antigens. Photomicrographs from left ventricular sections stained with *T. cruzi* antigens by peroxidase reaction. Panels (a) and (d): control nontreated mouse. Panels (b) and (e): chagasic nontreated mouse. Panels (c) and (f): chagasic mouse treated with pyridostigmine bromide. Top panels: magnification = 100x; bottom panels: magnification = 200x. Note the gray color labeling *T. cruzi* antigens throughout the sections in Panels (b), (c), (e), and (f).

low level, seems to play an important role in the pathogenesis of chronic Chagas disease because the low parasite load may continuously stimulate an immune response [38, 43]. Although antigens or DNA from *T. cruzi* were detected in the present study, no parasite pseudocysts or amastigote forms were observed in the heart tissue in either treated or nontreated chagasic mice. This lack of entire parasites at the site of cardiac lesions suggests the possibility of a remote niche for the parasites, such as smooth muscle cells, adipocytes, or skeletal muscle cells [43].

In conclusion, our results support the notion that autonomic dysfunction is a primary cause of the pro-/anti-inflammatory imbalance observed in inflammatory diseases, favoring the shift of immune response toward the predominance of proinflammatory response, thereby contributing to the pathogenesis of these diseases in general and Chagas heart disease in particular. Additionally, our findings showed the potential beneficial effects of anticholinesterasic agents, particularly pyridostigmine bromide, in increasing cardiac autonomic modulation and reducing inflammatory response to the heart.

Conflict of Interests

The authors declare no conflicts of Interests.

Authors' Contribution

Marilia Beatriz de Cuba and Marcus Paulo Ribeiro Machado equally contributed to this study.

Acknowledgments

This study was supported by the Ministero dell'Istruzione, Universita' e della Ricerca Scientifica PRIN 2007 Grant to

Nicola Montano and a Research Fellowship Grant (Proc. number 308016/2009-2) from the Conselho Nacional de Desenvolvimento Cientifico e Technologico (CNPq)-Brazil to Valdo Jose Dias da Silva.

References

[1] C. J. Chagas, "American trypanosomiasis," *Memórias do Instituto Oswaldo Cruz*, vol. 3, pp. 219–275, 1911.

[2] A. Prata, "Clinical and epidemiological aspects of Chagas disease," *The Lancet Infectious Diseases*, vol. 1, no. 2, pp. 92–100, 2001.

[3] J. R. Coura and P. A. Vīas, "Chagas disease: a new worldwide challenge," *Nature*, vol. 465, no. 7301, pp. S6–S7, 2010.

[4] J. A. Marin-Neto, E. Cunha-Neto, B. C. Maciel, and M. V. Simões, "Pathogenesis of chronic Chagas heart disease," *Circulation*, vol. 115, no. 9, pp. 1109–1123, 2007.

[5] S. A. Morris, H. B. Tanowitz, M. Wittner, and J. P. Bilezikian, "Pathophysiological insights into the cardiomyopathy of Chagas' disease," *Circulation*, vol. 82, no. 6, pp. 1900–1909, 1990.

[6] M. J. M. Alves and R. A. Mortara, "A century of research: What have we learned about the interaction of *Trypanosoma cruzi* with host cells?" *Memorias do Instituto Oswaldo Cruz*, vol. 104, supplement 1, pp. 76–88, 2009.

[7] C. A. Hunter, L. A. Ellis-Neyes, T. Slifer et al., "IL-10 is required to prevent immune hyperactivity during infection with *Trypanosoma cruzi*," *The Journal of Immunology*, vol. 158, no. 7, pp. 3311–3316, 1997.

[8] A. R. L. Teixeira, M. M. Hecht, M. C. Guimaro, A. O. Sousa, and N. Nitz, "Pathogenesis of Chagas' disease: parasite persistence and autoimmunity," *Clinical Microbiology Reviews*, vol. 24, no. 3, pp. 592–630, 2011.

[9] L. E. Ramirez, E. Lages-Silva, J. M. Soares Jr., and E. Chapadeiro, "Experimental hamster infection by *Trypanosoma cruzi*: the chronic phase," *Revista da Sociedade Brásileira de Medicina Tropical*, vol. 26, no. 4, pp. 253–254, 1993.

[10] V. J. D. da Silva, M. P. R. Machado, A. M. Rocha, R. M. Padilha, and L. E. Ramirez, "Analysis of cardiac autonomic function in hamsters with Chagas disease," *Revista da Sociedade Brasileira de Medicina Tropical*, vol. 36, supplement 2, pp. 11–12, 2003.

[11] A. R. Pérez, S. D. Silva-Barbosa, L. R. Berbert et al., "Immunoneuroendocrine alterations in patients with progressive forms of chronic Chagas disease," *Journal of Neuroimmunology*, vol. 235, no. 1-2, pp. 84–90, 2011.

[12] R. E. Kleiger, J. P. Miller, J. T. Bigger Jr., and A. J. Moss, "Decreased heart rate variability and its association with increased mortality after acute myocardial infarction," *The American Journal of Cardiology*, vol. 59, no. 4, pp. 256–262, 1987.

[13] A. Hamaad, M. Sosin, A. D. Blann, J. Patel, G. Y. H. Lip, and R. J. MacFadyen, "Markers of inflammation in acute coronary syndromes: association with increased heart rate and reductions in heart rate variability," *Clinical Cardiology*, vol. 28, no. 12, pp. 570–576, 2005.

[14] P. J. Hauptman, P. J. Schwartz, M. R. Gold et al., "Rationale and study design of the INcrease of Vagal TonE in Heart Failure study: INOVATE-HF," *The American Heart Journal*, vol. 163, no. 6, pp. 954–962, 2012.

[15] V. Papaioannou, I. Pneumatikos, and N. Maglaveras, "Association of heart rate variability and inflammatory response in patients with cardiovascular diseases: current strengths and limitations," *Front Physiol*, vol. 4, article 174, 2013.

[16] D. J. van Westerloo, I. A. J. Giebelen, S. Florquin et al., "The cholinergic anti-inflammatory pathway regulates the host response during septic peritonitis," *Journal of Infectious Diseases*, vol. 191, no. 12, pp. 2138–2148, 2005.

[17] K. J. Tracey, "Reflex control of immunity," *Nature Reviews Immunology*, vol. 9, no. 6, pp. 418–428, 2009.

[18] M. P. R. Machado, A. M. Rocha, L. F. de Oliveira et al., "Autonomic nervous system modulation affects the inflammatory immune response in mice with acute Chagas disease," *Experimental Physiology*, vol. 97, no. 11, pp. 1186–1202, 2012.

[19] V. M. Sanders, "The role of norepinephrine and beta-2-adrenergic receptor stimulation in the modulation of TH1, TH2, and B lymphocyte function," *Advances in Experimental Medicine and Biology*, vol. 437, pp. 269–278, 1998.

[20] I. J. Elenkov and G. P. Chrousos, "Stress hormones, Th1/Th2 patterns, pro/anti-inflammatory cytokines and susceptibility to disease," *Trends in Endocrinology and Metabolism*, vol. 10, no. 9, pp. 359–368, 1999.

[21] L. V. Borovikova, S. Ivanova, M. Zhang et al., "Vagus nerve stimulation attenuates the systemic inflammatory response to endotoxin," *Nature*, vol. 405, no. 6785, pp. 458–462, 2000.

[22] E. E. Benarroch, "Autonomic-mediated immunomodulation and potential clinical relevance," *Neurology*, vol. 73, no. 3, pp. 236–242, 2009.

[23] M. P. R. Machado and V. J. D. da Silva, "Autonomic neuroimmunomodulation in chagasic cardiomyopathy," *Experimental Physiology*, vol. 97, no. 11, pp. 1151–1160, 2012.

[24] M. Li, C. Zheng, T. Sato, T. Kawada, M. Sugimachi, and K. Sunagawa, "Vagal nerve stimulation markedly improves long-term survival after chronic heart failure in rats," *Circulation*, vol. 109, no. 1, pp. 120–124, 2004.

[25] Y. Okazaki, C. Zheng, M. Li, and M. Sugimachi, "Effect of the cholinesterase inhibitor donepezil on cardiac remodeling and autonomic balance in rats with heart failure," *The Journal of Physiological Sciences*, vol. 60, no. 1, pp. 67–74, 2010.

[26] S. M. Serra, R. V. Costa, R. R. Teixeira de Castro, S. S. Xavier, and A. C. Lucas da Nóbrega, "Cholinergic stimulation improves autonomic and hemodynamic profile during dynamic exercise in patients with heart failure," *Journal of Cardiac Failure*, vol. 15, no. 2, pp. 124–129, 2009.

[27] L. I. Zimerman, A. Liberman, R. R. T. Castro, J. P. Ribeiro, and A. C. L. Nóbrega, "Acute electrophysiologic consequences of pyridostigmine inhibition of cholinesterase in humans," *Brazilian Journal of Medical and Biological Research*, vol. 43, no. 2, pp. 211–216, 2010.

[28] R. R. T. Castro, G. Porphirio, S. M. Serra, and A. C. L. Nóbrega, "Cholinergic stimulation with pyridostigmine protects against exercise induced myocardial ischaemia," *Heart*, vol. 90, no. 10, pp. 1119–1123, 2004.

[29] R. R. T. Castro, S. M. Serra, G. Porphirio, F. S. N. S. Mendes, L. P. J. Oliveira, and A. C. L. Nóbrega, "Pyridostigmine reduces QTc interval during recovery from maximal exercise in ischemic heart disease," *International Journal of Cardiology*, vol. 107, no. 1, pp. 138–139, 2006.

[30] Z. Brener, "Therapeutic activity and criterion of cure on mice experimentally infected with Trypanosoma cruzi," *Revista do Instituto de Medicina Tropical de São Paulo*, vol. 4, pp. 389–396, 1962.

[31] Task Force of the European Society of Cardiology and the North American Society of Pacing and Electrophysiology, "Heart rate variability: standards of measurement, physiological

interpretation and clinical use," *Circulation*, vol. 93, pp. 1043–1065, 1996.

[32] N. Montano, A. Porta, C. Cogliati et al., "Heart rate variability explored in the frequency domain: a tool to investigate the link between heart and behavior," *Neuroscience and Biobehavioral Reviews*, vol. 33, no. 2, pp. 71–80, 2009.

[33] E. Chapadeiro, P. S. Beraldo, P. C. Jesus, W. P. Oliveira Júnior, and L. F. Junqueira Júnior, "Cardiac lesions in Wistar rats inoculated with various strains of *Trypanosoma cruzi*," *Revista da Sociedade Brasileira de Medicina Tropical*, vol. 21, no. 3, pp. 95–103, 1988.

[34] A. M. Macedo, M. S. Martins, E. Chiari, and S. D. J. Pena, "DNA fingerprinting of *Trypanosoma cruzi*: a new tool for characterization of strains and clones," *Molecular and Biochemical Parasitology*, vol. 55, no. 1-2, pp. 147–153, 1992.

[35] P. Wincker, M. Bosseno, C. Britto et al., "High correlation between Chagas' disease serology and PCR-based detection of *Trypanosoma cruzi* kinetoplast DNA in Bolivian children living in an endemic area," *FEMS Microbiology Letters*, vol. 124, no. 3, pp. 419–423, 1994.

[36] L. C. V. Ribeiro, A. A. Barbosa Jr., and Z. A. Andrade, "Pathology of intracardiac nerves in experimental chagas disease," *Memorias do Instituto Oswaldo Cruz*, vol. 97, no. 7, pp. 1019–1025, 2002.

[37] R. C. Ferreira, B. M. Ianni, L. C. J. Abel et al., "Increased plasma levels of tumor necrosis factor-alpha in asymptomatic/"indeterminate" and Chagas disease cardiomyopathy patients," *Memorias do Instituto Oswaldo Cruz*, vol. 98, no. 3, pp. 407–411, 2003.

[38] F. R. S. Gutierrez, P. M. M. Guedes, R. T. Gazzinelli, and J. S. Silva, "The role of parasite persistence in pathogenesis of chagas heart disease," *Parasite Immunology*, vol. 31, no. 11, pp. 673–685, 2009.

[39] A. S. de Melo, V. M. B. de Lorena, S. C. de Moura Braz, C. Docena, and Y. de Miranda Gomes, "IL-10 and IFN-γ gene expression in chronic Chagas disease patients after in vitro stimulation with recombinant antigens of *Trypanosoma cruzi*," *Cytokine*, vol. 58, no. 2, pp. 207–212, 2012.

[40] M. B. Soares and R. R. dos Santos, "Immunopathology of cardiomyopathy in the experimental Chagas disease," *Memórias do Instituto Oswaldo Cruz*, vol. 94, supplement 1, pp. 257–262, 1999.

[41] R. N. de la Fuente, B. Rodrigues, I. C. Moraes-Silva et al., "Cholinergic stimulation with pyridostigmine improves autonomic function in infarcted rats," *Clinical and Experimental Pharmacology and Physiology*, vol. 40, no. 9, pp. 610–616, 2013.

[42] C. Rocha-Resende, A. Roy, R. Resende et al., "Non-neuronal cholinergic machinery present in cardiomyocytes offsets hypertrophic signals," *Journal of Molecular and Cellular Cardiology*, vol. 53, no. 2, pp. 206–216, 2012.

[43] F. Nagajyothi, F. S. Machado, B. A. Burleigh et al., "Mechanisms of Trypanosoma cruzi persistence in Chagas disease," *Cellular Microbiology*, vol. 14, no. 5, pp. 634–643, 2012.

Hindawi Publishing Corporation
Mediators of Inflammation
Volume 2014, Article ID 683230, 11 pages
http://dx.doi.org/10.1155/2014/683230

Review Article

Chagas Disease Cardiomyopathy: Immunopathology and Genetics

Edecio Cunha-Neto[1,2,3] and Christophe Chevillard[4]

[1] *Heart Institute (InCor), University of São Paulo School of Medicine, Avenida Dr. Enéas de Carvalho Aguiar, 44 Bloco 2 9° Andar, 05406-000 São Paulo, SP, Brazil*
[2] *Institute for Investigation in Immunology (iii), INCT, São Paulo, SP, Brazil*
[3] *Division of Clinical Immunology and Allergy, University of São Paulo School of Medicine, 05406-000 São Paulo, SP, Brazil*
[4] *Aix-Marseille Université, INSERM, GIMP UMR_S906, 13385 Marseille, France*

Correspondence should be addressed to Edecio Cunha-Neto; edecunha@gmail.com

Received 11 June 2014; Revised 5 August 2014; Accepted 5 August 2014; Published 19 August 2014

Academic Editor: Marcelo T. Bozza

Chagas disease, caused by the protozoan *Trypanosoma cruzi*, is endemic in Latin America and affects ca. 10 million people worldwide. About 30% of Chagas disease patients develop chronic Chagas disease cardiomyopathy (CCC), a particularly lethal inflammatory cardiomyopathy that occurs decades after the initial infection, while most patients remain asymptomatic. Mortality rate is higher than that of noninflammatory cardiomyopathy. CCC heart lesions present a Th1 T-cell-rich myocarditis, with cardiomyocyte hypertrophy and prominent fibrosis. Data suggest that the myocarditis plays a major pathogenetic role in disease progression. Major unmet goals include the thorough understanding of disease pathogenesis and therapeutic targets and identification of prognostic genetic factors. Chagas disease thus remains a neglected disease, with no vaccines or antiparasitic drugs proven efficient in chronically infected adults, when most patients are diagnosed. Both familial aggregation of CCC cases and the fact that only 30% of infected patients develop CCC suggest there might be a genetic component to disease susceptibility. Moreover, previous case-control studies have identified some genes associated to human susceptibility to CCC. In this paper, we will review the immunopathogenesis and genetics of Chagas disease, highlighting studies that shed light on the differential progression of Chagas disease patients to CCC.

1. Introduction

Chagas disease (American trypanosomiasis) is caused by the protozoan parasite *Trypanosoma cruzi* and transmitted by the reduviid bug (called "barbeiro" in Brazil) in the poor, rural endemic areas of Latin America. The disease was discovered in 1909 by the Brazilian physician Carlos Chagas. Unfortunately, Chagas disease remains a neglected disease and a contemporary public health concern, with no vaccines available so far and only few antiparasitic drugs only proven efficient for treating the acute phase of the disease—but none has yet been shown to be effective in chronically infected adults, the stage when the great majority of patients are diagnosed. Approximately 8 million people are infected with *T. cruzi* in Central and South America [1]. At least 120 million are at risk from Chagas disease [2]. Chagas disease is a major cause of heart disease and cardiovascular-related deaths in endemic areas located in Latin America and causes significant economical burden in affected countries. Approximately 12,000 deaths attributable to Chagas disease occur annually, typically due to severe chronic Chagas disease cardiomyopathy (CCC) [1], which develops in ca. 30% of infected individuals decades after infection. The only available treatment for end-stage CCC patients is heart transplantation, a high-cost, high complexity intervention which is not available in a timely fashion for the majority of patients [3]. Chagas disease is now a global health issue. Thirteen million persons have migrated from endemic countries to the United States, and it is estimated that 0.3–1 million of which have chronic *T. cruzi* infection [4];

the European Community has also received large numbers of migrant from endemic areas. The World Health Organization estimates that 56 thousand new cases of Chagas disease occur every year [1, 3].

2. Natural History and Pathogenesis

The natural history of Chagas disease includes an acute and a chronic phase. The high parasite load typical of acute *T. cruzi* infection is dampened by the immune response into a low-grade chronic persistent infection [5]. CCC is an inflammatory cardiomyopathy that affects approximately 30% of infected individuals and occurs 5–30 years after acute infection, while the remaining patients develop digestive disorders (5–10%) or remain asymptomatic and free from cardiac or digestive disorders, (60–70%) the indeterminate phase (ASY). Approximately 1/3 of the CCC patients (or 10% of infected patients) develop a particularly lethal form of dilated cardiomyopathy (severe end-stage CCC) with ventricular dysfunction, heart failure, and arrhythmia. Clinical severity is correlated with the occurrence of myocarditis. ASY patients display minimal myocardial inflammation while patients with severe, end-stage CCC display frequent and intense myocarditis; moderate CCC patients display an intermediate level of myocarditis [6]. Our group has found a positive correlation between the cellularity of the infiltrate and degree of ventricular dilation in the Syrian hamster model of dilated Chagas disease cardiomyopathy with chronic *T. cruzi* infection ([7, 8] and data not shown). Survival in severe CCC is significantly shorter than clinically similar cardiomyopathies of noninflamammatory etiology, like idiopathic dilated cardiomyopathy (DCM) [9, 10]. Taken together, current literature suggests that myocarditis plays a major role in cardiomyocyte destruction, fibrosis, and disease progression [6, 11].

Histologically, CCC myocardium displays a diffuse myocarditis with foci of inflammatory infiltrate and heart fiber damage, prominent fibrosis, and scarcity of *T. cruzi* parasites (reviewed in [12]). The inflammatory infiltrate of CCC heart lesions is composed mainly of T cells displaying a Th1-type cytokine profile (2 : 1 ratio of CD8+/CD4+ T cell ratio) and macrophages [11, 13–17]. The list of cytokines and chemokines found to be increased in CCC is in Table 1. Chronic myocardial inflammation in CCC may be secondary to recognition of either *T. cruzi* antigen/DNA deposited/detected in hearts of both CCC and ASY patients [18] or myocardial antigens. Our group has identified both *T. cruzi*-specific [19] and *T. cruzi*-cross-reactive cardiac-myosin-specific T cells [20] in the myocardial inflammatory infiltrate, thus reactive to antigens that can be found in hearts of all Chagas disease patients.

3. Immunological Dynamics during the Acute and Chronic Phases of *T. cruzi* Infection

Shortly after the acute infection starts, *T. cruzi* components, including its DNA and membrane glycoconjugates, trigger innate immunity via Toll-like receptors in macrophages and dendritic cells, among other cell types [21]. Upon activation, such cells secrete proinflammatory cytokines and chemokines, express costimulatory receptors, and increase endocytosis and intracellular killing of parasites through release of reactive oxygen and nitrogen species. Released cytokines further activate other inflammatory cells [22, 23]. Macrophages and dendritic cells that have endocytosed the parasite subsequently elicit a strong T cell and antibody response against *T. cruzi*. IFN-γ-producing *T. cruzi*-specific T cells are thus generated [23], which migrate to sites of *T. cruzi*-induced inflammation, including the myocardium, in response to chemokines [24, 25] and blood parasitism. Silva et al. observed in a murine model of Chagas disease that CD8+ IFNγ+Perforin−T cells correlated with a less intense cardiac damage, whereas CD8+ IFNγ-Perforin+ T cells correlated with tissue damage 120 days postinfection. On the other hand, IL-10 and TGF-β are associated with susceptibility to *T. cruzi* infection in mice [26–28]. Recent data show that IL-17 and CD4+CD25+GITR+Foxp3+ regulatory T cells control the parasite-induced myocarditis and resistance to *T. cruzi* infection in mice [29, 30]. Patients with the acute phase of Chagas disease display increased circulating levels of IL-6 and TNF-α [31] and increased production of IFN-γ by mononuclear cells [32].

Th1/proinflammatory cytokines are also produced along the chronic phase *T. cruzi* infection, both in infected mice and in Chagas disease patients. Increased levels of plasma TNF-α and peripheral blood mononuclear cell-produced IFN-γ are detected in CCC and even in ASY patients [15, 33, 34], probably as a response to parasite persistence. Patients who develop Chagas cardiomyopathy display a particularly strong Th1-type immune response as compared to ASY patients. CCC patients show an increased number of CD4+ and CD8+ IFN-γ-producing T cells in the peripheral blood, with reduced numbers of IL-10-producing CD4+CD25+ regulatory T cells [15, 35, 36] and CD4+CD25+ FoxP3+ regulatory T cells [37] as compared with patients in the ASY form of Chagas disease. Taken together, this suggests that regulatory T cells may play a role in the control of the intensity of inflammation in chronic Chagas disease.

The exacerbated Th1 response observed in the peripheral blood of CCC patients is reflected on the Th1-rich inflammatory infiltrate predominantly secreting IFN-γ and TNFα, with lower production of IL-4, IL-6, IL-7, and IL-15 found in their heart tissue as evidenced by immunohistochemistry and mRNA expression studies [13–15, 17, 38–40]. Further to corroborate this, we recently observed significant expression of the hallmark Th1 transcription factor, T-bet, in the CCC myocardium (unpublished observations). Conversely, mRNA expressions GATA3, FoxP3, and RORγT, hallmark transcription factors of Th2, Treg, and Th17 populations, and their signature cytokines and molecular markers were low or undetectable [41]. This is in line with the reduced number of FoxP3+ cells in CCC myocardial tissue [37]. These results suggest the predominant Th1 infiltrate in CCC myocardium is essentially unopposed and suffers little regulation, which could explain its destructiveness, most likely due to excessive collateral damage by type-1 CD8 T cells as described for *T. cruzi*-infected mice [42]. We hypothesized that the

Table 1: Cytokine and chemokine expression in Chagas disease and animal models.

Cytokines/chemokines	Phase (acute/chronic/IND/severe/moderate CCC)	Host (mouse/human)	Organ/cell type	Reference
IFN-γ	Severe CCC	Human	Mononuclear cells	[15, 35]
IFN-γ	Severe CCC	Human	Myocardium	[39, 103]
IFN-γ	Severe CCC	Human	Heart-infiltrating T cells	[15]
IFN-γ	IND, Severe CCC	Human	Plasma	[15, 33, 81]
TNF-α	Severe CCC	Human	Mononuclear cells	[15, 35]
TNF-α	Severe CCC	Human	Heart-infiltrating T cells	[15]
TNF-α	Severe CCC	Human	Myocardium	[39, 103]
TNF-α	IND and Severe CCC	Human	Plasma	[15, 33, 81]
IFN-γ	Acute/chronic	Mouse	Heart	[104–106]
TNF-α	Acute/chronic	Mouse	Heart	[42]
IL-6	Severe CCC	Human	Heart-infiltrating T cells	[15, 39, 103]
IL-2	Severe CCC	Human	Heart-infiltrating T cells	[15, 39, 103]
IL-4	Severe CCC	Human	Heart-infiltrating T cells	[15, 39, 103]
IL-10	Severe CCC	Human	Heart-infiltrating T cells	[15, 39, 103]
IL-7	Severe CCC	Human	Myocardium	[40]
IL-15	Severe CCC	Human	Myocardium	[40]
IL-12	Acute	Mouse	Mononuclear cells	[75]
IL-18	Acute	Mouse	Mononuclear cells	[107]
IL-10	Acute	Mouse	Mononuclear cells	[26–28]
TGF-β	Acute	Mouse	Mononuclear cells	[26–28]
IL-17	Chronic	Mouse	Mononuclear cells	[29]
CCL2, CXCL10, CXCL9 (mRNA)	Severe CCC	Human	Myocardium	[38]
CCR2, CXCR3 (mRNA)	Severe CCC	Human	Myocardium	[38]
CCR5, CXCR3	Severe CCC, IND	Human	Mononuclear cells	[108]
CCL5, CXCL9, CXCL10	Chronic	Mouse	Cardiomyocytes	[109]
CCR5	Chronic	Mouse	Heart	[25, 83]
CCL5, CCL4, CXCR3 (mRNA)	Chronic	Dog	Heart	[110]

selective accumulation of Th1 T cells in CCC myocardium at the expense of other T cell types could be a result of an imbalance at the Th1-associated chemokine-chemokine receptor axes. We were able to detect mononuclear cells that express CXCR3, CCR5, CCR4, CXCL9, and CCL5 in the myocardium of CCC patients using confocal immunofluorescence, and real time qPCR analysis also showed increased mRNA expression of CCR2, CXCR3, CCR5, CCR4, CCR7, and their main chemokine ligands, including the monocyte-chemoattractant chemokine CCL2. CCL5 and CCL9 were the most upregulated chemokine genes in CCC heart tissue. Significantly, the intensity of the myocardial infiltrate was positively correlated with CXCL9 mRNA expression [38, 41]. These results were consistent with a major role of locally produced Th1-chemoattractant chemokines in the accumulation of Th1 T cells in CCC heart tissue.

In recent years, new-generation high-throughput or "omics" technologies have been widely applied in solving complex biological problems, by measuring multiple components simultaneously, in a data-driven, hypothesis-generating, large-scale research model. Systems biology approaches yield data that identify metabolic or signaling pathways involved in the pathogenesis of particular diseases, identifying therapeutic targets, as well as diagnosis and prognosis markers. Our group has used the "omics" approach to elucidate the pathogenesis of human CCC, especially the downstream events occurring in myocardial tissue that could be a consequence of Th1 T cell-driven myocardial inflammation. Cunha-Neto et al. analyzed the gene expression profiling of myocardial tissues of CCC, the noninflammatory idiopathic dilated cardiomyopathy (DCM), and heart donors with a cDNA microarray based on genes expressed in cardiovascular tissue [38]. Immune response-related genes were upregulated only in CCC patients. Multiple IFN-γ-inducible genes were strongly upregulated, indicating prominent IFN-γ signaling that included cardiomyocyte genes. We subsequently observed that IFN-γ and CCL2 treatment of cultured cardiomyocytes induced a strong increase in expression of atrial natriuretic factor (ANF) mRNA, a key member of the embryonic/hypertrophic cardiomyocyte gene expression program. Accordingly, although myocardium ANF mRNA levels were elevated in both disease groups, CCC myocardium expressed 6-fold higher ANF mRNA levels than DCM [37, 41]. The connection between myocardial

production of IFN-γ and cardiomyocyte gene expression changes leading to hypertrophy, ventricular dilation, and heart failure was previously unknown and unexpected and was only identified because of the use of a data-driven "omics"/systems biology approach. It is known that other inflammatory mediators such as TNF-α, CCL2 [38], IL-18, CCL21, and phosphorylated Smad2 involved in TGFβ signaling [43], upregulated in CCC myocardium, are able to induce cardiomyocyte hypertrophy and fibrosis [44, 45]. Taken together, data suggest that locally produced inflammatory mediators have nonimmunological effects on myocardial tissue distinct from direct tissue damage, which may play a significant pathogenic role in CCC, by modulating gene and protein expression in pathways essential to the development of CCC. Gene expression profiling also disclosed that lipid metabolism and mitochondrial oxidative phosphorylation genes were selectively modulated in CCC myocardial tissue, suggesting a specific energy imbalance. Using proteomic analysis (bidimensional electrophoresis and MALDI-TOF mass spectrometry), our group has established a proteomic inventory of >100 distinct myocardial proteins in CCC myocardial tissue [46]. Preliminary data from differential protein expression analysis in the myocardium of CCC, DCM, and ischemic cardiomyopathy (IC) patients as compared to control heart donor myocardial samples allowed the identification of prominently altered pathways, including cardiac remodeling and depressed energy metabolism. Validation studies have shown that both total creatine kinase activity and ATP synthase alpha chain protein levels were significantly lower in CCC samples than IC, IDC, and control samples [47], corroborating the results of the transcriptomic and proteomic analysis. It has been shown that IFN-γ may reduce expression of creatine kinase, which could be a possible mechanism for our findings in CCC hearts (reviewed in [12]). On the other hand, the finding that different degrees of myocardial inflammation were found in clinically similar end-stage CCC patients [41] suggests that noninflammatory factors, probably related to the heart itself, could potentially play a determinant role in disease progression. This is reinforced by findings on the Syrian hamster model of dilated Chagas cardiomyopathy. While the intensity of inflammation is correlated with ventricular dilation (i.e., disease progression), it is not different among animals who die from congestive heart failure or survivors ([7] and data not shown). This may suggest that additional, noninflammatory factors could contribute to severity or progression to death from CCC. Indeed, myocardial resilience, or the ability of myocardial tissue to withstand inflammatory and other stress, may be a key factor. One possible example of a myocardial resilience factor involves susceptibility to apoptosis. Some congenital heart diseases are associated with low levels of cardiomyocyte alpha-cardiac actin, which is related to increased susceptibility to apoptosis [48]. Apoptosis-inducing cytokines, abundant in end-stage CCC myocardium, will likely induce increased apoptosis in cardiomyocytes expressing low levels of cardiac actin. Significantly, we found that myocardial levels of cardiac actin protein are reduced in CCC myocardium. Indeed, Tostes et al. demonstrated the occurrence of significantly higher than normal levels of cardiomyocyte apoptosis in myocardial tissue from severe CCC cases [49]. It is also conceivable that reduced levels of alpha-cardiac actin could impact on Z-disc mechanosensor function and thereby enhance cardiomyocyte apoptosis. In a disease setting, this could accelerate progression to heart failure [50]. We thus consider that progression of chronic Chagas disease may be a result of multiple factors occurring in the affected myocardium including (i) the intensity of the myocardial inflammation, (ii) direct inflammatory damage, (iii) inflammatory mediator-induced changes in myocardial gene and protein expression, and (iv) the ability of the myocardial tissue to withstand inflammatory and other stress.

4. Genetic Polymorphisms and Susceptibility to CCC Development

Mechanisms underlying differential progression to CCC are still incompletely understood. Familial aggregation of CCC has been described [51], suggesting that there might be a genetic component to disease susceptibility [51]. This is also supported by the fact that only one-third of *T. cruzi*-infected individuals develop CCC. A possible role of polymorphisms is that the genetically heterogeneous *T. cruzi* parasite itself in disease outcome cannot be ruled out. CCC patients display a more intense inflammatory response than the asymptomatic patients, who seem to have a more regulated immune response. Given the importance of inflammatory mechanisms for CCC pathogenesis, genetic susceptibility to CCC may result from functionally relevant genetic polymorphisms that lead to variations in the intensity of the innate or acquired immune response and in inflammatory cytokines and chemokines involved in the pathogenesis of the disease.

A number of case-control genetic studies have found signs of association between gene polymorphisms and disease progression. Polymorphisms in the HLA class I and class II loci have been especially investigated in association with chronic Chagas cardiomyopathy. In a Venezuelan cohort Fernandez-Mestre et al. demonstrate the first evidence of association between Chagas disease and HLA genetic susceptibility when they analyzed HLA class II alleles in a sample of 67 serologically positive individuals with and without cardiomyopathy and compared with 156 healthy controls of similar ethnic origin [52]. The comparison of DRB1 and DQB1 allele frequencies among the patients and healthy control subjects showed a decreased frequency of DRB1$*$14 and DQB1$*$0303 in the patients, suggesting independent protective effects to the chronic infection in that population. Allele frequencies comparison between patients with and without cardiomyopathy showed a higher frequency of DRB1$*$01, DRB1$*$08, and DQB1$*$0501 and a decreased frequency of DRB1$*$1501 in the patients with arrhythmia and congestive heart failure [52]. These results suggest that HLA class II genes may be associated with the development of a chronic infection and with heart damage in Chagas disease. At the same time, Deghaide et al. have characterised a Brazilian population including 176 patients presenting with pure cardiomyopathy with heart failure ($N = 60$), cardiomyopathy

Table 2: Meta-analysis on the *TNFA*-308 polymorphism.

Study name	Statistics for each study			
	P value	Odds ratio	Lower limit	Upper limit
Rodríguez-Pérez et al. [59]	0.006	3.03	1.376	6.671
Drigo et al. [62]	0.701	1.129	0.608	2.097
Beraún et al. [61]	0.299	2.049	0.530	7.927
Meta-analysis (fixed effect)	0.025	1.687	1.067	2.668

without heart failure ($N = 18$), pure digestive tract manifestations ($N = 25$), cardiac plus digestive disease ($N = 40$), and asymptomatic patients with positive serology for chronic *T. cruzi* infection ($N = 33$) and noninfected individuals ($N = 448$). Serologic HLA class II analysis showed that HLA-DQ1 conferred susceptibility to while HLA-DQ7 antigen conferred protection against the development of the disease in the total group of patients. Oligonucleotide typing has shown that HLADQB1∗06 alleles were underrepresented in the total group and in the subgroups presenting with pure digestive or cardiac disease, conferring closely similar relative risks and preventive fractions. Asymptomatic patients showed a significant increase of HLA-DQB1∗0302 specificity [53]. Layrisse et al. have shown a strong association of HLA class I gene (HLAC∗03 allele) with CCC as compared with asymptomatic subjects in a Venezuelan cohort (the same population as Fernandez-Mestre et al.) [54]. After increasing their cohort (35 asymptomatic cases and 72 symptomatic cases), the authors confirmed their previous results and they have shown that the DPB1∗0401 allele frequency is also significantly increased in patients with heart disease while DPB1∗0101 frequency is higher among the asymptomatic group compared with CCC patients [55]. The results on DRB1 and DQB1 were partially confirmed on a Peruvian and Argentinean population [56, 57], whereas this replication failed on a Brazilian population [58]. Taken together, results suggest that HLA class II association may vary with the genetic background of the studied population, perhaps indicating differential linkage disequilibrium with functional variants in different populations. Genes in the MHC class III/*TNFA* region were also probed for association with Chagas disease progression. Association was detected with polymorphism *TNFA-308A/G* in a Mexican population (27 asymptomatic subjects, 27 patients with chronic cardiomyopathy, and 169 healthy individuals) [59]. Similarly, Campelo et al. have conducted an evaluation of genetic susceptibility to chronic disease in relationship of five microsatellite polymorphisms in and around a series of Brazilian chagasic patients stratified according to the clinical form of disease presentation, that is, cardiac, digestive, digestive plus cardiac, or indeterminate form (54 patients with cardiomyopathy with heart failure, 17 patients with cardiomyopathy without heart failure, 25 patients with pure digestive manifestations, 33 patients with digestive plus cardiac manifestations, 33 other patients characterized by indeterminate form, and 221 negative serology subjects). The relative risks associated with the susceptibility alleles ranged from 1.674 to 10.21, indicating that the individuals who possess these susceptibility alleles have almost 2 to 10 times higher risk of developing a given form of chronic disease if infected [60]. Twelve haplotype frequencies revealed significant differences when patients were considered as a whole or stratified according to the clinical variant and were compared to controls. All these results suggest that this chromosomal region is associated with susceptibility to or resistance against CCC forms. Even though this result was not confirmed into two independent studies performed on Peruvian [61] and Brazilian populations [62] a meta-analysis with data from the three studies disclosed a significant association on the *TNFA*-308 polymorphism with disease progression (Table 2). This indicates that this chromosomal region may indeed be involved in the genetic control of susceptibility to CCC development. The discrepancies between studies could have been due either to modest clinical group size or to differing genetic backgrounds, where the functional variant could be in strong linkage disequilibrium with the *TNFA*-308 polymorphism only in the Mexican population. Drigo et al. [63] have shown that end-stage CCC patients carrying *TNFA*-308A and/or TNFa microsatellite polymorphisms display a significantly shorter survival time compared to those carrying other alleles (166 CCC patients compared to 80 asymptomatic individuals employed as control group). Ramasawmy et al. have also focused their efforts on three other genes (UAP56, LTA, and IKBL) located into the HLA class III region, in proximity to the *TNFA* locus. For the polymorphism UAP56-22G/C, a significant difference in frequency between 154 Brazilian CCC patients and the 76 Brazilian asymptomatic patients was revealed at the genotype level [64]. The UAP56-22C allele seems to confer susceptibility to CCC. Lymphotoxin-α protein (encoded by LTA gene) is a proinflammatory cytokine which also induces adhesion molecules and cytokines from vascular endothelial cells and vascular smooth-muscle cells, which may contribute to the inflammation process. The LTA+80C/C genotype was significantly more common in CCC patients than asymptomatic patients [65]. This result was confirmed later on an independent Brazilian cohort [66]. A previous study done on hepatitis C virus infection has showed that a non-HLA gene block within the MHC class III region, including the IKBL, ATP6V1G2, BAT1, MICB, and MICA genes, was strongly associated with development of dilated cardiomyopathy. Among these genes, IKBL encodes an inhibitor of NF-κB which plays a key role in innate immunity. Ramasawmy et al. provide evidence that two variants (IKBL-62A/T and IKBL-262A/G) in the promoter region of the IKBL gene are associated with susceptibility to develop CCC [67]. Similar trend was observed for the

IKBL-262A homozygotes. A haplotype analysis led to the identification of a susceptibility haplotype (IKBL-262A IKBL-62A) more frequent in CCC patients [67].

On another side, polymorphisms in additional cytokine genes have been also investigated. On a Brazilian population, including hundred fifty-five patients in the chronic phase and 43 individuals without Chagas disease, the polymorphism IL10-1082G/A, which correlates with lower expression of IL-10, was associated with the development of Chagas disease cardiomyopathy [68]. An independent study including 104 CCC patients and 60 noninfected controls suggests that an epistasis between MHC and IL-10 is associated with susceptibility/resistance to Chagas disease [69]. The interleukin 1 (IL-1) is a primary inflammatory cytokine and has been implicated in mediating both acute and chronic pathologic inflammatory diseases [70]. A Colombian study (130 patients with cardiomyopathy and 130 asymptomatic subjects) has detected significant differences in the distribution of the *IL1B* +5810 genotypes between cardiomyopathic patients and asymptomatic individuals [71]. A haplotype covering the IL1A, IL1B, and IL1RN genes was associated with protection [71]. Putative association for the IL1 antagonist gene (IL1RN) was described on a Mexican population (58 CCC patients, 28 asymptomatic, 50 seronegative individuals with idiopathic dilated cardiomyopathy, and 109 healthy individuals) [72]. Interleukin-12 (IL-12) induces production of interferon-γ (IFN-γ) and favours the differentiation of T helper 1 (Th1). Different studies corroborate the crucial role of IL-12 in host resistance to *T. cruzi* infection [73–75]. The authors observed that the IL12+1188C allele was present at significantly higher frequency in the CCC population than in asymptomatic (Colombian population including 200 seronegative individuals, 260 serologically positive patients, 130 with Chagas cardiomyopathy, and 130 asymptomatic) [76]. However, this polymorphism does not discriminate the seropositive patients from the control individuals [76].

The TLRs play an important role in innate immunity by acting as sensors for invading pathogens. The intracellular signaling of TLRs is mediated by at least 5 adaptor proteins, including MyD88, MAL/TIRAP, TRIF, TICAM, and SARM [77]. On a Brazilian population including 169 patients with cardiomyopathy and 76 asymptomatic individuals, the frequency of homozygosity for the *MAL/TIRAP* 180S allele was significantly higher among patients with CCC than among asymptomatic patients, whereas the percentage of subjects homozygous for the *MAL/TIRAP* 180L allele was similar in both groups. The percentage of subjects heterozygous for *MAL/TIRAP* S180L among patients with CCC was significantly different from the percentage found in asymptomatic patients [78]. Migration inhibitory factor (MIF) protein is a pleiotropic cytokine produced by activated T cells, macrophages. For the polymorphism, MIF-173G/C, a statistically significant difference was detected between patients and controls in the Colombian cohort (240 chagasic patients and 199 controls). A similar association was found in the Peruvian cohort (74 chagasic patients and 85 controls). A meta-analysis has demonstrated that the MIF-173C allele confers a risk effect in Chagas patients. Moreover, a dose effect for the susceptibility allele was observed [79]. Locally produced chemokines such as CCL2, CCL5, and CXCL9 play a major role in inflammatory cell recruitment to the heart in *T. cruzi*-induced acute myocarditis in mice as well as chronic human Chagas disease myocarditis [24, 41, 80, 81]. Cytokine-mediated production of CCL2 by cardiomyocytes seems to participate in the killing of *T. cruzi* through a nitric oxide-dependent mechanism [82, 83]. Ramasawmy et al. showed an association between the *CCL2*-2518A/G polymorphism and CCC development [84]. Calzada et al. observed, on seropositive and seronegative Peruvian individuals, that the CCR5 59029A/G genotype was significantly increased in asymptomatic compared to CCC patients (85 seropositive and 87 seronegative individuals) [85]. An independent study, performed in Venezuela, indicates that a distinct genotype in the CCR5 gene is also associated with Chagas disease (asymptomatic versus arrhythmic and cardiomyopathic) [86]. Our group has found that the CCR5 rs1799988 CC genotype was significantly more frequent in the severe CCC than with the moderate CCC group, although polymorphisms in the CCL4, CCL5, CCL17, CCL19, and CXCR3 genes, all displaying upregulated expression in CCC myocardial tissue, were not associated with CCC [41].

Some functional polymorphisms have been identified. On a Brazilian population, including 149 asymptomatic subjects, 79 moderate CCC patients (EF > 40%), and 95 severe CCC patients (EF > 40%), our group has reported that chemokine gene polymorphisms *CXCL9* rs10336 *CC* and *CXCL10* rs3921 *GG* were significantly less frequent among the severe CCC patients with ventricular dysfunction as compared to moderate CCC patients in a Brazilian cohort study [41]. We then observed that myocardial explants of end-stage CCC patients submitted to heart transplantation carrying the lower risk genotypes displayed a 2–6-fold reduction in mRNA expression of CXCL9 and CXCL10 as compared to those with other *CXCL9/CXCL10* genotypes. However, only the *CXCL9 rs10336 GG* polymorphism was associated with reduced intensity of myocarditis; significantly, only myocardial mRNA levels of CXCL9 were strongly associated with intensity of myocarditis. Taken together, our results may suggest that genetic polymorphisms affecting local expression of CXCL9 and possibly CXCL10 control the intensity of myocarditis through modulation of CXCL9 and/or CXCL10 expression in the myocardium and the ensuing effects on the local expression of chemokine ligands of the CXCR3/CCR5/CCR4/CCR7. Considering that polymorphisms at the immunoregulatory CTLA-4 and PDCD1 genes may alter their inhibitory function, we investigated the association of alleles, genotypes, and haplotypes of polymorphic sites observed at the CTLA-4 and PDCD1 genes with different clinical manifestations of chronic Chagas disease (indeterminate, cardiac, digestive, and mixed). Dias et al. conduct a study on Brazilian subjects (90 Chagas disease patients with cardiac forms, 67 Chagas disease patients with digestive form, 39 Chagas disease patients with cardiac and digestive asymptomatic subjects, and 326 noninfected controls). They showed that alleles, genotypes, and haplotypes reported to increase the expression of the regulatory molecule CTLA-4 were associated with the indeterminate form of the disease [87].

Several studies on candidate genes putatively involved in the control of *T. cruzi* infection or myocardial function failed to display an association with CCC. This was reported for the TLR1, TLR2, TLR4, TLR5, TLR9 [88], PTPN22 [89], NRAMP1 [90], ACE [91], NOS2 [92], CCL4, CCL5, CCL17, CCL19, and CXCR3 [41], beta-cardiac myosin heavy chain [58], IL4 [93], and IFNG [94]. Such lack of association or fault positive association may be due either to the limited number of tested SNPs or to the low statistical power owing to limited cohort size. In order to avoid this bias, it is essential to set up large-scale genetic studies using new technologies on large study populations with clearly established phenotypes. In this way, we have enrolled a large Brazilian population and we performed a replication study (Brazilian population, 315 CCC patients and 118 asymptomatic individuals). Our genetic analysis focused on CCR5, CCL2, and MAL/TIRAP genes. The CCL2rs2530797A/A and TIRAPrs8177376A/A were associated with an increased susceptibility whereas the CCR5rs3176763C/C genotype is associated with protection of CCC [95]. Our data show that polymorphisms affecting key molecules involved in several immune parameters (innate immunity signal transduction and T cell/monocyte migration) play a role in genetic susceptibility to CCC development. This also points out to the multigenic character of CCC, each polymorphism imparting a small contribution [95]. In addition, recent results from our groups showed that a single nucleotide polymorphism in the promoter region of the alpha-cardiac actin gene (*ACTC1*) associated with CCC influences transcription factor binding, implying that the polymorphism may influence myocardial transcriptional levels of the highly relevant ACTC1 gene [96]. These results were obtained on a Brazilian population including 315 CCC patients and 118 asymptomatic individuals, and the same trend of association was found on a second independent cohort including 102 CCC patients and 36 asymptomatic individuals.

The first genome-wide association study (GWAS) on Chagas disease was published in 2013 [97]. This analysis included 600 Brazilian *T. cruzi* seropositive blood donors of different clinical forms and 488 Brazilian seronegative donors. Several phenotypes were analyzed, in addition to cardiomyopathy considered as the main trait. Authors also evaluated a limited number of specific parameters, including ejection fraction, PR interval, QRS duration (QRS), corrected QT interval (QTc), EIA signal/cutoff levels, and *T. cruzi* PCR status. Of the 600 *T. cruzi* seropositive donors cases, 221 were classified as having CCC, 311 had no cardiomyopathy, and 68 were inconclusive. For cardiomyopathy, two trends of association (after multiple comparison corrections) were detected for markers located around SLCO1B1 gene. SLCO1B1 is a membrane transporter that belongs to a solute carrier family and plays a role in drug metabolism. It is expressed in the liver, brain, heart, and kidney and transports organic anions, such as digoxin, bilirubin, methotrexate, and statins. In addition, loss-of-function mutations may be associated with impaired drug action in target tissues [98]. Moreover, a cluster of 12 SNPs within introns of COL14A1 was associated with PCR positivity. COL14A1 is a fibril-associated collagen which interacts with the fibril surface and regulates fibrillogenesis [99, 100]. Probably all these markers at this locus are in linkage disequilibrium. Furthermore, HSPB8 is a small heat shock protein whose heart specific overexpression induces myocardial hypertrophy [101]. HSPB8-transgenic mice bearing the K141N mutation expressed myocardial hypertrophy, ventricular dysfunction, and apical fibrosis—the latter being a hallmark of heart involvement in CCC [102]. Significantly, expression of HSPB8 is selectively increased in myocardial tissue from CCC patients, rather than in idiopathic dilated cardiomyopathy patients [38]. However, these indications remain suggestive due to the limited size of the studied cohort for a GWAS study. Surprisingly, no polymorphisms in immune-related genes were found.

The use of a systematic approach to identify genes proven to be pathogenetically relevant in CCC could greatly accelerate the finding of functional genetic polymorphisms. This would have a strong impact in the understanding of the pathogenic process in CCC, as well as in diagnosis, prognosis, and therapeutics.

Conflict of Interests

The authors declare that there is no conflict of interests regarding the publication of this paper.

Acknowledgments

This research was supported by the Brazilian Council for Scientific and Technological Development, CNPq, and the São Paulo State Research Funding Agency, FAPESP. Authors also received financial assistance from the Institut National de la Santé et de la Recherche Médicale (INSERM), the Aix-Marseille University, USP-COFECUB program, and the ARCUS II PACA Brésil program. Edecio Cunha-Neto and Christophe Chevillard were also recipients for an international program funded either by the French ANR (Br-Fr-CHAGAS) or by the Brazilian FAPESP agencies. Edecio Cunha-Neto is recipient of Brazilian Council for Scientific and Technological Development, CNPq, productivity awards. Christophe Chevillard was a recipient of a temporary professor position supported by the French consulate in Brazil and the University of São Paulo (USP).

References

[1] R. Salvatella, P. Irabedra, D. Sánchez, L. G. Castellanos, and M. Espinal, "South-south cooperation for Chagas disease," *The Lancet*, vol. 382, no. 9890, pp. 395–396, 2013.

[2] C. J. Schofield, J. Jannin, and R. Salvatella, "The future of Chagas disease control," *Trends in Parasitology*, vol. 22, no. 12, pp. 583–588, 2006.

[3] World Health Organisation, *Control of Chagas Disease*, World Health Organization Technical Report, WHO, Geneva, Switzerland, 2002.

[4] L. V. Kirchhoff and R. D. Pearson, "The emergence of chagas disease in the United States and Canada," *Current Infectious Disease Reports*, vol. 9, no. 5, pp. 347–350, 2007.

[5] U. O. Martín, D. Afchain, A. de Marteleur, O. Ledesma, and A. Caprón, "Circulating immune complexes in different developmental stages of Chagas' disease," *Medicina*, vol. 47, no. 2, pp. 159–162, 1987.

[6] M. de Lourdes Higuchi, C. F. de Morais, A. C. P. Barreto et al., "The role of active myocarditis in the development of heart failure in chronic Chagas' disease: a study based on endomyocardial biopsies," *Clinical Cardiology*, vol. 10, no. 11, pp. 665–670, 1987.

[7] A. M. B. Bilate, V. M. C. Salemi, F. J. A. Ramires et al., "The Syrian hamster as a model for the dilated cardiomyopathy of Chagas' disease: a quantitative echocardiographical and histopathological analysis," *Microbes and Infection*, vol. 5, no. 12, pp. 1116–1124, 2003.

[8] L. E. Ramirez, E. Lages-Silva, J. M. Soares Jr., and E. Chapadeiro, "The hamster (*Mesocricetus auratus*) as experimental model in Chagas' disease: parasitological and histopathological studies in acute and chronic phases of *Trypanosoma cruzi*infection," *Revista da Sociedade Brasileira de Medicina Tropical*, vol. 27, no. 3, pp. 163–169, 1994.

[9] R. B. Bestetti and G. Muccillo, "Clinical course of chagas' heart disease: a comparison with dilated cardiomyopathy," *International Journal of Cardiology*, vol. 60, no. 2, pp. 187–193, 1997.

[10] M. M. Barbosa, M. O. C. Rocha, F. A. Botoni, A. L. P. Ribeiro, and M. C. P. Nunes, "Is atrial function in Chagas dilated cardiomyopathy more impaired than in idiopathic dilated cardiomyopathy?" *European Journal of Echocardiography*, vol. 12, no. 9, pp. 643–647, 2011.

[11] J. Milei, R. Storino, G. F. Alonso, R. Beigelman, S. Vanzulli, and V. J. Ferrans, "Endomyocardial biopsies in chronic chagasic cardiomyopathy," *Cardiology*, vol. 80, no. 5-6, pp. 424–437, 1992.

[12] E. Cunha-Neto, L. G. Nogueira, P. C. Teixeira et al., "Immunological and non-immunological effects of cytokines and chemokines in the pathogenesis of chronic Chagas disease cardiomyopathy," *Memorias do Instituto Oswaldo Cruz*, vol. 104, supplement 1, pp. 252–258, 2009.

[13] M. de Lourdes Higuchi, P. S. Gutierrez, V. D. Aiello et al., "Immunohistochemical characterization of infiltrating cells in human chronic chagasic myocarditis: comparison with myocardial rejection process," *Virchows Archiv A: Pathological Anatomy and Histopathology*, vol. 423, no. 3, pp. 157–160, 1993.

[14] D. D. Reis, E. M. Jones, S. Tostes Jr. et al., "Characterization of inflammatory infiltrates in chronic chagasic myocardial lesions: presence of tumor necrosis factor-α+ cells and dominance of granzyme A+, CD8+ lymphocytes," *American Journal of Tropical Medicine and Hygiene*, vol. 48, no. 5, pp. 637–644, 1993.

[15] L. C. J. Abel, L. V. Rizzo, B. Ianni et al., "Chronic Chagas' disease cardiomyopathy patients display an increased IFN-γ response to Trypanosoma cruzi infection," *Journal of Autoimmunity*, vol. 17, no. 1, pp. 99–107, 2001.

[16] M. J. F. Morato, D. G. Colley, and M. R. Powell, "Cytokine profiles during experimental Chagas' disease," *Brazilian Journal of Medical and Biological Research*, vol. 31, no. 1, pp. 123–125, 1998.

[17] D. B. Rocha Rodrigues, M. A. dos Reis, A. Romano et al., "In situ expression of regulatory cytokines by heart inflammatory cells in Chagas' disease patients with heart failure," *Clinical & Developmental Immunology*, vol. 2012, Article ID 361730, 7 pages, 2012.

[18] N. Añez, H. Carrasco, H. Parada et al., "Myocardial parasite persistence in chronic chagasic patients," *American Journal of Tropical Medicine and Hygiene*, vol. 60, no. 5, pp. 726–732, 1999.

[19] S. G. Fonseca, H. Moins-Teisserenc, E. Clave et al., "Identification of multiple HLA-A*0201-restricted cruzipain and FL-160 $CD8^+$ epitopes recognized by T cells from chronically Trypanosoma cruzi-infected patients," *Microbes and Infection*, vol. 7, no. 4, pp. 688–697, 2005.

[20] E. Cunha-Neto and J. Kalil, "Autoimmunity in Chagas' heart disease," *São Paulo Medical Journal*, vol. 113, no. 2, pp. 757–766, 1995.

[21] A. Bafica, H. C. Santiago, R. Goldszmid, C. Ropert, R. T. Gazzinelli, and A. Sher, "Cutting edge: TLR9 and TLR2 signaling together account for MyD88-dependent control of parasitemia in *Trypanosoma cruzi* infection," *Journal of Immunology*, vol. 177, no. 6, pp. 3515–3519, 2006.

[22] V. Michailowsky, M. R. N. Celes, A. P. Marino et al., "Intercellular adhesion molecule 1 deficiency leads to impaired recruitment of T lymphocytes and enhanced host susceptibility to infection with *Trypanosoma cruzi*," *The Journal of Immunology*, vol. 173, no. 1, pp. 463–470, 2004.

[23] A. M. B. Bilate and E. Cunha-Neto, "Chagas disease cardiomyopathy: current concepts of an old disease," *Revista do Instituto de Medicina Tropical de São Paulo*, vol. 50, no. 2, pp. 67–74, 2008.

[24] M. M. Teixeira, R. T. Gazzinelli, and J. S. Silva, "Chemokines, inflammation and Trypanosoma cruzi infection," *Trends in Parasitology*, vol. 18, no. 6, pp. 262–265, 2002.

[25] A. P. M. P. Marino, A. da Silva, P. dos Santos et al., "Regulated on activation, normal T cell expressed and secreted (RANTES) antagonist (Met-RANTES) controls the early phase of trypanosoma cruzi-elicited myocarditis," *Circulation*, vol. 110, no. 11, pp. 1443–1449, 2004.

[26] J. S. Silva, D. R. Twardzik, and S. G. Reed, "Regulation of *Trypanosoma cruzi* infections in vitro and in vivo by transforming growth factor β (TGF-β)," *Journal of Experimental Medicine*, vol. 174, no. 3, pp. 539–545, 1991.

[27] R. R. dos Santos, M. A. Rossi, J. L. Laus, J. S. Silva, W. Savino, and J. Mengel, "Anti-CD4 abrogates rejection and reestablishes long-term tolerance to syngeneic newborn hearts grafted in mice chronically infected with Trypanosoma cruzi," *Journal of Experimental Medicine*, vol. 175, no. 1, pp. 29–39, 1992.

[28] C. Hölscher, M. Mohrs, W. J. Dai et al., "Tumor necrosis factor alpha-mediated toxic shock in *Trypanosoma cruzi*-infected interleukin 10-deficient mice," *Infection and Immunity*, vol. 68, no. 7, pp. 4075–4083, 2000.

[29] P. M. da Matta Guedes, F. R. S. Gutierrez, F. L. Maia et al., "IL-17 produced during Trypanosoma cruzi infection plays a central role in regulating parasite-induced myocarditis.," *PLoS neglected tropical diseases*, vol. 4, no. 2, Article ID e604, 2010.

[30] F. S. Mariano, F. R. S. Gutierrez, W. R. Pavanelli et al., "The involvement of CD4+CD25+ T cells in the acute phase of *Trypanosoma cruzi* infection," *Microbes and Infection*, vol. 10, no. 7, pp. 825–833, 2008.

[31] E. Moretti, B. Basso, L. Cervetta, A. Brigada, and G. Barbieri, "Patterns of cytokines and soluble cellular receptors in the sera of children with acute Chagas' disease," *Clinical and Diagnostic Laboratory Immunology*, vol. 9, no. 6, pp. 1324–1327, 2002.

[32] M. Samudio, S. Montenegro-James, M. de Cabral et al., "Differential expression of systemic cytokine profiles in Chagas' disease is associated with endemicity of Trypanosoma cruzi infections," *Acta Tropica*, vol. 69, no. 2, pp. 89–97, 1998.

[33] R. C. Ferreira, B. M. Ianni, L. C. J. Abel et al., "Increased plasma levels of tumor necrosis factor-α in asymptomatic "Indeterminate" and Chagas disease cardiomyopathy patients," *Memórias do Instituto Oswaldo Cruz*, vol. 98, no. 3, pp. 407–411, 2003.

[34] A. Talvani, M. O. C. Rocha, A. L. Ribeiro, R. Correa-Oliveira, and M. M. Teixeira, "Chemokine receptor expression on the surface of peripheral blood mononuclear cells in Chagas disease," *Journal of Infectious Diseases*, vol. 189, no. 2, pp. 214–220, 2004.

[35] J. A. S. Gomes, L. M. G. Bahia-Oliveira, M. O. C. Rocha, O. A. Martins-Filho, G. Gazzinelli, and R. Correa-Oliveira, "Evidence that development of severe cardiomyopathy in human Chagas' disease is due to a Th1-specific immune response," *Infection and Immunity*, vol. 71, no. 3, pp. 1185–1193, 2003.

[36] F. F. Araujo, J. A. S. Gomes, M. O. C. Rocha et al., "Potential role of $CD4^{+}CD25^{high}$ regulatory T cells in morbidity in Chagas disease," *Frontiers in Bioscience*, vol. 12, no. 8, pp. 2797–2806, 2007.

[37] A. B. M. da Silveira, F. F. de Araújo, M. A. R. Freitas et al., "Characterization of the presence and distribution of Foxp3+ cells in chagasic patients with and without megacolon," *Human Immunology*, vol. 70, no. 1, pp. 65–67, 2009.

[38] E. Cunha-Neto, V. J. Dzau, P. D. Allen et al., "Cardiac gene expression profiling provides evidence for cytokinopathy as a molecular mechanism in Chagas' disease cardiomyopathy," *The American Journal of Pathology*, vol. 167, no. 2, pp. 305–313, 2005.

[39] M. M. Reis, M. D. L. Higuchi, L. A. Benvenuti et al., "An in situ quantitative immunohistochemical study of cytokines and IL-2R+ in chronic human chagasic myocarditis: Correlation with the presence of myocardial Trypanosoma cruzi antigens," *Clinical Immunology and Immunopathology*, vol. 83, no. 2, pp. 165–172, 1997.

[40] S. G. Fonseca, M. M. Reis, V. Coelho et al., "Locally produced survival cytokines IL-15 and IL-7 may be associated to the predominance of CD8+ T cells at heart lesions of human chronic chagas disease cardiomyopathy," *Scandinavian Journal of Immunology*, vol. 66, no. 2-3, pp. 362–371, 2007.

[41] L. G. Nogueira, R. H. B. Santos, B. M. Ianni et al., "Myocardial chemokine expression and intensity of myocarditis in Chagas cardiomyopathy are controlled by polymorphisms in CXCL9 and CXCL10," *PLoS Neglected Tropical Diseases*, vol. 6, no. 10, Article ID e1867, 2012.

[42] M. A. Munoz-Fernandez and M. Fresno, "Activation of human macrophages for the killing of intracellular Trypanosoma cruzi by TNF-α and IFN-γ through a nitric oxide-dependent mechanism," *Immunology Letters*, vol. 33, no. 1, pp. 35–40, 1992.

[43] T. C. Araújo-Jorge, M. C. Waghabi, A. M. Hasslocher-Moreno et al., "Implication of transforming growth factor-β1 in Chagas disease myocardiopathy," *Journal of Infectious Diseases*, vol. 186, no. 12, pp. 1823–1828, 2002.

[44] L. Riol-Blanco, N. Sánchez-Sánchez, A. Torres et al., "The chemokine receptor CCR7 activates in dendritic cells two signaling modules that independently regulate chemotaxis and migratory speed," *The Journal of Immunology*, vol. 174, no. 7, pp. 4070–4080, 2005.

[45] R. Liu, C. Zhou, D. Wang et al., "Enhancement of DNA vaccine potency by sandwiching antigen-coding gene between secondary lymphoid tissue chemokine (SLC) and IgG Fc fragment genes," *Cancer Biology and Therapy*, vol. 5, no. 4, pp. 427–434, 2006.

[46] P. C. Teixeira, L. K. Iwai, A. C. K. Kuramoto et al., "Proteomic inventory of myocardial proteins from patients with chronic Chagas' cardiomyopathy," *Brazilian Journal of Medical and Biological Research*, vol. 39, no. 12, pp. 1549–1562, 2006.

[47] P. C. Teixeira, R. H. B. Santos, A. I. Fiorelli et al., "Selective decrease of components of the creatine kinase system and ATP synthase complex in chronic Chagas disease cardiomyopathy," *PLoS Neglected Tropical Diseases*, vol. 5, no. 6, Article ID e1205, 2011.

[48] H. Jiang, G. Qiu, J. Li-Ling, N. Xin, and K. Sun, "Reduced ACTC1 expression might play a role in the onset of congenital heart disease by inducing cardiomyocyte apoptosis," *Circulation Journal*, vol. 74, no. 11, pp. 2410–2418, 2010.

[49] S. Tostes Jr., D. B. Rocha-Rodrigues, G. de Araujo Pereira, and V. Rodrigues Jr., "Myocardiocyte apoptosis in heart failure in chronic Chagas' disease," *International Journal of Cardiology*, vol. 99, no. 2, pp. 233–237, 2005.

[50] R. S. Foo, K. Mani, and R. N. Kitsis, "Death begets failure in the heart," *The Journal of Clinical Investigation*, vol. 115, no. 3, pp. 565–571, 2005.

[51] F. Zicker, P. G. Smith, J. C. Almeida Netto, R. M. Oliveira, and E. M. S. Zicker, "Physical activity, opportunity for reinfection, and sibling history of heart disease as risk factors for Chagas' cardiopathy," *The American Journal of Tropical Medicine and Hygiene*, vol. 43, no. 5, pp. 498–505, 1990.

[52] M. T. Fernandez-Mestre, Z. Layrisse, S. Montagnani et al., "Influence of the HLA class II polymorphism in chronic Chagas' disease," *Parasite Immunology*, vol. 20, no. 4, pp. 197–203, 1998.

[53] N. H. S. Deghaide, R. O. Dantas, and E. A. Donadi, "HLA class I and II profiles of patients presenting with Chagas' disease," *Digestive Diseases and Sciences*, vol. 43, no. 2, pp. 246–252, 1998.

[54] Z. Layrisse, M. T. Fernandez, S. Montagnani et al., "HLA-C∗03 is a risk factor for cardiomyopathy in Chagas disease," *Human Immunology*, vol. 61, no. 9, pp. 925–929, 2000.

[55] I. A. Colorado, H. Acquatella, F. Catalioti, M. T. Fernandez, and Z. Layrisse, "HLA class II DRB1, DQB11, DPB1 polymorphism and cardiomyopathy due to *Trypanosoma cruzi* chronic infection," *Human Immunology*, vol. 61, no. 3, pp. 320–325, 2000.

[56] A. Nieto, Y. Beraún, M. D. Callado et al., "HLA haplotypes are associated with differential susceptibility to Trypanosoma cruzi infection," *Tissue Antigens*, vol. 55, no. 3, pp. 195–198, 2000.

[57] S. G. Borrás, C. Diez, C. Cotorruelo et al., "HLA class II DRB1 polymorphism in Argentinians undergoing chronic Trypanosoma cruzi infection," *Annals of Clinical Biochemistry*, vol. 43, no. 3, pp. 214–216, 2006.

[58] K. C. Faé, S. A. Drigo, E. Cunha-Neto et al., "HLA and β-myosin heavy chain do not influence susceptibility to Chagas' disease cardiomyopathy," *Microbes and Infection*, vol. 2, no. 7, pp. 745–751, 2000.

[59] J. M. Rodríguez-Pérez, D. Cruz-Robles, G. Hernández-Pacheco et al., "Tumor necrosis factor-alpha promoter polymorphism in Mexican patients with Chagas' disease," *Immunology Letters*, vol. 98, no. 1, pp. 97–102, 2005.

[60] V. Campelo, R. O. Dantas, R. T. Simões et al., "TNF microsatellite alleles in Brazilian chagasic patients," *Digestive Diseases and Sciences*, vol. 52, no. 12, pp. 3334–3339, 2007.

[61] Y. Beraún, A. Nieto, M. D. Collado, A. González, and J. Martín, "Polymorphisms at tumor necrosis factor (TNF) loci are not associated with Chagas' disease," *Tissue Antigens*, vol. 52, no. 1, pp. 81–83, 1998.

[62] S. A. Drigo, E. Cunha-Neto, B. Ianni et al., "Lack of association of tumor necrosis factor-α polymorphisms with Chagas disease in Brazilian patients," *Immunology Letters*, vol. 108, no. 1, pp. 109–111, 2007.

[63] S. A. Drigo, E. Cunha-Neto, B. Ianni et al., "TNF gene polymorphisms are associated with reduced survival in severe Chagas' disease cardiomyopathy patients," *Microbes and Infection*, vol. 8, no. 3, pp. 598–603, 2006.

[64] R. Ramasawmy, E. Cunha-Neto, K. C. Faé et al., "BAT1, a putative anti-inflammatory gene, is associated with chronic chagas cardiomyopathy," *Journal of Infectious Diseases*, vol. 193, no. 10, pp. 1394–1399, 2006.

[65] R. Ramasawmy, K. C. Fae, E. Cunha-Neto et al., "Polymorphisms in the gene for lymphotoxin-alpha predispose to chronic chagas cardiomyopathy," *Journal of Infectious Diseases*, vol. 196, no. 12, pp. 1836–1843, 2007.

[66] C. W. Pissetti, R. F. de Oliveira, D. Correia, G. A. N. Nascentes, M. M. Llaguno, and V. Rodrigues, "Association between the lymphotoxin-alpha gene polymorphism and chagasic cardiopathy," *Journal of Interferon and Cytokine Research*, vol. 33, no. 3, pp. 130–135, 2013.

[67] R. Ramasawmy, K. C. Faé, E. Cunha-Neto et al., "Variants in the promoter region of IKBL/NFKBIL1 gene may mark susceptibility to the development of chronic Chagas' cardiomyopathy among Trypanosoma cruzi-infected individuals," *Molecular Immunology*, vol. 45, no. 1, pp. 283–288, 2008.

[68] G. C. Costa, M. O. D. C. Rocha, P. R. Moreira et al., "Functional IL-10 gene polymorphism is associated with Chagas disease cardiomyopathy," *Journal of Infectious Diseases*, vol. 199, no. 3, pp. 451–454, 2009.

[69] M. Moreno, E. L. Silva, L. E. Ramírez, L. G. Palacio, D. Rivera, and M. Arcos-Burgos, "Chagas' disease susceptibility/resistance: linkage disequilibrium analysis suggest epistasis between major histocompatibility complex and interleukin-10," *Tissue Antigens*, vol. 64, no. 1, pp. 18–24, 2004.

[70] C. A. Petersen and B. A. Burleigh, "Role for interleukin-1β in Trypanosoma cruzi-induced cardiomyocyte hypertrophy," *Infection and Immunity*, vol. 71, no. 8, pp. 4441–4447, 2003.

[71] O. Flórez, G. Zafra, C. Morillo, J. Martín, and C. I. González, "Interleukin-1 gene cluster polymorphism in chagas disease in a Colombian case-control study," *Human Immunology*, vol. 67, no. 9, pp. 741–748, 2006.

[72] D. Cruz-Robles, J. P. Chvez-Gonzlez, M. M. Cavazos-Quero, O. Prez-Mndez, P. A. Reyes, and G. Vargas-Alarcn, "Association between IL-1B and IL-1RN gene polymorphisms and chagas' disease development susceptibility," *Immunological Investigations*, vol. 38, no. 3-4, pp. 231–239, 2009.

[73] M. I. Antúnez and R. L. Cardoni, "IL-12 and IFN-gamma production, and NK cell activity, in acute and chronic experimental Trypanosoma cruzi infections," *Immunology Letters*, vol. 71, no. 2, pp. 103–109, 2000.

[74] V. Michailowsky, N. M. Silva, C. D. Rocha, L. Q. Vieira, J. Lannes-Vieira, and R. T. Gazzinelli, "Pivotal role of interleukin-12 and interferon-γ axis in controlling tissue parasitism and inflammation in the heart and central nervous system during *Trypanosoma cruzi* infection," *The American Journal of Pathology*, vol. 159, no. 5, pp. 1723–1733, 2001.

[75] S. E. B. Graefe, T. Jacobs, I. Gaworski, U. Klauenberg, C. Steeg, and B. Fleischer, "Interleukin-12 but not interleukin-18 is required for immunity to *Trypanosoma cruzi* in mice," *Microbes and Infection*, vol. 5, no. 10, pp. 833–839, 2003.

[76] G. Zafra, C. Morillo, J. Martín, A. González, and C. I. González, "Polymorphism in the 3′ UTR of the IL12B gene is associated with Chagas' disease cardiomyopathy," *Microbes and Infection*, vol. 9, no. 9, pp. 1049–1052, 2007.

[77] L. A. J. O'Neill and A. G. Bowie, "The family of five: TIR-domain-containing adaptors in Toll-like receptor signalling," *Nature Reviews Immunology*, vol. 7, no. 5, pp. 353–364, 2007.

[78] R. Ramasawmy, E. Cunha-Neto, K. C. Fae et al., "Heterozygosity for the S180L variant of MAL/TIRAP, a gene expressing an adaptor protein in the toll-like receptor pathway, is associated with lower risk of developing chronic chagas cardiomyopathy," *Journal of Infectious Diseases*, vol. 199, no. 12, pp. 1838–1845, 2009.

[79] O. A. Torres, J. E. Calzada, Y. Beraún et al., "Association of the macrophage migration inhibitory factor -173G/C polymorphism with Chagas disease," *Human Immunology*, vol. 70, no. 7, pp. 543–546, 2009.

[80] P. Aukrust, T. Ueland, F. Müller et al., "Elevated circulating levels of C-C chemokines in patients with congestive heart failure," *Circulation*, vol. 97, no. 12, pp. 1136–1143, 1998.

[81] A. Talvani, M. O. C. Rocha, L. S. Barcelos, Y. M. Gomes, A. L. Ribeiro, and M. M. Teixeira, "Elevated concentrations of CCL2 and tumor necrosis factor-α in chagasic cardiomyopathy," *Clinical Infectious Diseases*, vol. 38, no. 7, pp. 943–950, 2004.

[82] F. Villalta, Y. Zhang, K. E. Bibb, J. C. Kappes, and M. F. Lima, "The cysteine-cysteine family of chemokines RANTES, MIP-1alpha, and MIP-1beta induce trypanocidal activity in human macrophages via nitric oxide," *Infection and Immunity*, vol. 66, no. 10, pp. 4690–4695, 1998.

[83] F. S. Machado, N. S. Koyama, V. Carregaro et al., "CCR5 plays a critical role in the development of myocarditis and host protection in mice infected with Trypanosoma cruzi," *Journal of Infectious Diseases*, vol. 191, no. 4, pp. 627–636, 2005.

[84] R. Ramasawmy, E. Cunha-Neto, K. C. Faé et al., "The monocyte chemoattractant protein-1 gene polymorphism is associated with cardiomyopathy in human Chagas disease," *Clinical Infectious Diseases*, vol. 43, no. 3, pp. 305–311, 2006.

[85] J. E. Calzada, A. Nieto, Y. Beraún, and J. Martín, "Chemokine receptor CCR5 polymorphisms and Chagas' disease cardiomyopathy," *Tissue Antigens*, vol. 58, no. 3, pp. 154–158, 2001.

[86] M. T. Fernández-Mestre, S. Montagnani, and Z. Layrisse, "Is the CCR5-59029-G/G genotype a protective factor for cardiomyopathy in Chagas disease?" *Human Immunology*, vol. 65, no. 7, pp. 725–728, 2004.

[87] F. C. Dias, S. Medina Tda, C. T. Mendes-Junior et al., "Polymorphic sites at the immunoregulatory CTLA-4 gene are associated with chronic chagas disease and its clinical manifestations," *PLoS ONE*, vol. 8, no. 10, Article ID e78367, 2013.

[88] G. Zafra, O. Flórez, C. A. Morillo, L. E. Echeverría, J. Martín, and C. I. González, "Polymorphisms of toll-like receptor 2 and 4 genes in Chagas disease," *Memórias do Instituto Oswaldo Cruz*, vol. 103, no. 1, pp. 27–30, 2008.

[89] G. Robledo, C. I. González, C. Morillo, J. Martín, and A. González, "Association study of PTPN22 C1858T polymorphism in *Trypanosoma cruzi* infection," *Tissue Antigens*, vol. 69, no. 3, pp. 261–264, 2007.

[90] J. E. Calzada, A. Nieto, M. A. López-Nevot, and J. Martín, "Lack of association between NRAMP1 gene polymorphisms and *Trypanosoma cruzi* infection," *Tissue Antigens*, vol. 57, no. 4, pp. 353–357, 2001.

[91] C. Pascuzzo-Lima, J. C. Mendible, and R. A. Bonfante-Cabarcas, "Angiotensin-converting enzyme insertion/deletion gene polymorphism and progression of Chagas ' cardiomyopathy," *Revista Espanola de Cardiologia*, vol. 62, no. 3, pp. 320–322, 2009.

[92] J. E. Calzada, M. A. López-Nevot, Y. Beraún, and J. Martín, "No evidence for association of the inducible nitric oxide synthase promoter polymorphism with Trypanosoma cruzi infection," *Tissue Antigens*, vol. 59, no. 4, pp. 316–319, 2002.

[93] O. Flórez, J. Martín, and C. I. González Rugeles, "Interleukin 4, interleukin 4 receptor-α and interleukin 10 gene polymorphisms in Chagas disease," *Parasite Immunology*, vol. 33, no. 9, pp. 506–511, 2011.

[94] O. A. Torres, J. E. Calzada, Y. Beraún et al., "Role of the *IFNG* +874T/A polymorphism in Chagas disease in a Colombian population," *Infection, Genetics and Evolution*, vol. 10, no. 5, pp. 682–685, 2010.

[95] A. F. Frade, C. W. Pissetti, B. M. Ianni et al., "Genetic susceptibility to Chagas disease cardiomyopathy: involvement of several genes of the innate immunity and chemokine-dependent migration pathways," *BMC Infectious Diseases*, vol. 13, article 587, 2013.

[96] A. F. Frade, P. C. Teixeira, B. M. Ianni et al., "Polymorphism in the alpha cardiac muscle actin 1 gene is associated to susceptibility to chronic inflammatory cardiomyopathy," *PLoS ONE*, vol. 8, Article ID e83446, 2013.

[97] X. Deng, E. C. Sabino, E. Cunha-Neto et al., "Genome wide association study (GWAS) of Chagas cardiomyopathy in Trypanosoma cruzi seropositive subjects," *PLoS ONE*, vol. 8, Article ID e79629, 2013.

[98] T. Ishikawa, "Genetic variants in the human SLCO1B1 gene and individual variations in methotrexate clearance," *Pharmacogenomics*, vol. 13, no. 9, pp. 993–994, 2012.

[99] H. L. Ansorge, X. Meng, G. Zhang et al., "Type XIV collagen regulates fibrillogenesis: premature collagen fibril growth and tissue dysfunction in null mice," *The Journal of Biological Chemistry*, vol. 284, no. 13, pp. 8427–8438, 2009.

[100] D. E. Birk, J. M. Fitch, J. P. Babiarz, K. J. Doane, and T. F. Linsenmayer, "Collagen fibrillogenesis in vitro: interaction of types I and V collagen regulates fibril diameter," *Journal of Cell Science*, vol. 95, part 4, pp. 649–657, 1990.

[101] C. Depre, M. Hase, V. Gaussin et al., "H11 kinase is a novel mediator of myocardial hypertrophy in vivo," *Circulation Research*, vol. 91, no. 11, pp. 1007–1014, 2002.

[102] A. Sanbe, T. Marunouchi, T. Abe et al., "Phenotype of cardiomyopathy in cardiac-specific heat shock protein B8 K141N transgenic mouse," *The Journal of Biological Chemistry*, vol. 288, no. 13, pp. 8910–8921, 2013.

[103] D. D. Reis, E. M. Jones, S. Tostes et al., "Expression of major histocompatibility complex antigens and adhesion molecules in hearts of patients with chronic Chagas' disease," *The American Journal of Tropical Medicine and Hygiene*, vol. 49, no. 2, pp. 192–200, 1993.

[104] J. C. Aliberti, M. A. Cardoso, G. A. Martins, R. T. Gazzinelli, L. Q. Vieira, and J. S. Silva, "Interleukin-12 mediates resistance to *Trypanosoma cruzi* in mice and is produced by murine macrophages in response to live trypomastigotes," *Infection and Immunity*, vol. 64, no. 6, pp. 1961–1967, 1996.

[105] F. Torrico, H. Heremans, M. T. Rivera, E. Van Marck, A. Billiau, and Y. Carlier, "Endogenous IFN-γ is required for resistance to acute Trypanosoma cruzi infection in mice," *Journal of Immunology*, vol. 146, no. 10, pp. 3626–3632, 1991.

[106] R. T. Gazzinelli, I. P. Oswald, S. L. James, and A. Sher, "IL-10 inhibits parasite killing and nitrogen oxide production by IFN-γ-activated macrophages," *Journal of Immunology*, vol. 148, no. 6, pp. 1792–1796, 1992.

[107] U. Müller, G. Köhler, H. Mossmann et al., "IL-12-independent IFN-γ production by T cells in experimental Chagas' disease is mediated by IL-18," *Journal of Immunology*, vol. 167, no. 6, pp. 3346–3353, 2001.

[108] J. A. S. Gomes, L. M. G. Bahia-Oliveira, M. O. C. Rocha et al., "Type 1 chemokine receptor expression in Chagas' disease correlates with morbidity in cardiac patients," *Infection and Immunity*, vol. 73, no. 12, pp. 7960–7966, 2005.

[109] F. S. Machado, G. A. Martins, J. C. S. Aliberti, F. L. A. C. Mestriner, F. Q. Cunha, and J. S. Silva, "Trypanosoma cruzi-infected cardiomyocytes produce chemokines and cytokines that trigger potent nitric oxide-dependent trypanocidal activity," *Circulation*, vol. 102, no. 24, pp. 3003–3008, 2000.

[110] P. M. M. Guedes, V. M. Veloso, A. Talvani et al., "Increased type 1 chemokine expression in experimental Chagas disease correlates with cardiac pathology in beagle dogs," *Veterinary Immunology and Immunopathology*, vol. 138, no. 1-2, pp. 106–113, 2010.

Hindawi Publishing Corporation
Mediators of Inflammation
Volume 2014, Article ID 573825, 7 pages
http://dx.doi.org/10.1155/2014/573825

Research Article

IL-17-Expressing CD4$^+$ and CD8$^+$ T Lymphocytes in Human Toxoplasmosis

Jéssica Líver Alves Silva,[1] Karine Rezende-Oliveira,[2] Marcos Vinicius da Silva,[1] César Gómez-Hernández,[3] Bethânea Crema Peghini,[1] Neide Maria Silva,[4] José Roberto Mineo,[5] and Virmondes Rodrigues Júnior[1]

[1] *Course of Tropical Medicine and Infectology, Laboratory of Immunology, Federal University of Triângulo Mineiro, Avenida Frei Paulino, No. 30, 38025-180 Uberaba, MG, Brazil*
[2] *Laboratory of Biomedical Sciences, Federal University of Uberlândia, Rua 20, No. 1600, 38304-402 Ituiutaba, MG, Brazil*
[3] *Course of Tropical Medicine and Infectology, Laboratory of Parasitology, Federal University of Triângulo Mineiro, Avenida Frei Paulino, No. 30, 38025-180 Uberaba, MG, Brazil*
[4] *Laboratory of Histology and Embryology, Federal University of Uberlândia, Avenida Pará, No. 1720, 38400-902 Uberlândia, MG, Brazil*
[5] *Laboratory of Immunology, Federal University of Uberlândia, Avenida Pará, No. 1720, 38400-902 Uberlândia, MG, Brazil*

Correspondence should be addressed to Karine Rezende-Oliveira; karinerezende.oliveira@gmail.com

Received 25 April 2014; Revised 11 July 2014; Accepted 12 July 2014; Published 17 August 2014

Academic Editor: Christophe Chevillard

This study aimed to measure the synthesis of Th1 and Th2 cytokines by mononuclear cells after culture with live *T. gondii* and identified Th17 (CD4$^+$) and Tc17 (CD8$^+$) cells in toxoplasma-seronegative and toxoplasma-seropositive parturient and nonpregnant women. Cytometric bead arrays were used to measure cytokine levels (IL-2, TNF-α, IFN-γ, IL-4, IL-5, and IL-10); immunophenotyping was used to characterize Th17 and Tc17 cells, and the cells were stained with antibodies against CD4$^+$ and CD8$^+$ T cells expressing IL-17. The addition of tachyzoites to cell cultures induced the synthesis of IL-5, IL-10, and TNF-α by cells from seronegative parturient women and of IL-5 and IL-10 by cells from seropositive, nonpregnant women. We observed a lower level of IL-17-expressing CD4$^+$ and CD8$^+$ T lymphocytes in cultures of cells from seronegative and seropositive parturient and nonpregnant women that were stimulated with tachyzoites, whereas analysis of the CD4$^+$ and CD8$^+$ T cell populations showed a higher level of CD4$^+$ T cells compared with CD8$^+$ T cells. These results suggest that the cytokine pattern and IL-17-expressing CD4$^+$ and CD8$^+$ T lymphocytes may have important roles in the inflammatory response to *T. gondii*, thus contributing to the maintenance of pregnancy and control of parasite invasion and replication.

1. Introduction

Toxoplasma gondii is an obligate intracellular protozoan that causes toxoplasmosis [1], which is an opportunistic infection that may manifest during the immunosuppression/immunodepression process of the infected patient [2]. Toxoplasmosis is considered to be a disease of major clinical importance to pregnant women [3] because the parasite can be transmitted through the placenta and cause abortion or fetal malformation [4].

The main mechanism of elimination of intracellular parasites is the host Th1 immune response, which results in the production of cytokines such as interleukin-2 (IL-2), interferon-gamma (IFN-γ), tumor necrosis factor-alpha (TNF-α), and interleukin-12 (IL-12) [5]. Th17 cells, another subset of effector T cells, produce the cytokines IL-17, IL-21, and IL-22 [6, 7] and contribute to the inflammatory response during parasite infection. IL-23 is produced by cells of the innate immune system [6] and is able to induce the generation and expansion of IL-17-producing T cells [8].

Cytotoxic $CD8^+$ T cells are essential for the development of specific immune responses and may be differentiated into effector subtypes that are characterized by their cytokine expression profiles after stimulation by antigens. A different subset of $CD8^+$ cells has been related to this process, but one type, known as Tc17, can express IL-17 in the presence or absence of IFN-γ and IL-4. Phenotypic analysis shows that Tc17 cells do not express perforin or granzyme B, and they are not capable of mediating a significant *in vitro* cell lysis process, regardless of the production of their standard cytokines [9].

Therefore, it is believed that Tc17 cells have a different chemotactic activity than that observed in Th17 cells; therefore, they may migrate to inflammatory sites in response to different chemokines [10] and can be defined as a different subset of $CD8^+$ T cells with their own phenotypic and functional characteristics [11].

It is known that maternal tolerance to fetal alloantigens is characterized by the response of regulatory T cells, which are prevalent during pregnancy, that produce cytokines such as IL-4, IL-5, IL-10, and TGF-β [12–14]. Although the inflammatory process is necessary for successful implantation, a severe inflammatory process may lead to embryo reabsorption. Cells that produce/express IL-17 are involved in this process; therefore, this cytokine may influence the pathophysiology of premature labor [15].

Taking into account the modulation characteristics of Th17/Tc17 cells, particularly their role in different inflammatory-infectious processes and the possible influences they may have on pregnancy stability, this study aimed to evaluate IL-17-expressing $CD4^+$ and $CD8^+$ T lymphocytes and the levels of cytokines synthesized by mononuclear cells of the peripheral blood of parturient and nonpregnant women that had been characterized as seropositive or seronegative for *T. gondii* infection.

2. Materials and Methods

2.1. Subjects. Sixty-two women aged 20–45 years were enrolled in the present study. Among them, 14 were parturient with negative serology for *Toxoplasma gondii*, 23 were parturient and seropositive for anti-*T. gondii* antibodies, 16 were nonpregnant women who were seronegative for *T. gondii*, and 9 were nonpregnant women who were seropositive for anti-*T. gondii* antibodies. The parturient patients (3rd trimester of pregnancy) were recruited from the Outpatient Clinic of Obstetrics at the General Hospital of Federal University of Triângulo Mineiro (UFTM). Students and Immunology Laboratory staff were invited to join the nonpregnant group. The volunteers did not have other inflammatory diseases and/or acute or chronic infections, and the parturient volunteers had no complications during pregnancy and did not use any medicine. The serology for IgG and IgM anti-*T. gondii* antibodies from each volunteer was determined using chemiluminescence (Biomerieux, São Paulo, SP, Brazil), and parturient and nonpregnant women who were serologically positive for IgM anti-*T. gondii* antibodies were excluded from the study.

All volunteers signed a consent form to take part in the study. This research project was approved by the Research Ethics Committee of Federal University of Triângulo Mineiro, Brazil, under protocol number 1348 in 2009 and was conducted in accordance with the Declaration of Helsinki (1964).

2.2. Peripheral Blood Mononuclear Cells (PBMCs) of the Patients. To obtain cell suspensions, 10 mL of peripheral blood samples was collected in heparinized tubes (Vacutainer). Mononuclear cells were isolated using Ficoll-Hypaque (density: 1.074) (Invitrogen, Grand Island, New York, USA) followed by centrifugation at 400 ×g for 25 minutes at 25°C. The mononuclear cell band was subjected to a washing procedure with sterile RPMI-1640 medium (Gibco BRL, Grand Island, USA) at 400 ×g for 10 minutes at 8°C. After washing, these cells were resuspended in RPMI-1640 culture medium supplemented with 10% fetal bovine serum (FBS) (Gibco BRL), 50 mM Hepes (Gibco BRL), and 40 μL/mL Gentamicin (Schering-Plough, São Paulo, SP, Brazil) (complete RPMI). The cells were counted in a Neubauer chamber, and the final concentration was adjusted to 5×10^5 cells/mL. Cell viability was determined by 0.2% Trypan blue exclusion. Cell suspensions with viability > 90% were used in both cell culture and immunophenotyping experiments.

2.3. Preparation of In Vitro Tachyzoites. Human foreskin fibroblast (HFF) cells were cultivated in RPMI-1640 culture medium (Gibco BRL) supplemented with 5% heat-inactivated fetal bovine serum (FBS) (Gibco BRL) and 40 mg/L Garamycin (Schering-Plough). Subsequently, the cells were incubated at 37°C in a CO_2 incubator. Live tachyzoites of the low-virulence ME49 strain of *T. gondii* were used. These parasites were kept in continuous culture in confluent monolayers of HFF cells that were then infected at a ratio of 3 tachyzoites/cell. After lysis of the infected cells, the culture supernatant was collected and subjected to centrifugation at 400 ×g for 10 minutes. The sediment was suspended in supplemented RPMI-1640 medium to obtain enriched preparations of tachyzoites.

2.4. Detection of IL-17-Expressing $CD4^+$ T and $CD8^+$ T Cells. After cell concentration adjustment in a Neubauer chamber (5×10^5 cells/mL), the cells were seeded into a 96-well plate (Sarstedt, Newton, North Carolina, USA) for culturing and later identification of IL-17-producing $CD4^+$ T and $CD8^+$ T cells.

Mononuclear cells in the culture of each subject were subjected to three conditions, as follows.

(1) Unstimulated PBMCs (Negative Control). Complete RPMI-1640 medium is in a final volume of 200 μL/well.

(2) Nonspecific Stimulation with Anti-$CD3^{\pm}$ (Positive Control). 50 μL of anti-CD3 (1 mg/mL) (mouse anti-human CD3, BD Pharmingen, San Diego, USA) was added to the culture plate and incubated for 40 minutes to allow for adhesion to the plate.

(3) Specific Stimulation with Live T. gondii Tachyzoites (ME49 Strain). The concentration of parasites used to infect mononuclear cell cultures (1×10^6 parasites/well) was adjusted after counting the cells in a Neubauer chamber.

The plates were incubated in a 5% CO_2 incubator at 37°C, and after 48 hours of culture, we added 100 mL of 10% RPMI-1640 complete medium into each well of the plate. Six hours before the end of the culture, we added 1 μL GolgiStop (BD Biosciences) into the wells submitted to culture conditions 2 and 3.

The supernatant was collected for later cytokine detection. The cells that remained in the wells were suspended in the plate in 1× phosphate-buffered saline (PBS), collected, and placed in cytometry tubes (BD Biosciences). Then, a PBS/skim milk solution was added to the tubes (to block nonspecific interactions), which were incubated for 20 minutes. Subsequently, 4 μL of CD4 mouse anti-human mAb conjugated to phycoerythrin ($CD4^+$-PE) (BD Pharmingen San Diego, USA) and 4 μL $CD8^+$ mouse anti-human mAb conjugated to CD8-peridinin chlorophyll protein (PerCP) (BD Pharmingen) were added to two tubes. These tubes were stored in a dark chamber at room temperature for 20 minutes. Next, the cell solutions were washed, and 100 μL of a cell fixative and permeabilizing solution (BD Cytofix/Cytoperm Plus Fixation Kit, BD Pharmingen) was added to the pellets of each tube. Then, the solutions were incubated in a dark chamber at room temperature for 20 minutes. After incubation, the tubes were washed again, the supernatants were discarded, and 100 μL of permeabilizing solution (BD Cytofix/Cytoperm Plus Fixation Kit, BD Pharmingen) was added to the pellets of each tube, followed by the addition of 3 μL intracellular anti-IL-17 (BD Pharmingen) and staining with fluorochrome Alexa Fluor 488. All tubes were incubated in a dark chamber at room temperature for 20 additional minutes. Finally, the cells were washed with an appropriate buffer solution, and 1% PBS/formaldehyde was added to the tube.

The cells were obtained by flow cytometry using a BD FACSCalibur (Becton & Dickinson) and analyzed using the CellQuest software. To quantify the T lymphocytes, we analyzed the forward-scattered light (FSC) and side-scattered light (SSC) parameters, and the cells in the mononuclear cell gate were selected and analyzed for CD4 and CD8 expression in the $CD4^+$ and $CD8^+$ T cell populations. This analysis allowed for the collection of statistical data on the cells in the corresponding quadrants, where a new gate was established to analyze the expression of IL-17 by these cells.

2.5. Quantification of the Cytokines in the Culture Supernatants. Quantification of the cytokines IL-2, IL-4, IL-5, IL-10, IFN-γ, and TNF-α in the culture supernatants was performed using a cytometric bead array (CBA, BD Pharmingen). The supernatants were incubated in cytometry tubes containing microspheres conjugated to capture and detect antibodies for each phycoerythrin-conjugated cytokine, and sandwich complexes were formed. A standard curve was concomitantly generated for each cytokine submitted to the assay. After incubation, analyses using a FACSCalibur (Becton & Dickson) and FCAP Array software were performed. The PE fluorescence intensity of each complex point determined the concentration of each cytokine in comparison with the standard curve. The data were calculated and expressed in pg/mL. The sensitivity ranged from 1.37 pg/mL to 12.500 pg/mL.

2.6. Statistical Analysis. The data were subjected to normality and homogeneity tests. For statistical analysis, STATVIEW software was used to perform Wilcoxon tests to evaluate the variation within the same group, the Mann-Whitney test was used to evaluate the differences between two groups, and the Kruskal-Wallis test was used to evaluate differences between four groups. Differences were considered statistically significant when $P < 0.05$.

3. Results

3.1. Expression of Th1 and Th2 Cytokines Produced by Mononuclear Cells of Parturient and Nonpregnant Women Who Were Seropositive or Seronegative for Anti-T. gondii Antibodies. The production of Th1 and Th2 cytokines was analyzed in culture supernatants of mononuclear cells of peripheral blood in the absence of stimuli or in the presence of *T. gondii* tachyzoites. Analyses were performed for each group taking into account, at first, the pregnancy parameter and then previous exposure to *T. gondii*.

As shown in Figure 1, the addition of live *T. gondii* tachyzoites to cell cultures of seronegative parturient women induced positive modulation of the synthesis of IL-5, IL-10, and TNF-α ($P = 0.012$, 0.033, and 0.050, resp.) by these cells, and these levels were compared with those produced by cells of seropositive parturient women. Moreover, there was a significant increase in the production of both IL-4 ($P = 0.044$) and IL-5 ($P = 0.001$) by cells of seropositive parturient women in comparison with seronegative parturient women in unstimulated cultures. Furthermore, in unstimulated cultures, the cells of seronegative nonpregnant women produced significant levels of IL-4 ($P = 0.024$) and IL-5 ($P = 0.001$) in comparison with the cells of seronegative parturient women. The detected IL-4 levels were lower than those of other cytokines (Figures 1(a) and 1(b)).

The addition of *T. gondii* tachyzoites to cell cultures of seropositive parturient and nonpregnant women led to increased synthesis of IL-5 ($P = 0.015$) and IL-10 ($P = 0.031$) by these cells in relation to the cells of seropositive parturient women.

We did not observe a significant difference between the groups when the syntheses of IFN-γ and IL-2 were analyzed (data not shown).

3.2. Cultured IL-17-Expressing $CD4^+$ or $CD8^+$ T Cells of Parturient or Nonpregnant Patients in the Presence or Absence of Live T. gondii Tachyzoites. As shown in Figure 2, PBMC cultures infected with live tachyzoites from seropositive nonpregnant patients had significantly higher levels of IL17-expressing $CD4^+$ T cells than unstimulated cultures ($P = 0.05$). The comparison of unstimulated cell cultures of

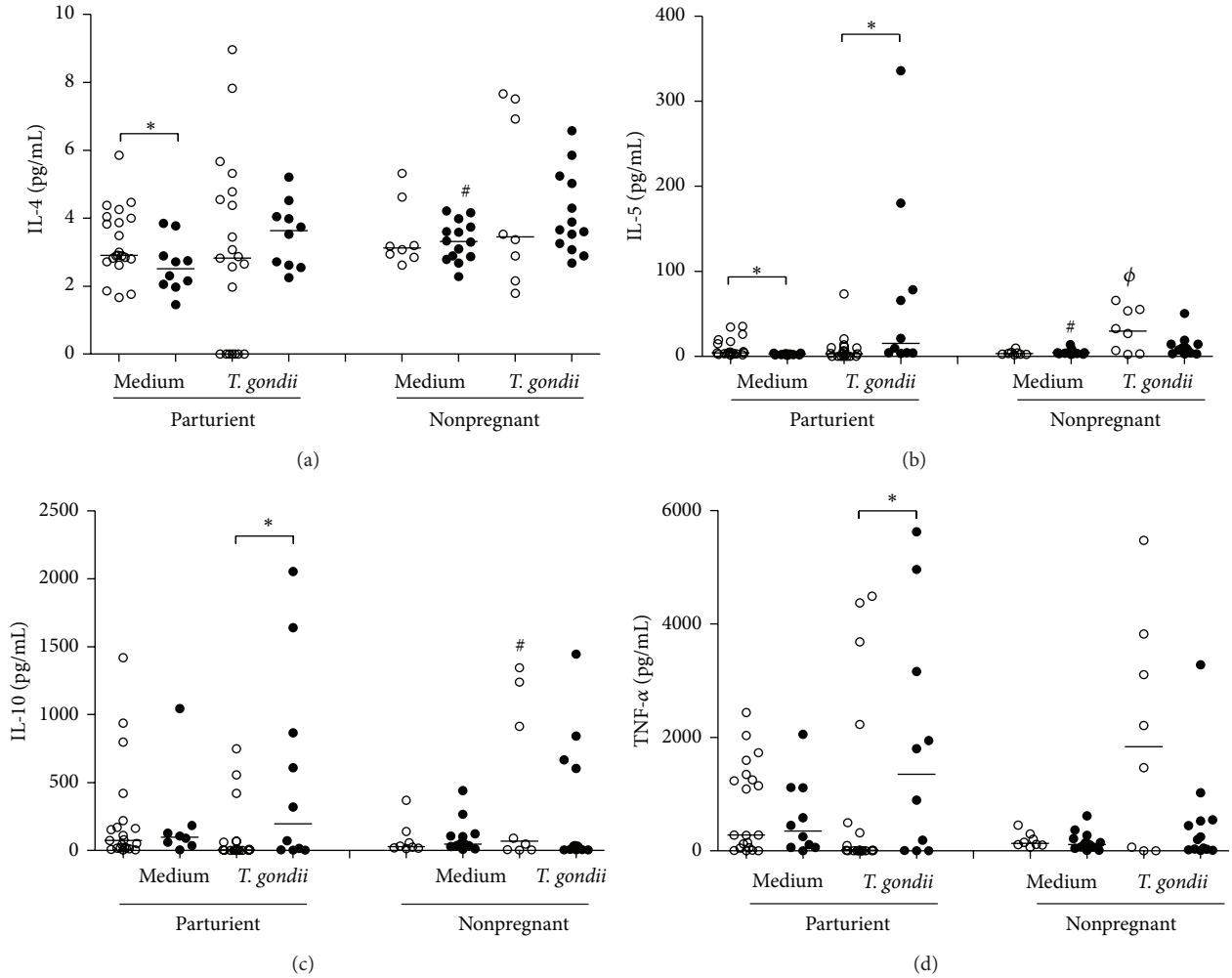

Figure 1: Cytokine production by PBMCs in culture supernatants stimulated with *T. gondii*. The horizontal line indicates the median, open circles indicate the *T. gondii* seronegative subjects, and filled circles indicate seropositive subjects. (a) *IL-4 expression from cells of seronegative and seropositive parturient women without the stimulus; $^{\#}$IL-4 expression from cells of seronegative parturient and nonpregnant women without the stimulus; (b) *IL-5 expression from cells of seronegative and seropositive parturient women without the stimulus and after stimulation with live tachyzoites; $^{\#}$IL-5 expression from cells of seronegative parturient or nonpregnant women without the stimulus; $^{\phi}$IL-5 expression from cells of seropositive parturient or nonpregnant women after stimulation with live tachyzoites; (c) *IL-10 expression from cells of seronegative or seropositive parturient women after stimulation with live tachyzoites; $^{\#}$IL-10 expression from cells of seropositive parturient or nonpregnant women after stimulation with live tachyzoites; (d) *TNF-α expression from cells of seropositive or seronegative parturient women after stimulation with live tachyzoites. ($^{*}P < 0.05$, Wilcoxon test). $^{\#,\phi}$Significant differences between the PMBCs of seropositive nonpregnant and parturient women stimulated with the *T. gondii* strain ($P < 0.05$, Mann-Whitney test).

seropositive parturient women in relation to those of nonpregnant women allowed us to observe a higher level of $CD4^+$ T cells expressing IL-17 in cultures from parturient women ($P = 0.045$) (Figures 2(a) and 2(b)).

$CD8^+$ T cell cultures from parturient women who were seropositive for anti-*T. gondii* antibodies that had not been subjected to stimuli had significant expression ($P = 0.05$) of IL-17 in comparison with nonpregnant women with the same serology (Figures 2(c) and 2(d)).

When comparing the IL-17 expression by $CD4^+$ T and $CD8^+$ T cells when live *T. gondii* tachyzoites were added or not added to the PBMC cultures of seropositive or seronegative parturient patients ($P = 0.0002$ and $P = 0.006$, resp.), a higher number of $CD4^+$ T cells than $CD8^+$ T cells expressing IL-17 were observed. After stimulation of PBMC cultures from nonpregnant women with live *T. gondii* tachyzoites, we observed a higher level of $CD4^+$ T cells than $CD8^+$ T cells expressing IL-17, regardless of the serology of the patients ($P = 0.007$) (Figure 2(e)).

4. Discussion

During pregnancy, cytokine production by maternal cells may vary according to the trimester of pregnancy [15]. Due to this variation in cytokine production, parturient women may become immunologically vulnerable and may be stricken by

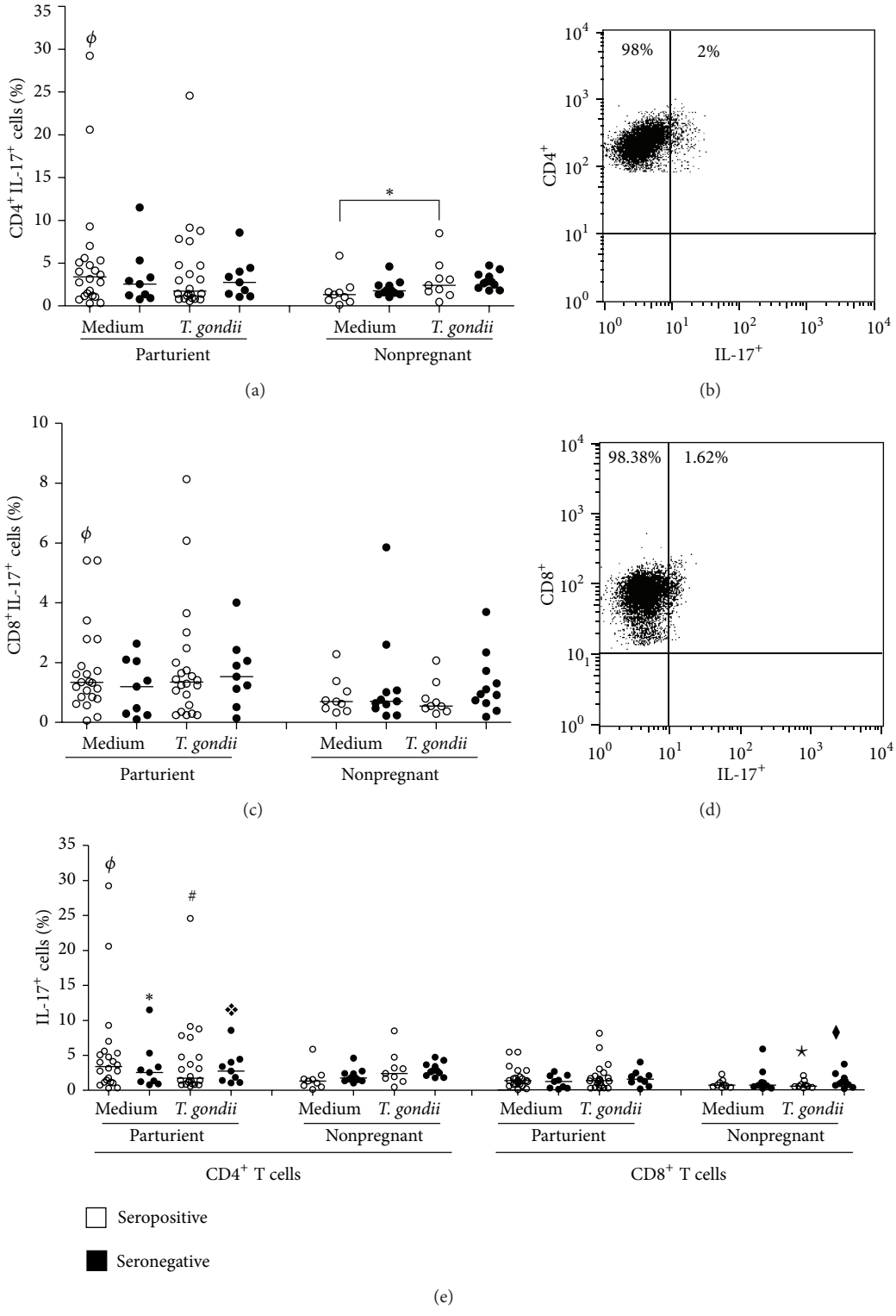

FIGURE 2: IL-17$^+$CD4$^+$ T cells and IL-17$^+$CD8$^+$ T cells from nonpregnant or parturient women. The horizontal line indicates the median, open circles indicate the *T. gondii* seronegative subjects, and filled circle indicate seropositive subjects. (a) The percentage of CD4$^+$ T cells expressing IL-17. (c) The percentage of CD8$^+$ T cells expressing IL-17. (e) Comparison CD4$^+$ T cells and CD8$^+$ T cell expressing IL-17. One representative dot-plot from each is shown ((b)—seropositive, nonpregnant, and unstimulated × *T. gondii* stimulated), ((d)—seropositive, parturient, unstimulated × seropositive, nonpregnant, and unstimulated). Gated on CD4$^+$ and CD8$^+$ T cells. The horizontal line indicates the median, bars indicate the 25% and 75% percentiles, and vertical lines indicate the 10% and 90% percentiles. ($^*P < 0.05$, Wilcoxon test). $^{\clubsuit,\star,\blacklozenge,\phi}$Significant differences between PMBCs of seropositive, nonpregnant and parturient women stimulated with *T. gondii* strain ($P < 0.05$, Mann-Whitney test).

diseases such as toxoplasmosis, which can be transmitted to the fetus during primary infection [16].

The present study showed that mononuclear cells of seronegative parturient women cultured with *T. gondii* tachyzoites produced significant levels of IL-5, IL-10, and TNF-α compared with the cells of seropositive parturient women. This work demonstrated the Th2 cytokine production after challenge by a nonvirulent strain of *T. gondii*, which makes this study distinct from the other by our group, where we analyzed the behavior and antigenic capacity of two distinct strains of *T. gondii* (a virulent and a nonvirulent strain) to stimulate the production of Th1 cytokines [17].

We noticed that the addition of tachyzoites to the culture led to a significant increase in the levels of TNF-α that were produced by cells of seronegative parturient women in relation to seropositive parturient women [17]. In another study, cells of seronegative nonpregnant women were shown to synthesize significant levels of IL-10 after the addition of tachyzoites to the culture. The present assay revealed that the addition of live parasites to the culture induced an increase in IL-10 synthesis by cells of seropositive nonpregnant women, which is an outcome that differs from the findings of our previous study. IL-10 has proved to be important in the preservation of tissue integrity in several experimental models of infectious diseases, including toxoplasmosis [18].

Matowicka-Karna et al. [19, 20] showed that nonpregnant women who were seropositive for *T. gondii* antibodies had significantly higher levels of IL-5 than seronegative women. Similar results were demonstrated in our study, which showed that cells from seropositive parturient women produced higher levels of IL-5 than those from seronegative parturient women. However, when the cell culture was infected with live tachyzoites, the IL-5 levels were reduced, suggesting that parasitic mechanisms may influence cytokine production.

The lower amounts of detected IL-4 may be related to gestational age (parturient), which is characterized by a proinflammatory or period of cell culture (nonpregnant). Even though they were at low levels, we observed increased IL-4 in the supernatant of seropositive parturient cells compared with seronegative cells, suggesting that the presence of a parasite can modulate cytokine synthesis, resulting in increased susceptibility to *T. gondii* infection.

The levels of IL-17 were not measured due to the period that the cells were maintained in culture when conducting this study.

In the present study, we found a higher level of $CD4^+$ T cells than $CD8^+$ T cells expressing IL-17 (Th17) in cell cultures of parturient and nonpregnant women, regardless of their serology status for anti-*T. gondii* antibodies. The analysis of IL-17 synthesis by $CD8^+$ and $CD4^+$ T cells in healthy adult individuals demonstrates that the level of IL-17-producing $CD8^+$ T cells was lower than that of $CD4^+$ T cells [21]. During pregnancy, significant amounts of IL-17-producing $CD4^+$ T cells are present, and there is no variation in the number of these cells between the second and third trimesters of pregnancy [21, 22].

The percentage of $CD4^+$ T cells that expressed IL-17 is significantly higher in the placenta of pregnant mice infected with *T. gondii* than in control mice [23]. In this study, we observed that there was a higher level of $CD4^+$ and $CD8^+$ T cells expressing IL-17 in PBMC cultures of seropositive parturient women who were infected with live *T. gondii* tachyzoites than in the unstimulated culture.

PBMC cultures of nonpregnant women who were seropositive for anti-*T. gondii* antibodies significantly expressed IL-17 by $CD4^+$ T cells (Th17) in cultures stimulated with live *T. gondii* tachyzoites, which is in consonance with results from Kelly et al. [24], who found that mice infected with *T. gondii* are capable of inducing a significant immune response, which is stimulated by IL-17, against parasites in the early stages of infection.

Furthermore, PBMC cultures of parturient and nonpregnant women, regardless of their serology, had a significant number of $CD8^+$ T cells expressing IL-17. Few studies have investigated the main functions in this cellular phenotype [25].

This is the first study about a repertoire of IL-17-expressing $CD4^+$ and $CD8^+$ T lymphocytes and the production of Th2 cytokines related to human pregnancy and *T. gondii* infection. Our results suggest that these cells and cytokines may display an important role in the inflammatory response by contributing to the process of pregnancy maintenance and control of parasite invasion and replication.

Conflict of Interests

The authors declare that there is no conflict of interests regarding the publication of this paper.

Authors' Contribution

Jéssica Líver Alves Silva and Karine Rezende-Oliveira contributed equally to this work.

Acknowledgments

The authors thank *Fundação de Ensino e Pesquisa de Uberaba* (FUNEPU, Research Foundation of Uberaba), *Coordenação de Aperfeiçoamento de Pessoal de Nivel Superior* (CAPES, Coordination for the Improvement of Higher Education Personnel Foundation), *Conselho Nacional de Desenvolvimento Cientifico e Tecnológico* (CNPq, National Counsel of Technological and Scientific Development), and *Fundação de Amparo a Pesquisa do Estado de Minas Gerais* (FAPEMIG, Research Foundation of the State of Minas Gerais) for financial support.

References

[1] C. Nicolle and L. Manceaux, "Sur un protozoaire nouveau du gondi: *toxoplasma*," *Seances Academy Scientific*, vol. 148, pp. 369–372, 1909.

[2] L. M. Weiss and K. Kim, *Toxoplasma Gondii. The Model Apicomplexan: Perspectives and Metods*, A. Press, 1st edition, 2007.

[3] J. P. Dubey, "Toxoplasmosis—a waterborne zoonosis," *Veterinary Parasitology*, vol. 126, no. 1-2, pp. 57–72, 2004.

[4] B. J. Luft and J. S. Remington, "Toxoplasmic encephalitis in AIDS," *Clinical Infectious Diseases*, vol. 15, no. 2, pp. 211–222, 1992.

[5] R. T. Gazzinelli, F. T. Hakim, S. Hieny, G. M. Shearer, and A. Sher, "Synergistic role of CD4+ and CD8+ T lymphocytes in IFN-γ production and protective immunity induced by an attenuated *Toxoplasma gondii* vaccine," *Journal of Immunology*, vol. 146, no. 1, pp. 286–292, 1991.

[6] T. Korn, E. Bettelli, M. Oukka, and V. K. Kuchroo, "IL-17 and Th17 cells," *Annual Review of Immunology*, vol. 27, pp. 485–517, 2009.

[7] D. Mesquita Junior, J. A. Araujo, T. T. Catelan et al., "Immune system—part II: basis of the immunological response mediated by T and B lymphocytes," *Revista Brasileira de Reumatologia*, vol. 50, no. 5, pp. 552–580, 2010.

[8] D. J. Cua, J. Sherlock, Y. Chen et al., "Interleukin-23 rather than interleukin-12 is the critical cytokine for autoimmune inflammation of the brain," *Nature*, vol. 421, no. 6924, pp. 744–748, 2003.

[9] H. R. Yen, T. J. Harris, S. Wada et al., "Tc17 CD8 T cells: functional plasticity and subset diversity," *Journal of Immunology*, vol. 183, no. 11, pp. 7161–7168, 2009.

[10] H. Tomiyama, H. Takata, T. Matsuda, and M. Takiguchi, "Phenotypic classification of human CD8+ T cells reflecting their function: Inverse correlation between quantitative expression of CD27 and cytotoxic effector function," *European Journal of Immunology*, vol. 34, no. 4, pp. 999–1010, 2004.

[11] M. Huber, S. Heink, H. Grothe et al., "Th17-like developmental process leads to $CD8^+$ Tc17 cells with reduced cytotoxic activity," *European Journal of Immunology*, vol. 39, no. 7, pp. 1716–1725, 2009.

[12] S. Saito, "Cytokine network at the feto-maternal interface," *Journal of Reproductive Immunology*, vol. 47, no. 2, pp. 87–103, 2000.

[13] P. Luppi, "How immune mechanisms are affected by pregnancy," *Vaccine*, vol. 21, no. 24, pp. 3352–3357, 2003.

[14] S. Schäfer-Somi, "Cytokines during early pregnancy of mammals: a review," *Animal Reproduction Science*, vol. 75, no. 1-2, pp. 73–94, 2003.

[15] S. Saito, A. Nakashima, T. Shima, and M. Ito, "Th1/Th2/Th17 and Regulatory T-Cell Paradigm in Pregnancy," *The American Journal of Reproductive Immunology*, vol. 63, no. 6, pp. 601–610, 2010.

[16] P. J. Gaddi and G. S. Yap, "Cytokine regulation of immunopathology in toxoplasmosis," *Immunology and Cell Biology*, vol. 85, no. 2, pp. 155–159, 2007.

[17] K. Rezende-Oliveira, N. M. Silva, J. R. Mineo, and V. Rodrigues Junior, "Cytokines and chemokines production by mononuclear cells from parturient women after stimulation with live *Toxoplasma gondii*," *Placenta*, vol. 33, no. 9, pp. 682–687, 2012.

[18] R. T. Gazzinelli, M. Wysocka, S. Hieny et al., "In the absence of endogenous IL-10, mice acutely infected with Toxoplasma gondii succumb to a lethal immune response dependent on CD4+ T cells and accompanied by overproduction of IL-12, IFN-γ, and TNF-α," *Journal of Immunology*, vol. 157, no. 2, pp. 798–805, 1996.

[19] J. Matowicka-Karna, V. Dymicka-Piekarska, and H. Kemona, "Does *Toxoplasma gondii* infection affect the levels of IgE and cytokines (IL-5, IL-6, IL-10, IL-12, and TNF-alpha)?" *Clinical and Developmental Immunology*, vol. 2009, Article ID 374696, 4 pages, 2009.

[20] J. Matowicka-Karna, H. Kemona, and A. Panasiuk, "The evaluations of concentrations IL-5 and IL-6 in toxoplasmosis," *Wiadomości Parazytologiczne*, vol. 50, no. 3, pp. 417–423, 2004.

[21] T. Kondo, H. Takata, F. Matsuki, and M. Takiguchi, "Cutting edge: Phenotypic characterization and differentiation of human $CD8^+$ T cells producing IL-171," *Journal of Immunology*, vol. 182, no. 4, pp. 1794–1798, 2009.

[22] A. Nakashima, M. Ito, A. Shiozaki, T. Hidaka, and S. Saito, "Circulating and decidual levels in healthy," *American Journal of Reproductive Immunology*, vol. 63, no. 2, pp. 104–109, 2009.

[23] H. Zhang, X. Hu, X. Liu, R. Zhang, Q. Fu, and X. Xu, "The Treg/Th17 imbalance in *Toxoplasma gondii*-infected pregnant mice," *American Journal of Reproductive Immunology*, vol. 67, no. 2, pp. 112–121, 2012.

[24] M. N. Kelly, J. K. Kolls, K. Happel et al., "Interteukin-17/interleukin-17 receptor-mediated signaling is important for generation of an optimal polymorphonuclear response against *Toxoplasma gondii* infection," *Infection and Immunity*, vol. 73, no. 1, pp. 617–621, 2005.

[25] S. P. Singh, H. H. Zhang, J. F. Foley, M. N. Hedrick, and J. M. Farber, "Human T cells that are able to produce IL-17 express the chemokine receptor CCR6," *Journal of Immunology*, vol. 180, no. 1, pp. 214–221, 2008.

Hindawi Publishing Corporation
Mediators of Inflammation
Volume 2014, Article ID 952857, 15 pages
http://dx.doi.org/10.1155/2014/952857

Research Article

Trypanosoma cruzi Infection in Genetically Selected Mouse Lines: Genetic Linkage with Quantitative Trait Locus Controlling Antibody Response

Francisca Vorraro, Wafa H. K. Cabrera, Orlando G. Ribeiro, José Ricardo Jensen, Marcelo De Franco, Olga M. Ibañez, and Nancy Starobinas

Laboratório de Imunogenética, Instituto Butantan, Avenida Vital Brasil 1500, 05503-900 São Paulo, SP, Brazil

Correspondence should be addressed to Nancy Starobinas; nancy.starobinas@butantan.gov.br

Received 24 April 2014; Revised 15 July 2014; Accepted 16 July 2014; Published 13 August 2014

Academic Editor: Christophe Chevillard

Trypanosoma cruzi infection was studied in mouse lines selected for maximal (AIRmax) or minimal (AIRmin) acute inflammatory reaction and for high (H_{III}) or low (L_{III}) antibody (Ab) responses to complex antigens. Resistance was associated with gender (females) and strain—the high responder lines AIRmax and H_{III} were resistant. The higher resistance of H_{III} as compared to L_{III} mice extended to higher infective doses and was correlated with enhanced production of IFN-γ and nitric oxide production by peritoneal and lymph node cells, in H_{III} males and females. We also analyzed the involvement of previously mapped Ab and *T. cruzi* response QTL with the survival of Selection III mice to *T. cruzi* infections in a segregating backcross [F1($H_{III} \times L_{III}$)×L_{III}] population. An Ab production QTL marker mapping to mouse chromosome 1 (34.8 cM) significantly cosegregated with survival after acute *T. cruzi* infections, indicating that this region also harbors genes whose alleles modulate resistance to acute *T. cruzi* infection.

1. Introduction

The protozoan *Trypanosoma cruzi*, the causative agent of Chagas' disease in humans, parasitizes several other mammalian species. After infection with *T. cruzi*, the parasites survive and multiply in nucleated cells as amastigotes, eventually reaching the bloodstream as trypomastigote forms. The acute infection phase is characterized by high levels of circulating parasites, while parasite proliferation is contained during the chronic phase [1].

Innate immune responses play critical roles in the control of parasite spreading and host survival. Toll-like receptor (TLR) family of pattern recognition receptors (PRRs) plays a central role in the recognition of *T. cruzi* by the immune system [2]; TLR4 [3], TLR2 [4–6], TLR9 [7], and TLR7 [8] initiate a signaling cascade that culminates in the activation of proinflammatory genes which are important for resistance to *T. cruzi* infection [9].

NOD1, a member of the cytosolic NOD-like receptor (NLR) family, also plays a role in controlling *T. cruzi* infection; *Nod1*−/− mice were shown to be very susceptible to *T. cruzi,* succumbing to the infection and displaying higher parasitemia and parasite loads in the spleen and heart tissues [10].

Recent works suggest that ASC inflammasomes are critical determinants of host resistance to *T. cruzi* infection [11]; moreover NLRP3 inflammasome controls parasitemia by inducing NO production via a caspase-1-dependent, IL-1R-independent pathway [12].

The early control of replication depends largely on nitric oxide (NO) induction in macrophages mediated by gamma-interferon (IFN-γ) and tumor necrosis factor alpha (TNF-α). IFN-γ is synthesized shortly after infection, mainly by IL-12 and TNF-α activated NK cells [13–16]. The *in vivo* inhibition of iNOS results in increased susceptibility to parasites [17, 18].

The effector mechanisms that control parasite loads and survival during the acute infection phase also depend on specific cell-mediated immune responses. Mice depleted or deficient in CD4 or CD8 lymphocytes show early mortality and increased numbers of parasites in their bloodstreams and

tissues [19–21]. As a mechanism of evasion during *T. cruzi* replication they release immunomodulatory molecules that delay parasite-specific responses mediated by effector T cells [22].

Resistance to *T. cruzi* infection in humans as well as mice may vary according to the genetic background of the host and the virulence of the parasite strain [23, 24]. Genetic control of responses to *T. cruzi* is governed by multiple genes, and mice of different strains can develop infections that evolve towards either early death or a chronic phase [25].

Silva et al. [26] recently analyzed the susceptibility of several inbred mouse lines to infection with the Y strain of *T. cruzi* and found that susceptibility varied among those lines, especially between A/J and C57BL/6 mice. A/J mice are extremely susceptible, with 100% death rates, whereas C57BL/6 mice are resistant. Data obtained with an F1 (A/J x C57BL/6J) population suggested the existence of one or more loci mapping on chromosome X that contribute to resistance to *T. cruzi* infections.

In addition to these inbred mouse lines, the involvement of different genetic backgrounds in infection control has been analyzed in mice lines selected for either high (H) or low (L) antibody responses and maximal (AIRmax) and minimal (AIRmin) acute inflammatory reactivity (AIR). Starting from a genetically heterogeneous founder population (F_0) of Albino Swiss mice, the selection of lines for antibody responsiveness (named Selection III) was carried out using assortative mating in successive generations based on secondary antibody response to *Salmonellae* flagellar antigens. This bidirectional selective pressure resulted in the accumulation of alleles at multiple quantitative trait loci (QTLs) in each H and L line endowed with opposite modulatory effects on the various steps of antibody biosynthesis [27]. The differences in antibody responses between H_{III} and L_{III} lines are not restricted just to the selection immunogen but encompass a wide range of complex antigens, showing evidence for multispecific effects of the relevant genes [28, 29]. Genetic analyses indicated that 5–10 QTLs regulate the antibody production phenotype, and a QTL mapping experiment using microsatellite markers yielded three highly significant QTLs on chromosomes 3, 8, and 9 [30]. H_{III} and L_{III} lines also show extreme divergence in other phenotypes, such as skin carcinogenesis [31] and pristane induced arthritis—PIA. Our group successfully detected a PIA-susceptibility QTL on chromosome 3 by examining the cosegregation of the most significant Ab QTL markers with arthritis phenotypes [32].

Selection for acute inflammatory response was carried out in a similar manner, using polyacrylamide beads (Biogel P-100), with induced local inflammatory influx and exudated protein concentrations as the selection phenotypes [33, 34]. Analysis of this selective process indicated that AIR regulation involves at least 11 QTLs [35]. Significant interline differences were also observed in response to several phlogistic agents, including carrageenan, zymosan, and inactivated bacteria [35]. These mouse lines have been used to study the effects of genetic control of nonspecific immunity on susceptibility to neoplastic [36], autoimmune [37], and infectious diseases [38].

The selective process did not affect specific immune responses, as both AIRmax and AIRmin mice produced similar amounts of antibodies after immunization with optimal doses of complex antigens (such as heterologous proteins and bacterial antigens). Cell-mediated immune responses, such as T-cell specific proliferation and delayed-type hypersensitivity reactions, were also similar in both lines. On the other hand, these lines differ in natural resistance to pristane induced arthritis [37], various bacterial infections [38], lung [39], kidney [40], and colon [41] chemical carcinogenesis, as well as wound-healing capacities [42].

The relative contributions of innate and specific immune responses to *T. cruzi* infections have not yet been determined, nor their genetic influences on infection susceptibility. In this study we analyzed the relationships between the genetic controls involved in antibody production and inflammatory responses and resistance to *T. cruzi* infection by examining the course of parasite infection in mice selected for high (H_{III}) and low (L_{III}) antibody responses (Selection III) or for maximal (AIRmax) and minimal (AIRmin) acute inflammatory responses (AIR).

2. Materials and Methods

2.1. Mice and Crosses. Male and female 8–12-week-old mice were used in all experiments. All stock mice and crosses used were developed and maintained at the animal facilities of the Immunogenetics Laboratory at the Butantan Institute, São Paulo State, Brazil. All animals received humane care according to criteria outlined in the Ethical Principles in Animal Research Guidelines adopted by the Brazilian College of Animal Experimentation. Experiments were approved (protocol no. 066/02) by the Committee on Ethics in the use of Animals of the Biomedical Sciences Institute—USP.

AIRmax and AIRmin mice were selected from a polymorphic foundation population constructed by the balanced intercrossing of eight inbred mouse lines (A/J, DBA2/J, SWR/J, CBA/J, SJL/J, BALB/cJ, P/J, and C57BL/6J), as described in detail elsewhere [35]. Although the formal stock designations are Ibut : AIRH and Ibut : AIRL, we refer to them in this paper and in previous publications as AIRmax and AIRmin, respectively.

The selection for high (H_{III}) and low (L_{III}) antibody responder mice (Selection III) was described in detail elsewhere [27].

Inbred H_{III} and L_{III} lines derived from their respective outbred stocks were used to produce F1 ($H_{III} \times L_{III}$) hybrid mice and 242 backcrossed ($F1 \times L_{III}$) segregating (Bc-L) mice for genetic studies.

Nonselected Swiss Albino male mice purchased from the Central Animal Facilities at the Butantan Institute were used for *in vivo* maintenance of *T. cruzi*.

2.2. Experimental Infections, Mortality Rates, and Parasitemia Determinations. The CL strain of *Trypanosoma cruzi* was used in all experiments. The parasite was maintained *in vivo* by serial passage of the parasite blood forms in Swiss Albino mice.

Mice were s.c. infected with *T. cruzi* blood forms diluted at the indicated concentrations in 100 μL PBS buffer and monitored daily for deaths. Parasitemia levels were determined by hemocytometer counts of trypomastigotes in fresh blood samples diluted in ammonium oxalate (1%).

2.3. Cell Cultures. Mice were euthanized at 0, 7, 15, and 20 days after infection with 1×10^2 parasites. Their peritoneal cavities were washed with 5 mL of PBS under sterile conditions, and the cells were pelleted and then resuspended in complete RPMI-1640 medium (RPMI-1640 supplemented with 2 mM L-glutamine, 10 g/mL gentamicin, and 10% fetal calf serum). The cells (2×10^5/well) were cultured for 48 h at 37°C and 5% CO_2 in a final volume of 100 μL/well in 96-well flat-bottom plates with or without stimulation with ConA (2.5 μg/mL).

Lymph node and spleen cell suspensions were obtained by homogenizing those organs in glass grinders with RPMI-1640 medium under sterile conditions and then washing and diluting the cells to 1×10^7 cells/mL in modified Click medium (RPMI-1640 supplemented with 0.05 mM 2-mercaptoethanol, 2 mM L-glutamine, 1 mM sodium pyruvate, 10 g/mL gentamicin, and 2% heat-inactivated normal mouse serum) to a final volume of 1 mL/well in 24-well flat-bottom plates. The cells were stimulated with ConA (2.5 μg/mL) and cultured for 48 h at 37°C and 5% CO_2. Cell-free culture supernatants were harvested and stored at −20°C.

2.4. IFN-γ Detection. Unlabeled XMG1.2 (5 μg/mL) and biotinylated AN-18 (5 μg/mL) rat anti-mouse IFN-γ monoclonal antibodies were used in two-site sandwich ELISA assays using an alkaline avidin-phosphatase and p-nitrophenyl phosphate substrate in Tris-NaCl buffer to detect IFN-γ contents in supernatants of 48-hour cultured lymph node or spleen cells. Absorbance at 405 nm was measured in a Multiskan MS plate reader (Labsystems, Finland), and IFN-γ concentrations were determined by comparisons with a standard curve obtained from serial dilutions of recombinant IFN-γ.

2.5. Nitric Oxide (NO) Quantification. Forty-eight-hour cell-free peritoneal culture supernatants were assayed for NO_2 using the Griess reaction. Briefly, 50 μL of culture supernatant was incubated with 50 μL of a mixture of 1% sulfanilamide and 0.1% N-(1-naphthyl) ethylenediamine dihydrochloride in 2.5% orthophosphoric acid (H_3PO_4) at room temperature for 10 min. Absorbance was measured at 540 nm using a Multiskan MS plate reader (Labsystems); the micromolar concentrations of NO_2 were determined by interpolation from a $NaNO_2$ standard curve.

2.6. Quantification of T. cruzi DNA in Cardiac Muscle by Real-Time PCR. Genomic DNA from mouse cardiac muscle was isolated using DNeasy Tissue kit (Qiagen, Germany) following the manufacturer's instructions. The primer pairs TCZ-F: 5′-GCT CTT GCC CAC CMG GGT GC-3′ (where M = A or C) and TCZ-R: 5′-CCA AGC AGC GGA TAG TTC AGG-3′ were used in qPCR to detect the target *T. cruzi* 195-bp repeat DNA in the cardiac muscles of infected mice. In parallel, primers for the murine specific TNF-single copy genomic sequence (TNF-5241: 5′-TCC CTC TCA TCA GTT CTA TGG CCC A-3′ and TNF-5411: 5′-CAG CAA GCA TCT ATG CAC TTA GAC CCC-3′) were used in a parallel assay as an internal control to normalize the amount of host DNA loaded in each reaction, as described by Cummings and Tarleton [43].

Normalization was obtained by calculating the ratios of the concentrations of target *T. cruzi* DNA and murine TNF-reference gene DNA in the same tissue sample.

Real-time PCR was carried out with 65 ng of sample DNA, 12.5 μL QuantiTect SYBR Green PCR Master Mix (Qiagen), 0.5 M of each primer, and nuclease-free water to a final volume of 25 μL. The reactions were run in a PTC-200 thermocycler (MJ Research, Inc., USA) with an initial step of 15 min at 95°C followed by 50 denaturation cycles (20 s at 95°C), annealing (20 s at 55°C), and extension (1 min. at 72°C). Fluorescence intensity was detected at the end of each extension phase using a Chromo 4 detector (MJ Research). Melt curves of the products were obtained after the amplification phase. All data was analyzed using Opticon Monitor Analysis Software v2.03 (MJ Research).

In order to estimate target *T. cruzi* DNA concentrations (and therefore the parasite load of each sample), a standard curve was constructed through serial dilutions (ranging from 10,000 to 10 parasite equivalents) of gDNA obtained from uninfected cardiac tissue with 10^4 *T. cruzi* trypomastigotes artificially added. The standard curve derived from these dilutions (log transformed) indicated the amounts of parasite equivalents in each sample (adapted from [43]).

2.7. Genotyping the Polymorphic Microsatellite Markers of Antibody-Controlling QTL (Ab QTL) in Selection III. For genomic DNA extraction, frozen mouse tail tips were incubated at 65°C for 1 h in 100 μL of lysis buffer containing 50 mM Tris-HCl (pH 8.0), 10 mM EDTA (pH 8.0), 0.5% SDS, with 1.5 mg/mL proteinase K (Invitrogen). Following another addition of 100 μL of lysis buffer, incubation for 15 min, and centrifugation (13,000 ×g/10 min), the supernatants were mixed with 0.1 volumes of 3 M sodium acetate (pH 5.2) and 2 volumes of 100% ethanol. The precipitated DNA was washed, dried at room temperature, and dissolved in sterile nuclease-free water.

The genotyping of the Ab QTL microsatellite markers, as described by De Souza et al. [30], was carried out by PCR amplification of 100 ng of DNA using specific primers (Research Genetics, Birmingham, CA). PCR reactions were incubated for 2 min at 94°C, followed by 35 cycles of 30 s/94°C, 35 s/55–57°C, and 45 s/72°C, followed by a final extension for 7 min at 72°C. Individual genotypes of the 242 backcrossed (Bc-L_{III}) mice for each marker were determined by comparing their PCR fragment sizes (as visualized in 4.5% agarose gels) with those of the parental lines.

2.8. Statistical and Genetic Analyses. Groups of infected mice were submitted to Survival Analysis. Means were compared by analysis of variance (ANOVA) and multiple comparison

Tukey post hoc tests. Differences between the groups were indicated when $P < 0.05$.

Individual genetic and phenotypic data from the 242 Bc-L_{III} segregant mice were analyzed using MapManager QTX software [44, 45] to determine the significance of the association between marker genotypes and the *T. cruzi* infection phenotypes. Due to the striking gender difference in infection survival, the $\log_n$ normalized data was analyzed considering sex as a covariate for traits.

Critical LRS (likelihood ratio statistic) values corresponding to suggestive ($P < 0.63$), significant ($P < 0.05$), or highly significant ($P < 0.001$) linkage [46] were determined by Random Permutation Testing [47].

3. Results

3.1. Mortality Rates. Mortality rates, monitored at doses ranging from 10 to 10^4 blood forms, showed marked gender-related differences in susceptibility to acute infection in all of the mouse lines analyzed. Males were more susceptible than their respective littermate females (Figures 1 and 2). In addition, we observed divergent levels of resistance in both the AIR (Figure 1) and Selection III (Figure 2) lines.

AIRmax males were significantly more resistant to infection with 10 parasites than AIRmin males (Figure 1(a)), while no differences were observed at higher infective doses (Figures 1(b) and 1(c)). AIRmax females were likewise more resistant than AIRmin females, showing no mortality when challenged with 10 and 10^2 parasites; AIRmin females inoculated with 10^2 trypomastigotes showed high mortality rates (Figure 1(b)) and different survival curves. Infection with more than 10^2 parasites, however, resulted in similar susceptibilities in females of both AIR lines (Figure 1(c)).

Both H_{III} and L_{III} male mice had high and similar mortality rates (Figures 2(a), 2(b), and 2(c)) when infected. L_{III} male mice died earlier than H_{III} animals, however, resulting in significantly different survival curves when infected with 10, 10^2, and 10^4 parasites.

Female H_{III} mice were more resistant than L_{III} females independent of the challenge dose, with clearly different survival curves and mortality rates (Figures 2(a), 2(b), and 2(c)). While only one H_{III} female died when challenged with the highest dose, mortality was already significant at the lowest dose among L_{III} females, reaching 100% after challenges with 10^4 parasites. Female L_{III} mice mortality was similar to that of the extremely susceptible L_{III} males (Figure 2(c)).

3.2. Parasitemia. Males and females of all mouse lines tested developed similar parasitemia peaks in acute *T. cruzi* infections, independent of initial parasite challenges (representative plots for the 10^2 dose are shown in Figure 3).

Differences related to both gender and lines were observed in parasite-clearance in these mice. Thus, except for a few AIRmax males that cleared blood parasite forms to undetectable levels, the other males died after acute infection (showing high levels of circulating parasites).

High percentages of females from AIRmin (60%) and L_{III} (100%) susceptible lines died without showing any effective control of parasitemia levels, whereas all females of resistant AIRmax and H_{III} lines cleared blood parasites during acute *T. cruzi* infection.

Differences in parasitemia control among H_{III} and L_{III} females in the acute infection phase were not correlated with parasite loads in cardiac tissue in the late phase (150 days after challenging) (Figure 4). This correlation could not be determined in males because all L_{III} males died during the acute phase. Gender-related differences were observed in H_{III} mice in terms of the amounts of *T. cruzi* genomic DNA found in their cardiac tissue, with higher values being found in males than in females of both lines (Figure 4). This data indicates that males differ from females not only in terms of the lethality of infection and of parasitemia control, but also in terms of parasite burdens in heart tissue.

3.3. Gamma Interferon and NO Production. Production of IFN-γ and nitric oxide (NO) in the acute phase of *T. cruzi* infection was investigated to evaluate whether these mediators were associated with the different levels of infection resistance in mice selected for AIR or Ab response phenotypes.

Increases in both IFN-γ and NO production were observed in infected AIRmax and AIRmin mice, but the increases were similar in both lines and did not correlate with either strain-related or gender-related differences in resistance (data not shown).

Lines selected for Ab response, on the other hand, showed distinct IFN-γ production patterns that increased significantly at 7 days and remained elevated 15 days after infection in H_{III} males and females; in L_{III} mice, IFN-γ production was similar to noninfected control levels at all time points (Figure 5(a)). Our data also suggests that IFN-γ production influences NO synthesis during acute infection as increases in this trypanocidal mediator were observed in both H_{III} males and females (Figure 5(b)) after, or at the same time as, IFN-γ detection. NO levels did not differ between infected and control L_{III} mice. Similar profiles of IFN-γ and NO secretion were observed with lymph node, peritoneal, and spleen cells (data not shown). Interestingly, we observed the same patterns of IFN-γ and NO production with males and their littermate females, so that no correlations between the production of these mediators and gender-related resistance to infection could be established in any of the mouse lines studied.

3.4. QTL Analyses of Responses to T. cruzi Infection. The quantitative trait *loci* (QTLs) controlling Ab production in Selection III lines had been previously mapped in genome-wide screening with polymorphic genetic markers (microsatellites) [18]. We therefore investigated the participation of these chromosomal regions in the response to *T. cruzi* infection. Inbred subpopulations of H_{III} and L_{III} lines that showed the same resistance pattern to *T. cruzi* infections as the outbred parental lines described above were used for this purpose.

F1 ($H_{III} \times L_{III}$) hybrids, obtained by reciprocal crosses (H_{III} males X L_{III} females or H_{III} females x L_{III} males), showed

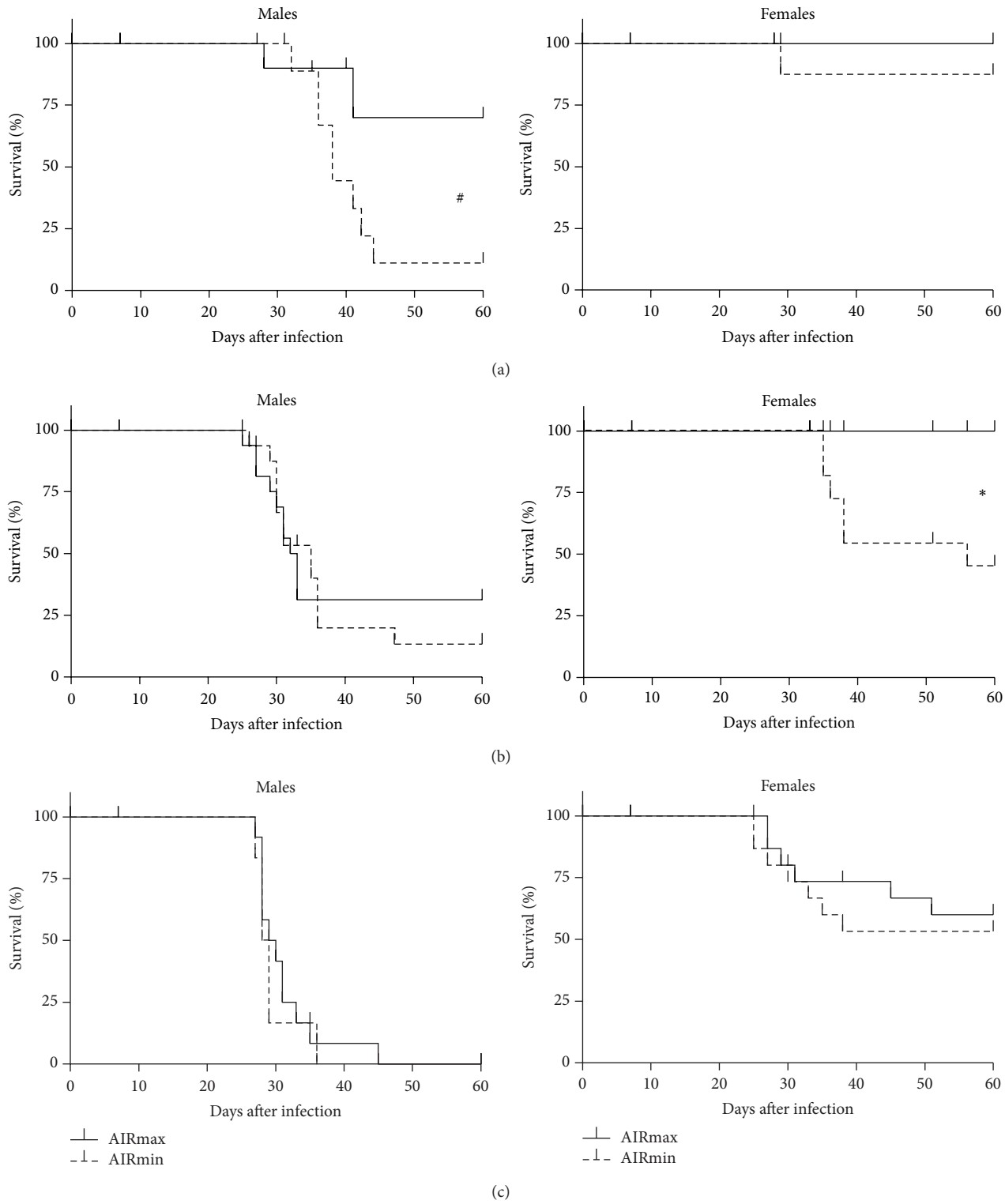

Figure 1: Survival curves of AIR mice after *T. cruzi* infection. AIRmax and AIRmin mice were infected (s.c.) with 10 (a), 10^2 (b), or 10^3 (c) of CL strain trypomastigote forms. Interline differences evaluated by survival curve analyses of each group ($n = 8$) are indicated for males ($^{\#}P = 0.04$) and females ($^{*}P = 0.003$).

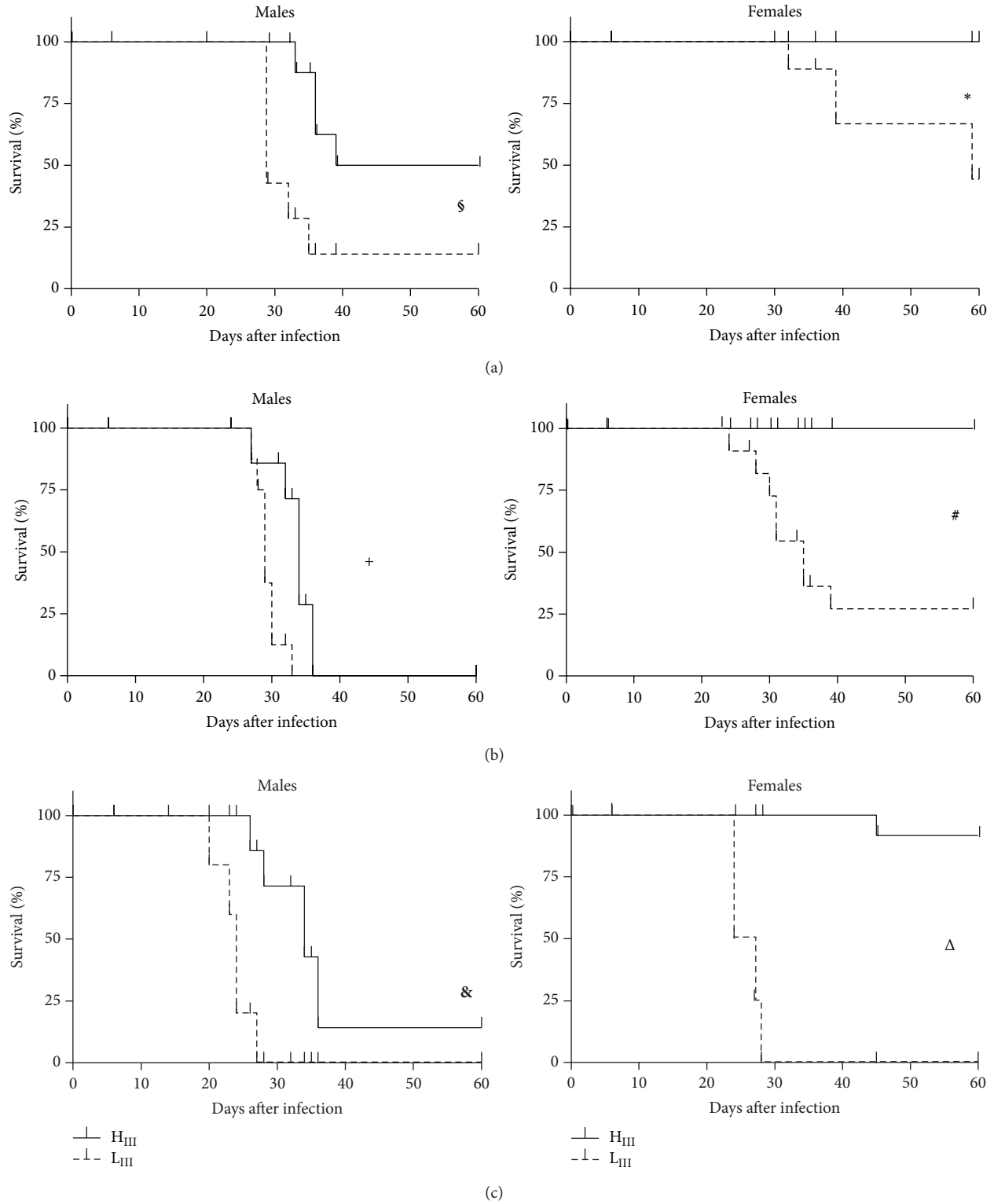

Figure 2: Survival curves of Selection III mice after *T. cruzi* infection. H_{III} and L_{III} mice (outbred stock) were infected (s.c.) with 10 (a), 10^2 (b), or 10^4 (c) of CL strain trypomastigote forms. Interline differences evaluated by survival curve analyses of each group ($n = 8$) are indicated for males ($^{\S}P = 0.018$; $^{+}P = 0.05$; $^{\&}P = 0.008$) and females ($^{*}P = 0.015$; $^{\#}P = 0.0008$; $^{\Delta}P < 0.0001$).

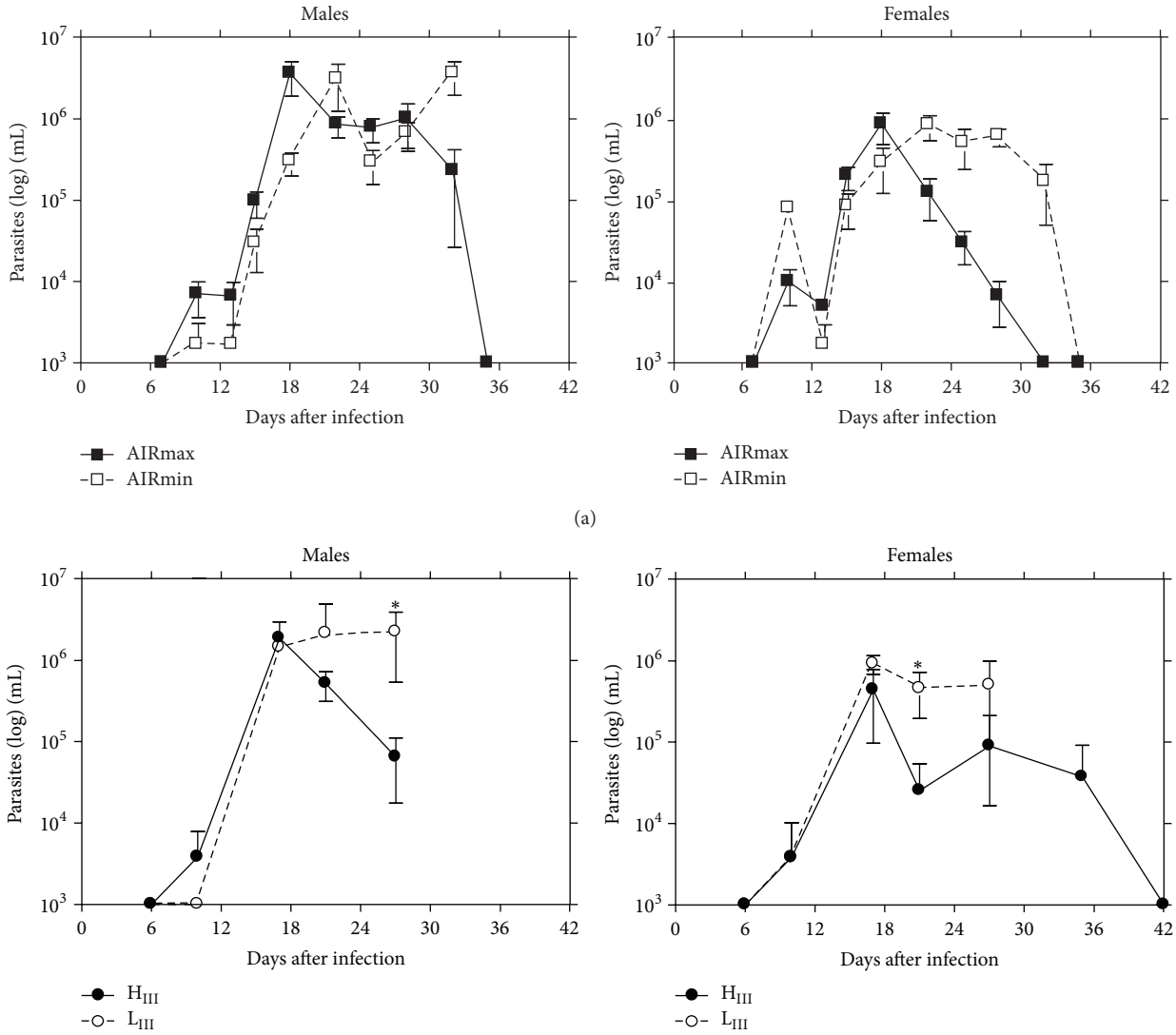

FIGURE 3: Parasitemia of (a) AIRmax, AIRmin mice ($n = 6$ animals/group), and (b) H_{III}, L_{III} mice ($n = 4$ animals/group) during the acute phase of infection with 10^2 trypomastigote forms of *T. cruzi* (CL strain). The results are expressed as the mean ± SE of each group of males and females and significant differences between AIRmax versus AIRmin and between H_{III} versus L_{III} mouse lines in parasitemia levels are indicated: $^*P < 0.05$.

identical resistance patterns to *T. cruzi* challenges (data not shown), indicating that there were no maternal or parental effects in determining resistance/susceptibility to infection. On the other hand, there was an overdominance effect of the resistance phenotype, with F1 hybrids showing greater resistance than the parental H_{III} line (Figures 6(a), 6(b), and 6(c)).

Due to the strong overdominance observed in F1 mice infected with 10^2 parasites (Figure 6(c)) and to a wide range of other challenge doses (data not shown), a segregating population of 242 mice was constructed by backcrossing F1 mice with the susceptible parental L_{III} line (Bc-L). Composite data related to the survival times of males and females from this backcross population (Figure 6(d)) were submitted to genetic analysis, considering sex as a covariate for that trait.

Of all microsatellites tested, the Ab QTL marker located at 34.8 cM on chromosome 1 (*D1Mit303*) attained significant cosegregation values for survival time (Table 1). A more distal peak in chromosome 1 (marked by three adjacent microsatellites) also involved in Ab regulation in H_{III} and L_{III} lines showed a suggestive level of cosegregation with mortality and survival rate.

4. Discussion

The present work demonstrated that polygenic regulation leading to high or low antibody production and maximal or minimal acute inflammatory responses affects host resistance against *T. cruzi* infections. Our results showed a positive

Table 1: Significance of cosegregation between mortality and survival time traits with microsatellites markers of Ab regulating QTLs (quantitative trait loci) from Selection III or with candidate region markers of *T. cruzi* infection susceptibility.

Chrom.	Marker	Cosegregation test Males and females Bc-L Location (Mb)[a]	(cM)[b]	Trait Mortality LRS[c]	Survival time[d] LRS[c]
1	D1Mit411	33220299–33220410	12.6	1.6	1.6
	D1Mit303	**62907596–62907723**	**34.8**	**7.4**	**9.1**[#]
	D1Mit286	128551097–128551241	67.0	3.4	3.9
	D1Mit102	147249520–147249632	79.0	5.3	5.6
	D1Mit36	169211172–169211344	92.3	3.9	5.6
	D1Mit149	172699229–172699330	94.2	3.9	5.7
3	D3Mit272	33007369–33007465	15.5	3	3.4
	D3Mit100	97081705–97081845	46.0	1.3	1.5
5	D5Mit122	150116320–150116477	85.0	0	0
6	D6Mit123	N/D	29.0	0.1	0.5
	D6Mit128	83471199–83471322	35.0	0.2	0.1
	D6Mit6	85277319–85277417	35.3	0.4	0.3
7	D7Mit176	63211190–63211340	27.0	0.3	0.1
9	D9Mit90	32500455–32500594	9.0	0.8	0.9
	D9Mit248	58362559–58362688	31.0	0	0
	D9Mit207	60573431–60573577	33.0	0.8	0.4
11	D11Mit4	68609257–68609504	37.0	0.2	0.9
12	D12Mit19	N/D	58.0	1.3	1.1
17	D17Mit177	48558951–48559063	24.0	1.8	1.1

[a]Megabases (mouse genome database); [b]CentiMorgans (mouse genome database); [c]likelihood ratio statistic; [d]survival time (days); N/D: not determined.
Critical LRS statistic values established by Random Permutation Test for the trait.
(i) Mortality: significant ≥ 8.8; highly significant ≥ 15.5; suggestive ≥ 2.7.
(ii) Survival time: [#]significant ≥ 7.9; highly significant ≥ 14.3; suggestive ≥ 2.8.

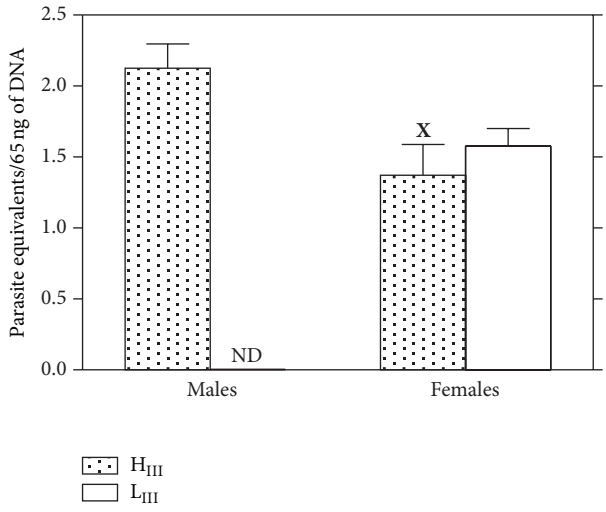

Figure 4: Parasite loads in the cardiac muscles of H_{III} and L_{III} male and female mice 150 days after infection (sc) with 10^3 trypomastigote forms of the CL strain of *T. cruzi*. Significant differences of the parasite loads in 65 ng of DNA isolated from cardiac tissue are indicated: $^{X}P = 0.0125$ (between H_{III} males and H_{III} females); ND: not determined (all male L_{III} mice die in the acute phase).

correlation between the resistance phenotype and mouse lines selected for high responses.

During acute infection, mice from both high-responder lines had lower mortality rates and showed greater capacities to control circulating parasites when compared to low-responder animals. This correlation was more evident among female mice.

Gender differences were also observed in mortality rates, with male mice being more susceptible than females. Male mice have been observed to be more susceptible to acute infections than females in other genetic mouse models, with significantly lower numbers of circulating parasites being observed in the latter [48], and hormones such as estrogen have been observed to reduce mortality in *T. cruzi* infected mice, presumably by their ability to stimulate macrophage activity [49]. Using *Calomys callosus* as an experimental model, Prado Jr. et al. [50, 51] showed that gonadectomy affected the courses of *T. cruzi* infections in females, with high parasitemia levels in the ovariectomized animals as compared to controls and sham-operated groups, indicating that sex hormones can influence natural immune mechanisms. The influence of gender on human susceptibility to *T. cruzi* has similarly been reported [52, 53].

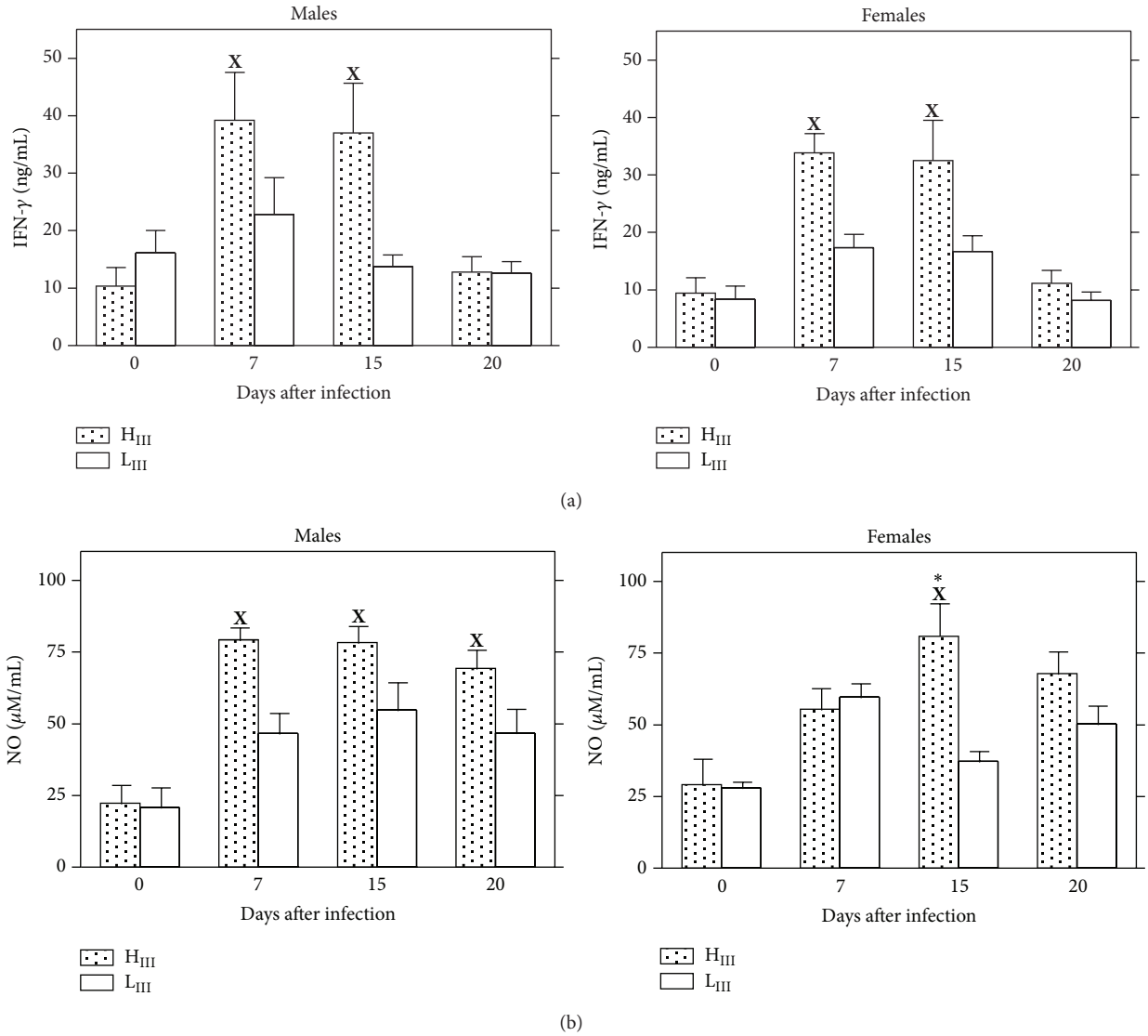

Figure 5: IFN-γ (a) and nitric oxide (NO) (b) production by lymph node (a) and peritoneal cells (b) during the acute phase of infection with 10^2 *T. cruzi* parasites (CL strain) in outbred H_{III} and L_{III} mice. Cells were stimulated in culture with ConA (2.5 μg/mL) for 48 h. Results are expressed as the means ± SE of each group ($n = 6$). Significant differences between infected and control mice (**X**) or between lines (∗) evaluated by ANOVA followed by Tukey multiple comparison tests are indicated when $P < 0.05$.

Recent work analyzing an F2 population obtained by intercrossing resistant and susceptible isogenic strains of mice found a significant association between parasitemia and mortality. By analyzing males and females separately, the authors found that males were more susceptible to death but parasitemia was similar in males and females. In fact they obtained a negative correlation of parasitemia with longevity in females but not in males, suggesting that additional factors independent of parasitemia cause early mortality in males during infection with *T. cruzi* [54].

In the present study, the selected mouse lines behaved like other mouse lines with susceptible male mice dying with higher numbers of blood trypomastigotes, while in females this association could not be done. The resistant mice enter the chronic phase without detectable parasites in their bloodstreams.

Some studies demonstrated that antibodies are responsible for the survival of susceptible animals in the initial phase of *T. cruzi* infection and for the maintenance of low levels of parasitemia in the chronic phase [55–57]. Despite the important effector role of antibody in the control of *T. cruzi* infection, resistant lines do not necessarily produce higher levels of specific antibody in comparison to susceptible lines [58, 59]. Elevation of specific antibody in the acute phase *T. cruzi* infection showed no correlation with the survival in isogenic mice. In the other hand, resistance correlated with enhance of some parasite-specific antibodies isotypes, particularly of IgG2b, [60–62].

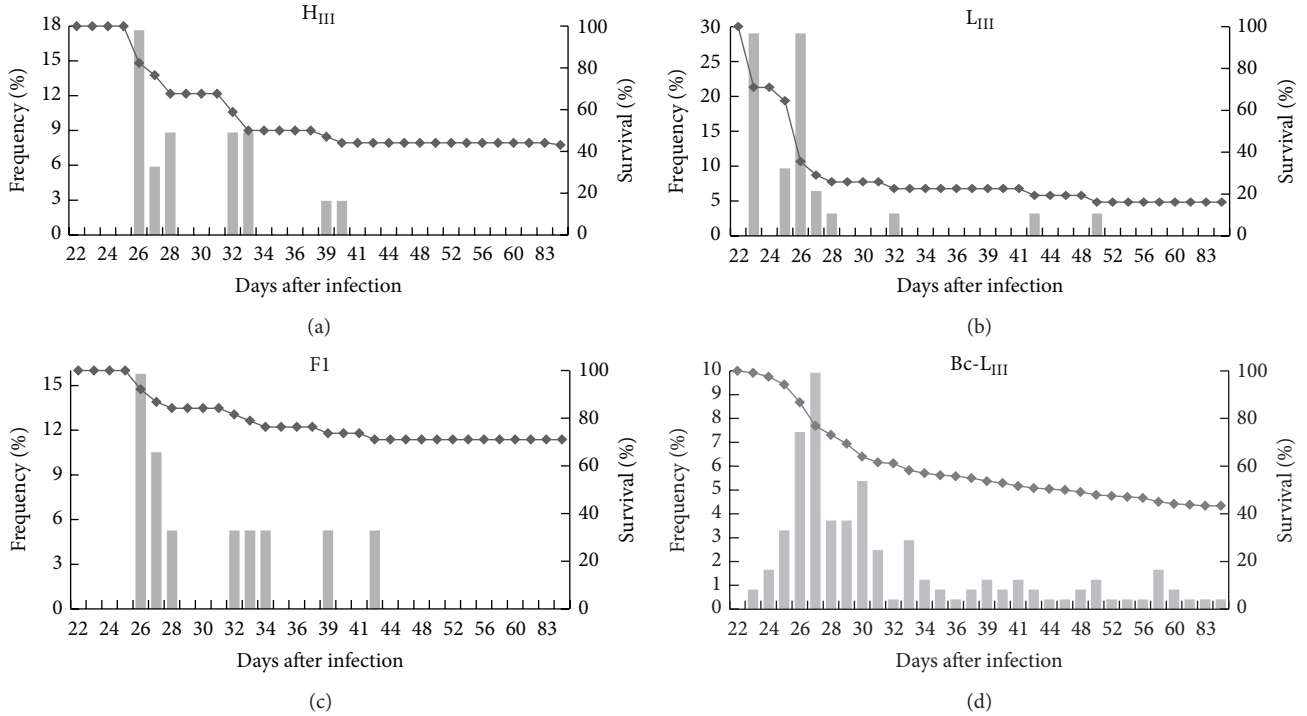

Figure 6: Survival curves and the mortality frequencies each day after *T. cruzi* infection. Males and females of inbred parental H_{III} (a) and L_{III} (b) lines, F1 ($H_{III} \times L_{III}$) hybrids (c), and backcrossed Bc-L (F1 $\times L_{III}$) mice populations (d). Mice were infected (s.c.) with 10^3 blood forms of the CL strain of *T. cruzi* and monitored daily for mortality.

It has been shown that an X-linked mutation (that prevents B1 cell development and specific and nonspecific immunoglobulins production) of Balb. Xid immunodeficient mice influences resistance to infection. Surprisingly, *T. cruzi* infected Xid mice were more resistant than wild-type mice, and the resistance was associated with the absence of IL-10 secreting B1 cells and increased production of IFN-γ [63, 64].

Cellular immune responses are considered important components of resistance to *T. cruzi* infection, with IFN-γ as a central mediator that activates NO-dependent parasiticidal mechanisms in macrophages [17, 65, 66].

In the present study, the increased levels of IFN-γ observed 7 and 15 days after infection in ConA-stimulated cells from H_{III} mice (Figure 5(a)) (as compared to cells from L_{III} mice) apparently trigger the higher NO levels observed in stimulated cells in those animals, suggesting an association between NO production and infection resistance. However, NO and IFN-γ were produced in significant levels in both resistant female and susceptible male mice of the H_{III} and AIRmax and AIRmin lines, indicating that IFN-γ and NO secretion are not the only parameters that contribute to gender differences in infection resistance and may not always correlate with survival, so that other mechanisms must be involved.

Wrightsman et al. [25] studied the genetic control of responses to *T. cruzi* infection and observed that multiple genes were involved in the control of parasitemia and survival, with female F1 hybrid mice from crosses of several susceptible and resistant mouse lines surviving the infections, indicating dominance of the resistance genes. Our results confirmed and extended these observations, indicating an overdominance of the resistance phenotype in F1 ($H_{III} \times L_{III}$) mice, with females being more resistant than males.

This data is in agreement with other genetic studies in which infection resistance was observed to be inherited in a dominant manner, with heterozygosity in crosses between susceptible and resistant inbred lines (or even between two susceptible lines) increasing resistance [24–26, 67]. Overall, these results indicate that, in addition to polygenic regulation, there is complementarity between different loci in determining the infection resistance phenotype.

The overdominance of the resistance phenotype in Selection III mouse lines led us to choose a segregating population Bc-L, created by backcrossing F1 [$H_{III} \times L_{III}$] with the susceptible parental L_{III} mice, to carry out the genetic linkage analysis. Backcrosses are more powerful than intercrosses for examining dominant/recessive traits because they eliminate interference from homozygous dominant genotypes in the analyses [68].

Susceptibility to infectious disease is influenced by multiple host genes, most of which are low penetrance QTLs that are difficult to map. So, the strategy that we chose for genetic analysis was to analyze the linkage between the mortality and survival phenotypes after infection of the Bc-L population with markers that were previously described as implicated in antibody production regulation as well as other markers implicated in resistance to *T. cruzi* infection

Microsatellite markers of QTLs for antibody production mapping on chromosomes 1, 3, 5, 6, 9, 11, and 12 were tested in this linkage analysis [30]. We also genotyped polymorphic

microsatellites among lines of Selection III mice that mark chromosomal regions related to resistance to acute infection by *T. cruzi* on chromosome 7 and near the H-2 locus on murine chromosome 17 [67, 69]. Two other markers on chromosome 1 were tested in a region associated with resistance to African trypanosomiasis (*Tir3b*) [70].

We detected a significant association between alleles of an Ab QTL on chromosome 1 (marked by microsatellite *D1Mit303* at 34.8 cM) with the survival phenotype after *T. cruzi* acute infection, obtaining a significant level of cosegregation in this region in spite of the strong influences on the phenotype of environmental factors such as sex hormones and limited population sizes.

Iraqi et al. [70] described one QTL (*Tir3a*) associated with African trypanosomiasis infection adjacent to the abovementioned QTL confidence interval. This region overlaps a QTL that controls antibody production in H_{III} and L_{III} mouse lines as well as a putative QTL for acute inflammatory response mapped in AIRmax and AIRmin mice [71]. Several genes map at the QTL interval that could interfere in the various steps of innate or adaptative immune response regulation.

A candidate gene in this region is *Slc11a1* (solute carrier family 11; proton-coupled divalent metal ion transporters, member 1 (formerly known as *Nramp1*)) which is a major gene regulating control of intracellular pathogen infections such as those caused by *Salmonella* Typhimurium, *Leishmania donovani*, and *Mycobacterium bovis* bacillus Calmette-Guerin (BCG) in mice and humans. This gene is also involved in inflammatory autoimmune diseases [72] and seems to interact with other genes to modulate this phenotype [73], as could be the case with *T. cruzi* infection in mice selected for acute inflammatory reaction.

However, this gene has no influence on the differential response of Selection III mice to *T. cruzi* because both lines have the resistance associated allele of this gene [74]. Despite this, H_{III} and L_{III} lines differ in susceptibility to *Salmonella* Typhimurium showing that the region that controls antibody production marked by the D1Mit303 microsatellite harbor genes involved in resistance to this bacterial infection [74] and also to *T. cruzi*, in absence of *Nramp*1 polymorphism. Also in humans a lack of association between *NRAMP1* gene polymorphism and *T. cruzi* infection was described [75].

Other genes located in this region, such as *Casp8*, *Icos* (induced T-cell costimulator), *CD28*, and chemokine receptors *Cxcr1* and *Cxcr2* (IL-8 receptor) could also be involved in this phenotype by regulating activation of the inflammatory and adaptive immune responses.

Genes evolved in apoptosis like *Casp8* may be implicated in the different resistance pattern we observed. Infection with *T. cruzi* triggers apoptosis of T and B lymphocytes, and lymphocyte apoptosis has immunoregulatory implications for host immune responses [22]. Treatment *in vivo* with a caspase inhibitor reduces lymphocyte apoptosis and improves protective immune responses in mice infected with *T. cruzi* [76].

Other studies assessed the involvement of caspase signaling in thymocyte death during *T. cruzi* infection and showed that caspase-8 and caspase-9 mediate thymocyte apoptosis in *Trypanosoma cruzi* acutely infected mice [77].

Another gene described in this region codes for CD28 molecule that mediates costimulatory signals required for T-cell activation. The involvement of CD28 in the modulation of protective immunity against *T. cruzi* was shown by mediating the activation of both CD4+ and CD8+ T cells, the production of IFN-γ, and, as a consequence, the production of NO efficient to control parasite growth during the acute phase of the infection. Mice knockout for CD28 presented high parasitemia and mortality [78]. However, when infected with the low virulent Sylvio X10/4 trypanosome strain CD28-KO mice exhibited resistant phenotype, with no parasitemia or mortality [79].

Chagasic patients lack CD28 expression on many of their circulating T lymphocytes [80].

The role of CXC chemokines in proinflammatory phenotype, developed by *T. cruzi* infection, was shown by experiments, in which tissue culture trypomastigotes activate innate sentinel cells via TLR2, releasing CXC chemokines, which in turn evoke neutrophil/CXCR2-dependent extravasation of plasma proteins, including high molecular weight kininogen, in parasite infected tissues [81, 82].

The QTL on chromosomes 3 and 9 that show the highest cosegregation significance with antibody production levels in H_{III} and L_{III} mice [30] were not involved in *T. cruzi* infection control. In previous studies with parasite infections, the response of Selection III lines to infection by the protozoan *Toxoplasma gondii* showed correlation with the potentiality of specific antibody production of their lines [83]. Also in the course of infection by Y strain of *T. cruzi*, minor mortality rates and more efficient control of parasitemia were associated with significant differences in *T. cruzi* specific IgG antibodies [84]. Herein, using CL strain, we quantified antibodies against *T. cruzi* antigen during the acute phase of infection but no differences in specific antibody production could be detected between lines, in spite of an increase of both IgM and IgG levels at 20 days of infection (data not shown), presumably due to a polyclonal activation induced by this parasite [85, 86].

The chromosome 5 Ab QTL located at 85 cM was not associated with the phenotypes analyzed here, although Graefe et al. [67, 87] described a locus on chromosome 5 at 58 cM associated with male mortality in the acute phase of *T. cruzi* Tulahuen strain infection [87]. Iraqi et al. [70] also described a QTL associated with survival of *T. congolense* infections adjacent to this region (at 42–44 cM). One reason for the failure to detect any association may be the large genetic distance between the marker and the published *T. cruzi* resistance QTL on this chromosome. The markers available in this 40–60 cM interval in the microsatellite panel used for mapping Ab QTL were not polymorphic among the H_{III} and L_{III} lines, and additional markers will need to be tested for polymorphism and any associations before definitive conclusions can be drawn.

The chromosome 11 QTL showed the highest significance among the resistance loci (survival) to the Y strain parasite in inbred mice [67]. These and other authors also described a QTL on chromosome 17 close to the H-2 complex as a determinant of responses to challenge with both *T. congolense* (*Tir1*) [70] and *T. cruzi* [66], although this region was not

associated with either *T. cruzi* infection control or antibody production phenotypes in H_{III} and L_{III} mouse lines in the present study [30, 88].

Differential gene expression was analyzed in the spleens of infected susceptible C57BL/6 and resistant (C57BL/6 X DBA/2) F1 mice using microarrays, and the results suggested that the differential transcription of certain genes involved in immune responses and inflammatory processes accounted for the differences in susceptibility to the Tulahuen strain of *T. cruzi* [87].

In humans many genetic linkages and association studies have attempted to identify genetic variations that are involved in immunopathogenesis of Chagas disease. However, causal genetic variants underlying susceptibility remain unknown due to complexity of parasite and host. Susceptibility/resistance to Chagas disease involves multiple genetic variants functioning jointly, each with small or moderate effects [89]. Polymorphism in the *ACTC1* gene of humans contributes to the progression to chronic autoimmune Chagas cardiomyopathy [90], and polymorphisms of other genes that affect several immune parameters such as innate immunity, signal transduction, and T-cell/monocyte migration to inflammatory regions play a role in genetic susceptibility to CCC development [91].

Our data suggest that one out of the several quantitative trait loci that regulate antibody production also contributes to the control of *T.cruzi* infection. Multiple genes control the several steps of antibody synthesis or of infection. The modifications in mechanisms that lead to differential immune response of H_{III} and L_{III} selected lines rather than the produced anti-*T.cruzi* antibodies might play a major role in infection outcome.

Overall, the results of this study demonstrated that an immunomodulatory QTL mapping on mouse chromosome 1 significantly cosegregated with the phenotype of survival time to acute *T. cruzi* infection. Therefore, our data indicates that a region controlling Ab production and inflammation on mouse chromosome 1 harbors genetic factors that also determine resistance to acute *T. cruzi* infections. This region had not previously been implicated with this disease, demonstrating the potential of this genetic model for dissecting complex multigenic regulated traits.

Conflict of Interests

The authors declare that there is no conflict of interests regarding the publication of this paper.

Acknowledgments

This work was supported by Fundação de Amparo à Pesquisa do Estado de São Paulo (FAPESP); Marcelo De Franco and Olga M. Ibañez were supported in part by Conselho Nacional de Pesquisas (CNPq).

References

[1] L. Hudson, "Immunobiology of *Trypanosoma cruzi* infection and Chagas' disease," *Transactions of the Royal Society of Tropical Medicine and Hygiene*, vol. 75, no. 4, pp. 493–498, 1981.

[2] R. T. Gazzinelli and E. Y. Denkers, "Protozoan encounters with Toll-like receptor signalling pathways: implications for host parasitism," *Nature Reviews Immunology*, vol. 6, no. 12, pp. 895–906, 2006.

[3] A. C. Oliveira, J. R. Peixoto, L. B. de Arrada et al., "Expression of functional TLR4 confers proinflammatory responsiveness to *Trypanosoma cruzi* glycoinositolphospholipids and higher resistance to infection with *T. cruzi*," *The Journal of Immunology*, vol. 173, no. 9, pp. 5688–5696, 2004.

[4] C. Ropert, L. R. P. Ferreira, M. A. S. Campos et al., "Macrophage signaling by glycosylphosphatidylinositol-anchored mucin-like glycoproteins derived from Trypanosoma cruzi trypomastigotes," *Microbes and Infection*, vol. 4, no. 9, pp. 1015–1025, 2002.

[5] I. C. Almeida, M. M. Camargo, D. O. Procópio et al., "Highly purified glycosylphosphatidylinositols from *Trypanosoma cruzi* are potent proinflammatory agents," *EMBO Journal*, vol. 19, no. 7, pp. 1476–1485, 2000.

[6] M. A. S. Campos, I. C. Almeida, O. Takeuchi et al., "Activation of toll-like receptor-2 by glycosylphosphatidylinositol anchors from a protozoan parasite," *Journal of Immunology*, vol. 167, no. 1, pp. 416–423, 2001.

[7] A. Bafica, H. C. Santiago, R. Goldszmid, C. Ropert, R. T. Gazzinelli, and A. Sher, "Cutting edge: TLR9 and TLR2 signaling together account for MyD88-dependent control of parasitemia in *Trypanosoma cruzi* infection," *Journal of Immunology*, vol. 177, no. 6, pp. 3515–3519, 2006.

[8] B. C. Caetano, B. B. Carmo, M. B. Melo et al., "Requirement of UNC93B1 reveals a critical role for TLR7 in host resistance to primary infection with *Trypanosoma cruzi*," *The Journal of Immunology*, vol. 187, no. 4, pp. 1903–1911, 2011.

[9] M. M. Rodrigues, A. C. Oliveira, and M. Bellio, "The immune response to *Trypanosoma cruzi*: role of toll-like receptors and perspectives for vaccine development," *Journal of Parasitology Research*, vol. 2012, Article ID 507874, 12 pages, 2012.

[10] G. K. Silva, F. R. S. Gutierrez, P. M. M. Guedes et al., "Cutting edge: nucleotide-binding oligomerization domain 1-dependent responses account for murine resistance against *Trypanosoma cruzi* infection," *The Journal of Immunology*, vol. 184, no. 3, pp. 1148–1152, 2010.

[11] GK. Silva, RS. Costa, TN. Silveira et al., "Apoptosis-associated speck-like protein containing a caspase recruitment domain inflammasomes mediate IL-1 β response and host resistance to *Trypanosoma cruzi* infection," *The Journal of Immunology*, vol. 191, pp. 3373–3383, 2013.

[12] V. M. Gonçalves, K. C. Matteucci, C. L. Buzzo et al., "NLRP3 controls *Trypanosoma cruzi* infection through a caspase-1-dependent IL-1R-independent NO production," *PLoS Neglected Tropical Diseases*, vol. 7, no. 10, Article ID e2469, 2013.

[13] C. A. Hunter, T. Slifer, and F. Araujo, "Interleukin-12-mediated resistance to *Trypanosoma cruzi* is dependent on tumor necrosis factor alpha and gamma interferon," *Infection and Immunity*, vol. 64, no. 7, pp. 2381–2386, 1996.

[14] J. C. S. Aliberti, M. A. G. Cardoso, G. A. Martins, R. T. Gazzinelli, L. Q. Vieira, and J. S. Silva, "Interleukin-12 mediates resistance to *Trypanosoma cruzi* in mice and is produced by murine macrophages in response to live trypomastigotes," *Infection and Immunity*, vol. 64, no. 6, pp. 1961–1967, 1996.

[15] F. Cardillo, J. C. Voltarelli, S. G. Reed, and J. S. Silva, "Regulation of *Trypanosoma cruzi* infection in mice by gamma interferon and interleukin 10: role of NK cells," *Infection and Immunity*, vol. 64, no. 1, pp. 128–134, 1996.

[16] J. S. Silva, G. N. R. Vespa, M. A. G. Cardoso, J. C. S. Aliberti, and F. Q. Cunha, "Tumor necrosis factor alpha mediates resistance to *Trypanosoma cruzi* infection in mice by inducing nitric oxide production in infected gamma interferon-activated macrophages," *Infection and Immunity*, vol. 63, no. 12, pp. 4862–4867, 1995.

[17] G. N. R. Vespa, F. Q. Cunha, and J. S. Silva, "Nitric oxide is involved in control of *Trypanosoma cruzi*-induced parasitemia and directly kills the parasite *in vitro*," *Infection and Immunity*, vol. 62, no. 11, pp. 5177–5182, 1994.

[18] J. S. Silva, F. S. Machado, and G. A. Martins, "The role of nitric oxide in the pathogenesis of chagas disease," *Frontiers in Bioscience*, vol. 8, pp. s314–s325, 2003.

[19] M. Russo, N. Starobinas, P. Minoprio, A. Coutinho, and M. Hontebeyrie-Joskowicz, "Parasitic load increases and myocardial inflammation decreases in *Trypanosoma cruzi*-infected mice after inactivation of helper T cells," *Annales de l'Institut Pasteur/Immunologie*, vol. 139, pp. 225–236, 1988.

[20] R. L. Tarleton, B. H. Koller, A. Latour, and M. Postan, "Susceptibility of β2-microglobulin-deficient mice to *Trypanosoma cruzi* infection," *Nature*, vol. 356, no. 6367, pp. 338–340, 1992.

[21] M. E. Rottenberg, A. Riarte, L. Sporrong et al., "Outcome of infection with different strains of *Trypanosoma cruzi* in mice lacking CD4 and/or CD8," *Immunology Letters*, vol. 45, no. 1-2, pp. 53–60, 1995.

[22] G. A. DosReis, "Evasion of immune responses by *Trypanosoma cruzi*, the etiological agent of Chagas disease," *Brazilian Journal of Medical and Biological Research*, vol. 44, no. 2, pp. 84–90, 2011.

[23] T. Trischmann, H. Tanowitz, M. Wittner, and B. Bloom, "*Trypanosoma cruzi*: role of the immune response in the natural resistance of inbred strains of mice," *Experimental Parasitology*, vol. 45, no. 2, pp. 160–168, 1978.

[24] T. M. Trischmann and B. R. Bloom, "Genetics of murine resistance to *Trypanosoma cruzi*," *Infection and Immunity*, vol. 35, no. 2, pp. 546–551, 1982.

[25] R. Wrightsman, S. Krassner, and J. Watson, "Genetic control of responses to *Trypanosoma cruzi* in mice: multiple genes influencing parasitemia and survival," *Infection and Immunity*, vol. 36, no. 2, pp. 637–644, 1982.

[26] G. K. Silva, L. D. Cunha, C. V. Horta et al., "A parent-of-origin effect determines the susceptibility of a non-informative F1 population to *Trypanosoma cruzi* infection in vivo," *PLoS ONE*, vol. 8, no. 2, Article ID e56347, pp. 1–10, 2013.

[27] M. Siqueira, A. Bandieri, M. S. Reis, O. A. Sant'anna, and G. Biozzi, "Selective breeding of mice for antibody responsiveness to flagellar and somatic antigens of *Salmonellae*," *European Journal of Immunology*, vol. 6, no. 4, pp. 241–249, 1976.

[28] M. Siqueira, M. B. Esteves, O. M. Ibanez et al., "Nonspecific genetic regulation of antibody responsiveness in the mouse," *European Journal of Immunology*, vol. 7, no. 4, pp. 195–203, 1977.

[29] G. Biozzi, D. Mouton, O. A. Sant'Anna et al., "Genetics of immunoresponsiveness to natural antigens in the mouse," *Current Topics in Microbiology and Immunology*, vol. 85, pp. 31–98, 1979.

[30] C. M. de Souza, L. Morel, W. H. K. Cabrera et al., "Quantitative trait loci in Chromosomes 3, 8, and 9 regulate antibody production against Salmonella flagellar antigens in the mouse," *Mammalian Genome*, vol. 15, no. 8, pp. 630–636, 2004.

[31] O. M. Ibañez, D. Mouton, O. G. Ribeiro et al., "Low antibody responsiveness is found to be associated with resistance to chemical skin tumorigenesis in several lines of Biozzi mice," *Cancer Letters*, vol. 136, no. 2, pp. 153–158, 1999.

[32] J. R. Jensen, L. C. Peters, A. Borrego et al., "Involvement of antibody production quantitative trait loci in the susceptibility to pristane-induced arthritis in the mouse," *Genes and Immunity*, vol. 7, no. 1, pp. 44–50, 2006.

[33] C. Stiffel, O. M. Ibanez, O. G. Ribeiro et al., "Genetic regulation of the specific and non-specific component of immunity," *Immunology Letters*, vol. 16, no. 3-4, pp. 205–217, 1987.

[34] C. Stiffel, O. M. Ibanez, O. G. Ribeiro et al., "Genetics of acute inflammation: inflammatory reactions in inbred lines of mice and in their interline crosses," *Experimental and Clinical Immunogenetics*, vol. 7, no. 4, pp. 221–233, 1990.

[35] O. M. Ibanez, C. Stiffel, O. G. Ribeiro et al., "Genetics of nonspecific immunity: I. Bidirectional selective breeding of lines of mice endowed with maximal or minimal inflammatory responsiveness," *European Journal of Immunology*, vol. 22, no. 10, pp. 2555–2563, 1992.

[36] G. Biozzi, O. G. Ribeiro, A. Saran et al., "Effect of genetic modification of acute inflammatory responsiveness on tumorigenesis in the mouse," *Carcinogenesis*, vol. 19, no. 2, pp. 337–346, 1998.

[37] N. D. Vigar, W. H. Cabrera, L. M. Araujo et al., "Pristane-induced arthritis in mice selected for maximal or minimal acute inflammatory reaction," *European Journal of Immunology*, vol. 30, pp. 431–437, 2000.

[38] L. M. M. Araujo, O. G. Ribeiro, M. Siqueira et al., "Innate resistance to infection by intracellular bacterial pathogens differs in mice selected for maximal or minimal acute inflammatory response," *European Journal of Immunology*, vol. 28, pp. 2913–2920, 1998.

[39] D. A. Maria, G. Manenti, F. Galbiati et al., "Pulmonary adenoma susceptibility 1 (Pas1) locus affects inflammatory response," *Oncogene*, vol. 22, no. 3, pp. 426–432, 2003.

[40] J. R. Jensen, A. Galvan, A. Borrego et al., "Genetic control of renal tumorigenesis by the mouse Rtm1 locus," *BMC Genomics*, vol. 14, article 724, 2013.

[41] R. F. Di Pace, S. Massa, O. G. Ribeiro et al., "Inverse genetic predisposition to colon versus lung carcinogenesis in mouse lines selected based on acute inflammatory responsiveness," *Carcinogenesis*, vol. 27, no. 8, pp. 1517–1525, 2006.

[42] M. de Franco, P. D. S. Carneiro, L. C. Peters et al., "Slc11a1 (Nramp1) alleles interact with acute inflammation loci to modulate wound-healing traits in mice," *Mammalian Genome*, vol. 18, no. 4, pp. 263–269, 2007.

[43] K. L. Cummings and R. L. Tarleton, "Rapid quantitation of *Trypanosoma cruzi* in host tissue by real-time PCR," *Molecular and Biochemical Parasitology*, vol. 129, no. 1, pp. 53–59, 2003.

[44] K. F. Manly and J. M. Olson, "Overview of QTL mapping software and introduction to map manager QT," *Mammalian Genome*, vol. 10, no. 4, pp. 327–334, 1999.

[45] K. F. Manly, R. H. Cudmore Jr., and J. M. Meer, "Map Manager QTX, cross-platform software for genetic mapping," *Mammalian Genome*, vol. 12, no. 12, pp. 930–932, 2001.

[46] E. Lander and L. Kruglyak, "Genetic dissection of complex traits: guidelines for interpreting and reporting linkage results," *Nature Genetics*, vol. 11, no. 3, pp. 241–247, 1995.

[47] G. A. Churchill and R. W. Doerge, "Empirical threshold values for quantitative trait mapping," *Genetics*, vol. 138, no. 3, pp. 963–971, 1994.

[48] W. L. Chapman Jr., W. L. Hanson, and V. B. Waits, "The influence of gonadectomy of host on parasitemia and mortality of mice infected with *Trypanosoma cruzi*," *Journal of Parasitology*, vol. 61, no. 2, pp. 213–216, 1975.

[49] F. Kierszenbaum, E. Knecht, D. B. Budzko, and M. C. Pizzimenti, "Phagocytosis: a defense mechanism against infection with *Trypanosoma cruzi*," *Journal of Immunology*, vol. 112, no. 5, pp. 1839–1844, 1974.

[50] J. Prado Jr., M. P. Leal, J. A. Anselmo-Franci, H. F. Andrade Jr., and J. K. Kloetzel, "Influence of female gonadal hormones on the parasitemia of female *Calomys collosus* infected with the "Y" strain of *Trypanosoma cruz*," *Parasitology Research*, vol. 84, pp. 100–105, 1998.

[51] Jr. do Prado J. C., A. M. A. de Levy, M. de Paula Leal, E. Bernard, and J. K. Kloetzel, "Influence of male gonadal hormones on the parasitemia and humoral response of male *Calomys callusus* infected with the Y strain of Trypanosoma cruzi," *Parasitology Research*, vol. 85, no. 10, pp. 826–829, 1999.

[52] A. C. Barretto, E. Arteaga, C. Mady, B. M. Ianni, G. Bellotti, and F. Pileggi, "Male sex. Prognostic factor in Chagas' disease," *Arquivos Brasileiros de Cardiologia*, vol. 60, no. 4, pp. 225–227, 1993.

[53] R. Espinosa, H. A. Carrasco, F. Belandria et al., "Life expectancy analysis in patients with Chagas' disease: prognosis after one decade (1973–1983)," *International Journal of Cardiology*, vol. 8, no. 1, pp. 45–56, 1985.

[54] T. L. M. Sanches, L. D. Cunha, G. K. Silva, P. M. M. Guedes, J. S. Silva, and D. S. Zamboni, "The use of a heterogeneously controlled mouse population reveals a significant correlation of acute phase parasitemia with mortality in Chagas disease," *PLoS ONE*, vol. 9, no. 3, Article ID e91640, 2014.

[55] L. F. Umekita, H. A. Takehara, and I. Mota, "Role of the antibody Fc in the immune clearance of *Trypanosoma cruzi*," *Immunology Letters*, vol. 17, no. 1, pp. 85–89, 1988.

[56] D. A. Bermejo, M. C. A. Vesely, M. Khan et al., "*Trypanosoma cruzi* infection induces a massive extrafollicular and follicular splenic B-cell response which is a high source of non-parasite-specific antibodies," *Immunology*, vol. 132, no. 1, pp. 123–133, 2011.

[57] M. C. A. Vesely, D. A. Bermejo, C. L. Montes, E. V. Acosta-Rodríguez, and A. Gruppi, "B-cell response during protozoan parasite infections," *Journal of Parasitology Research*, vol. 2012, Article ID 362131, 8 pages, 2012.

[58] E. N. de Gaspari, E. S. Umezawa, B. Zingales, A. M. Stolf, W. Colli, and I. A. Abrahamsohn, "Trypanosoma cruzi: serum antibody reactivity to the parasite antigens in susceptible and resistant mice.," *Memorias do Instituto Oswaldo Cruz*, vol. 85, no. 3, pp. 261–270, 1990.

[59] T. M. Trischmann, "Non-antibody-mediated control of parasitemia in acute experimental Chagas' disease," *Journal of Immunology*, vol. 130, no. 4, pp. 1953–1957, 1983.

[60] C. I. Brodskyn, A. M. M. Silva, H. A. Takehara, and I. Mota, "IgG subclasses responsible for immune clearance in mice infected with *Trypanosoma cruzi*," *Immunology and Cell Biology*, vol. 67, no. 6, pp. 343–348, 1989.

[61] H. A. Takehara, A. Perini, M. H. da Silva, and I. Mota, "*Trypanosoma cruzi*: role of different antibody classes in protection against infection in the mouse," *Experimental Parasitology*, vol. 52, no. 1, pp. 137–146, 1981.

[62] M. R. Powell and D. L. Wassom, "Host genetics and resistance to acute Trypanosoma cruzi infection in mice. I. Antibody isotype profiles," *Parasite Immunology*, vol. 15, no. 4, pp. 215–221, 1993.

[63] P. Minoprio, A. Coutinho, S. Spinella, and M. Hontebeyrie-Joskowicz, "Xid immunodeficiency imparts increased parasite clearance and resistance to pathology in experimental Chagas' disease," *International Immunology*, vol. 3, no. 5, pp. 427–433, 1991.

[64] P. Minoprio, M. C. El Cheikh, E. Murphy et al., "Xid-associated resistance to experimental Chagas' disease is IFN-γ dependent," *The Journal of Immunology*, vol. 151, no. 8, pp. 4200–4208, 1993.

[65] F. Plata, F. Garcia-Pons, and J. Wietzerbin, "Immune resistance to *Trypanosoma cruzi*: synergy of specific antibodies and recombinant interferon gamma *in vivo*," *Annales de l'Institut Pasteur—Immunology*, vol. 138, no. 3, pp. 397–415, 1987.

[66] R. T. Gazzinelli, I. P. Oswald, S. Hieny, S. L. James, and A. Sher, "The microbicidal activity of interferon-γ-treated macrophages against *Trypanosoma cruzi* involves an L-arginine-dependent, nitrogen oxide-mediated mechanism inhibitable by interleukin-10 and transforming growth factor-β," *European Journal of Immunology*, vol. 22, no. 10, pp. 2501–2506, 1992.

[67] S. E. B. Graefe, B. S. Meyer, B. Müller-Myhsok et al., "Murine susceptibility to Chagas' disease maps to chromosomes 5 and 17," *Genes and Immunity*, vol. 4, no. 5, pp. 321–325, 2003.

[68] A. Darvasi, "Experimental strategies for the genetic dissection of complex traits in animal models," *Nature Genetics*, vol. 18, no. 1, pp. 19–24, 1998.

[69] L. A. C. Passos, J. K. Sakurada, A. M. A. Guaraldo, S. C. B. C. Ortiz, H. A. Rangel, and J. L. Guenet, "Chagas Fenômeno da Resistência: Identificação de regiões do Genoma importantes no controle da doença," *Revista Biotecnologia Ciência & Desenvolvimento*, vol. 29, 2002.

[70] F. Iraqi, S. J. Clapcott, P. Kumari, C. S. Haley, S. J. Kemp, and A. J. Teale, "Fine mapping of trypanosomiasis resistance *loci* in murine advanced intercross lines," *Mammalian Genome*, vol. 11, no. 8, pp. 645–648, 2000.

[71] A. Galvan, F. Vorraro, W. Cabrera et al., "Association study by genetic clustering detects multiple inflammatory response *loci* in non-inbred mice," *Genes and Immunity*, vol. 12, no. 5, pp. 390–394, 2011.

[72] L. C. Peters, J. R. Jensen, A. Borrego et al., "*Slc11a1* (formerly *NRAMP1*) gene modulates both acute inflammatory reactions and pristane-induced arthritis in mice," *Genes and Immunity*, vol. 8, no. 1, pp. 51–56, 2007.

[73] M. De Franco, L. C. Peters, M. A. Correa et al., "Pristane-induced arthritis loci interact with the Slc11a1 gene to determine susceptibility in mice selected for high inflammation," *PLoS ONE*, vol. 9, no. 2, Article ID e88302, 2014.

[74] A. G. Trezena, C. M. Souza, A. Borrego et al., "Co-localization of quantitative trait loci regulating resistance to *Salmonella typhimurium* infection and specific antibody production phenotypes," *Microbes and Infection*, vol. 4, no. 14, pp. 1409–1415, 2002.

[75] J. E. Calzada, A. Nieto, M. A. López-Nevot, and J. Martín, "Lack of association between NRAMP1 gene polymorphisms and *Trypanosoma cruzi* infection," *Tissue Antigens*, vol. 57, no. 4, pp. 353–357, 2001.

[76] E. M. Silva, L. V. C. Guillermo, F. L. Ribiero-Gomes et al., "Caspase inhibition reduces lymphocyte apoptosis and improves host immune responses to *Trypanosoma cruzi* infection," *European Journal of Immunology*, vol. 37, no. 3, pp. 738–746, 2007.

[77] D. A. Farias-de-Oliveira, D. M. S. Villa-Verde, P. H. N. Panzenhagen et al., "Caspase-8 and caspase-9 mediate thymocyte apoptosis in *Trypanosoma cruzi* acutely infected mice," *Journal of Leukocyte Biology*, vol. 93, no. 2, pp. 227–234, 2013.

[78] G. A. Martins, A. P. Campanelli, R. B. Silva et al., "CD28 is required for T cell activation and IFN-gamma production by

CD4 + and CD8 + T cells in response to *Trypanosoma cruzi* infection," *Microbes and Infection*, vol. 6, no. 13, pp. 1133–1144, 2004.

[79] C. R. F. Marinho, L. N. Nuñez-Apaza, R. Martins-Santos et al., "IFN-γ, but not nitric oxide or specific IgG, is essential for the *in vivo* control of low-virulence Sylvio X10/4 Trypanosoma cruzi parasites," *Scandinavian Journal of Immunology*, vol. 66, no. 2-3, pp. 297–308, 2007.

[80] W. O. Dutra, O. A. Martins-Filho, J. R. Cançado et al., "Chagasic patients lack CD28 expression on many of their circulating T lymphocytes," *Scandinavian Journal of Immunology*, vol. 43, no. 1, pp. 88–93, 1996.

[81] V. Schmitz, E. Svensjö, R. R. Serra, M. M. Teixeira, and J. Scharfstein, "Proteolytic generation of kinins in tissues infected by *Trypanosoma cruzi* depends on CXC chemokine secretion by macrophages activated via Toll-like 2 receptors," *Journal of Leukocyte Biology*, vol. 85, no. 6, pp. 1005–1014, 2009.

[82] J. Scharfstein, D. Andrade, E. Svensjö, A. C. Oliveira, and C. R. Nascimento, "The kallikrein-kinin system in experimental Chagas disease: a paradigm to investigate the impact of inflammatory edema on GPCR-mediated pathways of host cell invasion by *Trypanosoma cruzi*," *Frontiers in Immunology*, vol. 3, article 396, 2012.

[83] M. Siqueira, L. S. Drumond, M. Gennari, V. C. Ferreira, M. H. Reis, and G. Biozzi, "Effect of genetic modification of antibody responsiveness on resistance to *Toxoplasma gondii* infection," *Infection and Immunity*, vol. 48, no. 2, pp. 298–302, 1985.

[84] A. C. Corsini, R. Braz, D. B. Ciampi, and M. R. L. Zucato, "Resistance to Trypanosoma cruzi infection in relation to the timing of IgG humoral response," *Zeitschrift fur Parasitenkunde*, vol. 68, no. 1, pp. 15–25, 1982.

[85] P. Minoprio, O. Burlen, P. Pereira et al., "Most B cells in acute *Trypanosoma cruzi* infection lack parasite specificity," *Scandinavian Journal of Immunology*, vol. 28, no. 5, pp. 553–561, 1988.

[86] P. Minoprio, A. Bandeira, P. Pereira, T. Mota Santos, and A. Coutinho, "Preferential expansion of Ly-1 B and CD4- CD8- T cells in the polyclonal lymphocyte responses to murine *T. cruzi* infection," *International Immunology*, vol. 1, no. 2, pp. 176–184, 1989.

[87] S. E. B. Graefe, T. Streichert, B. S. Budde et al., "Genes from Chagas susceptibility loci that are differentially expressed in *T. cruzi*-resistant mice are candidates accounting for impaired immunity," *PLoS ONE*, vol. 1, no. 1, article e57, 2006.

[88] O. A. Sant'Anna, V. C. Ferreira, M. H. Reis et al., "Genetic parameters of the polygenic regulation of antibody responsiveness to flagellar and somatic antigens of *Salmonellae*," *Journal of Immunogenetics*, vol. 9, no. 3, pp. 191–205, 1982.

[89] C. M. Ayo, M. M. O. Dalalio, J. E. L. Visentainer et al., "Genetic susceptibility to chagas disease: an overview about the infection and about the association between disease and the immune response genes," *BioMed Research International*, vol. 2013, Article ID 284729, 13 pages, 2013.

[90] A. F. Frade, P. C. Teixeira, B. M. Ianni et al., "Polymorphism in the alpha cardiac muscle actin 1 gene is associated to susceptibility to chronic inflammatory cardiomyopathy," *PLoS ONE*, vol. 19, Article ID e83446, 2013.

[91] A. F. Frade, C. W. Pissetti, B. M. Ianni et al., "Genetic susceptibility to chagas disease cardiomyopathy: involvement of several genes of the innate immunity and chemokine-dependent migration pathways," *BMC Infectious Diseases*, vol. 13, article 587, 2013.

Hindawi Publishing Corporation
Mediators of Inflammation
Volume 2014, Article ID 893634, 17 pages
http://dx.doi.org/10.1155/2014/893634

Research Article

The Acute Phase of *Trypanosoma cruzi* Infection Is Attenuated in 5-Lipoxygenase-Deficient Mice

Adriana M. C. Canavaci,[1] Carlos A. Sorgi,[1] Vicente P. Martins,[2] Fabiana R. Morais,[1] Érika V. G. de Sousa,[1] Bruno C. Trindade,[1] Fernando Q. Cunha,[3] Marcos A. Rossi,[4] David M. Aronoff,[5] Lúcia H. Faccioli,[1] and Auro Nomizo[1]

[1] *Departamento de Análises Clínicas, Toxicológicas e Bromatológicas, Faculdade de Ciências Farmacêuticas de Ribeirão Preto, Universidade de São Paulo, Avenida do Café, s/n, 14040-903 Ribeirão Preto, SP, Brazil*
[2] *Departamento de Biologia Celular, Instituto de Ciências Biológicas, Universidade de Brasília, Campus Darcy Ribeiro, 70910-900 Brasília, DF, Brazil*
[3] *Departamento de Farmacologia, Faculdade de Medicina de Ribeirão Preto, Universidade de São Paulo, Avenida Bandeirantes, No. 3900, 14049-900 Ribeirão Preto, SP, Brazil*
[4] *Departamento de Patologia, Faculdade de Medicina de Ribeirão Preto, Universidade de São Paulo, Avenida Bandeirantes, No. 3900, 14049-900 Ribeirão Preto, SP, Brazil*
[5] *Division of Infectious Diseases, Department of Medicine, Vanderbilt University Medical Center, Nashville, TN 37232, USA*

Correspondence should be addressed to Auro Nomizo; aunomizo@fcfrp.usp.br

Received 4 April 2014; Revised 12 June 2014; Accepted 17 June 2014; Published 3 August 2014

Academic Editor: Marcelo T. Bozza

In the present work we examine the contribution of 5-lipoxygenase- (5-LO-) derived lipid mediators to immune responses during the acute phase of *Trypanosoma cruzi* infection in 5-LO gene knockout (5-LO$^{-/-}$) mice and wild-type (WT) mice. Compared with WT mice, the 5-LO$^{-/-}$ mice developed less parasitemia/tissue parasitism, less inflammatory cell infiltrates, and a lower mortality. This resistance of 5-LO$^{-/-}$ mice correlated with several differences in the immune response to infection, including reduced PGE_2 synthesis; sustained capacity of splenocytes to produce high levels of interleukin (IL)-12 early in the infection; enhanced splenocyte production of IL-1β, IL-6, and IFN-γ; rapid T-cell polarization to secrete high quantities of IFN-γ and low quantities of IL-10; and greater numbers of $CD8^+CD44^{high}CD62L^{low}$ memory effector T cells at the end of the acute phase of infection. The high mortality in WT mice was associated with increased production of LTB_4/LTC_4, T cell bias to produce IFN-γ, high levels of serum nitrite, and marked protein extravasation into the peritoneal cavity, although survival was improved by treatment with a cys-LT receptor 1 antagonist. These data also provide evidence that 5-LO-derived mediators negatively affect host survival during the acute phase of *T. cruzi* infection.

1. Introduction

Infection with *Trypanosoma cruzi (T. cruzi)*, an obligate intracellular protozoan parasite, causes American trypanosomiasis or Chagas disease, a zoonosis endemic to Latin America. Approximately 60 million people live in areas with vector-borne transmission risk and the disease causes an estimated 14,000 deaths per year [1]. After entering the host, *T. cruzi* invades a variety of cell types, such as macrophages, heart muscle cells, skeletal muscle cells, and neurons, replicating within the cytoplasm [2]. The acute phase of the disease is characterized by a marked increase in parasite replication and migration to the blood, potentially leading to systemic infection. However, immunocompetent hosts are able to generate innate inflammatory and specific immune responses to acute secondary infection, thereby controlling the parasite burden [3]. These responses are primarily dependent on cytokine/chemokine mediated activation of infected phagocytes and/or tissue cells which leads to intracellular killing [4], although complete elimination of the parasite is rarely

achieved. Parasite persistence in tissues is followed by an asymptomatic or indeterminate phase, and chronic chagasic immunopathology develops in approximately 25% of cases [5].

The factors governing immunological resistance to acute trypanosomiasis are not fully understood. Host genetic background and parasite strain differences might be relevant [6]. Early, partial control of parasites within infected tissue is achieved by local production of type 1 IFNs [7], IL-1β [8], and β-chemokines [9]. Therefore, effective parasite control likely requires the participation of both innate and adaptive immune cells including macrophages, dendritic cells, and NK cells that secrete proinflammatory cytokines (e.g., IL-12 or IFN-γ) [10] and naive T cells for the generation of parasite-specific $CD4^+$ and $CD8^+$ effector T cells [11], which produce Th1 cytokines such as IFN-γ and, in lesser quantities, Th2 cytokines such as IL-4 and IL-10 [12, 13].

Although immune functions have been assigned to a number of polypeptide mediators (cytokines and chemokines) in host defense against *T. cruzi*, little attention has been paid to the role of lipid mediators. These lipid molecules are mainly eicosanoids that are generated through the effects of cyclooxygenases (COX) or 5-lipoxygenase (5-LO) and play a variety of roles in regulating host innate and adaptive immune responses [14]. The 5-LO pathway leads to the formation of two biologically relevant classes of leukotrienes (LTs): non-cysteinyl LTs such as LTB_4; and cysteinyl-LTs (cys-LTs) such as LTC_4, LTD_4, and LTE_4 [15]; and the activity of 5-LO seems to be a common step in LXA_4 synthesis [16]. LTs have been established to play protective roles during infection with many microbial pathogens, including *Salmonella typhimurium, Pseudomonas aeruginosa* [17], *Klebsiella pneumoniae* [18], vesicular stomatitis virus encephalitis [19], and *Histoplasma capsulatum* [20]. However, in other settings 5-LO products have been shown to play contradictory roles, for example, in *Mycobacterium tuberculosis* infection models [21, 22]. In addition, in a cecal ligation and puncture model of peritonitis, LTs exhibited beneficial effects on local immunity but exhibited deleterious effects on hemodynamic responses [23]. Immunoregulatory lipids, such as the arachidonic acid-derived eicosanoids, are increasingly implicated in the pathogenesis of parasitic infections [24, 25]. The 5-LO pathway products have also been implicated in modulating the pathogenesis of several parasitic infections and the results have also been contradictory. *In vitro*, LTB_4 and LTC_4 potentiate macrophages to kill *T. cruzi* [26, 27] and *Leishmania amazonensis* [28]. However, these mediators have been implicated in conferring susceptibility to *Schistosoma mansoni* [29], *Strongyloides venezuelensis* [30], and cerebral malaria [31], thereby suggesting that LTs play conflicting roles during parasite infection.

The immunoregulatory effects of 5-LO pathway eicosanoids are complex and context dependent. While their net effects are beneficial to host defense against some microbial pathogens, this is not necessarily true for all infections. In light of the importance in regulating immune responses to parasitic infections, and the contrasting roles exhibited by LTs in several infection models, we asked whether the 5-LO pathway activity could modulate the *T. cruzi* infection. To address this issue, here we studied specifically the acute phase of *T. cruzi* infection in 5-$LO^{-/-}$ mice.

2. Materials and Methods

2.1. Animals. Male mice (18–20 g) were used; the 5-$LO^{-/-}$ (129-*Alox5*^{tm1Fun}*/J*) and strain-matched WT mice (129-SF2/J) were purchased from Jackson Laboratories (Bar Harbor, ME). The animal colony was bred and maintained under specific pathogen-free conditions at the Faculdade de Ciências Farmacêuticas de Ribeirão Preto (Universidade de São Paulo, Brazil). This study was approved and carried out in strict accordance with the guidelines of the Animal Care Committee of the Universidade de São Paulo and Biosafety Committees (Process nos. 05.1.592.53.2 and CQB-0019/97). All euthanasia was performed under CO_2/O_2 excess atmosphere, and all efforts were made to minimize suffering.

2.2. Parasite Infection and Pharmacological Treatment. Mice were infected intraperitoneally with 200 units of the blood form of *T. cruzi* (Colombian strain) in 0.2 mL of 0.15 M PBS. Control mice received the same volume of sterile PBS. Parasites were counted in 5 μL of blood as previously described [32]. WT mice were previously subjected to *T. cruzi* infection [33]. In some experiments, the infected WT mice were treated with a cys-LT receptor 1 antagonist, montelukast (10 mg/kg, Singulair; Merck Sharp & Dohme, Campinas, Brazil) or its vehicle, carboxymethylcellulose (0.5% w/v), administered orally by gavage (300 μL/animal) on postinoculation days 14–32, starting on day 14 and given every 2 days. *T. cruzi* soluble antigens were obtained from trypomastigote forms (Colombian strain) and used for *in vitro* experiments [32]. Briefly, trypomastigotes were washed twice in cold PBS, subjected to six freeze-thaw cycles, and centrifuged (9000 ×g, 10 min, 4°C). The supernatant was filtered through a 0.22 μm pore size membrane filter, and the protein concentration was measured using a colorimetric assay (Pierce, Rockford, IL).

2.3. Histology and Quantitative Tissue Parasite Nest Determination. Histology and tissue parasite counts were performed as described elsewhere [11]. Briefly, tissue samples were fixed in 4% buffered formalin and processed for conventional paraffin embedding on day 16 after infection. Sections (8 μm) were deparaffinized and stained with hematoxylin and eosin. Intact parasite nests were evaluated in blinded samples by counting the number of parasites nests in 100 microscopic fields/sample of nonconsecutive sections.

2.4. Eicosanoid Levels in Peritoneal Cell Supernatants. Peritoneal cells were collected by intraperitoneal injection of 4 mL of cold PBS from uninfected controls, infected WT, and 5-$LO^{-/-}$ mice at various time points of infection. Cell concentration was adjusted to 10^6 cells mL^{-1} in Hank's buffered salt solution (HBSS; Sigma, St. Louis, MO) with Ca^{+2} and Mg^{+2}. Cells were stimulated with 0.5 μM of the calcium ionophore A23187 (Sigma, Saint Louis, EUA) for 15 min at 37°C in a

humidified atmosphere of 5% CO_2. The supernatants were harvested and PGE_2, LTB_4, and LTC_4 levels were determined by specific EIA kit, following the manufacturer's instructions (GE Healthcare, Little Chalfont, UK).

2.5. Spleen Cell Culture. Mice from experimental groups were euthanized on various days after inoculation. Single-cell suspensions were prepared by passing each spleen through a 70 μm cell strainer (Falcon, Sollentuna, Sweden). The splenocytes were washed 3 times with HBSS, counted with a hemocytometer, assessed for viability, and suspended in RPMI 1640 medium supplemented with 10% FCS, penicillin (100 U/mL), streptomycin (100 μg/mL), and gentamicin (50 μg/mL) (Gibco-Invitrogen, Carlsbad, CA) or HBSS supplemented with 5% FCS. The cell concentration was adjusted to 10^7 cells/mL and cultured in 24-well plates (Nalge Nunc, Rochester, NY) in 1 mL of supplemented RPMI medium, with 5 μg of anti-CD3ε or with 10–50 μg of soluble *T. cruzi* antigens at 37°C in an atmosphere of 5% CO_2 for 24–48 h. Supernatants were collected and stored at −70°C for further use.

2.6. Metabolic Assays. Splenocytes (4×10^5 cell/well) from different experimental groups were cultured in quintuplicate in flat 96-well microplates (Nalge Nunc, Rochester, NY) with supplemented RPMI medium. Cells were cultured alone or with anti-CD3ε IgG (1 μg/mL; BD Pharmingen, San Diego, CA) at 37°C in a humidified atmosphere of 5% CO_2. After 60 h, 10 μL (5 mg/mL) of MTT (Sigma, Saint Louis, EUA) was added to each well, and cells were incubated for an additional 4 h, followed by the addition of 50 μL of 20% SDS in PBS and stored in the dark overnight. Absorbance was measured at 570 nm using an automated microplate reader (μQUANT; BioTek Instruments, Winooski, VT).

2.7. Flow Cytometry. Spleen cells were isolated as described above and placed in ice-cold PBS supplemented with 5% FCS and 0.1% sodium azide. Staining was performed as previously described [11]. The following fluorochrome-conjugated monoclonal antibodies were used: anti-CD4 [H129.19]; anti-CD8 [53-6.7]; anti-CD19 [MB19-1]; anti-CD25 [7D4]; anti-CD44 [IM7]; anti-CD69 [H1.2F3]; anti-Gr-1/Ly6C/Ly6G [RB6-8C5]; anti-CD45RB [16A]; anti-CD62L [MEL-14]; anti-CD11b [M1/70] (BD Pharmingen, San Diego, CA); and anti-CD11c [HL3]—(Serotech, Raleigh, NC) anti-F4/80 [CI:A3-1] and anti-GITR [DTA-1] (eBioscience, San Diego, CA). After staining, the cells were fixed with 1% paraformaldehyde in PBS and analyzed using a FACSCanto (BD Biosciences, San Jose, CA), 50,000 events/sample recorded. Data were processed using FlowJo software (FlowJo LLC, Ashland, OR). Cell numbers were calculated using the percentage obtained by FACS analysis and the total numbers of leukocytes counted in a hemocytometer.

2.8. T. cruzi-Specific Antibodies. Specific IgG, IgG1, and IgG2a were determined in mouse sera by ELISA as previously described [32]. The individual titers were considered the highest serum dilutions that presented $OD_{492} > 0.1$.

2.9. Protein Extravasation. Protein extravasation was assessed as previously described [23]. Control mice or infected mice were i.v. injected with Evans blue dye (50 mg/kg in a volume of 0.1 mL; Sigma, Saint Louis, EUA). After 1 h, mice were euthanized by CO_2 inhalation, and the peritoneal exudates were recovered by injecting 2 mL of PBS. The peritoneal exudates were centrifuged for 10 min at 200 ×g, and the supernatant was saved for colorimetric determinations. The OD was determined at 630 nm in the automated microplate reader.

2.10. In Vitro Macrophage Infection. Peritoneal cells from WT and 5-$LO^{-/-}$ mice were collected, washed twice, and counted and the cell concentration was adjusted to 10^6 cells/mL in supplemented RPMI medium. Cells were attached on 13 mm-diameter glass coverslips placed to 24-well plates (Nalge Nunc, Rochester, NY), for 90 min at 37°C in an atmosphere of 5% CO_2. The nonadherent cells were removed by washings in warm supplemented RPMI medium. Peritoneal macrophages (PM) isolated by this procedure were >90% pure as measured by staining for $F4/80^+$ (data not shown). The PMs were stimulated for 6 h with 5 ng/mL of IFN-γ (BD Pharmingen, San Diego, CA) plus 0.1 μg/mL of LPS from *Escherichia coli* (Sigma, Saint Louis, EUA) and infected at a parasite-to-macrophage ratio of 5 : 1/well. After 2 h, the glass coverslips were washed five times in PBS to remove free parasites, fixed in absolute methanol, stained with Panoptic stain (Laborclin, Pinhais, Brazil), dried, mounted on glass slides, and examined microscopically for association (parasite adhered to macrophages plus internalized parasites) as previously described [26]. For killing assay, noninternalized parasites of infected macrophages wells were removed 24 h later by three gentle washes with warm supplemented RPMI medium. Fresh supplemented RPMI medium was added to each well, and infected macrophages were cultured at 37°C, in an atmosphere of 5% CO_2 for up to 10 days, 50% of the medium being removed and replaced with the same volume of supplemented RPMI medium every 48 h. After 7–11 days after infection, culture supernatants were collected daily to count the number of motile trypomastigotes/well.

2.11. Nitrite/Nitrate Concentration. Tail-vein blood samples were obtained at day 22 after inoculation. Nitrate in serum samples was converted to nitrite by nitrate reductase, and serum levels of nitrate/nitrite (Nitric oxide end-products or metabolites) were measured by absorbance using the Griess Reaction (Calbiochem, La Jolla, CA) [34]. The OD was determined at 540 nm in the μQUANT automated microplate reader. The nitriteconcentration was determined by reference to a standard (1–100 μM) sodium nitrite curve.

2.12. Cytokine ELISA. Levels of IL-1β, IL-2, IL-6, IL-10, IL-12, TNF-α, and IFN-γ were quantified by ELISA according to the manufacturer's instructions (BD Pharmingen, San Diego, CA) in the splenocytes culture supernatant. The lower limits of detection for those cytokines were 9.4 pg/mL.

2.13. Statistical Analysis. The results are presented as means ± SD, with the exception of those for parasitemia, shown as means ± SEM. The tests that were used to evaluate differences among groups are mentioned in the figure legends. Values of $P < 0.05$ were considered significant.

3. Results

3.1. Lipid Mediator Production by Infected Peritoneal Cells. Peritoneal cells from *T. cruzi*-infected mice (WT) released significantly more LTB_4 and PGE_2 upon calcium ionophore stimulation than did cells obtained from uninfected mice (Figures 1(a) and 1(b)). The potential of cells to produce LTB_4 was elevated at an early time point after inoculation (day 5) and increased gradually throughout the infection, peaking on day 19. This potential then decreased drastically toward the late phase of acute infection (day 26; Figure 1(a)).

The potential of peritoneal cells from *T. cruzi*-infected mice to produce PGE_2 was also increased (Figure 1(b)). Peritoneal cells from infected WT mice released PGE_2 at early time points (day 5) and increased markedly on subsequent days, peaking on day 12. PGE_2 levels decreased drastically by day 19 and increased again in the late phase of the acute infection by day 26. Peritoneal cells from infected 5-$LO^{-/-}$ mice also showed an enhanced production of PGE_2 (Figure 1(b)) but the pattern was different than observed for WT cells and did not suggest shunting of arachidonic acid towards the cyclooxygenase pathway. PGE_2 production by 5-$LO^{-/-}$ cells was not elevated on day 5 and increased on day 12 (albeit to levels below WT) to a level that was maintained throughout infection. Notably, the peritoneal cells from both WT and 5-$LO^{-/-}$ *T. cruzi*-infected mice appeared to produce more PGs than LTs, as evidenced by the fact that LTB_4 levels (Figure 1(a)) were far lower than those of PGE_2 (Figure 1(b)).

3.2. Control of Parasite Dissemination and Host Survival after Infection. As shown in Figure 1(c), infected 5-$LO^{-/-}$ mice presented a delay in the appearance of blood-circulating parasites and very low parasite numbers at the second peak of parasitaemia compared to WT mice. In addition, the number of intact parasite nests in heart muscle tissue was considerably lower in 5-$LO^{-/-}$ mice (Figure 1(d)). Furthermore, about 17% of the 5-$LO^{-/-}$ mice died on postinoculation days 16–19, whereas WT mice did not begin to die until day 19 (Figure 1(e)). In the acute phase of infection, only 30% of WT mice were capable of surviving the infection. In contrast, 82.3% of 5-$LO^{-/-}$ mice controlled parasite efficiently and survived the acute phase of infection (Figure 1(e)).

3.3. Inflammatory Infiltrate and Tissue Parasitism during the Acute Phase of T. cruzi Infection. Analysis of the histological samples of heart muscle tissue collected after 16 days after inoculation revealed that WT mice presented more intact parasite nests and more amastigote forms within those nests (Figure 2(a)) than did 5-$LO^{-/-}$ mice (Figure 2(b)). In addition, there were greater inflammatory mononuclear cell infiltrates in WT mice (Figure 2(c)) than in 5-$LO^{-/-}$ mice (Figure 2(d)).

3.4. Cytokine Production by Spleen Cells. In culture, the spleen cells of infected mice spontaneously produced IL-1β, IL-6, TNF-α, IL-10, IL-12, and IFN-γ (Figure 3). It is notable that the production of most of these cytokines was greater during the first two weeks of infection, peaking on day 12 after inoculation, correlating with parasitemia (Figure 1(c)). In general, the production of IL-6, IL-12, and IFN-γ was greater in spleen cells of infected 5-$LO^{-/-}$ than in WT cells. On day 5, the production of IL-1β, IL-6, IL-12, and IFN-γ was higher from 5-$LO^{-/-}$ cells than from WT cells but TNF-α production was lower. On day 12, IL-1β levels were comparably high in cell cultures from both mouse strains, while spleen cells from infected 5-$LO^{-/-}$ showed significantly greater production of IL-6, IL-12, IFN-γ, and TNF-α compared to the infected WT cells. The production of IL-10 showed the opposite trend (Figure 3(d)). In the late phase of infection (on days 19 and 26), 5-$LO^{-/-}$ spleen cells, in contrast to what was observed for WT spleen cells, showed a sustained elevation in the production of IL-1β (Figure 3(a)) and IL-10 (Figure 3(d)), higher levels of IL-12 (Figure 3(e)), and lower levels of IFN-γ (Figure 3(f)).

3.5. Cell Populations in the Spleen of Infected Mice. Infection of mice with *T. cruzi* led to the accumulation of $Gr1^+$ cells (i.e., neutrophils), $Gr1^+/CD11c^+$cells (i.e., plasmacytoid dendritic cells), $CD11b^+$cells (i.e., myeloid lineage cells), and $F4/80^+$cells (i.e., macrophages) in their spleens when compared with uninfected control mice (Figures 4(a)–4(d)). Greater numbers of $Gr1^+$, $Gr1^+/CD11c^+$, $CD11b^+$, and $F4/80^+$ cells were present in 5-$LO^{-/-}$ than in WT spleens at day 12 after infection (Figures 4(a)–4(c)). Macrophage ($F4/80^+$) numbers were higher in the spleens of 5-$LO^{-/-}$ mice on day 19 after infection compared with WT mice as well (Figure 4(d)). In addition, on day 5 after infection, plasmacytoid dendritic cell ($Gr1^+/CD11c^+$) counts were higher in infected 5-$LO^{-/-}$ mice, when compared with infected WT mice (Figure 4(b)). It is notable that myeloid lineage cells numbers were higher in the spleens of infected WT animals than the spleens of 5-$LO^{-/-}$ mice (Figure 4(c)).

3.6. Peritoneal Macrophage Infection. In the infected 5-$LO^{-/-}$ mice, PMs and IFN-γ both increased (Figures 4(d) and 3(f)). The *in vitro* infection of peritoneal LPS-plus IFN-γ-activated-macrophages from WT and 5-$LO^{-/-}$ mice showed differences in the association of macrophages with parasites (binding and internalization) and in their ability to kill intracellular parasites (Figures 4(e) and 4(f)). Compared with the activated PMs from WT mice, those from 5-$LO^{-/-}$ mice presented a greater capacity to associate with the blood form of the parasite, as evidenced by the higher numbers of bound and internalized parasites (Figure 4(e)). Activated PMs from 5-$LO^{-/-}$ mice were also more efficient at killing internalized parasites, as evidenced by the lower numbers of parasites recovered after *in vitro* infection as compared with WT PMs (Figure 4(f)).

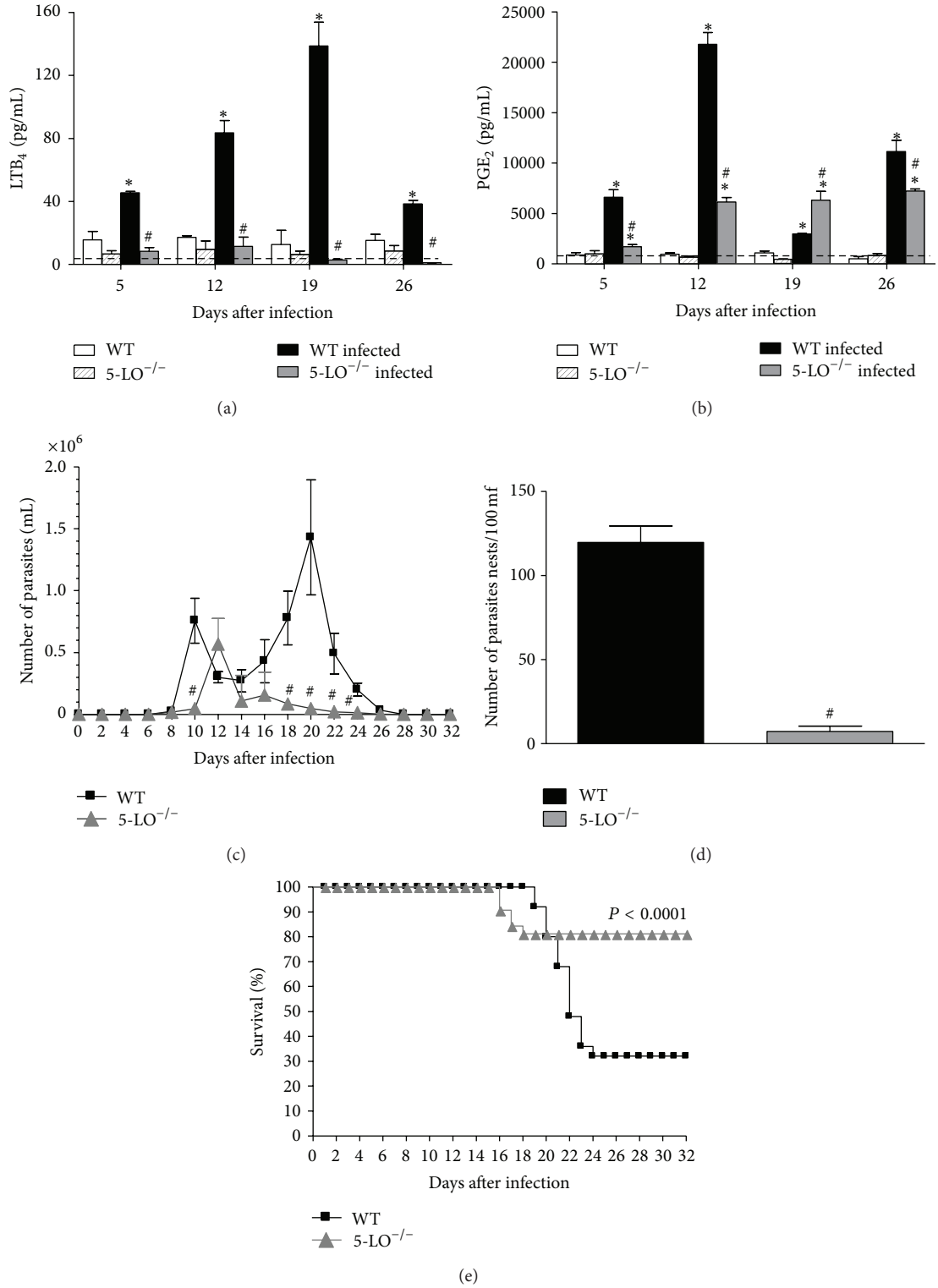

Figure 1: Lipid mediator production, parasitemia, tissue parasitism, and survival rate of WT and 5-LO$^{-/-}$ mice infected with *T. cruzi*: ((a) and (b)) LTB_4 and PGE_2: peritoneal cells were collected from control, infected WT, and infected 5-LO$^{-/-}$ mice ($n = 10$/group) and stimulated with calcium ionophore. $^{*}P < 0.01$ versus uninfected group; $^{\#}P < 0.01$ versus WT infected mice. (c) Parasitemia ($n = 10$ mice/group). $^{\#}P < 0.001$ versus infected WT mice. (d) Parasite nests in heart tissue on postinoculation day 16. $^{*}P < 0.001$ versus infected WT mice. (e) Survival: WT mice (squares) and 5-LO$^{-/-}$ mice (triangles), $n = 10$ animals/group. Wilcoxon signed-rank test (level of significance, $P < 0.001$). Data are representative of three independent experiments.

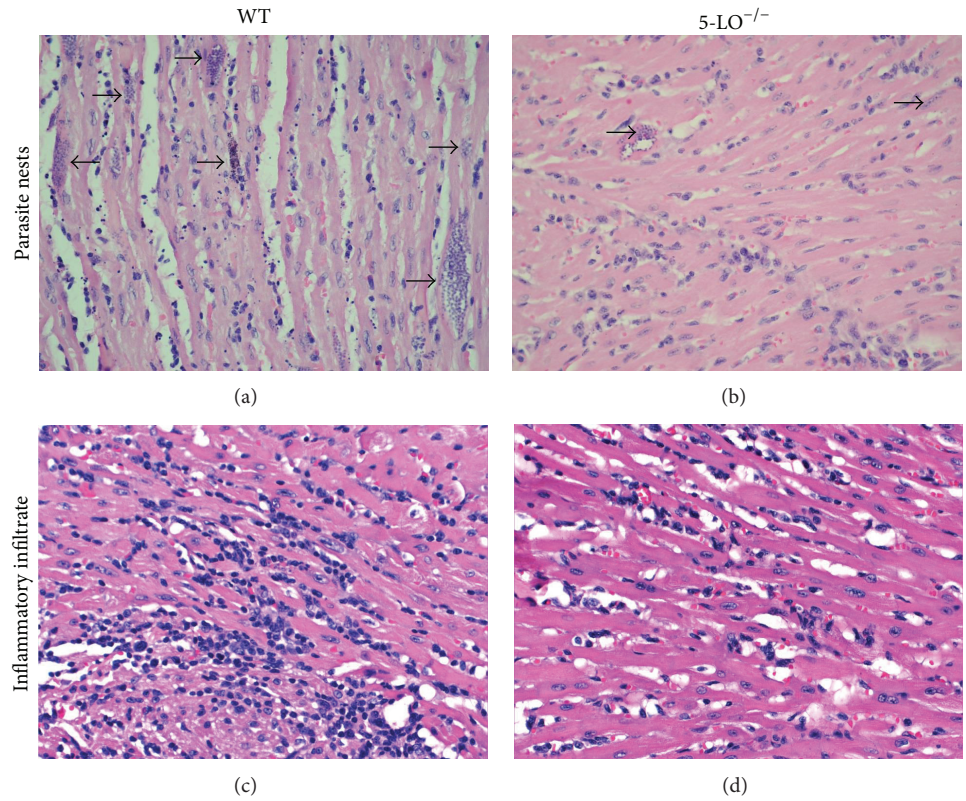

Figure 2: Histopathological analysis of heart tissue parasitism and inflammatory infiltrate in *T. cruzi*-infected WT and 5-LO$^{-/-}$ mice (n = 8/group) on postinoculation day 16 (staining with H&E; magnification, ×200): (a) section from a WT mouse, showing numerous large amastigote nests, (b) section from a 5-LO$^{-/-}$ mouse, showing fewer, smaller nests, (c) section from a WT mouse, showing intense mononuclear cell infiltration, (d) section from a 5-LO$^{-/-}$ mouse, showing less infiltration. Photomicrographs are from one experiment representative of three independent experiments.

3.7. Spleen B-Cell Counts and Serum Levels of Parasite-Specific Immunoglobulins. As shown in Figure 5(a), splenic CD19$^+$ B-cell counts were greater in mice infected with *T. cruzi* than in control mice. On day 5 after inoculation, splenic CD19$^+$ cell counts were elevated in infected WT mice and gradually returned to baseline values by the end of the acute phase of infection. In contrast, splenic CD19$^+$ cell counts increased significantly less in infected 5-LO$^{-/-}$ mice during the first two weeks of infection, gradually becoming significantly more elevated than WT mice in the later phase of infection.

Mice infected with *T. cruzi* produced detectable levels of parasite-specific IgG antibodies in a time-dependent manner during the later phase of infection (Figure 5(b)). The principal isotype produced during infection was IgG2a, and levels of IgG1 were low. Compared with WT mice, 5-LO$^{-/-}$ mice presented lower levels of parasite-specific IgG on day 26, as well as of parasite-specific IgG2a on days 19 and 26 of infection.

3.8. T-Cell Phenotypes in the Spleens of Infected Mice. As indicated in Figure 6, infected mice presented elevated CD4$^+$ and CD8$^+$ T-cell counts, the markers CD4$^+$CD69$^+$, CD8$^+$CD69$^+$, CD4$^+$CD25$^+$, CD4$^+$CD44$^+$, and CD8$^+$CD44$^+$, which indicate the presence of activated T-cells in the spleens of both WT and 5-LO$^{-/-}$ infected mice. In infected mice, the majority of the splenic T-cell populations presented the full/late T-cell activation markers CD4$^+$CD44$^+$ and CD8$^+$CD44$^+$ (Figures 6(c) and 6(d)). On day 5 after inoculation, numbers of all of these T-cell phenotypes were elevated in infected WT mice, gradually increasing over the course of infection and peaking on day 26, the study endpoint (Figure 6). In contrast, infected 5-LO$^{-/-}$ mice presented a delayed elevation in T-cell counts, and the increase of all of these activated T-cell phenotypes was less pronounced than observed in WT spleens. Infected 5-LO$^{-/-}$ mice presented a significant increase in CD4$^+$CD44$^+$ and CD8$^+$CD44$^+$ counts on day 12, a marked increase in the CD4$^+$CD69$^+$ count on day 19, and a slight but significant increase in CD8$^+$CD69$^+$ and CD4$^+$CD25$^+$ counts only on day 26.

3.9. T-Cells Properties, Cytokine Production, and CD4$^+$ Memory T Cells Expressing CD45RB^{low} and CD44^{high}CD62L^{low} in the Spleen. As shown in Figure 7(a), spleen cells from control mice proliferated after stimulation with anti-CD3ε, as expected, whereas spleen cells collected from infected WT mice on day 12 after inoculation and stimulated with anti-CD3ε presented a dramatic reduction in proliferation. However, spleen cells from infected 5-LO$^{-/-}$ mice on day 12

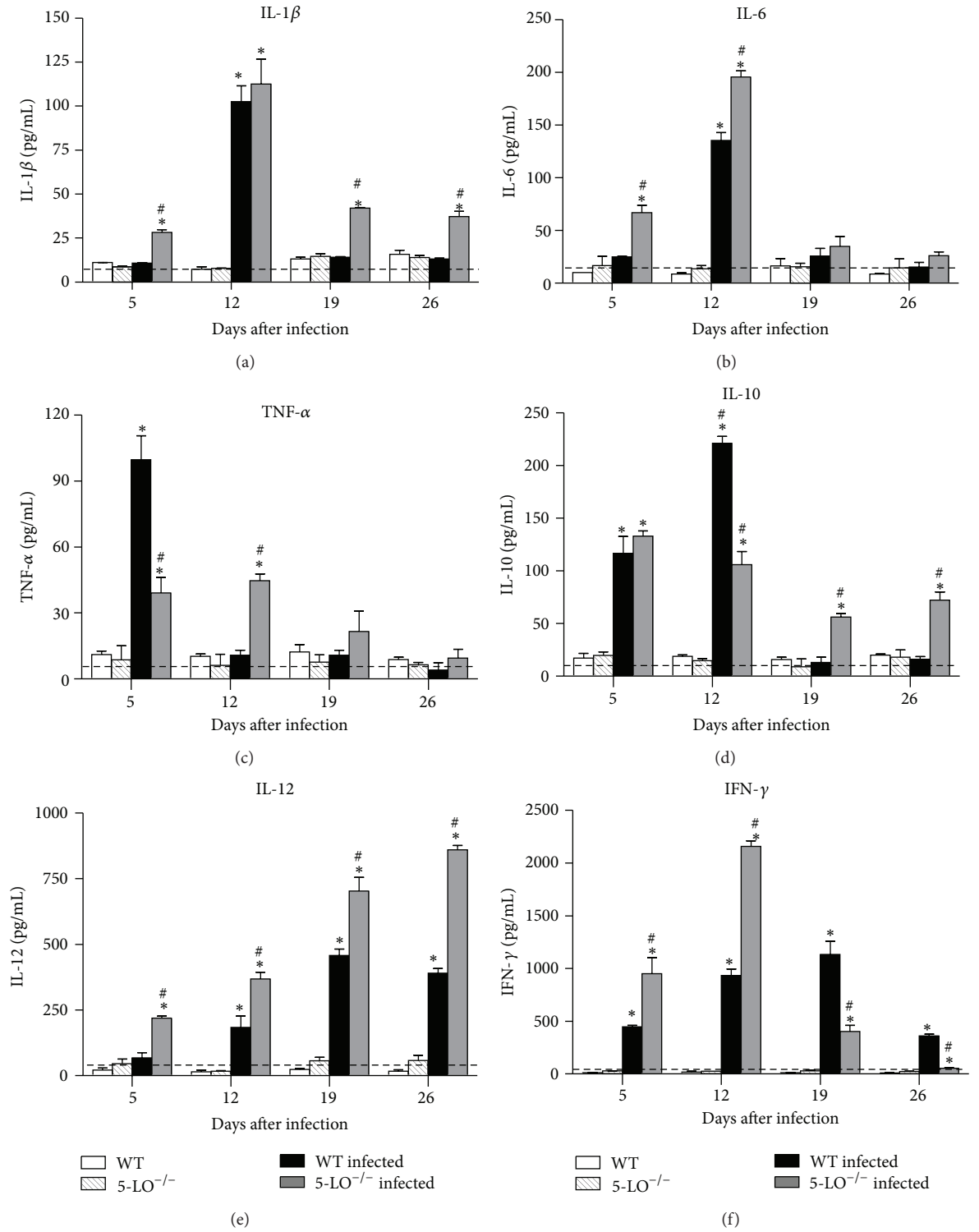

Figure 3: Cytokine production by spleen cells from *T. cruzi*-infected mice. Spleen cells from control, infected WT and infected 5-LO$^{-/-}$ mice (n = 10/group) cultured in medium alone. Data are from one of three independent experiments. Kruskal-Wallis test ($^{*}P < 0.01$ versus uninfected group; $^{\#}P < 0.05$ versus infected WT mice).

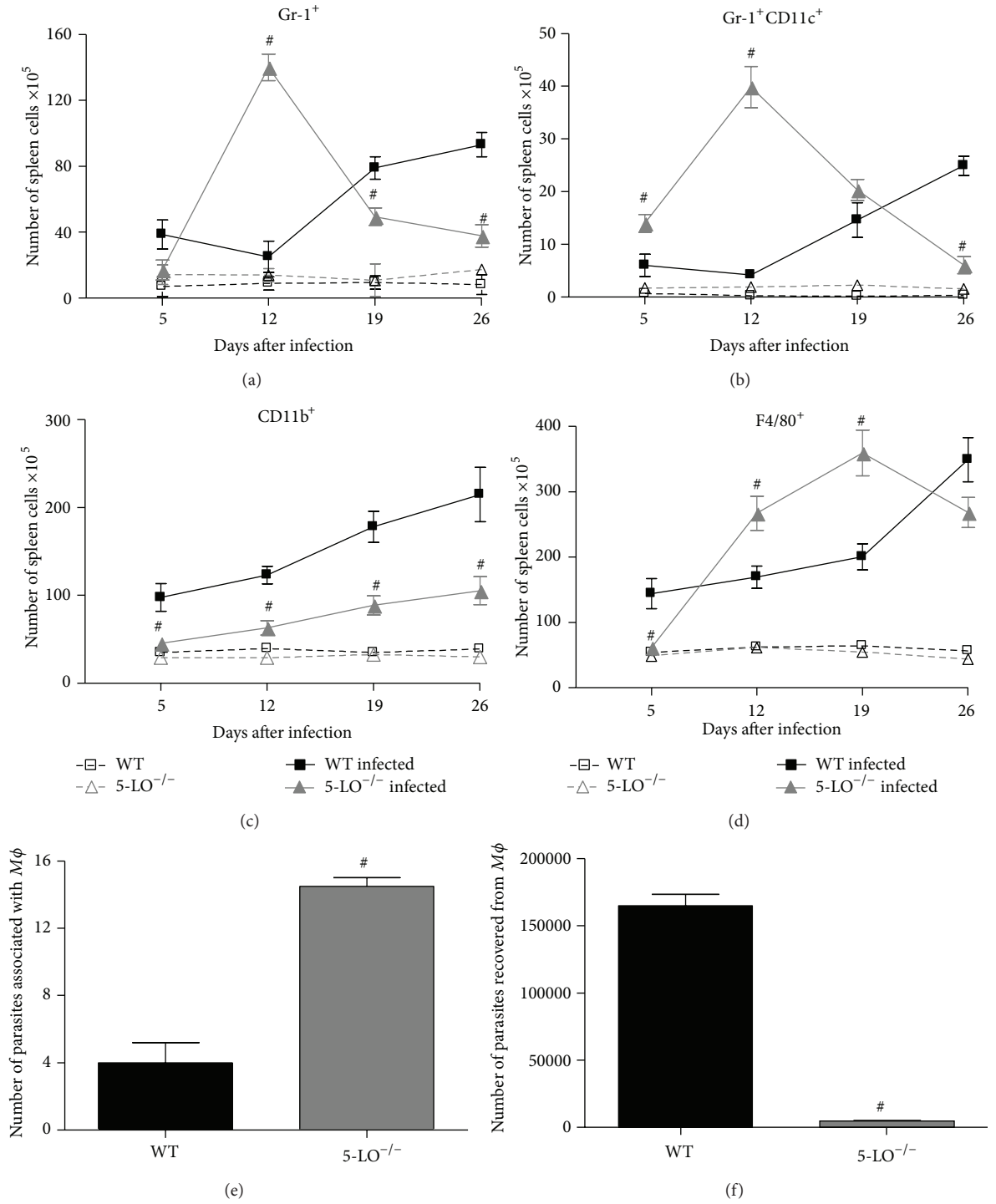

FIGURE 4: Quantitative and functional leukocyte responses to *T. cruzi* infection. (a) Gr1$^+$ cell (neutrophils); (b) Gr1$^+$CD11c$^+$ cell (pDC cells); (c) CD11b$^+$ cell (myeloid lineage cell marker, Mac-1); and (d) F4/80$^+$ cell (macrophages) numbers in the spleen.

and stimulated with anti-CD3ε presented a partially restored proliferative capacity.

Spleen cells were collected from infected mice on days 12 and 26 after inoculation, after which they were stimulated with anti-CD3ε. The supernatants were tested for the presence of IFN-γ and IL-10, the most abundant of the cytokines secreted spontaneously by spleen cells from infected mice that we measured (Figure 3), as well as for IL-2. Spleen cells collected from infected WT mice on day 12 and stimulated with anti-CD3ε produced significant amounts of the type 1 cytokine (Th1) IFN-γ, and the type 2 cytokine (Th2) IL-10, as well as very low levels of IL-2 (Figure 7(b)). In contrast, anti-CD3ε-stimulated spleen cells collected from infected 5-LO$^{-/-}$ mice on day 12 presented a bias to produce predominantly,

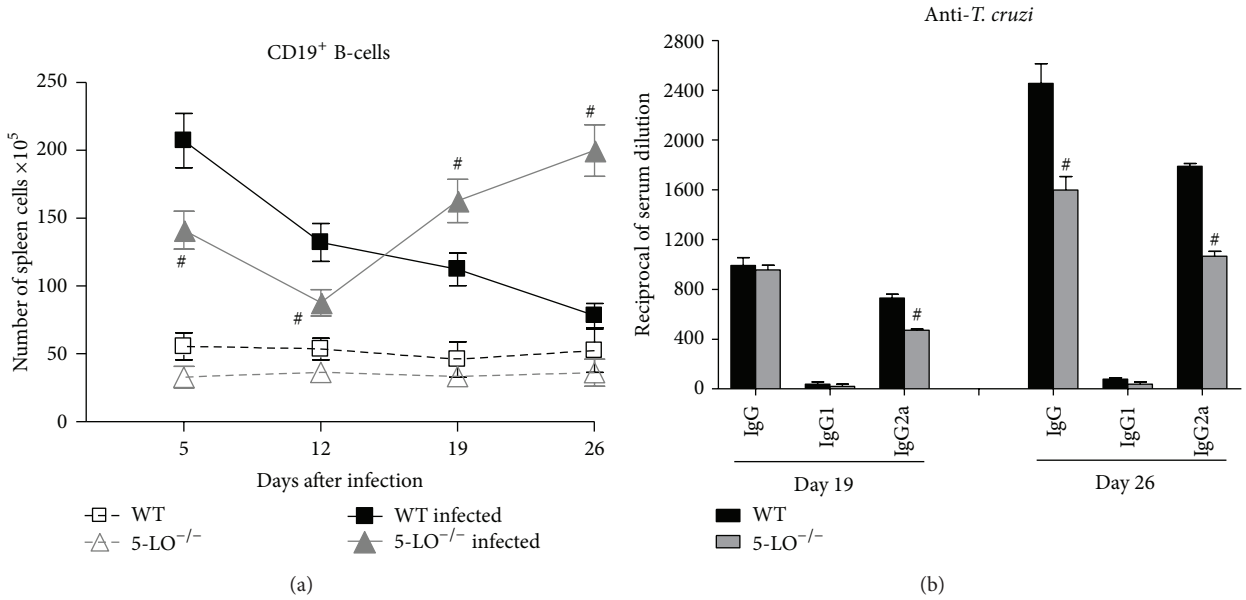

Figure 5: (a) Splenic CD19$^+$ B-cell counts in control, infected WT and infected 5-LO$^{-/-}$ mice (n = 10/group). Data are from one of three independent experiments. Student's t-test ($^{\#}P < 0.01$ versus infected WT mice). (b) *T. cruzi*-specific serum antibody titers in infected WT and 5-LO$^{-/-}$ mice (n = 10/group). Data are from one of two independent experiments. $^{\#}P < 0.001$ versus infected WT mice.

and in greater quantities, Th1 cytokines, producing lower quantities of Th2 cytokines and greater quantities of IL-2.

On day 26 after inoculation, infected WT mouse spleen cells stimulated with anti-CD3ε exhibited a bias to produce only the Th1 cytokine IFN-γ in quite high amounts (Figure 7(b)). However, infected 5-LO$^{-/-}$ mouse spleen cells receiving the same treatment presented no alterations in the cytokine production profile, a sustained capacity to produce detectable levels of IL-2, and high (and predominant) levels of Th1 cytokines, as well as low levels of Th2 cytokines, on day 12.

Since anti-CD3ε promotes a polyclonal T-cell stimulation, we investigated whether IFN-γ and IL-10 were produced by primed *T. cruzi*-specific cells. We tested the recall responses of spleen cells collected on day 12 after inoculation and cultured with soluble *T. cruzi* antigens. *T. cruzi*-specific cells from infected WT mice cultured with nominal antigens produced IFN-γ and IL-10, whereas *T. cruzi*-specific cells from infected 5-LO$^{-/-}$ mice produced a recall response, characterized by high levels of IFN-γ and lower levels of IL-10, in the same culture.

These results regarding the recall response suggested the presence of functional parasite-specific effector/memory T cells. Therefore, we sought to study the populations of effector/memory T cells. As shown in Figure 7, infected mice exhibited increased numbers of splenic effector/memory T cells in CD4$^+$ and CD8$^+$ subsets, including CD4$^+$CD45RB^{low}, CD4$^+$CD44^{high}CD62L^{low}, CD8$^+$CD45RB^{low}, and CD8$^+$CD44^{high}CD62L^{low}, on day 26 after inoculation. Interestingly, the numbers of effector/memory T cells CD4$^+$CD45RB^{low} and CD4$^+$CD44^{high}CD62L^{low} were higher in infected 5-LO$^{-/-}$ mice than in infected WT mice. However, we found no differences between infected 5-LO$^{-/-}$ mice and infected WT mice in terms of the numbers of CD8$^+$ effector/memory T cells.

We questioned whether the kinetic differences between infected 5-LO$^{-/-}$ mice and infected WT mice in terms of the increase in CD4$^+$CD25$^+$ T cell numbers (Figure 6(e)) were related to the involvement of regulatory T cells in this model. Figure 7(f) shows that *T. cruzi*-infected mice exhibited increased numbers of CD4$^+$CD25$^+$GITR$^+$regulatory T cells. However infected WT mice and 5-LO$^{-/-}$ mice exhibited similar numbers of splenic CD4$^+$CD25$^+$GITR$^+$ regulatory T cells. Unexpectedly, the numbers of CD4$^+$CD25$^+$GITR$^+$ in the spleen were lower in uninfected 5-LO$^{-/-}$ mice than in uninfected WT mice.

3.10. Levels of LTC$_4$, Serum Nitrite Levels, and Protein Extravasation into the Peritoneal Cavity during the Acute Phase of T. cruzi Infection. The cys-LTs mediate detrimental vascular effects in systemic infections such as sepsis [23]. Vasoactive mediators are produced and may also be involved in the mortality of animals during the acute phase of *T. cruzi* infection [35]. Thus, we next examined the levels of some vasoactive mediators such as NO metabolites, LTC$_4$, and measured the protein leak (as a marker of vascular permeability) at a time point when infected WT mice have a high mortality while infected 5-LO$^{-/-}$ mice do not. As illustrated in Figure 8, the capacity to produce LTC$_4$ was markedly upregulated in the peritoneal cells of infected WT mice on day 22 after inoculation, although, as expected, those of infected 5-LO$^{-/-}$ mice produced no detectable levels of

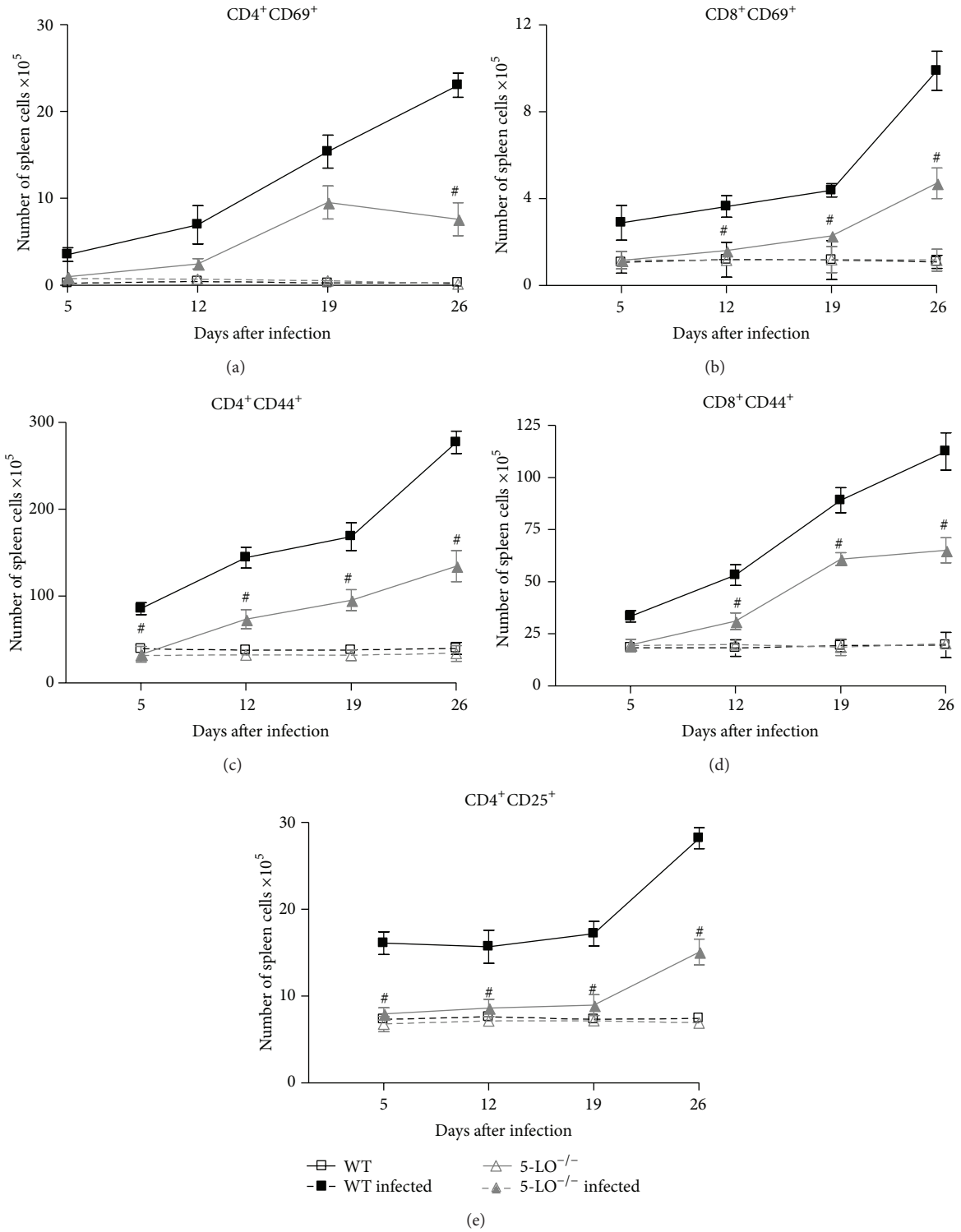

FIGURE 6: Splenic T-cell subpopulations in control, infected WT and infected 5-LO$^{-/-}$ mice (n = 8/group). Data are from one of three independent experiments. Student's t-test ($^{\#}P < 0.01$ versus infected WT mice).

LTC_4. At this time point, infected 5-LO$^{-/-}$ mice presented significantly lower serum nitrite levels than did infected WT mice. In addition, the peritoneal cavity protein extravasation assays (Figure 8(c)) indicated that on days 14 and 19, the degree of protein leakage was similar between the two groups of infected animals. Although the 5-LO$^{-/-}$ mice presented a tendency toward greater protein leakage than did the WT mice, the difference was not significant. However, on day

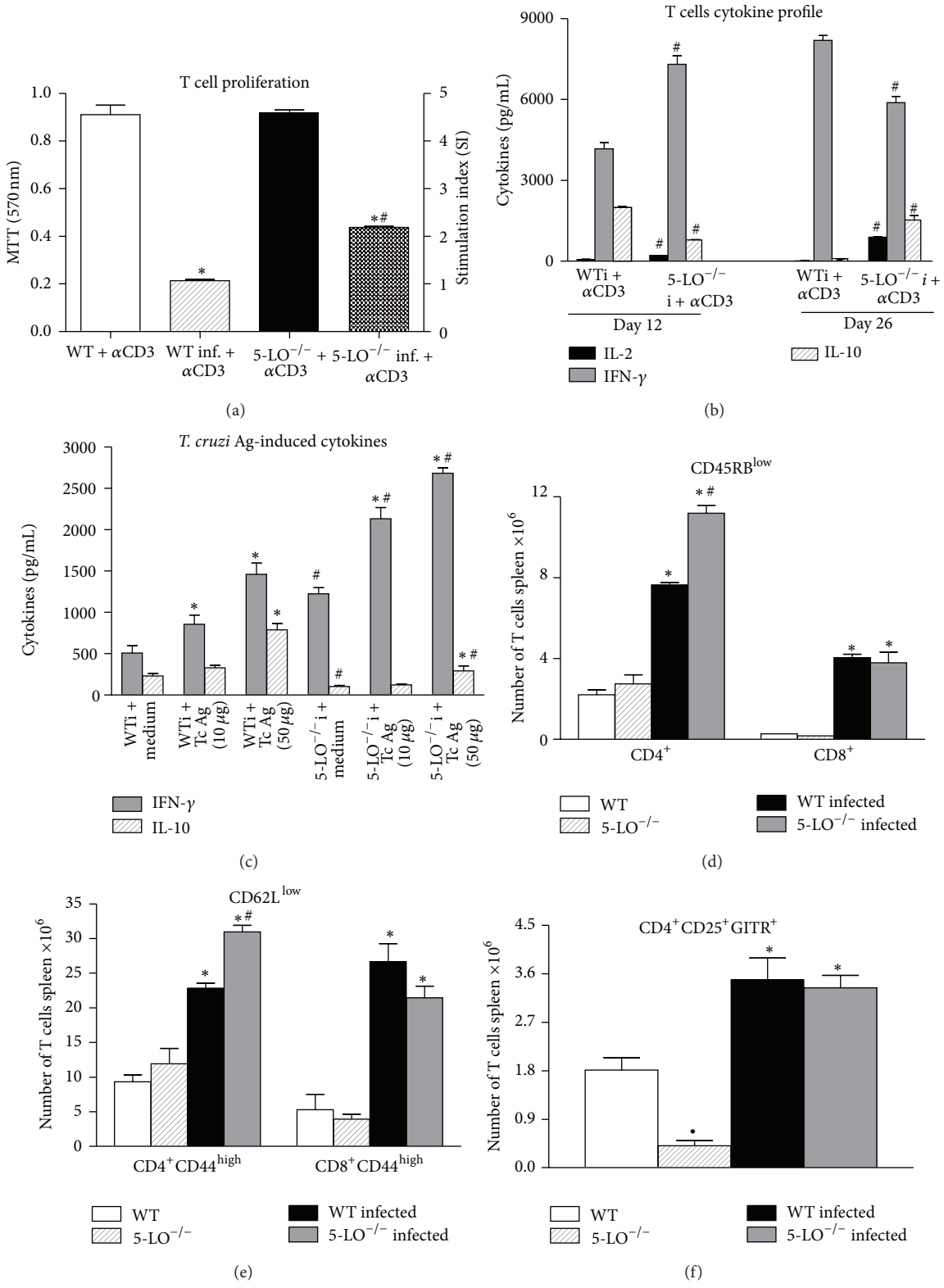

Figure 7: Splenic T-cell properties, effector/memory T cells, and regulatory T cells in control, infected WT and infected 5-LO$^{-/-}$ mice (n = 8/group): (a) proliferation; (b) cytokine production profile after anti-CD3 stimulation; and (c) Th1/Th2 cytokine recall response to soluble *T. cruzi* antigen. $^{*}P < 0.001$ versus uninfected group; $^{\#}P < 0.001$ versus infected WT mice. (d) CD4^{+}CD45RB^{low} and CD8^{+}CD45RB^{low}; (e) CD4^{+}CD44^{high}CD62L^{low} and CD8^{+}CD44^{high}CD62L^{low}; and (f) CD4^{+}CD25^{+}GITR^{+}. Stimulation index (SI) was generated by the ratio between the OD (570 nm) obtained in noninfected/infected cells. Data are from one of two independent experiments. Student's t-test ($^{\#}P < 0.01$ versus infected WT mice).

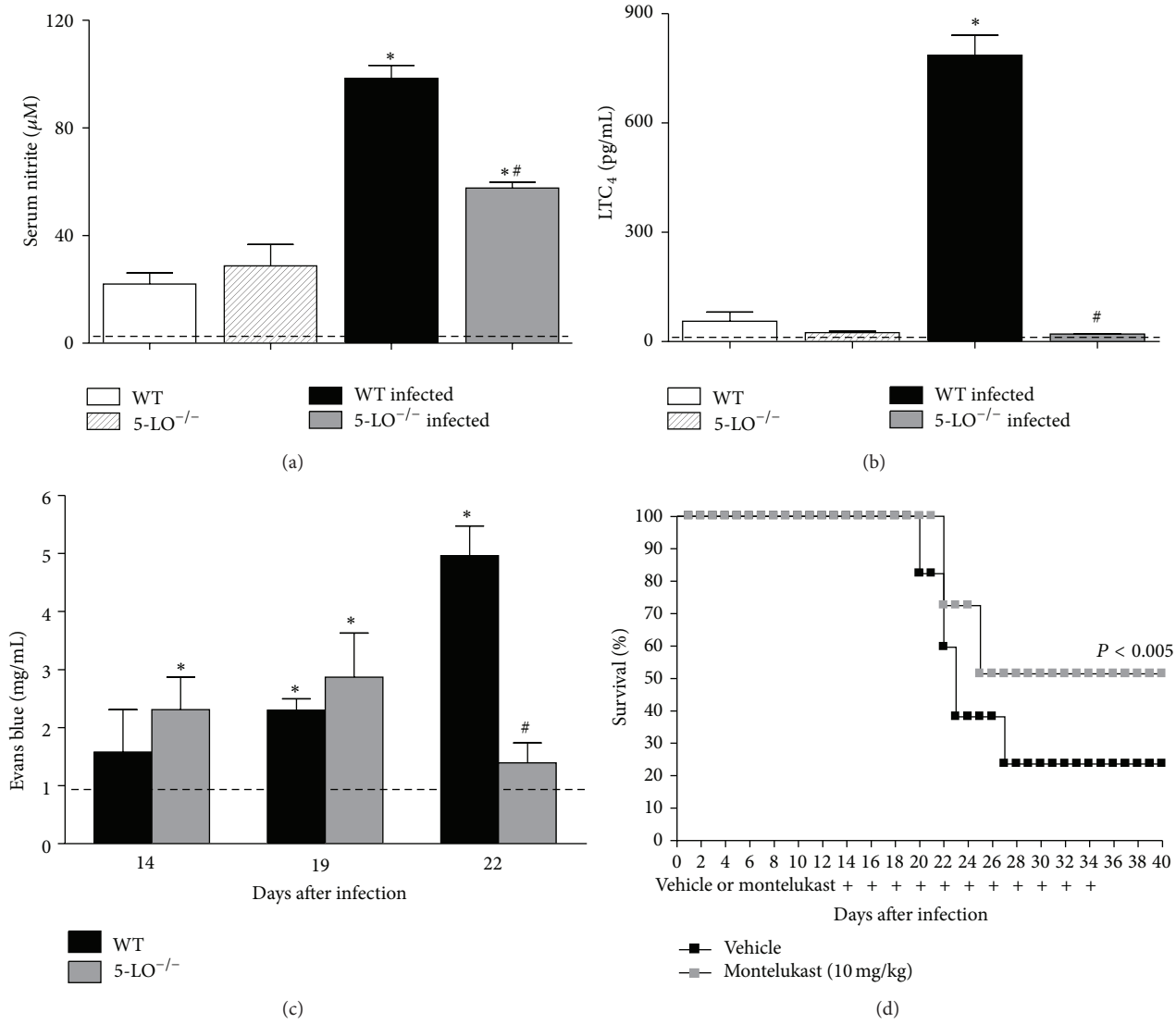

Figure 8: Levels of vasoactive/vasomotor mediators and relevance of cys-LTs in mice acutely infected with *T. cruzi* ($n = 10$/group): (a) total serum nitrite (nitrite/nitrate) levels and (b) LTC_4 production by peritoneal cells upon stimulation with calcium ionophore. Data are from one of three independent experiments. $^{\#}P < 0.001$ versus infected WT mice. (c) Protein extravasation in the peritoneal cavity (colorimetric assay of extravascular dye leakage). Dotted line indicates the mean Evans blue D.O. found in control mice. Data are from one experiment representative of three separate experiments. $^{\#}P < 0.05$ versus infected WT mice. (d) Effect of cys-LT receptor antagonist on survival in *T. cruzi*-infected mice: (black squares) vehicle-treated infected WT mice and (gray squares) infected WT mice treated with montelukast (10 mg/kg) from postinoculation day 14 to postinoculation day 34 and monitored for 26 days. Data are from one experiment representative of two separate experiments. Wilcoxon signed-rank test $^{\#}P < 0.005$ versus vehicle-treated infected WT mice.

22, protein leakage in the peritoneal cavity was considerably greater in the infected WT mice than in the infected 5-LO$^{-/-}$ mice.

3.11. Treatment of Infected Mice with cys-LTs Receptor Antagonist and Mortality. To determine whether cysLTs are involved in the mortality of *T. cruzi*-infected mice, WT mice were subjected to infection with *T. cruzi* and treated with the cysLT receptor antagonist montelukast from day 14 to day 34 after inoculation. On day 40 after inoculation, when mortality among the vehicle-treated control WT mice was 82%, a moderately significant degree of protection (reduction to 48% mortality) was achieved after treatment with montelukast (Figure 8(d)).

4. Discussion

Leukotrienes, products of the 5-LO pathway of arachidonic acid metabolism, are potent immunomodulatory lipids that are increasingly recognized to regulate innate and adaptive immune responses to parasitic infections [36]. Despite the relevance of LTs in *T. cruzi* killing by macrophages *in vitro* as well as in controlling blood parasite numbers *in vivo*

[26, 37, 38], the oxidative balance in 5-LO$^{-/-}$ *T. cruzi* infected mice has been related to be 5-LO-pathway independent [39]. Different results for NO and cytokines productions were observed during the acute phase of *T. cruzi* Y strain infection of 5-LO$^{-/-}$ mice and it has been related to resistance [40] or susceptibility [41]. The localized presence of TCD8$^+$ or TCD4$^+$ in the heart was demonstrated in *T. cruzi* 5-LO$^{-/-}$ infected mice [40], but other cell types and/or eicosanoid mediators were not investigated for a more complete immune response analysis. The novel finds in this study focus on the *in vivo* role of 5-LO metabolites in cells related to innate/adaptive immune responses, resistance, and mortality during the acute phase of *T. cruzi* murine infection. It is important to note that analysis performed after day sixteen after infection was done using infected mice that had survived up to that time point. Furthermore, we describe the results of 5-LO$^{-/-}$ mice infection, using *T. cruzi* Colombian strain, contributing to a better understanding of the immune response and pathology of the Chagas' disease.

Our data show that peritoneal cells from infected WT mice develop an enhanced capacity to produce LTB_4, LTC_4, and PGE_2 compared with cells obtained from uninfected mice, implicating LTs and PGs in the host response to *T. cruzi* parasitic infection. Compared with WT, 5-LO$^{-/-}$ mice developed significantly reduced parasitemia, lower tissue parasitism, and less inflammatory cell infiltrates, as well as a significant improvement in survival. Our curve of parasitemia showed a different profile compared with two previous publications [40, 41]. However, these publications are also different between them, what could be due to different trypomastigotes that were used to infect the experimental groups of mice, since one work used cell culture-derived trypomastigotes [40] and other used mice-derived trypomastigotes [41]. Moreover, both works used the Y strain of *T. cruzi*, while we used the Colombian strain.

These scenarios suggest that LTs deficiency renders mice more resistant to *T. cruzi* infection and conversely that 5-LO products confer susceptibility to *T. cruzi* virulence. The production of proinflammatory cytokines IL-1β, IL-6, IL-12, TNF-α, and IFN-γ and the presence of parasite-specific T cells generating predominantly IFN-γ and low levels of IL-10 were associated with an increased efficiency of 5-LO$^{-/-}$ mice to control the infection within the blood and tissue compartments. In fact, in the later phases of infection, parasitemia and tissue parasitism were significantly reduced in 5-LO$^{-/-}$ mice and it is in accordance with previous studies showing that cytokines such as IL-1β, IL-6, IL-12, TNF-α, and IFN-γ play a relevant role in host killing mechanisms against *T. cruzi* [8].

Consistent with our data, there is evidence that LTs induce TNF-α [38] and PGE_2 [42] release. In some models, it has been observed that drug-induced or genetic LTs deficiency increased PGE_2 levels [43]. We observed that 5-LO$^{-/-}$ mice presented a sustained potential to produce PGE_2 in the late phase of infection. In support of our findings that LTB_4 induced IL-6, healthy patients subjected to inhalation of swine house dust and treated with 5-LO inhibitor showed elevated IL-6 serum levels [44]. In addition, LTB_4 might induce IL-1β production [45]; although it is not seen as a unique inducer, we can presume that, in 5-LO$^{-/-}$ mice, IL-1β and IL-6 were induced by *T. cruzi* PAMPs (Pathogen Associated Molecular Patterns), as previously described [46].

In some murine models of fungal or bacterial infection, it was suggested that the pharmacological impairment of LT biosynthesis hindered the production of the Th1 cytokines IL-12 and IFN-γ [20, 21]. However, in our model, 5-LO$^{-/-}$ *T. cruzi* infected mice exhibited an increased capacity to produce IL-12 and IFN-γ. A similar result was obtained in other infection models using 5-LO$^{-/-}$ mice [22, 29, 30], and this capacity was found to be essential to achieving protective immunity against pathogens in these mice [22, 47]. Previous studies have demonstrated that the quality and quantity of inflammatory mediators such as IL-12, IFN-γ, and IL-10 released during the first two weeks of infection are critical to driving the generation of parasite-specific effector T cells [48] and we suggest that early IL-12 and IFN-γ production during infection was regulated by LTs. It is probable that splenic Gr-1$^+$CD11c$^+$ plasmacytoid dendritic cells, Gr-1$^+$ neutrophils, and F4/80$^+$ macrophages are sources of IL-12 and IFN-γ, since the numbers of these cells were found to be significantly higher in 5-LO$^{-/-}$ infected mice than in WT infected mice. These cell types have also been found to be increased by *T. cruzi* infection in other models [10, 49], and they are relevant source of IL-12 and IFN-γ in the setting of protozoal infection [50, 51]. Furthermore, IL-12-producing CD11c$^+$ cells were found to be elevated in 5-LO$^{-/-}$ model of *M. tuberculosis* infection [22].

There is evidence that LTs contribute to the process of T-cell activation/migration in different models [52, 53]. Our results demonstrated the importance of 5-LO products in T-cell activation during *T. cruzi* infection. Although a reduction in the numbers of activated splenic T cells was achieved in the infected 5-LO$^{-/-}$ mice, the T cells from these animals, as opposed to those from WT mice, presented a partially recovered capacity to proliferate after anti-CD3ε stimulation and also to produce IL-2 after anti-CD3ε stimulation or in the presence of *T. cruzi* soluble antigens. We are in accordance with previous studies showing that LTs may also inhibit T cell proliferation and IL-2 production [54] and that susceptibility to *T. cruzi* infection is associated with elevated numbers of polyclonal activated T cells in the spleen [55] or with splenic T cell unresponsiveness to mitogens and inability to secrete IL-2 [56]. Furthermore, the resistance to *T. cruzi* infection of 5-LO$^{-/-}$ mice, in contrast to the susceptibility of WT mice, correlated with elevated numbers of splenic effector/memory T cells, including CD4$^+$CD45RB^{low} and CD4$^+$CD44^{high} CD62L^{low}, at the end of the acute phase of infection. Elevated numbers of T cells expressing these phenotypes have been associated with IFN-γ production and resistance to *T. cruzi* infection [11].

The correlation between the resistance to infection and the Th1 bias of CD4$^+$ T cells has been identified in 5-LO$^{-/-}$ mice infected with other pathogens, including *M. tuberculosis* [22] and *T. gondii* [57]. The bias towards IFN-γ production by T cells from 5-LO$^{-/-}$ mice was also observed

following infections with typical Th2-inducing pathogens such as *S. mansoni* [29] and *S. venezuelensis* [30] leading these animals to become more resistant and susceptible to infection, respectively. The $CD4^+CD25^+$ T cells number abnormality found in *T. cruzi* 5-$LO^{-/-}$ infected mice led us to further investigate these $CD4^+CD25^+$ regulatory T cells. We found that WT and 5-$LO^{-/-}$ infected mice presented similar numbers of splenic $CD4^+CD25^+GITR^+$ regulatory T cells. This does not completely rule out the involvement of $CD4^+CD25^+$ regulatory T cells in the present model. In fact, it was recently demonstrated that $CD4^+CD25^+$ regulatory T cells play a limited role during the acute and chronic phases of *T. cruzi* infection [58].

Phagocytes have long been known to play an important role in the *T. cruzi* killing process [59]. It is also known that IFN-γ is one of the major mediators conferring resistance to *T. cruzi* [60]. Macrophage ($F4/80^+$) numbers and IFN-γ were found to be increased in *T. cruzi* 5-$LO^{-/-}$ infected mice. *In vitro* infection assays revealed that activated PMs from 5-$LO^{-/-}$ mice were strongly associated with more efficient parasite killing than WT macrophages. These results corroborate our *in vivo* findings that 5-$LO^{-/-}$ mice are more efficient at controlling parasitemia, but contrasts with previous *in vitro* findings showing LTs foster intracellular parasite killing [26, 38]. However, it is suggested in 5-$LO^{-/-}$ mice that an oxidative stress occurs by a leukotriene-independent pathway, since an increase in erythrocyte oxidative stress was observed in these animals [39]. Differences in experimental design between our study and previously published investigations warrant discussion. Some differences in results may be explained in part by the macrophage activation and/or responsiveness to LTs. We used classic activated macrophages (M1) *in vitro* [61], whereas previous studies showing enhanced pathogen-killing properties of LT-stimulated macrophages employed resident peritoneal macrophages [26, 37], thioglycollate-elicited macrophages [28, 38], or alveolar macrophages [18]. The functional differences among these different types of macrophages are remarkable and have been consistently described [62, 63]. The increased capacity of macrophages from 5-$LO^{-/-}$ mice to kill intracellular pathogens was previously described for *M. tuberculosis* [22]. These findings underscore the relevance of IFN-γ and the killing activity of macrophages in 5-$LO^{-/-}$ mice resistance to *T. cruzi* infection, although our data shed no light on whether LXA_4 is involved in the parasite resistance of mice, as has been described for *M. tuberculosis* infection [22].

Analysis of B cells indicated that *T. cruzi* 5-$LO^{-/-}$ infected mice developed smaller increases in the numbers of splenic $CD19^+$ B cells during the first two weeks than did WT mice, but this was followed by increased numbers of splenic $CD19^+$ B cells in the following weeks. The elevated numbers of $CD19^+$ B cells found in 5-$LO^{-/-}$ mice in the later phase of infection might indicate an accumulation of undifferentiated B cells in the splenic compartment. This hypothesis is supported by previous studies showing that antibody-secreting B cells lose their CD19 marker [64]. Previous *in vitro* findings showed that LTs are important in activating B cells in human and mouse models [65, 66] and suggest that this could be also relevant *in vivo*. The alteration in B cell activation observed in *T. cruzi* 5-$LO^{-/-}$ infected mice could explain the lower serum levels of parasite-specific IgG and IgG2a at the end of the acute phase of infection. It was previously described that LT deficiency altered specific-immunoglobulin class switching to specific pathogens *in vivo* [29, 30]. Indeed, LTs may affect parasite-specific antibody levels during infection and parasite-specific IgG and IgG2a might not be involved in 5-$LO^{-/-}$ mouse resistance to *T. cruzi* infection. This reinforces the previous observation that host resistance during the acute phase of *T. cruzi* infection can be achieved in the absence of B cells [67].

Animal mortality during the acute phase of *T. cruzi* infection has been associated with multiple factors, including parasite strain virulence [68], anemia [69], increased levels of TNF-α, and T-cell hyperactivity [70]. In fact, *T. cruzi*-infected mice have been shown to be extremely sensitive to sepsis-like inducers and to die with evidence of a shock syndrome [69]. We demonstrated that *T. cruzi*-infected WT mice presented, at the acute phase, an upregulated production of LTB_4 and LTC_4, as well as high serum nitrite levels. In addition, the analysis of protein extravasation in the peritoneal cavity revealed that infected WT mice exhibited stronger protein leakage as compared with 5-$LO^{-/-}$ mice. Previous studies showed that LTs induce NO production in macrophages and endothelial cells [38], and high levels of NO production have been associated with increased mortality in *T. cruzi*-infected mice [71]. LTs play a critical role in vascular events and mortality of mice subjected to the cecal ligation and puncture model of sepsis [23]. We observed that *T. cruzi*-infected WT mice treated with montelukast presented a significant reduction in mortality, providing evidence that cys-LTs are involved in vascular events associated with mortality of animals during the acute phase of *T. cruzi* infection. It is notable that montelukast treatment was less effective in increasing survival in contrast to what is observed in *T. cruzi*-infected 5-$LO^{-/-}$ mice. The deaths of some montelukast-treated animals might be attributable to the presence of other 5-LO products, such as LTB_4, and its indirect effect of inducing vasoactive mediators such as NO [72] and thromboxane [73]. However, unlike WT, 5-$LO^{-/-}$ infected mice sustain the production of TNF-α and IL-6. This finding is not surprising, since these cytokines have been shown to have vasoactive properties [35].

One reasonable mechanism to explain WT mice mortality during the acute phase of *T. cruzi* infection involves their capacity to produce LTs, which lead to the extreme bias of spleen cells and T-cells that secrete high levels of Th1 cytokines, such as IFN-γ, and very low levels of IL-10. In addition, downregulated production of PGE_2 might be relevant, since PGE_2 has been shown to induce IL-10 production [74], inhibit the production of IFN-γ during *T. cruzi* infection, and promote the increased production of NO [75]. The advantage in survival of *T. cruzi*-5-$LO^{-/-}$ infected mice represents a complex contribution of various effects on host defense, including their capacity to efficiently control the parasites and produce detectable levels of IL-10, the increase

in production of PGE_2, and lesser amounts of NO, as well as their inability to produce cys-LTs.

5. Conclusions

Our findings demonstrated that 5-LO deficiency altered eicosanoids and cytokines production during *T. cruzi* infection and favored the generation/maintenance of protective immune responses. Also, they provided evidence that 5-LO-derived lipid mediators have a negative effect on host survival during the acute phase of infection.

Conflict of Interests

The authors declare that there is no conflict of interests regarding the publication of this paper.

Authors' Contribution

Adriana M. C. Canavaci and Carlos A. Sorgi contributed equally to this work.

Acknowledgments

This work was supported by the *Fundação de Amparo a Pesquisa do Estado de São Paulo* (FAPESP, Foundation for the Support of Research in the State of São Paulo). Adriana M. C. Canavaci is the recipient of a fellowship from the Brazilian *Conselho Nacional de Desenvolvimento Científico e Tecnológico* (CNPq, National Council for Scientific and Technological Development).

References

[1] K. Senior, "Chagas disease: moving towards global elimination.," *The Lancet infectious diseases*, vol. 7, no. 9, p. 572, 2007.

[2] L. O. Andrade and N. W. Andrews, "The Trypanosoma cruzi-host-cell interplay: Location, invasion, retention," *Nature Reviews Microbiology*, vol. 3, no. 10, pp. 819–823, 2005.

[3] Z. Brener and R. T. Gazzinelli, "Immunological control of Trypanosoma cruzi infection and pathogenesis of Chagas' disease," *International Archives of Allergy and Immunology*, vol. 114, no. 2, pp. 103–110, 1997.

[4] R. T. Gazzinelli, I. P. Oswald, S. Hieny, S. L. James, and A. Sher, "The microbicidal activity of interferon-γ-treated macrophages against Trypanosoma cruzi involves an L-arginine-dependent, nitrogen oxide-mediated mechanism inhibitable by interleukin-10 and transforming growth factor-β," *European Journal of Immunology*, vol. 22, no. 10, pp. 2501–2506, 1992.

[5] C. A. Santos-Buch, "American trypanosomiasis: chagas' disease," *International Review of Experimental Pathology*, vol. 19, pp. 63–100, 1979.

[6] S. E. B. Graefe, T. Streichert, B. S. Budde et al., "Genes from Chagas susceptibility loci that are differentially expressed in T. cruzi-resistant mice are candidates accounting for impaired immunity," *PLoS ONE*, vol. 1, no. 1, article e57, 2006.

[7] S. V. de Avalos, I. J. Blader, M. Fisher, J. C. Boothroyd, and B. A. Burleigh, "Immediate/early response to *Trypanosoma cruzi* infection involves minimal modulation of host cell transcription," *The Journal of Biological Chemistry*, vol. 277, no. 1, pp. 639–644, 2002.

[8] L. E. Fichera, M. C. Albareda, S. A. Laucella, and M. Postan, "Intracellular growth of trypanosoma cruzi in cardiac myocytes is inhibited by cytokine-induced nitric oxide release," *Infection and Immunity*, vol. 72, no. 1, pp. 359–363, 2004.

[9] F. S. Machado, G. A. Martins, J. C. S. Aliberti, F. L. A. C. Mestriner, F. Q. Cunha, and J. S. Silva, "Trypanosoma cruzi-infected cardiomyocytes produce chemokines and cytokines that trigger potent nitric oxide-dependent trypanocidal activity," *Circulation*, vol. 102, no. 24, pp. 3003–3008, 2000.

[10] A. C. Monteiro, V. Schmitz, E. Svensjo et al., "Cooperative activation of TLR2 and bradykinin B_2 receptor is required for induction of type 1 immunity in a mouse model of subcutaneous infection by *Trypanosoma cruzi*," *The Journal of Immunology*, vol. 177, no. 9, pp. 6325–6335, 2006.

[11] A. Nomizo, F. Cardillo, E. Postól, L. P. de Carvalho, and J. Mengel, "Vγ1 $\gamma\delta$ T cells regulate type-1/type-2 immune responses and participate in the resistance to infection and development of heart inflammation in Trypanosoma cruzi-infected BALB/c mice," *Microbes and Infection*, vol. 8, no. 3, pp. 880–888, 2006.

[12] R. L. Tarleton, B. H. Koller, A. Latour, and M. Postan, "Susceptibility of β2-microglobulin-deficient mice to Trypanosoma cruzi infection," *Nature*, vol. 356, no. 6367, pp. 338–340, 1992.

[13] D. F. Hoft, A. R. Schnapp, C. S. Eickhoff, and S. T. Roodman, "Involvement of $CD4^+$ Th1 cells in systemic immunity protective against primary and secondary challenges with *Trypanosoma cruzi*," *Infection and Immunity*, vol. 68, no. 1, pp. 197–204, 2000.

[14] M. Peters-Golden, C. Canetti, P. Mancuso, and M. J. Coffey, "Leukotrienes: underappreciated mediators of innate immune responses," *The Journal of Immunology*, vol. 174, no. 2, pp. 589–594, 2005.

[15] M. Peters-Golden and T. G. Brock, "5-Lipoxygenase and FLAP," *Prostaglandins Leukotrienes and Essential Fatty Acids*, vol. 69, no. 2-3, pp. 99–109, 2003.

[16] C. N. Serhan, M. Hamberg, and B. Samuelsson, "Lipoxins: novel series of biologically active compounds formed from arachidonic acid in human leukocytes," *Proceedings of the National Academy of Sciences of the United States of America*, vol. 81, no. 17, pp. 5335–5339, 1984.

[17] T. Demitsu, H. Katayama, T. Saito-Taki, H. Yaoita, and M. Nakano, "Phagocytosis and bactericidal action of mouse peritoneal macrophages treated with leukotriene B4," *International Journal of Immunopharmacology*, vol. 11, no. 7, pp. 801–808, 1989.

[18] M. B. Bailie, T. J. Standiford, L. L. Laichalk, M. J. Coffey, R. Strieter, and M. Peters-Golden, "Leukotriene-deficient mice manifest enhanced lethality from Klebsiella pneumonia in association with decreased alveolar macrophage phagocytic and bactericidal activities," *Journal of Immunology*, vol. 157, no. 12, pp. 5221–5224, 1996.

[19] N. Chen, A. Restivo, and C. S. Reiss, "Leukotrienes play protective roles early during experimental VSV encephalitis," *Journal of Neuroimmunology*, vol. 120, no. 1-2, pp. 94–102, 2001.

[20] A. I. Medeiros, A. Sá-Nunes, E. G. Soares, C. M. Peres, C. L. Silva, and L. H. Faccioli, "Blockade of endogenous leukotrienes exacerbates pulmonary histoplasmosis," *Infection and Immunity*, vol. 72, no. 3, pp. 1637–1644, 2004.

[21] C. M. Peres, L. de Paula, A. I. Medeiros et al., "Inhibition of leukotriene biosynthesis abrogates the host control of Mycobacterium tuberculosis," *Microbes and Infection*, vol. 9, no. 4, pp. 483–489, 2007.

[22] A. Bafica, C. A. Scanga, C. Serhan et al., "Host control of *Mycobacterium tuberculosis* is regulated by 5-lipoxygenase-dependent lipoxin production," *The Journal of Clinical Investigation*, vol. 115, no. 6, pp. 1601–1606, 2005.

[23] C. F. Benjamin, C. Canetti, F. Q. Cunha, S. L. Kunkel, and M. Peters-Golden, "Opposing and hierarchical roles of leukotrienes in local innate immune versus vascular responses in a model of sepsis," *Journal of Immunology*, vol. 174, no. 3, pp. 1616–1620, 2005.

[24] H. D'Avila, C. G. Freire-de-Lima, N. R. Roque et al., "Host cell lipid bodies triggered by Trypanosoma cruzi infection and enhanced by the uptake of apoptotic cells are associated with prostaglandin E2 generation and increased parasite growth," *Journal of Infectious Diseases*, vol. 204, no. 6, pp. 951–961, 2011.

[25] L. Xiao, P. S. Patterson, C. Yang, and A. A. Lal, "Role of eicosanoids in the pathogenesis of murine cerebral malaria," *American Journal of Tropical Medicine and Hygiene*, vol. 60, no. 4, pp. 668–673, 1999.

[26] J. J. Wirth and F. Kierszenbaum, "Stimulatory effects of leukotriene B4 on macrophage association with and intracellular destruction of Trypanosoma cruzi," *Journal of Immunology*, vol. 134, no. 3, pp. 1989–1993, 1985.

[27] J. J. Wirth and F. Kierszenbaum, "Effects of leukotriene C4 on macrophage association with and intracellular fate of Trypanosoma cruzi," *Molecular and Biochemical Parasitology*, vol. 15, no. 1, pp. 1–10, 1985.

[28] C. H. Serezani, J. H. Perrela, M. Russo, M. Peters-Golden, and S. Jancar, "Leukotrienes are essential for the control of Leishmania amazonensis infection and contribute to strain variation in susceptibility," *Journal of Immunology*, vol. 177, no. 5, pp. 3201–3208, 2006.

[29] W. E. Secor, M. R. Powell, J. Morgan, T. A. Wynn, and C. D. Funk, "Mice deficient for 5-lipoxygenase, but not leukocyte-type 12- lipoxygenase, display altered immune responses during infection with Schistosoma mansoni," *Prostaglandins and Other Lipid Mediators*, vol. 56, no. 5-6, pp. 291–304, 1998.

[30] E. R. Machado, M. T. Ueta, E. V. Lourenço et al., "Leukotrienes play a role in the control of parasite burden in murine strongyloidiasis," *The Journal of Immunology*, vol. 175, no. 6, pp. 3892–3899, 2005.

[31] L. Xiao, P. S. Patterson, C. Yang, and A. A. Lal, "Role of eicosanoids in the pathogenesis of murine cerebral malaria," *The American Journal of Tropical Medicine and Hygiene*, vol. 60, no. 4, pp. 668–673, 1999.

[32] F. Cardillo, F. Q. Cunha, W. M. S. C. Tamashiro, M. Russo, S. B. Garcia, and J. Mengel, "NK 1.1+ Cells and T-cell activation in euthymic and thymectomized C57B1/6 mice during acute Trypanosoma cruzi infection," *Scandinavian Journal of Immunology*, vol. 55, no. 1, pp. 96–104, 2002.

[33] I. A. Abrahamsohn, A. P. G. da Silva, and R. L. Coffman, "Effects of interleukin-4 deprivation and treatment on resistance to Trypanosoma cruzi," *Infection and Immunity*, vol. 68, no. 4, pp. 1975–1979, 2000.

[34] G. N. R. Vespa, F. Q. Cunha, and J. S. Silva, "Nitric oxide is involved in control of Trypanosoma cruzi-induced parasitemia and directly kills the parasite in vitro," *Infection and Immunity*, vol. 62, no. 11, pp. 5177–5182, 1994.

[35] C. Hölscher, M. Mohrs, W. J. Dai et al., "Tumor necrosis factor α-mediated toxic shock in Trypanosoma cruzi-infected interleukin 10-deficient mice," *Infection and Immunity*, vol. 68, no. 7, pp. 4075–4083, 2000.

[36] A. P. Rogerio and F. F. Anibal, "Role of leukotrienes on protozoan and helminth infections," *Mediators of Inflammation*, vol. 2012, Article ID 595694, 13 pages, 2012.

[37] J. J. Wirth and F. Kierszenbaum, "Effects of leukotriene C_4 on macrophage association with and intracellular fate of *Trypanosoma cruzi*," *Molecular and Biochemical Parasitology*, vol. 15, no. 1, pp. 1–10, 1985.

[38] A. Talvani, F. S. Machado, G. C. Santana et al., "Leukotriene B4 induces nitric oxide synthesis in Trypanosoma cruzi-infected murine macrophages and mediates resistance to infection," *Infection and Immunity*, vol. 70, no. 8, pp. 4247–4253, 2002.

[39] C. L. Borges, R. Cecchini, V. L. H. Tatakihara et al., "5-Lipoxygenase plays a role in the control of parasite burden and contributes to oxidative damage of erythrocytes in murine Chagas' disease," *Immunology Letters*, vol. 123, no. 1, pp. 38–45, 2009.

[40] W. R. Pavanelli, F. R. S. Gutierrez, F. S. Mariano et al., "5-Lipoxygenase is a key determinant of acute myocardial inflammation and mortality during *Trypanosoma cruzi* infection," *Microbes and Infection*, vol. 12, no. 8-9, pp. 587–597, 2010.

[41] C. Panis, T. L. Mazzuco, C. Z. F. Costa et al., "*Trypanosoma cruzi*: effect of the absence of 5-lipoxygenase (5-LO)-derived leukotrienes on levels of cytokines, nitric oxide and iNOS expression in cardiac tissue in the acute phase of infection in mice," *Experimental Parasitology*, vol. 127, no. 1, pp. 58–65, 2011.

[42] A. Rossi, A. M. Acquaviva, F. Iuliano, R. di Paola, S. Cuzzocrea, and L. Sautebin, "Up-regulation of prostaglandin biosynthesis by leukotriene C4 in elicited mice peritoneal macrophages activated with lipopolysaccharide/ interferon-γ," *Journal of Leukocyte Biology*, vol. 78, no. 4, pp. 985–991, 2005.

[43] R. S. Byrum, J. L. Goulet, R. J. Griffiths, and B. H. Koller, "Role of the 5-lipoxygenase-activating protein (FLAP) in murine acute inflammatory responses," *Journal of Experimental Medicine*, vol. 185, no. 6, pp. 1065–1075, 1997.

[44] B. M. Larsson, M. Kumlin, B. M. Sundblad, K. Larsson, S. E. Dahlén, and L. Palmberg, "Effects of 5-lipoxygenase inhibitor zileuton on airway responses to inhaled swine house dust in healthy subjects," *Respiratory Medicine*, vol. 100, no. 2, pp. 226–237, 2006.

[45] Y. Kageyama, Y. Koide, S. Miyamoto, T. O. Yoshida, and T. Inoue, "Leukotrien B4-induced interleukin-1β in synovial cells from patients with rheumatoid arthritis," *Scandinavian Journal of Rheumatology*, vol. 23, no. 3, pp. 148–150, 1994.

[46] A. Talvani, C. S. Ribeiro, J. C. S. Aliberti et al., "Kinetics of cytokine gene expression in experimental chagasic cardiomyopathy: tissue parasitism and endogenous IFN-γ as important determinants of chemokine mRNA expression during infection with Trypanosoma cruzi," *Microbes and Infection*, vol. 2, no. 8, pp. 851–866, 2000.

[47] J. Aliberti, S. Hieny, C. Reis Sousa, C. N. Serhan, and A. Sher, "Lipoxin-mediated inhibition of IL-12 production by DCs: a mechanism for regulation of microbial immunity," *Nature Immunology*, vol. 3, no. 1, pp. 76–82, 2002.

[48] A. P. G. da Silva and I. de Almeida Abrahamsohn, "Interleukin-12 stimulation of lymphoproliferative responses in *Trypanosoma cruzi* infection," *Immunology*, vol. 104, no. 3, pp. 349–354, 2001.

[49] O. Goño, P. Alcaide, and M. Fresno, "Immunosuppression during acute *Trypanosoma cruzi* infection: involvement of Ly6G ($Gr1^+$)$CD11b^+$ immature myeloid suppressor cells," *International Immunology*, vol. 14, no. 10, pp. 1125–1134, 2002.

[50] C. H. Liu, Y. T. Fan, A. Dias et al., "Cutting edge: dendritic cells are essential for in vivo IL-12 production and development of resistance against Toxoplasma gondii infection in mice," *Journal of Immunology*, vol. 177, no. 1, pp. 31–35, 2006.

[51] D. G. Mordue and L. D. Sibley, "A novel population of $Gr\text{-}1^+$-activated macrophages induced during acute toxoplasmosis," *Journal of Leukocyte Biology*, vol. 74, no. 6, pp. 1015–1025, 2003.

[52] I. Prinz, C. Gregoire, H. Mollenkopf et al., "The type 1 cysteinyl leukotriene receptor triggers calcium influx and chemotaxis in mouse $\alpha\beta$- and $\gamma\delta$ effector T cells," *The Journal of Immunology*, vol. 175, no. 2, pp. 713–719, 2005.

[53] A. M. Tager, S. K. Bromley, B. D. Medoff et al., "Leukotriene B4 receptor BLT1 mediates early effector T cell recruitment," *Nature Immunology*, vol. 4, no. 10, pp. 982–990, 2003.

[54] J. S. Goodwin, "Regulation of T cell activation by leukotriene B4," *Immunologic Research*, vol. 5, no. 3, pp. 233–248, 1986.

[55] N. Nogueira, J. Ellis, S. Chaplan, and Z. Cohn, "Trypanosoma cruzi: In vivo and in vitro correlation between T-cell activation and susceptibility in inbred strains of mice," *Experimental Parasitology*, vol. 51, no. 3, pp. 325–334, 1981.

[56] A. Harel-Bellan, M. Joskowicz, D. Fradelizi, and H. Eisen, "Modification of T-cell proliferation and interleukin 2 production in mice infected with Trypanosoma cruzi," *Proceedings of the National Academy of Sciences of the United States of America*, vol. 80, no. 11, pp. 3466–3469, 1983.

[57] J. Aliberti, C. Serhan, and A. Sher, "Parasite-induced lipoxin A_4 is an endogenous regulator of IL-12 production and immunopathology in *Toxoplasma gondii* infection," *Journal of Experimental Medicine*, vol. 196, no. 9, pp. 1253–1262, 2002.

[58] J. Kotner and R. Tarleton, "Endogenous CD4+ CD25+ regulatory T cells have a limited role in the control of Trypanosoma cruzi infection in mice," *Infection and Immunity*, vol. 75, no. 2, pp. 861–869, 2007.

[59] D. M. Williams, S. Sawyer, and J. S. Remington, "Role of activated macrophages in resistance of mice to infection with *Trypanosoma cruzi*," *Journal of Infectious Diseases*, vol. 134, no. 6, pp. 610–614, 1976.

[60] F. Torrico, H. Heremans, M. T. Rivera, E. Van Marck, A. Billiau, and Y. Carlier, "Endogenous IFN-γ is required for resistance to acute Trypanosoma cruzi infection in mice," *Journal of Immunology*, vol. 146, no. 10, pp. 3626–3632, 1991.

[61] D. O. Adams and T. A. Hamilton, "Molecular transductional mechanisms by which IFNγ and other signals regulate macrophage development," *Immunological Reviews*, vol. 97, pp. 5–27, 1987.

[62] Y. Kita, T. Takahashi, N. Uozumi, L. Nallan, M. H. Gelb, and T. Shimizu, "Pathway-oriented profiling of lipid mediators in macrophages," *Biochemical and Biophysical Research Communications*, vol. 330, no. 3, pp. 898–906, 2005.

[63] Q. Wu, Y. Feng, Y. Yang et al., "Kinetics of the phenotype and function of murine peritoneal macrophages following acute inflammation," *Cellular & Molecular Immunology*, vol. 1, no. 1, pp. 57–62, 2004.

[64] F. Caligaris-Cappio, L. Bergui, L. Tesio et al., "Identification of malignant plasma cell precursors in the bone marrow of multiple myeloma," *The Journal of Clinical Investigation*, vol. 76, no. 3, pp. 1243–1251, 1985.

[65] K. A. Yamaoka, H. E. Claesson, and A. Rosen, "Leukotriene B4 enhances activation, proliferation, and differentiation of human B lymphocytes," *Journal of Immunology*, vol. 143, no. 6, pp. 1996–2000, 1989.

[66] C. Phillips, "Induction of leukotriene production before antigen challenge enhances antibody affinity in genetically selected mice," *Cellular Immunology*, vol. 136, no. 1, pp. 173–184, 1991.

[67] D. E. Burgess and W. L. Hanson, "*Trypanosoma cruzi*: the T-cell dependence of the primary immune response and the effects of depletion of T cells and Ig-bearing cells on immunological memory," *Cellular Immunology*, vol. 52, no. 1, pp. 176–186, 1980.

[68] V. Andrade, M. Barral-Netto, and S. G. Andrade, "Patterns of resistance of inbred mice to *Trypanosoma cruzi* are determined by parasite strain," *Brazilian Journal of Medical and Biological Research*, vol. 18, no. 4, pp. 499–506, 1985.

[69] M. C. G. Marcondes, P. Borelli, N. Yoshida, and M. Russo, "Acute *Trypanosoma cruzi* infection is associated with anemia, thrombocytopenia, leukopenia, and bone marrow hypoplasia: reversal by nifurtimox treatment," *Microbes and Infection*, vol. 2, no. 4, pp. 347–352, 2000.

[70] S. Hamano, K. Himeno, Y. Miyazaki et al., "WSX-1 is required for resistance to Trypanosoma cruzi infection by regulation of proinflammatory cytokine production," *Immunity*, vol. 19, no. 5, pp. 657–667, 2003.

[71] F. Cardillo, A. Nomizo, E. Postól, and J. Mengel, "NK1.1 cells are required to control T cell hyperactivity during Trypanosoma cruzi infection," *Medical Science Monitor*, vol. 10, no. 8, pp. BR259–BR267, 2004.

[72] H. Arndt, J. B. Russell, I. Kurose, P. Kubes, and D. N. Granger, "Mediators of leukocyte adhesion in rat mesenteric venules elicited by inhibition of nitric oxide synthesis," *Gastroenterology*, vol. 105, no. 3, pp. 675–680, 1993.

[73] K. Sakata, S.-E. Dahlén, and M. Bäck, "The contractile action of leukotriene B_4 in the guinea-pig lung involves a vascular component," *British Journal of Pharmacology*, vol. 141, no. 3, pp. 449–456, 2004.

[74] G. Strassmann, V. Patil-Koota, F. Finkelman, M. Fong, and T. Kambayashi, "Evidence for the involvement of interleukin 10 in the differential deactivation of murine peritoneal macrophages by prostaglandin E2," *Journal of Experimental Medicine*, vol. 180, no. 6, pp. 2365–2370, 1994.

[75] M. A. Michelin, J. S. Silva, and F. Q. C. Cunha, "Inducible cyclooxygenase released prostaglandin mediates immunosuppression in acute phase of experimental *Trypanosoma cruzi* infection," *Experimental Parasitology*, vol. 111, no. 2, pp. 71–79, 2005.

Hindawi Publishing Corporation
Mediators of Inflammation
Volume 2014, Article ID 914326, 9 pages
http://dx.doi.org/10.1155/2014/914326

Research Article

Myocardial Gene Expression of *T-bet*, *GATA-3*, *Ror-γt*, *FoxP3*, and Hallmark Cytokines in Chronic Chagas Disease Cardiomyopathy: An Essentially Unopposed T_H1-Type Response

Luciana Gabriel Nogueira,[1,2,3] Ronaldo Honorato Barros Santos,[4] Alfredo Inácio Fiorelli,[4] Eliane Conti Mairena,[1,2,3] Luiz Alberto Benvenuti,[5] Edimar Alcides Bocchi,[6] Noedir Antonio Stolf,[4] Jorge Kalil,[1,2,3] and Edecio Cunha-Neto[1,2,3]

[1] *Laboratory of Immunology, Heart Institute (InCor), University of São Paulo School of Medicine, 05403-000 São Paulo, SP, Brazil*
[2] *Division of Clinical Immunology and Allergy, University of São Paulo School of Medicine, 01246-903 São Paulo, SP, Brazil*
[3] *Institute for Investigation in Immunology (iii), INCT, University of São Paulo School of Medicine, 05403-000 São Paulo, SP, Brazil*
[4] *Division of Surgery, Heart Institute (InCor), University of São Paulo School of Medicine, 05403-000 São Paulo, SP, Brazil*
[5] *Division of Pathology, Heart Institute (InCor), University of São Paulo School of Medicine, 05403-000 São Paulo, SP, Brazil*
[6] *Transplantation and Heart Failure Unit, Heart Institute (InCor), University of São Paulo School of Medicine, 05403-000 São Paulo, SP, Brazil*

Correspondence should be addressed to Edecio Cunha-Neto; edecunha@gmail.com

Received 15 May 2014; Accepted 8 July 2014; Published 24 July 2014

Academic Editor: Christophe Chevillard

Background. Chronic Chagas disease cardiomyopathy (CCC), a late consequence of *Trypanosoma cruzi* infection, is an inflammatory cardiomyopathy with prognosis worse than those of noninflammatory etiology (NIC). Although the T cell-rich myocarditis is known to play a pathogenetic role, the relative contribution of each of the functional T cell subsets has never been thoroughly investigated. We therefore assessed gene expression of cytokines and transcription factors involved in differentiation and effector function of each functional T cell subset ($T_H1/T_H2/T_H17$/Treg) in CCC, NIC, and heart donor myocardial samples. *Methods and Results*. Quantitative PCR showed markedly upregulated expression of *IFN-γ* and transcription factor *T-bet*, and minor increases of *GATA-3*; *FoxP3* and *CTLA-4*; *IL-17* and *IL-18* in CCC as compared with NIC samples. Conversely, cytokines expressed by T_H2 cells (*IL-4*, *IL-5*, and *IL-13*) or associated with Treg (*TGF-β* and *IL-10*) were not upregulated in CCC myocardium. Expression of T_H1-related genes such as *T-bet*, *IFN-γ*, and *IL-18* correlated with ventricular dilation, *FoxP3*, and *CTLA-4*. *Conclusions*. Results are consistent with a strong local T_H1-mediated response in most samples, possibly associated with pathological myocardial remodeling, and a proportionally smaller $FoxP3^+CTLA4^+$ Treg cell population, which is unable to completely curb IFN-*γ* production in CCC myocardium, therefore fueling inflammation.

1. Introduction

Approximately 8 million people are infected with the protozoan parasite *Trypanosoma cruzi* [1] in Central and South America, with an estimated 300,000 cases in the USA alone due to migration. *T. cruzi* is a major cause of heart disease and cardiovascular-related deaths in endemic areas located in Latin America, with approximately 50,000 fatalities per year due to chronic Chagas cardiomyopathy (CCC) [2]. CCC, the most important clinical consequence of Chagas disease, is an inflammatory cardiomyopathy that affects around 30% of infected individuals and occurs 5–30 years after acute infection, while ca. 60% of those infected remain asymptomatic (ASY) [3]. The reasons why it takes so long after infection for development of full-blown CCC are still unknown. One-third of patients developing CCC present a particularly lethal form

of dilated cardiomyopathy with significant left ventricular dysfunction, and shorter survival than cardiomyopathies of noninflammatory etiology (NIC) [4]. CCC is characterized by a diffuse mononuclear cell myocarditis, with significant heart fiber damage, prominent fibrosis, and scarcity of *T. cruzi* parasites (reviewed in [5]). The inflammatory infiltrate of CCC heart lesions is mainly composed by CD4+ and CD8+ T cells and macrophages [6, 7]. The occurrence of myocarditis is correlated with clinical severity, ASY patients having minimal inflammation [8]. Evidence suggests that the presence or intensity of myocarditis plays a major pathogenic role in CCC development and severity.

The immune response to *T. cruzi* is triggered by persistent infection with an obligatory intracellular parasite. During acute *T. cruzi* infection, *T. cruzi* pathogen-associated molecular patterns (PAMPs) trigger innate immunity in multiple cell types [9], which release proinflammatory cytokines, such as IL-1, IL-6, IL-12, IL-18, and TNF-α, activating cascades of inflammatory cells [10] (reviewed [11]). Antigen-presenting cells subsequently elicit a strong T cell and antibody response against *T. cruzi*,where IL-12 and IL-18 drive the differentiation of IFN-γ-producing *T. cruzi*-specific T_H1-type T cells which migrate to sites of *T. cruzi*-induced inflammation, including the myocardium, in response to locally produced chemokines [11–13]. The T_H1-type T cell and antibody responses lead to control—but not complete elimination—of tissue and blood parasitism, establishing a low-grade chronic persistent infection by *T. cruzi*.

As a result of persistent infection, both CCC and ASY chronic Chagas disease patients show a skewed T_H1-type immune response [13–15] with reduced production of IL-4 by PBMC, but those who develop Chagas cardiomyopathy display a particularly strong T_H1-type immune response with increased numbers of IFN-γ-producing T cells in peripheral blood mononuclear cells (PBMC) [16–18] as well as plasma TNF-α in comparison with uninfected or ASY patients [14, 19].

In addition, CCC patients display a reduced number of $CD4^+CD25^{high}IL\text{-}10^+$ T cells and $CD4^+CD25^{high}FoxP3^+$ regulatory T cells in their peripheral blood as compared to patients in the ASY form of Chagas disease, suggesting that such cells may play a role in the control of the intensity of inflammation in chronic Chagas disease [14, 20, 21]. Furthermore, PBMC from CCC patients displayed increased numbers of $CD4^+CD25^{high}FoxP3^+CTLA\text{-}4^+$ T cells and decreased numbers of $CD4^+CD25^{high}IL\text{-}10^+$ T cells as compared to ASY patients. These reports suggest that a smaller $CD4^+CD25^+$ Treg compartment displays a deficient suppressive activity in CCC patients, leading to uncontrolled production of T_H1 cytokines [22]. Regarding T_H17 cells in Chagas disease, a recent study showed a lower frequency of circulating $CD4^+IL\text{-}17^+$ T cells in CCC patients as compared with ASY patients and noninfected individuals [23].

The exacerbated T_H1 response observed in the PBMC of CCC patients is reflected on the $CD4^+$ and $CD8^+$ T_H1-type T cell-rich myocardial inflammatory infiltrate, with mononuclear cells predominantly producing IFN-γ and TNF-α, with lower production of IL-4, IL-6, IL-7, and IL-15 [6, 7, 14, 16, 24, 25]. It has recently been shown by our group that $CCL5^+$, $CXCL9^+$, $CCR5^+$, and $CXCR3^+$ mononuclear cells were abundant in CCC myocardium, and mRNA levels of the T_H1-chemoattracting chemokines CXCL9, CXCL10, CCL3, CCL4, and CCL5 and their receptors were also found to be upregulated in CCC heart tissue [26]. Significantly, the intensity of the myocardial infiltrate was positively correlated with CXCL9 mRNA expression; moreover, a single nucleotide polymorphism in the *CXCL9* gene, associated with a reduced risk of developing severe CCC in a cohort study, was associated with reduced *CXCL9* expression and intensity of myocarditis in CCC [26]. These results are consistent with a major role of locally produced T_H1-chemoattractant chemokines in the accumulation of $CXCR3/CCR5^+T_H1$ T cells in CCC heart tissue. Significantly, CCC patients display increased numbers of *T. cruzi*-specific $CXCR3^+$ and $CCR5^+$ T cells coexpressing IFN-γ in the PBMC as compared to ASY subjects [27].

Although the presence of heart-infiltrating T_H1-type T cells has been well documented, relatively little is known about the presence or relative proportion of the other functional T cell subsets in CCC heart tissue, which may ultimately determine the local inflammatory status. Although studies with PBMC have established significant differences in the frequency of functional T cell subset differences between CCC and ASY, it does not necessarily follow that those findings will all apply to CCC heart tissue. The presence of different Treg populations in CCC heart tissue has been suggested by the findings of Foxp3 expression and TGF-β signaling (through Smad4 detection) in CCC compared to ASY heart tissue [28, 29]. Regarding production of IL-4 in CCC myocardium, there are conflicting results, where IL-4-producing mononuclear cells were either undetectable [14], prominent in autopsy samples [25], or outnumbered by IFN-γ-producing T cells [30]. So far, T_H17 cells have not yet been studied in human CCC myocardium.

We believe the elucidation of the balance of functional T cell lineages in CCC myocardium is of paramount importance to understand the pathogenesis of CCC, including the key elements for disease progression.

In order to evaluate the relative contribution of each functional T cell subset in the CCC myocardial inflammatory infiltrate, we assessed the mRNA expression of lineage-specifying transcription factors associated with differentiated $T_H1/T_H2/T_H17$ T cells (T-box expressed in T cells (T-bet), GATA-binding protein-3 (GATA-3), and retinoid-related orphan receptor γt (RORγ-T), respectively [31, 32] and the corresponding effector cytokines (IFNγ, IL-4, IL-5, IL-13, IL-17, and IL-23), along with genes associated with regulatory T cell function (FoxP3, TGF-β, CTLA-4, and IL-10), and proinflammatory and/or T_H1-inducing cytokines (IL-1, IL-6, IL-12p35, IL12p40, IL-18, and IL-23) in myocardial samples from CCC and NIC patients as well as heart donor controls.

2. Methods

2.1. Ethics Statement. The protocol was approved by the Institutional Review Board of the School of Medicine, University of São Paulo (Protocol number 739/2005) and written

Table 1: Characteristics of patients and control heart donors whose samples were used in this study.

	CCC	NIC	N
n	14	8	6
Age	47.2 ± 14.6	53.3 ± 7.5	32.2 ± 12.8
Sex (M/F)	5/9	0/9	0/6
EF	26.50 ± 8.96	22.73 ± 6.28	ND
Fibrosis	Moderate to intense	Moderate to intense	0
LVDD	71.64 ± 7.48	75.86 ± 15.84	ND
Hypertrophy	Yes	Yes	No
Myocarditis	Moderate to intense	Absent	0

Age (years); M (male); F (female); CCC (chronic Chagas cardiomyopathy); NIC (noninflammatory cardiomyopathy). Normal heart donors (N) were subject to ventilator and vasoactive drugs and had been under life support for an average of 48 hours. Characterization of the samples as myocarditis, fibrosis, and hypertrophy; reference values for the presence of myocarditis and fibrosis: absent; slight; moderate; intense; hypertrophy: Y (yes), N (no). ND (not done); EF (left ventricular ejection fraction) ≥ 55%; LVDD (left ventricle diastolic diameter); reference value: diameter 39–55 mm.

informed consent was obtained from the patients. In the case of samples from heart donors, written informed consent was obtained from their families.

2.2. Patients and Sample Collection. All Chagas disease patients were considered serologically positive for antibodies against *T. cruzi* on the basis of results of at least 2 of 3 independent tests as described [18]. All Chagas disease and NIC patients underwent standard electrocardiography and 2-dimension and M-mode echocardiography in the hospital setting as described [18]. Patients with CCC presented with typical electrocardiographic findings such as right bundle branch block and/or left anterior division hemiblock [33], in addition to ventricular dysfunction classified on the basis of left ventricular ejection fraction <40%. Myocardial left ventricular free wall heart samples were obtained from end-stage heart failure CCC patients (Table 1) and end-stage heart failure patients with noninflammatory cardiomyopathies (NIC, five patients with idiopathic dilated cardiomyopathy and three patients with ischemic cardiomyopathy, all seronegative for *T. cruzi;* Table 1). Control adult heart tissue from the left ventricular-free wall was obtained from nonfailing donor hearts (N, Table 1) not used for cardiac transplantation due to size mismatch with available recipients. This sample set is the same previously studied for myocardial chemokine expression [26]. Hearts were explanted at the time of heart transplantation at the Heart Institute-InCor, School of Medicine, University of São Paulo, São Paulo, SP, Brazil. For mRNA extraction, samples were quickly dissected, and myocardial tissue was frozen in liquid nitrogen and stored at −80°C.

2.3. RNA Isolation, Reverse Transcription, and Quantitative Real-Time Polymerase Chain Reaction (Real-Time qPCR). Total RNA was extracted from 5 × 5 × 5 mm myocardial samples using the Trizol method (Life Technologies Inc., Grand Island, NY). The RNA was quantified using NanoDrop Spectrophotometry (Thermo Scientific) and treated with Rnase-free DNase I (USB, Ohio, USA). cDNA was obtained from 5 μg total RNA using Super-script II Reverse Transcriptase (Invitrogen, Carlsbad, CA, USA). We designed forward and reverse primers for real-time qPCR assays using the Primer Express software (Applied Biosystems, Foster City, CA, USA; see Table S1 in supplementary materials available online at http://dx.doi.org/10.1155/2014/914326). Real-time qPCR reactions were carried out in an ABI Prism 7500 Sequence Detection system (Applied Biosystems) using the SYBR Green PCR Master Mix (Applied Biosystems), as described in [6]. PCR efficiency was measured in myocardial tissue for all real-time PCR primers. All the samples were tested in triplicate with the glyceraldehyde 3-phosphate dehydrogenase (GAPDH, reference gene) whose expression was previously shown to display little variance among human myocardial tissue samples [24], as the reference gene for normalization of data, and relative expression of each mRNA was calculated with the $2^{-\Delta\Delta Ct}$ method [34], using expression in six normal donor hearts as calibrator. A ratio between expression values of the *T-bet* and *GATA-3* genes was calculated as previously reported [32].

2.4. Statistical Analysis. Values of the relative expression of each mRNA in the CCC and NIC groups were compared with the Mann-Whitney *U* test and performed using the GraphPad Prism 5 software. Correlation analysis was performed by Spearman's rank correlation test with SPSS version 14.0 software (SPSS, Chicago, III).

3. Results

3.1. Patient and Sample Features. As previously observed with the same sample set studied here [26], while myocardial sections from both cardiomyopathy groups displayed cardiomyocyte hypertrophy and fibrosis upon histopathological analysis, lymphocytic myocarditis was only observed among samples from CCC patients (Table 1). No significant differences were found in age, ejection fraction (EF), or left ventricular diastolic diameter (LVDD) between the two groups. We have also previously observed positive correlations between the intensity of lymphocytic myocarditis and fibrosis and between EF and myocardial expression of *ANP* and *BNP* [26]. Myocardial tissue samples are rich in CD4+ and CD8+ T cells (photograph in [26]).

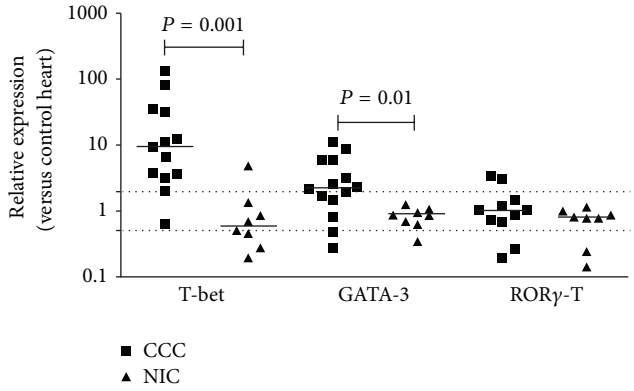

Figure 1: Expression of mRNA encoding transcription factors T-bet, Gata-3, and Rorγ-T in myocardium. Real-time qPCR analysis of mRNA expression in CCC and NIC myocardium. After normalization to GAPDH mRNA, relative increase was plotted in comparison to N group and data were calculated with the $2^{-\Delta\Delta Ct}$ method, as described in Methods section. The horizontal bar stands for the median; dotted lines indicate twofold increase or decrease of expression as compared with the control group.

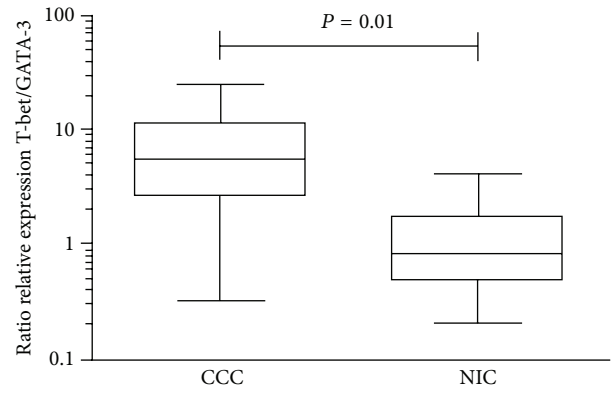

Figure 2: The ratio of mRNA encoding transcription factors T-bet and Gata-3 in myocardium. The ratio of relative expression of T-bet/GATA-3 in CCC and NIC group. The ratio of relative expression was plotted in comparison to N group and data were calculated with the $2^{-\Delta\Delta Ct}$ method, as described in Methods section.

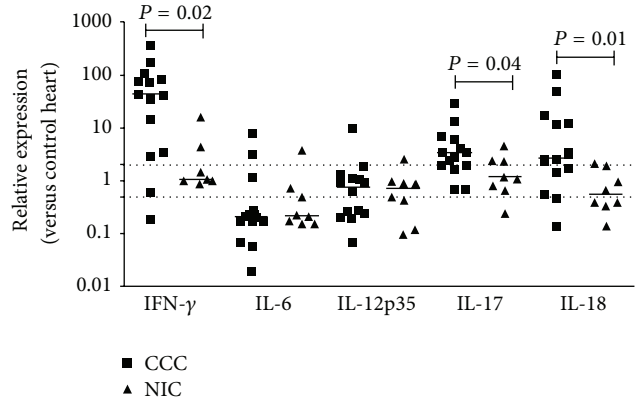

Figure 3: Myocardial expression of cytokine mRNA. Real-time qPCR analysis of mRNA expression in CCC and NIC myocardium. After normalization to GAPDH mRNA, relative increase was plotted in comparison to N group and data were calculated with the $2^{-\Delta\Delta Ct}$ method, as described in Methods section. The horizontal bar stands for the median. Dotted lines indicate twofold increase or decrease of expression as compared with the control group.

3.2. Expression of T_H1, T_H2, and T_H17 T Cell Lineage-Specific of Transcription Factors on Heart Tissue from CCC Patients. We evaluated the expression of the transcription factors associated with the T_H1, T_H2, and T_H17 effector T cell lineages. The expression of mRNA encoding the transcription factors *T-bet* and *GATA-3* was 10 and 2-fold higher in CCC samples than in NIC samples, respectively ($P = 0.001$ and $P = 0.01$, resp.; Figure 1). However, the expression of *RORγ*-T mRNA, the master transcription factor for T_H17 cells, was not significantly different in the myocardium of CCC patients when compared to heart of NIC patients and control individuals (Figure 1). The ratio of relative expression of *T-bet*/*GATA-3*, a putative index of T_H1/T_H2 imbalance [32], was significantly higher in the CCC than in the NIC group (Figure 2), indicating once again the skewed T_H1/T_H2 balance in CCC myocardium.

3.3. Hallmark T_H1, T_H2 and T_H17 Cytokine Expression in CCC Patient Myocardial Tissue. Given the evidence for the expression of *T-bet* and *GATA-3* mRNA in CCC myocardium, indicative of the presence of T_H1 and T_H2 cells, we also evaluated mRNA expression of hallmark T_H1, T_H2, and T_H17 cytokines. Expression levels of *IFN-γ* and the proinflammatory and pro-T_H1 cytokine *IL-18* were 42- and 3-fold higher in the heart tissue of CCC than NIC patients ($P = 0.02$ and $P = 0.01$, resp.; Figure 3). We observed a positive correlation between *T-bet* expression with that of *IFN-γ* and *IL-18*; significantly, mRNA expression of *T-bet* was also positively correlated with left ventricular diastolic diameter (LVDD), an index of global systolic ventricular dysfunction (Table 2). T_H2 cytokines *IL-4*, *IL-5*, and *IL-13* were undetectable in all samples, while *IL-17* expression was 3-fold higher among CCC than NIC samples ($P = 0.04$) (Figure 3 and data not shown). However, expression of other proinflammatory cytokines such as *IL-1β*, *IL-12p40*, *IL23p19*, and *IL-27*, which also has regulatory functions [35], was undetectable in all samples tested (data not shown), while expression of *IL-6* and *IL-12p35* both in the CCC and NIC groups was similar to that found in control samples (Figure 3).

3.4. Expression of Molecules Associated with Regulatory T Cell Function on Heart Tissue from CCC Patients. We next analyzed the expression of genes associated with regulatory T cell function in myocardial samples from the three groups. mRNA expression of *FoxP3* and *CTLA-4* was 3- and 5-fold higher in the heart tissue of CCC than in NIC patients, respectively ($P = 0.001$ and $P = 0.003$, resp.; Figure 4). On the other hand, there was no significant difference in the expression of *IL-10* and *TGF-β* in myocardial samples of CCC patients when compared to those of NIC patients and control individuals (Figure 4). We found a significant

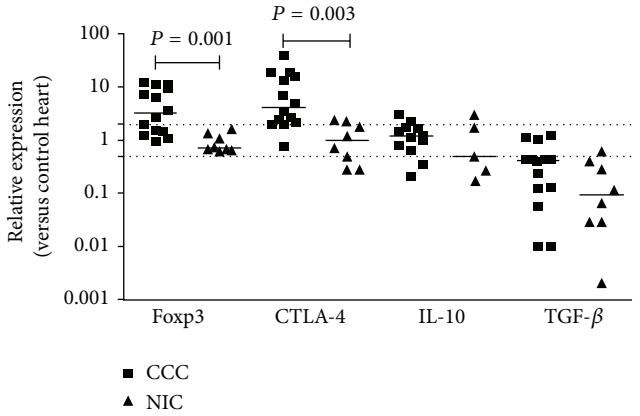

Figure 4: Expression of Foxp3, CTLA-4, IL-10, and TGF-β in myocardium. Real-time qPCR analysis of mRNA expression in CCC and NIC myocardium. After normalization to GAPDH mRNA, relative increase was plotted in comparison to N group and data were calculated with the $2^{-\Delta\Delta Ct}$ method, as described in Methods section. The horizontal bar stands for the median. Dotted lines indicate twofold increase or decrease of expression as compared with the control group.

Table 2: Correlation of mRNA expression of T cell lineage-associated molecules against each other and versus LVDD on heart tissue from CCC patients using Spearman's rank correlation.

mRNA expression	P	r
T-bet versus LVDD	0.043	0.546
T-bet versus Foxp3	0.047	0.538
T-bet versus CTLA-4	0.0001	0.903
IFN-γ versus Foxp3	0.004	0.714
IFN-γ versus CTLA-4	0.004	0.710
IL-18 versus T-bet	0.045	0.543
IL-18 versus IFN-γ	0.002	0.749
IL-18 versus Foxp3	0.009	0.670
IL-18 versus CTLA-4	0.007	0.648
Foxp3 versus CTLA-4	0.001	0.771

($r = 0.77$, $P = 0.001$) positive correlation between the mRNA expression of *FoxP3* and *CTLA-4* (Table 2), which is consistent with coexpression in the same cell population. Expression of genes associated with T_H1 cells, such as *IFN-γ*, *T-bet*, and *IL-18*, was positively correlated with the Treg-associated molecules *FoxP3* and *CTLA-4*; *T-bet* expression correlated highly significantly with *CTLA-4* ($r = 0.90$, $P = 0.001$) (Table 2).

4. Discussion

We report that CCC myocardial tissue displays significantly increased expression of mRNA encoding *IFN-γ* and *T-bet*, with less prominent increase in expression of *IL-17*, *GATA-3*, *FoxP3*, and *CTLA-4*. Among proinflammatory cytokines only *IL-18*, but not *IL1β*, *IL-6*, *IL-12*, *IL-23*, and *IL-27*, displayed increased expression in CCC heart tissue. mRNA expression of the T_H2 cytokines *IL-4*, *IL-5*, and *IL-13*, and cytokines associated with regulatory T cells, such as *IL-10* and *TGF-β*, was either similar to controls or undetectable. T_H1-associated genes such as *T-bet*, *IFN-γ*, and *IL-18* expression levels were found to correlate among themselves, as well as with *FoxP3*, *CTLA-4*, and, in the case of T-bet, with ventricular dilation. Transcription factor and cytokine expression patterns are consistent with a predominant T_H1-type inflammatory infiltrate, with antagonized T_H2 cells and a proportionately smaller $FoxP3^+CTLA\text{-}4^+$ Treg cell population which fails to completely suppress IFN-γ production and T_H1 inflammation in CCC myocardium. The correlation of T-bet and ventricular dysfunction further points out the role of inflammatory T_H1 responses in pathological myocardial hypertrophy/remodeling leading to disease progression.

The finding that the expression of *T-bet* is significantly upregulated in CCC myocardial tissue corroborates the predominance of T_H1-type of heart-infiltrating T cells in the CCC myocardium. The finding that the median *IFN-γ* mRNA expression was over 40-fold upregulated in CCC myocardial tissue is in line with previous studies of heart-infiltrating T cell lines and immunohistochemical studies [14, 25, 36]. Our group has recently shown that expression of IFN-γ- inducible chemokines *CXCL9* and *CXCL10* may be directly involved in the recruitment of large numbers of $CCR5^+$ and $CXCR3^+$ T_H1-type T cells to CCC myocardium [24, 26], suggesting that the local production of IFN-γ and IFN-γ inducible chemokines leads to the recruitment of effector T_H1-type T cells into heart tissue. The correlations between the T_H1-associated genes *T-bet*, *IFN-γ*, and *IL-18* and *CCR5*, *CXCR3*, and their IFN-γ-dependent chemokine ligands were described previously in the same sample set (Table S2) [26]. Although we measured static mRNA levels in a single time point, this can be a sign of a positive feedback loop. Increased numbers of cells capable of local production of IFN-γ and also IFN-γ-dependent chemoattractant molecules may result in the migration of additional $CCR5^+$, $CXCR3^+$, IFN-γ producing T1-type T cells. The correlation between *T-bet* expression levels and the left ventricular diastolic diameter, an index of ventricular dilation and disease severity, is consistent with the idea that the T_H1-type T cell compartment is a determinant factor in CCC progression. In support of this idea, associations between the intensity of the inflammatory infiltrate and disease progression have been previously described in Chagas disease patients [8] and in the chronic Syrian hamster model of CCC where the number of mononuclear cells also correlated with ventricular dilation (ECN and JK, unpublished data). This is further corroborated by the positive correlation between the intensity of lymphocytic myocarditis and fibrosis [26] and may be the pathogenetic translation of the ability of IFNγ to directly induce ANF expression in cardiomyocytes [24], the first step in the pathological hypertrophy pathway. Accordingly, a recent report has described that IFN-γ overexpressing transgenic mice develop mononuclear cell myocarditis, culminating in dilated cardiomyopathy [37].

The modest expression of *GATA-3*, together with the observed lack of expression of *IL-4*, *IL-5*, and *IL-13*, hallmark effector T_H2 cytokines, suggests that T_H2 cells may be relatively rare in the CCC myocardial infiltrate and failing to produce T_H2 cytokines, thus being nonfunctional possibly

due to antagonism by IFN-γ [38]. Our findings are in contrast with previous immunohistochemistry studies that, in spite of showing a majority of mononuclear cells staining with anti-IFN-γ, disclose a minority of mononuclear cells producing IL-4 in CCC myocardium [25, 30] but are in agreement with a previous study with T cell lines derived from CCC myocardium [13]. At any event, STAT4 mRNA was overexpressed in CCC patients with heart failure as compared with STAT6 levels in patients with presence or absence of heart failure [30], a further indication of T_H1 signaling [24]. The correlation found between *GATA-3* expression and CCR4 (Table S2) may suggest that infiltrating T_H2 cells effectively possess such a phenotype.

In the absence of *RORγ-T* expression, the finding of low-grade expression of *IL-17* suggests that there may be little or no differentiated T_H17 cells in CCC heart tissue. At any event, the correlation found between *IL-17* expression and *CCR4* (Table S2) may suggest that such putative infiltrating T_H17 cells effectively possess this phenotype. This may be in concert with the recent finding that CCC patients with low ejection fraction similar to the ones examined here had lower $IL17^+$ T cells in their PBMC than CCC patients without ventricular dysfunction [23].

Our finding of a modest increase in the mRNA expression of FoxP3 and CTLA-4, with no significant modulation of TGF-β and IL-10 expression, is in line with previous studies showing that FoxP3+ cells are significantly less abundant in myocardial sections from CCC than in ASY patients or noninfected individuals, suggesting that reduced numbers of Treg cells could be one important cause for the prevalent T_H1 response in CCC heart tissue [29]. Araujo et al. [21] have previously shown that PBMC from CCC patients displayed increased numbers of $CD4^+CD25^{high}Foxp3^+CTLA\text{-}4^+$ T cells and decreased numbers of $CD4^+CD25^{high}IL\text{-}10^+$ T cells, as compared to ASY patients, consistent with our findings in regulatory T cell molecules in CCC heart tissue [22]. Recently, CTLA-4 was found to be expressed in mononuclear cells infiltrating heart tissue sections from chronically infected subjects with severe myocarditis [39]. The finding that expression of FoxP3 and CTLA-4 displayed positive correlations with T_H1 chemokine receptors CCR5 and CXCR3 and their ligands, along with T-bet, IFN-γ, and IL-18 (Table S2), is in line with previous findings and indicates for the first time that the $FoxP3^+$ $CTLA4^+$ Treg compartment bears a relationship with the T_H1 infiltrate. However, in case the Treg compartment was effectively controlling the T_H1 infiltrate in at least some samples, one would expect to find a negative correlation between markers of the two T cell populations. Data thus suggest that a proportional but comparatively smaller or less functional $FoxP3^+$ $CTLA\text{-}4^+$ Treg compartment, possibly also bearing chemokine receptors CCR5 and/or CXCR3 [38], migrated to CCC heart tissue in a partially failed attempt to control T_H1-driven inflammation. However, since both FoxP3 and CTLA-4 can be transiently expressed in activated human T cells, we cannot formally exclude that the increased expression was merely due to the presence of activated T cells belonging to other functional subsets [40, 41]. Our findings of lack of upregulation of *TGF-β* in situ are in apparent contrast with the immunohistochemical study by Araújo-Jorge et al. [33] who have identified a low number of TGF-β^+ mononuclear cells infiltrating CCC myocardium. However, that report failed to show values from healthy control tissue samples, so it is not possible to assess whether the detected values were above baseline. A recent report showed that circulating TGF-β1 could be detected in CCC serum samples [42] which could be the source of activation of the TGF-β1 signaling pathway in CCC myocardium [28].

The selective increase of *IL-18* in the absence of any other proinflammatory cytokine in CCC myocardium is intriguing, since most proinflammatory cytokines are produced in response to shared stimuli, like Toll-like receptor ligands and IFN-γ [43]. The longer half-life of the *IL-18* mRNA [44] could partially explain our findings. The positive correlation between the mRNA expression of *IL-18* and *IFN-γ* is consistent with the described positive feedback loop between the two cytokines [45]. IL-18 has been reported to induce ANP gene expression and hypertrophy in cardiomyocytes, as previously described for IFN-γ, TNF-α, IL-1β, and CCL2 [24, 46]. IL-18 also induces fibroblast expression of fibronectin, a prominent extracellular matrix protein [47], a mechanism possibly involved in myocardial fibrosis.

Since all our CCC myocardium samples came from clinically similar end-stage patients submitted to transplantation, it could be argued that possessing a more or less intense expression of T-bet, a T_H1-associated expression profile or even a more significant inflammatory infiltrate by itself, may not be relevant for the progression of CCC. However, CCC is not a monogenic disease, and it is likely that the progression to overt inflammatory dilated cardiomyopathy may result from the combined effect and inadequate counterregulation of relevant genes and environmental factors. Polymorphisms in multiple innate immunity/inflammatory genes have been found to associate with risk for developing CCC (reviewed in [5, 11]). In addition to interference by other genes, differential myocardial resilience, including responses to hypertrophic/fibrogenic factors occurring in CCC heart tissue (*IL1β*, *TNF-α*, *IFN-γ*, *IL18*, *CCL2*,and *CCL21*)(reviewed in [5]), could explain why these few patients presenting less intense inflammation and a lower expression of T_H1 cytokines can nevertheless develop end-stage cardiomyopathy. Our group has recently observed that polymorphisms in the promoter region that bind to transcription factors of the cardiac actin gene, a cardiomyocyte gene associated with muscle contraction and resilience, whose dysfunction or altered expression levels lead to cardiomyocyte malfunction and apoptosis [48] associate with CCC development [49]. In the Syrian hamster model of chronic Chagas disease cardiomyopathy, although the intensity of chronic inflammation correlated with ventricular dilation, intensity of myocarditis was similar in hamsters dying from chronic *T. cruzi*-induced dilated cardiomyopathy and survivors euthanized 11 months after infection [5], suggesting the existence of additional factors related to disease progression or death from CCC.

It is likely that the interplay between the Treg and T_H1-type T cell populations is key towards the control of myocardial inflammation in chronic Chagas disease. Our findings suggest that the myocarditis in the chronic cardiac form of

Chagas disease is related to a strong T_H1 response in most cases, associated with a balanced regulatory T cell response and an antagonized T_H2 response. Our results are consistent with the hypothesis that a putative FoxP3$^+$ and CTLA-4$^+$ Treg heart-infiltrating T cell population fails to control the exacerbated IFN-γ production by T_H1-type T cells in the majority of end-stage CCC cases.

5. Conclusion

The T_H1-type T cell-rich mononuclear infiltrate plays a major role in the development and progression of chronic CCC. We found increased expression of T_H1-associated genes in CCC myocardial tissue, with minor upregulation, similar or even undetectable levels of mRNAs encoding associated T_H2, T_H17 and Treg associated genes. Our results show a limited role of T_H2-type T cells, and are consistent with the hypothesis that a putative FoxP3$^+$ and CTLA4$^+$ Treg heart-infiltrating T cell population fails to control the exacerbated IFN-γ production by T_H1-type T cells in the majority of end-stage CCC cases.

Conflict of Interests

The authors declare that there is no conflict of interests regarding the publication of this paper.

Acknowledgments

The authors thank Dr. Priscila Teixeira for helping in heart tissue collection and Dr. João Santana Silva for providing the sequences of the IL-17 primer.

References

[1] C. J. Schofield, J. Jannin, and R. Salvatella, "The future of Chagas disease control," *Trends in Parasitology*, vol. 22, no. 12, pp. 583–588, 2006.

[2] L. V. Kirchhoff, L. M. Weiss, M. Wittner, and H. B. Tanowitz, "Parasitic diseases of the heart," *Frontiers in Bioscience*, vol. 9, pp. 706–723, 2004.

[3] J. R. Coura, "Chagas disease: what is known and what is needed. A background article," *Memorias do Instituto Oswaldo Cruz*, vol. 102, supplement 1, pp. 113–122, 2007.

[4] R. B. Bestetti and G. Muccillo, "Clinical course of chagas' heart disease: a comparison with dilated cardiomyopathy," *International Journal of Cardiology*, vol. 60, no. 2, pp. 187–193, 1997.

[5] E. Cunha-Neto, L. G. Nogueira, P. C. Teixeira et al., "Immunological and non-immunological effects of cytokines and chemokines in the pathogenesis of chronic Chagas disease cardiomyopathy," *Memorias do Instituto Oswaldo Cruz*, vol. 104, supplement 1, pp. 252–258, 2009.

[6] S. G. Fonseca, M. M. Reis, V. Coelho et al., "Locally produced survival cytokines IL-15 and IL-7 may be associated to the predominance of CD8$^+$ T cells at heart lesions of human chronic chagas disease cardiomyopathy," *Scandinavian Journal of Immunology*, vol. 66, no. 2-3, pp. 362–371, 2007.

[7] M. de Lourdes Higuchi, P. S. Gutierrez, V. D. Aiello et al., "Immunohistochemical characterization of infiltrating cells in human chronic chagasic myocarditis: comparison with myocardial rejection process," *Virchows Archiv A: Pathological Anatomy and Histopathology*, vol. 423, no. 3, pp. 157–160, 1993.

[8] M. de Lourdes Higuchi, C. F. de Morais, A. C. P. Barreto et al., "The role of active myocarditis in the development of heart failure in chronic Chagas' disease: a study based on endomyocardial biopsies," *Clinical Cardiology*, vol. 10, no. 11, pp. 665–670, 1987.

[9] A. Bafica, H. C. Santiago, R. Goldszmid, C. Ropert, R. T. Gazzinelli, and A. Sher, "Cutting edge: TLR9 and TLR2 signaling together account for MyD88-dependent control of parasitemia in *Trypanosoma cruzi* infection," *Journal of Immunology*, vol. 177, no. 6, pp. 3515–3519, 2006.

[10] V. Michailowsky, N. M. Silva, C. D. Rocha, L. Q. Vieira, J. Lannes-Vieira, and R. T. Gazzinelli, "Pivotal role of interleukin-12 and interferon-γ axis in controlling tissue parasitism and inflammation in the heart and central nervous system during *Trypanosoma cruzi* infection," *The American Journal of Pathology*, vol. 159, no. 5, pp. 1723–1733, 2001.

[11] A. M. B. Bilate and E. Cunha-Neto, "Chagas disease cardiomyopathy: current concepts of an old disease," *Revista do Instituto de Medicina Tropical de Sao Paulo*, vol. 50, no. 2, pp. 67–74, 2008.

[12] M. M. Teixeira, R. T. Gazzinelli, and J. S. Silva, "Chemokines, inflammation and *Trypanosoma cruzi* infection," *Trends in Parasitology*, vol. 18, no. 6, pp. 262–265, 2002.

[13] A. P. M. P. Marino, A. Da Silva, P. dos Santos et al., "Regulated on activation, normal T cell expressed and secreted (RANTES) antagonist (Met-RANTES) controls the early phase of *Trypanosoma cruzi*-elicited myocarditis," *Circulation*, vol. 110, no. 11, pp. 1443–1449, 2004.

[14] L. C. J. Abel, L. V. Rizzo, B. Ianni et al., "Chronic Chagas' disease cardiomyopathy patients display an increased IFN-γ response to *Trypanosoma cruzi* infection," *Journal of Autoimmunity*, vol. 17, no. 1, pp. 99–107, 2001.

[15] M. Ribeirao, V. L. Pereira-Chioccola, L. Rénia, A. A. F. Filho, S. Schenkman, and M. M. Rodrigues, "Chagasic patients develop a type 1 immune response to *Trypanosoma cruzi* trans-sialidase," *Parasite Immunology*, vol. 22, no. 1, pp. 49–53, 2000.

[16] D. D. Reis, E. M. Jones, S. Tostes et al., "Expression of major histocompatibility complex antigens and adhesion molecules in hearts of patients with chronic Chagas' disease," *The American Journal of Tropical Medicine and Hygiene*, vol. 49, no. 2, pp. 192–200, 1993.

[17] F. F. de Araújo, R. Corrêa-Oliveira, M. O. C. Rocha et al., "Foxp3$^+$CD25 high CD4$^+$ regulatory T cells from indeterminate patients with Chagas disease can suppress the effector cells and cytokines and reveal altered correlations with disease severity," *Immunobiology*, vol. 217, no. 8, pp. 768–777, 2012.

[18] E. Cunha-Neto and J. Kalil, "Heart-infiltrating and peripheral T cells in the pathogenesis of human Chagas' disease cardiomyopathy," *Autoimmunity*, vol. 34, no. 3, pp. 187–192, 2001.

[19] A. Talvani, M. O. C. Rocha, A. L. Ribeiro, R. Correa-Oliveira, and M. M. Teixeira, "Chemokine receptor expression on the surface of peripheral blood mononuclear cells in Chagas disease," *The Journal of Infectious Diseases*, vol. 189, no. 2, pp. 214–220, 2004.

[20] J. A. S. Gomes, L. M. G. Bahia-Oliveira, M. O. C. Rocha, O. A. Martins-Filho, G. Gazzinelli, and R. Correa-Oliveira, "Evidence that development of severe cardiomyopathy in human Chagas' disease is due to a Th1-specific immune response," *Infection and Immunity*, vol. 71, no. 3, pp. 1185–1193, 2003.

[21] F. F. Araujo, J. A. S. Gomes, M. O. C. Rocha et al., "Potential role of $CD4^+CD25^{HIGH}$ regulatory T cells in morbidity in Chagas disease," *Frontiers in Bioscience*, vol. 12, no. 8, pp. 2797–2806, 2007.

[22] P. M. M. Guedes, F. R. S. Gutierrez, G. K. Silva et al., "Deficient regulatory T cell activity and low frequency of IL-17-producing T cells correlate with the extent of cardiomyopathy in human Chagas' disease," *PLoS Neglected Tropical Diseases*, vol. 6, no. 4, Article ID e1630, 2012.

[23] L. M. D. Magalhães, F. N. A. Villani, M. D. C. P. Nunes, K. J. Gollob, M. O. C. Rocha, and W. O. Dutra, "High interleukin 17 expression is correlated with better cardiac function in human chagas disease," *The Journal of Infectious Diseases*, vol. 207, no. 4, pp. 661–665, 2013.

[24] E. Cunha-Neto, V. J. Dzau, P. D. Allen et al., "Cardiac gene expression profiling provides evidence for cytokinopathy as a molecular mechanism in Chagas' disease cardiomyopathy," *The American Journal of Pathology*, vol. 167, no. 2, pp. 305–313, 2005.

[25] M. M. Reis, M. D. L. Higuchi, L. A. Benvenuti et al., "An in situ quantitative immunohistochemical study of cytokines and $IL\text{-}2R^+$ in chronic human chagasic myocarditis: correlation with the presence of myocardial *Trypanosoma cruzi* antigens," *Clinical Immunology and Immunopathology*, vol. 83, no. 2, pp. 165–172, 1997.

[26] L. G. Nogueira, R. H. B. Santos, B. M. Ianni et al., "Myocardial chemokine expression and intensity of myocarditis in chagas cardiomyopathy are controlled by polymorphisms in CXCL9 and CXCL10," *PLoS Neglected Tropical Diseases*, vol. 6, no. 10, Article ID e1867, 2012.

[27] J. A. S. Gomes, L. M. G. Bahia-Oliveira, M. O. C. Rocha et al., "Type 1 chemokine receptor expression in Chagas' disease correlates with morbidity in cardiac patients," *Infection and Immunity*, vol. 73, no. 12, pp. 7960–7966, 2005.

[28] T. C. Araújo-Jorge, M. C. Waghabi, A. M. Hasslocher-Moreno et al., "Implication of transforming growth factor-β1 in Chagas disease myocardiopathy," *The Journal of Infectious Diseases*, vol. 186, no. 12, pp. 1823–1828, 2002.

[29] F. F. de Araújo, A. B. M. da Silveira, R. Correa-Oliveira et al., "Characterization of the presence of $Foxp3^+$ T cells from patients with different clinical forms of Chagas' disease," *Human Pathology*, vol. 42, no. 2, pp. 299–301, 2011.

[30] D. B. Rocha Rodrigues, M. A. dos Reis, A. Romano et al., "*In situ* expression of regulatory cytokines by heart inflammatory cells in Chagas' disease patients with heart failure," *Clinical and Developmental Immunology*, vol. 2012, Article ID 361730, 7 pages, 2012.

[31] S. A. Miller and A. S. Weinmann, "Common themes emerge in the transcriptional control of T helper and developmental cell fate decisions regulated by the T-box, GATA and ROR families," *Immunology*, vol. 126, no. 3, pp. 306–315, 2009.

[32] L. Dong, M. Chen, Q. Zhang, L. Li, X. Xu, and W. Xiao, "T-bet/GATA-3 ratio is a surrogate measure of Th1/Th2 cytokine profiles and may be novel targets for CpG ODN treatment in asthma patients," *Chinese Medical Journal*, vol. 119, no. 16, pp. 1396–1399, 2006.

[33] M. T. Jorge, T. A. A. Macedo, R. S. Janones, D. P. Carizzi, R. A. G. Heredia, and R. E. S. Achá, "Types of arrhythmia among cases of American trypanosomiasis, compared with those in other cardiology patients," *Annals of Tropical Medicine and Parasitology*, vol. 97, no. 2, pp. 139–148, 2003.

[34] S. A. Bustin, V. Benes, J. A. Garson et al., "The MIQE guidelines: minimum information for publication of quantitative real-time PCR experiments," *Clinical Chemistry*, vol. 55, no. 4, pp. 611–622, 2009.

[35] C. A. Hunter and R. Kastelein, "Interleukin-27: balancing protective and pathological immunity," *Immunity*, vol. 37, no. 6, pp. 960–969, 2012.

[36] D. D. Reis, E. M. Jones, S. Tostes Jr. et al., "Characterization of inflammatory infiltrates in chronic chagasic myocardial lesions: presence of tumor necrosis factor-α+ cells and dominance of granzyme A+, CD8+ lymphocytes," *The American Journal of Tropical Medicine and Hygiene*, vol. 48, no. 5, pp. 637–644, 1993.

[37] M. Torzewski, P. Wenzel, H. Kleinert et al., "Chronic inflammatory cardiomyopathy of interferon γoverexpressing transgenic mice is mediated by tumor necrosis factor-α," *The American Journal of Pathology*, vol. 180, no. 1, pp. 73–81, 2012.

[38] L. K. Teixeira, B. P. F. Fonseca, B. A. Barboza, and J. P. B. Viola, "The role of interferon-γ on immune and allergic responses," *Memórias do Instituto Oswaldo Cruz*, vol. 100, supplement 1, pp. 137–144, 2005.

[39] R. J. Argüello, M. C. Albareda, M. G. Alvarez et al., "Inhibitory receptors are expressed by *Trypanosoma cruzi*-specific effector T cells and in hearts of subjects with chronic Chagas disease," *PLoS one*, vol. 7, no. 5, p. e35966, 2012.

[40] M. Kmieciak, M. Gowda, L. Graham et al., "Human T cells express CD25 and Foxp3 upon activation and exhibit effector/memory phenotypes without any regulatory/suppressor function," *Journal of Translational Medicine*, vol. 7, article 89, 2009.

[41] S. Sakaguchi, K. Wing, Y. Onishi, P. Prieto-Martin, and T. Yamaguchi, "Regulatory T cells: how do they suppress immune responses?" *International Immunology*, vol. 21, no. 10, pp. 1105–1111, 2009.

[42] R. M. Saraiva, M. C. Waghabi, M. F. Vilela et al., "Predictive value of transforming growth factor-beta1in Chagas disease: towards a biomarker surrogate of clinical outcome," *Transactions of the Royal Society of Tropical Medicine and Hygiene*, vol. 107, pp. 518–525, 2013.

[43] K. Nakanishi, T. Yoshimoto, H. Tsutsui, and H. Okamura, "Interleukin-18 regulates both Th1 and Th2 responses," *Annual Review of Immunology*, vol. 19, pp. 423–474, 2001.

[44] M. Tone, S. A. J. Thompson, Y. Tone, P. J. Fairchild, and H. Waldmann, "Regulation of IL-18 (IFN-γ-inducing factor) gene expression," *Journal of Immunology*, vol. 159, no. 12, pp. 6156–6163, 1997.

[45] C. A. Dinarello and G. Fantuzzi, "Interleukin-18 and host defense against infection," *The Journal of Infectious Diseases*, vol. 187, supplement 2, pp. S370–S384, 2003.

[46] B. Chandrasekar, S. Mummidi, L. Mahimainathan et al., "Interleukin-18-induced human coronary artery smooth muscle cell migration is dependent on NF-κB- and AP-1-mediated matrix metalloproteinase-9 expression and is inhibited by atorvastatin," *The Journal of Biological Chemistry*, vol. 281, no. 22, pp. 15099–15109, 2006.

[47] V. S. Reddy, R. E. Harskamp, M. W. van Ginkel et al., "Interleukin-18 stimulates fibronectin expression in primary human cardiac fibroblasts via PI3K-Akt-dependent NF-κB activation," *Journal of Cellular Physiology*, vol. 215, no. 3, pp. 697–707, 2008.

[48] H. Jiang, G. Qiu, J. Li-Ling, N. Xin, and K. Sun, "Reduced *ACTC1* expression might play a role in the onset of congenital heart disease by inducing cardiomyocyte apoptosis," *Circulation Journal*, vol. 74, no. 11, pp. 2410–2418, 2010.

[49] A. F. Frade, P. C. Teixeira, B. M. Ianni et al., "Polymorphism in the alpha cardiac muscle actin 1 gene is associated to susceptibility to chronic inflammatory cardiomyopathy," *PLoS ONE*, Article ID e83446, 2013.

Hindawi Publishing Corporation
Mediators of Inflammation
Volume 2014, Article ID 798078, 16 pages
http://dx.doi.org/10.1155/2014/798078

Research Article

Tumor Necrosis Factor Is a Therapeutic Target for Immunological Unbalance and Cardiac Abnormalities in Chronic Experimental Chagas' Heart Disease

Isabela Resende Pereira,[1] Glaucia Vilar-Pereira,[1] Andrea Alice Silva,[2] Otacilio Cruz Moreira,[3] Constança Britto,[3] Ellen Diana Marinho Sarmento,[1] and Joseli Lannes-Vieira[1]

[1] *Laboratório de Biologia das Interações, Instituto Oswaldo Cruz/Fiocruz, Avenida Brasil 4365, 21045-900 Rio de Janeiro, RJ, Brazil*
[2] *Departamento de Patologia, Universidade Federal Fluminense, 24033-900 Niterói, RJ, Brazil*
[3] *Laboratório de Biologia Molecular e Doenças Endêmicas, IOC/Fiocruz, 21045-900 Rio de Janeiro, RJ, Brazil*

Correspondence should be addressed to Joseli Lannes-Vieira; joselilannes@gmail.com

Received 14 April 2014; Revised 24 June 2014; Accepted 26 June 2014; Published 22 July 2014

Academic Editor: Christophe Chevillard

Background. Chagas disease (CD) is characterized by parasite persistence and immunological unbalance favoring systemic inflammatory profile. Chronic chagasic cardiomyopathy, the main manifestation of CD, occurs in a TNF-enriched milieu and frequently progresses to heart failure. *Aim of the Study*. To challenge the hypothesis that TNF plays a key role in *Trypanosoma cruzi*-induced immune deregulation and cardiac abnormalities, we tested the effect of the anti-TNF antibody Infliximab in chronically *T. cruzi*-infected C57BL/6 mice, a model with immunological, electrical, and histopathological abnormalities resembling Chagas' heart disease. *Results*. Infliximab therapy did not reactivate parasite but reshaped the immune response as reduced TNF mRNA expression in the cardiac tissue and plasma TNF and IFNγ levels; diminished the frequency of IL-17A$^+$ but increased IL-10$^+$ CD4$^+$ T-cells; reduced TNF$^+$ but augmented IL-10$^+$ Ly6C$^+$ and F4/80$^+$ cells. Further, anti-TNF therapy decreased cytotoxic activity but preserved IFNγ-producing VNHRFTLV-specific CD8$^+$ T-cells in spleen and reduced the number of perforin$^+$ cells infiltrating the myocardium. Importantly, Infliximab reduced the frequency of mice afflicted by arrhythmias and second degree atrioventricular blocks and decreased fibronectin deposition in the cardiac tissue. *Conclusions*. Our data support that TNF is a crucial player in the pathogenesis of Chagas' heart disease fueling immunological unbalance which contributes to cardiac abnormalities.

1. Introduction

Immunological unbalance with high levels of cytokines in the serum [1–5] is detected in patients with the cardiac form of Chagas disease (DC), a neglected tropical disease caused by the protozoan parasite *Trypanosoma cruzi* [6]. Importantly, increased plasma tumor necrosis factor (TNF) levels are related to the degree of left ventricular dysfunction in patients with chronic chagasic cardiomyopathy (CCC), the most frequent manifestation of CD [1, 3]. Chagas' heart disease is marked by persistence of low parasite load in the cardiac tissue and progressive fibrosis with remodeling of the myocardium and vasculature, which commonly progresses to heart failure and dilation [6]. In patients with CCC, the low-grade heart inflammation occurs in an inflammatory milieu enriched in the inflammatory cytokines TNF and interferon (IFN)γ [7]. Importantly, the number of TNF-producing cells in the cardiac tissue is associated with the presence of heart failure in CD patients [8]. In noninfectious conditions, the participation of TNF in ischemic and dilated heart disorders is supported by several observations, including elevated plasma TNF levels, and raised the proposal

of using TNF blocking as immunotherapeutic strategy for improving the severity of heart diseases [9]. Antagonists of TNF as Etanercept (soluble dimeric human TNFR2/p75-IgG1 Fc fusion protein that binds to TNF and members of lymphotoxin family, neutralizing soluble TNF and LTα3 with similar potency) and Infliximab (chimeric monoclonal antibody with human IgG1κ Fc and murine variable regions that binds to both soluble and transmembrane TNF) have shown efficacy in a variety of immune-mediated inflammatory diseases [10, 11].

In experimental acute *T. cruzi* infection, the frequencies of TNF^+ and TNF receptor $1/p55^+$ ($TNFR1^+$) cells are increased [12]. Additionally, in acute *T. cruzi* infection TNFR1 signaling is crucial for parasite resistance [13] but also involved in heart tissue damage [12]. Moreover, the treatment of acutely *T. cruzi*-infected mice with the anti-TNF antibody Infliximab did not impact heart parasitism but reduced fibronectin (FN) deposition in the heart and ameliorated cardiomyocyte lesion in association with reduced CD8-enriched myocarditis [12]. These and other circumstantial findings led to the hypothesis that TNF signaling plays a role in the pathogenesis of heart tissue damage in *T. cruzi* infection [14]. This idea was previously challenged by administration of the soluble TNFR2 Etanercept to chronically infected hamsters with signs of CCC. This therapy did not alter blood and cardiac parasitism but significantly aggravated CCC in hamsters [15]. Interestingly, short treatment with Infliximab initiated three-month postinfection diminished cardiac TNF mRNA expression and CD8-enriched myocarditis in *T. cruzi*-infected rats, without evidence of parasitism reactivation but in presence of increased circulating IL-10 levels [16]. This regulatory cytokine was associated with the benign evolution of Chagas' heart disease [17].

Recently, we proposed that perforin $(Pfn)^+$ and $IFN\gamma^+$ $CD8^+$ T-cells infiltrating the cardiac tissue play antagonist roles in CCC [18]. *In vitro* experiments support that Infliximab depletes a Pfn^+CD8^+ T-cell population which express TNF on cell surface [19]. More recently, in patients with a chronic inflammatory condition TNF neutralization was shown to downregulate IL-17 [20], a cytokine upregulated in cardiopathic CD patients [4]. Based on these data, we hypothesized that *in vivo* therapeutic intervention targeting TNF could selectively interfere with the nonbeneficial Pfn^+CD8^+ T-cells invading the cardiac tissue and also downregulate the Th17 profile associated with CCC. We, therefore, challenged the hypothesis that TNF fuels immunological unbalance which promotes Chagas' heart disease. For that, we used an experimental model of CCC occurring in parallel to high plasma TNF levels [18, 21] and short treatment with the monoclonal antibody Infliximab aiming to block TNF biological activities.

2. Materials and Methods

2.1. Ethical Information. Mice obtained from the animal facilities of the Oswaldo Cruz Foundation (CECAL/Fiocruz, Rio de Janeiro, Brazil) were housed under specific pathogen-free conditions in a 12-hour light-dark cycle with access to food and water *ad libitum*. Our protocols were approved by the Institutional Committee for Animal Ethics of Fiocruz (CEUA/Fiocruz, License 004/09). All presented data were obtained from three independent experiments (D2, T3, and T4, Experiment Register Books number 4 and number 5, LBI/IOC-Fiocruz).

2.2. Experimental Infection. Five- to seven-week-old female C57BL/6 ($H\text{-}2^b$) mice were intraperitoneally infected with 100 blood trypomastigotes (bt) of the Colombian strain of *T. cruzi*, and parasitemia was employed as a parameter to establish acute and chronic phases [18]. Sex- and age-matched noninfected mice were kept in parallel. Each experimental group was composed of three to fifteen animals.

2.3. Anti-TNF Therapy. C57BL/6 mice were given subcutaneous injections of 0.1 mL of apyrogenic saline (BioManguinhos, Fiocruz, Rio de Janeiro, RJ, Brazil) containing 10 μg of anti-human TNF blocking antibody (Infliximab, Remicade), a gift from Schering-Plough of Brazil, 48-hour intervals from 120 to 150 days postinfection (dpi). Infliximab was previously shown to block *in vivo* TNF biological activities in murine and rat models [16, 22]. For injection control, sex- and age-matched noninfected mice received apyrogenic saline, according to our therapeutic schemes (Figure 1(a)). This group is, thereafter, referred to as noninfected (NI) controls.

2.4. Reagents and Antibodies. For functional assays, the $H\text{-}2K^b$-restricted VNHRFTLV peptide from the amastigote surface protein 2 (ASP2) [18] was synthesized by GenScript USA Inc. (USA). For ELISpot anti-mouse IFNγ (clone R4-6A2) was used for capture, and biotin-conjugated anti-mouse IFNγ antibody (clone XMG1.2) and alkaline phosphatase-labeled streptavidin for detection were obtained from BD PharMingen (USA). For immunohistochemical staining (IHS) we use the polyclonal rabbit anti-mouse FN (Gibco-BRL, USA), anti-mouse F4/80 (CALTAG, USA), anti-mouse CD8a (53-6.7), and anti-mouse CD4 (clone GK1.5) supernatants were produced in our laboratory (LBI/IOC-Fiocruz, Brazil), biotinylated anti-rabbit immunoglobulin, biotinylated anti-rat immunoglobulin, and peroxidase-streptavidin complex were purchased form Amersham (UK). The monoclonal antibodies anti-mouse Pfn (clone CB5.4, Alexis Biochemicals, USA) and anti-IFNγ (clone R4-6A2, BD PharMingen, USA) produced in rat were also used in IHS. For flow cytometry studies, the reagents and antibodies recognizing mouse molecules purchased from BD Pharmingen (USA) were PE-Cy7-anti-TCR$\alpha\beta$ (clone H57-597), APC-anti-CD8a (clone 53-6.7), FITC-anti-CD4 (clone GK1.5), APC-anti-Ly6C (clone HK1.4), PE-Cy7-anti-TNF (clone MP6-XT22), PerCP-anti-CD4 (clone GK1.5), PE-anti-CD8a (clone 53-6.7), FITC-anti-IL-17A (clone eBio17B7), APC-anti-IL-10 (clone JES5-16E3), APC-streptavidin, FITC-anti-CD8a (clone 53-6.7), and PE-anti-TNF (clone MP6-XT22). The PE-Texas-red-anti-F4/80 (clone BM8) was made by Invitrogen (USA), the PE-anti-IL-10 (clone JES5-2A5) was made by CALTAG Laboratories, and PE-conjugated anti-TNFR1/p55/CD120a

(clone 55R-286) was purchased from BioLegend (USA). Appropriate controls were prepared by replacing the antibodies with the corresponding serum, purified immunoglobulin, or fluorochrome-matched isotype. All antibodies and reagents were used according to the manufacturers' instructions.

2.5. Real-Time Quantitative RT-PCR for Detection of Cytokines mRNA. For real-time quantitative RT-PCR (qRT-PCR), the hearts were harvested, washed to remove blood clots, weighed, and frozen in RNAlater (number AM7021, Life Technologies, USA). The total RNA was extracted from the same sample used for DNA extraction for parasite detection using TRI-Reagent (Sigma-Aldrich, USA). All reverse transcriptase reactions were performed using a SuperScript III Kit (number 18080-051) and qRT-PCR was performed using TaqMan gene expression assays for the cytokine TNF (number Mm00443258_m1) and the endogenous housekeeping control genes glyceraldehyde 3-phosphate dehydrogenase (GAPDH) (number Mm99999915_g1) and HPRT (number Mm01545399_m1), purchased from Life Technologies (USA). The reactions were performed and analyzed as previously described [21].

2.6. Real-Time Quantitative PCR for Parasite Detection. Hearts were collected and processed as described in Section 2.5. Total DNA was extracted from heart samples using TRI-Reagent (Sigma-Aldrich, USA). The purified DNA was analyzed by real-time quantitative PCR (qPCR) using primers Cruzi 1 (5′-AST CGG CTG ATC GTT TTC GA-3′) and Cruzi 2 (5′-AAT TCC TCC AAG CAG CGG ATA-3′) for *T. cruzi* nuclear satellite DNA and GAPDH gene (GAPDH Fw 5′-CCA CTC ACG GCA AAT TCA ACG GC-3′ and GAPDH Rv 5′-CCA CCC TTC AAG TGG GCC CCG-3′), as an internal control from the mouse DNA. Parasitic load quantification was obtained by absolute quantification of *T. cruzi* DNA, following normalization by heart weight. The standard curve for the absolute quantification was generated by a 1 : 10 serial dilution of DNA extracted from the Colombian strain epimastigote culture stocks, ranging from 10^6 to 10 parasite equivalents. All procedures and analyses were performed as previously described [23].

2.7. Detection of Cytokines in the Serum. A mouse cytometric bead array (CBA; Inflammation Kit (number 560485, Becton & Dickinson, USA)) was used to quantify cytokines in the serum according to the manufacturer's instructions. The fluorescence produced by the CBA beads was measured with a FACSCalibur instrument (Becton Dickinson, USA) and analyzed using FCAP Array software. Standard curves (1 pg/mL to 100 ng/mL) were generated in parallel. This method consistently detected concentrations above 10 pg/mL.

2.8. Nitric Oxide Quantification. Nitrate and nitrite (NO_x) were determined in serum samples from NI and infected mice using Griess reagent and vanadium chloride III with a standard curve of 0.8–100 μM $NaNO_2$ and $NaNO_3$ [23].

2.9. Flow Cytometry Analysis. Spleens were minced, and the red blood cells were removed using lysis buffer (Sigma, USA). The splenocytes were labeled, 100,000 to 300,000 events were acquired with a Beckman Coulter CyAn 7 Color flow cytometer (USA), and the data were analyzed with the Summit v.4.3 Build 2445 program (Dako, USA), as described elsewhere [18].

2.10. IFNγ Enzyme-Linked Immunospot (ELISpot) Assay. The ELISpot assay for the enumeration of IFNγ-producing cells was performed in triplicate as previously described [18]. Briefly, plates were coated with the capture anti-mouse IFNγ antibody (clone R4-6A2). Antigen-presenting cells were primed with the immunodominant H-2K^b-restricted VNHRFTLV amastigote surface protein 2 (ASP2) peptide, incubated with freshly isolated splenocytes from experimental mice (5×10^5 cells/well), incubated for 20 hours at 37°C and 5% CO_2, and cytokine was detected using biotin-conjugated anti-mouse and revealed as previously described alkaline phosphatase-labeled streptavidin in presence of a solution of NBT and BCIP (Sigma, USA). The mean number of spots in triplicate wells was determined for each experimental condition and the number of specific IFNγ-secreting T-cells was calculated by estimating the stimulated spot count/10^6 cells using a CTL OHImmunoSpot A3 Analyzer (USA), as previously described [18].

2.11. In Vivo Cytotoxicity Assay. For the *in vivo* cytotoxicity assays, splenocytes from naïve C57BL/6 mice were divided into two populations and labeled with the fluorogenic dye CFSE (Molecular Probes, USA) at a final concentration of 10 μM (CFSE^{high}) or 0.1 μM (CFSE^{low}). CFSE^{high} cells were coated with 2.5 μM of the VNHRFTLV ASP2 peptide for 40 minutes at 37°C. The CFSE^{low} cells remained uncoated. Subsequently, the CFSE^{high} cells were washed and mixed with equal numbers of CFSE^{low} cells before intravenous injection (1-2 $\times$ 10^7 cells per mouse) into C57BL/6 recipients sedated with ketamine and xylazine (100 mg/kg and 5 mg/kg, resp.). Spleen cells were collected from the recipient mice at 20 hours after adoptive cell transfer and fixed using 1.0% paraformaldehyde. All samples were acquired using a Beckman Coulter CyAn 7 Color flow cytometer (USA) and analyzed using the Summit v.4.3 Build 2445 program (Dako, Denmark) and the percentage of specific lysis was determined as previously described [18].

2.12. Immunohistochemistry. The animals were euthanized under anesthesia at 150 dpi and the hearts were removed, embedded in the tissue-freezing medium Tissue-Tek (Miles Laboratories, USA), and stored in liquid nitrogen. Three sections were analyzed per heart tissue. The phenotypes of the inflammatory cells colonizing the heart tissue and the FN deposition were characterized and analyzed as previously described [18, 24]. The numbers of CD4$^+$, CD8$^+$, F4/80$^+$ (macrophages), IFNγ^+, and Pfn$^+$ inflammatory cells were counted in 100 microscopic fields (400X magnification) per

section. The FN-positive areas in 25 fields (12.5 mm^2) per section were evaluated with a digital morphometric apparatus. The images were digitized using a color view XS digital video camera adapted to a Zeiss microscope and analyzed with AnalySIS AUTO Software (Soft Imaging System, USA). The data are presented as the percent of FN positive area in the cardiac tissue.

2.13. Electrocardiogram (ECG) Registers. Mice were tranquilized with diazepam (10 mg/kg) and transducers were placed subcutaneously (DII). The traces were recorded for 2 min using a digital power lab 2/20 system connected to a bioamplifier at 2 mV for 1 second (PanLab Instruments, Spain). The filters were standardized between 0.1 and 100 Hz and the traces were analyzed using Scope software for Windows V3.6.10 (PanLab Instruments, Spain). The ECG parameters were analyzed as previously described [18].

2.14. Statistical Analysis. The data are expressed as arithmetic means ± standard deviation. Student's t-tests, ANOVA, or other appropriate tests were used to analyze the statistical significance of the observed differences. The Kaplan-Meier method was used to compare the survival times of the studied groups. All statistical tests were performed with GraphPad Prism. Differences were considered statistically significant when $P < 0.05$.

3. Results

3.1. Anti-TNF Therapy Does Not Affect Body Weight but Reduced the T. cruzi-Induced Splenomegaly. To test the hypothesis that TNF is a hub in the immunological and cardiac abnormalities, therapy with Infliximab was initiated at 120 dpi; when high TNF levels in the serum [21], splenomegaly and signs of CCC as cardiomegaly and electrical abnormalities [18] are detected. We used a therapeutic scheme with 48-hour interval injections; all parameters were analyzed at 150 dpi (Figure 1(a)), when all saline-injected and anti-TNF-treated *T. cruzi*-infected C57BL/6 mice were alive (data not shown). Infliximab and saline administration did not affect the body temperature (data not shown) and weight of *T. cruzi*-infected C57BL/6 mice (Figure 1(b)). Indeed, at 150 dpi, there was no difference in body weight when *T. cruzi*-infected mice (injected with saline or treated with anti-TNF) were compared to age-matched NI controls (Figure 1(c)). Short Infliximab therapy significantly decreased (3.95 ± 0.33 mg/g; $P < 0.01$) the cardiomegaly detected in not-treated (4.8 ± 0.38 mg/g) chronically infected mice. However, there was no difference when Infliximab-treated mice were compared with saline-injected (4.31 ± 0.66 mg/g; $P = 0.156$) chronically infected mice (Figure 1(d)). At 120 dpi, a remarkable splenomegaly due to increased number of splenocytes is noticed in Colombian-infected C57BL/6 mice compared to noninfected mice [18]. At 150 dpi, splenomegaly was also detected in saline-injected mice. However, anti-TNF therapy significantly reduced the number of total splenocytes (data not shown) and splenomegaly (Figure 1(e)).

3.2. Anti-TNF Therapy Does Not Reactivate T. cruzi Infection. At 150 dpi, heart tissue parasitism, detected by qPCR for genomic parasite DNA, persisted low in the chronic phase of *T. cruzi* infection of C57BL/6 mice (Figure 2(a)). Importantly, anti-TNF therapy with Infliximab did not reactivate *T. cruzi* infection in the central nervous tissue systemically (data not shown) and in the cardiac tissue of chronically infected mice (Figure 2(a)).

3.3. Treatment with Infliximab Reduces TNF mRNA Expression in the Heart Tissue. At 150 dpi, the expression of TNF mRNA was upregulated in the cardiac tissue of *T. cruzi*-infected mice compared to age-matched NI controls (Figure 2(b)). Notably, this TNF mRNA overexpression was significantly diminished after short anti-TNF therapy (Figure 2(b)).

3.4. TNF Neutralization Decreases the Levels of Inflammatory Cytokines but Preserves IL-10 Levels in the Serum. Chronic chagasic patients with severe myocardial involvement present a systemic inflammatory profile revealed as increased levels of cytokines (TNF, IFNγ, IL-10, IL-17, and IL-6) and the inflammatory mediator NO_x in the serum [4]. These features were reproduced in the experimental model of CCC in Colombian-infected C57BL/6 mice in comparison with age-matched NI controls (Figure 2(c) and Figures S1(a) and S1(b) available online at http://dx.doi.org/10.1155/2014/798078). Anti-TNF therapy tended to decrease the levels of IL-17A, IL-6, and NO_x in the serum (Figures S1(a) and S1(b)). Importantly, administration of Infliximab from 120 to 150 dpi significantly reduced the levels of TNF and IFNγ but did not influence the levels of IL-10 in the serum (Figure 2(c)). Consequently, anti-TNF therapy increased the IL-10/TNF and IL-10/IFNγ ratios in chronically infected mice (Figure 2(d)).

3.5. TNF Blocking Reduces the Accumulation of $CD8^+$ Cells in the Heart Tissue. At 120 dpi, chronically Colombian-infected C57BL/6 mice show CD8-enriched myocarditis [18]. Anti-TNF therapy did not diminish the general inflammatory foci composed of $CD8^+$, $CD4^+$, and $F4/80^+$ (macrophages) (Figure S2(a)) but reduced the number of $CD8^+$ cells infiltrating the cardiac tissue (Figures S2(b) and S2(c)). Therefore, we tested whether it was a site restricted effect examining the cell composition of a secondary lymphoid tissue. The frequencies of $CD4^+$ and $CD8^+$ T-cells in the spleen persisted unchanged after anti-TNF administration (Figure S2(d)).

3.6. TNF Neutralization with Infliximab Reduces TNFR1 Expression on $CD4^+$ and $CD8^+$ T-Cells. The frequencies of TNF^+ and $TNFR1^+$ splenic cells are upregulated in acute *T. cruzi* infection [12]. The frequencies of TNF-expressing $CD4^+$ and $CD8^+$ T-cells, which were also upregulated in chronically *T. cruzi*-infected mice, were not significantly modified by short therapy with anti-TNF (data not shown). The frequencies of $CD4^+TNFR1^+$ and $CD8^+TNFR1^+$ splenic T-cells were also markedly increased in chronically infected C57BL/6 mice compared to NI controls (Figure 3). Interestingly, anti-TNF therapy significantly decreased the frequency

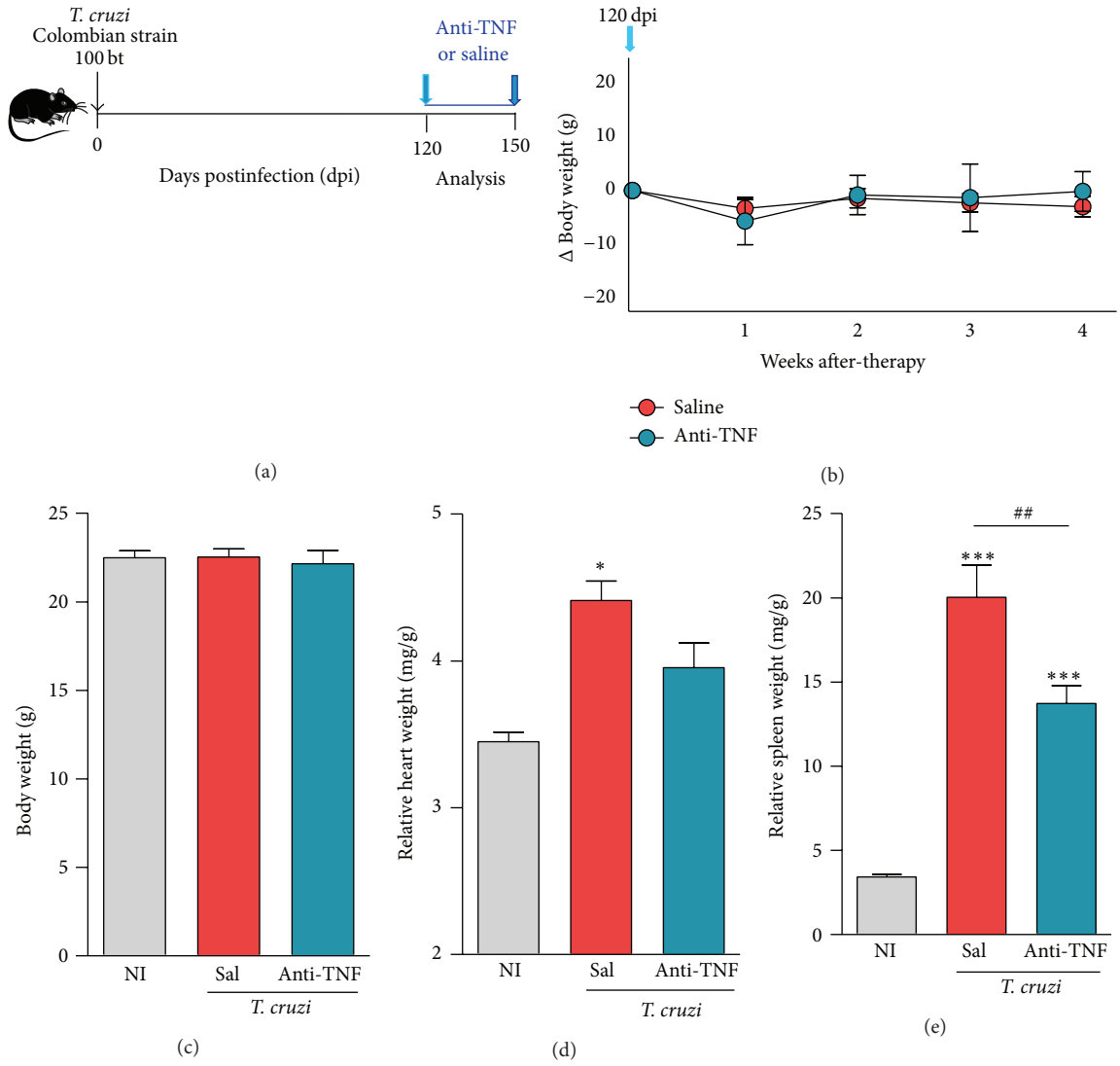

Figure 1: Anti-TNF therapy reduces *Trypanosoma cruzi*-induced splenomegaly in experimental model of chronic Chagas' heart disease. (a) C57BL/6 mice were infected with 100 bt of the Colombian *T. cruzi* strain and received saline or anti-TNF Infliximab 48-hour intervals from 120 (light blue arrow) to 150 days postinfection (dpi); noninfected mice received saline injections; all mice were analyzed at 150 (dark blue arrow) dpi. (b) Treatments were initiated at 120 dpi (blue arrow) and variation of body weight (g) was registered weekly. (c) Body weight (g), (d) relative heart weight (mg/g), and (e) relative spleen weight (mg/g) were analyzed at 150 dpi. $^{*}P < 0.05$ and $^{***}P < 0.001$, *T. cruzi*-infected mice (saline injected or anti-TNF treated) compared to NI controls. $^{\#\#}P < 0.01$, anti-TNF-treated compared to saline-injected *T. cruzi*-infected mice. Bar represents the mean ± SD of the studied group (9 to 15 mice). Representative data from three independent experiments are shown.

of TNFR1-bearing $CD4^+$ and $CD8^+$ T-cells compared with saline injection (Figure 3).

3.7. Anti-TNF Decreases TNF While Favors IL-10 Expression by $Ly6C^+$ and $F4/80^+$ Cells. Monocytes from cardiopathic CD patients seem to be committed to high TNF production, while monocytes from patients with the indeterminate (IND) form of CD display modulatory profile with high IL-10 production [17]. Therefore, we tested the effect of anti-TNF therapy on inflammatory (TNF) and regulatory (IL-10) profiles of $Ly6C^+$ and $F4/80^+$ splenic cells in chronic *T. cruzi* infection. In comparison with NI controls, chronically saline-injected *T. cruzi*-infected mice presented a remarkable increase in the frequency of TNF^+ cells among $Ly6C^+$ (Figure 4(a)) and $F4/80^+$ (Figure 4(b)) in R1(SSCxFSC) gated mononuclear splenocytes. Anti-TNF therapy significantly reduced the frequency of TNF-producing $Ly6C^+$ (Figure 4(a)) and $F4/80^+$ (Figure 4(b)) cells. Further, treatment with Infliximab upregulated the frequencies of $IL\text{-}10^+$ single-positive and $TNF^+IL\text{-}10^+$ double-positive cells among $Ly6C^+$ (Figure 4(a)) and $F4/80^+$ (Figure 4(b)) cells. Interestingly, short anti-TNF therapy reestablished the IL-10/TNF ratio among $Ly6C^+$ mononuclear splenocytes (means: 2.11 in NI controls; 0.54 in saline-injected versus 2.32 in anti-TNF-treated infected mice; Figure 4(a)).

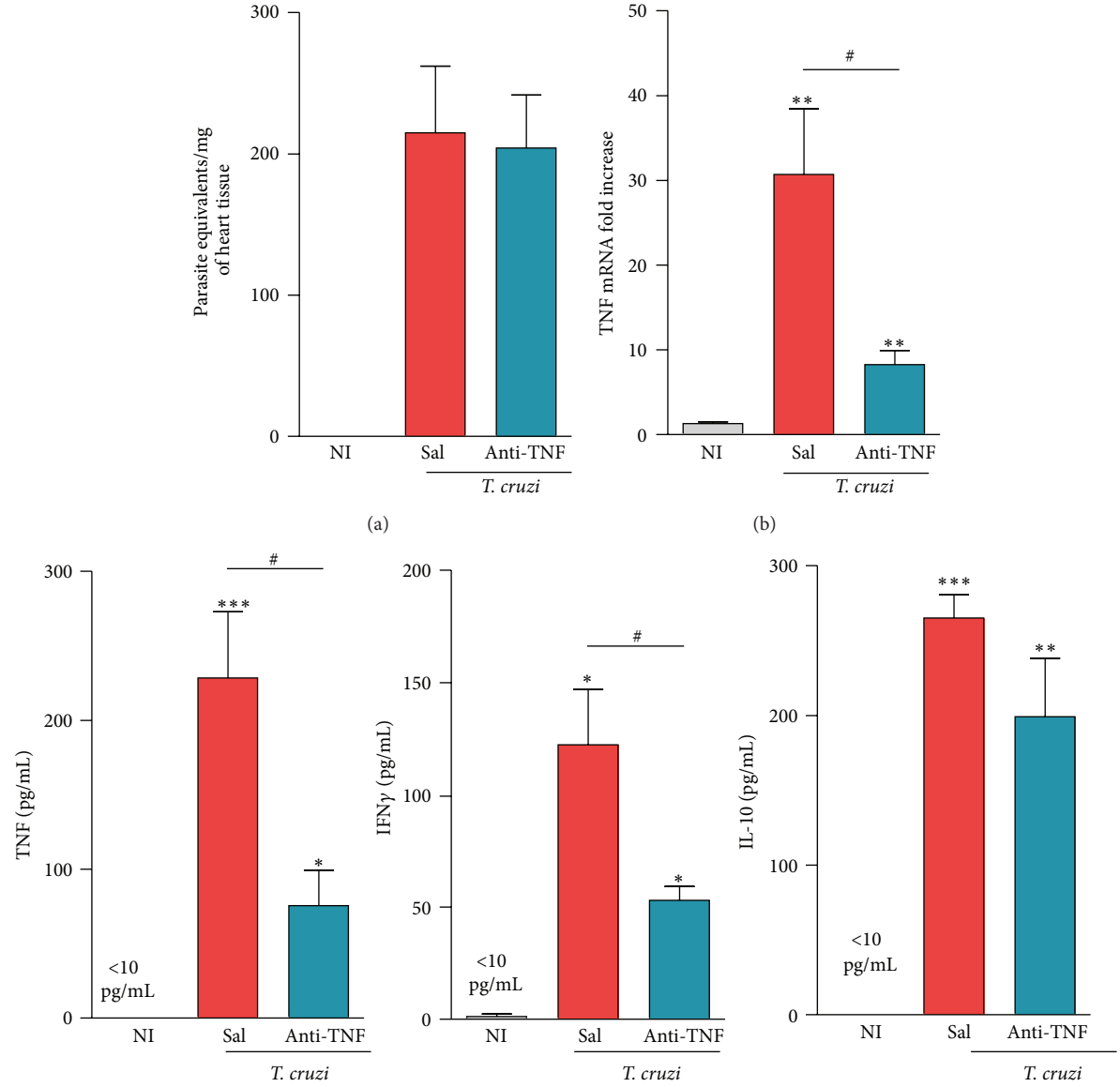

Ratio	IL-10/TNF	IL-10/IFNγ
T. cruzi + saline	1.16	2.63
T. cruzi + anti-TNF	2.17	3.75

(d)

Figure 2: Therapy with Infliximab does not reactivate *Trypanosoma cruzi* but reduces TNF mRNA expression in the heart tissue and inflammatory cytokine profile in the serum of chronically infected mice. C57BL/6 mice infected with 100 bt of the Colombian *T. cruzi* strain were treated from 120 to 150 dpi and analyzed at 150 dpi. (a) Detection of parasite DNA (equivalents/mg) in the cardiac tissue. (b) Expression of TNF mRNA (fold increase) in the heart tissue. (c) Measure of cytokine concentrations in the serum. (d) Relative ratios of IL-10/TNF and IL-10/IFNγ levels in the serum in saline-injected and anti-TNF treated infected mice. $^{*}P < 0.05$, $^{**}P < 0.01$, and $^{***}P < 0.001$, *T. cruzi*-infected mice (saline injected or anti-TNF treated) compared to NI controls. $^{\#}P < 0.05$, anti-TNF-treated compared to saline-injected *T. cruzi*-infected mice. Bar represents the mean ± SD of the studied group (3 to 5 mice). These data represent three independent experiments.

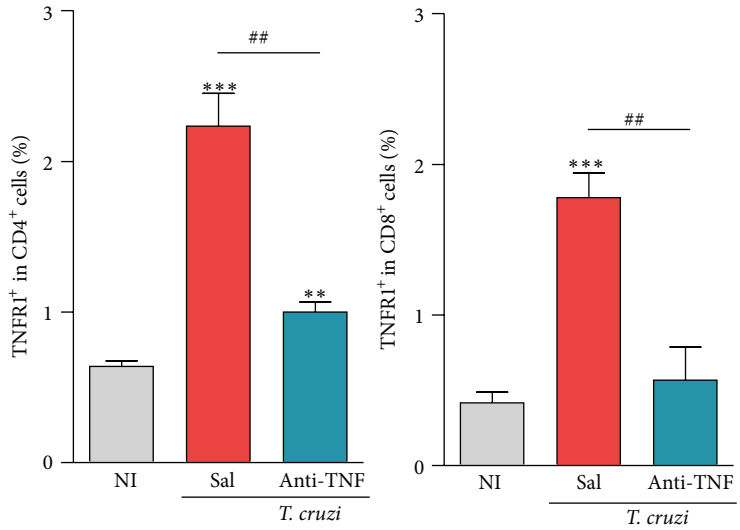

FIGURE 3: Anti-TNF administration reduces the frequency of TNFR1-expressing $CD4^+$ and $CD8^+$ T-cells in chronically *Trypanosoma cruzi*-infected mice. C57BL/6 mice infected with 100 bt of the Colombian *T. cruzi* strain were treated from 120 to 150 dpi and analyzed at 150 dpi. Frequency of $TNFR1^+$ cells among $CD4^+$ and $CD8^+$ T-cells in the spleen [R1 (SSCxFSC) gated]. $^{**}P < 0.01$ and $^{***}P < 0.001$, *T. cruzi*-infected mice (saline injected or anti-TNF treated) compared to NI controls. $^{\#\#}P < 0.01$, anti-TNF-treated compared to saline-injected *T. cruzi*-infected mice. Bar represents the mean ± SD of the studied group (4 to 6 mice). These data represent two independent experiments.

3.8. TNF Neutralizing Antibody Diminishes the Frequency of IL-17A$^+$ but Increased IL-10$^+$ CD4$^+$ T-Cells. Increased frequency of IL-$17A^+$ $CD4^+$ cells was noticed in chronically infected mice compared to age-matched NI controls (Figure 5(a)). Recently, anti-TNF therapy was shown to downregulate IL-17 expression and the frequency of Th17 cells in ankylosing spondylitis patients [20]; therefore, we tested whether it was also the case in chronic *T. cruzi* infection. Interestingly, Infliximab administration reduced the frequency of IL-$17A^+$ cells (Figure 5(a)). Conversely, anti-TNF therapy significantly enhanced the frequency of IL-10^+ $CD4^+$ cells, which was already upregulated during the chronic infection (Figure 5(b)). Interestingly, short anti-TNF therapy reestablished the IL-17A/IL-10 ratio among $CD4^+$ T splenocytes (means: 1.31 in NI controls; 3.03 in saline-injected versus 1.23 in anti-TNF-treated infected mice; Figure 5(c)).

3.9. TNF Neutralization Reduces Cytotoxic Activity but Preserves IFNγ-Producing Parasite-Specific CD8$^+$ T-Cells. Recently, we proposed that Pfn^+ and IFNγ^+ $CD8^+$ T-cells play antagonist roles in CCC [18]. Further, *in vitro* stimulus of $CD8^+$ T-cells with *Mycobacterium* lysed in the presence of anti-TNF antibody reduced the effector cytotoxic activity [19]. Therefore, we hypothesized that *in vivo* therapeutic intervention targeting TNF could selectively interfere with distinct $CD8^+$ T-cells modulating $CD8^+Pfn^+$ and cytotoxic $CD8^+$ T-cell effectors (CTL) in chronic *T. cruzi* infection. Herein, we challenged this hypothesis. When compared to age-matched NI controls, there was a significant increase in *in vivo* CTL activity (Figure 6(a)) and IFNγ-producing (Figure 6(b)) $CD8^+$ T-cells which recognize the immunodominant H-$2K^b$-restricted VNHRFTLV ASP2 peptide in chronically infected mice, at 150 dpi. More importantly, short anti-TNF therapy reduced CTL activity (Figure 6(a)) but preserved IFNγ-producing (Figure 6(b)) $CD8^+$ T-cells specific for the immunodominant VNHRFTLV ASP2 peptide.

3.10. Infliximab Administration Reduces the Number of Pfn$^+$ Cells Infiltrating the Cardiac Tissue. We, then, examined whether anti-TNF therapy influenced the balance of cytotoxic (Pfn^+) and inflammatory (IFNγ^+) cells composing the chronic *T. cruzi*-induced myocarditis. Compared to saline-injected mice, anti-TNF-treated mice showed reduced number of Pfn^+ cells (Figure 6(c)) but similar number of IFNγ^+ cells (Figure 6(d)) infiltrating the cardiac tissue, supporting that Infliximab remolded chronic *T. cruzi*-induced myocarditis.

3.11. Anti-TNF Treatment Improves Chronic ECG Abnormalities. Based on our results that anti-TNF downmodulates the expression of TNF and CTL activity, immune effectors hypothesized to be protagonist players of CCC pathogenesis [14, 18], we examined the effects of Infliximab in chronically *T. cruzi*-induced electrical abnormalities. At 120 dpi, when treatment with Infliximab was initiated, electrical abnormalities were already established in Colombian-infected C57BL/6 mice [18]. At 150 dpi, chronically infected C57BL/6 mice not-treated (data not shown) or injected with saline presented abnormalities in the electrical conduction system (Figure 7(a)), including low heart rate and prolonged PR, corrected QT (QTc) and QRS intervals (Figure 7(b)). Further, compared to NI controls, chronically infected mice showed a high proportion of mice afflicted by arrhythmias (ART), second-degree atrioventricular block (AVB2), and other ECG abnormalities (Figure 7(c)), including a low frequency of mice showing first-degree atrioventricular block (AVB1) and

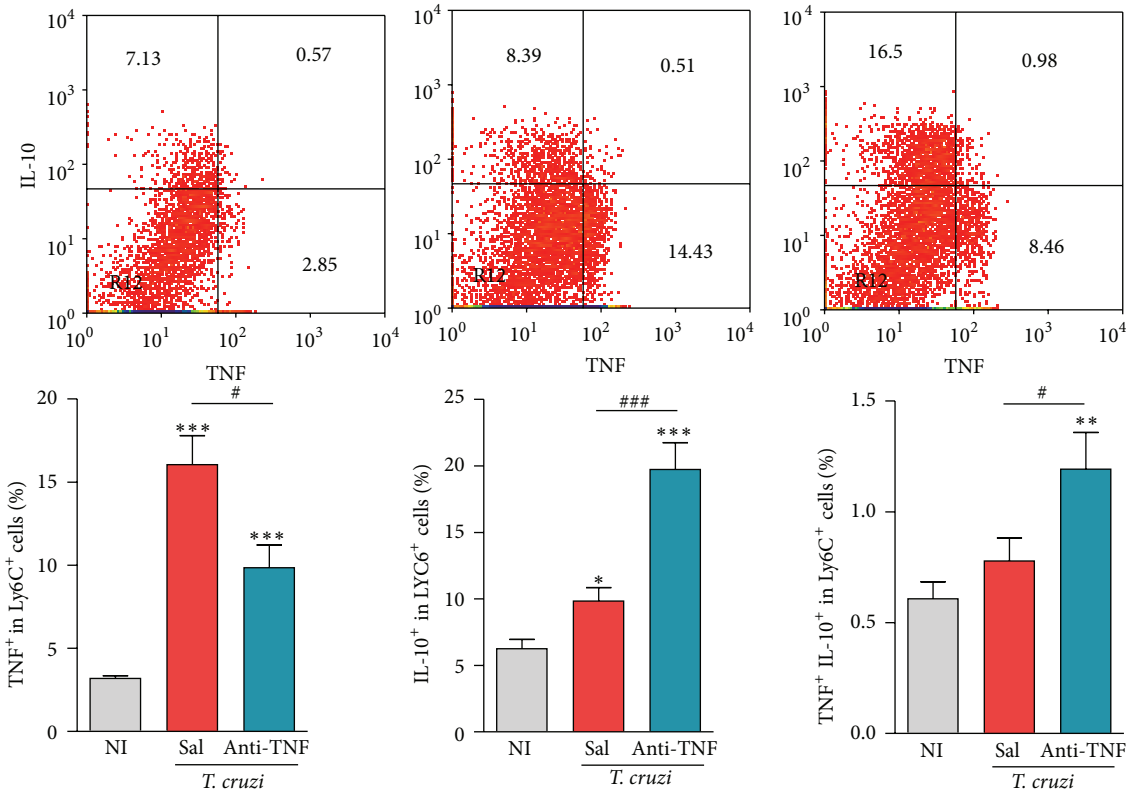

Ratio	IL-10/TNF
NI controls	0.85–3.47 (2.11)
T. cruzi + saline	0.23–1.69 (0.54)
T. cruzi + anti-TNF	1.68–3.30 (2.32)

(a)

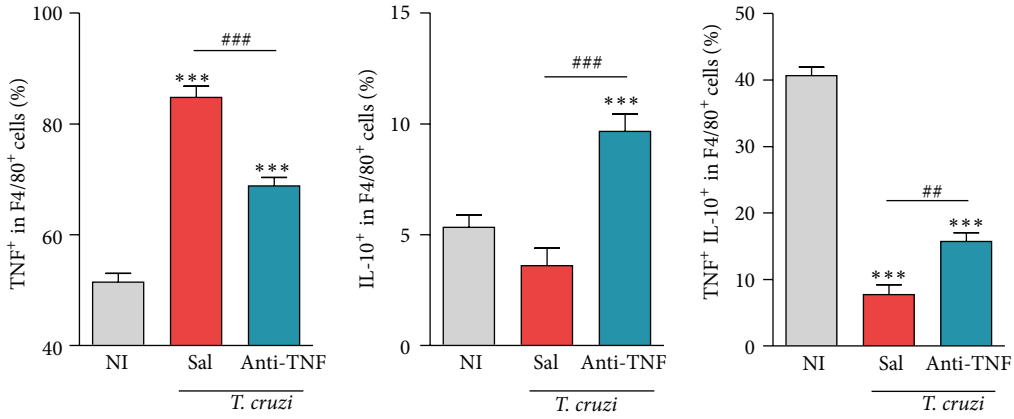

(b)

Figure 4: Anti-TNF therapy reduces the frequency of TNF$^+$ cells but increases the frequency of IL-10$^+$ and IL-10$^+$TNF$^+$ cells among Ly6C$^+$ and F4/80$^+$ macrophages in chronically *Trypanosoma cruzi*-infected mice. C57BL/6 mice infected with 100 bt of the Colombian *T. cruzi* strain were treated from 120 to 150 dpi and analyzed at 150 dpi. (a) Representative dot plots, frequency of TNF$^+$, IL-10$^+$, and TNF$^+$ IL-10$^+$ cells among Ly6C$^+$ in the spleen [R1 (SSCxFSC) mononuclear cells gated], and ranges (means) of the IL-10/TNF relative ratios are shown. (b) Frequency of TNF$^+$, IL-10$^+$, and TNF$^+$ IL-10$^+$ double-positive cells among F4/80$^+$ in the spleen [R1 (SSCxFSC) mononuclear cells gated]. $^{*}P < 0.05$, $^{**}P < 0.01$, and $^{***}P < 0.001$, *T. cruzi*-infected mice (saline injected or anti-TNF treated) compared to NI controls. $^{\#}P < 0.05$, $^{\#\#}P < 0.01$, and $^{\#\#\#}P < 0.001$, anti-TNF-treated compared to saline-injected *T. cruzi*-infected mice. Bar represents the mean ± SD of the studied group (4 to 6 mice). These data represent two independent experiments.

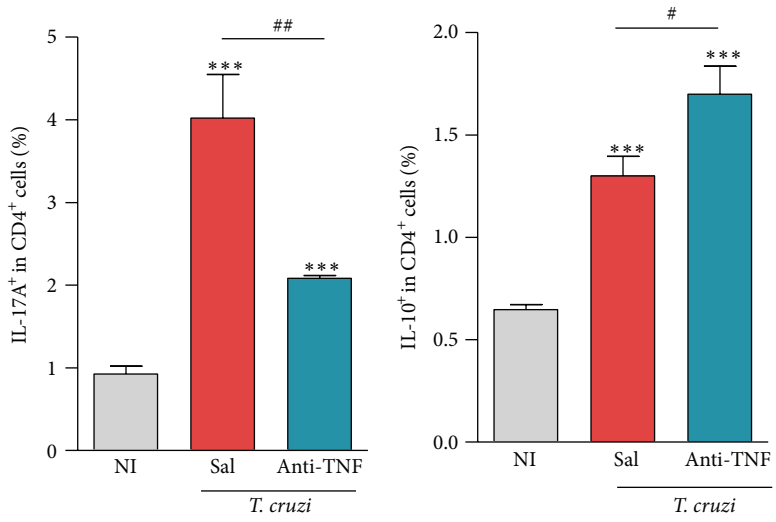

(a) (b)

Ratio	IL-17/IL-10
NI controls	1.03–1.60 (1.31)
T. cruzi + saline	2.03–5.14 (3.03)
T. cruzi + anti-TNF	0.86–1.54 (1.23)

(c)

Figure 5: Anti-TNF therapy reduces the frequency of IL-17A$^+$ CD4$^+$ cells but increases the frequency of IL-10$^+$ CD4$^+$ cells in chronically *Trypanosoma cruzi*-infected mice. C57BL/6 mice infected with 100 bt of the Colombian *T. cruzi* strain were treated from 120 to 150 dpi and analyzed at 150 dpi. (a) Frequencies of IL-17A$^+$ and (b) IL-10$^+$ cells among CD4$^+$ cells in the spleen [R1 (SSCxFSC)/R2 (TCR$\alpha\beta$/CD4) gated]. (c) Relative ratios of IL-17A/IL-10 in saline-injected and anti-TNF treated infected mice. $^{***}P < 0.001$, *T. cruzi*-infected mice (saline injected or anti-TNF treated) compared to NI controls. $^{\#}P < 0.05$ and $^{\#\#}P < 0.01$, anti-TNF-treated compared to saline-injected *T. cruzi*-infected mice. Bar represents the mean ± SD of the studied group (4 to 6 mice). These data represent three independent experiments.

rare cases of fibrillation (data not shown). Importantly, anti-TNF therapy restored the normal heart rate, P wave duration (data not shown), and PR, QTc, and QRS intervals (Figure 7(b)). Notably, compared with their counterparts anti-TNF therapy reduced the proportions of mice afflicted by ART, AVB2, and any ECG abnormalities (Figure 7(c)).

3.12. Anti-TNF Treatment Ameliorates Chronic T. cruzi-Induced Heart Tissue Damage. At 150 dpi, all chronically infected C57BL/6 mice not-treated [25] or injected with saline present increased FN deposition in the heart tissue compared to NI controls (Figure 8). More importantly, anti-TNF therapy significantly reduced the frequency of areas positively stained for FN deposition in the cardiac tissue (Figure 8).

4. Discussion

Here we used the immunomodulatory strategy with the anti-TNF Infliximab antibody to investigate the influence of TNF on unbalanced immune response and cardiac tissue damage in chronic experimental Chagas' heart disease. TNF blocking therapy did not interfere with *T. cruzi* growth control but reshaped the broad immunological unbalance associated with CCC severity. Anti-TNF therapy selectively downregulated inflammatory cytokines but favored the expression of IL-10. Further, TNF neutralization reshaped parasite-specific CD8$^+$ T-cells as CTL activity was reduced but IFNγ production preserved. Additionally, Infliximab remodeled chronic myocarditis as the number of Pfn$^+$ cells was reduced but IFNγ^+ cells were unaffected. Moreover, therapy with Infliximab ameliorated ECG abnormalities and cardiac tissue damage. Therefore, we highlighted the contribution of TNF signaling as a hub in the immunological unbalance associated with the cardiac form of chronic *T. cruzi* infection.

When C57BL/6 mice were infected with low inoculum of the Colombian *T. cruzi* strain, 80–85% of mice survived the acute phase and developed CCC featured by low-grade cardiac tissue parasitism and CD8-enriched inflammation [18, 26]. Moreover, this model of chronic CD recapitulated ECG abnormalities and cardiac tissue injuries [18] found in chagasic patients [6] and non-human primates [23]. Similarly to CD patients [1–5], high TNF levels are detected in the serum of chronically Colombian-infected C57BL/6 mice paralleling CCC [18, 21, 25]. Therefore, this was an appropriated model to approach TNF influence on CCC pathogenesis.

Previous data showed cachexia and death in acutely *T. cruzi*-infected mice injected with the anti-TNF TN3 antibody

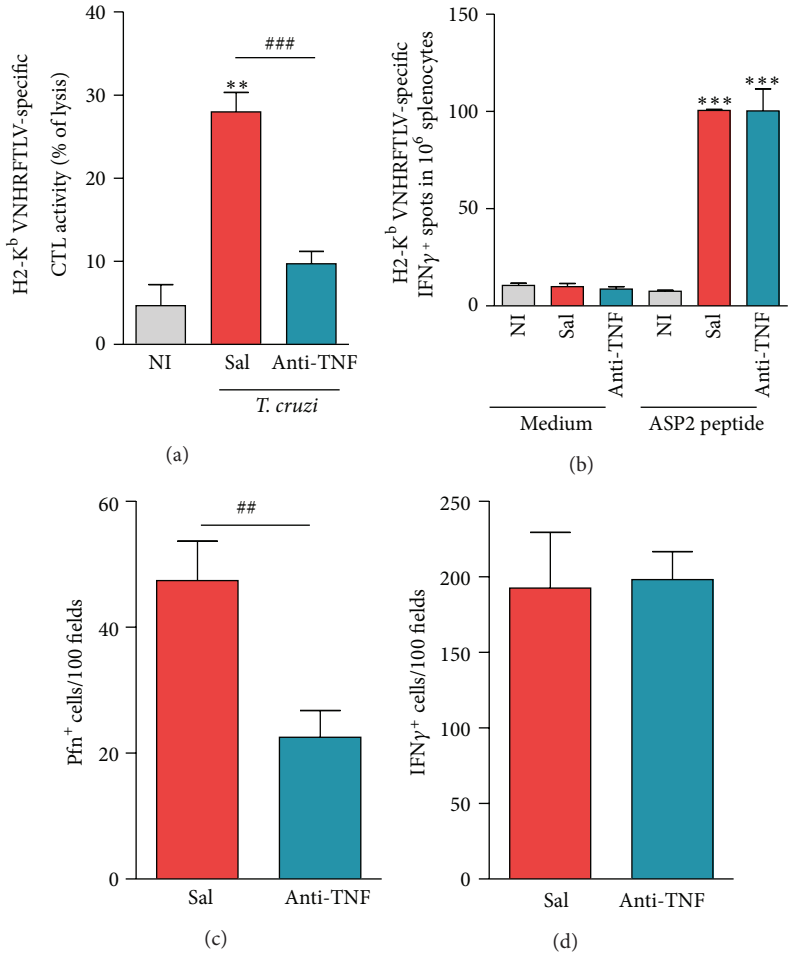

Figure 6: Anti-TNF therapy reshapes *Trypanosoma cruzi*-specific CTL activity and IFNγ-producing cells in spleen and the composition of Pfn$^+$ and IFNγ^+ cells invading the cardiac tissue in chronically *Trypanosoma cruzi*-infected mice. C57BL/6 mice infected with 100 bt of the Colombian *T. cruzi* strain were treated from 120 to 150 dpi and analyzed at 150 dpi. (a) Frequency of *in vivo* specific lysis of H-2K^b-restricted VNHRFTLV ASP2 peptide-labeled target cells in spleen. (b) Numbers of H-2K^b-restricted VNHRFTLV ASP2 peptide IFNγ^+ cells (spots) among splenocytes. Immunohistochemical staining of (c) Pfn$^+$ and (d) IFNγ^+ cells infiltrating the cardiac tissue, at 150 dpi. $^{**}P < 0.01$ and $^{***}P < 0.001$, *T. cruzi*-infected mice (saline injected or anti-TNF treated) compared to NI controls. $^{\#\#}P < 0.01$ and $^{\#\#\#}P < 0.001$, anti-TNF-treated compared to saline-injected *T. cruzi*-infected mice. Bar represents the mean ± SD of the studied group (3 to 6 mice). These data represent three independent experiments.

[27] and remarkable body weight loss in chronically infected hamsters treated with the TNF blocker Etanercept [15]. Here, we showed that anti-TNF therapy with Infliximab was not toxic to chronically infected mice, as they survived and did not lose body weight. Importantly, Infliximab administration to chronically infected C57BL/6 mice significantly reduced *T. cruzi*-induced splenomegaly, a cue previously associated with *T. cruzi*-induced T- and B-cell polyclonal activation [28]; therefore, anti-TNF therapy interfered with an immunological hallmark of *T. cruzi* infection.

The low-grade CD8-enriched CCC [29] is reproduced in Colombian-infected C57BL/6 mice [18, 26]. Anti-TNF therapy was shown to reduce the CD8-enriched myocarditis in acute *T. cruzi* infection in mouse [12] and chronic infection in rats [16]. Corroborating these findings, Infliximab administration also reduced the number of CD8$^+$ cells infiltrating the cardiac tissue of Colombian-infected C57BL/6 mice. Considering that part of the CD8$^+$ cells infiltrating the cardiac tissue play a role in the control of *T. cruzi* growth [18], the anti-TNF-induced reduction of myocarditis was expected to have a deleterious result on *T. cruzi* parasitism. However, anti-TNF therapy did not abrogate parasite control systemically or in the cardiac tissue of chronically infected C57BL/6 mice, reinforcing previous study [16].

TNF mRNA expression is related to protein production in the cardiac tissue in experimental CCC [24, 30]; therefore, increased TNF mRNA expression in the heart tissue of Colombian-infected C57BL/6 mice supports that this model mimics the TNF-enriched milieu of patients with CCC [7, 8]. Importantly, blockade of TNF activity by Infliximab directly or indirectly reverberated in TNF mRNA expression. Although significantly reduced in Infliximab-treated mice

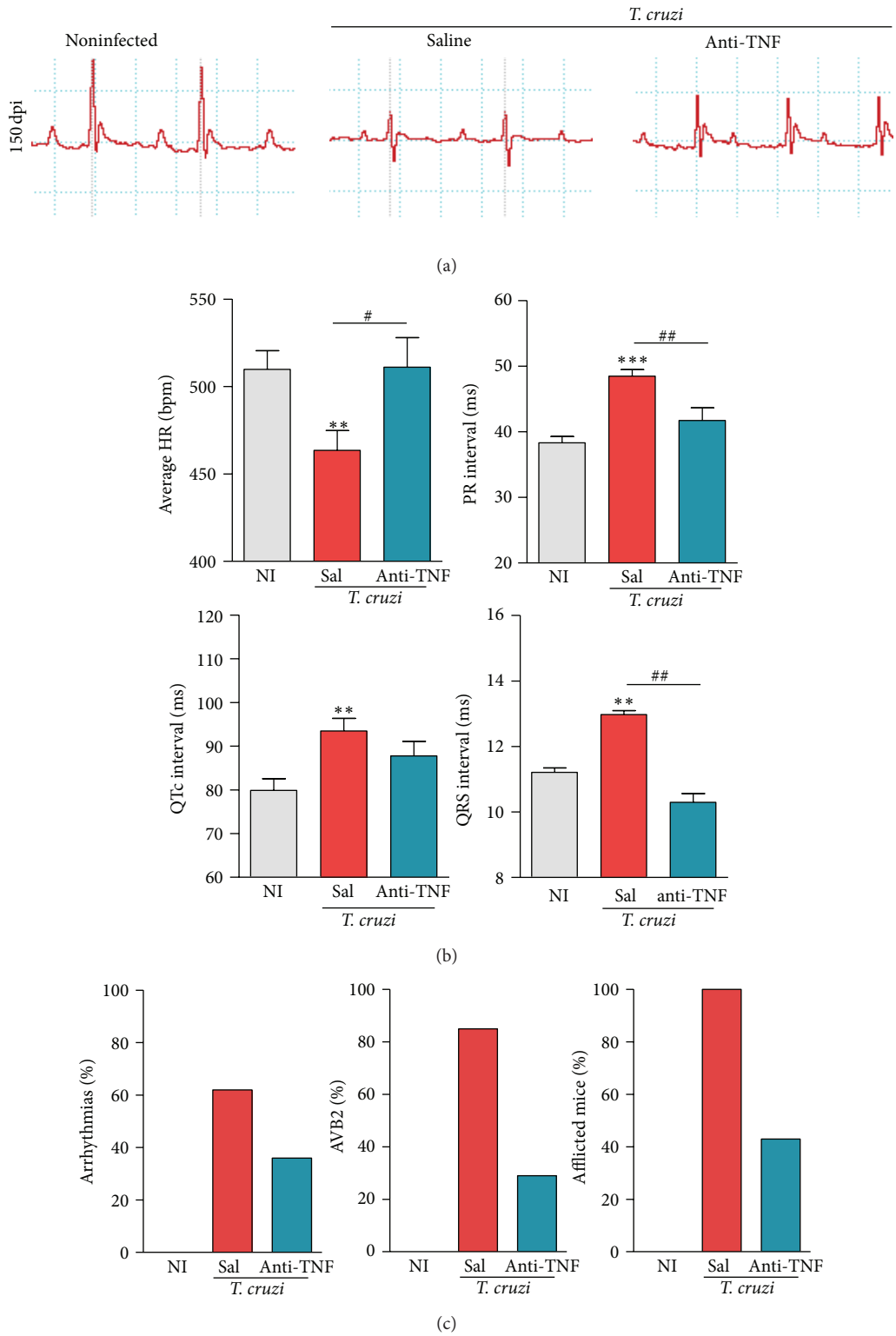

Figure 7: Anti-TNF therapy ameliorates electrical abnormalities in chronically *Trypanosoma cruzi*-infected mice. C57BL/6 mice infected with 100 bt of the Colombian *T. cruzi* strain were treated from 120 to 150 dpi and analyzed at 150 dpi. (a) Representative ECG register segments of sex- and age-matched NI controls and *T. cruzi*-infected mice injected with saline or anti-TNF, at 150 dpi. (b) Group data for the ECG records showing the heart rate (beats per minute, bpm), variation in the PR, QTc, and QRS intervals. (c) Summary of the group data from NI and *T. cruzi*-infected mice (injected with saline or anti-TNF) showing the frequency of mice presenting ART, AVB2 and afflicted by any ECG alterations. $^{**}P < 0.01$ and $^{***}P < 0.001$, *T. cruzi*-infected mice (saline injected or anti-TNF treated) compared to NI controls. $^{\#}P < 0.05$ and $^{\#\#}P < 0.01$, anti-TNF-treated compared to saline-injected *T. cruzi*-infected mice. Bar represents the mean ± SD of the studied group (10 to 15 mice). These data represent three independent experiments.

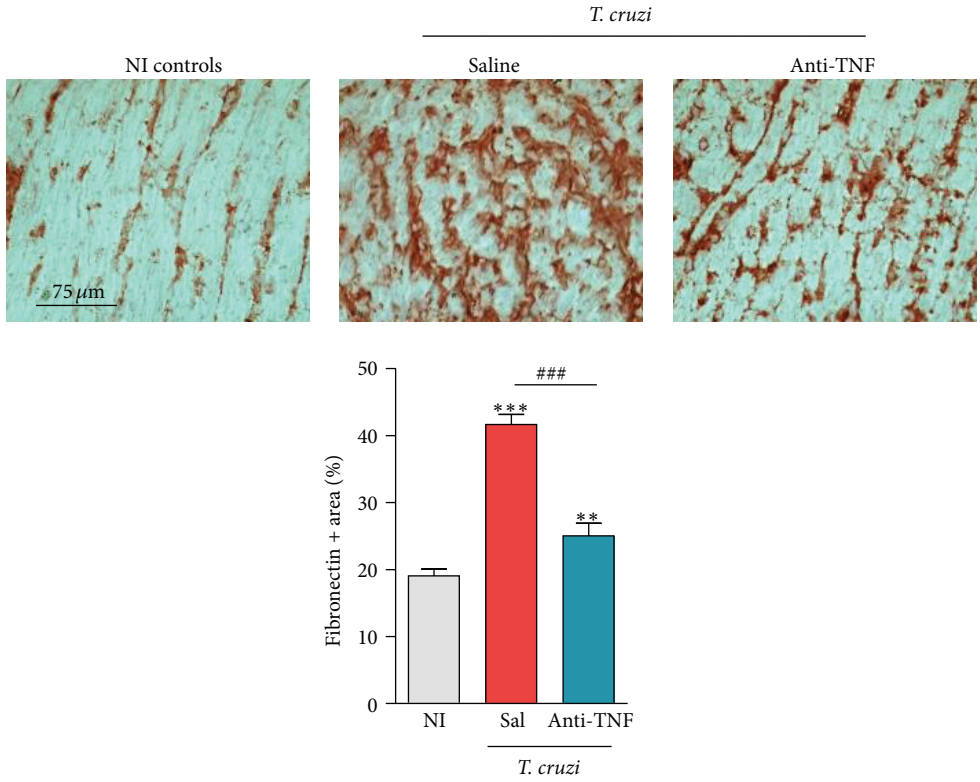

Figure 8: Anti-TNF therapy decreases fibronectin expression in the cardiac tissue of chronically *Trypanosoma cruzi*-infected mice. C57BL/6 mice infected with 100 bt of the Colombian *T. cruzi* strain were treated from 120 to 150 dpi and analyzed at 150 dpi. Representative heart sections from each experimental group analyzed by immunohistochemical staining to detect FN are shown. Data are expressed as percentage of FN-stained area (%).$^{**}P < 0.01$ and $^{***}P < 0.001$, *T. cruzi*-infected mice (saline injected or anti-TNF treated) compared to NI controls. $^{\#\#\#}P < 0.001$, anti-TNF-treated compared to saline-injected *T. cruzi*-infected mice. Bar represents the mean ± SD of the studied group (3 to 5 mice). These data represent three independent experiments.

compared to saline-injected ones, TNF mRNA expression was not abolished in the heart tissue. Hence, after the initial trigger by *T. cruzi* infection the elevated local TNF production may contribute to maintain high TNF mRNA expression in the cardiac tissue. The source of TNF mRNA expression in the cardiac tissue is unclear; however, both myocardial [31] and heart infiltrating inflammatory cells [7] may contribute to amplify local TNF production in chagasic infection. Notably, as TNF expression is not abolished by anti-TNF therapy, the remnant cytokine may contribute to parasite growth control [13, 31], explaining the absence of parasite burden after immunotherapy with Infliximab.

Along with the increased plasma TNF levels, we showed that chronically infected C57BL/6 mice present a broader systemic inflammatory profile with increased levels of IFNγ, IL-10, IL17A, IL-6, and NO_x in the serum, reproducing features of cardiopathic CD patients [1–5]. Although anti-TNF therapy reduced the circulating TNF and IFNγ levels, the production of these cytokines was not abolished. Moreover, the anti-TNF effect on cytokine production was selective as the high plasma IL-10 levels persisted and, consequently, after TNF blocking therapy the IL-10/TNF and IL-10/IFNγ ratios increased. These findings emphasize that the effectiveness of immune mediators involved in *T. cruzi* control [32] is disconnected from the systemic inflammatory profile [4, 5] and preserved after anti-TNF therapy. Indeed, no reactivation of *T. cruzi* in the heart and, mostly, in the central nervous system, which depends on preservation of the IFNγ axis [33], was detected after anti-TNF therapy.

TNF signals via TNFR1 and TNFR2 and TNFR1 signaling mediate most of the biological activities of TNF [34]. Due to TNFR1 upregulation on T-cells in chronically infected mice, we explored the effect of anti-TNF on TNFR1 expression. Indeed, TNF blockage abrogated *T. cruzi*-triggered TNFR1 upregulation on splenic $CD4^+$ and $CD8^+$ T-cells. Although not tested, it is reasonable to expect a similar effect on other cell types, including cardiomyocytes. TNFR1, but not TNFR2, signaling participates in *T. cruzi* control during acute infection [13, 35] and in acute heart injury [12]. Our data support that TNFR1 signaling is not crucial for parasite control during chronic infection. Importantly, TNF by acting on TNFR1, but not TNFR2, aggravates noninfectious heart failure [36, 37]. Therefore, TNFR1 downmodulation may be a favorable effect of anti-TNF on Chagas' heart disease. It is feasible that the beneficial effects of the anti-TNF therapy are due to an intervention in the positive feedback circuit

triggered by an increase in TNF induced by *T. cruzi* infection, which may promote TNFR1 expression and the TNF/TNFR1 signaling that fuels TNF overproduction. Therefore, the downregulatory effect of anti-TNF on TNFR1 expression may contribute to reduce the responsiveness of activated cells to TNF in chronic chagasic infection and, therefore, disrupting or, at least, quelling the continuous TNF/TNFR1 signaling.

In chronic *T. cruzi* infection, TNF production by innate ($Ly6C^+$ and $F4/80^+$) immune cells was significantly enhanced. Interestingly, TNF production by $Ly6C^+$ and $F4/80^+$ monocytic cells was significantly reduced after anti-TNF therapy. Moreover, TNF neutralization increased the frequencies of $IL\text{-}10^+$ and $TNF^+IL\text{-}10^+$ multifunctional producers among $Ly6C^+$ and $F4/80^+$ splenic cells. Again, the IL-10/TNF ratio was favored by Infliximab administration in the chronic phase of chagasic infection. However, it remains to be explored whether anti-TNF therapy alters the balance between classically activated inflammatory (M1) and alternatively activated regulatory (M2) macrophages in chronic *T. cruzi* infection, as recently shown in *Leishmania* infection [38]. Importantly, the study of chronic patients with polar clinical forms of CD showed that monocytes from IND patients display regulatory profile with high IL-10 production, whereas monocytes from cardiopathic patients may be committed to induction of inflammatory responses related to high TNF expression [17]. Further, the development of CCC in a canine model was related to high IFNγ and TNF and low IL-10 production systemically and in the heart tissue in the acute *T. cruzi* infection [39]. Therefore, our data support that the fate of the chronic Chagas' heart disease may be altered even after it had apparently been sealed.

Adaptive immune cells, particularly $CD4^+$ and $CD8^+$ T-cells, contribute to the inflammatory/regulatory cytokine balance in chronic CD [40]. In chronically *T. cruzi*-infected C57BL/6 mice the short anti-TNF therapy did not impact the increased TNF expression by T-cells. Increased frequencies of $IL\text{-}17A^+$ and $IL\text{-}10^+$ splenic $CD4^+$ T-cells were also detected in chronically infected mice. The anti-TNF therapy downregulated the frequency of Th17 cells in these mice, corroborating previous findings in ankylosing spondylitis patients [20]; therefore, downmodulation of IL-17 is a conserved effect of TNF blocking. IL-17A contributes to protection against bacterial and fungal infections [41, 42]. In acute *T. cruzi* infection, IL-17 shaping the Th1 differentiation, cytokine and chemokine production, regulates the influx of inflammatory cells to the cardiac tissue involved in parasite resistance and myocardial destruction [43]. Here we demonstrated that high IL-17A production in the chronic phase of infection is not essential to anti-*T. cruzi* immunity. Importantly, IL-17A amplifies TNF signals by promoting mRNA stabilization of TNF-induced genes as chemokines and cytokines [44]; therefore, in breaking this circuit the beneficial effect of anti-TNF reducing the systemic inflammatory profile in chronic *T. cruzi* infection may reside. Nevertheless, anti-TNF therapy increased the frequency of IL-10-producing splenic $CD4^+$ T-cells, favoring a more regulatory balance. Actually, IL-10-production by T-cells promotes *T. cruzi* control and protection from fatal acute myocarditis [45] and, thus, may concur to the beneficial effects of anti-TNF in chronic infection. More importantly, higher IL-10 expression was associated with better left ventricular ejection fraction and left ventricular diastolic diameter values in CD patients [5]. Our data support that anti-TNF therapy alters the inflammatory/regulatory balance in innate and adaptive immune effectors during chronic *T. cruzi* infection. Interestingly, considering the overall cytokine profile of innate and adaptive immune cells from CD patients, 80% of CCC patients are high inflammatory (e.g., IFNγ, TNF) cytokine producers and 75% of IND patients are high regulatory (e.g., IL-10) cytokine producers [40]. Therefore, our data support that the blend of inflammatory/regulatory cytokines in different sources and compartments of the host may contribute to the generation but also to the perpetuation of pathological features of chronic Chagas' heart disease, as previously hypothesized [46]. Moreover, our data support that the inflammatory scenario can be reshaped by appropriate therapeutic intervention.

The complete abrogation of TNF production or activity may not be required for the beneficial effect of TNF-based therapy on CCC and may even be harmful in *T. cruzi* infection. Nonbeneficial effects of anti-TNF immunotherapy in chronic inflammatory diseases (as rheumatoid arthritis and ankylosing spondylitis) associated with reactivation of *Mycobacterium* infection may be attributed to the depletion of the cytolytic $CD8^+perforin^+/granulysin^+$ CTL population by Infliximab [19]. In chronically *T. cruzi*-infected mice treated with anti-TNF, the frequency of H2-K^b-restricted VNHRFTLV-specific CTL activity effectors was decreased but IFNγ producers were preserved. In *T. cruzi* infection, $CD8^+$ $IFN\gamma^+$ cells are protective and, conversely, $CD8^+Pfn^+$ cells are detrimental to electrical conduction and cardiac tissue injury [18]. Moreover, anti-TNF therapy in the chronic infection reduced the number of Pfn^+ but preserved $IFN\gamma^+$ cells invading the heart tissue. Thus, the remolded immune response in the cardiac tissue may contribute to avoid parasite burden and, moreover, may improve electrical conduction, as we previously hypothesized [18].

To our knowledge, this is the first description of a beneficial effect of anti-TNF therapy on major immunological features previously shown to parallel CCC [1–5]. In *T. cruzi* infection, anti-TNF therapy reduced acute cardiomyocyte lesion [12] and reversed chronic depressive-like behavior [21]. Here, we demonstrated that in chronically *T. cruzi*-infected C57BL/6 mice, anti-TNF ameliorated important signs of Chagas' heart disease, including bradycardia, prolonged P wave duration and PR interval, ART and AVB2, and remarkable CD features [6]. In CD, the severity of heart failure parallels plasma TNF levels [1–5]. Recently, we showed that in murine models of severe and mild CCC disease severity paralleled TNF and NO levels in the serum [25]. Also, in chagasic patients the severity of myocardial scarring, assessed by magnetic resonance, was related to ECG QRS score [47]. Importantly, the prolonged QRS in Colombian-strain C57BL/6 infected mice was reduced by anti-TNF therapy paralleling the inhibition of FN overdeposition in the heart tissue. Lastly, enhanced FN deposition in the cardiac tissue

reveals fibrosis in CD [48, 49]. These data reinforce the idea that *T. cruzi*-induced cardiac fibrosis can be ameliorated if the trigger of the process subsides [23] and posed TNF as a pivotal player in cardiac tissue injury and electrical abnormalities, supporting an even broader action of TNF signaling in chronic *T. cruzi* infection.

There is a consensus that *T. cruzi* persistence and parasite-driven deregulation of the immune response are key players in the establishment of CCC [29]. However, neither the intensity of parasitism nor the intensity of inflammation in the cardiac tissue seems to be crucial factors concurring to severity of chronic Chagas' heart disease. As hypothesized [18], the presence of Pfn^+ cells in the cardiac inflammation, probably fuelled by TNF, is a key player in CCC pathogenesis. Furthermore, TNF itself may trigger and/or maintain the nonbeneficial systemic inflammatory profile and the detrimental cardiac inflammation, which may crucially contribute to the pathogenesis of the heart disease in chronic *T. cruzi* infection, supporting that these are interconnected events.

5. Conclusions

The short anti-TNF therapeutic scheme used was safe and prevented progression of and, moreover, reversed heart injury and ECG abnormalities in association with the reshape of immunological unbalance. Further, TNF blocking inhibits the harmful immune circuits involved in heart injury but preserves the beneficial antiparasitic immunity. Therefore, anti-TNF might be a viable treatment for chronic Chagas' heart disease combined with a trypanocidal drug. Although the molecular mechanisms linking TNF to major *T. cruzi*-induced immunological abnormalities remain to be clarified, our data open a new pathway to be explored to comprehend the pathogenesis of Chagas' heart disease.

Conflict of Interests

All authors have no conflict of interests.

Acknowledgments

The authors are grateful to Dr. Cynthia Cascabulho for CBA data acquisition and analysis and the support of ELISpot and Cytometry Platforms of IOC/Fiocruz. The authors would like to thank Dr. Maria do Carmo Leite de Moraes and Dr. Veronica Schmitz Pereira for providing support to their discussion. This work was supported in part by grants from FAPERJ (Grants nos. APQ1-E-26/111.756/2008, CNE/E-26/101.549/2010, E-26/110.153/2013, and E-26/111.709/2013), the Brazilian Research Council/CNPq (Grants nos. 474234/2012-6-Universal and 302534/2008-3), and National Institute for Science and Technology for Vaccines–INCTV/CNPq (Grant no. 403979/2012-9-DECIT). I. R. Pereira is Research Fellow from FAPERJ. C. Britto and J. Lannes-Vieira are Research Fellows of the CNPq.

References

[1] R. C. Ferreira, B. M. Ianni, L. C. J. Abel et al., "Increased plasma levels of tumor necrosis factor-alpha in asymptomatic/"indeterminate" and Chagas disease cardiomyopathy patients," *Memorias do Instituto Oswaldo Cruz*, vol. 98, no. 3, pp. 407–411, 2003.

[2] R. Pérez-Fuentes, J. F. Guégan, C. Barnabé et al., "Severity of chronic Chagas disease is associated with cytokine/antioxidant imbalance in chronically infected individuals," *International Journal for Parasitology*, vol. 33, no. 3, pp. 293–299, 2003.

[3] A. Talvani, M. O. C. Rocha, A. L. Ribeiro, R. Correa-Oliveira, and M. M. Teixeira, "Chemokine receptor expression on the surface of peripheral blood mononuclear cells in Chagas disease," *Journal of Infectious Diseases*, vol. 189, no. 2, pp. 214–220, 2004.

[4] A. R. Pérez, S. D. Silva-Barbosa, L. R. Berbert et al., "Immunoneuroendocrine alterations in patients with progressive forms of chronic Chagas disease," *Journal of Neuroimmunology*, vol. 235, no. 1-2, pp. 84–90, 2011.

[5] G. R. Sousa, J. A. Gomes, R. C. Fares et al., "Plasma cytokine expression is associated with cardiac morbidity in Chagas disease," *PLoS ONE*, vol. 9, no. 3, Article ID e87082, 2014.

[6] A. Rassi Jr., A. Rassi, and J. A. Marin-Neto, "Chagas disease," *The Lancet*, vol. 375, no. 9723, pp. 1388–1402, 2010.

[7] L. C. J. Abel, L. V. Rizzo, B. Ianni et al., "Chronic Chagas' disease cardiomyopathy patients display an increased IFN-γ response to Trypanosoma cruzi infection," *Journal of Autoimmunity*, vol. 17, no. 1, pp. 99–107, 2001.

[8] D. B. Rocha Rodrigues, M. A. dos Reis, A. Romano et al., "In situ expression of regulatory cytokines by heart inflammatory cells in Chagas' disease patients with heart failure.," *Clinical & developmental immunology*, vol. 2012, Article ID 361730, 7 pages, 2012.

[9] K. Sliwa, A. Woodiwiss, V. N. Kone et al., "Therapy of ischemic cardiomyopathy with the immunomodulating agent pentoxifylline: results of a randomized study," *Circulation*, vol. 109, no. 6, pp. 750–755, 2004.

[10] M. Wong, D. Ziring, Y. Korin et al., "TNFα blockade in human diseases: mechanisms and future directions," *Clinical Immunology*, vol. 126, no. 2, pp. 121–136, 2008.

[11] P. C. Taylor, "Pharmacology of TNF rheumatoid arthritis and other chronic inflammatory," *Current Opinion in Pharmacology*, vol. 10, no. 3, pp. 308–315, 2010.

[12] K. Kroll-Palhares, J. C. Silvério, A. A. Da Silva et al., "TNF/TNFR1 signaling up-regulates CCR5 expression by CD8+ T lymphocytes and promotes heart tissue damage during *Trypanosoma cruzi* infection: beneficial effects of TNF-α blockade," *Memorias do Instituto Oswaldo Cruz*, vol. 103, no. 4, pp. 375–385, 2008.

[13] J. C. S. Aliberti, J. T. Souto, A. P. M. P. Marino et al., "Modulation of chemokine production and inflammatory responses in IFN-γ and TNF-R1 deficient mice during *Trypanosoma cruzi* infection," *American Journal of Pathology*, vol. 158, no. 4, pp. 1433–1440, 2001.

[14] J. Lannes-Vieira, I. R. Pereira, N. F. Vinagre, and L. E. A. Arnez, "TNF-α and TNFR in chagas disease: from protective immunity to pathogenesis of chronic cardiomyopathy," *Advances in Experimental Medicine and Biology*, vol. 691, pp. 221–230, 2011.

[15] A. M. B. Bilate, V. M. Salemi, F. J. Ramires et al., "TNF blockade aggravates experimental chronic Chagas disease cardiomyopathy," *Microbes and Infection*, vol. 9, no. 9, pp. 1104–1113, 2007.

[16] A. R. Pérez, G. H. Fontanella, A. L. Nocito, S. Revelli, and O. A. Bottasso, "Short treatment with the tumour necrosis factor-α blocker infliximab diminishes chronic chagasic myocarditis in rats without evidence of Trypanosoma cruzi reactivation," *Clinical and Experimental Immunology*, vol. 157, no. 2, pp. 291–299, 2009.

[17] P. E. A. Souza, M. O. C. Rocha, E. Rocha-Vieira et al., "Monocytes from patients with indeterminate and cardiac forms of Chagas' disease display distinct phenotypic and functional characteristics associated with morbidity," *Infection and Immunity*, vol. 72, no. 9, pp. 5283–5291, 2004.

[18] J. C. Silverio, I. R. Pereira, M. D. C. Cipitelli et al., "CD8+ T-cells expressing interferon gamma or perforin play antagonistic roles in heart injury in experimental trypanosoma cruzi-elicited cardiomyopathy," *PLoS Pathogens*, vol. 8, no. 4, Article ID e1002645, 2012.

[19] H. Bruns, C. Meinken, P. Schauenberg et al., "Anti-TNF immunotherapy reduces CD8+ T cell-mediated antimicrobial activity against Mycobacterium tuberculosis in humans," *Journal of Clinical Investigation*, vol. 119, no. 5, pp. 1167–1177, 2009.

[20] L. Xueyi, C. Lina, W. Zhenbiao, H. Qing, L. Qiang, and P. Zhu, "Levels of circulating Th17 cells and regulatory T cells in ankylosing spondylitis patients with an inadequate response to anti-TNF-α therapy.," *Journal of clinical immunology*, vol. 33, no. 1, pp. 151–161, 2013.

[21] G. Vilar-Pereira, A. A. D. Silva, I. R. Pereira et al., "*Trypanosoma cruzi*-induced depressive-like behavior is independent of meningoencephalitis but responsive to parasiticide and TNF-targeted therapeutic interventions," *Brain, Behavior, and Immunity*, vol. 26, no. 7, pp. 1136–1149, 2012.

[22] K. Redlich, S. Hayer, A. Maier et al., "Tumor necrosis factor α-mediated joint destruction is inhibited by targeting osteoclasts with osteoprotegerin," *Arthritis and Rheumatism*, vol. 46, no. 3, pp. 785–792, 2002.

[23] C. M. E. Carvalho, J. C. Silverio, A. A. da Silva et al., "Inducible nitric oxide synthase in heart tissue and nitric oxide in serum of Trypanosoma cruzi-infected rhesus monkeys: Association with heart injury," *PLoS Neglected Tropical Diseases*, vol. 6, no. 5, Article ID e1644, 2012.

[24] G. A. Medeiros, J. C. Silvério, A. P. M. P. Marino et al., "Treatment of chronically *Trypanosoma cruzi*-infected mice with a CCR1/CCR5 antagonist (Met-RANTES) results in amelioration of cardiac tissue damage," *Microbes and Infection*, vol. 11, no. 2, pp. 264–273, 2009.

[25] I. R. Pereira, G. Vilar-Pereira, A. A. Silva, and J. Lannes-Vieira, "Severity of chronic experimental Chagas' heart disease parallels tumour necrosis factor and nitric oxide levels in the serum: models of mild and severe disease," *Memórias do Instituto Oswaldo Cruz*, vol. 109, no. 3, pp. 289–298, 2014.

[26] A. Talvani, C. S. Ribeiro, J. C. S. Aliberti et al., "Kinetics of cytokine gene expression in experimental chagasic cardiomyopathy: tissue parasitism and endogenous IFN-γ as important determinants of chemokine mRNA expression during infection with Trypanosoma cruzi," *Microbes and Infection*, vol. 2, no. 8, pp. 851–866, 2000.

[27] C. Truyens, F. Torrico, R. Lucas, P. de Baetselier, W. A. Buurman, and Y. Carlier, "The endogenous balance of soluble tumor necrosis factor receptors and tumor necrosis factor modulates cachexia and mortality in mice acutely infected with *Trypanosoma cruzi*," *Infection and Immunity*, vol. 67, no. 11, pp. 5579–5586, 1999.

[28] P. Minoprio, "Parasite polyclonal activators: new targets for vaccination approaches?" *International Journal for Parasitology*, vol. 31, no. 5-6, pp. 588–591, 2001.

[29] M. D. L. Higuchi, L. A. Benvenuti, M. M. Reis, and M. Metzger, "Pathophysiology of the heart in Chagas'disease: current status and new developments," *Cardiovascular Research*, vol. 60, no. 1, pp. 96–107, 2003.

[30] P. V. A. dos Santos, E. Roffê, H. C. Santiago et al., "Prevalence of $CD8^{+}\alpha\beta$ T cells in *Trypanosoma cruzi*-elicited myocarditis is associated with acquisition of $CD62L^{Low}LFA\text{-}1^{High}VLA\text{-}4^{High}$ activation phenotype and expression of IFN-γ-inducible adhesion and chemoattractant molecules," *Microbes and Infection*, vol. 3, no. 12, pp. 971–984, 2001.

[31] F. S. Machado, G. A. Martins, J. C. S. Aliberti, F. L. A. C. Mestriner, F. Q. Cunha, and J. S. Silva, "*Trypanosoma cruzi*-infected cardiomyocytes produce chemokines and cytokines that trigger potent nitric oxide-dependent trypanocidal activity," *Circulation*, vol. 102, no. 24, pp. 3003–3008, 2000.

[32] C. Junqueira, B. Caetano, D. C. Bartholomeu et al., "The endless race between *Trypanosoma cruzi* and host immunity: lessons for and beyond Chagas disease," *Expert Reviews in Molecular Medicine*, vol. 12, article e29, 2010.

[33] V. Michailowsky, N. M. Silva, C. D. Rocha, L. Q. Vieira, J. Lannes-Vieira, and R. T. Gazzinelli, "Pivotal role of interleukin-12 and interferon-γ axis in controlling tissue parasitism and inflammation in the heart and central nervous system during Trypanosoma cruzi infection," *The American Journal of Pathology*, vol. 159, no. 5, pp. 1723–1733, 2001.

[34] G. Chen and D. V. Goeddel, "TNF-R1 signaling: a beautiful pathway," *Science*, vol. 296, no. 5573, pp. 1634–1635, 2002.

[35] E. Castaños-Velez, S. Maerlan, L. M. Osorio et al., "*Trypanosoma cruzi* infection in tumor necrosis factor receptor p55-deficient mice," *Infection and Immunity*, vol. 66, no. 6, pp. 2960–2968, 1998.

[36] A. M. Feldman and D. McNamara, "Myocarditis," *The New England Journal of Medicine*, vol. 343, no. 19, pp. 1388–1398, 2000.

[37] T. Hamid, Y. Gu, R. V. Ortines et al., "Divergent tumor necrosis factor receptor-related remodeling responses in heart failure: role of nuclear factor-κB and inflammatory activation," *Circulation*, vol. 119, no. 10, pp. 1386–1397, 2009.

[38] G. S. Ashcroft, M. J. Jeong, J. J. Ashworth et al., "Tumor necrosis factor-alpha (TNF-α) is a therapeutic target for impaired cutaneous wound healing," *Wound Repair and Regeneration*, vol. 20, no. 1, pp. 38–49, 2012.

[39] P. M. M. Guedes, V. M. Veloso, L. C. C. Afonso et al., "Development of chronic cardiomyopathy in canine Chagas disease correlates with high IFN-γ, TNF-α, and low IL-10 production during the acute infection phase," *Veterinary Immunology and Immunopathology*, vol. 130, no. 1-2, pp. 43–52, 2009.

[40] D. M. Vitelli-Avelar, R. Sathler-Avelar, A. Teixeira-Carvalho et al., "Strategy to assess the overall cytokine profile of circulating leukocytes and its association with distinct clinical forms of human Chagas disease," *Scandinavian Journal of Immunology*, vol. 68, no. 5, pp. 516–525, 2008.

[41] Y. Iwakura, H. Ishigame, S. Saijo, and S. Nakae, "Functional specialization of interleukin-17 family members," *Immunity*, vol. 34, no. 2, pp. 149–162, 2011.

[42] A. S. Wareham, J. A. Tree, and P. D. Marsh, "Th17 cells and iron homeostasis in protective immunity against tuberculosis in cynomolgus macaques," *PLoS ONE*, vol. 9, no. 2, Article ID e88149, 2014.

[43] P. M. da Matta Guedes, F. R. S. Gutierrez, F. L. Maia et al., "IL-17 produced during *Trypanosoma cruzi* infection plays a central role in regulating parasite-induced myocarditis.," *PLoS Neglected Tropical Diseases*, vol. 4, no. 2, article e604, 2010.

[44] J. Hartupee, C. Liu, M. Novotny, X. Li, and T. Hamilton, "IL-17 enhances chemokine gene expression through mRNA stabilization," *Journal of Immunology*, vol. 179, no. 6, pp. 4135–4141, 2007.

[45] E. Roffê, A. G. Rothfuchs, H. C. Santiago et al., "IL-10 limits parasite burden and protects against fatal myocarditis in a mouse model of *Trypanosoma cruzi* infection," *Journal of Immunology*, vol. 188, no. 2, pp. 649–660, 2012.

[46] R. Corrêa-Oliveira, J. Gomes, and E. M. Lemos, "The role of the immune response on the development of severe clinical forms of human Chagas disease," *Memórias do Instituto Oswaldo Cruz*, vol. 94, supplement 1, pp. 235–253, 1999.

[47] D. G. Strauss, S. Cardoso, J. A. C. Lima, C. E. Rochitte, and K. C. Wu, "ECG scar quantification correlates with cardiac magnetic resonance scar size and prognostic factors in Chagas' disease," *Heart*, vol. 97, no. 5, pp. 357–361, 2011.

[48] S. G. Andrade, J. B. Magalhães, and A. L. Pontes, "Therapy of the chronic phase of the experimental infection by *Trypanosoma cruzi* with benzonidazole and nifurtimox," *Revista da Sociedade Brasileira de Medicina Tropical*, vol. 22, no. 3, pp. 113–118, 1989.

[49] M. de Lourdes Higuchi, S. Fukasawa, T. de Brito, L. C. Parzianello, G. Bellotti, and J. A. F. Ramires, "Different microcirculatory and interstitial matrix patterns in idiopathic dilated cardiomyopathy and Chagas'disease: a three dimensional confocal microscopy study," *Heart*, vol. 82, no. 3, pp. 279–285, 1999.

Hindawi Publishing Corporation
Mediators of Inflammation
Volume 2014, Article ID 728939, 6 pages
http://dx.doi.org/10.1155/2014/728939

Research Article

Circumsporozoite Protein-Specific K^d-Restricted CD8+ T Cells Mediate Protective Antimalaria Immunity in Sporozoite-Immunized MHC-I-K^d Transgenic Mice

Jing Huang,[1] Tiffany Tsao,[1] Min Zhang,[2] and Moriya Tsuji[1]

[1] *HIV and Malaria Vaccine Program, Aaron Diamond AIDS Research Center, Affiliate of The Rockefeller University, 455 First Avenue, New York, NY 10016, USA*
[2] *Department of Pathology, New York University School of Medicine, 545 First Avenue, New York, NY 10016, USA*

Correspondence should be addressed to Jing Huang; jhuang@adarc.org and Moriya Tsuji; mtsuji@adarc.org

Received 24 April 2014; Accepted 23 June 2014; Published 15 July 2014

Academic Editor: Mauricio Martins Rodrigues

Although the roles of CD8+ T cells and a major preerythrocytic antigen, the circumsporozoite (CS) protein, in contributing protective antimalaria immunity induced by radiation-attenuated sporozoites, have been shown by a number of studies, the extent to which these players contribute to antimalaria immunity is still unknown. To address this question, we have generated C57BL/6 (B6) transgenic (Tg) mice, expressing K^d molecules under the MHC-I promoter, called MHC-I-K^d-Tg mice. In this study, we first determined that a single immunizing dose of IrPySpz induced a significant level of antimalaria protective immunity in MHC-I-K^d-Tg mice but not in B6 mice. Then, by depleting various T-cell subsets *in vivo*, we determined that CD8+ T cells are the main mediator of the protective immunity induced by IrPySpz. Furthermore, when we immunized (MHC-I-K^d-Tg × CS-Tg) F1 mice with IrPySpz after crossing MHC-I-K^d-Tg mice with PyCS-transgenic mice (CS-Tg), which are unable to mount PyCS-specific immunity, we found that IrPySpz immunization failed to induce protective antimalaria immunity in (MHC-I-K^d-Tg × CS-Tg) F1 mice, thus indicating the absence of PyCS antigen-dependent immunity in these mice. These results indicate that protective antimalaria immunity induced by IrPySpz in MHC-I-K^d-Tg mice is mediated by CS protein-specific, K^d-restricted CD8+ T cells.

1. Introduction

Malaria is a severe disease that ranks among the most prevalent infections in tropical areas throughout the world. Approximately 250–300 million people become infected yearly with relatively high rates of morbidity and mortality. The WHO estimates that every year nearly one million children die of malaria in Africa alone [1]. The widespread occurrence and the increasing incidence of malaria in many countries, caused by drug resistant parasites and insecticide resistant vectors (*Anopheles* mosquitoes), underscore the need for developing new methods of controlling this disease, which include more effective vaccines.

Most vaccine efforts are directed against the preerythrocytic stages (sporozoites (Spz) and liver stages) and blood stages [2]. The finding that vaccination with radiation-attenuated sporozoites (IrSpz) can induce complete protection (i.e., sterile immunity) against malaria infection not only in experimental animals but also in man [3–7] demonstrated the feasibility of effective vaccination against this disease. A number of mouse studies to date using *Plasmodium yoelii* and *P. berghei* parasites for challenge have shown that protective immunity against preerythrocytic stages is mediated in part by T cells, particularly CD8+ T cells. Firstly, the major role for CD8+ T cells was shown by studies in which *in vivo* depletion of CD8+ T cells abrogated Spz-induced protective immunity in mice [8, 9]. Secondly, the adoptive transfer of CD8+ T-cell clones specific for the immunodominant CD8+ T-cell epitope, SYVPSAEQI, of the *P. yoelii* circumsporozoite (PyCS) protein, a major Spz antigen, confers protection

against Spz challenge in naïve mice [10, 11]. More recently, by using transgenic (Tg) mice expressing a T-cell receptor (TCR), based on the TCR sequence of CD8+ T cells recognizing the SYVPSAEQI epitope, transgenic CD8+ T cells were shown to mediate protection against malaria [12]. Finally, Hoffman's group has recently shown that intravenous (IV) immunization of IrSpz vaccine is very effective in inducing a high frequency of malaria-specific CD8+ T cells in the liver of nonhuman primates and mice and, furthermore, conferring protection in mice [13]. More recently the same group showed that immunization of multiple doses of their IrPfSPZ vaccine by IV conferred protection in six out of six vaccines against malaria challenge [14].

Thus, a number of studies have shown that CD8+ T cells can significantly contribute to the protective immunity against the liver stages of malaria parasites in mice [8–16]. However, it is still largely unknown to which extend CD8+ T cells, particularly those specific for the CS protein, can mediate the protection induced by IrSpz. To address this key question, we have taken a novel approach. C57BL/6 (B6) mice express MHC-class-I molecule, H-2K^b (K^b), but lack H-2K^d (K^d) molecule, whereas BALB/c mice express the K^d molecules. We have generated transgenic (Tg) B6 mice that express the K^d molecules on all nucleated cells under the major histocompatibility complex- (MHC-) I promoter, which we call MHC-I-K^d-Tg mice [17]. As described above, the immunodominant T-cell epitope of the PyCS protein, SYVPSAEQI, is presented by H-2K^d molecules to CD8+ T cells and is known to be the only epitope that can induce protective CD8+ T cells against malaria [10, 11], underscoring the importance of generating MHC-I-K^d-Tg mice. These MHC-I-K^d-Tg mice were used to further refine the role of CD8+ T cells in protective antimalaria immunity induced by IrPySpz. Furthermore, by crossing our MHC-I-K^d-Tg mice with PyCS-transgenic mice (CS-Tg), in which mice are unable to induce PyCS-specific immunity [18], we have generated (MHC-I-K^d-Tg × CS-Tg) F1 mice and used it to study the role of CS antigen in mediating protective antimalaria immunity induced in IrPySpz-immunized MHC-I-K^d-Tg mice.

2. Materials and Methods

2.1. Mice. B6 mice and BALB/c mice were purchased from the Jackson Laboratory (Bar Harbor, ME). Transgenic mice (MHC-I-K^d) expressing H-2K^d shared allele by BALB/c mice under the control of the H-2K^b promoter on the B6 background were derived as previously described [17]. CS transgenic mice expressing CS gene of *P. yoelii* (17X NL) on the B6 background, CS-Tg mice [18], were kindly provided to us by Dr. Victor Nussenzweig at New York University. (MHC-I-K^d-Tg × CS-Tg) F1 mice were generated by crossing CS-Tg mice to MHC-I-K^d-Tg mice.

2.2. Antibodies. The following monoclonal antibodies (mAb) were purchased from BioLegend (San Diego, CA) and used for a flow cytometric analysis: purified anti-CD16/32 (clone 93), Alexa Fluor 647-labeled anti-H-2K^d (clone SF1-1.1), Pacific Blue-labeled anti-F4/80 (clone BM8), PE-Cy7-labeled anti-CD11b (clone M1/70), PerCP-Cy5.5-labeled anti-I-A^b (clone AF6-120.1), PE-labeled anti-CD11c (clone N418), FITC-labeled anti CD3 (17A2), APC-labeledanti-CD4 (clone RM4-5), and Pacific Blue-labeled anti-CD8 (clone 53-6.7).

2.3. Flow Cytometric Analysis. Murine cells were incubated with unlabeled anti-CD16/CD32 mAb for 10 min at RT and later incubated with the respective mAbs described in the preceding section. All cells were costained with propidium iodide (Sigma-Aldrich, St. Louis, MO) to exclude nonviable cells. Flow cytometric data collection was performed using an LSR II Flow Cytometer (BD Biosciences, San Jose, CA). Subsequent data analyses were performed using FlowJo software (Tree Star Inc.).

2.4. Parasites and Immunization. Female *Anopheles stephensi* mosquitoes infected with *P. yoelii* 17×NL strain were purchased from the New York University insectary. *P. yoelii* sporozoites were isolated from the salivary glands of infected *A. stephensi* mosquitoes 14 days after the mosquitoes had received an infectious blood meal. Sporozoites for immunization were attenuated after giving 15,000 rads by a gamma-irradiator. Mice were immunized with 5×10^4 to 1×10^5 irradiated sporozoites suspended in RPMI with 2% mouse sera by IV or intramuscular (IM) injection.

2.5. Depletion of T-Cell Subsets In Vivo. MHC-I-K^d-Tg mice were intraperitoneally injected with 250 μg or 500 μg of rat mAbs against CD4 (clone GK 1.5) or CD8 (clone YTS 169), respectively, on day −3 and day −1 prior to challenge with live *P. yoelii* sporozoites. The status of *in vivo* depletion of the corresponding T-cell subsets was assessed by flow cytometric assay, using anti-CD4 (clone RM4-5) and anti-CD8 (clone 53-6.7) mAbs.

2.6. Sporozoite Challenge and Assessment of Parasite Burden in the Liver. Mice were challenged by IV injection of viable *P. yoelii* sporozoites with varied doses from 1×10^4 to 5×10^4 per mouse. Parasite burden in the liver was determined 42 h after the challenge by measuring parasite-specific 18S rRNA using a quantitative real-time reverse transcription-PCR method with the 7500 Fast Real-Time PCR System (Applied Biosystems). Parasite burden was described as a ratio of the absolute copy number of parasite-specific 18S rRNA to that of mouse GAPDH.

2.7. Statistics. All of the statistical analyses were done using GraphPad Prism (version 5.03) (GraphPad Software Inc.). In the challenge experiment, parasite load in the liver was determined by a real-time RT-PCR. The values were then log-transformed and analyzed by 1-way ANOVA, followed by Dunnett's test. $P < 0.01$ is considered statistically significant.

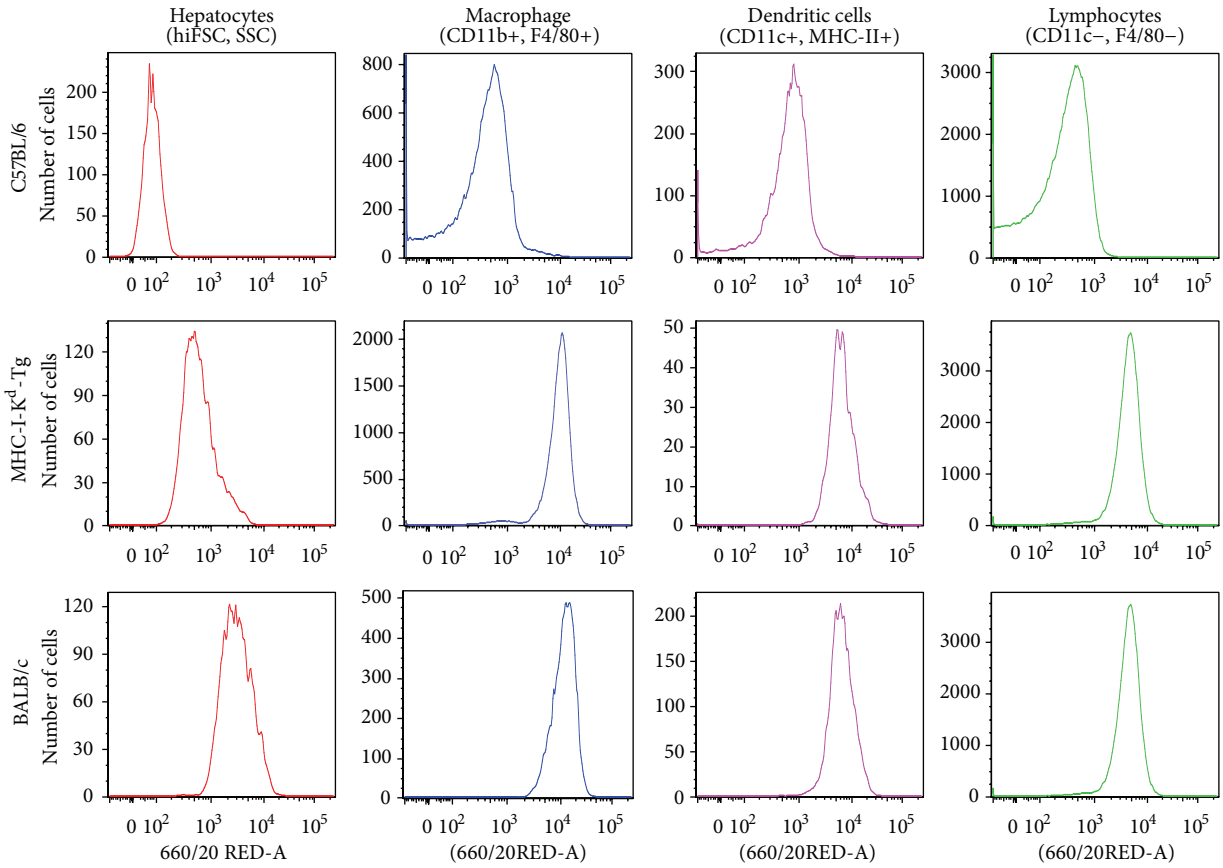

FIGURE 1: *Phenotype of MHC-I-K^d-Tg mice*. Histograms show H-2K^d expression levels on hepatocytes, macrophages, dendritic cells, and lymphocytes of C57BL/6 (B6), MHC-I-K^d-Tg, and BALB/c. Hepatocytes were isolated from mouse liver and then gated based on high FSC/SSC parameters. Macrophages were gated on CD11b+/F4/80+ and CD11c+/MHC II+ were used to define dendritic cells. Lymphocytes were identified by CD11c−/F4/80−.

3. Results and Discussion

MHC-I-K^d-Tg mice that express BALB/c mouse-derived H-2K^d allele under the control of the H-2K^b promoter on the B6 background were established previously in our laboratory [17]. The K^d expression profile of MHC-I-K^d-Tg mice was extensively investigated by flow cytometric analysis in various cells including hepatocytes, macrophages, dendritic cells, and lymphocytes as shown in Figure 1. B6 mice and BALB/c mice were used as K^d negative control and K^d positive control, respectively. As shown in Figure 1, K^d expression level on hepatocytes of MHC-I-K^d-Tg mice was only slightly lower than that of BALB/c mice but still significantly higher than that of B6 mice lacking K^d expression. In Figure 1, MHC-I-K^d-Tg mice showed similar expression levels of K^d on macrophages, dendritic cells, and lymphocytes as that on the corresponding cells of BALB/c mice. This suggests that, as expected, the MHC-I-K^d-Tg mice express K^d to the extent very similar to that of BALB/c mice, even with B6 mice background.

The protection between MHC-I-K^d-Tg mice and B6 mice against challenge of infectious *P. yoelii* sporozoites was evaluated after immunization with radiation-attenuated *P. yoelii* sporozoites (IrPySpz) by route of either IV or IM injections. As shown in Figure 2, IrPySpz immunization resulted in a statistically significant reduction ($P < 0.01$) in parasite load via both IV and IM injections in the livers of MHC-I-K^d-Tg mice. There was no such reduction in those of B6 mice in either IV or IM IrPySpz immunization routes. This is presumably because B6 mice lack K^d molecules that can present PyCS-derived CD8+ T-cell epitope for the induction of protective antimalarial CD8+ T cells. The challenge results in Figure 2 also showed that IrPySpz immunization in MHC-I-K^d-Tg mice via IV injection provided significantly more protection ($P < 0.01$) by way of liver stage parasite load reduction than the same immunization via IM injection. This finding corroborates the finding recently observed in humans showing that vaccination by IV of irradiated *P. falciparum* sporozoites induced protection [14].

In order to investigate which type of lymphocytes mediates the protective immunity against preerythrocytic stages of malaria, we depleted either CD4+ T cells or CD8+ T cells from MHC-K^d-Tg mice immunized IM with a single dose of IrPySpz. As shown in Figure 3(a), depletion of CD8+ T cells

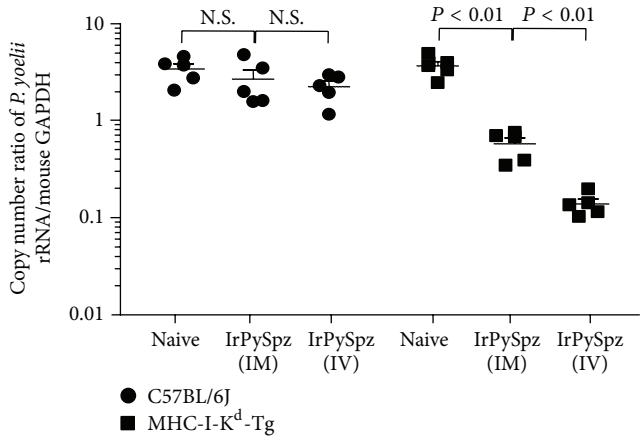

Figure 2: *Protection against malaria infection after a single immunizing dose of IrPySpz*. Groups of naive B6 mice and MHC-I-K^d-Tg mice (5 per group) were immunized with 1×10^5 IrPySpz via IV or IM injection. Protection assay was performed by challenge with 5×10^4 viable *P. yoelii* sporozoites via IV injection 2 weeks after immunization. Naïve B6 mice and MHC-I-K^d-Tg mice were also challenged as infection control. Parasite burden was described as a ratio of the absolute copy number of parasite-specific 18s rRNA to that of mouse GAPDH. $P < 0.01$ is considered statistically significant, whereas N.S. means "not significant" in Figures 2–4.

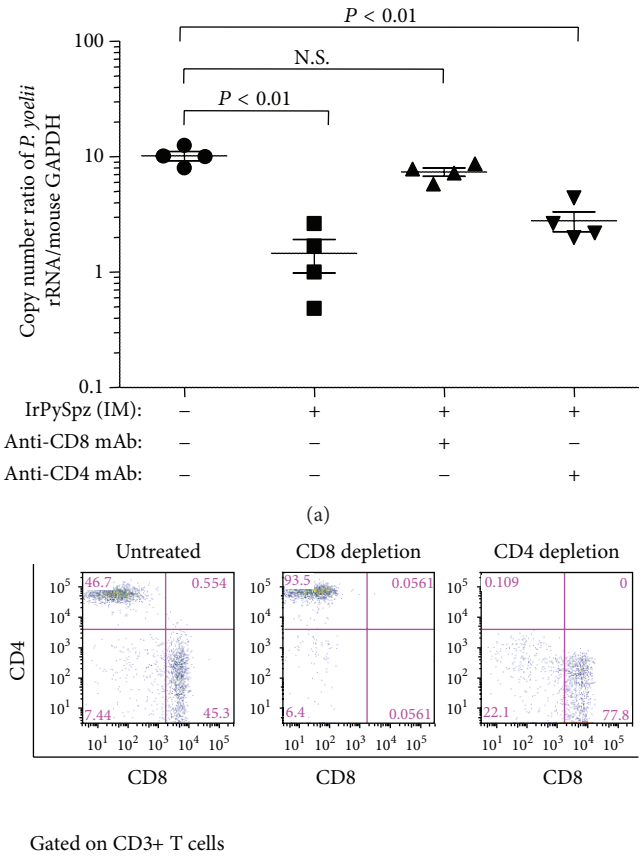

Figure 3: *Protection against plasmodium infection in IrPySpz-immunized MHC-I-K^d-Tg mice after depletion of CD8+ T cells or CD4+ T cells*. (a) Groups of MHC-I-K^d-Tg mice (4 per group) were immunized with 1×10^5 IrPySpz via IM injection following challenge with 5×10^4 viable *P. yoelii* sporozoites via IV injection at 2 weeks after immunization. Some cohorts of mice were treated with rat anti-CD4 mAb (GK1.5) or anti-CD8 mAb (YTS 169) 3 days and 1 day prior to challenge with *P. yoelii* sporozoites. Naive MHC-I-K^d-Tg mice were challenged as infection control. The value of parasite burden was described previously. (b) The dot plots by flow cytometric analysis represent the frequency of total CD4+ and CD8+ T cells among the CD3+ T-cell population of splenocytes, following the indicated antibody treatment to IrPySpz-immunized MHC-I-K^d-Tg mice.

remarkably abolished the inhibition of the liver stage development in IrPySpz-immunized MHC-I-K^d-Tg mice followed by live PySpz challenge. The levels of parasite load in CD8+ T-cell-depleted, IrPySpz-immunized mice were very similar to that of unimmunized naïve mice, following infectious PySpz challenge. The depletion of CD4+ T cells, meanwhile, significantly diminished but failed to abolish the inhibition observed in IrPySpz-immunized, PySpz-challenged MHC-I-K^d-Tg mice (Figure 3(a)). Figure 3(b) shows that the *in vivo* administration of monoclonal antibody against CD4+ or CD8+ T cells efficiently depleted each respective T-cell population. This finding corroborates a previous study, in which BALB/c mice carrying H-2d haplotype were immunized intravenously with IrPySpz [9], and strongly suggests that IrPySpz-induced antimalaria protection observed in MHC-I-K^d-Tg mice is largely dependent on CD8+ T cells but not on CD4+ T cells. CD8+ T-cell-dependent protection observed in MHC-I-K^d-Tg mice would make sense in view of the presence of K^d molecules in MHC-I-K^d-Tg mice, which should be able to present an immunodominant CD8+ T-cell epitope, SYVPSAEQI, derived from the PyCS protein, thus eliciting potent and protective CD8+ T-cell response against malaria.

However, it is still unclear to which extent a single immunizing dose of IrPySpz would induce protective immunity mediated by PyCS antigen-specific CD8+ T-cell response. Although a whole sporozoite consists of more than one thousand antigens, CS protein is shown to be a dominant antigen that can mediate the protective immunity against preerythrocytic stages of malaria. This was verified by using PyCS antigen transgenic mice (CS-Tg mice) that were tolerant to CS-T-cell epitopes, as PyCS-specific CD8+ T-cell response was not detected in the CS-Tg mice with BALB/c background upon IrPySpz immunization [18]. Therefore, in order to determine the contribution of PyCS antigen in overall protective antimalaria immunity induced by IrPySpz, we decided to cross MHC-I-K^d-Tg mice with CS-Tg mice and generated (MHC-I-K^d-Tg × CS-Tg) F1 mice. Then we immunized (MHC-I-K^d-Tg × CS-Tg) F1 mice, as well as MHC-I-K^d-Tg mice, with a single dose of IrPySpz and compared the level of protective antimalaria immunity between the two groups of mice upon challenge with live PySpz. Figure 4

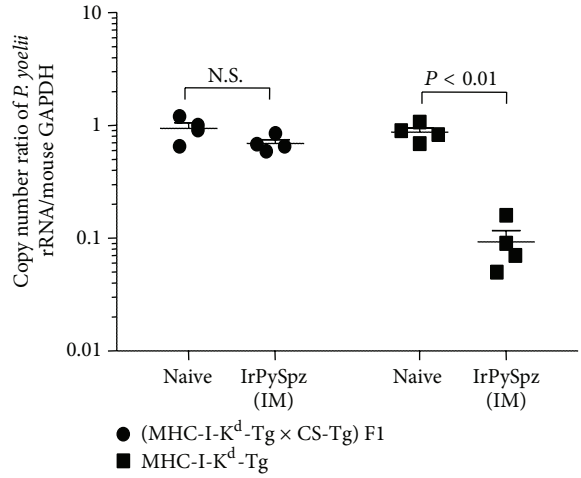

Figure 4: *Protection against plasmodium infection in IrPySpz-immunized MHC-I-K^d-Tg mice and (MHC-I-K^d-Tg × CS-Tg) F1 mice*. (MHC-I-K^d-Tg × CS-Tg) F1 mice were generated by crossing CS-Tg mice to MHC-I-K^d-Tg mice. Groups (4 mice per group) of naive MHC-I-K^d-Tg mice and MHC-I-K^d-Tg × CS-Tg mice were immunized with 5×10^4 IrPySpz via IM injection. Protection assay was performed by challenge with 1×10^4 infectious *P. yoelii* sporozoites via IV injection 2 weeks after immunization. Naïve MHC-I-K^d-Tg mice and (MHC-I-K^d-Tg × CS-Tg) F1 mice were also challenged as infection controls. The value of parasite burden was described previously.

shows that, in contrast to the significant level of protective antimalaria immunity observed in IrPySpz-immunized MHC-I-K^d-Tg mice, a single immunizing dose of IrPySpz failed to mount a significant level of protective immunity in (MHC-I-K^d-Tg × CS-Tg) F1 mice. These findings suggest that the protective antimalaria immunity induced in MHC-K^d-Tg mice by a single immunizing dose of IrPySpz is dependent on the immunity against the PyCS antigen.

4. Conclusions

Using transgenic B6 mice expressing K^d molecules in all nucleated cells under MHC-class-I promoter, we investigated in the current studies the nature of protective antimalaria immunity induced by immunization with radiation-attenuated *P. yoelii* sporozoites, IrPySpz. Firstly, we found that a single immunizing dose of IrPySpz could induce a significant level of antimalaria protective immunity in MHC-I-K^d-Tg mice, but not in B6 mice, likely due to the presence of K^d molecule. Then we determined that CD8+ T cells are the main mediators of the protective immunity induced by IrPySpz by depleting various T-cell subsets *in vivo* from IrPySpz-immunized MHC-I-K^d-Tg mice. Furthermore, when we generated (MHC-I-K^d-Tg × CS-Tg) F1 mice, by crossing the MHC-I-K^d-Tg mice with PyCS-transgenic (CS-Tg) mice that fail to mount PyCS-specific immunity, and immunized them with IrPySpz, we found that IrPySpz failed to induce protective antimalaria immunity in (MHC-I-K^d-Tg × CS-Tg) F1 mice, indicating that the protective immunity observed in MHC-I-K^d-Tg mice depends on the immunity specific for the PyCS antigen. Altogether, in summary, our current studies indicate that IrPySpz-induced, protective antimalaria immunity in MHC-I-K^d-Tg mice is dependent on CS protein-specific, K^d-restricted CD8+ T cells.

Conflict of Interests

The authors declare that there is no conflict of interests regarding the publication of this paper.

Acknowledgments

The authors thank Drs. Ruth Nussenzweig and Victor Nussenzweig for their support. They also thank Drs. Xiangming Li and Vincent Sahi for their help with performing various assays. This work was supported by a Grant from NIH, AI10289.

References

[1] *Malaria*, Fact Sheet No 94, WHO, Geneva, Switzerland, 2008.

[2] P. D. Crompton, S. K. Pierce, and L. H. Miller, "Advances and challenges in malaria vaccine development," *Journal of Clinical Investigation*, vol. 120, no. 12, pp. 4168–4178, 2010.

[3] D. F. Clyde, V. C. McCarthy, R. M. Miller, and R. B. Hornick, "Specificity of protection of man immunized against sporozoite induced falciparum malaria," *American Journal of the Medical Sciences*, vol. 266, no. 6, pp. 398–403, 1973.

[4] R. W. Gwadz, A. H. Cochrane, V. Nussenzweig, and R. S. Nussenzweig, "Preliminary studies on vaccination of rhesus monkeys with irradiated sporozoites of Plasmodium knowlesi and characterization of surface antigens of these parasites," *Bulletin of the World Health Organization*, vol. 57, no. 1, pp. 165–173, 1979.

[5] D. Herrington, J. Davis, E. Nardin et al., "Successful immunization of humans with irradiated malaria sporozoites: humoral and cellular responses of the protected individuals," *The American Journal of Tropical Medicine and Hygiene*, vol. 45, no. 5, pp. 539–547, 1991.

[6] S. L. Hoffman, L. M. L. Goh, T. C. Luke et al., "Protection of humans against malaria by immunization with radiation-attenuated *Plasmodium falciparum* sporozoites," *Journal of Infectious Diseases*, vol. 185, no. 8, pp. 1155–1164, 2002.

[7] R. S. Nussenzweig, J. Vanderberg, H. Most, and C. Orton, "Protective immunity produced by the injection of X-irradiated sporozoites of plasmodium berghei," *Nature*, vol. 216, no. 5111, pp. 160–162, 1967.

[8] L. Schofield, J. Villaquiran, A. Ferreira, H. Schellekens, R. Nussenzweig, and V. Nussenzweig, "γ Interferon, CD8+ T cells and antibodies required for immunity to malaria sporozoites," *Nature*, vol. 330, no. 6149, pp. 664–666, 1987.

[9] W. R. Weiss, M. Sedegah, R. L. Beaudoin, L. H. Miller, and M. F. Good, "CD8+ T cells (cytotoxic/suppressors) are required for protection in mice immunized with malaria sporozoites," *Proceedings of the National Academy of Sciences of the United States of America*, vol. 85, no. 2, pp. 573–576, 1988.

[10] M. M. Rodrigues, A.-S. Cordey, G. Arreaza et al., "$CD8^+$ cytolytic T cell clones derived against the Plasmodium yoelii circumsporozoite protein protect against malaria," *International Immunology*, vol. 3, no. 6, pp. 579–585, 1991.

[11] W. R. Weiss, J. A. Berzofsky, R. A. Houghten, M. Sedegah, M. Hollindale, and S. L. Hoffman, "A T cell clone directed at the circumsporozoite protein which protects mice against both Plasmodium yoelii and Plasmodium berghei," *Journal of Immunology*, vol. 149, no. 6, pp. 2103–2109, 1992.

[12] G. Sano, J. C. R. Hafalla, A. Morrot, R. Abe, J. J. Lafaille, and F. Zavala, "Swift development of protective effector functions in naive CD8+ T cells against malaria liver stages," *Journal of Experimental Medicine*, vol. 194, no. 2, pp. 173–179, 2001.

[13] J. E. Epstein, K. Tewari, K. E. Lyke et al., "Live attenuated malaria vaccine designed to protect through hepatic $CD8^+$ T cell immunity," *Science*, vol. 334, no. 6055, pp. 475–480, 2011.

[14] R. A. Seder, L. Chang, M. E. Enama et al., "Protection against malaria by intravenous immunization with a non-replicating sporozoite vaccine," *Science*, vol. 341, no. 6152, pp. 1359–1365, 2013.

[15] M. Tsuji and F. Zavala, "T cells as mediators of protective immunity against liver stages of Plasmodium," *Trends in Parasitology*, vol. 19, no. 2, pp. 88–93, 2003.

[16] M. Tsuji, "Re-evaluating the role of T cells for the development of T cell-based malaria vaccine," *Experimental Parasitology*, vol. 126, pp. 421–425, 2010.

[17] J. Huang, X. Li, K. Kohno et al., "Generation of tissue-specific H-$2K^d$ transgenic mice for the study of K^d-restricted malaria epitope-specific $CD8^+$ T-cell responses *in vivo*," *Journal of Immunological Methods*, vol. 387, no. 1-2, pp. 254–261, 2013.

[18] K. Arun Kumar, G. Sano, S. Boscardin et al., "The circumsporozoite protein is an immunodominant protective antigen in irradiated sporozoites," *Nature*, vol. 444, no. 7121, pp. 937–940, 2006.

Hindawi Publishing Corporation
Mediators of Inflammation
Volume 2014, Article ID 754965, 7 pages
http://dx.doi.org/10.1155/2014/754965

Review Article

Innate Immunity to *Leishmania* Infection: Within Phagocytes

Marcela Freitas Lopes, Ana Caroline Costa-da-Silva, and George Alexandre DosReis

Carlos Chagas Filho Institute of Biophysics, Federal University of Rio de Janeiro, 21941-900 Rio de Janeiro, RJ, Brazil

Correspondence should be addressed to Marcela Freitas Lopes; marcelal@biof.ufrj.br

Received 30 April 2014; Accepted 17 June 2014; Published 7 July 2014

Academic Editor: Edecio Cunha-Neto

Infection by *Leishmania* takes place in the context of inflammation and tissue repair. Besides tissue resident macrophages, inflammatory macrophages and neutrophils are recruited to the infection site and serve both as host cells and as effectors against infection. Recent studies suggest additional important roles for monocytes and dendritic cells. This paper addresses recent experimental findings regarding the regulation of *Leishmania major* infection by these major phagocyte populations. In addition, the role of IL-4 on dendritic cells and monocytes is discussed.

1. Introduction

Infection of humans with *Leishmania* surmounts 1.3 million new cases each year. Parasites infect and survive within phagolysosomal vesicles in host macrophages. Following infection with *Leishmania*, macrophages produce reactive oxygen species (ROS), cytokines, and chemokines and recruit an early inflammatory reaction [1, 2]. Interactions with inflammatory neutrophils either increase or decrease *L. major* replication in macrophages depending on host genotype and through mechanisms involving TGF-β or neutrophil elastase [3–5]. Recent studies suggest that additional phagocytes such as monocytes and dendritic cells (DCs) play important roles in infection, both as host and as effector cells. Here we discuss recent experimental findings regarding regulation of *L. major* infection by these major phagocyte populations. In addition, the role of IL-4 on DC and monocyte responses to infection is discussed.

2. Macrophage Activation

In response to microbial stimulation, macrophages differentiate into distinct M1 and M2 phenotypes [6, 7]. Both M1 and M2 macrophages are induced in the course of *Leishmania* infection. Microbial stimulation following priming with the Th1 cytokine IFN-γ leads to classically activated or M1-type macrophages [6]. M1 macrophages express nitric oxide (NO)-dependent leishmanicidal activity and are important for control of *Leishmania* infection [7]. By contrast, M2-type macrophages, induced by the Th2 cytokine IL-4, express arginase and play an important role in tissue repair [6]. Expression of PPAR-γ is also required for induction of M2 macrophages [8]. Mice lacking M2 or alternatively activated macrophages due to genetic deficiency of either the IL-4 receptor or PPAR-γ are more resistant to *L. major* infection [8, 9]. In addition, host IgG promotes infection by *Leishmania* due to early effects on macrophage differentiation [10]. Ligation of Fcγ receptors by IgG immune complexes induces IL-10 production and imprints a regulatory or M2b phenotype in macrophages, which is permissive for *Leishmania* replication [7, 11]. These results suggest that *L. major* takes advantage of M2 macrophages to replicate in the host.

Infection by *L. major* takes place in the context of inflammation and tissue repair induced by the insect bite [12–14]. Insect salivary molecules play an important role in the establishment of infection. Maxadilan, an insect derived salivary peptide, modulates the immune response of the host and reprograms dendritic cell maturation to facilitate infection [15, 16]. In addition, molecular and cellular elements recruited by the inflammatory reaction modulate

macrophage/*Leishmania* interactions. Tissue repair is a conserved response to injury characterized by an initial influx of neutrophils, followed by monocyte/macrophages and fibroblasts. Repair cannot be completed until inflammation is resolved, and, in the case of *L. major* infection, chronic ulcers are associated with persisting infiltrates of neutrophils [13]. Dynamic intravital microscopy of *L. major* infection site indicates that, after 1 day of infection, parasites localize mainly inside neutrophils [14]. Later, neutrophils are cleared and parasites become localized to monocyte/macrophages [14]. Interestingly, viable parasites are released from apoptotic neutrophils in the vicinity of macrophages [14]. Therefore, it is possible that *Leishmania* hides in neutrophils until apoptosis forces the parasites to infect a macrophage.

3. Early Macrophage Responses following Infection with *L. major*

Infection of resident macrophages plays an important sentinel role in early stages of *Leishmania* infection. Macrophages respond to infectious stress by either adapting or undergoing apoptosis. We investigated the role of cellular stress and apoptosis in macrophages infected with *L. major* in both susceptible and resistant mice. FasL plays a major role in early responses of susceptible BALB/c mice to infection. Infection induces FasL-dependent apoptosis of Mac-1/CD11b^{hi} resident macrophages, concomitant with secretion of chemokines KC and MIP-1α, and neutrophil extravasation [4]. Apoptosis and chemokine secretion induced by *L. major* in resident macrophages can be prevented with a neutralizing antibody specific for FasL, and neutrophil extravasation is reduced in FasL-deficient *gld* mutant mice [4]. These results agree with studies showing resident macrophage demise, chemokine secretion, and neutrophil extravasation following FasL stimulation of macrophages [17].

In contrast, early responses of resistant mice to infection are independent of FasL. Macrophages from B6 mice do not undergo apoptosis upon *L. major* infection. Chemokine secretion is independent of FasL expression, and neutrophil extravasation induced by infection is preserved in FasL-deficient mice [18]. In addition, we found no sign of macrophage death, and infected B6 macrophages remained viable as judged by constitutive secretion of lysozyme [18]. The reason for the different role of FasL in these mouse strains is unknown. However, BALB/c and B6 mice express a genetic polymorphism in FasL that affects biological activity, and B6 FasL has less cytotoxic activity than BALB FasL [19].

Although infection with *Leishmania* fails to induce apoptosis, it induces a cellular stress response in resident B6 macrophages characterized by increased production of ROS, activation of the stress activated protein kinases JNK, activation of c-Jun, and increased expression of FasL in resident macrophages [18]. Infection increased secretion of cytokines/chemokines TNF-α, IL-6, TIMP-1, IL-1RA, G-CSF, TREM, KC, MIP-1α, MIP-1β, MCP-1, and MIP-2 in resident macrophages. Secretion of KC is blocked either by addition of antioxidants or by a JNK inhibitor, suggesting that the stress response is involved in chemokine secretion. Interestingly, antioxidants and JNK inhibitor also blocked the intracellular growth of parasites [18], although the mechanisms involved remain to be determined. These results suggest that a cellular stress response by resident B6 macrophages recruits inflammatory cells but also promotes the intracellular survival/growth of the parasite [18].

4. Infection with *L. major* Interferes with Cytokine-Induced Macrophage Differentiation

In response to cytokines, macrophages differentiate to effector functions. Macrophages treated with a combination of IFN-γ plus IL-4 express leishmanicidal activity [20] and, following restimulation with LPS, secrete nitrites and IL-12, two markers of M1 differentiation [21]. We investigated the effect of prior *Leishmania* infection on cytokine induced macrophage differentiation. Macrophages treated with IFN-γ plus IL-4 produced increased levels of NO and IL-12p40 following restimulation with LPS (Figure 1(a)). Prior infection with *L. major* substantially reduced the ability to produce NO and IL-12p40 (Figure 1(a)). Prior infection did not reduce TNF-α response (Figure 1(a)), arguing against a defect in the response to LPS and suggesting a specific defect in IL-12 and nitrite secretion. We also investigated expression of LIGHT, a marker of M2b macrophage differentiation [7]. Prior infection with *L. major* increased expression of LIGHT in macrophages treated with IFN-γ plus IL-4 (Figure 1(b)). Therefore, prior infection with *L. major* reduces expression of M1 differentiation markers, whereas it increases expression of M2 differentiation marker. Interestingly, infection with *L. major* after treatment with IFN-γ did not modulate expression of differentiation markers (results not shown). Together, these data suggest that *L. major* modulates macrophage differentiation to ensure its intracellular survival. Interestingly, production of ROS is required for inducing M2, but not M1 macrophage differentiation [22], suggesting that the initial stress response could be involved.

5. Engulfment of Neutrophils Regulates Infection of Macrophages

Neutrophils play important roles in the innate immune response. Neutrophils are short lived cells that undergo spontaneous apoptosis following transmigration of blood vessels [23]. Neutrophil apoptosis induces phagocytic clearance and secretion of cytokines by macrophages, which are important for resolution of inflammation and tissue repair [23]. Interestingly, different outcomes of *L. major* infection and cytokine production are observed in macrophages engulfing apoptotic neutrophils, depending on host genetic background [3]. Engulfment of apoptotic BALB/c neutrophils induces production of TGF-β, but not TNF-α in macrophages, and increases growth of *L. major* in a manner dependent on PGE_2 and TGF-β [3]. Depletion of neutrophils with anti-Gr1 antibody reduces, and adoptive transfer of apoptotic neutrophils increases infection in lymph nodes of BALB/c mice, suggesting a disease promoting role of neutrophils

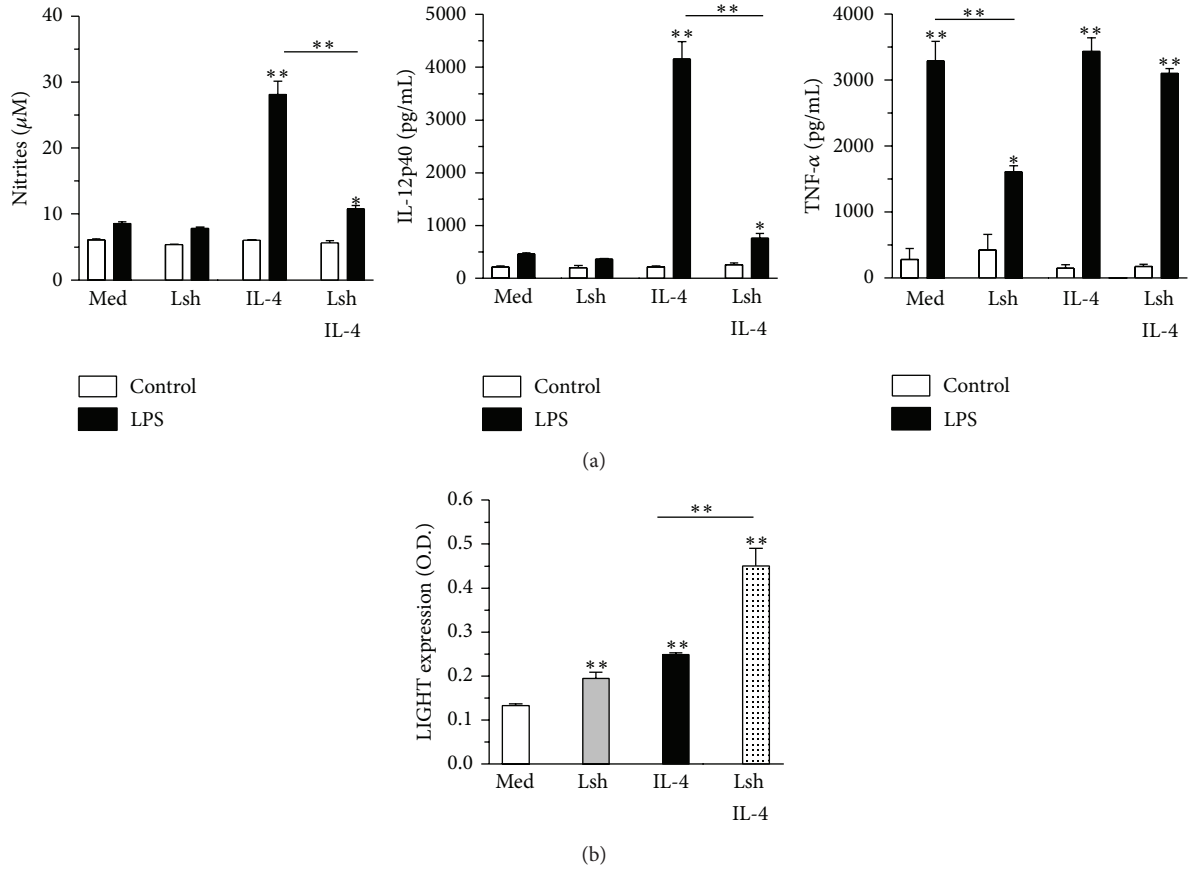

Figure 1: Infection with *L. major* reduces production of NO and IL-12 and increases expression of M2 marker LIGHT by differentiated macrophages. (a-b) Bone marrow derived macrophages (BMDM from B6 mice) were infected or not with *L. major* after 6 days. Next day, all BMDM were treated with IFN-γ, and next day, some of the BMDM cultures were treated with IL-4. (a) After 3 d, cells were washed and restimulated with medium (control) or LPS. After 2 additional days, the levels of nitrites, IL-12p40, and TNF-α were determined. (b) After 3 d, expression of LIGHT was evaluated by cellular ELISA. Results are expressed as mean and SE of triplicates (a) or quadruplicates (b), $^{*}P < 0.05$, $^{**}P < 0.01$.

[3]. On the other hand, engulfment of B6 neutrophils induces production of TNF-α, and not TGF-β, in infected macrophages and reduces *L. major* intramacrophagic load in a manner dependent on TNF-α [3]. Depletion of neutrophils with anti-Gr1 antibody increases, and adoptive transfer of apoptotic neutrophils decreases infection in lymph nodes of B6 mice, role. Neutralization of neutrophil elastase (NE) with a specific inhibitor peptide abrogates the inflammatory clearance of B6 neutrophils and increases infection in lymph nodes [3].

6. Macrophage Activation and Differentiation Induced by Neutrophil Engulfment and Neutrophil Elastase

Clearance of apoptotic cells can be proinflammatory in the presence of additional innate immune stimuli, such as TLR ligands [24, 25]. This observation helps to explain the puzzling proinflammatory effects of phagocytosis of apoptotic B6 neutrophils. NE triggers proinflammatory responses through TLR4 [26, 27]. Purified NE triggers TNF-α production by macrophages and induces leishmanicidal activity in a manner dependent on TLR4 [5]. Interestingly, B6 neutrophils release 2-3-fold more NE than BALB/c neutrophils. In addition, mutant *pallid* B6 neutrophils, which fail to release NE, do not induce killing of *L. major* [5]. These results suggest that the proinflammatory and leishmanicidal activities of B6 neutrophils are due to efficient amounts of released NE and perhaps other released granule proteins.

One important question is whether neutrophil engulfment imprints a particular phenotype in macrophages. Our results indicate that proinflammatory, but not antiinflammatory clearance of neutrophils induces a sustained regulatory or M2b phenotype in macrophages, characterized by low IL-12p70 and high IL-10 production following restimulation with LPS, increased expression of LIGHT, induction of Th2 responses, and permissive replication of *L. major* [21]. As expected, the ability of senescent neutrophils to induce the regulatory phenotype requires NE activity and TLR4 expression [21]. Moreover, previous injection of senescent neutrophils enhances subsequent infection *in vivo* [21]. These

results suggest that induction of regulatory macrophages plays a permissive role in establishment of infection.

7. Monocytes and DCs as Phagocytes and Effector Cells

Monocytes are crucial to immunity against *L. major* infection as precursors of macrophages and inflammatory DCs. On the other hand, the role of monocytes as key effectors of parasite killing remains elusive, since current monocyte depletion models fail to spare the other cell types. Accordingly, CCR2 is required for mobilization of monocytes from bone marrow [28] and for effective control of *L. major* infection [29–31]. Whether CCR2-dependent immunity to *L. major* relies on direct effector role of monocytes, in the generation of effector macrophages/DCs, or both is still debatable [29–32]. Conversely, attempts to deplete only neutrophils by using antibody against Gr1, which encompasses both Ly6C (monocyte) and Ly6G (neutrophil) epitopes, more likely result in monocyte depletion as well.

Infection with *L. major* increases both myelopoiesis and the number of circulating myeloid precursors [33]. In addition, purified blood monocytes are already able to phagocytose *L. major* parasites [34]. Blood monocytes, however, may not match the activation state of elicited monocytes in the infection site [34, 35]. More important, different degrees of monocyte maturation, either in the bone marrow or in the infection site, might confer susceptibility or resistance to *L. major* infection in BALB/c versus B6 mice [13, 36, 37].

Immature myeloid cells were once considered as "safe targets" for *Leishmania* infection [33, 38]. Indeed, immature macrophages expressing myeloid markers were found as major parasite reservoirs in skin lesions of BALB/c mice infected with *L. major* even 4 weeks after infection [13, 36, 38]. Recent evidences indicate that monocytes/macrophages predominate as infected cells at early (3 days) and late (4 wks) time points in skin lesions, whereas infected DCs accumulate at 4 weeks in lesions and are always dominant in B6 or BALB/c draining lymph nodes [32, 39]. In spite of differences in phagocyte populations in different sites and routes of infection [40], detailed analyses in B6 mice show that $Ly6C^{hi}$ monocytes are the major infected cell at the ear infection site from 1 day to 1 week postinfection, remaining infected thereafter, whereas DCs/macrophages predominate as infected cells upon 2 weeks of infection [41]. Recent results also suggest that both monocytes and monocyte-derived dendritic cells (Mo-DCs) may either express effector activity against *Leishmania* parasites or contribute to infection in different models. For example, Mo-DCs became infected at the infection site and migrate to LN to induce Th1 responses [32]. By contrast, DCs that were infected through uptake of infected neutrophils fail as APCs for CD4 T cells [41].

Nonetheless, the effector functions of both monocytes and DCs were recently evidenced in the *L. major* model (Table 1). Following *L. major* infection and platelet activation, $Gr1^{+}$ monocytes from B6 mice are recruited to infection site through the CCR2 receptor [31]. Phagocytosis of *L. major* by monocytes ensues, followed by killing/disappearance of *L. major* parasites both *in vitro* and *in vivo* [31]. Although other mechanisms were not addressed, monocytes eliminated *L. major* infection in a Phox-dependent manner *in vitro* [31]. $Ly6C^{hi}$ monocytes elicited by *L. major* infection can also kill parasites *in vitro* by producing NO [42]. A possible explanation to reconcile these apparently discrepant results is that peroxynitrites derived from both NO and ROS are involved as a more effective killing mechanism [43]. Injection of purified monocytes at the time of infection also helped infected B6 mice to control skin lesions and *L. major* parasites [42]. Treatment with all-*trans*-retinoic acid (ATRA) to induce monocyte maturation into macrophages releases T cell proliferation from suppression mediated by NO-producing immature monocytes [42]. However, treatment with ATRA also reduces parasite killing *in vitro* and promotes infection *in vivo* [42]. These results indicate that monocytes from B6 mice are authentic effector cells against *L. major* infection and that failure to recruit monocytes in CCR2 deficient mice has a major contribution to susceptibility to infection [31, 42]. Resistance to *L. major* infection has also been attributed to monocyte derived INOS-producing inflammatory DCs [30, 39]. However, activated monocytes share many markers with inflammatory DCs, including CD11c [44], and current markers fail to achieve a clear distinction between these phenotypes in the infection site [32]. Although CD11c has been considered as a key marker for DCs, a recent investigation on depletion of cells in a CD11c-DTR model indicates that monocytes are also depleted and that conclusions drawn from these models should be interpreted with caution [44]. In any case, DCs predominate in lymph nodes where they help immunity both as NO-producing effector cells [30, 39] and APCs to induce Th1 responses in *L. major* infection [32].

8. Protective Effects of IL-4 in *L. major* Infection

New evidence has challenged the role of IL-4 as the canonical Th2 cytokine that favors *L. major* infection. Early injection of IL-4 in susceptible mice promotes Th1 responses and resistance to *L. major* infection, through stimulation of DCs to produce IL-12 [45]. Similarly, in concert with TLR ligands, IL-4 and IL-4Rα induce priming of Th1 responses by DCs [46]. Nonetheless, IL-4 also alternatively activates DCs in Th2 responses [46], in analogy to IL-4-alternatively activated macrophages [9]. Therefore, the role of IL-4 is target cell and context dependent. Interestingly, BALB/c mice deficient for IL-4Rα expression on $CD11c^{+}$ cells are highly susceptible to *L. major* infection [39]. These studies suggest that IL-4/IL-4Rα signaling accounts for resistance in the acute phase of infection, by promoting DC-induced Th1 responses and classical macrophage activation [39]. As discussed here, however, IL-4Rα deficiency in $CD11c^{+}$ activated monocytes could also account for susceptibility to *L. major* infection. By contrast, defective IL-4Rα expression in macrophages results in increased resistance to *L. major* by blocking alternative activation of macrophages [9].

Table 1: The role of phagocytes and IL-4 in immunity to *L. major* infection.

Phagocytes	Role in immunity	Experimental model	Outcome to infection	Ref.
Monocytes	APCs	Injected in B6 mice 4 wks upon infection	Generation of Mo-DCs/APCs (Th1 responses)	[32]
Monocytes	NO-producing effector cells	Injected in B6 mice upon infection	Resistance to acute infection	[42]
Monocytes	ROS-producing effector cells	B6-CCR2.KO	Susceptibility	[31]
DCs	APCs	B6-CCR2.KO	Susceptibility/Th2 response	[29]
DCs	APCs/NO-producing effector cells	B6-CCR2.KO	Defective recruitment of DCs to LN	[30]
DCs	APCs/NO-producing effector cells	$CD11c^{cre}IL\text{-}4R\alpha^{flox/-}$	Susceptibility/Th2 response	[39]
Macrophages	NO-producing effector cells	$LysM^{cre}IL\text{-}4R\alpha^{flox/-}$	Resistance to acute infection	[9]

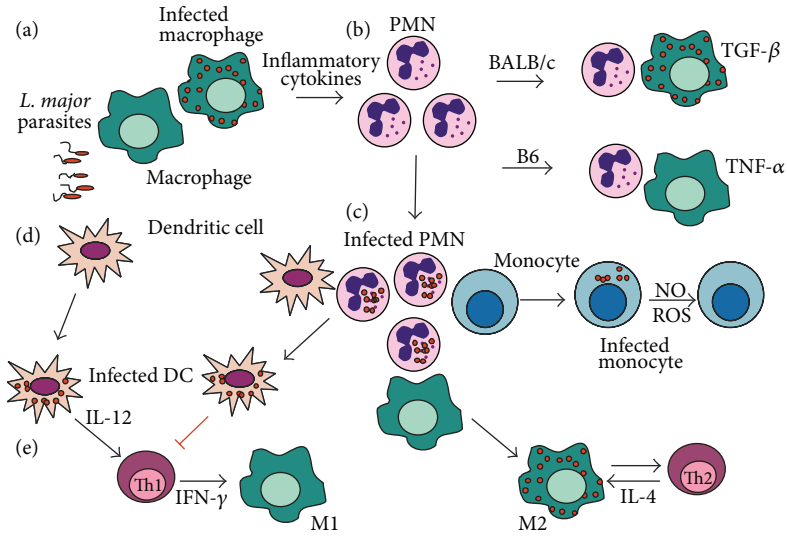

Figure 2: (a) Interactions among phagocytes in *L. major* infection. Upon *L. major* infection, tissue resident macrophages produce inflammatory cytokines and chemokines [4, 18] that recruit neutrophils and monocytes, which act as effector cells [31, 42] or give rise to inflammatory macrophages and DCs [30, 32]. (b) Neutrophils may either help or prevent parasite clearance by macrophages from B6 and BALB/c mice, respectively [3, 5]. (c) In addition, infected neutrophils help to propagate infection to macrophages, monocytes, and DCs [14, 41]. Moreover, macrophages primed by apoptotic neutrophils became permissive to subsequent infection and induce Th2 responses [21]. (d) DCs infected through efferocytosis of neutrophils fail to activate T lymphocytes [41]. Otherwise, infected DCs go to lymph nodes and induce Th1 responses [29, 32]. (e) Th1 cytokines activate M1 macrophages to kill parasites, whereas Th2 responses induce parasite-permissive M2 macrophages [6, 7].

Recent studies demonstrate that exacerbated Th2 responses help resistance to *L. major* in Th1-biased B6 model and that late treatment with anti-IL-4 (2–4 wks) increases susceptibility to infection [47]. Interestingly, NO-producing $Gr1^+$ monocytes accumulate in the spleens of *L. major*-infected mice in this mixed Th1/Th2 model (unpublished results). Moreover, similar to findings with macrophages [9, 20, 48], monocytes elicited by *L. major* can be stimulated with a combination of IL-4 and IFN-γ to kill parasites in a NO-dependent manner [42]. IL-4 and IL-13, which share the same IL-4Rα, induce myelomonopoiesis and therefore play a role both in the generation [49, 50] and the activation [51] of monocytes under certain conditions.

9. Concluding Remarks

Different phagocyte populations can be infected by *L. major* and express distinct responses that affect immunoregulation (Figure 2). Taken together, the studies discussed here also open new questions to the controversial role of IL-4/IL-4Rα in *L. major* model [52]. Furthermore, monocytes and DCs

can be relocated to the core of this issue, with direct implications for the development of new vaccines to Leishmaniasis [53].

Conflict of Interests

The authors declare that there is no conflict of interests regarding the publication of this paper.

Acknowledgments

The authors' cited work was financed by the Brazilian National Research Council (CNPq), the Rio de Janeiro State Science Foundation (FAPERJ), and the National Institutes of Science and Technology Initiative (INCT).

References

[1] C. Matte and M. Olivier, "*Leishmania*-induced cellular recruitment during the early inflammatory response: modulation of proinflammatory mediators," *Journal of Infectious Diseases*, vol. 185, no. 5, pp. 673–681, 2002.

[2] I. Rabhi, S. Rabhi, R. Ben-Othman et al., "Transcriptomic signature of *Leishmania* infected mice macrophages: a metabolic point of view," *PLoS Neglected Tropical Diseases*, vol. 6, no. 8, Article ID e1763, 2012.

[3] F. L. Ribeiro-Gomes, A. C. Otero, N. A. Gomes et al., "Macrophage interactions with neutrophils regulate *Leishmania major* infection," *Journal of Immunology*, vol. 172, no. 7, pp. 4454–4462, 2004.

[4] F. L. Ribeiro-Gomes, M. C. A. Moniz-De-Souza, V. M. Borges et al., "Turnover of neutrophils mediated by Fas ligand drives *Leishmania major* infection," *Journal of Infectious Diseases*, vol. 192, no. 6, pp. 1127–1134, 2005.

[5] F. L. Ribeiro-Gomes, M. C. A. Moniz-de-Souza, M. S. Alexandre-Moreira et al., "Neutrophils activate macrophages for intracellular killing of *Leishmania major* through recruitment of TLR4 by neutrophil elastase," *Journal of Immunology*, vol. 179, no. 6, pp. 3988–3994, 2007.

[6] F. O. Martinez, L. Helming, and S. Gordon, "Alternative activation of macrophages: an immunologic functional perspective," *Annual Review of Immunology*, vol. 27, pp. 451–483, 2009.

[7] D. M. Mosser and J. P. Edwards, "Exploring the full spectrum of macrophage activation," *Nature Reviews Immunology*, vol. 8, no. 12, pp. 958–969, 2008.

[8] J. I. Odegaard, R. R. Ricardo-Gonzalez, M. H. Goforth et al., "Macrophage-specific PPARγ controls alternative activation and improves insulin resistance," *Nature*, vol. 447, no. 7148, pp. 1116–1120, 2007.

[9] C. Hölscher, B. Arendse, A. Schwegmann, E. Myburgh, and F. Brombacher, "Impairment of alternative macrophage activation delays cutaneous leishmaniasis in nonhealing BALB/c mice," *The Journal of Immunology*, vol. 176, no. 2, pp. 1115–1121, 2006.

[10] M. M. Kane and D. M. Mosser, "The role of IL-10 in promoting disease progression in Leishmaniasis," *Journal of Immunology*, vol. 166, no. 2, pp. 1141–1147, 2001.

[11] S. A. Miles, S. M. Conrad, R. G. Alves, S. M. B. Jeronimo, and D. M. Mosser, "A role for IgG immune complexes during infection with the intracellular pathogen *Leishmania*," *Journal of Experimental Medicine*, vol. 201, no. 5, pp. 747–754, 2005.

[12] A. A. Filardy, D. R. Pires, and G. A. Dosreis, "Macrophages and neutrophils cooperate in immune responses to *Leishmania* infection," *Cellular and Molecular Life Sciences*, vol. 68, no. 11, pp. 1863–1870, 2011.

[13] W. J. Beil, G. Meinardus-Hager, D.-C. Neugebauer, and C. Sorg, "Differences in the onset of the inflammatory response to cutaneous leishmaniasis in resistant and susceptible mice," *Journal of Leukocyte Biology*, vol. 52, no. 2, pp. 135–142, 1992.

[14] N. C. Peters, J. G. Egen, N. Secundino et al., "*In vivo* imaging reveals an essential role for neutrophils in leishmaniasis transmitted by sand flies," *Science*, vol. 321, no. 5891, pp. 970–974, 2008.

[15] R. V. Morris, C. B. Shoemaker, J. R. David, G. C. Lanzaro, and R. G. Titus, "Sandfly maxadilan exacerbates infection with *Leishmania major* and vaccinating against it protects against *L. major* infection," *Journal of Immunology*, vol. 167, no. 9, pp. 5226–5230, 2001.

[16] W. H. Wheat, K. E. Pauken, R. V. Morris, and R. G. Titus, "*Lutzomyia longipalpis* salivary peptide maxadilan alters murine dendritic cell expression of CD80/86, CCR7, and cytokine secretion and reprograms dendritic cell-mediated cytokine release from cultures containing allogeneic T cells," *Journal of Immunology*, vol. 180, no. 12, pp. 8286–8298, 2008.

[17] A. M. Hohlbaum, M. S. Gregory, S. T. Ju, and A. Marshak-Rothstein, "Fas ligand engagement of resident peritoneal macrophages in vivo induces apoptosis and the production of neutrophil chemotactic factors," *Journal of Immunology*, vol. 167, no. 11, pp. 6217–6224, 2001.

[18] A. A. Filardy, A. C. Costa-da-Silva, C. M. Koeller et al., "Infection with *Leishmania major* induces a cellular stress response in macrophages," *PLoS ONE*, vol. 9, no. 1, Article ID e85715, 2014.

[19] N. Kayagaki, N. Yamaguchi, F. Nagao et al., "Polymorphism of murine Fas ligand that affects the biological activity," *Proceedings of the National Academy of Sciences of the United States of America*, vol. 94, no. 8, pp. 3914–3919, 1997.

[20] C. Bogdan, S. Stenger, M. Rollinghoff, and W. Solbach, "Cytokine interactions in experimental cutaneous leishmaniasis. Interleukin 4 synergizes with interferon-γ to activate murine macrophages for killing of *Leishmania majoramastigotes*," *European Journal of Immunology*, vol. 21, no. 2, pp. 327–333, 1991.

[21] A. A. Filardy, D. R. Pires, M. P. Nunes et al., "Proinflammatory clearance of apoptotic neutrophils induces an IL-12^{low}IL-10^{high} regulatory phenotype in macrophages," *Journal of Immunology*, vol. 185, no. 4, pp. 2044–2050, 2010.

[22] Y. Zhang, S. Choksi, K. Chen, Y. Pobezinskaya, I. Linnoila, and Z. G. Liu, "ROS play a critical role in the differentiation of alternatively activated macrophages and the occurrence of tumor-associated macrophages," *Cell Research*, vol. 23, no. 7, pp. 898–914, 2013.

[23] J. Savill, I. Dransfield, C. Gregory, and C. Haslett, "A blast from the past: clearance of apoptotic cells regulates immune responses," *Nature Reviews Immunology*, vol. 2, no. 12, pp. 965–975, 2002.

[24] L. Zheng, M. He, M. Long, R. Blomgran, and O. Stendahl, "Pathogen-induced apoptotic neutrophils express heat shock proteins and elicit activation of human macrophages," *The Journal of Immunology*, vol. 173, no. 10, pp. 6319–6326, 2004.

[25] M. B. Torchinsky, J. Garaude, A. P. Martin, and J. M. Blander, "Innate immune recognition of infected apoptotic cells directs T H17 cell differentiation," *Nature*, vol. 458, no. 7234, pp. 78–82, 2009.

[26] J. M. Devaney, C. M. Greene, C. C. Taggart, T. P. Carroll, S. J. O'Neill, and N. G. McElvaney, "Neutrophil elastase up-regulates interleukin-8 via toll-like receptor 4," *FEBS Letters*, vol. 544, no. 1–3, pp. 129–132, 2003.

[27] R. Benabid, J. Wartelle, L. Malleret et al., "Neutrophil elastase modulates cytokine expression: contribution to host defense against *pseudomonas aeruginosa* induced pneumonia," *The Journal of Biological Chemistry*, vol. 287, no. 42, pp. 34883–34894, 2012.

[28] N. V. Serbina and E. G. Pamer, "Monocyte emigration from bone marrow during bacterial infection requires signals mediated by chemokine receptor CCR2," *Nature Immunology*, vol. 7, no. 3, pp. 311–317, 2006.

[29] N. Sato, S. K. Ahuja, M. Quinones et al., "CC chemokine receptor (CCR)2 is required for langerhans cell migration and localization of T helper cell type 1 (Th1)-inducing dendritic cells: absence of CCR2 shifts the *Leishmania major*—resistant phenotype to a susceptible state dominated by Th2 cytokines, B cell outgrowth, and sustained neutrophilic inflammation," *Journal of Experimental Medicine*, vol. 192, no. 2, pp. 205–218, 2000.

[30] C. de Trez, S. Magez, S. Akira, B. Ryffel, Y. Carlier, and E. Muraille, "iNOS-producing inflammatory dendritic cells constitute the major infected cell type during the chronic *Leishmania major* infection phase of C57BL/6 resistant mice," *PLoS Pathogens*, vol. 5, no. 6, Article ID e1000494, 2009.

[31] R. Goncalves, X. Zhang, H. Cohen, A. Debrabant, and D. M. Mosser, "Platelet activation attracts a subpopulation of effector monocytes to sites of *Leishmania major* infection," *Journal of Experimental Medicine*, vol. 208, no. 6, pp. 1253–1265, 2011.

[32] B. León, M. López-Bravo, and C. Ardavín, "Monocyte -derived dendritic cells formed at the infection site control the induction of protective T helper 1 responses against *Leishmania*," *Immunity*, vol. 26, no. 4, pp. 519–531, 2007.

[33] A. M. Mirkovich, A. Galelli, A. C. Allison, and F. Z. Modabber, "Increased myelopoiesis during *Leishmania major* infection in mice: generation of "safe targets", a possible way to evade the immune mechanism," *Clinical & Experimental Immunology*, vol. 64, no. 1, pp. 1–7, 1986.

[34] C. Sunderkötter, T. Nikolic, M. J. Dillon et al., "Subpopulations of Mouse Blood Monocytes Differ in Maturation Stage and Inflammatory Response," *Journal of Immunology*, vol. 172, no. 7, pp. 4410–4417, 2004.

[35] F. Geissmann, S. Jung, and D. R. Littman, "Blood monocytes consist of two principal subsets with distinct migratory properties," *Immunity*, vol. 19, no. 1, pp. 71–82, 2003.

[36] C. Sunderkotter, M. Kunz, K. Steinbrink et al., "Resistance of mice to experimental leishmaniasis is associated with more rapid appearance of mature macrophages in vitro and in vivo," *The Journal of Immunology*, vol. 151, no. 9, pp. 4891–4901, 1993.

[37] K. Steinbrink, F. Schönlau, U. Rescher et al., "Ineffective elimination of *Leishmania major* by inflammatory (MRP14-positive) subtype of monocytic cells," *Immunobiology*, vol. 202, no. 5, pp. 442–459, 2000.

[38] Y. Goto, C. Sanjoba, N. Arakaki et al., "Accumulation of macrophages expressing MRP8 and MRP14 in skin lesions during *Leishmania major* infection in BALB/c and RAG-2 knockout mice," *Parasitology International*, vol. 56, no. 3, pp. 231–234, 2007.

[39] R. Hurdayal, N. E. Nieuwenhuizen, M. Revaz-Breton et al., "Deletion of IL-4 receptor alpha on dendritic cells renders BALB/c mice hypersusceptible to *Leishmania major* infection," *PLOS Pathogens*, vol. 9, no. 10, Article ID e1003699, 2013.

[40] F. L. Ribeiro-Gomes, E. H. Roma, M. B. Carneiro, N. A. Doria, D. L. Sacks, and N. C. Peters, "Site dependent recruitment of inflammatory cells determines the effective dose of *Leishmania major*," *Infection and Immunity*, vol. 82, no. 7, pp. 2713–2727, 2014.

[41] F. L. Ribeiro-Gomes, N. C. Peters, A. Debrabant, and D. L. Sacks, "Efficient capture of infected neutrophils by dendritic cells in the skin inhibits the early anti-leishmania response," *PLoS Pathogens*, vol. 8, no. 2, Article ID e1002536, 2012.

[42] W. F. Pereira, F. L. Ribeiro-Gomes, L. V. C. Guillermo et al., "Myeloid-derived suppressor cells help protective immunity to *Leishmania major* infection despite suppressed T cell responses," *Journal of Leukocyte Biology*, vol. 90, no. 6, pp. 1191–1197, 2011.

[43] E. Linares, S. Giorgio, R. A. Mortara, C. X. C. Santos, A. T. Yamada, and O. Augusto, "Role of peroxynitrite in macrophage microbicidal mechanisms in vivo revealed by protein nitration and hydroxylation," *Free Radical Biology and Medicine*, vol. 30, no. 11, pp. 1234–1242, 2001.

[44] M. M. Meredith, K. Liu, G. Darrasse-Jeze et al., "Expression of the zinc finger transcription factor zDC (Zbtb46, Btbd4) defines the classical dendritic cell lineage," *Journal of Experimental Medicine*, vol. 209, no. 6, pp. 1153–1165, 2012.

[45] T. Biedermann, S. Zimmermann, H. Himmelrich et al., "IL-4 instructs THI responses and resistance to *Leishmania major* in susceptible BALB/c mice," *Nature Immunology*, vol. 2, no. 11, pp. 1054–1060, 2001.

[46] P. C. Cook, L. H. Jones, S. J. Jenkins, T. A. Wynn, J. E. Allen, and A. S. MacDonald, "Alternatively activated dendritic cells regulate CD4+ T-cell polarization in vitro and in vivo," *Proceedings of the National Academy of Sciences of the United States of America*, vol. 109, no. 25, pp. 9977–9982, 2012.

[47] W. F. Pereira-Manfro, F. L. Ribeiro-Gomes, A. A. Filardy et al., "Inhibition of caspase-8 activity promotes protective Th1- and Th2-mediated immunity to *Leishmania major* infection," *Journal of Leukococyte Biology*, vol. 95, no. 2, pp. 347–355, 2014.

[48] S. Stenger, W. Solbach, M. Rollinhoff, and C. Bogdan, "Cytokine interactions in experimental cutaneous leishmaniasis. II. Endogenous tumor necrosis factor-α production by macrophages is induced by the synergistic action of interferon (IFN)-γ and interleukin (IL) 4 and accounts for the antiparasitic effect mediated by IFN-γ and IL 4," *European Journal of Immunology*, vol. 21, no. 7, pp. 1669–1675, 1991.

[49] Y. H. Lai, J. Heslan, S. Poppema, J. F. Elliott, and T. R. Mosmann, "Continuous administration of IL-13 to mice induces extramedullary hemopoiesis and monocytosis," *Journal of Immunology*, vol. 156, no. 9, pp. 3166–3173, 1996.

[50] S. E. W. Jacobsen, C. Okkenhaug, O. P. Veiby, D. Caput, P. Ferrara, and A. Minty, "Interleukin 13: novel role in direct regulation of proliferation and differentiation of primitive hematopoietic progenitor cells," *Journal of Experimental Medicine*, vol. 180, no. 1, pp. 75–82, 1994.

[51] G. Gallina, L. Dolcetti, P. Serafini et al., "Tumors induce a subset of inflammatory monocytes with immunosuppressive activity on $CD8^+$ T cells," *Journal of Clinical Investigation*, vol. 116, no. 10, pp. 2777–2790, 2006.

[52] R. Hurdayal and F. Brombacher, "The role of IL-4 and IL-13 in cutaneous Leishmaniasis," *Immunology Letters*, vol. 161, no. 1, 2014.

[53] A. Masic, R. Hurdayal, N. E. Nieuwenhuizen, F. Brombacher, and H. Moll, "Dendritic cell-mediated vaccination relies on interleukin-4 receptor signaling to avoid tissue damage after Leishmania major infection of BALB/c mice," *PLoS Neglected Tropical Diseases*, vol. 6, no. 7, Article ID e1721, 2012.

Hindawi Publishing Corporation
Mediators of Inflammation
Volume 2014, Article ID 636039, 10 pages
http://dx.doi.org/10.1155/2014/636039

Research Article

Involvement of Different CD4$^+$ T Cell Subsets Producing Granzyme B in the Immune Response to *Leishmania major* Antigens

Ikbel Naouar,[1,2] Thouraya Boussoffara,[1,2] Melika Ben Ahmed,[1,2] Nabil Belhaj Hmida,[1,2] Adel Gharbi,[1,2] Sami Gritli,[3] Afif Ben Salah,[1,2] and Hechmi Louzir[1,2]

[1] *Laboratory of Transmission, Control, and Immunobiology of Infections-LR11IPT02, Pasteur Institute of Tunis, 13 Place Pasteur, 1002 Tunis, Tunisia*
[2] *University of Tunis El Manar, 1068 Tunis, Tunisia*
[3] *Department of Pathology, Charles Nicolle Hospital, Boulevard 9 Avril 1938, 1006 Tunis, Tunisia*

Correspondence should be addressed to Hechmi Louzir; hechmi.louzir@pasteur.rns.tn

Received 4 April 2014; Revised 10 June 2014; Accepted 10 June 2014; Published 2 July 2014

Academic Editor: Mauricio Martins Rodrigues

The nature of effector cells and the potential immunogenicity of *Leishmania major* excreted/secreted proteins (*Lm*ES) were evaluated using peripheral blood mononuclear cells (PBMCs) from healed zoonotic cutaneous leishmaniasis individuals (HZCL) and healthy controls (HC). First, we found that PBMCs from HZCL individuals proliferate and produce high levels of IFN-γ and granzyme B (GrB), used as a marker of activated cytotoxic T cells, in response to the parasite antigens. IFN-γ is produced by CD4$^+$ T cells, but unexpectedly GrB is also produced by CD4$^+$ T cells in response to stimulation with *Lm*ES, which were found to be as effective as soluble *Leishmania* antigens to induce proliferation and cytokine production by PBMCs from immune individuals. To address the question of regulatory T cell (Tregs) involvement, the frequency of circulating Tregs was assessed and found to be higher in HZCL individuals compared to that of HC. Furthermore, both CD4$^+$CD25$^+$ and CD4$^+$CD25$^-$ T cells, purified from HZCL individuals, produced IFN-γ and GrB when stimulated with *Lm*ES. Additional experiments showed that CD4$^+$CD25$^+$CD127$^{dim/-}$ Tregs were involved in GrB production. Collectively, our data indicate that *Lm*ES are immunogenic in humans and emphasize the involvement of CD4$^+$ T cells including activated and regulatory T cells in the immune response against parasite antigens.

1. Introduction

Cutaneous leishmaniasis is endemic in the tropics and neotropics. It is often referred to as a group of diseases because of the varied spectrum of clinical manifestations, which range from small cutaneous nodules to gross mucosal tissue destruction. Cutaneous leishmaniasis can be caused by several *Leishmania* spp and is transmitted to humans and animals by sandflies [1].

Zoonotic cutaneous leishmaniasis (ZCL), a highly prevalent disease in North Africa, sub-Saharan West Africa, Middle East, and Central Asia, is caused by *Leishmania major* [2]. In humans, previous studies have reported that healing of cutaneous leishmaniasis is generally associated with the development of a cellular immune response against the parasite, as well as a positive leishmanin skin test (LST) reactivity [1, 3]. Moreover, healing is usually correlated with resistance to a subsequent symptomatic infection [4, 5] demonstrating that immunity against leishmaniasis is possible and can be achieved through vaccination. The prevailing view is that Th1 responses are essential for the control of parasite multiplication. Previously, we have demonstrated that parasite-specific cytotoxic immune responses are developed by individuals living in areas of *L. major* transmission and could play a crucial role in resistance to reinfection [6, 7]. Therefore, it seems that elucidation of the specific effective immunological

Table 1: Clinical and immunological features of the study population.

	HZCL Individuals ($n = 15$)	HC ($n = 13$)
Age, mean ± SD (range), years	37.6 ± 12.9 (15–52)	27.6 ± 3.6 (22–33)
ZCL scars, yes/no	11/4	0/13
Male/female	6/9	2/11
LST induration, mean ± SD (range), mm	10.5 ± 4.6 (5–17.5)	Not available
LST positive[a]	12/15	Not available
SLA-specific lymphoproliferation (IS) mean ± SD (range)	31.8 ± 22 (8.8–78.2)	2.2 ± 0.6 (0.5–2.9)

ZCL: zoonotic cutaneous leishmaniasis; LST: leishmanin skin test; IS: index of stimulation.
[a]Number of individuals with a positive LST result/total number of tested individuals.

mechanisms and the cell populations operating in the resistance against human *Leishmania* infection is fundamental for vaccine development.

In this setting, we were interested in the excreted/secreted proteins of *Leishmania major*. Indeed, it has previously been hypothesized that the secreted and surface molecules are mainly important for the establishment of infection, protecting the parasite from the early action of the host immune system and acting as invasive/evasive determinants [8]. In addition, it was reported in animal models that excreted/secreted molecules from other intracellular pathogens, such as *Mycobacterium tuberculosis* and *Toxoplasma gondii,* contain highly immunogenic and protective antigens [9–11]. Furthermore, there is evidence that *Leishmania* promastigote culture filtrate proteins eliciting a strong protective immunity against the infection in BALB/c mice [12–14]. Similarly, in dogs, *L. infantum* excreted/secreted antigens inducing a long lasting and strong immune response against canine visceral leishmaniasis [15–17].

In the present study, we aimed at better evaluating the nature of the cellular effectors involved in *Leishmania* infection by focusing on the cytotoxic immune response induced by the parasite antigens, and at validating *Lm*ES as potential target of this immune response.

2. Materials and Methods

2.1. Study Population and Samples. Peripheral blood samples were obtained from 15 individuals living in Sidi Bouzid Governorate (Central Tunisia); an endemic area of *L. major* infection. These HZCL individuals had characteristic scars of leishmaniasis on skin examination and/or a positive LST (mean induration > 5 mm) and/or a positive lymphoproliferative response to soluble *Leishmania* antigens (SLA) (Table 1). Thirteen healthy individuals living in Tunis, a nonendemic region for ZCL, were included as healthy controls (HC), (Table 1). All subjects provided written informed consent for participation in the study and sample collection and analyses. The protocol was approved by the Institutional Review Board of the Pasteur Institute of Tunis.

2.2. Leishmania major Excreted/Secreted Proteins and Soluble Leishmania Antigen Preparation. L. major parasites (MHOM/TN/94/GLC94, zymodeme MON25) were cultured on Novy-Nicolle-McNeal medium at 26°C and progressively adapted to RPMI 1640 medium (Sigma, St. Louis, MO) containing 2 mM L-glutamine (Sigma, St. Louis, MO), 100 U/mL penicillin (Sigma, St. Louis, MO), 100 mg/mL streptomycin (Sigma, St. Louis, MO), and 10% heat-inactivated fetal calf serum (FCS) (Invitrogen, Cergy-Pontoise, France). Stationary-phase promastigotes were used for preparation of SLA as previously described [18]. Preparation of *Lm*ES was performed as described by Chenik and collaborators [19]. Proteins were analyzed by SDS-PAGE and their concentrations were determined with a Bradford protein assay.

2.3. Leishmanin Skin Test. LST was performed by intradermal injection of 100 μL of leishmanin suspension containing 5×10^6 *L. major* promastigotes/mL in 0.5% phenol saline. After 72 h, the induration was measured along 2 diameters by the ballpoint pen technique. Induration with a diameter of 5 mm or more indicated a positive test.

2.4. Isolation of Human PBMCs and T Cell Subsets. PBMCs were separated from heparinized blood samples using Ficoll-Paque (GE Healthcare, Uppsala, Sweden) density gradient centrifugation. In some experiments, $CD8^+$ or $CD4^+$ T cells were depleted directly from PBMCs according to the manufacturer's recommendations (Miltenyi Biotec GmbH, Bergisch Gladbach, Germany). $CD4^+CD25^+$ T-lymphocytes were purified by a two-step immunomagnetic technique: purification of $CD4^+$ T-lymphocytes using a mAb-cocktail (Miltenyi Biotec GmbH, Bergisch Gladbach, Germany) and positive selection of $CD4^+CD25^+$ T-lymphocytes using anti-CD25 magnetic microbeads.

The isolation of $CD4^+CD25^+CD127^{dim/-}$ regulatory T cells was also performed in a two-step procedure. First, the non-$CD4^+$ and $CD127^{high}$ cells are indirectly magnetically labeled with a cocktail of biotin-conjugated antibodies. In the second step, the $CD4^+CD25^+CD127^{dim/-}$ regulatory T cells are directly labeled with CD25 MicroBeads and isolated by positive selection from the preenriched $CD4^+$ T cell fraction. The purity of each depleted fraction was assessed by flow cytometry and was above 85% for all samples.

2.5. Lymphoproliferative Tests. Total or depleted PBMCs were cultured in 96-well plates at a concentration of

1×10^6 cells/mL in a final volume of 200 μL of complete medium containing RPMI 1640 medium (Sigma, St. Louis, MO) supplemented with 2 mM L-glutamine (Sigma, St. Louis, MO), 100 U/mL penicillin (Sigma, St. Louis, MO), 100 μg/mL streptomycin (Sigma, St. Louis, MO), and 10% (v/v) heat-inactivated human AB serum (Sigma, St. Louis, MO), 1% HEPES (0.01 M), (Invitrogen, Cergy-Pontoise, France), 1% sodium pyruvate (1 mM) (Invitrogen, Cergy-Pontoise, France), 1% MEM Non-Essential Amino Acids (Invitrogen, Cergy-Pontoise, France), 1Ğ 2-Mercaptoethanol (10^{-2} M), (Invitrogen, Cergy-Pontoise, France), and 0.2% gentamicin (20 μg/mL) (Invitrogen, Cergy-Pontoise, France). PBMCs were stimulated with *Lm*ES (10 μg/mL) or SLA (10 μg/mL) for five days. The uptake of [^{3}H]-thymidine (Amersham, Saclay, France) was measured after adding 1 mCi/well for the last 6 h and evaluated for cell proliferation in a liquid scintillation counter (Rack Beta, LKB Wallace, Australia). Results were expressed as a proliferation index: mean counts of triplicates in antigen-stimulated cultures/mean counts of triplicates in unstimulated cultures.

2.6. Antigen-Presenting Cell Preparation and Co-Culture with Effector Cells. PBMCs were treated with 50 μg/mL mitomycin C (Sigma, St. Louis, MO) at 2×10^6 cells/mL in RPMI supplemented with 10% FCS for 1 h at 37°C followed by 3 washes with RPMI 1640 medium. These cells were used as antigen-presenting cells (APCs) and incubated in the presence of *Lm*ES (10 μg/mL), alone or with $CD4^+CD25^+$, $CD4^+CD25^-$, or $CD4^+CD25^+CD127^{dim/-}$ T cells at different ratio of effector cells/APCs (5/1 to 50/1). The number of APCs was kept constant and the number of effector cells was increasing according to the appropriate ratios. Supernatants were collected after 5 days of culture and stored at −80°C until use.

2.7. GrB and IFN-γ Detection in Culture Supernatants. Measurement of GrB was carried out using commercially available Human Granzyme B ELISA set (Mabtech AB, Nacka Strand, Sweden) according to the manufacturer's recommendations. OptEIA set ELISA Set (BD Biosciences, San Jose, CA) was used to detect IFN-γ. The results were interpolated from a standard curve using recombinant cytokines and expressed in pg/mL.

2.8. Flow Cytometry Analyses. PBMCs (2×10^6 cells/well) were stimulated *in vitro* for 16 h in presence of *Lm*ES (10 μg/mL), or medium alone with Golgistop (BD Biosciences, San Jose, CA) added for the last 6 h of culture. Cells were surface stained (with PerCP-CD3, PE-Cy7-CD4, anti-CD28, anti-CD25, anti-CD57, and anti-CD16 coupled to FITC), fixed, and permeabilized using BD Cytoperm/cytofix plus kit (BD Biosciences, San Jose, CA) according to the manufacturer's recommendations and stained with PE-conjugated anti-human GrB (Fitzgerald Industries Inc., BioLegend, London, UK) and APC-conjugated anti-human IFN-γ (BD Biosciences, San Jose, CA). A total of 100,000 events were acquired for all samples. Analyses were performed with a FACS Canto flow cytometer using the FACS Diva software (BD Biosciences, San Jose, CA).

2.9. ELISpot Assay Specific for GrB and IFN-γ. The dual ELISpot assay specific for GrB and IFN-γ was performed to quantify *Lm*ES-specific T cells. In brief, PBMCs or purified $CD4^+$ and $CD8^+$ T cells were cultured at room temperature for 30 min in the presence or absence of *Lm*ES at a final concentration of 10 μg/mL. For positive controls, cells were stimulated with 10 μg/mL phytohaemagglutinin (Sigma, St. Louis, MO). Cells under stimulation were then transferred in a PVDF-bottomed-well ELISpot plate coated with IFN-γ and GrB capture antibodies (Abcam, Cambridge, MA) and incubated overnight in a humidified 5% CO_2 incubator at 37°C. The plates were further washed and incubated with anti-FITC HRP and streptavidin-alkaline phosphatase conjugates for 1 h at 37°C. The plates were then developed, first using AEC buffer and then BCIP/NBT buffer. Spots were analyzed using CTL ImmunoSpot reader (CTL Analyzers, Shaker Hights, OH). Data were expressed as the mean spot-forming units (SFU) per 10^6 cells calculated after subtracting spots of the negative controls.

2.10. Statistical Analyses. Mann-Whitney test was used for comparison of lymphoproliferative response and induction of GrB and IFN-γ between the different study groups. Correlation between GrB and IFN-γ levels was estimated using Spearman's rank order correlation coefficient. Statistical analyses were performed using SPSS 10.0 statistical program (IBM, Armork, NY). Statistical significance was assigned to a value of $P < 0.05$.

3. Results

3.1. A Strong Correlation Is Observed Between IFN-γ and GrB Production in Response to Leishmania Antigens. The effect of *Leishmania* proteins on IFN-γ and GrB production by immune cells was studied in 15 HZCL individuals in whom PBMCs proliferate when stimulated with *Leishmania* antigens (*Lm*ES and SLA) and 6 HC who do not show any PBMC cell proliferation (Figure 1(a)). *Leishmania* antigens induced significantly high levels of IFN-γ and GrB in culture supernatants of PBMCs from HZCL individuals compared to those of HC ($P < 0.001$ and $P = 0.009$, resp.), (Figures 1(b) and 1(c)). Interestingly, a highly significant correlation was found between the levels of GrB and IFN-γ produced by *Leishmania* antigen-stimulated PBMCs (Spearman's rank correlation coefficient; $r = 0.816$, $P < 0.0001$), (*data not shown*).

3.2. GrB Induced by Leishmania Antigens Are Unexpectedly Produced by $CD4^+$ T Cells. In an attempt to better define the features of the cellular population activated by *Leishmania* antigens and more specifically, to determine the effector cells producing IFN-γ and GrB, cell depletion experiments were done using PBMCs obtained from four representative HZCL individuals and five donors from the HC group. We first

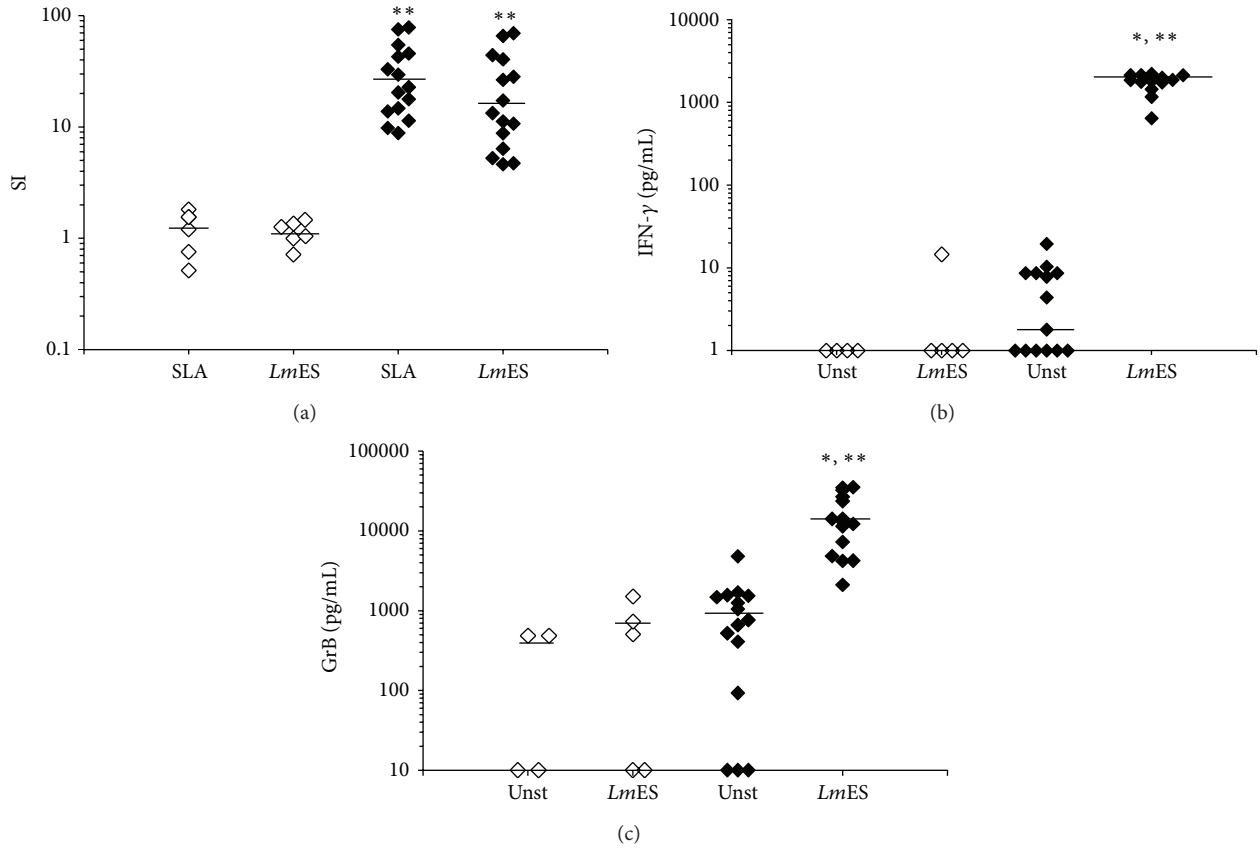

Figure 1: PBMCs response induced by *Lm*ES. PBMCs from HZCL and HC were stimulated with *Lm*ES (10 μg/mL) or SLA (10 μg/mL) during 5 days. (a) Proliferation was assessed by [^{3}H]-thymidine uptake. Results were expressed as an index of proliferation (SI) (mean counts of triplicates in antigen-stimulated cultures/mean counts of triplicates in unstimulated cultures) in all tested individuals. IFN-γ (b) and GrB (c) levels were evaluated in supernatants of cultures by ELISA tests at day 5. Results were expressed as cytokine concentrations in pg/mL. Bars represent median values. Statistical analysis: $^*P < 0.05$, when comparing the stimulated cells to the unstimulated cells (Unst) and $^{**}P < 0.05$, when comparing HZCL to HC.

demonstrated that only CD8-depleted PBMCs (-CD8) from HZCL individuals proliferate in response to *Leishmania* antigens (Figure 2(a)). Accordingly, no significant proliferation of CD4-depleted PBMCs (-CD4) was observed in response to stimulation with such antigens. In addition, only total PBMCs or (-CD8) from HZCL individuals produced high levels of IFN-γ and GrB in response to *Leishmania* antigen stimulation (Figures 2(b) and 2(c)). In contrast, for the (-CD4), GrB and IFN-γ were detected at low levels and no significant differences were observed between unstimulated and stimulated conditions ($P > 0.05$). Altogether, our results suggest that in response to *Leishmania* antigens, the main effector cells were CD4$^+$ T cells in term of cell proliferation and IFN-γ and GrB production.

3.3. IFN-γ and GrB Are Produced by Different CD4$^+$ T Cell Subset. In order to assess if GrB and IFN-γ are produced by the same populations of CD4$^+$ T cells, intracellular production of IFN-γ and GrB in stimulated PBMCs was studied. Flow cytometry analyses performed in 7 HZCL individuals confirmed that stimulation of PBMCs with *Leishmania* antigen proteins induces the production of IFN-γ and GrB by CD4$^+$ T lymphocytes in most HZCL individuals (Figure 3). In fact, a significant high percentage of CD4$^+$ T cells positive for GrB was obtained following *Lm*ES stimulation when compared to that of the unstimulated cells ($P = 0.044$). A similar result was found with regard to the percentage of CD4$^+$ T cells positive for IFN-γ in PBMCs from HZCL individuals stimulated with *Lm*ES ($P < 0.0001$). Although a high percentage of CD8$^+$ T cells and CD57$^+$ cells (NKT cells) positive for GrB was found in HZCL individuals compared to that of HC, this percentage did not augment after *Lm*ES stimulation. Similarly, a high percentage of CD4$^+$ T cells positive for GrB or IFN-γ was found in response to *Lm*ES stimulation in HZCL individuals, yet the absence of a double positive staining of CD4$^+$ T cells demonstrated by flow cytometry suggests that both molecules are produced by different CD4$^+$ T cell subsets (Figures 4(a) and 4(b)). To confirm these results and for further characterization of this response, we used the Dual color ELISpot assay. CD4$^+$ T cells were isolated from PBMCs obtained from four HZCL individuals, challenged with *LmES*, and tested separately for

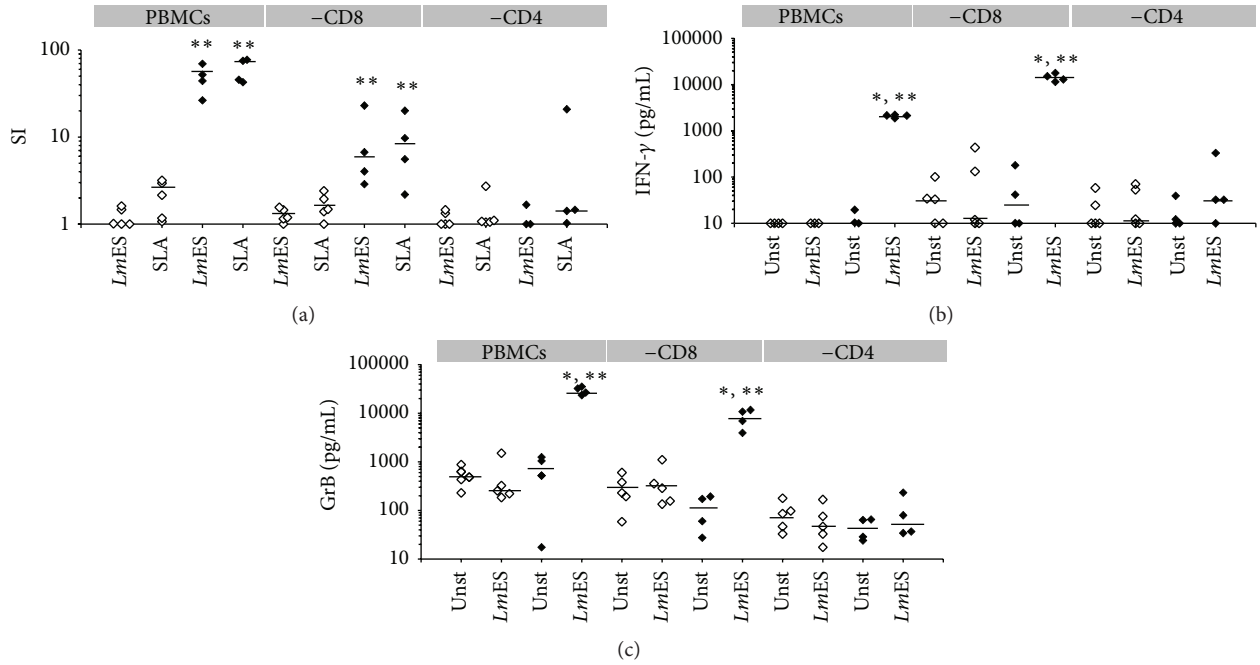

Figure 2: Immune response induced by *Lm*ES in total PBMCs or PBMCs depleted of $CD4^+$ or $CD8^+$ T cells. Whole PBMCs or those depleted of $CD4^+$ (-CD4) or $CD8^+$ T cells (-CD8) from 4 HZCL (♦) and 5 HC (◊) were stimulated with *Lm*ES (10 μg/mL) for 5 days. (a) Proliferative responses were assessed by $[^3H]$-thymidine uptake. IFN-γ (b) and GrB (c) secretion was evaluated in supernatants of cultures at day 5 using ELISA tests. Bars represent median values. Statistical analysis: $^*P < 0.05$, when comparing the stimulated cells to the unstimulated cells, (Unst) and $^{**}P < 0.05$, when comparing HZCL to HC.

IFN-γ and GrB production. Mitomycin C-treated PBMCs were used as APCs. In response to *Lm*ES stimulation, the mean number of GrB positive spots was 1219.91 (±DS = 979.81) SFU/10^6 $CD4^+$ T cells and 9.26 (±DS = 7.09) SFU/10^6 $CD4^+$ T cells for IFN-γ (Figure 4(c)). Interestingly, no double positive IFN-γ^+GrB$^+$ spots were detected.

3.4. $CD4^+CD25^+$ and $CD4^+CD25^-$ T Cells Produce IFN-γ and GrB in Response to LmES. Considering the fact that $CD4^+CD25^+$ Treg cells might have cytolytic effects on target T cells, as well as on APCs through the secretion of GrB and perforin [20], we attempted to track their involvement in the production of GrB induced by *Leishmania* antigen stimulation. Therefore, the $CD4^+CD25^+$ and $CD4^+CD25^-$ T cells from 4 HZCL individuals and 3 HC were immunomagnetically purified and cultured with autologous PBMCs treated with mitomycin C (APCs) at different ratios in presence of *Lm*ES, then GrB and IFN-γ production was evaluated. As shown in Figure 5, both $CD4^+CD25^+$ and $CD4^+CD25^-$ T subsets from immune individuals produced IFN-γ and GrB after *Lm*ES stimulation. IFN-γ and GrB levels were enhanced in parallel to the increase of effector cell/APC ratio and reached the highest levels at the ratio of 50/1. At this ratio, IFN-γ generated by both T cell populations from HZCL individuals was significantly higher than in HC subjects ($P = 0.028$ and $P = 0.024$ for $CD4^+CD25^+$ and $CD4^+CD25^-$ T cells, resp.). Likewise, significant differences were obtained for GrB levels when comparing HZCL individuals to HC ($P = 0.034$ and $P = 0.034$ for $CD4^+CD25^+$ and $CD4^+CD25^-$ T cells, resp.).

To test whether $CD4^+CD25^+$ T cells activated by *Lm*ES correspond to regulatory T cells, $CD4^+CD25^+CD127^{dim/-}$ peripheral regulatory T cells were isolated from cryopreserved cells from the same donors and used in a similar experiment. No IFN-γ was detected in supernatants of $CD4^+CD25^+CD127^{dim/-}$ peripheral regulatory T cells in all tested conditions (*data not shown*). In contrast, GrB was detected in Treg cell culture supernatants, yet with low levels comparing to the previous experiment, and a significant difference was found between unstimulated and stimulated conditions at the ratio of 50/1 ($P = 0.024$) (Figure 6).

Taken together, our data suggest that stimulation by *Leishmania* antigens activates a $CD4^+CD25^+$ regulatory T cell population that produces GrB.

4. Discussion

The rationale for *Leishmania* vaccine development is provided by the evidence that most individuals that had leishmaniasis or symptomless infection are resistant to subsequent symptomatic infections. However, no effective vaccine for human use is currently available. This is mostly due to the difficulties in defining the immunopathological and protective mechanisms in *Leishmania* infections, the nature of effector cells involved in the resistance, and the parasite antigens targeted by this immune response.

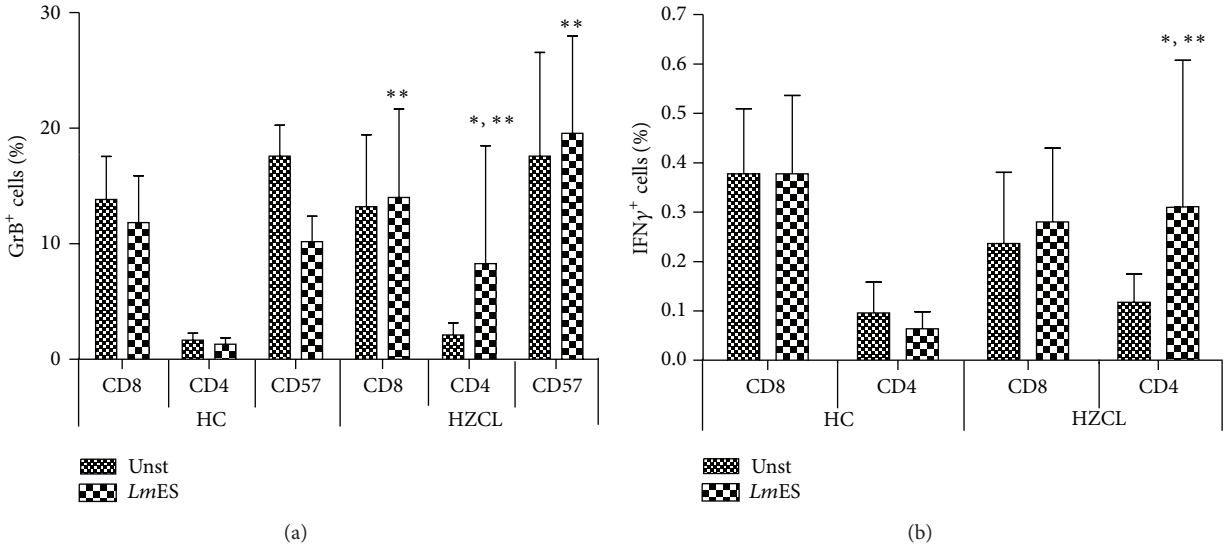

Figure 3: Phenotyping of cells producing GrB and IFN-γ. Percentage of cells positive for GrB (a) or IFN-γ (b) analyzed *ex-vivo* in PBMCs of HZCL or HC. Results are shown as percentages of positive cells inside the $CD3^+$ T cells gate. Results are expressed as the mean ± standard error of the mean of levels. Statistical analysis: $^*P < 0.05$, when comparing the stimulated cells to the unstimulated cells (Unst) and $^{**}P < 0.05$, when comparing HZCL to HC.

In the present study, we aimed at investigating the potential existence of cytotoxic immune response through GrB production against *Leishmania* antigens *ex vivo*, using cells from individuals with a confirmed previous contact with the parasite.

In addition to *Leishmania* soluble antigens, we have chosen to use *Leishmania* excreted/secreted antigens as previous reports have shown that such proteins, released by the parasite in the phagolysosomal compartment, may constitute interesting targets for the host cellular Th1 and cytotoxic immune responses and have been shown to be strongly immunogenic and protective in mice and dogs [12–17]. In humans, few reports have described the cellular immunity against *Leishmania* excreted/secreted proteins [14].

Herein, we report two important findings. The first is that *Leishmania* excreted/secreted antigens are able to induce a similar cellular immune response to that induced by SLA, in terms of intensity of proliferation and cytokine production. Indeed, as these antigens are released into the host cell phagosomes, they might be processed to generate both MHC class II and class I binding peptides and be presented to effector cells. Our results showed evidence of immunogenicity of these proteins in humans, corroborating the previously published data in different experimental models [12–17], and suggest that they are target of a cellular immune response.

Our second finding is that GrB is significantly and specifically produced in response to *Leishmania* antigens in immune individuals. However, unexpectedly, the main source of GrB seems to be $CD4^+$ T cells and not $CD8^+$ T cells as usually described. In fact, depletion experiments showed that $CD4^+$ are as expected the main source of IFN-γ, but they also produce high levels of GrB in response to *Leishmania* antigens. Interestingly, IFN-γ and GrB production in culture supernatants of stimulated cells from such individuals showed a strong positive correlation ($r = 0.8$), though the absence of double positive IFN-γ^+GrB$^+$ cells in ELISpot and flow cytometry analyses showed that GrB and IFN-γ are produced by different $CD4^+$ T cell subsets.

Flow cytometry analyses also showed high percentages of $CD8^+$ T and $CD57^+$ T cells (NKT cells) positive for GrB in HZCL individuals compared with those of HC, but it appears that this increase in percentages is independent of the antigen stimulation and no difference was observed between *Lm*ES-stimulated and -unstimulated PBMCs. Nevertheless, the percentage of $CD4^+GrB^+$ T cells is significantly increased specifically in response to our antigens and these percentages are higher in HZCL individuals compared to those of HC.

To better define these effector cells and check whether regulatory T cells are the source of GrB, additional analyses were performed on $CD4^+$ T cells. In fact, studies using mice and human cells suggest that a subset of $CD4^+CD25^+$ T cells can have cytolytic activity. $CD4^+CD25^+$ T cells isolated from human subjects have been shown to express perforin and GrB and exhibit cytotoxicity against a variety of autologous target cells including $CD4^+$ and $CD8^+$ T cells, $CD14^+$ monocytes, and dendritic cells [21]. Our results showed that purified $CD4^+CD25^+$ and $CD4^+CD25^-$ T cell subsets were both able to produce GrB and IFN-γ at high levels in HZCL individuals compared to HC. Finally, in order to discriminate between regulatory and activated T cells, $CD4^+CD25^+CD127^{dim/-}$ peripheral regulatory T cells were purified. Our data showed their capacity to produce GrB but not IFN-γ in response to *Leishmania* antigens in HZCL individuals. Yet, low levels of GrB were detected in culture supernatant of Treg cells. This could be explained by the use of lower numbers of cells after cell sorting from cryopreserved cells. Altogether, our findings may suggest that regulatory T cells are involved, among other cell populations, in GrB production in response to

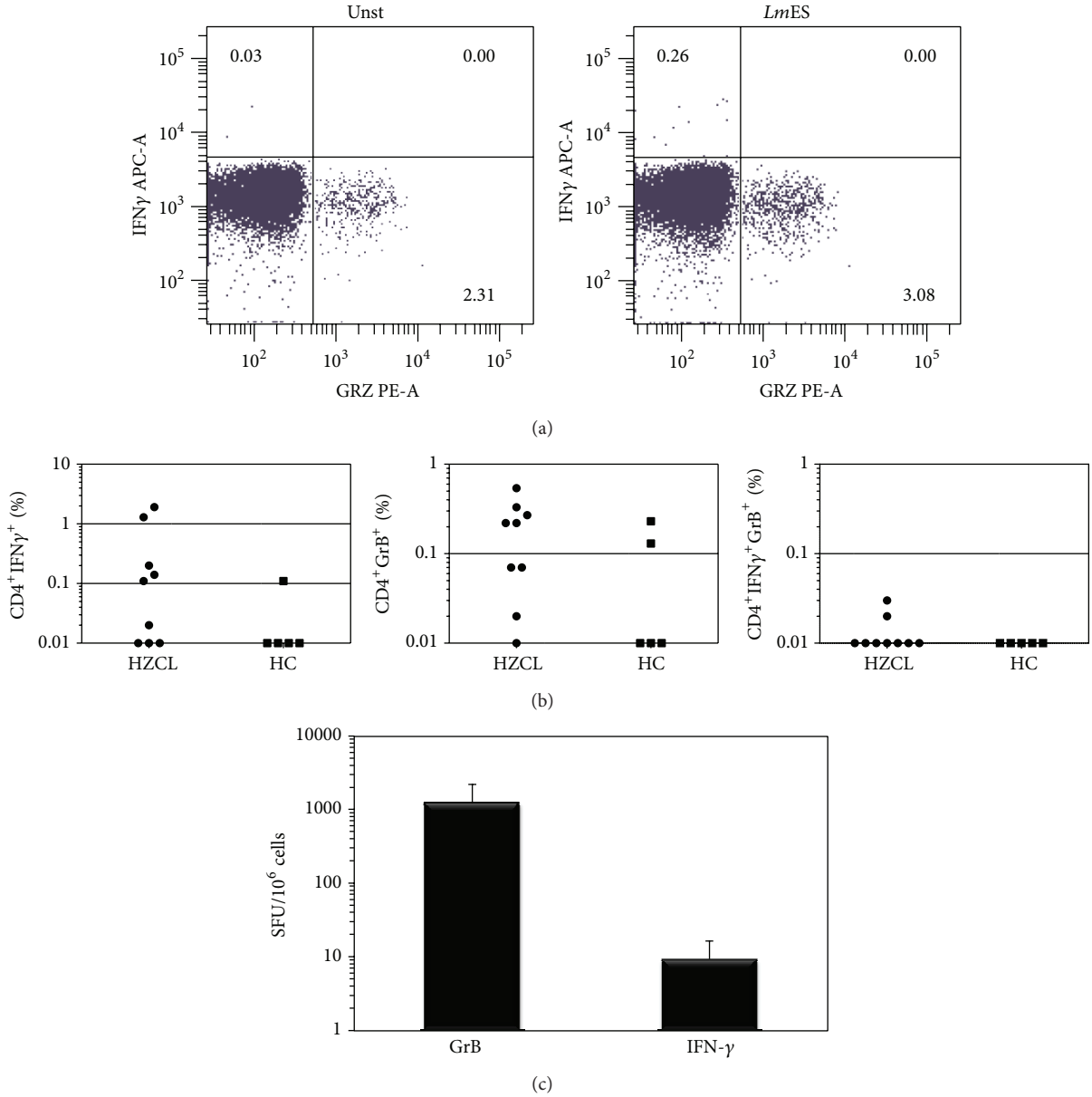

Figure 4: GrB and IFN-γ are produced by different subsets of $CD4^+$ T cells. (a) Representative example of FACS analyses of PBMCs from HZCL incubated in culture medium alone (Unst) or in presence of proteins (*Lm*ES) and analyzed for the expression of GrB and IFN-γ. Results are shown as percentages of positive cells inside the $CD4^+$ T cells gate. (b) shows percentages of $CD4^+$ T cells positive for GrB, IFN-γ and those double positive in 9 HZCL and 5 HC. Results are expressed as the mean ± standard error of the mean of levels. (c) $CD4^+$ T cells were purified from the peripheral blood of 4 HZCL incubated with *Lm*ES *in vitro* in presence of mitomycin C-treated autologous PBMCs (APCs) and analysed by a dual color ELISpot specific for GrB and IFN-γ. Results are expressed as the mean ± standard error of the mean of SFU/10^6 cells.

Leishmania antigens, suggesting a potential role of a cytotoxic pathway in Treg cell immune regulation in leishmaniasis. Further experiments are in progress to confirm such hypothesis.

Besides their cytotoxic activity, Treg cells have been reported to use several mechanisms to suppress the activation and proliferation of conventional T cells [22]. They can modulate the functions of APCs or proceed through the secretion of inhibitory cytokines, such as TGF-β, IL-10, and IL-35 [22]. These mechanisms have not been addressed in the present study. In human cutaneous leishmaniasis, there is a strong correlation between activation of different T cell subsets and disease outcome. The Th1 response is characterized by secretion of proinflammatory cytokines, while Th2 response is associated with anti-inflammatory cytokines, such as IL-10 and TGF-β, which promote macrophage inactivation and prevent excessive production of protective cytokines [1]. The role of regulatory T cells in cutaneous leishmaniasis has only recently been investigated. Several groups have shown that

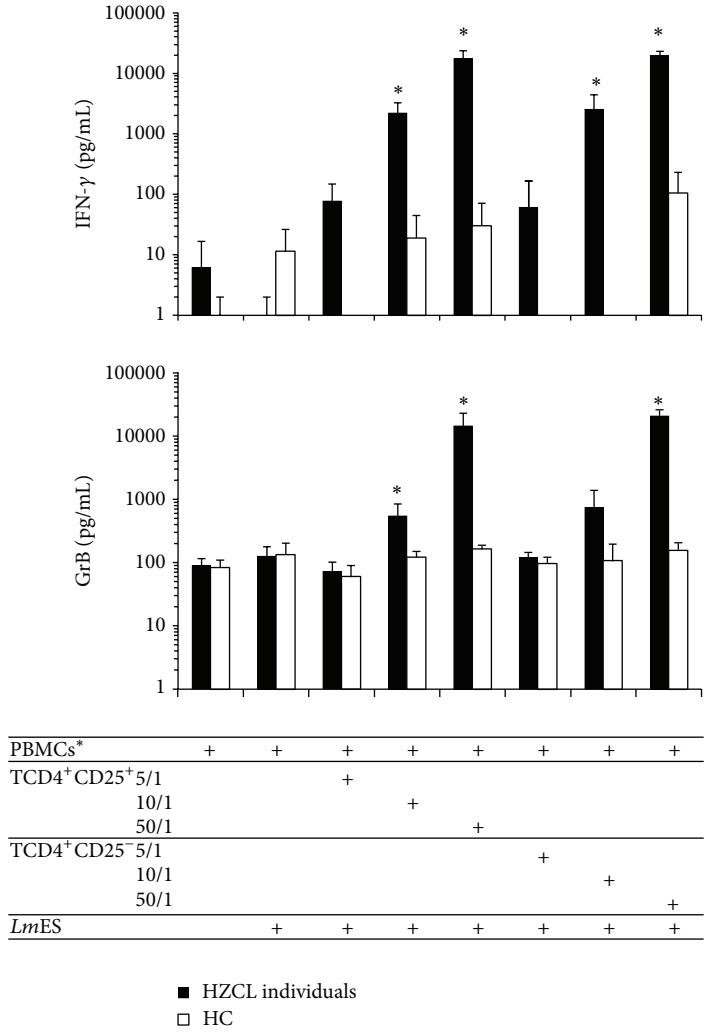

FIGURE 5: Both $CD4^+CD25^+$ and $CD4^+CD25^-$ T cell subsets produce IFN-γ and GrB in response to *Lm*ES *in vitro*. T cell subsets $CD4^+CD25^+$ and $CD4^+CD25^-$ were purified from the peripheral blood of 4 HZCL and 3 HC. The cells were stimulated with *Lm*ES *in vitro* in presence of mitomycin C-treated autologous PBMCs (APCs) at different Effector/APC ratios for 5 days. Culture supernatants were used to determine IFN-γ (a) and GrB (b) concentrations using ELISA tests. Results are expressed as the mean ± standard error of the mean of levels. Statistical analysis: $^*P < 0.05$ when comparing HZCL to HC.

during *L. major* infection, $CD4^+CD25^+$ Treg cells accumulate at the primary infection site in both humans and mice where they suppress parasite elimination by $CD4^+CD25^-$ effector cells and mediate chronicity, and their depletion leads to parasite clearance [23–25]. The balance between Th1, Th2, Treg, and other effector cells will determine the disease outcome.

In the present study, while we expected a classical cytotoxic immune response where the main effectors are $CD8^+$ T cells, our results surprisingly showed that $CD4^+$ T cell populations, including Treg cells, are rather the ones involved in the immune response against *Leishmania* antigens. These $CD4^+$ T cells are different from the IFN-γ-producing Th1 cells.

Cytotoxic $CD4^+$ T cells have been described in several studies and have been implicated in the control of a variety of persistent viral infections, such as EBV, HCV, and HIV-1 infections [26]. Analyses of cytotoxic $CD4^+$ T cells indicate that they have lytic granules containing cytotoxic factors, such as granzymes and perforin, and are characterized by a loss of CD28 surface expression [26]. The involvement of such $CD28^-$ cytotoxic T lymphocytes in *Leishmania* infection is currently under investigation in our laboratory.

5. Conclusion

Our study provides new insights and strong evidence regarding the involvement of $CD4^+$ T cells producing GrB in the immune response against *Leishmania* antigens. This cell population deserves further consideration during *Leishmania* infection to figure out whether they are actually involved in the promotion of or protection against leishmaniasis development.

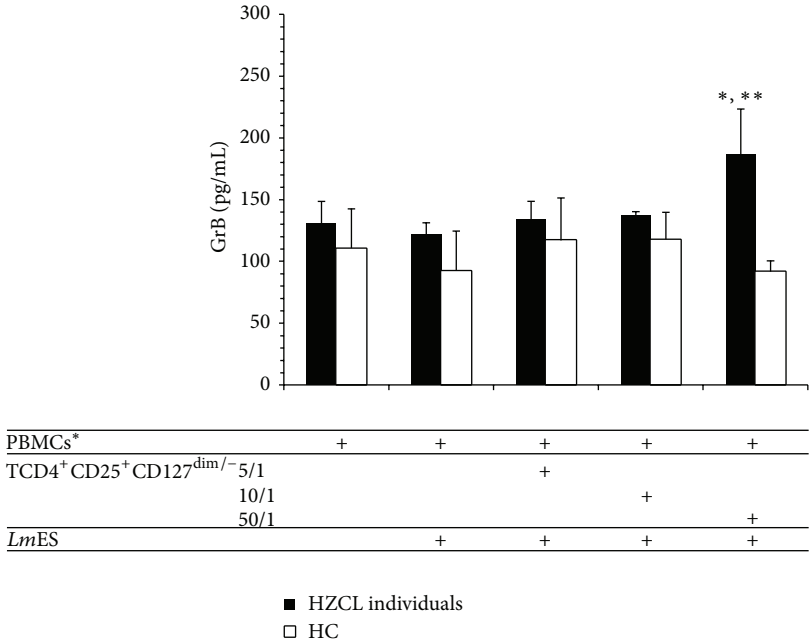

Figure 6: *Lm*ES induce GrB production by $CD4^+CD25^+CD127^{dim/-}$ regulatory T in HZCL. $CD4^+CD25^+CD127^{dim/-}$ regulatory T cells were purified from peripheral blood of 4 HZCL and 3 HC and stimulated with *Lm*ES (10 μg/mL) *in vitro* in the presence of mitomycin C-treated PBMCs (APCs) at different Effector/APC ratios for 5 days. Culture supernatants were used to determine GrB concentration. Results are expressed as the mean ± standard error of the mean of levels. Statistical analysis: $^*P < 0.05$ when comparing HZCL to HC.

Conflict of Interests

The authors declare that they have no conflict of interests regarding the publication of this paper.

Authors' Contribution

Ikbel Naouar and Thouraya Boussoffara contributed equally to this work.

Acknowledgments

The authors are indebted to the individuals who participated in the study. This work was supported by the NIH/NIAID Grant no. SP50AI074178.

References

[1] R. Reithinger, J. C. Dujardin, H. Louzir, C. Pirmez, B. Alexander, and S. Brooker, "Cutaneous leishmaniasis," *Lancet Infectious Diseases*, vol. 7, no. 9, pp. 581–596, 2007.

[2] R. W. Ashford, "The leishmaniases as emerging and reemerging zoonoses," *International Journal for Parasitology*, vol. 30, no. 12-13, pp. 1269–1281, 2000.

[3] F. Y. Liew and C. A. O'Donnell, "Immunology of leishmaniasis," *Advances in Parasitology*, vol. 32, pp. 161–259, 1993.

[4] S. Y. Guirges, "Natural and experimental re-infection of man with Oriental sore," *Annals of Tropical Medicine and Parasitology*, vol. 65, no. 2, pp. 197–205, 1971.

[5] C. R. Davies, E. A. Llanos-Cuentas, S. D. M. Pyke, and C. Dye, "Cutaneous leishmaniasis in the Peruvian Andes: an epidemiological study of infection and immunity," *Epidemiology and Infection*, vol. 114, no. 2, pp. 297–318, 1995.

[6] T. Bousoffara, H. Louzir, A. Ben Salah, and K. Dellagi, "Analysis of granzyme B activity as a surrogate marker of Leishmania-specific cell-mediated cytotoxicity in zoonotic cutaneous leishmaniasis," *Journal of Infectious Diseases*, vol. 189, no. 7, pp. 1265–1273, 2004.

[7] H. Louzir, T. Bousoffara, A. Ben Salah et al., "Leishmania specific cytotoxic cellular immune response as a new correlate for human protection against infection," in *Proceedings of the 3rd World Congress on Leishmaniosis (Worldleish '05)*, Terrasini , Italy, 2005.

[8] N. Santarém, R. Silvestre, J. Tavares et al., "Immune response regulation by *Leishmania* secreted and non-secreted antigens," *Journal of Biomedicine and Biotechnology*, vol. 2007, no. 6, pp. 85154–85164, 2007.

[9] T. A. Costa-Silva, C. S. Meira, I. M. R. Ferreira, R. M. Hiramoto, and V. L. Pereira-Chioccola, "Evaluation of immunization with tachyzoite excreted-secreted proteins in a novel susceptible mouse model (A/Sn) for Toxoplasma gondii," *Experimental Parasitology*, vol. 120, no. 3, pp. 227–234, 2008.

[10] J. E. Grotzke, A. C. Siler, D. A. Lewinsohn, and D. M. Lewinsohn, "Secreted immunodominant *Mycobacterium tuberculosis* antigens are processed by the cytosolic pathway," *Journal of Immunology*, vol. 185, no. 7, pp. 4336–4343, 2010.

[11] H. Lv, Y. Gao, Y. Wu et al., "Identification of a novel cytotoxic T lymphocyte epitope from CFP21, a secreted protein of *Mycobacterium tuberculosis*," *Immunology Letters*, vol. 133, no. 2, pp. 94–98, 2010.

[12] R. Rosa, O. R. Rodrigues, C. Marques, and G. M. Santos-Gomes, "*Leishmania infantum*: soluble proteins released by the parasite exert differential effects on host immune response," *Experimental Parasitology*, vol. 109, no. 2, pp. 106–114, 2005.

[13] R. Rosa, C. Marques, O. R. Rodrigues, and G. M. Santos-Gomes, "Immunization with *Leishmania infantum* released proteins confers partial protection against parasite infection with a predominant Th1 specific immune response," *Vaccine*, vol. 25, no. 23, pp. 4525–4532, 2007.

[14] W. K. Tonui and R. G. Titus, "*Leishmania major* soluble exo-antigens (*Lm*SEAgs) protect neonatal BALB/c mice from a subsequent challenge with *L. major* and stimulate cytokine production by Leishmania-naïve human peripheral blood mononuclear cells," *Journal of Parasitology*, vol. 92, no. 5, pp. 971–976, 2006.

[15] J. Lemesre, P. Holzmuller, M. Cavaleyra, R. B. Gonçalves, G. Hottin, and G. Papierok, "Protection against experimental visceral leishmaniasis infection in dogs immunized with purified excreted secreted antigens of *Leishmania infantum* promastigotes," *Vaccine*, vol. 23, no. 22, pp. 2825–2840, 2005.

[16] J. Lemesre, P. Holzmuller, R. B. Gonçalves et al., "Long-lasting protection against canine visceral leishmaniasis using the LiESAp-MDP vaccine in endemic areas of France: double-blind randomised efficacy field trial," *Vaccine*, vol. 25, no. 21, pp. 4223–4234, 2007.

[17] P. Holzmuller, M. Cavaleyra, J. Moreaux et al., "Lymphocytes of dogs immunised with purified excreted-secreted antigens of *Leishmania infantum* co-incubated with *Leishmania* infected macrophages produce IFN gamma resulting in nitric oxide-mediated amastigote apoptosis," *Veterinary Immunology and Immunopathology*, vol. 106, no. 3-4, pp. 247–257, 2005.

[18] A. Sassi, H. Louzir, A. B. Salah, M. Mokni, A. B. Osman, and K. Dellagi, "Leishmanin skin test lymphoproliferative responses and cytokine production after symptomatic or asymptomatic *Leishmania major* infection in Tunisia," *Clinical and Experimental Immunology*, vol. 116, no. 1, pp. 127–132, 1999.

[19] M. Chenik, S. Lakhal, N. Ben Khalef, L. Zribi, H. Louzir, and K. Dellagi, "Approaches for the identification of potential excreted/secreted proteins of *Leishmania major* parasites," *Parasitology*, vol. 132, no. 4, pp. 493–509, 2006.

[20] Y. Rochman, R. Spolski, and W. J. Leonard, "New insights into the regulation of T cells by γ_c family cytokines," *Nature Reviews Immunology*, vol. 9, no. 7, pp. 480–490, 2009.

[21] W. J. Grossman, J. W. Verbsky, W. Barchet, M. Colonna, J. P. Atkinson, and T. J. Ley, "Human T regulatory cells can use the perforin pathway to cause autologous target cell death," *Immunity*, vol. 21, no. 4, pp. 589–601, 2004.

[22] D. A. A. Vignali, L. W. Collison, and C. J. Workman, "How regulatory T cells work," *Nature Reviews Immunology*, vol. 8, no. 7, pp. 523–532, 2008.

[23] C. F. Anderson, S. Mendez, and D. L. Sacks, "Nonhealing infection despite Th1 polarization produced by a strain of *Leishmania* major in C57BL/6 mice," *Journal of Immunology*, vol. 174, no. 5, pp. 2934–2941, 2005.

[24] A. P. Campanelli, A. M. Roselino, K. A. Cavassani et al., "$CD4^+CD25^+$ T cells in skin lesions of patients with cutaneous leishmaniasis exhibit phenotypic and functional characteristics of natural regulatory T cells," *Journal of Infectious Diseases*, vol. 193, no. 9, pp. 1313–1322, 2006.

[25] E. Bourreau, C. Ronet, E. Darcissac et al., "Intralesional regulatory T-Cell suppressive function during human acute and chronic cutaneous leishmaniasis due to *Leishmania guyanensis*," *Infection and Immunity*, vol. 77, no. 4, pp. 1465–1474, 2009.

[26] D. Z. Soghoian and H. Streeck, "Cytolytic $CD4^+$ T cells in viral immunity," *Expert Review of Vaccines*, vol. 9, no. 12, pp. 1453–1463, 2010.

Hindawi Publishing Corporation
Mediators of Inflammation
Volume 2014, Article ID 912965, 9 pages
http://dx.doi.org/10.1155/2014/912965

Review Article

Chagas Disease: Still Many Unsolved Issues

José M. Álvarez,[1] Raissa Fonseca,[1] Henrique Borges da Silva,[1] Cláudio R. F. Marinho,[2] Karina R. Bortoluci,[3] Luiz R. Sardinha,[4] Sabrina Epiphanio,[5] and Maria Regina D'Império Lima[1]

[1] *Department of Immunology, Biomedical Sciences Institute, University of São Paulo, 05508-000 São Paulo, SP, Brazil*
[2] *Department of Parasitology, Biomedical Sciences Institute, University of São Paulo, 05508-000 São Paulo, SP, Brazil*
[3] *Department of Biological Sciences, UNIFESP (Campus Diadema), 09972-270 Diadema,SP, Brazil*
[4] *Hospital Israelita Albert Einstein, 05652-000 São Paulo, SP, Brazil*
[5] *Department of Clinical and Toxicological Analyses, Faculty of Pharmaceutical Sciences, University of São Paulo, 05508-000 São Paulo, SP, Brazil*

Correspondence should be addressed to José M. Álvarez; jmamosig@icb.usp.br

Received 22 April 2014; Accepted 15 June 2014; Published 29 June 2014

Academic Editor: Edecio Cunha-Neto

Over the past 20 years, the immune effector mechanisms involved in the control of *Trypanosoma cruzi*, as well as the receptors participating in parasite recognition by cells of the innate immune system, have been largely described. However, the main questions on the physiopathology of Chagas disease remain unanswered: "Why does the host immune system fail to provide sterile immunity?" and "Why do only a proportion of infected individuals develop chronic pathology?" In this review, we describe the mechanisms proposed to explain the inability of the immune system to eradicate the parasite and the elements that allow the development of chronic heart disease. Moreover, we discuss the possibility that the inability of infected cardiomyocytes to sense intracellular *T. cruzi* contributes to parasite persistence in the heart and the development of chronic pathology.

1. A Brief Overview of Chagas Disease

Chagas disease is caused by *Trypanosoma cruzi* and represents an important health problem in Latin America, with approximately 8 million chronically infected people [1]. Recently, as a consequence of human migrations, Chagas disease has become a potential public health issue in developed countries, and significant increases in confirmed cases have been reported in the USA, Canada, Europe, Japan, and Australia [2]. The invasion of the human host frequently occurs by the passage through damaged skin or intact mucosa of metacyclic trypomastigotes released with the feces of infected triatomines after their blood meal. Alternatively, infection through other routes, such as oral, congenital, and blood transfusion/organ transplantation, also occurs. Because it is an obligate intracellular parasite, *T. cruzi* can be found in the vertebrate host as amastigotes, the intracellular replicative form, and as extracellular trypomastigotes circulating freely in the blood and tissues. The infection has a self-limiting acute phase, with patent (or subpatent) parasitemia, which goes unnoticed in many infected individuals. At this stage, the parasites actively replicate in many different cell types, such as macrophages; smooth, striated, and cardiac muscle cells; adipocytes; and cells of the central nervous system [3].

While a small proportion of patients succumbs to the acute phase of the disease, the development of the adaptive immune response typically provides control of the *T. cruzi* infection, albeit nonsterile control. Failing to completely eradicate the parasite, individuals remain infected for life and establish a dynamic equilibrium with the parasite that results in different clinical outcomes. Thus, while many chronically infected individuals remain in the asymptomatic indeterminate phase, a significant proportion (30–35%) of patients develop the cardiac or digestive manifestations of chronic disease: cardiomyopathy that may lead to congestive heart failure, arrhythmia and, eventually, patient death, and esophageal or colonic megasyndromes. These are irreversible pathological changes that occur despite parasite scarcity.

Recapitulating human chagasic myocarditis, mice surviving long-term infection by certain stocks of *T. cruzi* develop chronic myocardial lesions [4, 5].

2. The Host Immune Response against *T. cruzi*

The immune system is well equipped to detect and control *T. cruzi* parasites through the combined effect of diverse branches of the immune response. $CD4^+$ and $CD8^+$ T cells, as well as B cells, contribute to control the parasite through cytokine secretion, cellular cytotoxicity, and specific antibody production [6–8]. From the end of the acute phase and throughout chronic infection, *T. cruzi*-specific IgG antibodies actively participate in the removal of extracellular parasites released from ruptured tissue nests, an effect that presumably occurs by promoting parasite phagocytosis by macrophages and neutrophils. In addition, specific IgG antibodies mediate the removal of blood trypomastigotes, a clearance process in which complement and mononuclear phagocytes from the liver, spleen, and lungs appear to be involved [9–11]. The IFN-γ produced by activated $CD4^+$ and $CD8^+$ T cells, NK cells, and $CD4^-CD8^-\gamma\delta$ T cells plays a crucial role in parasite elimination [12, 13]. IFN-γ potentiates the effector activity of macrophages by inducing the transcription of the inducible nitric oxide synthase (iNOS) gene, notably increasing the production of nitric oxide, which has a potent effect on *T. cruzi* killing [14, 15]. In addition, IFN-γ promotes the immunoglobulin switch to IgG subclasses with high opsonizing and complement-activating potential. Lastly, cytotoxic $CD8^+$ T cells also contribute to *T. cruzi* control through the recognition and destruction of cells that harbor intracellular forms of the parasite [16].

3. Limitations to the Innate and Acquired Immune Responses That Contribute to Parasite Persistence

One of the most intriguing questions of human and experimental *T. cruzi* infection is why the immune system fails to totally eradicate the parasite. At first glance, the inability of the infected host to attain sterility suggests that the immune effector activity directed against the parasite is insufficient or inappropriate due to defective activation of the specific immune response or excessive regulation of this response.

In this context, we outline in this section the different escape mechanisms employed by *T. cruzi* parasites and discuss the hypothesis generated to explain an immune system failure. At the beginning of the infection (before development of the parasite-specific response), *T. cruzi* trypomastigotes escape lysis by the complement system, an evasion strategy that results from the presence of complement-regulatory molecules on the parasite surface [17]. In addition, internalized parasites of diverse *T. cruzi* strains escape the phagocytic vacuole of unprimed resident macrophages [18], a strategy that relies on a variety of molecules with antioxidant properties [19, 20]. Nevertheless, as infection progresses, these two evasion strategies are largely circumvented by the development of the specific humoral response and the induction of macrophage activation by IFN-γ and other cytokines. Because *T. cruzi* strains display different levels of antioxidant activity that directly correlate with strain virulence [21], it remains unclear whether IFN-γ confers effective macrophage protection against any *T. cruzi* parasite or results in different degrees of intracellular parasite destruction for different isolates.

Pattern recognition receptors (PRRs), such as toll-like receptors (TLRs) 2, 4, 7, and 9, nucleotide-binding oligomerization domain-like receptor (NOD) 1 and NATCH, LRR, and PyD domains-containing protein 3 (NLRP3) have been shown to participate in *T. cruzi* detection by macrophages and dendritic cells [22–27]. However, a deficient innate immune response due to poor PRR signaling by pathogen-associated molecular patterns (PAMPs) has been proposed as a mechanism involved in parasite escape. This hypothesis is supported by data showing that, compared with mice infected by wild-type *T. cruzi* parasites, mice infected with transgenic *T. cruzi* expressing *Salmonella typhimurium* flagellin (fliC) display an increased innate response mediated by macrophages and dendritic cells and notably enhanced adaptive immunity [28]. More importantly, in the chronic phase, mice infected with fliC-transgenic *T. cruzi* display notably reduced parasite levels in relation to those infected with wild-type parasites.

Parasite persistence has also been attributed to the relatively slow development of *T. cruzi*-specific $CD8^+$ T effector cells [29], a phenomenon explained by diverse factors, including the postulated poor PAMP activity of *T. cruzi* [28] and the induction of a strong Fas expression on *T. cruzi*-specific $CD8^+$ T cells [30]. Another possible reason for the failure to acquire sterile immunity is the clonal dominance of the lymphocyte response to *T. cruzi* infection. This is illustrated by the observation that the $CD8^+$ T cell response to the abundantly expressed *T. cruzi* antigen amastigote surface protein-2 (ASP2) is restricted to a small number of clones [31]. Narrowing the scope of parasite peptides that are recognized by $CD8^+$ T cells may impair complete parasite eradication during chronic infection and the control of reinfection, which frequently occurs in endemic areas.

An alternative mechanism that restricts the efficiency of adaptive immunity in eliminating *T. cruzi* parasites is the negative regulation of effector lymphocytes because of persistent stimulation. The senescence of $CD4^+$ T cells [32] and exhaustion of $CD8^+$ T cells that infiltrate the heart or striated muscle of chronically infected hosts have been observed during chronic infection [33, 34]. In this context, it was suggested that the parasite can survive inside myocardial or striated muscle cells because following migration to the tissues $CD8^+$ T cells lose their cytotoxic and IFN-γ-producing capacities [35]. Also suggesting the negative regulation of the effector response, Albareda and cols [36] reported that $CD4^+$ T cells from patients with long-term chronic infection are primarily monofunctional, whereas in children in the early chronic stage of infection, multifunctional responses are also observed. Last, the expression of PD-1 and PD-L1 regulatory molecules has been shown to downmodulate the effector activity of $CD4^+$ and $CD8^+$ T cells in *T. cruzi*-infected mice [37]. While PD-L1-PD-1 regulatory interaction was observed in the acute phase of infection, its roles in limiting parasite

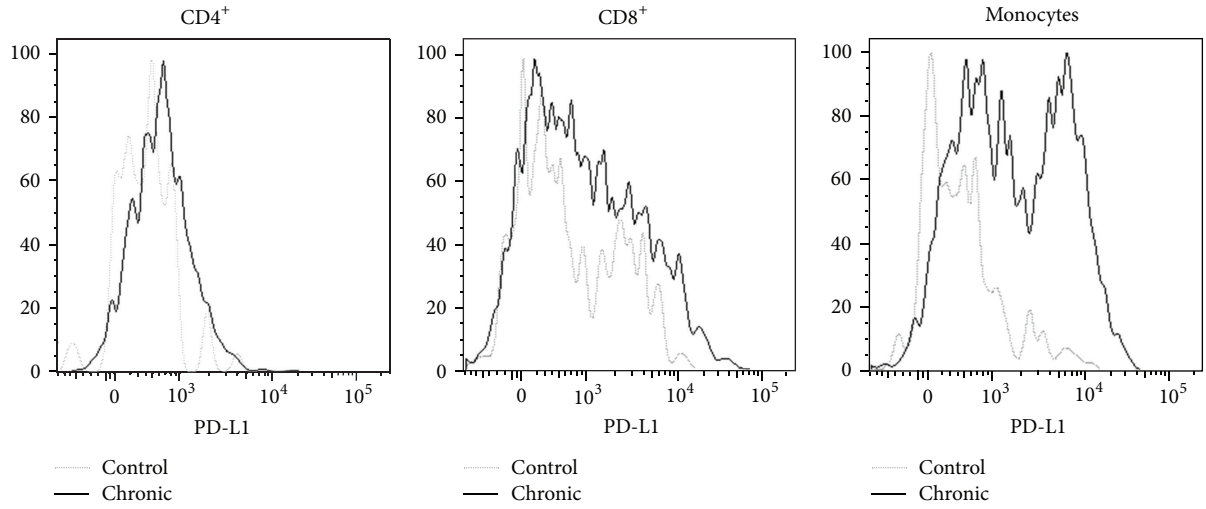

Figure 1: Expression of PD-L1 by infiltrating leukocytes in a chronically infected heart. C3H/HePAS mice were infected with 4×10^5 Sylvio X10/4 trypomastigotes obtained from LLCMK2 cultures. At day 400 postinfection, mice were sacrificed, and the heart tissue was digested with collagenase to isolate the infiltrating leukocytes. PD-L1 expression was analyzed by flow cytometry. Heart leukocytes from a pool of age-matched noninfected mice were also included.

elimination and permitting the perpetuation of lesions in the chronic phase remain to be determined. In this respect, our data showing the intense expression of PD-L1 in the heart-infiltrating leukocytes of mice chronically infected by Sylvio X10/4 *T. cruzi* parasites suggest the involvement of this regulatory circuit in parasite persistence (Figure 1).

The mechanisms of parasite escape discussed above refer to limitations of the innate or acquired protective immune response to *T. cruzi* that appear to operate in all infected individuals. However, in addition to these general elements, we must consider that individuals differ in the intensity/effectiveness of their anti-*T. cruzi* humoral and cellular responses, a consequence of polymorphisms in genes associated with the immune response [38]; these polymorphisms influence the intensity of the anti-*T. cruzi* effector activity, yielding different levels of residual parasites and undesired tissue lesions in chronically infected human patients. In addition, these polymorphisms influence the residual parasite distribution in different tissues/organs, an element closely connected to the development of the different forms of the disease.

The isogenic strains of mice also differ in the immune response to *T. cruzi*. These differences are often critical for acute phase survival [39] and most likely determine the parasite load in the chronic phase. However, not a single mouse strain has been reported to promote the complete elimination of the parasite. Therefore, regardless of the mouse/parasite strain combination, the inevitable outcome of murine infection by *T. cruzi* appears to be parasite persistence, a result analogous to that observed in human patients.

4. Only a Proportion of *T. cruzi*-Infected Individuals Show Chronic Pathologies

A significant proportion of chronically infected individuals develop the cardiac and digestive forms of the disease, but the largest fraction present the indeterminate form. Importantly, although many indeterminate patients remain asymptomatic for the rest of their lives, it is estimated that, each year, 2.5% of infected individuals evolve from the indeterminate to the clinical forms [40]. Chronic chagasic cardiomyopathy (CCC) represents the main cause of death in *T. cruzi*-infected patients. Moreover, this clinical form represents an important social burden in terms of lost labor hours and hospital costs. The situation of CCC patients is worrisome because the specific anti-*T. cruzi* drugs, currently limited to benznidazol and nifurtimox, show limited efficacy in chronically infected patients.

Because of parasite scarcity in the inflamed heart, CCC was long considered an autoimmune disease directed against self-epitopes showing cross-reactivity with parasite antigens [41]. According to this view, lesions were thought to occur as a result of T cell reactivity against myosin and other heart-derived proteins [42] as well as humoral reactivity to the beta-1-adrenergic and M2 cholinergic receptors, leading to autonomic nervous system imbalance [43]. However, in the last 20 years, cumulative evidence has promoted a change in our understanding of this process. First, immunohistochemistry data showed that, in patients with CCC, the level of *T. cruzi* antigen correlated with the intensity of the inflammatory infiltrate [44]. Furthermore, *T. cruzi* DNA was found in the heart of diseased CCC patients but not in the heart of patients with the indeterminate form [45]. In contrast, patients with megaesophagus, one of the digestive forms of the disease, displayed positive PCR for *T. cruzi* kinetoplast DNA in the esophagus [46]. Confirming the human studies, in mice chronically infected by *T. cruzi*, we previously observed that live parasites were only detected in the heart of mice with cardiomyopathy, although these mice displayed subpatent blood parasite levels similar to those in mice with no heart pathology [47]. Based on the data from these and other important reports, at present, it is largely

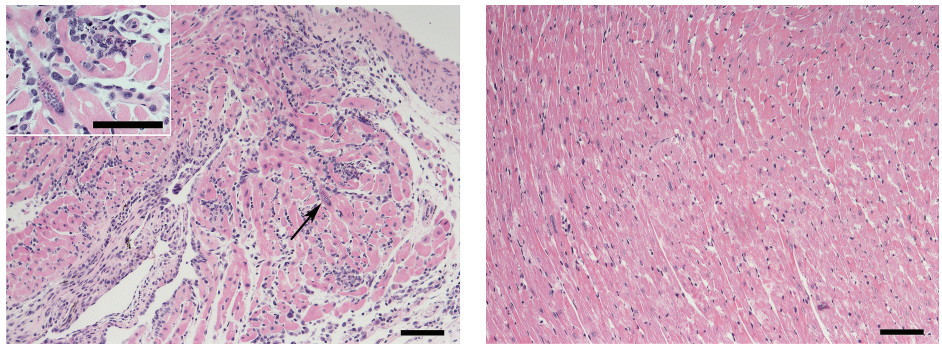

(a) (b)

Figure 2: Parasite persistence is not the necessary outcome of heart infection by *T. cruzi* parasites. C57BL/6 mice were infected with 10^3 *T. cruzi* blood trypomastigotes of the Y strain. At days 18 (a) and 180 (b) postinfection, mice were sacrificed, and the heart tissue was formalin-fixed, included in paraffin, and stained with hematoxylin/eosin. Arrow in the figure shows an amastigote nest, which is magnified at the insert. Bars in figures correspond to 200 μm and to 100 μm at the insert.

agreed that the inflammatory infiltrate in CCC is caused by a response directed toward locally persisting parasites [48]. Still, because Chagas disease is a highly heterogeneous process influenced by host genetics, we cannot discard that the immune response in the heart of CCC patients could include, besides leukocyte reactivity towards locally persisting parasites, different degrees of autoreactivity. Furthermore, it is possible that a proportion of CCC patients shows cardiac pathology in the absence of locally persisting infection. This last possibility is illustrated by a recent report using bioluminescence imaging, in which mice chronically infected with luciferase expressing *T. cruzi* parasites display mild heart inflammation in the absence of local parasitism [49]. Further studies on the contribution of autoimmunity are required for a full comprehension of CCC physiopathology. These studies may eventually reveal alternative therapeutic approaches to attenuate heart tissue inflammation in chagasic patients.

Nonetheless, because most data suggest the association of chronic cardiac pathology with local parasite persistence, CCC is presently understood as an expression of the host's incapacity to totally eliminate the heart parasitism, a particularity of the host's failure to eradicate *T. cruzi* from the organism. This leads us to question why heart parasitism occurs in only a fraction of *T. cruzi* chronically infected individuals.

5. Where Does *T. cruzi* Persist in the Chronically Infected Host?

The tissue distribution of *T. cruzi* parasites varies among chronically infected individuals. As indicated above, patients with cardiomyopathy and megaesophagus harbor parasites in the heart and esophagus, respectively. However, are there in these patients, as well as in those with the indeterminate form, other locations where the parasite is relatively safe from complete elimination by the immune system? *A priori*, because parasite persistence is the rule, it is reasonable to hypothesize that immune-privileged *T. cruzi* reservoirs must exist in all chronically infected hosts. One of these parasite niches could be the central adrenal vein, which, in autopsy studies of patients with chronic Chagas disease, has been found to frequently harbor amastigote nests; further, the presence of these nests shows a close correlation with heart pathology parameters such as the intensity of leukocyte infiltration and myocardial fibrosis [50]. Additionally, both brown and white adipose tissues, as well as the colon and stomach, have been described as locations where *T. cruzi* parasites chronically persist [49, 51, 52]. Moreover, because of parasite persistence in the cardiac tissue of CCC patients, the heart could be one of these niches for a fraction of the infected population.

Another issue is whether parasite dissemination through the blood or by spreading from neighboring tissues occurs in the chronic host. Are the *T. cruzi* found in the hearts of CCC patients the consequence of chronic phase dispersion from other tissues or do they result from the perpetuation of heart colonization during the acute phase? This is an important question because chronic phase reinvasion could readdress the problem of heart parasite persistence outside the cardiac tissue.

On the other hand, it is important to note the observation made by different research groups that mice from certain strains can eliminate *T. cruzi* from the heart. This occurs in C57BL/6 mice infected with a sublethal dose of Y strain parasites; these mice exhibit strong leukocyte infiltration with the presence of amastigote nests in the heart in the late acute phase but no signs of infection or pathology in this organ in the chronic phase (Figure 2). This observation indicates that parasite persistence is not the necessary outcome of heart infection. Moreover, these results open the possibility that the indeterminate group of human patients might include patients in whom the cardiac infection was resolved in addition to individuals in whom the heart was never colonized by the parasite.

6. Elements Involved in Parasite Persistence in the Heart or Other Tissues: Parasite Tropism

T. cruzi displays a broad heterogeneity, being currently classified in six different groups (I-VI) [53] that show discrete

correlations with the sylvatic or peridomestic forms of transmission as well as with the occurrence (or lack thereof) of different chronic pathologies. Mixed infections by multiple *T. cruzi* isolates are frequently observed in chronic chagasic patients.

Parasite tropism was originally defined as the preferential invasion of a cell type by a *T. cruzi* clone/isolate. Nevertheless, because the infected host exhibits considerable variability in its tissue responses to the parasite, tropism has to be redefined as the outcome of the interaction of a defined *T. cruzi* clone/isolate in a particular individual, a process largely dependent on the parasite and host genetics. The importance of the host in the development of chronic heart pathology by a single *T. cruzi* parasite is clearly illustrated in the murine model of infection by parasites of the *T. cruzi* clone Sylvio X10/4, which results in chronic cardiomyopathy in C3H/HePAS mice but not in C57BL/6 or A/J mice [47].

Therefore, while (at least for mice and men) the lack of a spontaneous cure and, consequently, the persistence of the parasite are general problems associated with *T. cruzi* infection, independent of parasite and host diversity, the development of chronic heart disease appears to be limited to particular host-parasite combinations.

7. Is Parasite Persistence Merely the Result of a Deficit in the Local Immune Response?

Different research groups have analyzed the heart-infiltrating leukocytes of CCC patients and mice with chronic cardiomyopathy [54–58]. These studies have yielded valuable data regarding the distribution of leukocyte populations, surface marker expression, and the production of cytokines, chemokines, and other mediators. Nonetheless, the gathered information did not help to determine whether a local immune deficit exists because the characteristics of an effective local immune response are undefined. This is because in those chronic settings in which an effective response could eventually occur, such as in chronically infected mice with no cardiac pathology or in patients with the indeterminate form, there are by definition no heart infiltrates to dissect. Therefore, if there is a defect in the local immune response in the heart of CCC patients, it has yet to be found.

Immune response analysis of the blood of patients with the cardiac and indeterminate forms has been used as an indirect means of searching for the presumed local immune defect, aiming to reveal a special immune signature that would explain why the parasite persists in the heart of CCC patients. Remarkably, these studies have revealed that the production of IFN-γ and other proinflammatory cytokines is higher in CCC patients than in indeterminate form patients [59–61] and that asymptomatic patients exhibit augmented T_{REG} numbers and IL-10 levels [59, 62]. Because a proinflammatory response is considered the appropriate approach to eliminate *T. cruzi* parasites, these results conflict with the hypothesis that parasite evasion is the result of a deficient immune response. Furthermore, while systemic studies do not suggest a local deficit in the anti-*T. cruzi* immune response of CCC patients, they do indicate that these patients display an aggressive deregulated response that may explain the presence of tissue damage in the affected heart [63].

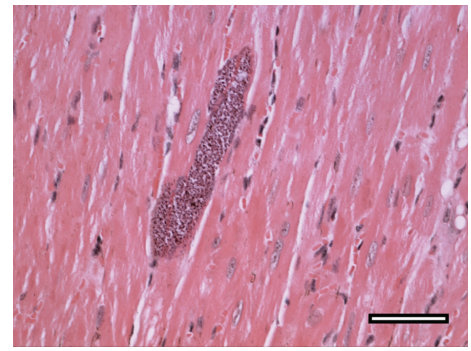

Figure 3: Lack of sensing of amastigote nests could contribute to parasite perpetuation and pathology in the chronically infected heart. Lack of sensing could occur independently of the origin of cardiomyocyte-invading trypomastigotes, that is, from a local ruptured nest or metastasis from a distant niche. The heart picture shown corresponds to a C3H/HePAS mouse infected for more than 200 days with 10^6 Sylvio X10/4 trypomastigotes. The tissue section was stained with hematoxylin-eosin. Bar corresponds to 100 μm (reproduced from C. R. F. Marinho, *Microbes and Infection* [64] with permission from Elsevier).

What, then, is missing? How can we explain why patients with greater proinflammatory responses to *T. cruzi* are those with lower heart parasite control? An interesting possibility is that *T. cruzi* persistence in the heart (and in other relatively immunoprivileged locations) is not merely the consequence of a defective local immune response but that it, to a large extent, derives from the parasite's ability to remain unnoticed inside the structural cells, safe from the effector activity of cytotoxic $CD8^+$ T cells [64]. Illustrative evidence of this possibility is shown in Figure 3, where an amastigote nest can be observed amid myocardial fibers in a mouse infected for more than 200 days, that is, in an animal with a high level of anti-*T. cruzi* immune effector activity. While a notable feature of this picture is the nest size, the most impressive aspect is the absence of leukocytes surrounding it. This suggests a deficiency in signaling for leukocyte recruitment, a condition that allows the parasite to temporarily evade the immune system. Anecdotally, the presence of heart amastigote nests undetected by the inflammatory response was described by Vianna [65] in 1911, one year after the discovery of Chagas disease. From these observations, we can postulate that, independently of the cardiomyocyte-invading parasites originating from a local ruptured nest or a distant niche, the failure to attain sterile immunity in the heart may to a large extent result from an intrinsic or acquired deficit of the cardiomyocytes in sensing the intracellular parasite. Because leukocyte recruitment requires infected cardiomyocytes to signal the presence of an infection through the secretion of chemotactic molecules, we can speculate that, in patients with chronic cardiac disease, this mechanism is largely suppressed. Meanwhile, *T. cruzi*-infected neonatal cardiomyocytes have been shown *in vitro* to transcribe the genes for the chemokines MCP-1, RANTES, KC/GRO, MIP-2, MIG, and IP-10 together with those for the cytokines

TNF-α and IL-1β [66]. A way to reconcile these *in vitro* and *in vivo* findings is that the failure of cardiomyocyte signaling *in vivo* could be an adaptive trait that develops during the course of infection in only certain parasite-host combinations. The possibility that *T. cruzi* interferes with the physiology of infected structural cells is supported by other studies. In this manner, cruzipain, an enzyme abundantly found in *T. cruzi* parasites, has been shown to interfere with cardiomyocyte apoptosis through activation of the NFκB and PI3K/Akt and MEK1/ERK1/2 pathways in the host cell, which lead to increased expression of antiapoptotic Bcl-2 molecules and increased arginase expression [67]. It is therefore conceivable that the crosstalk of the intracellular parasite with the signaling pathways of these structural cells might negatively impact the production of chemotactic molecules.

A deficit in intracellular parasite sensing, although important, is insufficient to guarantee *T. cruzi* evasion in the chronically infected heart. This is the case given that, sooner or later, an undetected amastigote nest will spontaneously disrupt, releasing extracellular parasites that, after detection by antibodies, will cause complement and resident macrophages to generate mediators for leukocyte recruitment. Thus, for long-term parasite perpetuation to occur, it is predictable that a small fraction of nest-released trypomastigotes will reinvade relatively distant cardiomyocytes, where they may remain unnoticed and out of the reach of cytotoxic $CD8^+$ T cells in the newly formed infiltrate.

As stated above, defective parasite sensing by cardiomyocytes could be an adaptive process of the heart tissue that develops with the length of infection. This process most likely exhibits a great degree of variability, reflecting the genetics of the host and the parasite. Moreover, its occurrence in the cardiac tissue is not surprising because the heart is a vital organ that must have special mechanisms designed to protect its integrity.

8. Local Parasite Destruction versus Immunopathology

Theoretically, if two hosts are unable to control tissue parasites, the one with a greater local inflammatory response will pay a higher price by provoking greater damage of the infected tissue [68]. Therefore, if defective local sensing occurs in CCC patients, strong local immune responses would clearly represent a detrimental factor in the induction of pathology, thus explaining the reported associations between high levels of cardiac dysfunction and genotypes associated with high reactivity [69, 70]. Furthermore, the inverse correlation observed in CCC patients between the intensity of electrocardiogram abnormalities and IL-10 plasma levels [59] reinforces this view. That is, to respond strongly when there is a gap in local *T. cruzi* control clearly represents a deleterious manner of dealing with the parasite.

Entering into a persistent cycle of an intense local effector response with no resolution is, to a certain extent, a form of autoaggression, considering the high price paid by the organism in terms of tissue damage. It is not, however, an aggression specifically directed against self-antigens but the unwanted price for unceasingly attempting to completely eliminate a small number of parasites that persist in a fraction of chronically infected individuals. Paradoxically, to protect heart integrity, cardiomyocytes may allow parasite persistence, which indirectly results in tissue damage every time a nest breaks open and new leukocyte infiltrates are formed.

A deficit in the interaction of *T. cruzi* parasites with tissue structural cells could also be involved in parasite persistence at locations other than the heart. This could occur in any infected patient, independent of whether the infection is cardiac, digestive, or indeterminate. In contrast to the heart, however, in many of these locations, the bystander tissue damage resulting from the persistent immune reaction against parasites might not be sufficient to compromise the function of the infected tissue.

Future Perspectives

While extensive research has deciphered the local and systemic immune responses of chronically *T. cruzi*-infected hosts in the last two decades, future studies will need to focus on the *in vivo* interaction of parasites with structural cells, in both the heart and other tissues. Although these studies currently face great technical challenges, they will be of great importance to improve our knowledge about Chagas disease pathology.

Disclosure

Figure 3 is reprinted with permission from Elsevier from Microbes and Infection [64].

Conflict of Interests

The authors declare that there is no conflict of interests regarding the publication of this paper.

Acknowledgments

The authors extend their thanks to Rogério Silva do Nascimento and Bernardo Paulo Albe for providing technical support. Financial support was provided by Grants FAPESP 2013/08199-0 and CNPq 303269/2010-3.

References

[1] OMS, "Chagas disease (American trypanosomiasis)," Fact Sheet 340, 2013, http://www.who.int/mediacentre/factsheets/fs340/en/index.html.

[2] J. R. Coura and P. A. Vĩas, "Chagas disease: a new worldwide challenge," *Nature*, vol. 465, no. 7301, pp. S6–S7, 2010.

[3] A. L. Bombeiro, L. A. Gonçalves, C. Penha-Gonçalves et al., "IL-12p40 deficiency leads to uncontrolled Trypanosoma cruzi dissemination in the spinal cord resulting in neuronal death and motor dysfunction," *PLoS ONE*, vol. 7, no. 11, Article ID e49022, 2012.

[4] S. G. Andrade and Z. A. Andrade, "Pathology of prolonged experimental Chagas' disease," *Revista do Instituto de Medicina Tropical de Sao Paulo*, vol. 10, no. 3, pp. 180–187, 1968.

[5] R. P. Laguens, P. C. Meckert, and R. J. Gelpi, "Chronic Chagas disease in the mouse. I. Electrocardiographic and morphological patterns of the cardiopathy.," *Medicina B*, vol. 41, no. 1, pp. 35–39, 1981.

[6] F. G. Araujo, "Development of resistance to *Trypanosoma cruzi* in mice depends on a viable population of L3T4+ (CD4+) T lymphocytes," *Infection and Immunity*, vol. 57, no. 7, pp. 2246–2248, 1989.

[7] R. L. Tarleton, B. H. Koller, A. Latour, and M. Postan, "Susceptibility of β_2-microglobulin-deficient mice to *Trypanosoma cruzi* infection," *Nature*, vol. 356, no. 6367, pp. 338–340, 1992.

[8] A. M. Rodriguez, F. Santoro, D. Afchain, H. Bazin, and A. Capron, "Trypanosoma cruzi infection in B-cell-deficient rats," *Infection and Immunity*, vol. 31, no. 2, pp. 524–529, 1981.

[9] L. F. Umekita, H. A. Takehara, and I. Mota, "Role of the antibody Fc in the immune clearance of *Trypanosoma cruzi*," *Immunology Letters*, vol. 17, no. 1, pp. 85–89, 1988.

[10] I. Mota and L. F. Umekita, "The effect of C3 depletion on the clearance of *Trypanosoma cruzi* induced by IgG antibodies," *Immunology Letters*, vol. 21, no. 3, pp. 223–226, 1989.

[11] L. R. Sardinha, T. Mosca, R. M. Elias et al., "The liver plays a major role in clearance and destruction of blood trypomastigotes in Trypanosoma cruzichronically infected mice," *PLoS Neglected Tropical Diseases*, vol. 4, no. 1, article e578, 2010.

[12] F. Cardillo, J. C. Voltarelli, S. G. Reed, and J. S. Silva, "Regulation of Trypanosoma cruzi infection in mice by gamma interferon and interleukin 10: role of NK cells," *Infection and Immunity*, vol. 64, no. 1, pp. 128–134, 1996.

[13] L. R. Sardinha, R. M. Elias, T. Mosca et al., "Contribution of NK, NK T, $\gamma\delta$ T, and $\alpha\beta$ T cells to the gamma interferon response required for liver protection against *Trypanosoma cruzi*," *Infection and Immunity*, vol. 74, no. 4, pp. 2031–2042, 2006.

[14] R. E. McCabe, S. G. Meagher, and B. T. Mullins, "Endogenous interferon-γ, macrophage activation, and murine host defense against acute infection with Trypanosoma cruzi," *Journal of Infectious Diseases*, vol. 163, no. 4, pp. 912–915, 1991.

[15] R. T. Gazzinelli, I. P. Oswald, S. Hieny, S. L. James, and A. Sher, "The microbicidal activity of interferon-γ-treated macrophages against Trypanosoma cruzi involves an L-arginine-dependent, nitrogen oxide-mediated mechanism inhibitable by interleukin-10 and transforming growth factor-β," *European Journal of Immunology*, vol. 22, no. 10, pp. 2501–2506, 1992.

[16] H. P. Low, M. A. M. Santos, B. Wizel, and R. L. Tarleton, "Amastigote surface proteins of *Trypanosoma cruzi* are targets for $CD8^+$ CTL," *Journal of Immunology*, vol. 160, no. 4, pp. 1817–1823, 1998.

[17] K. A. Joiner, W. D. daSilva, M. T. Rimoldi, C. H. Hammer, A. Sher, and T. L. Kipnis, "Biochemical characterization of a factor produced by trypomastigotes of *Trypanosoma cruzi* that accelerates the decay of complement C3 convertases," *The Journal of Biological Chemistry*, vol. 263, no. 23, pp. 11327–11335, 1988.

[18] N. Nogueira and Z. Cohn, "Trypanosoma cruzi: mechanism of entry and intracellular fate in mammalian cells," *Journal of Experimental Medicine*, vol. 143, no. 6, pp. 1402–1420, 1976.

[19] H. Castro and A. M. Tomás, "Peroxidases of trypanosomatids," *Antioxidants and Redox Signaling*, vol. 10, no. 9, pp. 1593–1606, 2008.

[20] L. Piacenza, M. P. Zago, G. Peluffo, M. N. Alvarez, M. A. Basombrio, and R. Radi, "Enzymes of the antioxidant network as novel determiners of Trypanosoma cruzi virulence," *International Journal for Parasitology*, vol. 39, no. 13, pp. 1455–1464, 2009.

[21] L. Piacenza, M. N. Alvarez, G. Peluffo, and R. Radi, "Fighting the oxidative assault: the Trypanosoma cruzi journey to infection," *Current Opinion in Microbiology*, vol. 12, no. 4, pp. 415–421, 2009.

[22] M. A. S. Campos, I. C. Almeida, O. Takeuchi et al., "Activation of toll-like receptor-2 by glycosylphosphatidylinositol anchors from a protozoan parasite," *Journal of Immunology*, vol. 167, no. 1, pp. 416–423, 2001.

[23] A. Oliveira, J. R. Peixoto, L. B. de Arrada et al., "Expression of functional TLR4 confers proinflammatory responsiveness to Trypanosoma cruzi glycoinositolphospholipids and higher resistance to infection with T. cruzi," *Journal of Immunology*, vol. 173, no. 9, pp. 5688–5696, 2004.

[24] B. C. Caetano, B. B. Carmo, M. B. Melo et al., "Requirement of UNC93B1 reveals a critical role for TLR7 in host resistance to primary infection with *Trypanosoma cruzi*," *Journal of Immunology*, vol. 187, no. 4, pp. 1903–1911, 2011.

[25] G. K. Silva, F. R. S. Gutierrez, P. M. M. Guedes et al., "Cutting edge: nucleotide-binding oligomerization domain 1-dependent responses account for murine resistance against Trypanosoma cruzi infection," *Journal of Immunology*, vol. 184, no. 3, pp. 1148–1152, 2010.

[26] G. K. Silva, R. S. Costa, T. N. Silveira et al., "Apoptosis-associated speck-like protein containing a caspase recruitment domain inflammasomes mediate IL-1β response and host resistance to *Trypanosoma cruzi* infection," *The Journal of Immunology*, vol. 191, no. 6, pp. 3373–3383, 2013.

[27] V. M. Gonтalves, K. C. Matteucci, C. L. Buzzo et al., "NLRP3 controls *Trypanosoma cruzi* infection through a caspase-1-dependent IL-1R-independent NO production," *PLoS Neglected Tropical Diseases*, vol. 7, no. 10, article e2469, 2013.

[28] S. P. Kurup and R. L. Tarleton, "Perpetual expression of PAMPs necessary for optimal immune control and clearance of a persistent pathogen," *Nature Communications*, vol. 4, article 2616, 2013.

[29] F. Tzelepis, B. C. G. De Alencar, M. L. O. Penido, R. T. Gazzinelli, P. M. Persechini, and M. M. Rodrigues, "Distinct kinetics of effector $CD8^+$ cytotoxic T cells after infection with Trypanosoma cruzi in naïve or vaccinated mice," *Infection and Immunity*, vol. 74, no. 4, pp. 2477–2481, 2006.

[30] J. R. Vasconcelos, O. Bruña-Romero, A. F. Araújo et al., "Pathogen-induced proapoptotic phenotype and high CD95 (Fas) expression accompany a suboptimal CD8+ T-cell response: reversal by adenoviral vaccine," *PLoS Pathogens*, vol. 8, no. 5, Article ID e1002699, 2012.

[31] F. Tzelepis, B. C. G. de Alencar, M. L. O. Penido et al., "Infection with Trypanosoma cruzi restricts the repertoire of parasite-specific CD8+ T cells leading to immunodominance," *Journal of Immunology*, vol. 180, no. 3, pp. 1737–1748, 2008.

[32] M. C. Albareda, G. C. Olivera, S. A. Laucella et al., "Chronic human infection with *Trypanosoma cruzi* drives $CD4^+$ T cells to immune senescence," *The Journal of Immunology*, vol. 183, no. 6, pp. 4103–4108, 2009.

[33] J. K. Leavey and R. L. Tarleton, "Cutting edge: dysfunctional CD8+ T cells reside in nonlymphoid tissues during chronic Trypanosoma cruzi infection," *Journal of Immunology*, vol. 170, no. 5, pp. 2264–2268, 2003.

[34] D. L. Martin, D. B. Weatherly, S. A. Laucella et al., "CD8+ T-cell responses to *Trypanosoma cruzi* are highly focused on strain-variant trans-sialidase epitopes," *PLoS Pathogens*, vol. 2, no. 8, pp. 731–740, 2006.

[35] D. L. Martin, M. Postan, P. Lucas, R. Gress, and R. L. Tarleton, "TGF-β regulates pathology but not tissue CD8$^+$ T cell dysfunction during experimental Trypanosoma cruzi infection," *European Journal of Immunology*, vol. 37, no. 10, pp. 2764–2771, 2007.

[36] M. C. Albareda, A. M. de Rissio, G. Tomas et al., "Polyfunctional T cell responses in children in early stages of chronic *Trypanosoma cruzi* infection contrast with monofunctional responses of long-term infected adults," *PLoS Neglected Tropical Diseases*, vol. 7, no. 12, article e2575, 2013.

[37] F. R. Gutierrez, F. S. Mariano, C. J. Oliveira et al., "Regulation of *Trypanosoma cruzi*-induced myocarditis by programmed death cell receptor 1," *Infection and Immunity*, vol. 79, no. 5, pp. 1873–1881, 2011.

[38] C. M. Ayo, M. M. Dalalio, J. E. Visentainer et al., "Genetic susceptibility to Chagas disease: an overview about the infection and about the association between disease and the immune response genes," *BioMed Research International*, vol. 2013, Article ID 284729, 13 pages, 2013.

[39] C. Sanoja, S. Carbajosa, M. Fresno, and N. Gironès, "Analysis of the dynamics of infiltrating CD4$^+$ T cell subsets in the heart during experimental *Trypanosoma cruzi* infection," *PLoS ONE*, vol. 8, no. 6, Article ID e65820, 2013.

[40] J. C. Pinto Dias, "The indeterminate form of human chronic Chagas' disease. A clinical epidemiological review," *Revista da Sociedade Brasileira de Medicina Tropical*, vol. 22, no. 3, pp. 147–156, 1989.

[41] R. Ribeiro-Dos-Santos, J. O. Mengel, E. Postol et al., "A heart-specific CD4+ T-cell line obtained from a chronic chagasic mouse induces carditis in heart-immunized mice and rejection of normal heart transplants in the absence of *Trypanosoma cruzi*," *Parasite Immunology*, vol. 23, no. 2, pp. 93–101, 2001.

[42] E. Cunha-Neto, M. Duranti, A. Gruber et al., "Autoimmunity in Chagas disease cardiopathy: biological relevance of a cardiac myosin-specific epitope crossreactive to an immunodominant Trypanosoma cruzi antigen," *Proceedings of the National Academy of Sciences of the United States of America*, vol. 92, no. 8, pp. 3541–3545, 1995.

[43] L. Sterin-Borda and E. Borda, "Role of neurotransmitter autoantibodies in the pathogenesis of chagasic peripheral dysautonomia," *Annals of the New York Academy of Sciences*, vol. 917, pp. 273–280, 2000.

[44] M. D. L. Higuchi, M. M. Reis, V. D. Aiello et al., "Association of an increase in CD8+ T cells with the presence of *Trypanosoma cruzi* antigens in chronic, human, chagasic myocarditis," *American Journal of Tropical Medicine and Hygiene*, vol. 56, no. 5, pp. 485–489, 1997.

[45] E. M. Jones, D. G. Colley, S. Tostes, E. R. Lopes, C. L. Vnencak-Jones, and T. L. McCurley, "Amplification of a Trypanosoma cruzi DNA sequence from inflammatory lesions in human chagasic cardiomyopathy," *American Journal of Tropical Medicine and Hygiene*, vol. 48, no. 3, pp. 348–357, 1993.

[46] A. R. Vago, A. M. Macedo, S. J. Adad, D. D'Avila Reis, and R. Correa-Oliveira, "PCR detection of *Trypanosoma cruzi* DNA in oesophageal tissues of patients with chronic digestive Chagas' disease," *The Lancet*, vol. 348, no. 9031, pp. 891–892, 1996.

[47] C. R. F. Marinho, D. Z. Bucci, M. L. Z. Dagli et al., "Pathology affects different organs in two mouse strains chronically infected by a *Trypanosoma cruzi* clone: a model for genetic studies of Chagas'disease," *Infection and Immunity*, vol. 72, no. 4, pp. 2350–2357, 2004.

[48] R. L. Tarleton, "Parasite persistence in the aetiology of Chagas disease," *International Journal for Parasitology*, vol. 31, no. 5-6, pp. 550–554, 2001.

[49] M. D. Lewis, A. F. Francisco, M. C. Taylor et al., "Bioluminescence imaging of chronic *Trypanosoma cruzi* infections reveals tissue-specific parasite dynamics and heart disease in the absence of locally persistent infection," *Cellular Microbiology*, 2014.

[50] V. de Paula Antunes Teixeira, V. Hial, R. A. da Silva Gomes et al., "Correlation between adrenal central vein parasitism and heart fibrosis in chronic chagasic myocarditis," *American Journal of Tropical Medicine and Hygiene*, vol. 56, no. 2, pp. 177–180, 1997.

[51] T. P. Combs, S. Mukherjee, C. J. G. De Almeida et al., "The adipocyte as an important target cell for *Trypanosoma cruzi* infection," *The Journal of Biological Chemistry*, vol. 280, no. 25, pp. 24085–24094, 2005.

[52] A. V. Ferreira, M. Segatto, Z. Menezes et al., "Evidence for *Trypanosoma cruzi* in adipose tissue in human chronic Chagas disease," *Microbes and Infection*, vol. 13, no. 12-13, pp. 1002–1005, 2011.

[53] B. Zingales, S. G. Andrade, M. R. S. Briones et al., "A new consensus for *Trypanosoma cruzi* intraspecific nomenclature: second revision meeting recommends TcI to TcVI," *Memorias do Instituto Oswaldo Cruz*, vol. 104, no. 7, pp. 1051–1054, 2009.

[54] L. G. Nogueira, R. H. B. Santos, B. M. Ianni et al., "Myocardial chemokine expression and intensity of myocarditis in Chagas cardiomyopathy are controlled by polymorphisms in *CXCL9* and *CXCL10*," *PLoS Neglected Tropical Diseases*, vol. 6, no. 10, Article ID e1867, 2012.

[55] D. B. Rocha Rodrigues, M. A. dos Reis, A. Romano et al., "In situ expression of regulatory cytokines by heart inflammatory cells in Chagas' disease patients with heart failure," *Clinical and Developmental Immunology*, vol. 2012, Article ID 361730, 7 pages, 2012.

[56] E. Cunha-Neto, V. J. Dzau, P. D. Allen et al., "Cardiac gene expression profiling provides evidence for cytokinopathy as a molecular mechanism in Chagas'disease cardiomyopathy," *The American Journal of Pathology*, vol. 167, no. 2, pp. 305–313, 2005.

[57] M. M. Reis, M. D. L. Higuchi, L. A. Benvenuti et al., "An in situ quantitative immunohistochemical study of cytokines and IL-2R+ in chronic human chagasic myocarditis: correlation with the presence of myocardial *Trypanosoma cruzi* antigens," *Clinical Immunology and Immunopathology*, vol. 83, no. 2, pp. 165–172, 1997.

[58] J. C. Silverio, I. R. Pereira, M. D. C. Cipitelli et al., "CD8+ T-cells expressing interferon gamma or perforin play antagonistic roles in heart injury in experimental *Trypanosoma cruzi*-elicited cardiomyopathy," *PLoS Pathogens*, vol. 8, no. 4, Article ID e1002645, 2012.

[59] G. R. Sousa, J. A. Gomes, R. C. Fares et al., "Plasma cytokine expression is associated with cardiac morbidity in chagas disease," *PLoS ONE*, vol. 9, no. 3, Article ID e87082, 2014.

[60] J. A. S. Gomes, L. M. G. Bahia-Oliveira, M. O. C. Rocha, O. A. Martins-Filho, G. Gazzinelli, and R. Correa-Oliveira, "Evidence

that development of severe cardiomyopathy in human Chagas' disease is due to a Th1-specific immune response," *Infection and Immunity*, vol. 71, no. 3, pp. 1185–1193, 2003.

[61] C. Poveda, M. Fresno, N. Gironés et al., "Cytokine profiling in Chagas disease: towards understanding the association with infecting *Trypanosoma cruzi* discrete typing units (A BENEFIT TRIAL SubStudy)," *PLoS ONE*, vol. 9, no. 3, Article ID e0091154, 2014.

[62] F. F. de Araújo, R. Corrêa-Oliveira, M. O. C. Rocha et al., "Foxp3$^+$CD^{25} high CD4$^+$ regulatory T cells from indeterminate patients with Chagas disease can suppress the effector cells and cytokines and reveal altered correlations with disease severity," *Immunobiology*, vol. 217, no. 8, pp. 768–777, 2012.

[63] W. O. Dutra, C. A. S. Menezes, F. N. A. Villani et al., "Cellular and genetic mechanisms involved in the generation of protective and pathogenic immune responses in human Chagas disease," *Memorias do Instituto Oswaldo Cruz*, vol. 104, no. 1, pp. 208–218, 2009.

[64] C. R. F. Marinho, L. N. Nuñez-Apaza, K. R. Bortoluci et al., "Infection by the Sylvio X10/4 clone of Trypanosoma cruzi: relevance of a low-virulence model of Chagas' disease," *Microbes and Infection*, vol. 11, no. 13, pp. 1037–1045, 2009.

[65] G. Vianna, "Contribuição para o estudo da Anatomia Patológica da Molestia de Carlos Chagas," *Memorias do Instituto Oswaldo Cruz*, vol. 3, p. 276, 1911.

[66] F. S. Machado, G. A. Martins, J. C. S. Aliberti, F. L. A. C. Mestriner, F. Q. Cunha, and J. S. Silva, "Trypanosoma cruzi-infected cardiomyocytes produce chemokines and cytokines that trigger potent nitric oxide-dependent trypanocidal activity," *Circulation*, vol. 102, no. 24, pp. 3003–3008, 2000.

[67] M. D. P. Aoki, R. C. Cano, A. V. Pellegrini et al., "Different signaling pathways are involved in cardiomyocyte survival induced by a *Trypanosoma cruzi* glycoprotein," *Microbes and Infection*, vol. 8, no. 7, pp. 1723–1731, 2006.

[68] L. Råberg, D. Sim, and A. F. Read, "Disentangling genetic variation for resistance and tolerance to infectious diseases in animals," *Science*, vol. 318, no. 5851, pp. 812–814, 2007.

[69] R. Ramasawmy, K. C. Fae, E. Cunha-Neto et al., "Polymorphisms in the gene for lymphotoxin-α predispose to chronic chagas cardiomyopathy," *Journal of Infectious Diseases*, vol. 196, no. 12, pp. 1836–1843, 2007.

[70] G. Zafra, C. Morillo, J. Martín, A. González, and C. I. González, "Polymorphism in the 3′ UTR of the IL12B gene is associated with Chagas' disease cardiomyopathy," *Microbes and Infection*, vol. 9, no. 9, pp. 1049–1052, 2007.

Hindawi Publishing Corporation
Mediators of Inflammation
Volume 2014, Article ID 605023, 13 pages
http://dx.doi.org/10.1155/2014/605023

Research Article

Genetic Vaccination against Experimental Infection with Myotropic Parasite Strains of *Trypanosoma cruzi*

Adriano Fernando Araújo,[1,2] Gabriel de Oliveira,[3] Juliana Fraga Vasconcelos,[4,5] Jonatan Ersching,[1,2] Mariana Ribeiro Dominguez,[1,2] José Ronnie Vasconcelos,[1,2,6] Alexandre Vieira Machado,[7] Ricardo Tostes Gazzinelli,[7,8,9] Oscar Bruna-Romero,[10] Milena Botelho Soares,[4,5] and Mauricio Martins Rodrigues[1,2]

[1] *Centro de Terapia Celular e Molecular (CTCMol), Escola Paulista de Medicina, UNIFESP, Rua Mirassol, 207 04044-010 São Paulo, SP, Brazil*
[2] *Departmento de Microbiologia, Imunologia e Parasitologia, Escola Paulista de Medicina, Universidade Federal de São Paulo, Rua Mirassol, 207 04044-010 São Paulo, SP, Brazil*
[3] *Laboratório Biologia Celular, Instituto Oswaldo Cruz (FIOCRUZ), Avenida Brasil, 4365—Manguinhos, 21040-360 Rio de Janeiro, RJ, Brazil*
[4] *Centro de Pesquisas Gonçalo Moniz, FIOCRUZ, Rua Waldemar Falcão, 121, 40296-710 Salvador, BA, Brazil*
[5] *Hospital São Rafael, Avenida São Rafael 2152, São Marcos, 41253-190 Salvador, BA, Brazil*
[6] *Departamento de Biociências, Instituto de Saúde e Sociedade, UNIFESP, Campus Baixada Santista, 11015-020 Santos, SP, Brazil*
[7] *Centro de Pesquisas René Rachou, FIOCRUZ, Avenida Augusto de Lima 1.715, Barro Preto, 30190-002 Belo Horizonte, MG, Brazil*
[8] *Departamento de Bioquímica e Imunologia, Instituto de Ciências Biológicas, Universidade Federal de Minas Gerais, Avenida Presidente Antônio Carlos, 6627, Pampulha, 31270-901 Belo Horizonte, MG, Brazil*
[9] *Division of Infectious Disease and Immunology, Department of Medicine, University of Massachusetts Medical School, 55 Lake Avenue North, Worcester, MA 01655, USA*
[10] *Departamento de Microbiologia, Imunologia e Parasitologia, Universidade Federal de Santa Catarina, Campus Universitário da Trindade, 88040-900 Florianopolis, SC, Brazil*

Correspondence should be addressed to Mauricio Martins Rodrigues; mrodrigues@unifesp.br

Received 26 March 2014; Accepted 25 May 2014; Published 26 June 2014

Academic Editor: Marcelo T. Bozza

In earlier studies, we reported that a heterologous prime-boost regimen using recombinant plasmid DNA followed by replication-defective adenovirus vector, both containing *Trypanosoma cruzi* genes encoding *trans*-sialidase (TS) and amastigote surface protein (ASP) 2, provided protective immunity against experimental infection with a reticulotropic strain of this human protozoan parasite. Herein, we tested the outcome of genetic vaccination of F1 (CB10XBALB/c) mice challenged with myotropic parasite strains (Brazil and Colombian). Initially, we determined that the coadministration during priming of a DNA plasmid containing the murine IL-12 gene improved the immune response and was essential for protective immunity elicited by the heterologous prime-boost regimen in susceptible male mice against acute lethal infections with these parasites. The prophylactic or therapeutic vaccination of resistant female mice led to a drastic reduction in the number of inflammatory infiltrates in cardiac and skeletal muscles during the chronic phase of infection with either strain. Analysis of the electrocardiographic parameters showed that prophylactic vaccination reduced the frequencies of sinus arrhythmia and atrioventricular block. Our results confirmed that prophylactic vaccination using the TS and ASP-2 genes benefits the host against acute and chronic pathologies caused by *T. cruzi* and should be further evaluated for the development of a veterinary or human vaccine against Chagas disease.

1. Introduction

Chagas disease is an acute and chronic illness caused by *Trypanosoma cruzi*, an obligatory intracellular protozoan parasite that is endemic in the Americas. The disease currently affects millions of people who are chronically infected. Thousands of new cases are also estimated to occur every year [1, 2]. Prophylactic measures aimed at eliminating transmission by the vector (kissing bugs) have been very successful in many countries [3]. Considering their success and the highly neglected state of Chagas disease research, vaccine development has often been considered a difficult and expensive strategy for disease control and eradication.

Despite this general consideration, recent theoretical studies have shown a divergent perspective on the problem, indicating that the development of a vaccine against Chagas disease would be cost effective even if the efficacy is not high and the transmission is low [4, 5]. In moving toward the development of vaccines against Chagas disease, several laboratories have described a number of antigens and delivery systems capable of providing some degree of protective immunity against experimental infections. These systems include genetically attenuated parasites, recombinant protein in adjuvant systems, and genetically modified bacteria or viral vectors (reviewed in [6–12]). The antigens pursued for recombinant vaccines include *T. cruzi trans*-sialidase, cruzain (a cysteine proteinase), and the amastigote surface proteins 2, 3, 4, TcG1, TcG2, TcG4, TSA-1, and Tc24 (reviewed in [6–12]).

Our group in particular has been working for many years on the development of genetic vaccines against *T. cruzi* infection. We initially used the gene encoding the catalytic domain of the parasite *trans*-sialidase (TS, [13, 14]). More recently, we have described studies using a heterologous prime-boost regimen consisting of priming with plasmid DNA followed by a booster injection with replication-defective recombinant human adenovirus type 5. Both the prime and the boost contained the gene encoding the amastigote surface protein (ASP)-2 antigen of *T. cruzi*. This regimen successfully vaccinated highly susceptible A/Sn and resistant C57BL/6 mice against infection with the reticulotropic Y strain of *T. cruzi* [15–18]. Protective immunity was mediated by long-lived $CD4^+$ and $CD8^+$ T Effector or effector memory cells [15, 19, 20].

T. cruzi infection in mammalian hosts leads to diverse clinical manifestations. Among the most relevant factors influencing this diversity is the existence of biologically different parasite strains. *T. cruzi* intraspecific nomenclature was established in 2009, and the isolates and strains are assigned to one of six genetic groups or discrete typing units, named TcI to TcVI [21]. Among domestic transmission cycles, TcI occurs predominantly in northern South America, while TcII, TcV, and TcVI are more often observed in the Southern Cone countries [22]. Considering this genetic variability, it is important that studies of vaccination or chemotherapy are conducted in different experimental models using distinct parasite strains. Because our previous studies of vaccination have been performed with the reticulotropic Y strain (TcII), it was our intention to extend these studies using experimental infections with two myotropic strains of the parasites belonging to TcI (Colombian) and TcII (Brazil).

2. Materials and Methods

2.1. Ethics Statement. This study was carried out in strict accordance with the recommendations in the Guide for the Care and Use of Laboratory Animals of the Brazilian National Council of Animal Experimentation (http://www.cobea.org.br/). The protocol was approved by the Committee on the Ethics of Animal Experiments of the Institutional Animal Care and Use Committee at the Federal University of Sao Paulo (Id # CEP 0426/09).

2.2. Mice and Parasites. Female or male 5- to 8-week-old F1 (CB10XBALB/c) mice were purchased from CEDEME (Federal University of São Paulo). Bloodstream trypomastigotes of the Colombian or Brazil strain of *T. cruzi* were obtained from mice infected 21–28 days earlier. The concentration of parasites was estimated and adjusted to 10^4 parasites/mL. Each mouse was inoculated with 10^3 trypomastigotes diluted in 0.1 mL PBS and administrated subcutaneously (s.c.) in the base of the tail.

2.3. Peptides. Synthetic peptides (Genscript, Piscataway, New Jersey) were higher than 90% pure. The immunodominant epitopes of ASP-2 or TS were represented by AA VNHRFTLV or IYNVGQSVI, respectively.

2.4. Genetic Vaccination. The plasmid (pWRG3169) containing coding sequences for the p35 and p40 subunits of murine (m) IL-12 was generated as earlier described [23]. Plasmids p154/13 (TS gene) or pIgSPclone9 (ASP-2 gene) were generated, grown, and purified as described earlier [13, 24]. Human replication deficient adenovirus type 5 expressing the ASP-2 gene (AdASP-2) or TS gene (AdTS) was generated and produced as described earlier [25] Control mice were immunized with pcDNA3 and human replication deficient adenovirus type 5 expressing β-galactosidase (Adβ-gal). F1 (CB10XBALB/c) mice were immunized i.m. in each *tibialis anterioris* muscle with plasmid DNA. For priming, control mice received plasmid pcDNA3 (300 μg), a second group was immunized with a mixture of pIgSPCl9 and p154/13 (200 μg), and the third, a mixture of pIL12, pIgSPCl9, and p154/13 (300 μg). Twenty-one days later, these mice received in these same spots 100 μL of viral suspension containing a total of 2×10^8 plaque forming units (pfu) of rec. adenovirus. For boosting, control mice received adenovirus Adβgal; other mouse groups were immunized with a mixture of rec. adenovirus AdASP-2 and Ad-TS. Immunological assays were performed 14 days after viral inoculation.

Therapeutic vaccination was performed as follows. F1 (CB10XBALB/c) female mice were challenged s.c. with 1,000 trypomastigotes of the indicated parasite strain. Thirty days later, control mice received a mixture of plasmid pcDNA3 and of pIL12 (300 μg) and second mice group was immunized with a mixture of pIL12pIgSPCl9 and p154/13 (300 μg). Twenty days later, these mice received in these same spots

100 μL of viral suspension containing a total of 2×10^8 pfu of rec. adenovirus. For boosting, control mice received adenovirus Adβgal and the other mice were immunized with a mixture of rec. adenovirus AdASP-2 and Ad-TS.

2.5. Immunological Assays. For the surface intracellular expression of cytokines (IFNγ and TNF, ICS) or translocation of CD107a to the membrane, splenocytes collected from immune mice were treated with ACK buffer. ICS and surface mobilization of CD107a were evaluated after *in vitro* culture of splenocytes in the presence or absence of the antigenic stimulus. Cells were washed 3 times in plain RPMI and resuspended in cell culture medium consisting of RPMI 1640 medium, pH 7.4, supplemented with 10 mM Hepes, 0.2% sodium bicarbonate, 59 mg/L of penicillin, 133 mg/L of streptomycin, and 10% Hyclone fetal bovine sera (Hyclone, Logan, Utah). The viability of the cells was evaluated using 0.2% trypan blue exclusion dye to discriminate between live and dead cells. Cell concentration was adjusted to 5×10^6 cells/mL in cell culture medium containing FITC-labeled anti-CD107a (2 μg/mL), anti-CD28 (2 μg/mL), BdGolgiPlug, and monensin (5 μg/mL). In part of the cultures, a final concentration of 10 μM of the VNHRFTLV or IYNVGQSVI peptides was added. The cells were cultivated in flat-bottom 96-well plates (Corning) in a final volume of 200 μL in duplicate, at 37°C in a humid environment containing 5% CO_2. After 12 h incubation, cells were stained for surface markers with PerCP-labeled anti-CD8, on ice for 20 min. To detect IFNγ and TNF by intracellular staining, cells were then washed twice in buffer containing PBS, 0.5% BSA, and 2 mM EDTA, fixed and permeabilized with BD perm/wash buffer. After being washed twice with BD perm/wash buffer, cells were stained for intracellular markers using APC-labeled anti-IFNγ (Clone XMG1.2) and PE-labeled anti-TNF (clone MP6-XT22). Finally, cells were washed twice with BD perm/wash buffer and fixed in 1% PBS-paraformaldehyde. At least 300,000 cells were acquired on a BD FacsCanto flow cytometer and then analyzed with FlowJo.

2.6. Electrocardiogram (ECG). Mice were i.p. tranquilized with diazepan (20 mg/kg) and transducers were carefully placed under the skin in accordance with chosen preferential derivation (DII). Traces were recorded using a digital system (Power Lab 2/20) connected to a bioamplifier in 2 mV for 1 s (PanLab Instruments). Filters were standardized between 0.1 and 100 Hz and traces were analyzed using the Scope software for Windows V3.6.10 (PanLab Instruments). We measured heart rate (beats per minute—bpm), duration of the PR, QRS, and QT intervals, and P wave in ms (millisecond) on 222 dpi. The relationship between the QT interval and RR interval was individually assessed to obtain physiologically relevant values for the heart rate-corrected QT interval (QTc) through Bazzet's formula.

2.7. Morphometric Analyses. Analyses were performed essentially as described in [26]. Briefly, heart sections were analyzed by light microscopy after paraffin embedding, followed by standard hematoxylin and eosin staining. Inflammatory cells infiltrating heart tissue were counted using a digital morphometric evaluation system. Images were digitized using a color digital video camera (CoolSnap, Photometrics, Montreal, QC, Canada) adapted to a BX41 microscope (Olympus, Tokyo, Japan). Morphometric analyses were performed using the software Image-Pro Plus v.7.0 (Media Cybernetics, San Diego, CA, USA). The inflammatory cells were counted in 10 fields (×400 view)/heart. All of the analyses were performed in a blinded fashion.

2.8. Statistical Analysis. For the purpose of comparing the different mouse groups, we used the statistical analyses suggested by [27]. The values were compared using One Way ANOVA followed by Tukey's HSD tests or Fisher exact probability test (http://faculty.vassar.edu/lowry/VassarStats.html/). The Logrank test was used to compare mouse survival rates after challenge with *T. cruzi* (http://bioinf.wehi.edu.au/software/russell/logrank/). The differences were considered significant when the P value was <0.05.

3. Results

3.1. Addition of pIL-12 during Priming Improved the Immune Response Mediated by CD8$^+$ T Cells and Increased Protective Immunity against Acute Infection. A previous study has reported that the coadministration of plasmid DNA expressing IL-12 during priming improves the efficacy of a heterologous prime-boost vaccination regimen, as estimated by protective immunity against SIV infection [28]. We, therefore, decided to determine whether this strategy could also improve the immune response and protective immunity against *T. cruzi* infection in the mouse model. Mice were immunized with the following: (i) pcDNA3 followed by a booster injection of Adβgal (G1, control); (ii) p154/13 and pIgSPCl9 followed by a booster injection of AdASP-2 and AdTS (G2); (iii) pIL-12, p154/13 and pIgSPCl9 followed by a booster injection of AdASP-2 and AdTS (G3).

To compare the different mouse groups, we stained CD8$^+$ spleen cells following *in vitro* peptide stimulation for the surface mobilization of CD107a, a marker for T cell degranulation, and intracellular effector cytokines (IFNγ and TNF, ICS). Figure 1(a) depicts examples of the frequency estimates of peptide-specific CD8$^+$ spleen cells that mobilized CD107a to their surface and expressed IFNγ. The frequencies of CD8$^+$ cells that mobilized CD107a to the cell surface and expressed IFNγ were higher in G3. Control mice (G1) had a negligible number of specific CD8$^+$CD107a$^+$IFNγ^+ cells. These frequencies were dependent on the presence of peptide in culture because the frequency of CD8$^+$CD107a$^+$IFNγ^+ cells was very small in the absence of peptide in all groups.

We made a similar observation when we estimated the frequencies of splenic peptide-specific CD8 cells that expressed IFNγ or IFNγ and TNF. These frequencies were higher in G3 mice (Figure 1(b)). As described above, control mice (G1) had a negligible number of specific CD8$^+$IFNγ^+ or CD8$^+$IFNγ^+TNF$^+$ cells. The numerical differences and the statistical significances are depicted in Figures 1(c)–1(f). As shown in Figures 1(d) and 1(f), following peptide

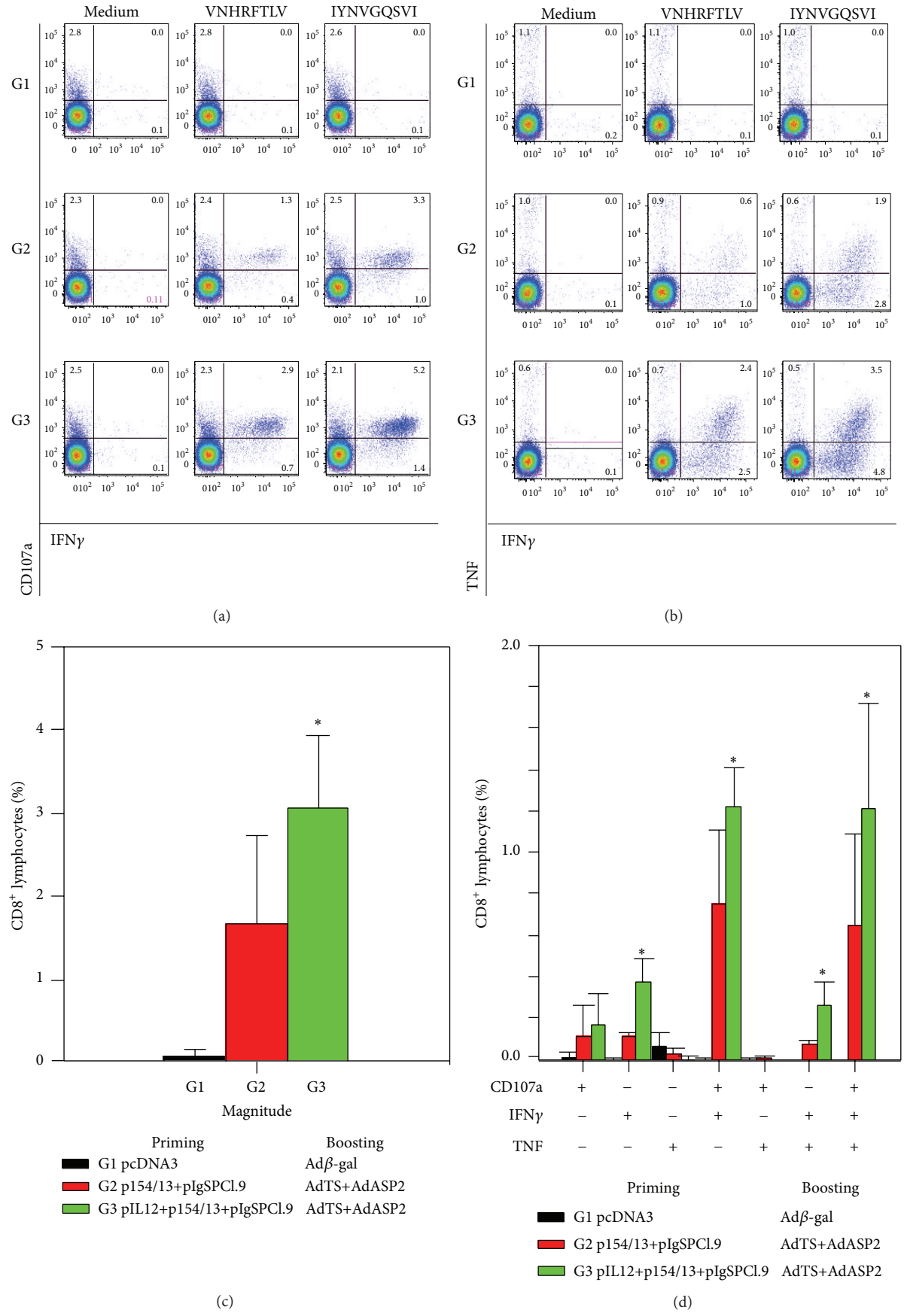

Figure 1: Continued.

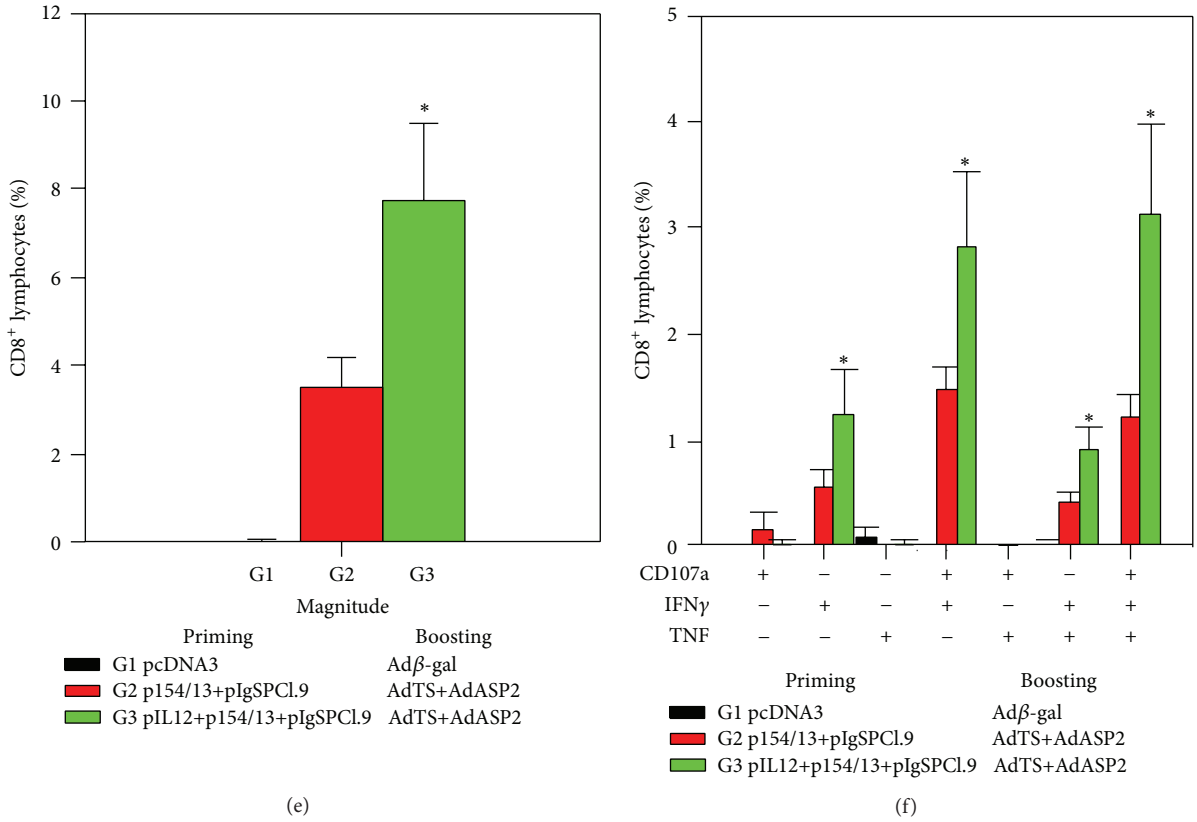

Figure 1: Frequencies of specific cytokine-secreting splenic $CD8^+$ T cells in mice vaccinated with the heterologous prime-boost vaccination regimen. F1 (CB10XBALB/c) mice were immunized i.m. in each *tibialis anterior* muscle with plasmid DNA. For priming, G1 received control plasmid pcDNA3 (300 μg), G2 was immunized with a mixture of pIgSPCl9 and p154/13 (200 μg), and G3 received a mixture of pIL-12, pIgSPCl9, and p154/13 (300 μg). Twenty-one days later, these mice received, in these same spots, 100 μL of a viral suspension containing a total of 2×10^8 pfu of rec. adenovirus. For boosting, G1 received control adenovirus Adβgal, and G2 and G3 were immunized with a mixture of rec. adenovirus AdASP-2 and Ad-TS. Immunological assays were performed 14 days after viral inoculation. Spleen cells were restimulated *in vitro* in the presence or absence of the peptides VNHRFTLV or IYNVGQSVI, anti-CD107a, anti-CD28, BdGolgiPlug, and monensin. After 12 h, the cells were stained with anti-CD8, anti-IFNγ, and anti-TNF. (a) The histograms show FACS analysis of CD8+ cells. The numbers represent the frequencies of cells stained for CD107a and/or IFNγ. The results are a representative of 4 mice per group (Median). (b) Frequencies of CD8+ cells stained for IFNγ and/or TNF. The results are a representative of 4 mice per group (Median). (c) Total frequencies of CD8+ cells specific for the peptide VNHRFTLV and stained for CD107a or IFNγ or TNF. The results are representative of 4 mice per group (Mean ± SD). (d) Frequencies of CD8+ cells specific for the peptide VNHRFTLV and stained for each marker (CD107a, IFNγ, or TNF). The results are representative of 4 mice per group (Mean ± SD). (e) Same as in (c) for CD8+ cells specific for the peptide IYNVGQSVI. The results are representative of 4 mice per group (Mean ± SD). (f) Same as in (d) for CD8+ cells specific for the peptide IYNVGQSVI. All three groups were compared statistically by one-way ANOVA followed by Tukey HSD (c–e). The values of G2 and G3 mice were always higher than those of G1 mice ($P < 0.01$ in all cases). Asterisks denote that the values of G3 mice were higher than those of G2 mice ($P < 0.05$). The results are representative of three independent experiments.

stimulation *in vitro*, most of the $CD8^+$ cells were either $CD107a^+IFN\gamma^+TNF^+$ or $CD107a^+IFN\gamma^+$.

To determine whether this improvement in the frequencies of specific $CD8^+$ T cells would impact protective immunity, we vaccinated susceptible male mice and challenged them with trypomastigotes of either the Brazil or Colombian strain. As shown in Figures 2(a) and 2(c), mice vaccinated with the TS and ASP-2 genes (G2 and G3) presented a statistically significant reduction in peak parasitemia. A comparison between these two groups also showed that the parasitemia in G3 was significantly lower than that in G2. Not only did mice from G3 display lower parasitemia, but vaccination also significantly reduced mouse mortality (Figures 2(b) and 2(d)). While all G3 mice survived the experimental challenge, most control (G1) and G2 mice died after challenge with the Brazil or Colombian parasite strain. Based on these results, we concluded that the use of pIL-12 for priming significantly improved the immune response and the protective immunity against acute infection with the myotropic Brazil and Colombian strains.

3.2. Impact of Genetic Vaccination against Chronic Infection. To evaluate the impact of genetic vaccination on the chronic symptoms of the experimental infection, resistant female mice were treated according to the following protocols: (i) naïve (G1); (ii) pIL-12 and pcDNA3 followed by a booster

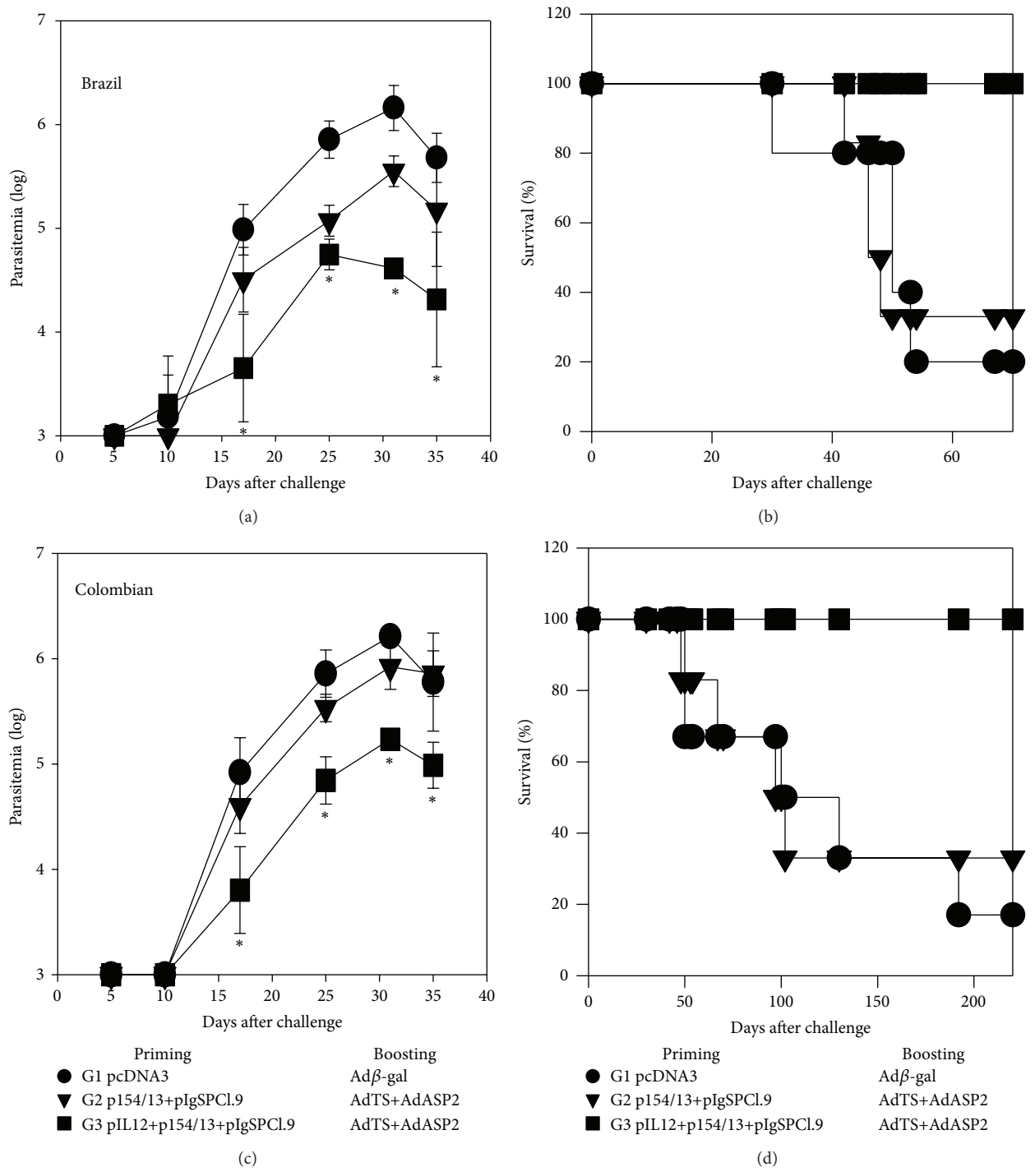

Figure 2: The protective immunity elicited by heterologous prime-boost vaccination in susceptible mice. F1 (CB10XBALB/c) male mice were immunized i.m. exactly as described in the legend of Figure 1. Fourteen days later, mice were challenged s.c. with 1,000 trypomastigotes of the indicated parasite strain. (a) Mean parasitemia ± SD of each mouse group ($n = 6$) challenged with parasites of the Brazil strain. The values of G2 and G3 mice at days 21, 25 and 35 were lower than those of G1 mice ($P < 0.01$ in all cases, one-way ANOVA, Tukey HSD). Asterisks denote that the values of G3 mice were lower than those of G2 mice ($P < 0.05$); (b) The Kaplan-Meier survival curves of the different groups were compared, and the results showed that G3 survived significantly longer ($P < 0.01$) than the two other groups; (c) Mean parasitemia ± SD of each mouse group ($n = 6$) challenged with parasites of the Colombian strain. The values of G2 and G3 mice at days 25 and 31 were lower than those of G1 mice ($P < 0.01$ in all cases). Asterisks denote that the values of G3 mice were lower than those of the G2 mice ($P < 0.05$); (d) The Kaplan-Meier survival curves of the different groups were compared, and the results showed that G3 survived significantly longer ($P < 0.01$) than the two other groups. The results were obtained from one of two independent experiments.

Table 1: Summary of the ECG records.

Days after challenge	Strain	Sinus arrhythmia mouse groups			*P* values		
		G1	G2	G3	G1 × G2	G1 × G3	G2 × G3
80	Brazil	0/6	0/6	0/6	NS	NS	NS
150	Brazil	0/6	19/6	0/6	*0.001*	NS	*0.001*
240	Brazil	0/6	20/6	3/6	*0.001*	NS	*0.026*
80	Colombian	0/6	0/6	0/5	NS	NS	NS
150	Colombian	0/6	1/6	1/5	NS	NS	NS
240	Colombian	0/6	9/6	1/5	*0.017*	NS	*0.093*
Days after challenge	Strain	Atrioventricular block			*P* values		
		G1	G2	G3	G1 × G2	G1 × G3	G2 × G3
80	Brazil	0/6	0/6	0/6	NS	NS	NS
150	Brazil	0/6	4/6	2/6	*0.03*	NS	NS
240	Brazil	0/6	59/6	7/6	*0.001*	*0.004*	*0.003*
80	Colombian	0/6	19/6	0/5	*0.001*	NS	NS
150	Colombian	0/6	14/6	6/5	*0.001*	*0.002*	NS
240	Colombian	0/6	39/6	10/5	*0.001*	*0.002*	NS

ECG record of mice genetically vaccinated and challenged as described in the legend of Figure 5(a). Values represent the number of episodes (sinus arrhythmia or atrioventricular block) recorded during one minute per total of mice analyzed and were compared by Fisher exact probability test.

injection of Adβgal (G2, control); (iii) pIL-12, p154/13 and pIgSPCl9 followed by a booster injection of AdASP-2 and AdTS (G3).

G2 and G3 mice were subsequently challenged with parasites of either the Brazil or the Colombian strain, as depicted in Figure 3(a). We estimated the level of parasitemia for each mouse group. G3 mice presented a lower peak parasitemia at day 27 ($P = 0.02$) after infection with parasites of the Brazil strain (Figure 3(b)). In the case of mice challenged with parasites of the Colombian strain, there was a statistically significant reduction in the levels of parasitemia at days 13, 20, 24, 28, and 31 ($P < 0.05$ in all cases, Figure 3(c)).

Individual ECGs were evaluated at days 80, 150, and 240 following infection. As shown in Table 1, the primary abnormalities we detected were sinus arrhythmia and atrioventricular block. Significantly lower frequencies of sinus arrhythmia were observed in G3 mice when compared with G2 mice following infection with the Brazil or Colombian strains. These differences were observed at later days (150 or 240 days) following challenge. Similarly, significantly lower frequencies of atrioventricular block were observed in G3 mice when compared with G2 mice following infection with parasites of the Brazil strain. In the case of mice challenged with parasites of the Colombian strain, the differences were smaller and not statistically significant.

At day 240 after challenge, the mice were euthanized, and morphometric analyses of the heart and skeletal muscle were performed. The number of inflammatory cells within the skeletal muscle, but not the heart, of G3 mice challenged with parasites of the Brazil strain was significantly lower (Figure 4(b)). In G3 mice challenged with parasites of the Colombian strain, we found significantly lower numbers of inflammatory cells within the skeletal muscle and heart when compared to G2 mice (Figure 4(c)).

We then evaluated the impact of therapeutic genetic vaccination on the chronic symptoms of experimental infection. Resistant female mice were infected and then treated according to the protocols described in Figures 5(a) and 6(a). Mice received the following treatments: (i) pIL-12 and pcDNA3 followed by a booster injection of Adβgal (G2, control); (ii) pIL-12, p154/13 and pIgSPCl9 followed by a booster injection of AdASP-2 and AdTS (G3).

The estimation of parasitemia until day 50 did not reveal any difference between G2 or G3 mice infected with parasites of the Brazil or Colombian strains (Figures 5(b) and 5(c), resp.). We concluded that the plasmid administration at day 30 after challenge did not elicit immunity that could reduce the ongoing parasitemia. Individual ECGs were evaluated at days 90, 120, 150, and 180 following infection. As shown in Table 2, we detected differences in the frequencies of sinus arrhythmia, but not atrioventricular block, in G3 mice when compared with G2 mice following infection with the Brazil strain of *T. cruzi*. However, this difference was observed only on days 90 and 120. Later (150 and 180 days), G3 mice also developed sinus arrhythmia. G3 mice infected with parasites of the Colombian strain had significantly lower frequencies of sinus arrhythmia at days 120 and 180, when G2 mice developed a significant number of events. However, the occurrence of atrioventricular block in G3 mice was similar to that in G2. At day 180 after challenge, the mice were euthanized, and morphometric analyses of the heart and skeletal muscle were performed. The numbers of inflammatory cells within the skeletal muscle and heart of G3 mice challenged with parasites of the Brazil or Colombian strains were significantly lower than the frequencies in the tissues of G2 mice (Figures 6(b) and 6(c), resp.).

4. Discussion

The present study evaluated the outcome of experimental infection with two myotropic *T. cruzi* strains in F1 (CB10XBALB/c) mice genetically vaccinated with TS and ASP-2 following a heterologous DNA prime-adenovirus boost regimen. Prophylactic vaccination reduced the acute

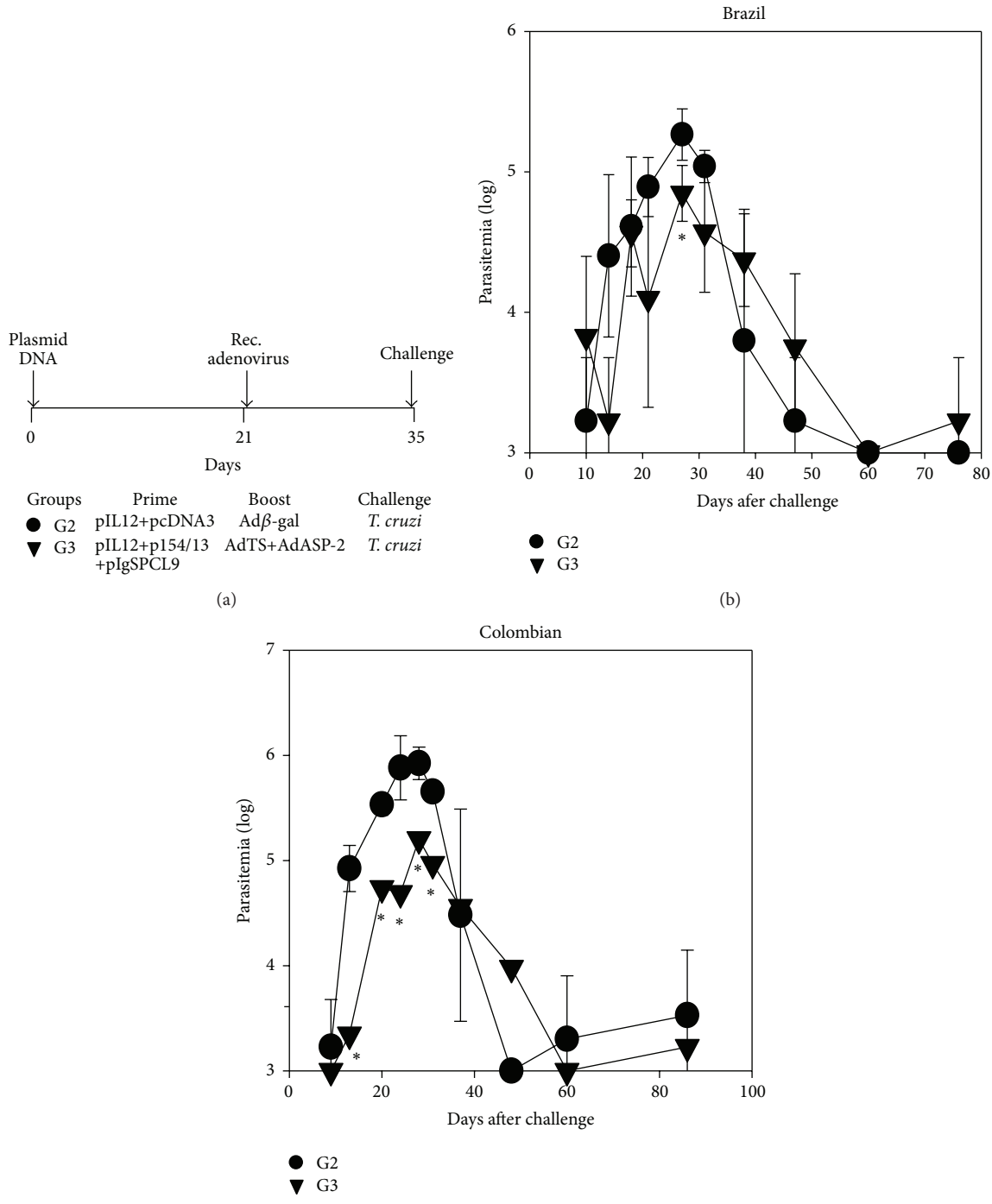

Figure 3: The protective immunity elicited by heterologous prime-boost vaccination in resistant mice. (a) F1 (CB10XBALB/c) female mice were immunized i.m. as depicted. For priming, G2 mice received a mixture of control plasmid pcDNA3 and of pIL-12 (300 μg), and G3 mice were immunized with a mixture of pIL-12, pIgSPCl9 and p154/13 (300 μg). Twenty-one days later, these mice received, in these same spots, 100 μL of a viral suspension containing a total of 2×10^8 pfu of rec. adenovirus. For boosting, G2 mice received control adenovirus Adβgal, and G3 mice were immunized with a mixture of rec. adenovirus AdASP-2 and Ad-TS. Fourteen days later, mice were challenged s.c. with 1,000 trypomastigotes of the indicated parasite strain. (b) Mean parasitemia ± SD of each mouse group ($n = 6$) challenged with parasites of the Brazil strain. Asterisk denotes that at day 37, the values of G3 mice were lower than those of G2 mice ($P < 0.05$, one-way ANOVA, Tukey HSD); (c) Mean parasitemia ± SD of each mouse group ($n = 6$) challenged with parasites of the Colombian strain. Asterisks denote that at days 13 to 31, the values of G3 mice were lower than those of G2 mice ($P < 0.05$).

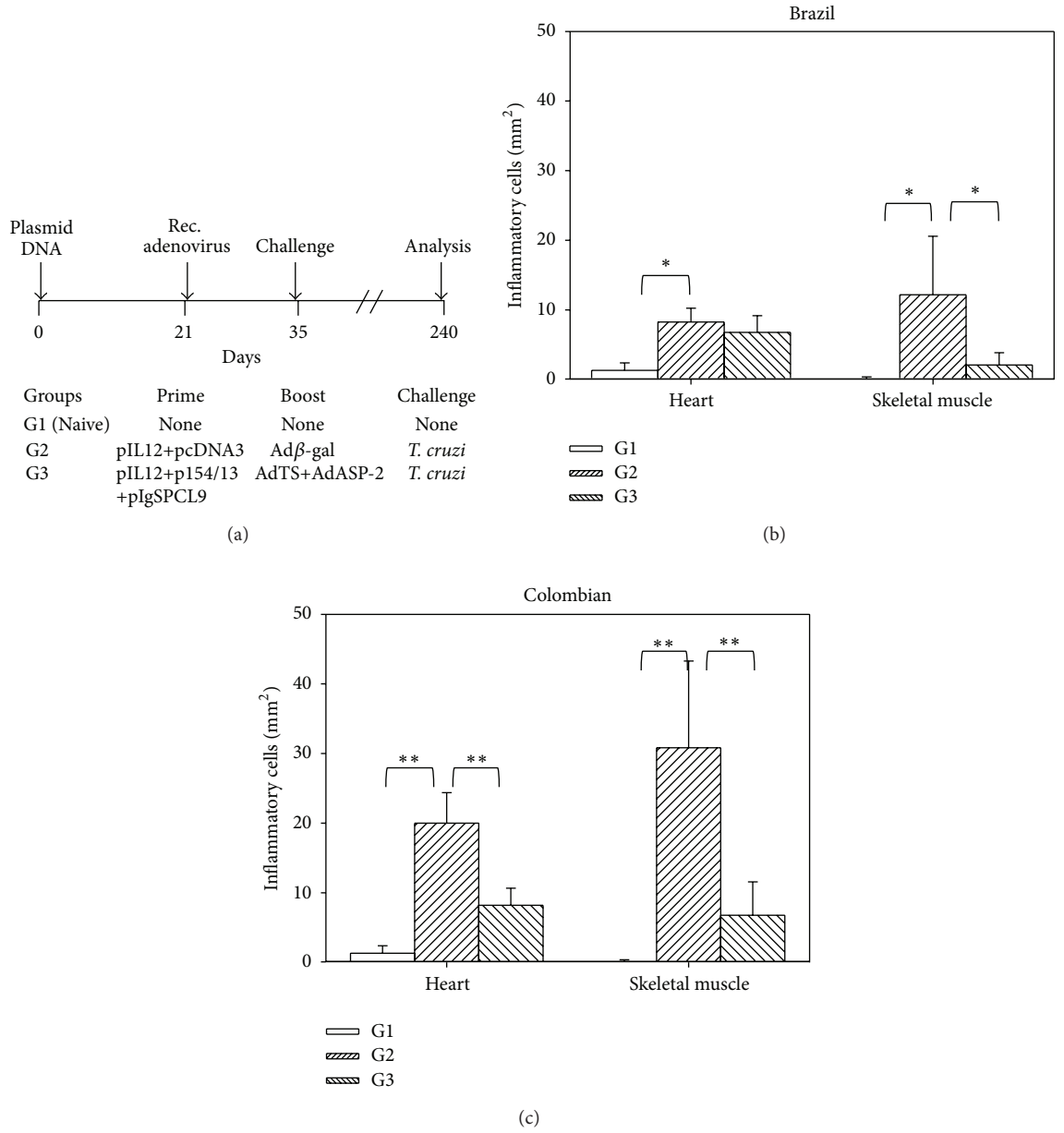

Figure 4: Frequencies of inflammatory cells in the hearts and skeletal muscles of resistant mice vaccinated by the heterologous prime-boost regimen. (a) F1 (CB10XBALB/c) female mice were immunized i.m., as depicted. Details on the dose are shown in Figure 3(a). (b) At 240 days, heart and skeletal muscle sections of mice challenged with the Brazil strain were stained with hematoxylin and eosin, and the number of inflammatory cells was quantified. Bars represent the mean of 6 mice/group ± SD. Asterisks denote that there was a significant difference between the indicated groups ($^{*}P < 0.05$ or $^{**}P < 0.01$). (c) The same as above, except that the mice were challenged with parasites of the Colombian strain. Bars represent the mean of 5 mice/group ± SD.

phase symptoms, as estimated by parasitemia and mortality. In addition, ECG analysis demonstrated that prophylactic vaccination also reduced some of the chronic phase signs. These results essentially confirm and extend our previous observations in mice challenged with a reticulotropic *T. cruzi* strain [15–20].

In contrast to prophylactic vaccination, the therapeutic use of our vaccine had a much lower impact on the chronic phase signs evaluated by ECG. The treatment reduced sinus arrhythmia earlier in mice challenged with the Brazil strain. Additionally, most mice challenged with the Colombian strain never developed episodes of sinus arrhythmia. Despite this observation, no differences were detected in the frequencies of episodes of atrioventricular block. It is important to highlight that these ECG alterations occurred in mice with a reduced number of inflammatory cells in their heart. This dichotomy most likely reflects the successful control by vaccination of the inflammatory reactions later during

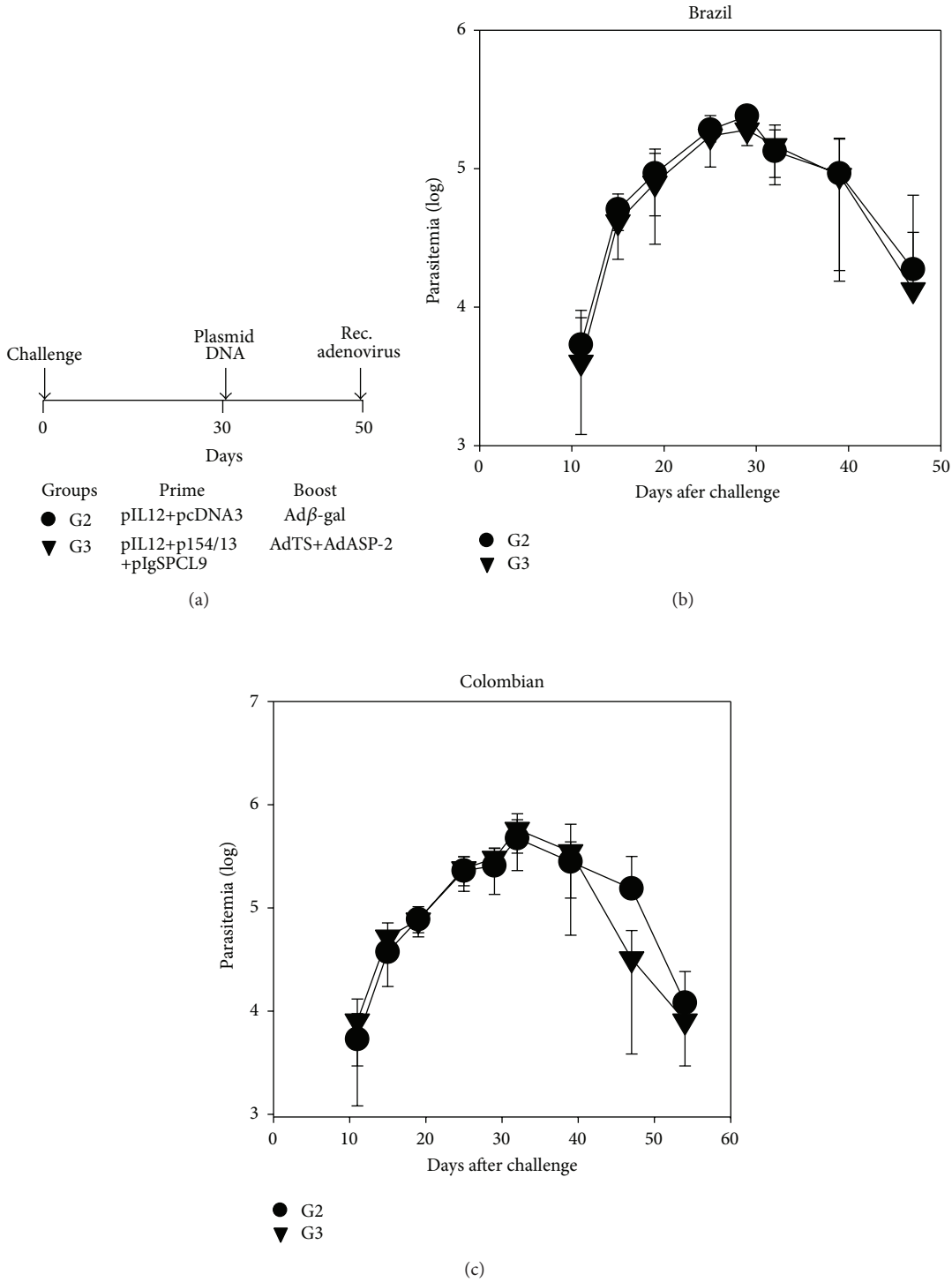

Figure 5: Impact of therapeutic vaccination in the immunity of resistant mice. (a) F1 (CB10XBALB/c) female mice were challenged s.c. with 1,000 trypomastigotes of the indicated parasite strain. Thirty days later, G2 mice received a mixture of control plasmid pcDNA3 and of pIL-12 (300 μg), and G3 mice were immunized with a mixture of pIL-12, pIgSPCl9, and p154/13 (300 μg). Twenty days later, these mice received, in these same spots, 100 μL of a viral suspension containing a total of 2×10^8 pfu of rec. adenovirus. For boosting, G2 mice received control adenovirus Adβgal, and G3 mice were immunized with a mixture of rec. adenovirus AdASP-2 and Ad-TS. (b) Mean parasitemia ± SD of each mouse group ($n = 6$) challenged with parasites of the Brazil strain. (c) Mean parasitemia ± SD of each mouse group ($n = 6$) challenged with parasites of the Colombian strain.

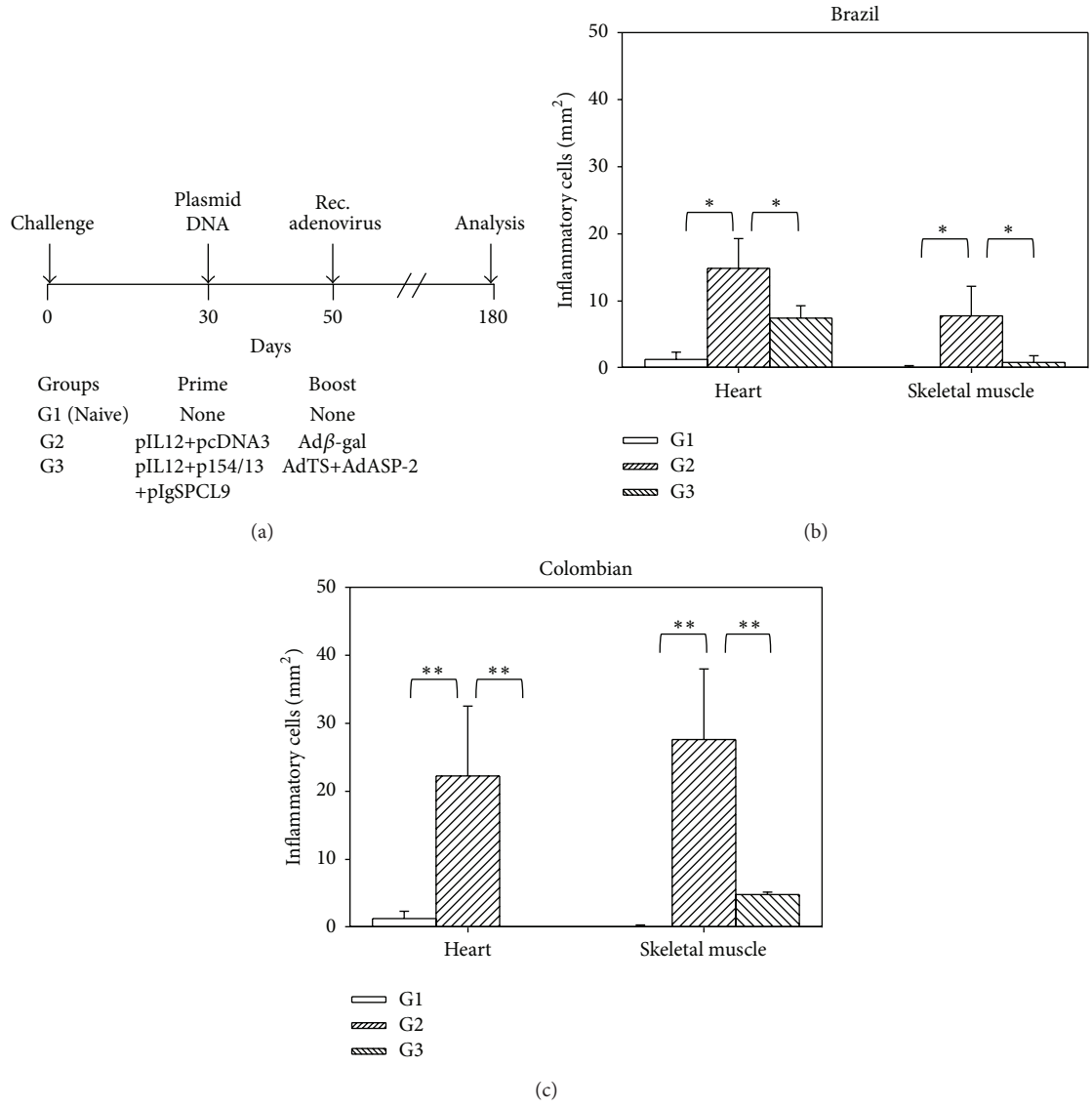

Figure 6: Frequencies of inflammatory cells in the hearts and skeletal muscles of resistant mice treated by the heterologous prime-boost regimen. (a) F1 (CB10XBALB/c) female mice were immunized i.m., as depicted. Details on the dose are shown Figure 5(a). (b) At 180 days, heart and skeletal muscle sections of mice challenged with the Brazil strain were stained with hematoxylin and eosin, and the number of inflammatory cells was quantified. Bars represent the mean of 6 mice/group ± SD. Asterisks denote that there was a significant difference between the indicated groups ($^{*}P < 0.05$ or $^{**}P < 0.01$). (c) The same as above, except that the mice were challenged with parasites of the Colombian strain.

infection, when the mice were euthanized. However, the damage to the heart had been established earlier and could no longer be reversed.

The reason why the T cells elicited by therapeutic genetic vaccination are not capable of reducing the symptoms is unknown at present. One possibility is that following infection, specific T cells are already committed to express the death receptor CD95, as we have recently described [29]. Once these cells express CD95, their viability is impaired, and they can no longer expand properly. It will be important to test this possibility because it has implications for the use of T cell vaccines for therapeutic purposes during this or other chronic diseases [30–36].

The protective immune mechanisms mediating the effects of our new vaccination regimen were not addressed in the present study. However, it is plausible that $CD4^{+}$ and $CD8^{+}$ T cells participate in this immune response, as we have previously described [15]. Corroborating this hypothesis is the fact that the addition of pIL-12 during priming led to a significant increase in the frequencies of multifunctional $CD8^{+}$ T cells and a parallel increase in the protective immunity against acute infection.

Table 2: Summary of the ECG records.

Days after challenge	Strain	Sinus arrhythmia mouse groups			*P* values		
		G1	G2	G3	G1 × G2	G1 × G3	G2 × G3
90	Brazil	0/6	10/6	0/6	*0.001*	NS	*0.012*
120	Brazil	0/6	10/6	1/6	*0.001*	NS	*0.044*
150	Brazil	0/6	11/6	5/6	*0.001*	*0.007*	NS
180	Brazil	0/6	4/6	4/6	0.03	0.03	NS
90	Colombian	0/6	3/6	1/5	NS	NS	NS
120	Colombian	0/6	3/6	0/5	NS	NS	NS
150	Colombian	0/6	12/6	0/5	*0.001*	NS	*0.013*
180	Colombian	0/6	16/6	1/5	*0.001*	NS	*0.022*
Days after challenge	Strain	Atrioventricular block mouse groups			*P* values		
		G1	G2	G3	G1 × G2	G1 × G3	G2 × G3
90	Brazil	0/6	36/6	46/6	*0.001*	*0.001*	NS
120	Brazil	0/6	19/6	22/6	*0.001*	*0.001*	NS
150	Brazil	0/6	5/6	6/6	*0.007*	*0.001*	NS
180	Brazil	0/6	5/6	3/6	*0.007*	NS	NS
90	Colombian	0/6	20/6	30/5	*0.001*	*0.001*	NS
120	Colombian	0/6	27/6	15/5	*0.001*	*0.001*	NS
150	Colombian	0/6	6/6	2/5	*0.001*	NS	NS
180	Colombian	0/6	10/6	10/5	*0.001*	*0.001*	NS

ECG record of mice challenged and treated as described in the legend of Figure 6(a). Values represent the number of episodes (sinus arrhythmia or atrioventricular block) recorded during one minute per total of mice analyzed and were compared by Fisher exact probability test.

In conclusion, this study reinforces and extends our previous work by demonstrating the improvement in acute and chronic symptoms after prophylactic genetic vaccination against *T. cruzi* infection using a vector expressing the TS and ASP-2 antigens.

Conflict of Interests

Ricardo Tostes Gazzinelli, Mauricio Martins Rodrigues, Alexandre Vieira Machado, and Oscar Bruna-Romero are named inventors on patent applications covering *Trypanosoma cruzi* vectored vaccines and immunization regimens. The other authors have no conflict of interests.

Acknowledgments

This work was supported by Grants from Fundação de Amparo à Pesquisa do Estado de São Paulo (2009/06820-4, 2013/13668/0, and 2012/22514-3) and Instituto Nacional de Ciência e Tecnologia em Vacina (INCTV-CNPq). Adriano Fernando Araújo, José Ronnie Vasconcelos, Mariana Ribeiro Dominguez, and Jonatan Ersching were recipients of fellowship from FAPESP. Oscar Bruna-Romero, Ricardo Tostes Gazzinelli, Milena Botelho Soares, and Mauricio Martins Rodrigues are recipients of fellowships from CNPq.

References

[1] P. J. Hotez, M. E. Bottazzi, C. Franco-Paredes, S. K. Ault, and M. R. Periago, "The neglected tropical diseases of Latin America and the Caribbean: a review of disease burden and distribution and a roadmap for control and elimination," *PLoS Neglected Tropical Diseases*, vol. 2, no. 9, article e300, 2008.

[2] K. Stuart, R. Brun, S. Croft et al., "Kinetoplastids: related protozoan pathogens, different diseases," *Journal of Clinical Investigation*, vol. 118, no. 4, pp. 1301–1310, 2008.

[3] A. R. L. Teixeira, M. M. Hecht, M. C. Guimaro, A. O. Sousa, and N. Nitz, "Pathogenesis of chagas' disease: parasite persistence and autoimmunity," *Clinical Microbiology Reviews*, vol. 24, no. 3, pp. 592–630, 2011.

[4] B. Y. Lee, K. M. Bacon, D. L. Connor, A. M. Willig, and R. R. Bailey, "The potential economic value of a *Trypanosoma cruzi* (Chagas disease) vaccine in Latin America," *PLoS Neglected Tropical Diseases*, vol. 4, no. 12, article e916, 2010.

[5] B. Y. Lee, K. M. Bacon, A. R. Wateska, M. E. Bottazzi, E. Dumonteil, and P. J. Hotez, "Modeling the economic value of a Chagas' disease therapeutic vaccine," *Human Vaccines and Immunotherapeutics*, vol. 8, no. 9, pp. 1293–1301, 2012.

[6] Y. Miyahira, "Trypanosoma cruzi infection from the view of $CD8^+$ T cell immunity—an infection model for developing T cell vaccine," *Parasitology International*, vol. 57, no. 1, pp. 38–48, 2008.

[7] S. I. Cazorla, F. M. Frank, and E. L. Malchiodi, "Vaccination approaches against *Trypanosoma cruzi* infection," *Expert Review of Vaccines*, vol. 8, no. 7, pp. 921–935, 2009.

[8] J. C. Vázquez-Chagoyán, S. Gupta, and N. J. Garg, "Vaccine development against *Trypanosoma cruzi* and Chagas disease," *Advances in Parasitology*, vol. 75, pp. 121–146, 2011.

[9] I. Quijano-Hernandez and E. Dumonteil, "Advances and challenges toward a vaccine against Chagas disease," *Human Vaccines*, vol. 7, no. 11, pp. 1184–1191, 2011.

[10] M. M. Rodrigues, A. C. Oliveira, and M. Bellio, "The immune response to *Trypanosoma cruzi*: role of toll-like receptors and perspectives for vaccine development," *Journal of Parasitology Research*, vol. 2012, Article ID 507874, 12 pages, 2012.

[11] E. Dumonteil, M. E. Bottazzi, and B. Zhan, "Accelerating the development of a therapeutic human Chagas disease: rationale and prospects," *Expert Reviews Vaccines*, vol. 11, pp. 1043–1055, 2012.

[12] C. P. Brandan and M. A. Basombrío, "Genetically attenuated *Trypanosoma cruzi* parasites as a potential vaccination tool," *Bioengineered*, vol. 3, no. 4, pp. 242–246, 2012.

[13] F. Costa, G. Franchin, V. L. Pereira-Chioccola, M. Ribeirão, S. Schenkman, and M. M. Rodrigues, "Immunization with a plasmid DNA containing the gene of trans-sialidase reduces *Trypanosoma cruzi* infection in mice," *Vaccine*, vol. 16, no. 8, pp. 768–774, 1998.

[14] A. E. Fujimura, S. S. Kinoshita, V. L. Pereira-Chioccola, and M. M. Rodrigues, "DNA sequences encoding $CD4^+$ and $CD8^+$T-cell epitopes are important for efficient protective immunity induced by DNA vaccination with a *Trypanosoma cruzi* gene," *Infection and Immunity*, vol. 69, no. 9, pp. 5477–5486, 2001.

[15] B. C. De Alencar, P. M. Persechini, F. A. Haolla et al., "Perforin and gamma interferon expression are required for CD4+ and CD8+ T-cell-dependent protective immunity against a human parasite, *Trypanosoma cruzi*, elicited by heterologous plasmid DNA prime-recombinant adenovirus 5 boost vaccination," *Infection and Immunity*, vol. 77, no. 10, pp. 4383–4395, 2009.

[16] F. A. Haolla, C. Claser, B. C. G. de Alencar et al., "Strain-specific protective immunity following vaccination against experimental *Trypanosoma cruzi* infection," *Vaccine*, vol. 27, no. 41, pp. 5644–5653, 2009.

[17] M. R. Dominguez, E. L. Silveira, J. R. de Vasconcelos et al., "Subdominant/cryptic CD8 T cell epitopes contribute to resistance against experimental infection with a human protozoan parasite," *PLoS ONE*, vol. 6, no. 7, Article ID e22011, 2011.

[18] M. R. Dominguez, J. Ersching, R. Lemos et al., "Re-circulation of lymphocytes mediated by sphingosine-1-phosphate receptor-1 contributes to resistance against experimental infection with the protozoan parasite *Trypanosoma cruzi*," *Vaccine*, vol. 30, no. 18, pp. 2882–2891, 2012.

[19] P. O. Rigato, B. C. de Alencar, J. R. C. de Vasconcelos et al., "Heterologous plasmid DNA prime-recombinant human adenovirus 5 boost vaccination generates a stable pool of protective long-lived CD^{8+} T effector memory cells specific for a human parasite, *Trypanosoma cruzi*," *Infection and Immunity*, vol. 79, no. 5, pp. 2120–2130, 2011.

[20] J. R. Vasconcelos, M. R. Dominguez, R. L. Neves et al., "Adenovirus vector-induced $CD8^+$ T effector memory cell differentiation and recirculation, but not proliferation, are important for protective immunity against experimental *Trypanosoma cruzi* infection," *Human Gene Therapy*, vol. 25, no. 4, pp. 350–363, 2014.

[21] B. Zingales, S. G. Andrade, M. R. S. Briones et al., "A new consensus for Trypanosoma cruzi intraspecific nomenclature: second revision meeting recommends TcI to TcVI," *Memórias do Instituto Oswaldo Cruz*, vol. 104, no. 7, pp. 1051–1054, 2009.

[22] M. A. Miles, M. S. Llewellyn, M. D. Lewis et al., "The molecular epidemiology and phylogeography of Trypanosoma cruzi and parallel research on *Leishmania*: looking back and to the future," *Parasitology*, vol. 136, no. 12, pp. 1509–1528, 2009.

[23] A. L. Rakhmilevich, J. Turner, M. J. Ford et al., "Gene gun-mediated skin transfection with interleukin 12 gene results in regression of established primary and metastatic murine tumors," *Proceedings of the National Academy of Sciences of the United States of America USA*, vol. 93, no. 13, pp. 6291–6296, 1996.

[24] S. B. Boscardin, S. S. Kinoshita, A. E. Fujimura, and M. M. Rodrigues, "Immunization with cDNA expressed by amastigotes of *Trypanosoma cruzi* elicits protective immune response against experimental infection," *Infection and Immunity*, vol. 71, no. 5, pp. 2744–2757, 2003.

[25] A. V. Machado, J. E. Cardoso, C. Claser, M. M. Rodrigues, R. T. Gazzinelli, and O. Bruna-Romero, "Long-term protective immunity induced against *Trypanosoma cruzi* infection after vaccination with recombinant adenoviruses encoding amastigote surface protein-2 and *trans*-sialidase," *Human Gene Therapy*, vol. 17, no. 9, pp. 898–908, 2006.

[26] J. F. Vasconcelos, B. S. Souza, and T. F. Lins, "Administration of granulocyte colony-stimulating factor induces immunomodulation, recruitment of T regulatory cells, reduction of myocarditis and decrease of parasite load in a mouse model of chronic Chagas disease cardiomyopathy," *FASEB Journal*, vol. 27, no. 12, pp. 4691–4702, 2013.

[27] C. H. Olsen, "Statistics in infection and immunity revisited," *Infection and Immunity*, vol. 82, no. 3, pp. 916–920, 2014.

[28] N. Winstone, A. J. Wilson, G. Morrow et al., "Enhanced control of pathogenic Simian immunodeficiency virus SIVmac239 replication in macaques immunized with an interleukin-12 plasmid and a DNA prime-viral vector boost vaccine regimen," *Journal of Virology*, vol. 85, no. 18, pp. 9578–9587, 2011.

[29] J. R. Vasconcelos, O. Bruña-Romero, A. F. Araújo et al., "Pathogen-induced proapoptotic phenotype and high CD95 (Fas) expression accompany a suboptimal $CD8^+$ T-cell response: reversal by adenoviral vaccine," *PLoS Pathogen*, vol. 8, no. 5, Article ID e1002699, 2012.

[30] P. Stephens, "Vaccine R&D: past performance is no guide to the future," *Vaccine*, vol. 32, no. 19, pp. 2139–2142, 2014.

[31] E. S. Pronker, T. C. Weenen, H. Commandeur, E. H. Claassen, and A. D. Osterhaus, "Risk in vaccine research and development quantified," *PLoS ONE*, vol. 8, no. 3, Article ID e57755, 2013.

[32] M. Karkada, N. L. Berinstein, and M. Mansour, "Therapeutic vaccines and cancer: focus on DPX-0907," *Biologics*, vol. 8, pp. 27–38, 2014.

[33] D. Majhen, H. Calderon, N. Chandra et al., "Adenovirus-based fighting infectious diseases and cancer: progress in the field," *Human Gene Therapy*, vol. 25, no. 4, pp. 301–317, 2014.

[34] G. Carcelain and B. Autran, "Immune interventions in HIV infection," *Immunological Reviews*, vol. 254, no. 1, pp. 355–371, 2013.

[35] C. Montagnani, E. Chiappini, L. Galli, and M. de Martino, "Vaccine tuberculosis: what's new?" *BMC Infectious Diseases*, vol. 14, supplement 1, article S2, 2014.

[36] J. R. Vasconcelos, M. R. Dominguez, A. F. Ara et al., "Relevance of long-lived CD8(+) T effector memory cells for protective immunity elicited by heterologous prime-boost vaccination," *Frontiers in Immunology*, vol. 3, p. 358, 2012.

Hindawi Publishing Corporation
Mediators of Inflammation
Volume 2014, Article ID 580919, 9 pages
http://dx.doi.org/10.1155/2014/580919

Research Article

Aspirin Modulates Innate Inflammatory Response and Inhibits the Entry of *Trypanosoma cruzi* in Mouse Peritoneal Macrophages

Aparecida Donizette Malvezi,[1] Rosiane Valeriano da Silva,[1] Carolina Panis,[1] Lucy Megumi Yamauchi,[2] Maria Isabel Lovo-Martins,[1] Nagela Ghabdan Zanluqui,[1] Vera Lúcia Hideko Tatakihara,[1] Luiz Vicente Rizzo,[3] Waldiceu A. Verri Jr.,[4] Marli Cardoso Martins-Pinge,[5] Sueli Fumie Yamada-Ogatta,[2] and Phileno Pinge-Filho[1]

[1] *Laboratório de Imunopatologia Experimental, Departamento de Ciências Patológicas, Centro de Ciências Biológicas, Universidade Estadual de Londrina, 86057-970 Londrina, PR, Brazil*
[2] *Laboratório de Biologia Molecular de Microrganismos, Departamento de Microbiologia, Centro de Ciências Biológicas, Universidade Estadual de Londrina, 86057-970 Londrina, PR, Brazil*
[3] *Instituto Israelita de Ensino e Pesquisa Albert Einstein, 056510-901 São Paulo, SP, Brazil*
[4] *Departamento de Ciências Patológicas, Centro de Ciências Biológicas, Universidade Estadual de Londrina, 86057-970 Londrina, PR, Brazil*
[5] *Departamento de Ciências Fisiológicas, Centro de Ciências Biológicas, Universidade Estadual de Londrina, 86057-970 Londrina, PR, Brazil*

Correspondence should be addressed to Phileno Pinge-Filho; pingefilho@uel.br

Received 3 March 2014; Revised 13 May 2014; Accepted 20 May 2014; Published 19 June 2014

Academic Editor: Marcelo T. Bozza

The intracellular protozoan parasite *Trypanosoma cruzi* causes Chagas disease, a serious disorder that affects millions of people in Latin America. Cell invasion by *T. cruzi* and its intracellular replication are essential to the parasite's life cycle and for the development of Chagas disease. Here, we present evidence suggesting the involvement of the host's cyclooxygenase (COX) enzyme during *T. cruzi* invasion. Pharmacological antagonist for COX-1, aspirin (ASA), caused marked inhibition of *T. cruzi* infection when peritoneal macrophages were pretreated with ASA for 30 min at 37°C before inoculation. This inhibition was associated with increased production of IL-1β and nitric oxide ($NO^{\bullet}$) by macrophages. The treatment of macrophages with either NOS inhibitors or prostaglandin E_2 (PGE_2) restored the invasive action of *T. cruzi* in macrophages previously treated with ASA. Lipoxin ALX-receptor antagonist Boc2 reversed the inhibitory effect of ASA on trypomastigote invasion. Our results indicate that PGE_2, $NO^{\bullet}$, and lipoxins are involved in the regulation of anti-*T. cruzi* activity by macrophages, providing a better understanding of the role of prostaglandins in innate inflammatory response to *T. cruzi* infection as well as adding a new perspective to specific immune interventions.

1. Introduction

Trypanosoma cruzi is an intracellular protozoan parasite causing Chagas disease, which affects millions of people in Latin America. During the acute inflammatory phase of the *T. cruzi* infection, high-level expression of inducible nitric oxide synthase (iNOS) [1], proinflammatory cytokines [2], and arachidonic acid- (AA-) derived lipids such as leukotrienes, lipoxins (LXs), H (P) ETEs, prostaglandins, and thromboxane is prevalent [3, 4]. In the early *T. cruzi* infection, nitric oxide ($NO^{\bullet}$) and arachidonic acid metabolites could be attributed to resistance, but later on to tissue damage [4].

Prostaglandins (PGs) are oxygenated lipid mediators formed from the ω6 essential fatty acid, arachidonic acid

(AA). The committed step in PG biosynthesis is the conversion of AA to PG H_2 (PGH_2), catalyzed by either PG endoperoxide H synthase-1 or -2, commonly known as cyclooxygenase-1 (COX-1) and cyclooxygenase-2 (COX-2), respectively [5, 6]. Both COX-1 and COX-2 are nonselectively inhibited by nonsteroidal anti-inflammatory drugs (NSAIDs) such as aspirin and ibuprofen, whereas COX-2 activity is selectively blocked by COX-2 inhibitors called coxibs (e.g., celecoxib) [7, 8]. The relevance of these enzymes and the bioactive lipids that they produce are not well understood in parasitic disease, although the role of eicosanoids in the pathogenesis of Chagas disease is becoming more defined [3]. Pharmacological antagonists of COX-1 (aspirin, ASA), COX-2 (celecoxib), or both (indomethacin) have been found to increase mortality and parasitemia (parasite load in peripheral blood and cardiac tissue) regardless of which mouse or *T. cruzi* strains were used [9–13]. Moreover, evidence suggests that administration of NSAIDs may enhance mortality in chagasic patients [12]. Conversely, others have found that inhibition of PG synthesis/release reduces parasitemia and extends survival of mice infected with *T. cruzi* [14–17]. This was often associated with a decrease in the levels of circulating inflammatory cytokines (such as TNF-α, IFN-γ, and IL-10) [16]. More recently, treatment with ASA during chronic infection was found to be beneficial with no increase in mortality and substantial improvement in cardiac function [13]. Additionally, the protective effect of ASA could be mediated by the synthesis of 15-epi-lipoxin A_4 (15-epi-LXA_4) [18].

Given the increasing interest in the role of eicosanoids in *T. cruzi* infection, we decided to investigate the effect of prostaglandin synthesis inhibition with ASA on inflammatory response and macrophage invasion by *T. cruzi*.

2. Material and Methods

2.1. Animals. Six- to eight-week-old BALB/c female and male mice were supplied by the Multi-Institutional Center for Biological Investigation, State University of Campinas, Brazil. Mice were maintained under standard conditions in the animal house of the Department of Pathological Sciences, Center for Biological Sciences, State University of Londrina. Commercial rodent diet (Nuvilab-CR1, Quimtia-Nuvital, Colombo, Brazil) and sterilized water were available *ad libitum*.

All animal procedures were performed in accordance with the guidelines of the Brazilian Code for the Use of Laboratory Animals. The protocols were approved by the Internal Scientific Commission and the Ethics in Animal Experimentation Committee of Londrina State University (Approval Number: CEEA 5492.2012.22).

2.2. Parasites. T. cruzi Y [19] was maintained by weekly intraperitoneal inoculation of Swiss mice with 2×10^5 trypomastigotes. To conduct our experiments, blood from previously infected mice was obtained by cardiac puncture without anticoagulant. The blood was centrifuged at 1,500 ×g for 1 min and allowed to stand at 37°C for 60 min. The supernatant serum containing most of the *T. cruzi* was centrifuged at 1,200 ×g for 15 min. The sediment was resuspended in 1 mL of RPMI 1640 medium (GIBCO, Gran Island, NY) containing 10% inactivated fetal bovine serum (FBS), 100 units of penicillin, and 100 μg streptomycin (GIBCO, Gran Island, NY).

Trypomastigotes were derived from the supernatant of *T. cruzi*-infected LLC-Mk2 culture cells (ATCC CCL-7; American Type Culture Collection, Rockville, MD) grown in RPMI 1640 medium containing 10% inactivated fetal bovine serum (FBS), 40 $\mu g\,mL^{-1}$ gentamicin, 100 units of penicillin, and 100 μg streptomycin (GIBCO, Gran Island, Y). Subconfluent cultures of LLC-Mk2 were infected with 5×10^6 trypomastigotes. Free parasites were removed after 24 h and cultures were maintained in 10% FBS-RPMI 1640. Five days postinfection, free trypomastigote forms could be found in the cell supernatants.

2.3. Macrophage Culture. Mice were inoculated intraperitoneally with 2 mL of 5% thioglycollate and, 4 days later, the elicited cells from the peritoneal exudates were harvested in cold PBS. Mouse peritoneum was washed with 5 mL ice-cold, serum-free RPMI. Peritoneal cells from 3–6 mice were pooled and left to adhere in complete medium (RPMI, 2 mM glutamine, 1 mM sodium pyruvate, 40 $\mu g\,mL^{-1}$ gentamicin, and 10 mM HEPES) for 24 h in 24-well plates at 2×10^5 cells/well. Each suspension of pooled peritoneal cells was plated in triplicate wells. Then, nonadherent cells were washed away and adherent cells received complete medium. The macrophages were plated onto 13 mm round glass coverslips and washed in warm phosphate-buffered saline (PBS) before the interaction assays. In addition, 2.0×10^5 macrophages were plated onto 96-well dishes. One set of plates was used to quantify IL-1β and the other set for $NO^{\bullet}$ detection.

2.4. Treatment of Macrophages with Drugs and Macrophage Invasion Assay. Before the experiments, peritoneal macrophages previously washed were incubated for 30 min at 37°C in a 5% CO_2 atmosphere in the presence of different concentrations of ASA (2.5 mM, 1.25 mM, and 0.625 mM) to test its effect on internalization of the parasite into the host cell. After incubation, the medium containing ASA was removed, and macrophages were allowed to interact with trypomastigote forms added in a ratio of 5 parasites per cell. The interaction was allowed to proceed for 2 h, at 37°C in a 5% CO_2 atmosphere. The cells were then washed three times, fixed with Bouin's fixative, stained with Giemsa (Merck) stain, and observed with a light microscope at 1000x magnification. Other treatments included incubation with aminoguanidine (1 mM) or L-NAME (1.0 mM) for 60 min at 37°C with or without ASA.

The internalization index was calculated by multiplying the percentage of infected cells by the mean number of parasites per infected cell [20]. All internalization indices were normalized. Experiments were performed in triplicate,

and six independent experiments were completed. All experiments included untreated, infected peritoneal macrophages as controls. The quantification was carried out using light microscopy where a total of 500 cells were randomly counted. The viability of the cells obtained from the cultures before and after incubation experiments was determined using MTT (Sigma-Aldrich) assay, showing the mitochondrial activity of living cells. The culture medium was aspirated, and MTT ($0.5\,mg\,mL^{-1}$) was added to the cells prior to incubation at 37°C for 4 h. The supernatant was aspirated and dimethyl sulfoxide (Sigma-Aldrich) was added to the wells. Insoluble crystals were dissolved by mixing and the plates were read using a BioRad multiplate reader (Hercules, CA), at a test wavelength of 570 nm and a reference wavelength of 630 nm.

2.5. Nitrite Measurements. Production of nitric oxide ($NO^{\bullet}$) was determined by measuring the level of accumulated nitrite, a metabolite of $NO^{\bullet}$ in the culture supernatant using Griess reagent (Sigma-Aldrich). After 24 h of treatment with ASA (0.625 mM), the culture supernatants were collected and mixed with an equal volume of Griess reagent in 96-well culture plates and incubated at room temperature for 10 min. The absorbance was measured at 540 nm and nitrite concentrations were calculated by reference to a standard curve generated by known concentrations of sodium nitrite.

2.6. Immunocytochemistry Labeling for iNOS. Immunocytochemistry for iNOS was performed on coverslip-adherent cells using the labeled streptavidin biotin method with a LSAB KIT (DAKO Japan, Kyoto, Japan) without microwave accentuation. The coverslips were incubated with 10% Triton X-100 solution for 1 h, washed 3 times in PBS, and treated for 40 min at room temperature with 10% BSA. The coverslips were then incubated overnight at 4°C with the primary antibody (anti-iNOS rabbit monoclonal antibody diluted 1 : 200, BD Biosciences, catalog number 610599), followed by secondary antibody treatment for 2 h at room temperature. Horseradish peroxidase activity was visualized by treatment with H_2O_2 and 3,3′-diaminobenzidine (DAB) for 5 min. At the last step, the sections were weakly counterstained with Harry's hematoxylin (Merck). For each case, negative controls were prepared by omitting the primary antibody. Intensity and localization of immune reaction against primary antibody used were examined on all coverslips using a photomicroscope (Olympus BX41, Olympus Optical Co., Ltd., Tokyo, Japan). For the image analysis study, photomicroscopic color slides of representative areas (magnification, 40x) were digitally acquired. After conversion of the images into grey scale (Adobe Photoshop) iNOS-positive pixels and total pixels became thresholds and were processed by Image J program. Positive immunostained area was calculated as the proportion of positive pixels to total pixels (%).

2.7. ELISA for IL-1β. Culture supernatants from peritoneal macrophages in 96-well plates treated with ASA (0.625 mM) or untreated, either infected or not infected with *T. cruzi*, were incubated for 24 h. Levels of IL-1β in 100 μL medium were measured by commercial ELISA kits (Ready-SET-Go! eBioscience, San Diego, CA), according to the manufacturer's instructions.

2.8. Statistical Analysis. The statistical analysis was conducted using one way ANOVA with Bonferroni's multiple comparison test. Values are presented as ± standard error of mean. The results were considered significant when $P < 0.05$. Statistical analysis was performed using the GraphPad Prism 5.0 computer software application (GraphPad Software, San Diego, CA, USA).

3. Results

3.1. Aspirin Inhibits T. cruzi Entry into Macrophages. To determine whether COX-derived mediators are involved in *T. cruzi* entry into host cells, cells were treated with increasing amounts of ASA for 30 min and after treatment, the medium containing ASA was removed before macrophage invasion assay in order to guarantee that ASA affected only the host cell and not the parasites. After 2 h of incubation with parasites, which provides sufficient time for them to enter into macrophages, the free parasites were removed. Aspirin irreversibly inhibits COX-1 by acetylation of a single serine residue on the enzyme [21] and this inactivation persists, that is, ≥24 hours. In some cases, the medium with increasing ASA concentrations was added every 24 hours until the end of the *T. cruzi* infection period (7 days, Figure 4(d)). Figure 1(a) shows that ASA markedly inhibited the internalization of trypomastigote by macrophages at all concentrations tested ($P < 0.0001$). Thus, PGE_2 synthesis inhibition using ASA improves macrophage response against *T. cruzi* infection. The cytotoxicity of ASA in macrophages was evaluated by MTT assay (Figure 1(a), insert). ASA did not induce cell death, as the concentrations of ASA used in all experiments reported were too low to cause cytotoxicity [22]. Light microscopy observations confirm *T. cruzi* inhibition invasion of ASA treated cells (Figure 1(c)).

3.2. COX-2 Inhibition Together with Aspirin Restores the Infectivity of Trypomastigotes in Peritoneal Macrophages. We examined the combined effect of celecoxib (COX-2 selective inhibitor) and ASA on the entry of *T. cruzi* into phagocytic cells. Peritoneal macrophages were incubated separately, with or without drugs (ASA and celecoxib) either alone or in combination. Figure 1(b) shows that the drugs in combination significantly ($P < 0.01$) restored the invasive capacity of trypomastigotes. None of the drugs (ASA, celecoxib, or their combination) showed cytotoxicity against uninfected peritoneal macrophages (data not shown). These results indicate that the enzyme activities of COX-1 and COX-2 favor invasion, but simultaneous inhibition of both activities also favors parasite invasion, probably by allowing a new panorama of eicosanoids production.

3.3. Aspirin Decreases Trypomastigotes Release to Culture Supernatants from T. cruzi-Infected Macrophages. Four days postinfection, macrophages began releasing trypomastigotes into the supernatant (Figure 4(d)). Trypomastigotes release

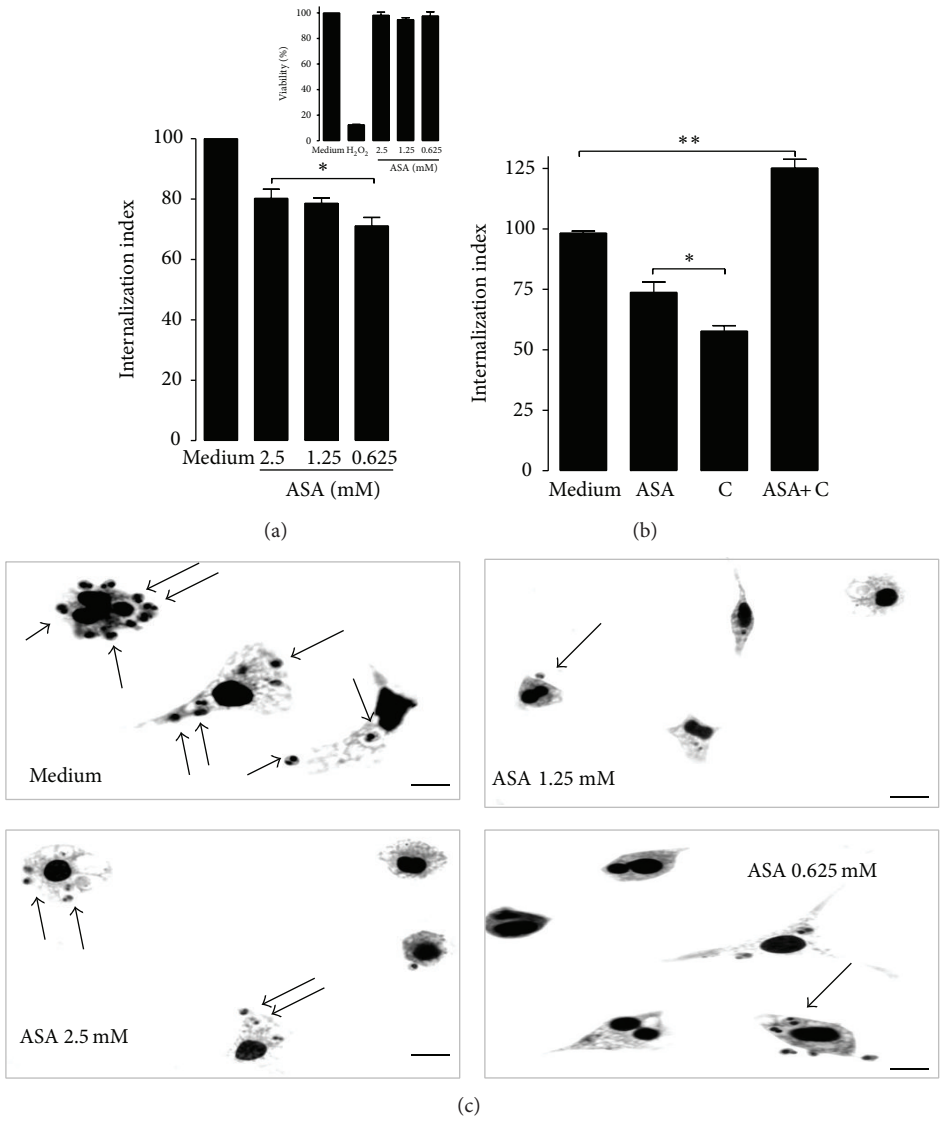

Figure 1: Aspirin (ASA) impairs *Trypanosoma cruzi* internalization by peritoneal macrophages. (a) Internalization index of the interaction process between macrophages treated for 30 minutes with increasing concentrations of ASA (0.625, 1.25, and 2.5 mM) and exposed to *T. cruzi* (Y strain). After treatment with ASA, peritoneal macrophages interacted with 5 : 1 trypomastigotes for 2 hours, after which they are washed, fixed with Bouin's fixative, and stained with Giemsa. Quantification was carried out under a light microscope where the number of intracellular parasites was counted in a total of at least 500 cells. MTT assay to measure cell viability in macrophages after treatment with ASA at 0.625 to 2.5 mM concentrations. H_2O_2 (1000 μM) was used as negative control (insert). Values are the means ± standard error of mean of 10 experiments or two experiments (MTT assay). $^{*}P < 0.0001$ for a comparison with infected cells cultured in medium alone. (b) The combined effect of celecoxib and aspirin on the entry of *T. cruzi* into phagocytic cells. Macrophages were treated for 30 minutes with celecoxib (0.625 mM) and ASA (0.625 mM) exposed to *T. cruzi* as describe above. Results are the mean ± standard error for triplicate determinations and are representative of three independent experiments. $^{*}P < 0.0001$, $^{**}P < 0.001$ for a comparison with infected cells cultured in medium alone. (c) Light microscopy observations confirm *T. cruzi* inhibition invasion of ASA treated cells. Observation after Giemsa staining by light microscopy of the interaction process between peritoneal macrophages treated (or not) with different concentration of ASA and exposed to trypomastigotes forms of *T. cruzi*. The black arrows indicate internalized parasites. Bars = 10 μm.

to culture supernatants from *T. cruzi*-infected macrophages was diminished by ASA (0.625 mM). This result is in agreement with previous reports, showing that aspirin and other COX inhibitors decrease *T. cruzi* infection *in vitro* [14–16, 23].

3.4. Aspirin Inhibits T. cruzi Entry into Macrophages via ALX. Lipoxins (LXs) are endogenous lipid mediators with potent anti-inflammatory and proresolving actions [24, 25]. Native LXs and their stable analogues exert their biological effects by binding to a G-protein-coupled receptor, denoted as ALX [26, 27]. The effect of ASA has been associated, in part, to a switch to the AA pathway linked to the acetylation of the COX-2 isoenzyme. This reaction enables COX-2 to synthesize LXs as 15-epi-LXs (15-epi-LXA4) [22]. To evaluate

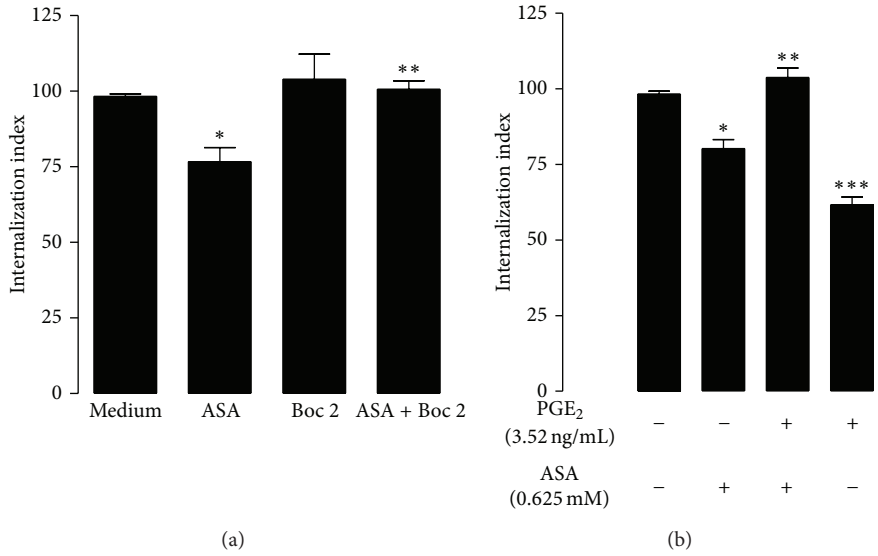

Figure 2: The effect of ASA on the entry of *T. cruzi* into macrophages was prevented by Boc-2. (a) Internalization index of the interaction process between macrophages treated for 30 minutes separately either with or without drugs (0.625 μM ASA or 100 μM Boc-2). Results are the mean ± standard error for triplicate determinations and are representative of two independent experiments. $^{*}P < 0.01$, for a comparison with infected cells cultured in medium alone. $^{**}P < 0.001$, for a comparison with infected cell treated with ASA. (b) PGE_2 restores aspirin effect on *T. cruzi* entry into macrophages. Macrophages were treated for 30 minutes separately either with or without PGE_2 (35.2, 3.52, or 0.35 ng mL^{-1}) alone or in combination (ASA 0.625 mM + PGE_2 3.52 ng mL^{-1}). Results are the mean ± standard error and are representative of two independent experiments. $^{*}P < 0.001$ for a comparison with infected cells cultured in medium alone. $^{**}P < 0.05$ for comparison with infected cell treated with ASA or PGE_2 alone. $^{***}P < 0.05$ for a comparison with infected cells cultured in medium alone.

the effect of ASA-triggered LXs on the entry of *T. cruzi* into phagocytic cells, peritoneal macrophages were incubated separately either with or without drugs (ASA or Boc-2, a specific antagonist of the 15-epi-LXs) either alone or in combination. The inhibitory effect of ASA on the entry of *T. cruzi* into macrophages was prevented by Boc-2 demonstrating that the effect of ASA on the entry of *T. cruzi* into macrophages could be mediated by the synthesis of 15-epi-LXA4. Furthermore, Boc-2 did not have any effect on the entry of *T. cruzi* into macrophages when used alone (Figure 2(a)).

3.5. PGE_2 Restores Aspirin Effect on T. cruzi Entry into Macrophages. Figure 2(b) (insert) shows that treatment of macrophages with high concentrations of PGE_2 causes inhibition of *T. cruzi* entry into macrophages. When PGE_2 (3.52 ng mL^{-1}) was added alone or in combination with ASA, the effect of ASA was inhibited, indicating that PGE_2 is involved in the internalization of *T. cruzi* trypomastigotes into peritoneal macrophages.

3.6. Aspirin Modulates Innate Inflammatory Response of Macrophages Infected with T. cruzi. The internalization of *T. cruzi* into macrophages stimulated the release of IL-1β while ASA increased IL-1β production by infected macrophages (Figure 3(a)). The effect of ASA on $NO^{\bullet}$ production was evaluated by detection of nitrite in *T. cruzi*-infected macrophage supernatants using Griess reaction (Figure 3(b)). $NO^{\bullet}$ production in macrophages was stimulated by *T. cruzi* and was also increased by prior treatment of macrophages with ASA.

In addition, we observed that ASA treatment stimulated iNOS expression in *T. cruzi*-infected macrophages (Figure 4(a)). To confirm that the effect of ASA on macrophage activity depends on $NO^{\bullet}$ levels, we assessed the entry of trypomastigotes into macrophages incubated with aminoguanidine (AG, iNOS inhibitor) or with L-NAME (c-NOS inhibitor). We found that both inhibitors reversed the effects of ASA (Figures 4(b) and 4(c)).

4. Discussion

Previous studies have shown that the release of eicosanoids during infection with *T. cruzi* regulates host responses and controls disease progression [3, 10, 11, 13, 14, 28–31]. PGs, together with $NO^{\bullet}$ and TNF-α, participate in a complex circuit that controls lymphoproliferative and cytokine responses in *T. cruzi* infection [10]. However, the involvement of COX-mediated PG production in the entry of *T. cruzi* into macrophages is largely unexplored. The data shown herein demonstrates that the treatment of macrophages with ASA significantly inhibits internalization of *T. cruzi* trypomastigotes and strongly supports the idea that the COX pathway plays a fundamental role in the process of parasite invasion. In fact, PGE_2production increases significantly in *T. cruzi*-infected macrophages as compared to uninfected macrophages [32] and synergistically enhances the activity of nifurtimox and benznidazole on infected RAW 264.7 cells [23].

Ours results suggest that the actions of ASA depend on COX-2-derived biosynthesis of products. This is

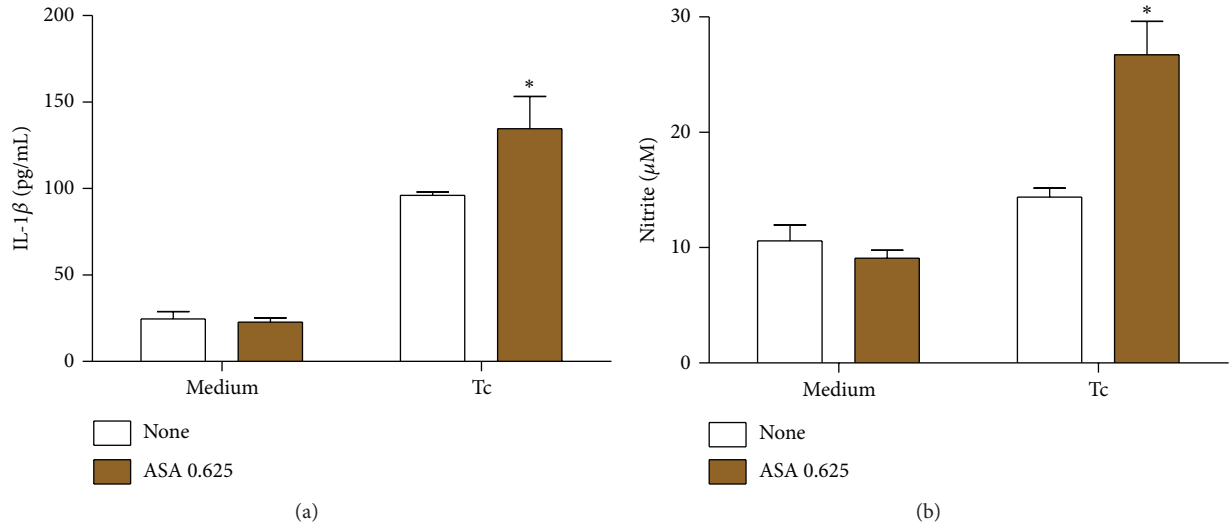

Figure 3: Effects of ASA upon IL-1β and nitrite production in *T. cruzi*-infected macrophages. Macrophages were treated for 30 minutes with ASA (0.625 mM) and exposed to *T. cruzi* (Y strain). After treatment with ASA, cells interacted with 5 : 1 trypomastigotes for 2 hours, after which they are cultured at 37°C in 5% CO_2 during 24 h. Afterwards, IL-1β (a) and nitrite (b) levels in supernatant were measured with a specific enzyme-linked immunosorbent assay and by Griess reaction, respectively. Results are the mean ± standard error for duplicate determinations and are representative of four independent experiments. $^*P < 0.05$ for a comparison with cell culture in medium alone.

demonstrated by the observation that celecoxib reversed the aspirin-induced inhibition of entry of *T. cruzi* into macrophages. The problem of NSAIDs coadministration is actively discussed in literature in the context of uncertainty of the resulting therapeutic and side effects arising from such combinations. The mechanism of such a suppression of aspirin inhibitory effect on COX-1 by other NSAIDs has been difficult to satisfactorily explain. This could be due to celecoxib binding strongly to a monomer of COX-1 without affecting AA oxygenation [7]. In fact, a related study has shown that celecoxib prevented ASA inhibition in a dog model of thrombosis [33]. However, the application of our approach to investigate the combined effect of aspirin and celecoxib on COX-1 during coadministration confirmed the ability of celecoxib to suppress the aspirin-mediated inhibition of COX-1 *in vitro* conditions [7].

In addition, the effects of ASA on *T. cruzi* infection have been associated in part, to a switch to the AA pathway linked to the acetylation of the COX-2 isoenzyme [18]. Such modification promotes the synthesis of the 15-R-HETE intermediate, which can be transformed by 5-lipooxygenase to 15-epi-LXA4, a lipid involved in the resolution of inflammation [34]. Accordingly, we assessed the effect of Boc-2 (a specific antagonist of the 15-epi-LXs) on low doses of ASA, indicating that 15-epi-LXA4 is probably involved in the inhibitory effect exerted by ASA on the internalization of *T. cruzi* by macrophages.

Interestingly, when macrophages were treated with PGE_2 concentration as high as 3.52 ng mL^{-1}, we observed a reduction in the entry of parasites, but when we used low concentration of PGE_2 (0.35 ng mL^{-1}), the entry of *T. cruzi* was similar to that observed in untreated macrophages. In addition, we found reversal of ASA effect, even when PGE_2 concentration as low as 3.52 ng mL^{-1} was used, indicating that PGE_2 has an important role in ASA effect. Inhibition of COX activity may increase $NO^\bullet$ levels, thus restoring the antiparasitic activity of macrophages [23]. Our results are in agreement with this hypothesis. To confirm that the effect of ASA on macrophage activity depends upon restoring $NO^\bullet$ levels, we assessed the invasive capacity of *T. cruzi* when cells were incubated with aminoguanidine (AG), an iNOS inhibitor. We found that 1.0 mM AG reverses ASA effect totally. In addition, we showed that iNOS expression in macrophages was increased with ASA treatment, suggesting that iNOS-dependent $NO^\bullet$ production is responsible for ASA effects. We did find reversal of ASA effect with L-NAME (1.0 mM), indicating the role of cNOS in ASA activity. This can be explained as high concentrations of L-NAME may interfere in the selectivity for cNOS and can inhibit other isoforms of NOS, such as nNOS and iNOS. So, $NO^\bullet$ deficiency induced by L-NAME could be explaining our results.

Additionally, polyamines seem to be crucial for trypomastigote internalization process in, at least, some cellular types and infection progression [35]. In *T. cruzi*-infected macrophages, COX is related to the increase of ornithine decarboxylase (ODC) activity [15], which might increase the polyamine content in macrophages. Since *T. cruzi* uses these polyamines to synthesize trypanothione (an enzyme that participates in the hydroperoxide detoxification of *T. cruzi*), the inhibition of COX by ASA probably resulted in a reduction in polyamine levels caused by inhibition of ODC, indirectly contributing to decrease trypanothione synthesis in *T. cruzi*, as suggested by López-Muñoz and collaborators [23].

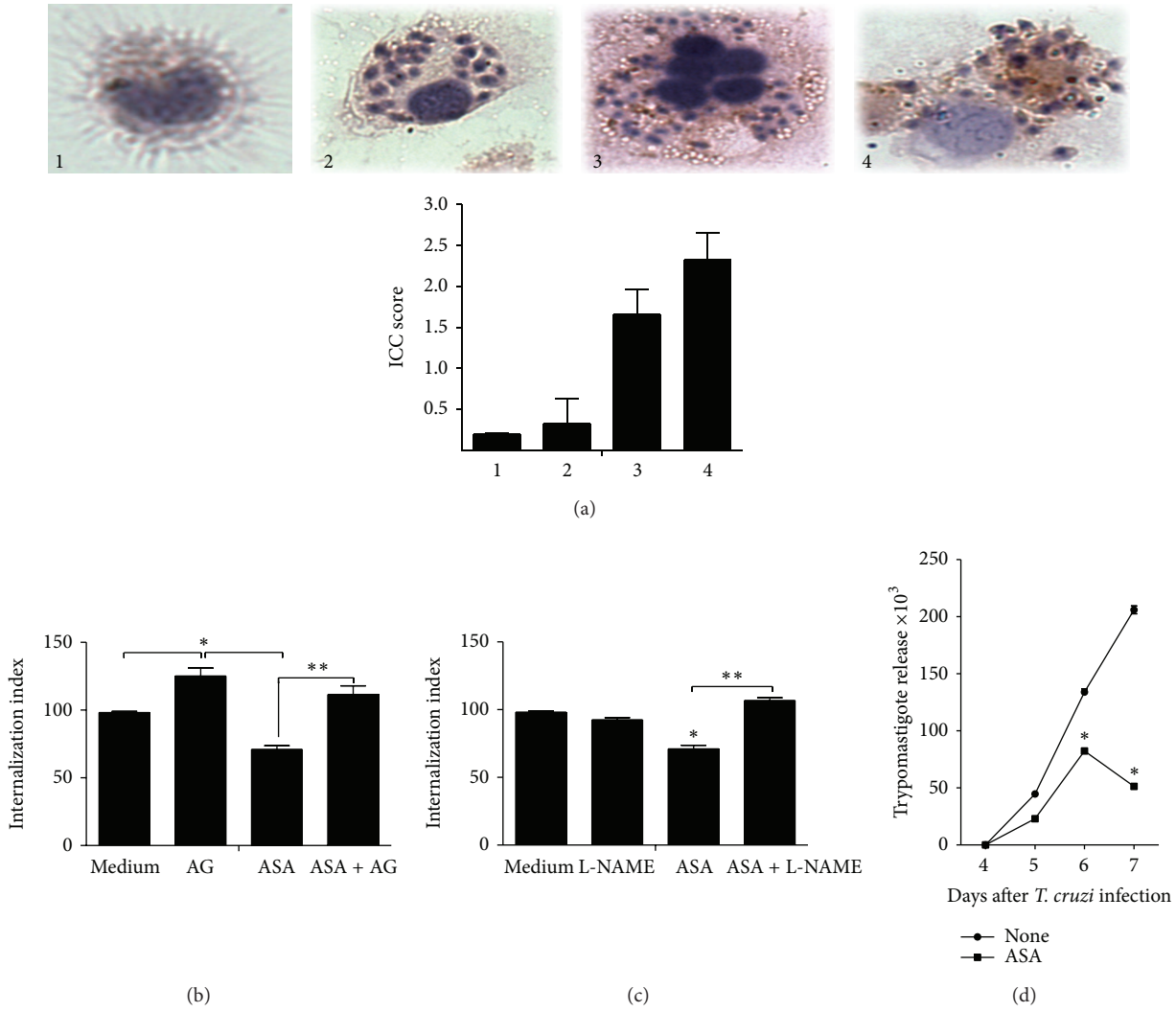

Figure 4: Effect of ASA on macrophage activity depends on $NO^{\bullet}$ production. (a) Aspirin treatment stimulated iNOs expression in *T. cruzi*-infected macrophages. Immunocytochemistry for iNOS was performed on coverslip-adherent cells using the labeled streptavidin biotin method with a LSAB KIT (DAKO Japan, Kyoto, Japan) without microwave accentuation. (1) Intracellular iNOS protein cannot be detected by immunocytochemistry in uninfected (control) macrophages, (2) *T. cruzi*-infected cell, (3) ASA (0.625 mM) was an effective inducer of iNOS expression in peritoneal macrophages, and (4) the addition of PGE_2 (3.52 ng mL^{-1}) to culture media increased iNOS mRNA expression in macrophages infected. Macrophages were treated for 30 minutes separately with 0.625 μM ASA. After treatment, macrophages were washed and incubated with aminoguanidine (AG, 1.0 mM) (b) or L-NAME (c) at 1.0 mM for 1 h at 37°C. After treatment, macrophages were washed again and interacted with 5 : 1 trypomastigotes for 2 hours at 37°C, after which they are washed, fixed with Bouin's fixative, and stained with Giemsa. Quantification was carried out under a light microscope where the number of intracellular parasites was counted in a total of at least 500 cells. Results are the mean ± standard error for triplicate determinations and are representative of two independent experiments. (d) Effect of aspirin upon trypomastigote release in aspirin-treated *T. cruzi*-infected macrophages. Cells were infected with *T. cruzi* trypomastigotes and treated daily with ASA at 0.625 mM; after 4 days of treatment, trypomastigotes release to supernatants was found and was measured until day 7 after infection. Results are the mean ± standard error for triplicate determinations and are representative of two independent experiments. $^{*}P < 0.01$ for a comparison with infected cells cultured in medium alone. $^{**}P < 0.01$ for a comparison with infected cells cultured treated with ASA.

Finally, in *T. cruzi*-infected macrophages, COX inhibition by ASA was related to the increase of IL-1β, which also might explain the increase of antiparasitic activity of macrophages treated with ASA. In fact, IL-1β is critical for the restriction of *Leishmania amazonensis* infection [36] and it recently was demonstrated that macrophages treated with IL-1β released fewer trypomastigotes than untreated macrophages and IL-1β triggered $NO^{\bullet}$ release by *T. cruzi*-infected macrophages in a dose dependent manner [37].

5. Conclusion

In conclusion, this is the first report, to our knowledge, showing the *in vitro* effect of aspirin on *T. cruzi* entry into

peritoneal macrophages and the influence of COX pathway on innate inflammatory response to *T. cruzi* infection, adding a new perspective to immune interventions against Chagas disease.

Conflict of Interests

The authors declare no conflict of interests.

Authors' Contribution

P. Pinge-Filho, S. F. Yamada-Ogatta, M. C. Martins-Pinge, and L. V. Rizzo participated in research design. A. D. Malvezi, C. Panis, R. Valeriano da Silva, M. I. Lovo-Martins, N. G. Zanluqui, and V. L. H. Tatakihara conducted experiments. W. A. Verri Jr., and L. M. Yamauchi contributed to the new reagents or analytical tools. A. D. Malvezi, C. Panis, R. Valeriano da Silva, M. I. Lovo-Martins, and P. Pinge-Filho performed data analysis. A. D. Malvezi, C. Panis, and P. Pinge-Filho contributed to the writing of the paper.

Acknowledgments

This work was supported by the Conselho Nacional de Desenvolvimento Científico e Tecnológico, Brazil (CNPq, 302097/2010-474792/2011-0), Coordenação de Aperfeiçoamento de Pessoal de Nível Superior (CAPES), and the Fundação Araucaria (Convênio 419/2009). LVR, WAVJ, MCMP, and PPF received research fellowships from CNPq.

References

[1] M. E. Rottenberg, E. Castaños-Velez, R. de Mesquita, O. G. Laguardia, P. Biberfeld, and A. Örn, "Intracellular co-localization of *Trypanosoma cruzi* and inducible nitric oxide synthase (iNOS): evidence for dual pathway of iNOS induction," *European Journal of Immunology*, vol. 26, no. 12, pp. 3203–3213, 1996.

[2] J. A. Gomes, A. M. Molica, T. S. Keesen et al., "Inflammatory mediators from monocytes down-regulate cellular proliferation and enhance cytokines production in patients with polar clinical forms of Chagas disease," *Human Immunology*, vol. 75, no. 1, pp. 20–28, 2014.

[3] F. S. Machado, S. Mukherjee, L. M. Weiss, H. B. Tanowitz, and A. W. Ashton, "Bioactive lipids in *Trypanosoma cruzi* infection," *Advances in Parasitology*, vol. 76, pp. 1–31, 2011.

[4] R. L. Cardoni and M. I. Antúnez, "Circulating levels of cyclooxygenase metabolites in experimental *Trypanosoma cruzi* infections," *Mediators of Inflammation*, vol. 13, no. 4, pp. 235–240, 2004.

[5] B. Rocca and G. A. FitzGerald, "Cyclooxygenases and prostaglandins: shaping up the immune response," *International Immunopharmacology*, vol. 2, no. 5, pp. 603–630, 2002.

[6] J. Y. Park, M. H. Pillinger, and S. B. Abramson, "Prostaglandin E_2 synthesis and secretion: the role of PGE_2 synthases," *Clinical Immunology*, vol. 119, no. 3, pp. 229–240, 2006.

[7] G. Rimon, R. S. Sidhu, D. A. Lauver et al., "Coxibs interfere with the action of aspirin by binding tightly to one monomer of cyclooxygenase-1," *Proceedings of the National Academy of Sciences of the United States of America*, vol. 107, no. 1, pp. 28–33, 2010.

[8] I. Pountos, T. Georgouli, H. Bird, and P. V. Giannoudis, "Nonsteroidal anti-inflammatory drugs: prostaglandins, indications, and side effects," *International Journal of Interferon, Cytokine and Mediator Research*, vol. 3, no. 1, pp. 19–27, 2011.

[9] A. M. Celentano, G. Gorelik, M. E. Solana, L. Sterin-Borda, E. Borda, and S. M. González Cappa, "PGE_2 involvement in experimental infection with *Trypanosoma cruzi* subpopulations," *Prostaglandins*, vol. 49, no. 3, pp. 141–153, 1995.

[10] P. Pinge-Filho, C. E. Tadokoro, and I. D. A. Abrahamsohn, "Prostaglandins mediate suppression of lymphocyte proliferation and cytokine synthesis in acute *Trypanosoma cruzi* infection," *Cellular Immunology*, vol. 193, no. 1, pp. 90–98, 1999.

[11] V. L. Hideko Tatakihara, R. Cecchini, C. L. Borges et al., "Effects of cyclooxygenase inhibitors on parasite burden, anemia and oxidative stress in murine *Trypanosoma cruzi* infection," *FEMS Immunology and Medical Microbiology*, vol. 52, no. 1, pp. 47–58, 2008.

[12] L. Sterin-Borda, G. Gorelik, N. Goren, S. Gonzalez Cappa, A. M. Celentano, and E. Borda, "Lymphocyte muscarinic cholinergic activity and PGE_2 involvement in experimental *Trypanosoma cruzi* infection," *Clinical Immunology and Immunopathology*, vol. 81, no. 2, pp. 122–128, 1996.

[13] S. Mukherjee, F. S. Machado, H. Huang et al., "Aspirin treatment of mice infected with *Trypanosoma cruzi* and implications for the pathogenesis of chagas disease," *PLoS ONE*, vol. 6, no. 2, Article ID e16959, 2011.

[14] G. K. Abdalla, G. E. L. Faria, K. T. Silva, E. C. C. Castro, M. A. Reis, and M. A. Michelin, "*Trypanosoma cruzi*: the role of PGE_2 in immune response during the acute phase of experimental infection," *Experimental Parasitology*, vol. 118, no. 4, pp. 514–521, 2008.

[15] C. G. Freire-de-Lima, D. O. Nascimento, M. B. P. Soares et al., "Erratum: uptake of apoptotic cells drives the growth of a pathogenic trypanosome in macrophages (Nature (2000) 403 (199-203))," *Nature*, vol. 404, no. 6780, p. 904, 2000.

[16] M. A. Michelin, J. S. Silva, and F. Q. C. Cunha, "Inducible cyclooxygenase released prostaglandin mediates immunosuppression in acute phase of experimental *Trypanosoma cruzi* infection," *Experimental Parasitology*, vol. 111, no. 2, pp. 71–79, 2005.

[17] C. N. Paiva, R. H. Arras, L. P. Lessa et al., "Unraveling the lethal synergism between *Trypanosoma cruzi* infection and LPS: a role for increased macrophage reactivity," *European Journal of Immunology*, vol. 37, no. 5, pp. 1355–1364, 2007.

[18] A. Molina-Berríos, C. Campos-Estrada, N. Henriquez et al., "Protective role of acetylsalicylic acid in experimental *Trypanosoma cruzi* infection: evidence of a 15-epi-lipoxin A4-mediated effect," *PLoS Neglected Tropical Diseases*, vol. 7, no. 4, Article ID e2173, 2013.

[19] L. H. P. Silva and V. Nussenzweig, "Sobre uma cepa de *Trypanosoma cruzi* altamente virulenta para o camundongo branco," *Folia Clinica et Biológica*, vol. 20, pp. 191–203, 1953.

[20] E. S. Barrias, L. C. Reignault, W. de Souza, and T. M. U. Carvalho, "Dynasore, a dynamin inhibitor, inhibits *Trypanosoma cruzi* entry into peritoneal macrophages," *PLoS ONE*, vol. 5, no. 1, Article ID e7764, 2010.

[21] W. L. Smith, "Nutritionally essential fatty acids and biologically indispensable cyclooxygenases," *Trends in Biochemical Sciences*, vol. 33, no. 1, pp. 27–37, 2008.

[22] P. F. T. Cezar-De-Mello, A. M. Vieira, V. Nascimento-Silva, C. G. Villela, C. Barja-Fidalgo, and I. M. Fierro, "ATL-1, an analogue of aspirin-triggered lipoxin A 4, is a potent inhibitor of several steps in angiogenesis induced by vascular endothelial growth factor," *British Journal of Pharmacology*, vol. 153, no. 5, pp. 956–965, 2008.

[23] R. López-Muñoz, M. Faúndez, and S. Klein, "*Trypanosoma cruzi*: in vitro effect of aspirin with nifurtimox and benznidazole," *Experimental Parasitology*, vol. 124, no. 2, pp. 167–171, 2010.

[24] C. N. Serhan, N. Chiang, and T. E. van Dyke, "Resolving inflammation: dual anti-inflammatory and pro-resolution lipid mediators," *Nature Reviews Immunology*, vol. 8, no. 5, pp. 349–361, 2008.

[25] C. D. Russell and J. Schwarze, "The role of pro-resolution lipid mediators in infectious disease," *Immunology*, vol. 141, no. 2, pp. 166–173, 2014.

[26] S. Fiore, G. Antico, M. Aloman, and S. Sodin-Semrl, "Lipoxin A4 biology in the human synovium. Role of the ALX signaling pathways in modulation of inflammatory arthritis," *Prostaglandins Leukotrienes and Essential Fatty Acids*, vol. 73, no. 3-4, pp. 189–196, 2005.

[27] N. Chiang, C. N. Serhan, S.-E. Dahlén et al., "The lipoxin receptor ALX: potent ligand-specific and stereoselective actions in vivo," *Pharmacological Reviews*, vol. 58, no. 3, pp. 463–487, 2006.

[28] J. Clària, M. H. Lee, and C. N. Serhan, "Aspirin-triggered lipoxins (15-epi-LX) are generated by the human lung adenocarcinoma cell line (A549)-neutrophil interactions and are potent inhibitors of cell proliferation," *Molecular Medicine*, vol. 2, no. 5, pp. 583–596, 1996.

[29] A. W. Ashton, S. Mukherjee, F. N. U. Nagajyothi et al., "Thromboxane A2 is a key regulator of pathogenesis during *Trypanosoma cruzi* infection," *Journal of Experimental Medicine*, vol. 204, no. 4, pp. 929–940, 2007.

[30] C. L. Borges, R. Cecchini, V. L. H. Tatakihara et al., "5-Lipoxygenase plays a role in the control of parasite burden and contributes to oxidative damage of erythrocytes in murine Chagas'disease," *Immunology Letters*, vol. 123, no. 1, pp. 38–45, 2009.

[31] C. Panis, T. L. Mazzuco, C. Z. F. Costa et al., "*Trypanosoma cruzi*: effect of the absence of 5-lipoxygenase (5-LO)-derived leukotrienes on levels of cytokines, nitric oxide and iNOS expression in cardiac tissue in the acute phase of infection in mice," *Experimental Parasitology*, vol. 127, no. 1, pp. 58–65, 2011.

[32] M. M. Borges, J. K. Kloetzel, H. F. Andrade Jr., C. E. Tadokoro, P. Pinge-Filho, and I. Abrahamsohn, "Prostaglandin and nitric oxide regulate TNF-α production during *Trypanosoma cruzi* infection," *Immunology Letters*, vol. 63, no. 1, pp. 1–8, 1998.

[33] J. K. Hennan, J. Huang, T. D. Barrett et al., "Effects of selective cyclooxygenase-2 inhibition on vascular responses and thrombosis in canine coronary arteries," *Circulation*, vol. 104, no. 7, pp. 820–825, 2001.

[34] Y.-P. Wang, Y. Wu, L.-Y. Li et al., "Aspirin-triggered lipoxin A4attenuates LPS-induced pro-inflammatory responses by inhibiting activation of NF-κB and MAPKs in BV-2 microglial cells," *Journal of Neuroinflammation*, vol. 8, article no. 95, 2011.

[35] F. Kierszenbaum, J. J. Wirth, P. P. McCann, and A. Sjoerdsma, "Impairment of macrophage function by inhibitors of ornithine decarboxylase activity," *Infection and Immunity*, vol. 55, no. 10, pp. 2461–2464, 1987.

[36] D. S. Lima-Junior, D. L. Costa, V. Carregaro et al., "Inflammasome-derived IL-1β production induces nitric oxide-mediated resistance to Leishmania," *Nature Medicine*, vol. 19, no. 7, pp. 909–915, 2013.

[37] G. K. Silva, R. S. Costa, T. N. Silveira, and B. C. Caetano, "Apoptosis-associated speck-like protein containing a caspase recruitment domain inflammasomes mediate IL-1β response and host resistance to *Trypanosoma cruzi* infection," *Journal of Immunology*, vol. 191, pp. 3373–3383, 2013.

Hindawi Publishing Corporation
Mediators of Inflammation
Volume 2014, Article ID 362605, 6 pages
http://dx.doi.org/10.1155/2014/362605

Review Article

Immune Evasion Strategies of Pre-Erythrocytic Malaria Parasites

Hong Zheng, Zhangping Tan, and Wenyue Xu

Department of Pathogenic Biology, Third Military Medical University, Chongqing 400038, China

Correspondence should be addressed to Wenyue Xu; xuwenyue@gmail.com

Received 8 January 2014; Revised 25 March 2014; Accepted 27 March 2014; Published 7 May 2014

Academic Editor: Mauricio M. Rodrigues

Malaria is a mosquito-borne infectious disease of humans. It begins with a bite from an infected female *Anopheles* mosquito and leads to the development of the pre-erythrocytic and blood stages. Blood-stage infection is the exclusive cause of clinical symptoms of malaria. In contrast, the pre-erythrocytic stage is clinically asymptomatic and could be an excellent target for preventive therapies. Although the robust host immune responses limit the development of the liver stage, malaria parasites have also evolved strategies to suppress host defenses at the pre-erythrocytic stage. This paper reviews the immune evasion strategies of malaria parasites at the pre-erythrocytic stage, which could provide us with potential targets to design prophylactic strategies against malaria.

1. Developmental Bottlenecks at the Pre-Erythrocytic Stage

After the infected female *Anopheles* mosquitoes bite and inject sporozoites into the host skin, the deposited sporozoites spread from the injection site within several hours [1]. Although approximately 20% of sporozoites are drained into the lymphatic system, most sporozoites enter the blood circulation [1]. To invade hepatocytes, sporozoites in the blood must safely cross the Kupffer cells (KCs), which are interspersed throughout the sinusoidal lining [2]. After passing through the sinusoidal cell layer, sporozoites traverse several hepatocytes until they ultimately settle in the final one. Inside the final hepatocyte, sporozoites are enclosed by a parasitophorous vacuole and develop into schizonts [3]. Finally, merozoites exit the hepatocyte in the form of merosomes [4].

During this process, sporozoites encounter host robust innate immune responses. Up to 20–30% of sporozoites entering the lymphatic system are impeded at the proximal lymph node, and most parasites are degraded within DCs [5]. It is still unknown about the sensor involved in this process, but our recent data suggested that sporozoite might be recognized by Toll-like receptor 2 (TLR2) on the innate immune cells, as sporozoite lysate could activate TLR2 and knockout of TLR2 significantly promoted the development of the exoerythrocyte form (unpublished data). Even inside the liver, hepatocyte damage during sporozoite transmigration releases DAMPs (damage-associated molecular pattern molecules) and triggers innate immune responses that suppress the pre-erythrocytic stage [6]. Very recently, exoerythrocyte form (EEF) RNA was reported to be recognized by Mda5 in hepatocyte, leading to the production of IFN-α/β, which triggered a type I IFN response in the innate immune cells to limit the development of liver-stage [7]. Consistently, innate immune cells, such as NK, $\gamma\delta$T, and $CD4^-$ $CD8^-$ NK1.1+ $TCR\alpha\beta^{int}$ cells, have been known to be activated and inhibit the development of intrahepatic parasites during primary infection [8–10]. By an unknown mechanism, the ongoing blood-stage infection induces the expression of the host iron regulatory hormone hepcidin, which impairs the growth of subsequently inoculated sporozoites [11]. These results indicated that innate immune responses create several bottlenecks that inhibit the development of sporozoites into EEF. Although an average of only 123 sporozoites is injected by the bite of a single infected mosquito, a successful infection can be established [12], suggesting that sporozoites overcome these bottlenecks. Growing evidence shows that sporozoites have developed several strategies to escape host defenses during the development of the pre-erythrocytic stage, and we will discuss this issue in the following text.

2. Concealed Sporozoites Resist Phagocytes and Develop in the Skin

The skin membrane barrier is one of the most important parts of innate immunity, acting as the first line of defense against invading organisms. However, biting mosquitoes liberate many different soluble components, such as antihistamines, vasodilators, anticoagulants, platelet aggregation inhibitors, and immunomodulators, from their salivary glands. All of these components assist in sporozoite survival and facilitate their inoculation.

After inoculation, sporozoites stay in the skin for several hours [1, 13] and are activated into a state of readiness for the hepatic stages after they shift from the mosquito to the mammalian host [14]. However, their capacity for migration allows sporozoites to avoid destruction by phagocytes and growth arrest by nonphagocytic cells in the host dermis. Some sporozoites that are deficient in cell migration, such as spect (sporozoite microneme protein essential for cell traversal)−/− or spect2−/− sporozoites, are immobilized in the dermis, associated with CD11b+ cells, and destroyed by phagocytes [15]. Interestingly, ~10% of sporozoites transform into EEFs within the epidermis or the dermis, especially in the immune-privileged hair follicles [16]. However, subsequent overwhelming data showed that EEFs developing in the skin may not lead to a blood-stage infection [17], and their development in the skin remained to be confirmed in human malaria infection. Most sporozoites leaving the injection site invade the dermal blood circulation and travel to the liver; some entering the lymphatic system are degraded inside the DCs after a short differentiation period [5]. However, it is unknown whether sporozoites are phagocytized by DCs or actively invade DCs; it is also unknown whether it is beneficial for the host to elicit immune responses to clear the parasites or for malaria parasites to suppress the host immune responses.

3. Suppression of the Function of Kupffer Cells by Sporozoites

Once inside the circulatory system, sporozoites rapidly reach the liver. Sporozoites, however, are initially arrested in the sinusoid by specific binding of the stellate cell-derived ECM (extracellular matrix) proteoglycans, which extend from the Disse space through EC (endothelial cell) fenestrations [18, 19]. To invade hepatocytes, sporozoites must cross the continuous cell layer lining the sinusoids. The arrested sporozoites then glide freely for several minutes along the sinusoidal endothelium until meeting a KC, the resident macrophage of the liver. Previous intravital microscopy and electron microscopy supported that sporozoites actively pass through KCs but not ECs, and the interaction of CSP (circumsporozoite protein) with chondroitin and heparan sulfate proteoglycans on the surface of KCs allows entry to the liver parenchyma [2, 20]. However, multiplicity of sporozoite crossing mechanisms was revealed recently by using spinning-disk confocal imaging. It was found that most sporozoites penetrate the sinusoidal barrier through ECs (53%), and some specifically cross KCs (~24%). Some sporozoites can cross the gaps between ECs or between an EC and a KC, independent of their cell-transversal capacity. Thus, gap crossing may be observed for the cell crossing-deficient sporozoite mutants SPECT, SPECT2, and CelTOS (cell-traversal protein for ookinetes and sporozoites), which all induce a blood infection, though with reduced efficiency [21–24].

It is puzzling that sporozoites safely traverse KCs, which provide innate immunity against microorganisms invading hepatocytes. The mechanisms responsible for this migration are becoming clearer. The binding of sporozoite CSP to the LRP-1 (low-density lipoprotein receptor-related protein) and proteoglycans on the KC surface increases the levels of intracellular cAMP/EPAC and prevents the formation of ROS (reactive oxygen species) [25]. Sporozoite contacting with KC also downregulates the inflammatory cytokines TNF-α, IL-6, and MCP-1 and upregulates the anti-inflammatory cytokine IL-10 after stimulation with IFN-γ or LPS [26]. In addition, the binding of sporozoites also induced KC apoptosis [26]. Further study found that the ability to migrate across cells is not only required for the malaria parasite to reach the liver [15], but also for its resistance to clearance by KCs, as sporozoites with high cell-crossing capacities kill KCs during this process [24]. In addition, the antigen-presentation activity of KCs, including the expression of MHC-I and IL-12, is severely reduced in mice challenged with sporozoites compared with those immunized with irradiation-attenuated sporozoites [27]. We previously showed that pretreatment with TLR agonists, especially CpG, significantly inhibits sporozoite development into EEF, potentially by enhancing the phagocytic capacity of KCs [28]; this result also suggested that sporozoites suppress KC function, and they could actively penetrate KCs if the phagocytic function of KCs is suppressed by sporozoites (Figure 1).

It is assumed that sporozoites traverse KCs without forming parasitophorous vacuoles [24]. However, previous study showed that sporozoites in KCs are isolated in parasitophorous vacuoles, which are formed to avoid lysosomal degradation [29]. CSP in parasitophorous vacuoles is released into the cytoplasm of host hepatocytes via its PEXEL domain [30] and inhibits host cell protein synthesis [31]. Therefore, it is interesting to investigate whether CSP could also suppress the function of KCs through inhibiting protein synthesis.

4. The Manipulation of Hepatocytes

After penetrating the sinusoidal cell layer, sporozoites invade hepatocytes and develop into EEFs. Unlike many other microbial organisms that utilize the phagocytic properties of their host cells for invasion, sporozoites actively invade hepatocytes. Sporozoites possibly use the cholesterol uptake pathway to invade hepatocytes. In addition to tetraspanin CD81 [32] and CD9 [33], the successful invasion of hepatocytes by sporozoites requires the host hepatocyte SR-BI (scavenger receptor BI) [34], which mediates the selective uptake of cholesteryl esters from both high- and low-density lipoprotein. However, sporozoites always pass through several hepatocytes prior to the final hepatocyte in which they develop

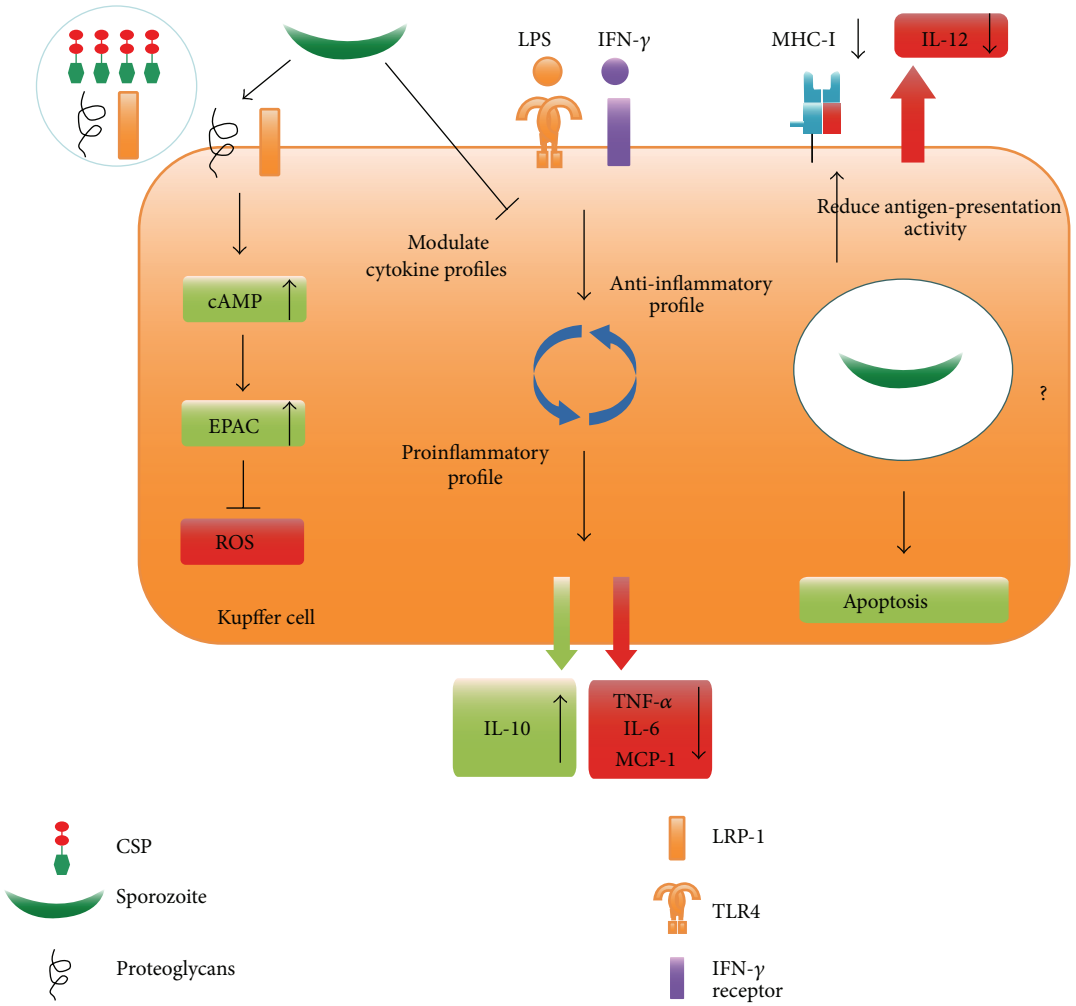

Figure 1: Sporozoites suppress the function of KCs. The binding of sporozoite CSP to proteoglycans and LRP-1 upregulates cAMP/EPAC and prevents the formation of ROS (left). Exposure to sporozoites downregulates the inflammatory cytokines TNF-α, IL-6, and MCP-1 and upregulates the anti-inflammatory cytokine IL-10 after stimulation with IFN-γ or LPS (middle). Sporozoite infection also downregulates MHC I and IL-12p40 and induces apoptosis in KCs (right).

[3]. Although the reason for this process is not well defined, it is likely that sporozoites choose the best environment for their differentiation into merozoites. The migration through hepatocytes increases sporozoite competency for differentiation by inducing the exocytosis of sporozoite apical organelles that are involved in the formation of an intracellular vacuole for infection [35]. The exocytosis of apical organelles during sporozoite migration is mediated by the malaria parasite adenylyl cyclase α and cAMP signaling [36]. Hepatocyte damage caused by transmigration is essential for making neighboring hepatocytes more susceptible to early parasite development; this process occurs by the activation of a HGF (hepatocyte growth factor)/cMET-dependent pathway and reorganization of host cell actin cytoskeleton [37]. However, SPECT1- [23] or SPECT2-defective [22] sporozoites, which cannot cross cells, infect hepatocytes *in vitro*, suggesting that transmigration may not be indispensable for the development of sporozoites in hepatocytes. Migration and invasion are two different sporozoite phenotypes that are regulated by the interaction of the sporozoite main surface protein CSP [38] and HSPGs (heparan sulfate proteoglycans). When CSP binds to low-sulfate HSPGs on dermal fibroblasts or endothelial cells, sporozoites transmigrate the host cells without parasitophorous vacuole formation. If CSP interacts with high-sulfate HSPGs on hepatocytes, it will be cleaved and supposed to expose the TSR (thrombospondin repeat) domain, and the binding of TSR domain to HSPGs leads to sporozoite invasion of hepatocytes [39, 40]. Once inside the final hepatocyte, a sporozoite is enclosed in a parasitophorous vacuole [3], which is separated from the lysosome to avoid degradation by the endocytic/lysosome system.

To survive and develop in the parasitophorous vacuole, the parasite has developed several strategies to suppress hepatocyte function while preventing cell death. For instance, cleaved CSP escapes from the parasitophorous vacuole into hepatocyte cytoplasm using its PEXEL domain [30]. Cleaved CSP that is translocated into the cytoplasm inhibits host cell protein synthesis by binding ribosomes, which might be

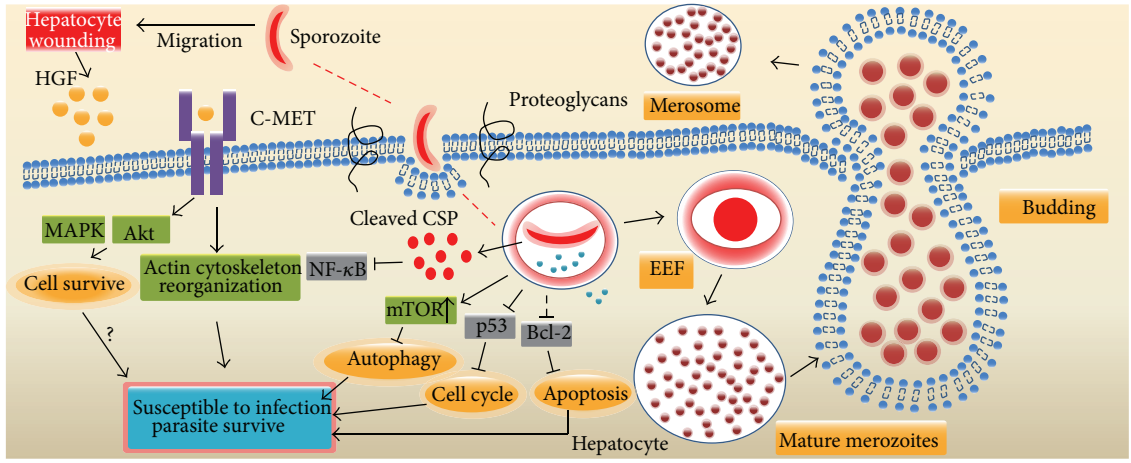

FIGURE 2: The manipulation of hepatocytes by sporozoites. Sporozoites transmigrate several hepatocytes prior to settling in a final cell. Transmigrated hepatocytes release HGF, which binds to the C-MET receptor, making the hepatocyte susceptible to infection and resistant to apoptosis by upregulation of MAPK, and Akt (left). The interaction of CSP with high levels of HSPGs triggers the cleavage of CSP and encapsulation of sporozoites in parasitophorous vacuoles. Cleaved CSP escapes from the parasitophorous vacuole into the cytoplasm, where it inhibits the NF-κB activation and host protein synthesis. Sporozoite invasion upregulates mTOR and downregulates p53, and Bcl-2 which block autophagy, cell cycle progression and Apoptosis, respectively (middle). To avoid destruction by KCs and DCs during release from hepatocytes, merozoites bud from the hepatocytes in merosomes, which are covered with host cell-derived membranes, and PS exposure on the outer leaflet of the dying hepatocytes is blocked (right).

beneficial for the development of the sporozoite [31]. CSP released into the cytoplasm possibly promotes parasite development through the suppression of NF-κB [30]. Furthermore, *P. berghei* sporozoites infection inhibited hepatocyte apoptosis [41], and external HGF/cMET signaling is also involved in this process through upregulation of MAPK and PI3-kinase/Akt [42]. Very recently, Kaushansky et al. found that the majority of hepatocytes infected with wildtype but not attenuated liver-stage parasites can resist Fas-mediated apoptosis via an antiapoptotic mitochondrial protein [43]. Using protein lysate microarrays, they also found that hepatocyte regulatory pathways involved in cell survival (Bcl-2), proliferation, and autophagy (mTOR) were significantly perturbed by the *P. yoelii* sporozoite infection. Notably, the prodeath protein p53 was substantially decreased in infected hepatocytes, which allowed parasite survival [44].

Autophagy is a bulk degradation system that delivers cytoplasmic constituents and organelles into lysosomes for hydrolysis. It is originally thought to be essential for cell survival, development, and homeostasis, but growing evidence supported that autophagy could also restrict viral infections and the replication of intracellular bacteria and parasites [45]. Although autophagy was found to be involved in the transformation of sporozoites into the liver stage [46], the role of hepatocyte autophagy on the development of the pre-erythrocytic stage has not been reported. It is, therefore, interesting to investigate whether the sporozoite infection could induce hepatocyte autophagy and its effect on pre-erythrocytic stage development.

In addition to the period when sporozoites develop into merozoites in hepatocytes, merozoites also evade host defenses when they exit hepatocytes. To access the bloodstream, liver-stage merozoites must leave hepatocytes and cross both the Disse and sinusoid spaces, where they are vulnerable to be attacked by phagocytes including KCs and DCs. To avoid host cell defense mechanisms, merozoites bud from detached hepatocytes in merosomes [4, 47], which are covered with host cell-derived membranes [48]. During this process, the infected hepatocyte dies, but merozoites uptake Ca^{2+} and maintain low Ca^{2+} levels in the host cell to block the exposure of PS (phosphatidylserine) on the outer leaflet of the dying cells [4, 47]. Thus, dying hepatocytes avoid recognition by phagocytes, and merosomes are safely shielded from the hepatocytes. Merosomes eventually disintegrate inside pulmonary capillaries, which liberate merozoites into the bloodstream and for erythrocyte invasion [49] (Figure 2).

5. Concluding Remarks

Sporozoite infection elicits robust innate immune responses to limit its development into the erythrocytic stage. However, this parasite has evolved several escape strategies at each step of the liver-stage infection. For example, sporozoites could suppress the immune functions in KCs to ensure their safe passage through the sinusoidal cell layer of the liver. Once inside the hepatocyte, sporozoites could also inhibit the apoptosis of the infected hepatocyte to foster their development into EEFs, but they also induce host cell death after their release from the liver in merosomes. However, sporozoite challenge upregulates HO-1 (heme oxygenase-1), which promotes the development of the liver stage by inducing anti-inflammatory cytokines [50]. Although great progress has been made in recent years, some questions still remain. For instance, do molecules other than CSP escape from the PV to the cytoplasm and suppress hepatocyte functions? Does sporozoite infection induce hepatocyte autophagy?

What is the effect of autophagy on pre-erythrocytic stage development? Answering these questions will not only help us to further understand the immune evasion strategies of sporozoites but will also provide us with novel targets for preventing malaria. For example, our previous study showed that preactivation of innate immune cells, such as KC, by individual TLRs agonists could significantly prevent the development of the pre-erythrocytic stage [28, 51].

Conflict of Interests

The authors declare that there is no conflict of interests regarding the publication of this paper.

Acknowledgments

The authors would like to thank Ana Rodriguez for her critical reading of and suggestions for the paper. This research was supported by the Natural Science Foundation of China (81271859 and 81000747) and the Natural Science Foundation of the Military (CWS12J093).

References

[1] L. M. Yamauchi, A. Coppi, G. Snounou, and P. Sinnis, "*Plasmodium* sporozoites trickle out of the injection site," *Cellular Microbiology*, vol. 9, no. 5, pp. 1215–1222, 2007.

[2] U. Frevert, S. Engelmann, S. Zougbédé et al., "Intravital observation of *Plasmodium berghei* sporozoite infection of the liver," *PLoS Biology*, vol. 3, no. 6, Article ID e192, 2005.

[3] M. M. Mota, G. Pradel, J. P. Vanderberg et al., "Migration of *Plasmodium* sporozoites through cells before infection," *Science*, vol. 291, no. 5501, pp. 141–144, 2001.

[4] A. Sturm, R. Amino, C. van de Sand et al., "Manipulation of host hepatocytes by the malaria parasite for delivery into liver sinusoids," *Science*, vol. 313, no. 5791, pp. 1287–1290, 2006.

[5] R. Amino, S. Thiberge, B. Martin et al., "Quantitative imaging of *Plasmodium* transmission from mosquito to mammal," *Nature Medicine*, vol. 12, no. 2, pp. 220–224, 2006.

[6] R. Torgler, S. E. Bongfen, J. C. Romero, A. Tardivel, M. Thome, and G. Corradin, "Sporozoite-mediated hepatocyte wounding limits *Plasmodium* parasite development via MyD88-mediated NF-κB activation and inducible NO synthase expression," *The Journal of Immunology*, vol. 180, no. 6, pp. 3990–3999, 2008.

[7] P. Liehl, V. Zuzarte-Luis, J. Chan et al., "Host-cell sensors for *Plasmodium* activate innate immunity against liver-stage infection," *Nature Medicine*, vol. 20, no. 1, pp. 47–53, 2014.

[8] S. Pied, J. Roland, A. Louise et al., "Liver $CD4^{-}CD8^{-}$ $NK1.1^{+}$ TCR$\alpha\beta$ intermediate cells increase during experimental malaria infection and are able to exhibit inhibitory activity against the parasite liver stage in vitro," *The Journal of Immunology*, vol. 164, no. 3, pp. 1463–1469, 2000.

[9] K. C. McKenna, M. Tsuji, M. Sarzotti, J. B. Sacci Jr., A. A. Witney, and A. F. Azad, "$\gamma\delta$ T cells are a component of early immunity against preerythrocytic malaria parasites," *Infection and Immunity*, vol. 68, no. 4, pp. 2224–2230, 2000.

[10] J. Roland, V. Soulard, C. Sellier et al., "NK cell responses to *Plasmodium* infection and control of intrahepatic parasite development," *The Journal of Immunology*, vol. 177, no. 2, pp. 1229–1239, 2006.

[11] S. Portugal, C. Carret, M. Recker et al., "Host-mediated regulation of superinfection in malaria," *Nature Medicine*, vol. 17, no. 6, pp. 732–737, 2011.

[12] D. L. Medica and P. Sinnis, "Quantitative dynamics of *Plasmodium yoelii* sporozoite transmission by infected anopheline mosquitoes," *Infection and Immunity*, vol. 73, no. 7, pp. 4363–4369, 2005.

[13] C. Kebaier, T. Voza, and J. Vanderberg, "Kinetics of mosquito-injected *Plasmodium* sporozoites in mice: fewer sporozoites are injected into sporozoite-immunized mice," *PLoS Pathogens*, vol. 5, no. 4, Article ID e1000399, 2009.

[14] A. Siau, O. Silvie, J.-F. Franetich et al., "Temperature shift and host cell contact up-regulate sporozoite expression of *Plasmodium falciparum* genes involved in hepatocyte infection," *PLoS Pathogens*, vol. 4, no. 8, Article ID e1000121, 2008.

[15] R. Amino, D. Giovannini, S. Thiberge et al., "Host cell traversal is important for progression of the malaria parasite through the dermis to the liver," *Cell Host & Microbe*, vol. 3, no. 2, pp. 88–96, 2008.

[16] P. Gueirard, J. Tavares, S. Thiberge et al., "Development of the malaria parasite in the skin of the mammalian host," *Proceedings of the National Academy of Sciences of the United States of America*, vol. 107, no. 43, pp. 18640–18645, 2010.

[17] T. Voza, J. L. Miller, S. H. Kappe, and P. Sinnis, "Extrahepatic exoerythrocytic forms of rodent malaria parasites at the site of inoculation: clearance after immunization, susceptibility to primaquine, and contribution to blood-stage infection," *Infection and Immunity*, vol. 80, no. 6, pp. 2158–2164, 2012.

[18] G. Pradel, S. Garapaty, and U. Frevert, "Proteoglycans mediate malaria sporozoite targeting to the liver," *Molecular Microbiology*, vol. 45, no. 3, pp. 637–651, 2002.

[19] G. Pradel, S. Garapaty, and U. Frevert, "Kupffer and stellate cell proteoglycans mediate malaria sporozoite targeting to the liver," *Comparative Hepatology*, vol. 3, supplement 1, article S47, 2004.

[20] G. Pradel and U. Frevert, "Malaria sporozoites actively enter and pass through rat Kupffer cells prior to hepatocyte invasion," *Hepatology*, vol. 33, no. 5, pp. 1154–1165, 2001.

[21] T. Kariu, T. Ishino, K. Yano, Y. Chinzei, and M. Yuda, "CelTOS, a novel malarial protein that mediates transmission to mosquito and vertebrate hosts," *Molecular Microbiology*, vol. 59, no. 5, pp. 1369–1379, 2006.

[22] T. Ishino, Y. Chinzei, and M. Yuda, "Two proteins with 6-cys motifs are required for malarial parasites to commit to infection of the hepatocyte," *Molecular Microbiology*, vol. 58, no. 5, pp. 1264–1275, 2005.

[23] T. Ishino, K. Yano, Y. Chinzei, and M. Yuda, "Cell-passage activity is required for the malarial parasite to cross the liver sinusoidal cell layer," *PLoS Biology*, vol. 2, no. 1, article e4, 2004.

[24] J. Tavares, P. Formaglio, S. Thiberge et al., "Role of host cell traversal by the malaria sporozoite during liver infection," *The Journal of Experimental Medicine*, vol. 210, no. 5, pp. 905–915, 2013.

[25] I. Usynin, C. Klotz, and U. Frevert, "Malaria circumsporozoite protein inhibits the respiratory burst in Kupffer cells," *Cellular Microbiology*, vol. 9, no. 11, pp. 2610–2628, 2007.

[26] C. Klotz and U. Frevert, "*Plasmodium yoelii* sporozoites modulate cytokine profile and induce apoptosis in murine Kupffer cells," *International Journal for Parasitology*, vol. 38, no. 14, pp. 1639–1650, 2008.

[27] N. Steers, R. Schwenk, D. J. Bacon, D. Berenzon, J. Williams, and U. Krzych, "The immune status of Kupffer cells profoundly

influences their responses to infectious *Plasmodium berghei* sporozoites," *European Journal of Immunology*, vol. 35, no. 8, pp. 2335–2346, 2005.

[28] J. Chen, W. Xu, T. Zhou, Y. Ding, J. Duan, and F. Huang, "Inhibitory role of toll-like receptors agonists in *Plasmodium yoelii* liver stage development," *Parasite Immunology*, vol. 31, no. 8, pp. 466–473, 2009.

[29] J. F. Meis, J. P. Verhave, P. H. Jap, R. E. Sinden, and J. H. Meuwissen, "Ultrastructural observations on the infection of rat liver by *Plasmodium berghei* sporozoites in vivo," *Journal of Protozoology*, vol. 30, no. 2, pp. 361–366, 1983.

[30] A. P. Singh, C. A. Buscaglia, Q. Wang et al., "*Plasmodium* circumsporozoite protein promotes the development of the liver stages of the parasite," *Cell*, vol. 131, no. 3, pp. 492–504, 2007.

[31] U. Frevert, M. R. Galinski, F.-U. Hügel et al., "Malaria circumsporozoite protein inhibits protein synthesis in mammalian cells," *The EMBO Journal*, vol. 17, no. 14, pp. 3816–3826, 1998.

[32] O. Silvie, E. Rubinstein, J.-F. Franetich et al., "Hepatocyte CD81 is required for *Plasmodium falciparum* and *Plasmodium yoelii* sporozoite infectivity," *Nature Medicine*, vol. 9, no. 1, pp. 93–96, 2003.

[33] S. Charrin, S. Yalaoui, B. Bartosch et al., "The Ig domain protein CD9P-1 down-regulates CD81 ability to support *Plasmodium yoelii* infection," *The Journal of Biological Chemistry*, vol. 284, no. 46, pp. 31572–31578, 2009.

[34] C. D. Rodrigues, M. Hannus, M. Prudêncio et al., "Host scavenger receptor SR-BI plays a dual role in the establishment of malaria parasite liver infection," *Cell Host & Microbe*, vol. 4, no. 3, pp. 271–282, 2008.

[35] M. M. Mota, J. C. R. Hafalla, and A. Rodriguez, "Migration through host cells activates *Plasmodium* sporozoites for infection," *Nature Medicine*, vol. 8, no. 11, pp. 1318–1322, 2002.

[36] T. Ono, L. Cabrita-Santos, R. Leitao et al., "Adenylyl cyclase α and cAMP signaling mediate *Plasmodium* sporozoite apical regulated exocytosis and hepatocyte infection," *PLoS Pathogens*, vol. 4, no. 2, Article ID e1000008, 2008.

[37] M. Carrolo, S. Giordano, L. Cabrita-Santos et al., "Hepatocyte growth factor and its receptor are required for malaria infection," *Nature Medicine*, vol. 9, no. 11, pp. 1363–1369, 2003.

[38] S. H. I. Kappe, C. A. Buscaglia, and V. Nussenzweig, "*Plasmodium* sporozoite molecular cell biology," *Annual Review of Cell and Developmental Biology*, vol. 20, pp. 29–59, 2004.

[39] A. Coppi, C. Pinzon-Ortiz, C. Hutter, and P. Sinnis, "The *Plasmodium* circumsporozoite protein is proteolytically processed during cell invasion," *The Journal of Experimental Medicine*, vol. 201, no. 1, pp. 27–33, 2005.

[40] A. Coppi, R. Tewari, J. R. Bishop et al., "Heparan sulfate proteoglycans provide a signal to *Plasmodium* sporozoites to stop migrating and productively invade host cells," *Cell Host & Microbe*, vol. 2, no. 5, pp. 316–327, 2007.

[41] C. van de Sand, S. Horstmann, A. Schmidt et al., "The liver stage of *Plasmodium berghei* inhibits host cell apoptosis," *Molecular Microbiology*, vol. 58, no. 3, pp. 731–742, 2005.

[42] P. Leirião, S. S. Albuquerque, S. Corso et al., "HGF/MET signalling protects *Plasmodium*-infected host cells from apoptosis," *Cellular Microbiology*, vol. 7, no. 4, pp. 603–609, 2005.

[43] A. Kaushansky, P. G. Metzger, A. N. Douglass et al., "Malaria parasite liver stages render host hepatocytes susceptible to mitochondria-initiated apoptosis," *Cell Death & Disease*, vol. 4, Article ID e762, 2013.

[44] A. Kaushansky, A. S. Ye, L. S. Austin et al., "Suppression of host p53 is critical for *Plasmodium* liver-stage infection," *Cell Reports*, vol. 3, no. 3, pp. 630–637, 2013.

[45] P. Kuballa, W. M. Nolte, A. B. Castoreno, and R. J. Xavier, "Autophagy and the immune system," *Annual Review of Immunology*, vol. 30, pp. 611–646, 2012.

[46] I. Coppens, "Metamorphoses of malaria: the role of autophagy in parasite differentiation," *Essays in Biochemistry*, vol. 51, pp. 127–136, 2011.

[47] A. F. Cowman and S. H. I. Kappe, "Malaria's stealth shuttle," *Science*, vol. 313, no. 5791, pp. 1245–1246, 2006.

[48] S. Graewe, K. E. Rankin, C. Lehmann et al., "Hostile takeover by *Plasmodium*: reorganization of parasite and host cell membranes during liver stage egress," *PLoS Pathogens*, vol. 7, no. 9, Article ID e1002224, 2011.

[49] K. Baer, C. Klotz, S. H. I. Kappe, T. Schnieder, and U. Frevert, "Release of hepatic *Plasmodium yoelii* merozoites into the pulmonary microvasculature," *PLoS Pathogens*, vol. 3, no. 11, Article ID e171, 2007.

[50] S. Epiphanio, S. A. Mikolajczak, L. A. Gonçalves et al., "Heme oxygenase-1 is an anti-inflammatory host factor that promotes murine *Plasmodium* liver infection," *Cell Host & Microbe*, vol. 3, no. 5, pp. 331–338, 2008.

[51] X. Wen-Yue, W. Xing-Xiang, Q. Jie, D. Jian-Hua, and H. Fu-Sheng, "*Plasmodium yoelii*: influence of immune modulators on the development of the liver stage," *Experimental Parasitology*, vol. 126, no. 2, pp. 254–258, 2010.